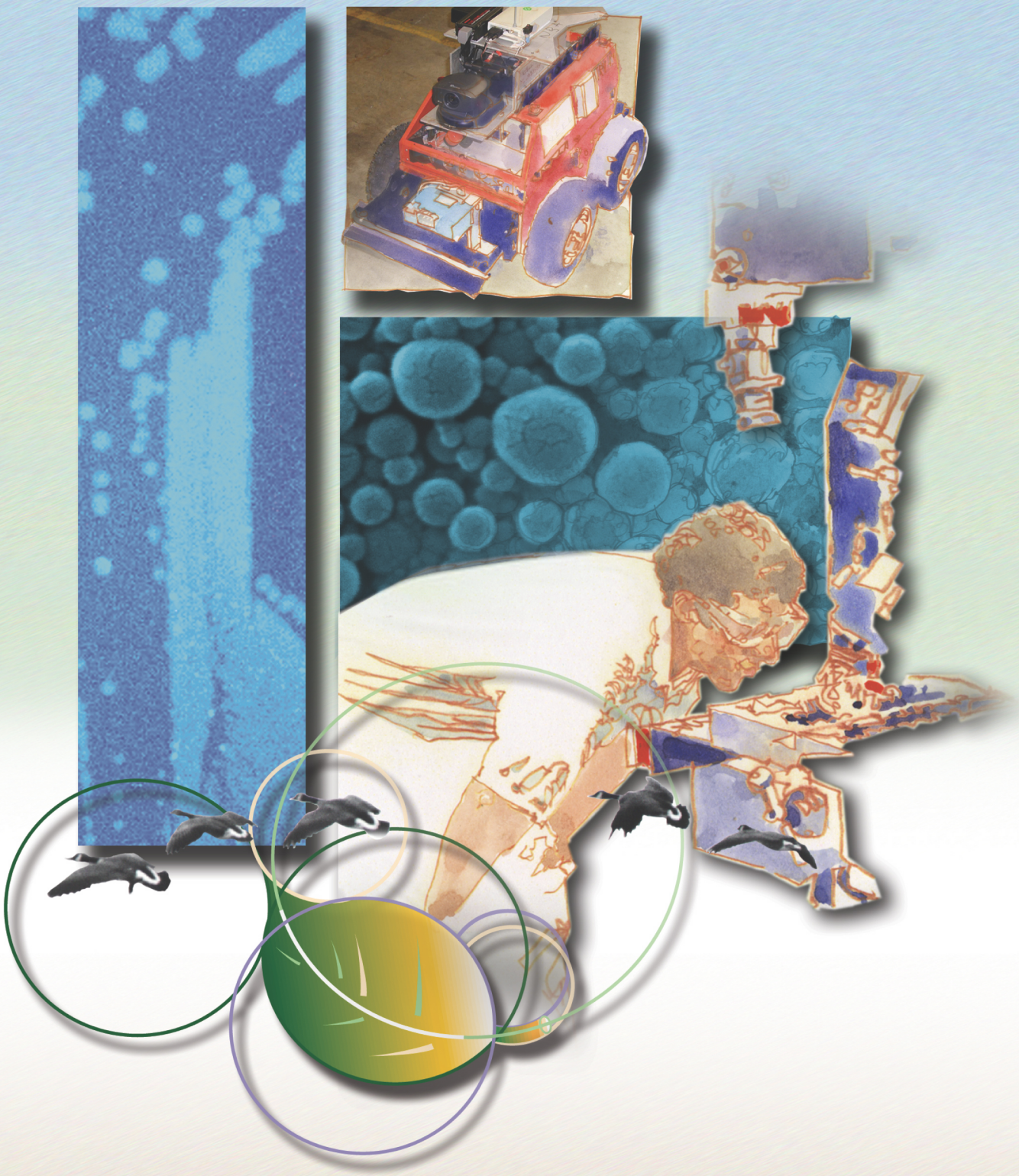

# Laboratory-Directed Research and Development

## Annual Report for FY-2002

Idaho National Engineering & Environmental Laboratory

# To Our Stakeholders

It is my pleasure to submit the fiscal year 2002 Annual Report for the Laboratory Directed Research and Development (LDRD) Program at the Idaho National Engineering and Environmental Laboratory (INEEL). This report summarizes our discretionary research portfolio in support of the mission areas of the Department of Energy (DOE) and the INEEL's strategic focus as detailed in our Institutional Plan.

Our technologies continue to earn national recognition through prestigious awards such as Research & Development 100, Technical Review 100, and Federal Laboratory Consortium for Technology Transfer. The INEEL developed and deployed 107 new technologies to assist with environmental cleanup work and created six successful spin-off companies. A number of researchers hold leadership positions, or were honored by technical and professional societies for their research accomplishments. Many of these successes are attributable to the investment in LDRD.

As a multi-program national laboratory, the INEEL continues to deliver advances in science and technology that support DOE's missions in energy, national defense, and science. We continue to strengthen existing partnerships and build new alliances with other national laboratories, government agencies, academia, and private industry. These relationships are essential to stimulating intellectual vitality, leveraging knowledge and resources, and generally increasing the value of science and technology delivered to DOE.

The fiscal year 2002 INEEL LDRD research portfolio reflects priorities of the DOE in support of national needs. In keeping with INEEL's past strong support of DOE's environmental mission, and in response to aggressive changes in the environmental cleanup program initiative by Jesse Roberson, the Assistant Secretary for Environmental Management (EM), a large percentage of INEEL's LDRD research in fiscal year 2002 focused on environmental science.

In July 2002, Spencer Abraham, DOE Secretary of Energy established the INEEL as the nation's leading center for nuclear energy research and development (R&D). This action recognized and expanded the laboratory's role in national and energy security. Energy security is fundamental to our nation's well being, and the INEEL's rich history of technical and scientific expertise in nuclear energy engineering, research, and analysis provides a strong platform for national leadership. In partnership with the DOE Office of Nuclear Energy, Science, and Technology, we look forward to taking a leadership role in defining and implementing a new era of nuclear R&D, and our LDRD portfolio reflects this commitment.

The progress achieved by LDRD researchers in fiscal year 2002 is summarized in this report. INEEL LDRD research not only helps us to meet existing needs, but also to anticipate future needs of DOE and the nation.

*Billy D. Shipp, Ph. D.*

Laboratory Director and General Manager

INEEL/EXT-03-00390

# Acknowledgments

This annual report provides an overview of the Laboratory Directed Research and Development (LDRD) Program at the Idaho National Engineering and Environmental Laboratory (INEEL). Summarized in this report are 136 technical research projects conducted in fiscal year 2002. The LDRD Program at the INEEL is managed for the laboratory by Dr. Richard Jacobsen, Associate Laboratory Director, Strategic Management and Chief Scientist. Dr. Ray S. Enge is the director for Strategic Planning and LDRD. Dr. Debonny Shoaf is the LDRD Program Manager.

Many people contributed to this report; particular thanks go to the principal investigators who conduct the cutting-edge research so important to this laboratory.

**Managing Editor:** Mary Catherine Thelen
**Associate Editor:** Lonnie Martinell
**Science Writer:** Diane Salisbury
**Designer:** Shaun C. Eames

Prepared for the U.S. Department of Energy
Assisatant Secretary for Environmental Management
Under DOE Idaho Operations Office
Contract DE-AC07-99ID13727

# Table of Contents


## *Overview* ..... *13*

Feature Article ..... 15

## *Energy* ..... *23*

Hydrogen Production from High Temperature Nuclear Reactors ..... 25
Co-Firing of Coal and Refuse-Derived Fuel with Oil Shale for Improved Production and Control of Environmental Contaminants: Laboratory Studies ..... 27
Two-Phase Mass Flow Measurement for Geothermal Wells ..... 31
Clean Cold Start Technology for Conventional, Electric, and Hybrid Vehicles ..... 33
Novel Solid Electrolyte Materials for Lithium Batteries ..... 35
Active Neutron Spectroscopy for Neutron Capture Beam Characterization ..... 38
Characterization and Modeling of a Grain Combine Harvester ..... 41
Development of Analytical Decision-Making Tools for Energy Efficient Agricultural Biomass Production ..... 44
Hydrogen Technologies R&D ..... 47
Carbon Dioxide Sequestration in Geologic Coal Formations ..... 49
Dependence of Coal Bed Permeability on Pore Pressure and Adsorbed Gas Content ..... 52
Thermal Studies of Potential Increased ATR Power Margins ..... 55
High-Temperature Flow Measurement of Molten Salts ..... 57
Energy Efficient Building Simulation and Technologies ..... 60
Friction Stir Welding of Lightweight Materials ..... 63
Genetic Control of Straw Stem Ultrastructure that Affects the Biomechanics of Stem Separation ..... 65
Laser Ultrasonic Characterization of Irradiated Ceramics ..... 68
Laser Ultrasonic Corrosion Monitor ..... 71
Removal of Minerals from Wheat Straw for Increased Straw Utilization for Bioenergy and Bioproducts ..... 74
Computational Fluid Dynamics Model Based Control of Two-Phase Flow ..... 78
Acidophilic Bioprocess for Production of Organic Acids from Biomass ..... 81
An Innovative Gas-Cooled Fast Reactor ..... 83
Characterization of Methane Hydrate Deposits ..... 86

## *Environmental* ..... *89*

Elemental Tracers and Multi-Variate Receptor Modeling Methods in Assessing Air Pollution ..... 91
Improving Stakeholders Interactions: A Stakeholder-Based Research Methodology for Reaching Decisions on Polarized Issues ..... 94
Biologically Based Catalysts for Processing and Detection in Harsh Service Conditions ..... 97
New Ion Injection Technologies for Ion Trap Secondary Ion Mass Spectrometry ..... 100
Ion Mobility Spectrometry ..... 103
Advanced Control Architectures for Human-Robot Synergy in Complex Domains ..... 107
Detection of Buried Objects Using Imaging Laser Acoustics ..... 110
Behavioral and Control Modeling for Large-Scale Micro-Robot Systems ..... 113
Characterization of Legacy Risk ..... 116
Controlled Growth of Nanowires ..... 118

Use of Engineered Nano-Particles for Nutrient Delivery and Bioremediation in Subsurface Environments ..... 119
High Intensity Perrhenate Ion Gun for Use as a Primary Ion Beam in SIMS
(Secondary Ion Mass Spectroscopy) ..... 122
Enhanced Transport in Nano-Crystalline Ceramic Films ..... 126
Making Sustainable Decisions Using the KONVERGENCE Framework ..... 128
Nucleation and Growth of Nanoparticle Materials in Supercritical Fluid Processes ..... 130
Elucidating the Photo-Physics of Complex Metal Ions Trapped in a Fourier Transform Mass Spectrometer ..... 132
Recombinant Adhesive Protein Production and Investigation into Alternate Natural Adhesive Systems in
Marine Mussels ..... 135
Integrated Experimental and Mathematical Analysis of Complex Chemical and Biological Systems ..... 137
Nanostructure Characterization for Sensing ..... 139
Trace Chemical Species Detection and Analysis Using Femtosecond OHD-RIKES ..... 142
Mechanical and Flow Properties of Dry Granular Media ..... 144
Carbon Fractionation Potential of Soils Via CO2/Water Gradient Fractionation ..... 147

*National Defense ..... 151*

Second Generation Neutron/Gamma Sensor ..... 153
Multipath Propagation Analysis, Simulation, and Prediction in Wireless Environments ..... 156
Selected Release of Polymer Degradation Agents by Photoinitiation ..... 159
Information Visualization by Query ..... 162
A Compton-Backscatter Photon Source for Tunable, Monoenergetic, Hard X-rays ..... 165
Mechanical, Physical and Metallurgical Factors Affecting Liquid-Metal Embrittlement of Steels ..... 168
Cermet Filters for Hazardous Material, Chemical, and Biological Weapon Agent Destruction ..... 169
Distant Neutron Source Detection and Location ..... 172
Microantenna Infrared Tags ..... 175
Ultrasonic Detection and Characterization of Buried Objects: Air-Coupled Techniques ..... 177
Novel Cyclodextrin-Based Sorbent Materials for EM Waste Separation Needs ..... 179
Probalistic Risk Monitoring Software for SAPHIRE ..... 181
Technical Advancement for the INEEL CIP SCADA Test Bed ..... 183
Cutting of Structural Materials using Energetic Materials ..... 184
Novel Selective Matrix for Collection and Identification of Priority Pathogens ..... 185
Imaging Applications of Photon Beams Produced with Compton Backscatter of Laser Beams ..... 187
Classified Cluster Computing ..... 190
Plasma Spray Processing Development for Energetic Materials ..... 192
Assessment of Long-Term Variations in Soil Moisture and Regional Groundwater Flow Patterns within the
Snake River Plain Aquifer System in Response to Potential Climate Changes ..... 195
Mechanisms of Liquid Metal Embrittlement in Steels ..... 199
Porous Crystalline Silica (Gubka) Based Ion Exchange Sorbents ..... 201
Exploring Applications of Wavelet Theory: Groundwater Dynamical Systems,
Gamma Spectral Analysis, Acoustic Resonance Spectrometry ..... 204

## *Advanced Computing and Simulation Initiative* ..... *207*

Development and Validation of Advanced Simulation and Collaboration Capability ..... 209
Parallel Computing with Cluster Technology ..... 211
Aerospace Situation Awareness and
Risk Monitor Tool ..... 215
Improving Numerical Model Efficiency of a Simulation Model ..... 217

## *Advanced Waste Management Solutions Initiative* ..... *219*

An Energy-Dispersive, X-Ray Fluorescence Excitation Source for the
In-Field Analysis ..... 221
Enhanced Sample Based Modeling Techniques for Non Destructive Analysis and
Long-Term Stewardship ..... 224
Direct Dissolution of Plutonium and Neptunium Using Complexing Agents in
Carbon Dioxide ..... 226
Cold-Crucible Design Parameters for Next Generation High Level Waste Melters ..... 228
Steam Reforming in Micro Rectors for Destruction of Hazardous Organic Materials ..... 231
Model-Based Decision Making ..... 233
Advanced Formulation for Homogenization of Refractory Components
in Glass and Ceramic Phases ..... 235
Polyacrylonitrile-Based Ion Exchange Sorbents ..... 238

## *Critical Infrastructure Protection Initiative* ..... *241*

Use of Thermally Sprayed Traces for Damage Detection and Data Transmission ..... 243
Development of Blast- and Penetration-Resistant Materials and Systems for
Comprehensive Protection of Vehicles, Personnel and Buildings ..... 246
Critical Infrastructure Critical Sub-network ..... 250
Survivable Networks of Dynamic Systems ..... 253

## *Environmental Stewardship Initiative* ..... *257*

Airborne Contaminant Gradient Mapping System ..... 259
Long Term Record Storage For Long Term Stewardship ..... 261
Uptake and Translocation Patterns of Strontium by Sagebrush Steppe
Ecosystem Plants ..... 262

DOE Complex-Wide Long-Term Stewardship Options Analysis System ..... 265
Development of an Integrated Watershed Information Management Tool for Long-term Facilities Stewardship ..... 267
Use of Genetic Markers for Ecological Risk Assessment ..... 270
Development of Collaborative Approaches to Long Term Environmental Stewardship ..... 273

## *Generation IV Nuclear Reactor Initiative* ..... 277

Advanced Transient Analysis Capabilities for Generation IV Reactors ..... 279
Advanced Nuclear Fuels for Enhanced Proliferation Resistance ..... 281
Design of an Actinide Burning, Lead or Lead-Bismuth Reactor That Produces Low Cost Electricity ..... 283
Development of a Nodal Diffusion Method for the General Cylindrical Geometry Reactor Core ..... 288
Modular Pebble Bed Reactor ..... 290
Generation IV Gas-Cooled Reactor System Analysis Tools ..... 293

## *Subsurface Science Initiative* ..... 297

Development of Sensors for Detection of Metal-Reducing Bacteria in Mesoscale and Field Experiments ..... 299
Use of Molecular Markers for Detection and Tracking of Environmental Bacteria ..... 302
Characterizing Microbial Population Shifts in Response to Alternative Electron Donors and their Effect on Trichloroethylene Dechlorination Efficiency ..... 304
Characterization of Dense Non-Aqueous Phase Liquids Adsorption/Desorption to Geological Media ..... 307
Residual Hazards Management: Decisions Leading Toward Success or Failure ..... 309
Hybrid Nanocomposite Materials as Subsurface Permeable Reactive Barriers ..... 311
Advanced Technology for Mapping Subsurface Water Conductivity ..... 314
Electrical Resistivity Imaging to Define Preferred Flow Paths in a Heterogeneous, Layered Vadose Zone ..... 317
Quantitative Deep-Reading Vadose Zone Moisture Characterization ..... 319
Application of New Borehole Geophysical Methods for Stratigraphic Correlation and Identification of Non-Aqueous-Phase Contaminants ..... 322
A New Hydrogeophysical Method for Characterizing and Monitoring Preferential Flow Paths in Complex Layered and Fractured Basalt ..... 324
Advanced Simulation Method Development ..... 326
Demonstration of Spatially Resolved Molecular Approach to Detect Specific Microbial Activity on Mineral Surfaces ..... 329
Nonaqueous-Phase Fluid Behavior in the Vadose Zone: Model Development & Testing ..... 331
Investigation of the Movement and Fate of Chlorinated Hydrocarbons ..... 333
Investigation of the Effects of Microbial Growth on Unsaturated Hydraulic Properties ..... 335
Modeling of Flow and Colloid Behavior in Subsurface Fractures ..... 337
Natural and Synthetic Subsurface Colloids ..... 339
Fundamental Studies on Gas Contaminant Mobility in the Vadose Zone from Atmospheric Pressure Fluctuations ..... 341
Enhanced Techniques for Evaluating Colloidal Processes ..... 344
Chemical Modification of Atomic Force Microscope Probes for Imaging Patterned Molecular Architectures ..... 346
Evaluating Microelectrodes and Fiber-Optic Probes for Use in Mesoscale Experiments ..... 350
In Situ Bioremediation of Explosives in the Vadose Zone ..... 352
Kinetics and Mechanisms of Inter-Surface Transfer, and Solid-Solution Partitioning, of Surface-Complexed Metals in Colloidal Systems ..... 353
Organic Co-Solvent and Co-Contaminant Effects on Sorption of Uranyl and Cesium to Metal Oxide Surfaces ..... 356

Computational Experiments of Hysteretic Chemical and Moisture Migration ..... 358
Development of Imaging Fourier Transform Mass Spectrometer Capabilities for Analyses of Complex & Heterogeneous Samples ..... 361
Dual Electrodes and Defining the Electrically Disturbed Region in Induced Polarization Measurements ..... 364
Improving Soil Water Flux Estimates in the Deep Vadose Zone ..... 366
Regional Setting and Flow Dynamics of the Snake River Plain Aquifer ..... 368
Development of Techniques for In situ Measurement of Groundwater Contaminant Source Strength ..... 370
Improved Osmotic Tensiometer Components and Parameters ..... 372
Development and Application of Custom Flow Models for Understanding Flow in Porous and Fractured Matrices with Biological Components ..... 374
Characterization of Nonlinear Complex Resistivity Spectra during Biochemical Reduction of Cr+6 to Cr+3 ..... 376
Development of Biosensors for Environmental Applications ..... 379
Calibration and Enhancement of Geophysical Imaging Tools in a Mesoscale Experimental Facility ..... 382
Fracture Prediction, Characterization, and Detection in Snake River Basalts – A Modeling and Field Approach ..... 384
Advanced Borehole Seismic Sources for High-Resolution Subsurface Imaging and Characterization for Environmental Applications ..... 386
Modeling an Earth-Borehole System for Physical Property Determination in Shallow Subsurface Environments with Emphasis on Vadose Zone Applications ..... 388
Carbon Fractionation Potential of Soils Via CO2/Water Gradient Fractionation ..... 391

*Appendices* ..... *395*

Appendix A–Authors ..... 397
Appendix B–Refereed Publications ..... 401
Appendix C–Key Terms ..... 409
Appendix D–Project Performance ..... 417
Appendix E–Relevence to Major DOE Missions ..... 428
Appendix F–Relevence to Major DOE Missions ..... 437

# Overview

## LDRD Annual Report for FY-2002

Idaho National Engineering & Environmental Laboratory

# Overview and Feature Article

*The INEEL's mission involves the following elements:*

- Deliver science-based, engineered solutions to the challenges of DOE's missions areas, other federal agencies, and industrial clients.
- Complete environmental cleanup responsibly and cost-effectively using innovative science and engineering capabilities.
- Provide leadership and support to optimize the value of EM investments and strategic partnerships throughout the DOE complex.
- Enhance scientific and technical talent, facilities, and equipment to best serve national and regional interests.

National laboratories and their Laboratory Directed Research and Development (LDRD) programs are a crucial part of this nation's ability to rapidly solve ever-changing research needs. The LDRD program was instituted by Congress to provide DOE laboratories the flexibility to perform cutting edge research that addresses DOE missions and national needs. Recently, the Department of Energy's (DOE) mission was redirected to address and solve national security concerns. Through LDRD, each national laboratory has the ability to redirect research to address these new and important needs with speed and agility.

LDRD is managed by DOE under Order 413.2A which describes the purpose, limitations and guidelines for the program. This annual report fulfills one of the program requirements specified in that Order.

At the INEEL, LDRD research provides a number of benefits:

1) development of new and innovative scientific and technological ideas;

2) enhances the scientific and technological vitality of the laboratory;

3) assists in development of strategic direction; and

4) development and retention of new workforce capabilities.

LDRD plays a seminal role in attracting and retaining the most qualified scientists and engineers. LDRD is considered a unique resource for scientists newly hired by the laboratory. In FY02, LDRD supported 178 postdoctoral fellows, graduate students, and university faculty. Approximately 55% of all the postdoctoral fellows at the laboratory were sponsored by LDRD research.

LDRD is used to initiate research programs and build technical capabilities. Veteran researchers at the laboratory value LDRD for enabling the exploration of ideas believed to be of importance, but not yet sufficiently developed to attract programmatic support. The program also enables researchers to establish important partnerships with universities and industrial research groups that enliven and diversify the intellectual approaches to the research. LDRD is responsible for some of the highest quality research conducted at the laboratory. A significant number of the technical publications, presentations, invention disclosures and patents are derived from LDRD. Likewise, many of the national awards and recognition of INEEL researchers occurred because of accomplishments on LDRD projects. Performance and Program statistics about the fiscal year 2002 projects can be found on the next page.

This Annual Report contains progress summaries of all the research sponsored by the INEEL LDRD Program in fiscal year 2002. It represents some of the most exciting research conducted at the INEEL that addresses complex technical problems facing DOE and the nation. Some notable examples that are found in this report are:

- In July 2002, Department of Energy Secretary Abraham established the INEEL as the nation's leading center for nuclear energy research and development. The INEEL has a 50 year history of contributions to nuclear energy R&D, ranging from building, testing, and demonstrating the country's first nuclear reactors to its current

involvement in the development of the next generation of nuclear reactors. LDRD has played a pivotal role in the ability of the INEEL to address this critical national need. The feature article "Anticipating the Future" (which follows this introduction) sets into historical context the cluster of LDRD projects devoted to the support of this initiative.

- The effective management of radioactive waste persists as one of DOE's greatest challenges. The LDRD project "Cold Crucible Design Parameters for Next Generation High Level Waste Melters" is one of several addressing the issue of treatment of high level radioactive waste. This particular project involves use of a cold-crucible induction melter that is more corrosion-resistant, smaller in size, and less costly than current technologies available.
- The INEEL's Subsurface Science Initiative is a major research undertaking to develop a better understanding of the movement and interaction of contaminants in the subsurface over time. Such understanding is essential to the development and validation of models of water and contaminant flow in fractured heterogeneous media, and for predicting the viability of underground waste storage strategies. Through LDRD project "Hybrid Nanocomposite Materials as Subsurface Permeable Reactive Barriers," researchers are making progress on the investigation of novel barrier materials (molecular composites) that show very promising mechanical, physical, and chemical properties for capture and sequestration of certain species of contaminants.
- In an article entitled "Tools You Can Use: Easier-to-Use-Interfaces are a Top Priority as Information Technology Grows in Sophistication" (*Federal Computer Week*, September 30, 2002), author Brian Robinson observes, "In the past year's discussions about the use of technology to boost homeland security efforts, one consistently understated issue is the usability of that technology… the so-called human factor." He describes Jerry Harbour's LDRD "Model Based Decision Making" as an example of "…emphasizing simplicity and power so that systems that provide high-level modeling and predictive capabilities can be used by people with differing skill levels."

## FY02 Performance Statistics

| | |
|---|---|
| Refereed publications | 80 |
| Symposia chaired or organized | 21 |
| Invited presentations | 75 |
| Invention disclosures | 28 |
| Patents awarded | 2 |
| University personnel | 178 |

## FY02 Program Statistics

| | |
|---|---|
| Total projects | 136 |
| Smallest project | $20K |
| Largest project | $640K |

In addition to individual project summaries, this report includes a number of Appendices. These Appendices provide a portrait of the INEEL LDRD research portfolio. Appendix A cross-references authors with progress reports. Appendix B is a list of publications. Appendix C is a key term index. Appendix D lists performance indicators such as number of publications, patents, national awards, students and postdoctoral fellows supported. Appendix E describes the relevance of each project to DOE missions, and Appendix F describes the relevance to major national programs.

An Annual Report focuses on achievements in a single fiscal year, and does not illustrate the impact of a 10 or 20-year retrospective. Nevertheless, even from a 12-month perspective, it is evident that LDRD makes a unique contribution to the laboratory's ability to serve all of DOE's missions and the nation. LDRD provides the ability to invest in long-term, higher risk research that has a potentially high payoff. It is essential to INEEL's ability to attract and retain the best researchers. By its exploratory nature, LDRD allows researchers to anticipate technological needs and envision and test the potential value of novel ideas. The INEEL LDRD Program will continue to evolve to support emerging national needs and future DOE missions.

## Feature Article

# Anticipating the Future

In December 1951, an experimental reactor at the Argonne National Laboratory-West, National Reactor Testing Station (now the Idaho National Engineering and Environmental Laboratory, INEEL) produced the first electric power from the atom, lighting four light bulbs. Today, nuclear power produces 16% of the world's electricity and 20% of the electricity in the United States. Ongoing operating, maintenance and fuel costs are industry-competitive, resulting in low-cost electricity that is second only to hydroelectric power. Nuclear energy also provides substantial environmental benefits that contribute to clean air by reducing dependency on coal-burning power plants. Since the mid 1970s, nuclear power use has helped the nation avoid over three billion tons of air pollutants.

Plentiful, affordable energy is critical to a healthy world economy and an improved standard of living for future generations. Forecasts suggest the world electricity demand will increase by 50% over the next 20 to 25 years, possibly doubling by 2050. Rapidly developing and growing economies in Asia and Latin America will drive much of this increase. In addition, the U.S. and Europe will need new generating capacity, as aging power plants (primarily fossil fueled) are replaced to address environmental concerns and meet energy and economic security needs. With the large economies of the world currently using the lion's share of electricity output, developed nations like the United States have a moral obligation to take the lead in the deployment of advanced, clean-energy technologies that preserve the world's fossil fuels and assure abundant energy supplies for the future.

The outlook for worldwide energy demand indicates that nuclear energy should play an increasing role as the one technology capable of large-scale, near-term deployment without greenhouse gas emissions. However, to take its rightful place in the energy mix, nuclear technology must respond to several challenges. It is widely recognized as providing low operating costs, but continues to be burdened with high capital costs that inhibit growth. Public opinion of nuclear power – though overall positive — is fragile, hinging on perceptions of safety and physical protection. Finally, nuclear power must adequately address questions about waste disposal and concerns about nonproliferation of growing inventories of spent nuclear fuel.

Funding from Laboratory-Directed Research and Development (LDRD) at the INEEL has been a key contributor in building the nuclear energy expertise the nation now calls upon from the INEEL to meet these challenges. Researchers at the INEEL anticipate the technology and science needs of tomorrow and LDRD

## *Goals for Generation IV Nuclear Energy Systems (Gen IV)*

- *SUSTAINABILITY:* Gen IV nuclear energy systems will provide sustainable energy generation that meets clean-air objectives and promotes long-term availability of systems and effective fuel utilization for worldwide energy production. These energy systems will minimize and manage their nuclear waste and notably reduce the long-term stewardship burden, thereby improving protection for the public health and the environment.
- *ECONOMICS:* Gen IV nuclear energy systems will have a clear life cycle cost advantage over other energy sources. The level of financial risk will be comparable to other energy projects.
- *SAFETY & RELIABILITY:* Gen IV nuclear energy systems operations will excel in safety and reliability, and have a low likelihood and degree of reactor core damage. These systems will eliminate the need for offsite emergency response.
- *PROLIFERATION RESISTANCE & PHYSICAL PROTECTION:* Gen IV nuclear energy systems will increase the assurance that they are a very unattractive and the least desirable route for diversion or theft of weapons-usable materials, and provide increased physical protection against acts of terrorism.

fosters this exploration by providing discretionary funds for creative and innovative research and development. LDRD also fosters the development of the human capabilities that will be needed to address some of the most challenging technical problems facing DOE and the Nation. Collaboration with university and commercial partners through LDRD-funded projects attracts outstanding young scientists and engineers, creating a new generation of world-class science and technology talent. INEEL LDRD funding has supported the nuclear technology development agenda of the DOE through the investigation of advanced reactor concepts, fuel cycle development, hydrogen research, nuclear waste management, plutonium reuse and nonproliferation.

The INEEL is at the center of a new era in nuclear energy development. In 2000, the INEEL played a highly influential role in a worldwide discussion among technical leaders on the future of nuclear technologies. The Generation IV International Forum was created as a platform that joined ten countries (Argentina, Brazil, Canada, France, Japan, the Republic of Korea, the Republic of South Africa, Switzerland, the United Kingdom and the United States) in conversation about where the nuclear industry has been and where it needs to go to come closer to addressing the world's energy problems. The discussions are essential steps along the path leading to reliable, competitively priced energy products that address safety, waste, proliferation and public perception concerns. The INEEL also played a substantive role in the development of a roadmap for the six most promising next-generation (Gen IV) nuclear reactor systems, building a solid technical foundation for sustainable international design and development efforts.

Nuclear power as a major source of electrical energy and a growing source of hydrogen transportation fuel can have a significant impact on human health, climate, preservation of fossil fuels, and the availability of affordable electricity for generations to come. The INEEL investment in LDRD helps the laboratory fulfill its leadership role in the development of nuclear energy technology that will deliver a bright energy future for the U.S. and the world.

*Discovery begins with imagination. Imagine non-polluting vehicles powered by hydrogen made with nuclear energy. Imagine fast reactors that can recycle their fuels to extract 100 times more energy than what is obtained today. Imagine nuclear power plants so safe they don't need traditional containment structures.*

The following LDRD projects are examples of INEEL technologies exploring answers to the challenges of nuclear energy.

*The energy from one pound of nuclear fuel could provide the hydrogen equivalent of 250,000 gallons of gasoline with no carbon emissions.*

## *Powering Vehicles with Nuclear-Generated Hydrogen*

Tomorrow's nuclear power plants may be generating electricity by day and hydrogen by night, providing large quantities of clean hydrogen. Advanced nuclear power plants capable of hydrogen generation could be in operation as early as 2010. With increased availability in the near future, hydrogen is gaining increased attention – as witnessed by President Bush's emphasis on hydrogen fuel in his recent State of the Union address — for use as a non-polluting transportation fuel, replacing U.S. dependence on imported oil and reducing use of fossil fuels.

To realize the potential of the "hydrogen economy," new technologies must be developed for hydrogen generation, storage, transportation and utilization. LDRD NE125 *(Hydrogen Technologies R&D – Advanced Materials for Hydrogen Storage p. 47)* looks at materials that can be used in high-pressure hydrogen gas storage tanks to absorb large amounts of hydrogen. The hydrogen is then converted into either mechanical energy (using a combustion engine) or electrical energy (using a fuel cell) to power the vehicle. Currently, these high-pressure fuel tanks can only store enough hydrogen to offer a vehicle range of about 80 miles –enough to get you around town, but not enough to inspire widespread conversion.

The advanced materials (intercalated graphite and new-generation carbon nanotubes) being researched in this LDRD project could absorb significantly larger quantities of hydrogen, increasing storage capacity by two to four times with no increase in tank size or hydrogen pressure. With a per-tank range of 200 to 400 miles, hydrogen-powered vehicles become commercially viable and will likely gain wider acceptance. Increasing hydrogen storage capacity of fuel tanks also enables more efficient transportation of hydrogen from generating stations for other uses.

"Vehicle manufacturers, like General Motors, already have target dates for introducing hydrogen-powered vehicles with fuel-cell engines," says principal investigator Paul Lessing. "If successful, we might see this type of technology in use within seven to ten years."

## *Improved Economics for Nuclear Energy*

What if switching to a supercritical coolant could decrease nuclear plant size by as much as 30%? What if using passive safety systems instead of those that require mechanical or electrical means could make nuclear

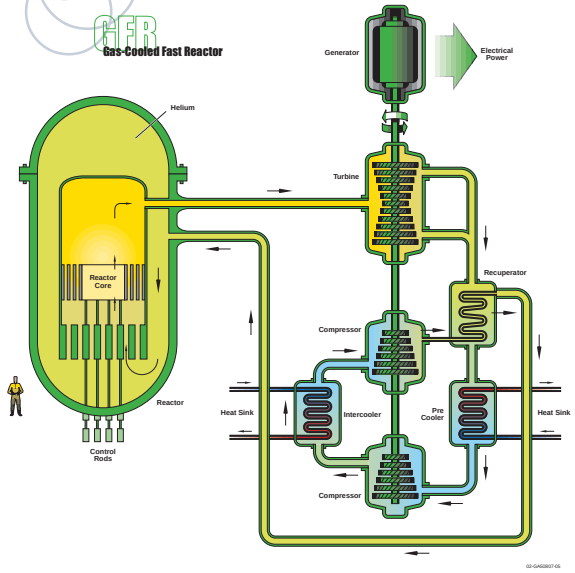


*The GFR features a fast neutron spectrum and closed fuel cycle for efficient management of actinides and conversion of fertile uranium. This system is primarily envisioned for electricity production, and may be able to economically support hydrogen production as well. The GFR system brings excellent benefits in the minimization of waste and efficient use of uranium resources.*

plants more fail-proof, improving public confidence? These are two questions addressed in LDRD NE122 *(An Innovative Gas-Cooled Fast Reactor p. 83)* that could result in smaller, more economical fast spectrum reactors with advanced safety features and a closed fuel cycle for waste management.

A focus of this project is investigation of carbon dioxide at supercritical pressures to replace helium as the coolant in new Generation IV Gas-Cooled Fast Reactor (GFR) designs. Because the supercritical carbon dioxide can operate at lower temperatures for the same high thermal efficiencies as helium gas, it could improve the capacity of future large-scale plants while enabling smaller, cost-effective plant designs as well.

Research is also being accomplished on the shift from "active" to "passive" safety systems. Though current safety systems have proven extremely reliable, they depend on mechanical or electrical means for activation (e.g., an electrical impulse to start a blower). Taking a cue from nature, new safety systems are being reviewed that use gravity, natural cooling and flow as simple, fail-proof methods for accomplishing safety-related tasks. Investigation into different fuel forms (carbide, nitride and metallic) that offer very high fuel densities is also embedded in this research.

This project supports development of fast reactors that are expected to be very good at management of actinides — the uranium, plutonium and other radioactive elements present in spent nuclear fuel. Fast spectrum reactors are designed to recycle these long-lived wastes into new nuclear fuel, extending our fuel resources and reducing the availability of weapons-usable materials. Existing uranium stockpiles mixed with actinides from spent nuclear fuel is all that will be needed to run these reactors indefinitely.

"Generation IV requires a different way of thinking for nuclear reactor people," says principal investigator Kevan Weaver. "This LDRD will result in materials analyses and two to three reactor designs to meet different mission needs for fast reactors."

*The average electricity production cost in 2000 for nuclear energy was 1.76 cents per kilowatt-hour, for coal-fired plants 1.79 cents, for oil 5.28 cents, and for gas 5.69 cents.*

The pebble-bed fuel concept is one of two being considered for the Generation IV Very High Temperature Reactor (VHTR). In the pebble bed design, fuel particles are pressed into cue ball-shaped "pebbles" that move through the core over time. The fuel is made in a chemical vapor deposition process. Each fuel particle has

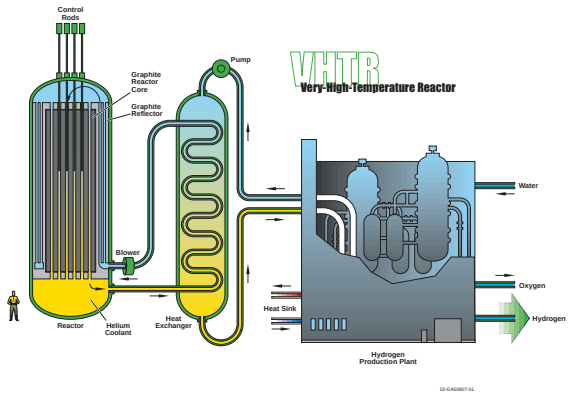


*The VHTR is targeted for nearer-term deployment and may be in operation by the end of the decade. This reactor concept uses helium coolant and produces the very high coolant outlet temperatures (1000° C) to incorporate a water-cracking cycle for the production of hydrogen. Other benefits of this design include passive safety systems, high thermal efficiency and process heat applications.*

a coating layer that acts as its own little pressure vessel. Because of this phenomenon, the fuel is considered very safe and may enable reactor design without traditional containment buildings. Though this technology holds great promise as a safe fuel for future implementation in the VHTR, current modeling tools do not confidently predict fuel performance.

LDRD GE101 *(Modular Pebble Bed Reactor)* is providing the modeling tools to benchmark pebble-bed fuel. Specifically, this research will model how the fuel is burned as it moves through the reactor to predict power levels and improve efficiency. State-of-the-art modeling tools are being extended to pebble bed designs to evaluate safety, and new modeling tools are being developed to help understand the stresses that develop in fuel, forecasting when and how it will fail. In addition, models are being developed to determine whether the fuel's "built in" containment properties can be statistically verified for the billions of particles that comprise these fuel pebbles.

"This fuel is considered so good that many believe it can act as its own containment," says principal investigator David Petti. "If conformity among each fuel particle to these very high standards can be statistically proven through this testing and modeling effort, the potential exists for the next generation of pebble bed reactors to be built without containment buildings and possibly as modular units for significant cost savings."

## *Ongoing Evaluation of Safety and Design*

The Generation IV reactor concepts will feature improvements in fuel cycle and operating efficiencies, use different fuels, materials and coolant fluids, and some will be used in new energy applications such as hydrogen production. Because these new designs have fundamentally different characteristics than the current generation of reactors, their analysis requires extensions or additions to existing analysis tools. LDRD GE102 *(Advanced Transient Analysis Capabilities for Generation IV Reactors p. 279)* is developing new modeling capabilities in support of development and demonstration of the new Generation IV reactor technologies.

*Of all energy sources, nuclear energy has perhaps the lowest impact on the environment, including water, land, habitat, species and air resources.*

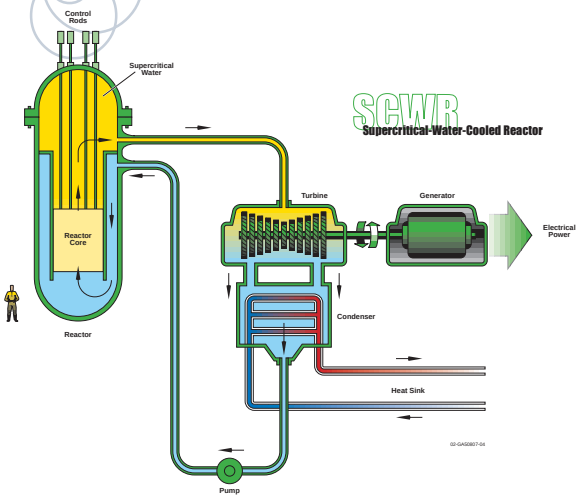


*The SCWR system uses a high temperature, high-pressure water-cooled reactor that achieves a thermal efficiency near 45% in a simplified plant design. Primarily aimed at electricity production, the system's high thermal efficiency and plant simplification may provide a breakthrough in system economics.*

Very High Temperature Reactors (VHTR) are targeted for nearer-term deployment with a focus on hydrogen production. Operating at an efficiency of about 50%, such a plant could produce more than 200 metric tons of hydrogen per day – the equivalent of over 300,000 gallons of gasoline. The Supercritical Water-Cooled Reactor (SCWR) features a simplified plant design that is expected to provide a breakthrough in system economics. The transient operations modeled with this important new software will provide ongoing evaluation of safety and design issues to support the VHTR, SCWR and other new reactor designs as they move forward.

"Our work is extending the existing code capabilities used for reactor transient analyses in a variety of areas," says principal investigator Ed Harvego. "This research has primarily focused on the extension of current INEEL analysis capabilities to address the unique transient analysis needs of Gen IV High-Temperature Gas-Cooled and Supercritical Water-Cooled Reactors."

# Energy

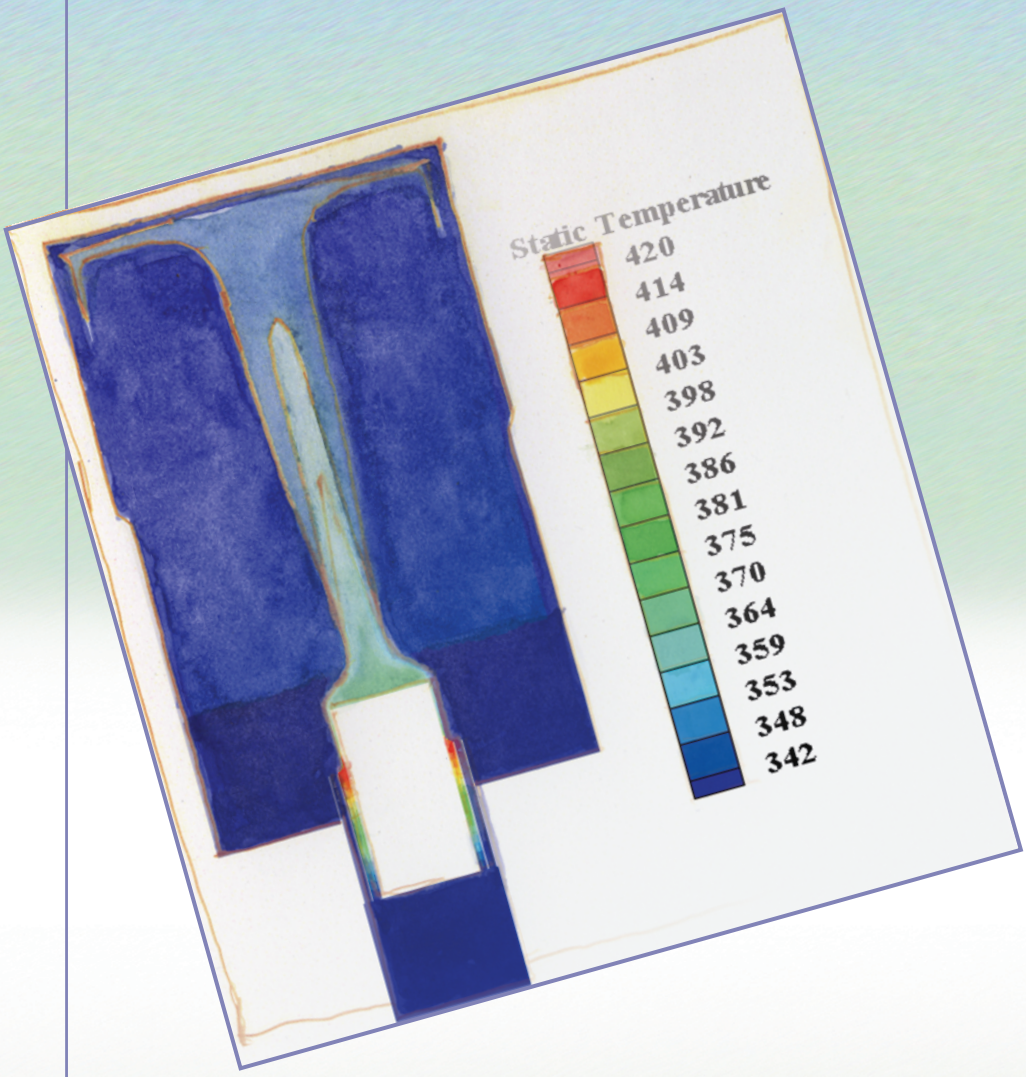


# LDRD Annual Report for FY-2002

Idaho National Engineering & Environmental Laboratory

# Hydrogen Production from High Temperature Nuclear Reactors

*Raymond P. Anderson, J. Stephen Herring, Robert A. Carrington, David E. Shropshire*

## *Removing barriers to hydrogen energy production*

NE120

Hydrogen is reported to be the fastest growing commodity with growth expected to accelerate as hydrogen begins to be used as an energy carrier for transportation, power generation, and combined heat and power generation. Drivers for using hydrogen as an energy carrier are improved energy efficiency (fuel cells are more efficient than internal combustion engines), energy security (can be produced from domestic energy resources), and environmental constraints (fuel cells emit only water as a byproduct). However, carbon dioxide, a greenhouse gas, is liberated when hydrogen is produced from fossil fuels.

Compelling reasons for using nuclear energy for hydrogen production are that it depends only on domestic resources, does not consume our finite supply of fossil fuels, and does not release carbon dioxide. A number of thermochemical cycles or thermochemical/electrochemical cycles may be used for the splitting of water to oxygen and hydrogen using nuclear heat or heat/electricity as the energy source. These water-splitting processes require quite high temperatures (up to 850° C) and use corrosive chemicals (e.g., sulfuric acid, halogens and halogen acids).

This LDRD project is identifying technological barriers to the most promising cycles for hydrogen production using nuclear energy, and putting forth a research plan to address barriers in the areas of high temperature reaction rates, high temperature materials, electrolysis, and separations. The objective of this research is not to develop thermochemical water-splitting processes but to demonstrate technology to enable engineering-scale demonstration of the leading candidate technologies.

Technical objectives for fiscal year 2002:

- Assess current state-of-the-art on the use of nuclear energy for hydrogen production through literature survey, participation in workshops, and contact with other researchers.
- Identify critical technological barriers to using thermochemical or thermochemical/electrochemical processes for the production of hydrogen with nuclear energy.
- Develop a research plan to address the most critical technological barriers.
- Form an external advisory committee to evaluate the proposed research areas, suggest additional needed R&D, and assist in prioritization of research issues.
- Prepare a research report addressing the path forward.

Domestic production of hydrogen is now nine million tons/year and worldwide production is 40 million tons per year. Hydrogen is now the fastest growing commodity. The largest markets for hydrogen are in ammonia-based fertilizer production and petroleum refining. Current growth is primarily in the petroleum refining area and is due to refining of heavier crudes with increasing sulfur contents and increasingly strict environmental restrictions on gasoline and diesel quality. Hydrogen growth is expected to accelerate as hydrogen begins to be used as a transportation fuel and for electricity generation.

Currently, most hydrogen is produced from the steam reforming of natural gas. In a carbon-constrained economy, other non-fossil energy resources will have to be used to meet future demands for hydrogen production. The advantages of using nuclear energy for hydrogen production are that it relies on a domestic resource, it does not consume our finite supply of fossil fuels, and it does not emit carbon dioxide, a greenhouse gas.

There are several methods by which hydrogen can be produced using nuclear energy. This LDRD project is limited to the use of thermochemical or hybrid thermochemical-electrochemical cycles for the splitting of water to hydrogen and oxygen. A previous study (General Atomics, Inc., Sandia, University of Kentucky) evaluated 115 thermochemical or hybrid cycles that can be used to accomplish water splitting. The cycles were evaluated and ranked using a number of evaluation criteria.

The INEEL study is focusing on the four top-ranked cycles identified in the General Atomics (GA) study: the two top-ranked thermochemical and the two top-ranked thermochemical-electrochemical cycles. Typically these cycles require temperatures higher than those for the chemical process industry (up to 850° C) and use

corrosive chemicals. In the following (Table 1), the number-one ranked cycle (the GA sulfur iodine cycle) accomplishes water splitting (reaction 1) by reactions 2-4.

| | |
|---|---|
| Reaction 1. (water splitting) | $2H_2O \rightarrow 2H_2 + O_2$ (requires a minimum of 2000° C) |
| Reaction 2. 850° C | $2H_2SO_4 \rightarrow 2SO_2 + 2H_2O + O_2$ |
| Reaction 3. 450° C | $2HI \rightarrow I_2 + H_2$ |
| Reaction 4. 120° C | $I_2 + SO_2 + 2H_2O \rightarrow 2HI + H_2SO_4$ |
| Net Result | $2H_2O \rightarrow 2H_2 + O_2$ 02-GA51349-041a |

*TABLE 1. General Atomic sulfur iodine cycle water splitting reactions.*

The other top-ranked cycles include:

- The Westinghouse cycle, which involves a two-step process including the same sulfuric acid decomposition step plus an electrolysis step to convert sulfurous acid to hydrogen with regeneration of sulfuric acid;
- The University of Tokyo process, which is a four-step process based on solid beds and involves compounds of calcium and iron along with bromine and hydrobromic acid; and
- The Ispra Mark 13 process, which is a three-step process including the sulfuric acid decomposition, electrolysis of hydrobromic acid to bromine and hydrogen, and the regeneration of hydrobromic acid and sulfuric acid).

To a large degree, these cycles share the common attributes of processing conditions and chemistry that by conventional industrial standards would be considered as harsh and difficult to implement and operate.

Reviewing available literature and other information identified technological barriers to physical implementation of the selected cycles. Potential barriers for each of the four cycles were itemized in a spreadsheet and cross cutting issues common to the various processes were identified. What appeared to be potential problems were discussed first with in-house experts in the various technology areas. External experts with experience in research and development related to the use of nuclear energy for hydrogen production were then contracted to evaluate the proposed research areas, suggest other R&D that may have been overlooked, and assist in the prioritization of research issues and key opportunities. As a result of the internal and external assessments, the following research and development areas were identified for the INEEL LDRD program.

- Investigation of sulfuric acid decomposition to identify limiting mechanisms and improve reaction rates or lower reaction temperatures.
- Materials selection/fabrication for critical components and subsystems; effects of impurities, manufacturing and joining issues.
- Improved separation processes.
- Electrolysis step of the Westinghouse process.

Factors in the selection of the above research areas were to provide enabling solutions to produce hydrogen by the thermochemical splitting of water using nuclear heat and, through this, build INEEL capabilities in high temperature technologies (thermochemical cycles, kinetics, electrolysis, and materials). Safety is obviously an important consideration in the implementation of hydrogen production using nuclear energy. However, it was decided not to have a separate safety analysis task, though safety will be an important consideration in the above research efforts.

The growth of the “hydrogen economy” and the required R&D to support the transition to hydrogen as an energy carrier is a significant growth opportunity for the INEEL. This LDRD will assist in obtaining recognition of INEEL as a player in the hydrogen arena. Special effort will be made for each of the research tasks to not duplicate the efforts of General Atomics and others, but to take maximum benefit from previous and current studies. To this end, it will be useful to establish a continuing relationship with GA, Oak Ridge National Laboratory (ORNL) and others in this research area.

# Co-Firing of Coal and Refuse-Derived Fuel with Oil Shale for Improved Production and Control of Environmental Contaminants: Laboratory Studies

*Richard D. Boardman, Robert A. Carrington*

## *Using an abundant underdeveloped natural resource to address pollutants*

NE121

The development of cost-effective sorbents to remove sulfur and chlorine pollutants and toxic metals (especially mercury) from coal combustion and gasifier offgas continues to lead DOE and EPA objectives. Oil shale is an abundant, underdeveloped natural resource that has sorbent properties, and its ash has natural cementitious properties.

Prior research indicates that oil shale can enhance power generation by:

- Adding heating value to the fuel input, whereas other sorbents constitute an energy drain.
- Serving as a natural, highly effective acid-gas absorbent for both coal and mixed solid waste (MSW) offgas.
- Creating a cementitious ash that reduces the potential for leaching "hazardous" components from the ash, and possibly serving as a viable building material.
- Relieving the strain on available landfills.

An additional hypothetical benefit recognized by the INEEL is the potential to use the sulfidated oil shale as a sorbent for mercury emissions.

This LDRD is establishing a better fundamental understanding of oil shale pollutant sorption reactions under both fuel-lean and fuel-rich conditions, and as a function of temperature, gas composition, and residence time. The first phase of research involves the setup of a differential reactor to measure the rate of finely ground oil shale devolatilization/calcination, followed by the sorption rate of $SO_2$ (fuel-lean conditions) and $H_2S$ (fuel-rich conditions), $HCl/Cl_2$, and then mercury vapors. A mechanistic pollutant sorption model for reacting particles will then be developed and incorporated into a comprehensive computer code for reacting flows. The code will be used to determine and optimize technically viable coal and mixed solid waste applications. Future deployment of such applications will improve energy efficiency while cost-effectively reducing pollutant emissions in the U.S.

Technical objectives for fiscal year 2002:

- Perform comprehensive review of calcium-based pollutant sorbent studies.
- Obtain several kilograms of oil shale from the Colorado-A (C-A) mine site and prepare for the differential reactor tests.
- Perform analysis of the ground oil shale particles to measure the sample volatile, carbon, ash, and moisture content in addition to heating value, elemental analysis (including 18 metals), radiochemical analysis (gamma scan and gross alpha-beta), BET surface and pore volume of unreacted and heated (i.e., devolatilized and calcined) samples, and thermo-gravimetric/calorimetry.
- Complete detailed test plan and work authorization package in preparation for setting up the experimental equipment and conducting the kinetic tests.
- Fabricate a differential quartz reactor and fabricate/purchase other experimental equipment and supplies, including compressed gases, low-volume precision mass flow controllers/meters, and a personnel safety gas monitor (for $H_2S$, $SO_2$, HCl, CO, and LEL).
- Perform cursory economical evaluation of proposed commercial applications to justify completion of the science studies necessary to determine technical feasibility.
- Perform differential reactor kinetic tests. (Delayed to FY03 due to curtailment of funding.)
- Summarize findings for intellectual property claims, relevant publications and peer discussions.

Even though there is much high-level talk about the need for energy security, some of our greatest and most accessible domestic resources such as coal and oil shale are being overlooked or downgraded in the public debate due to concern over $CO_2$ release, nitrogen oxide and sulfur pollutants, and mercury emissions. Current industrial practice for sulfur pollutant is to slurry limestone for flue-gas scrubbing or inject pulverized limestone into the combustor or reheat zone of an entrained-flow boiler. Activated carbon and other novel sorbents are being studied for injection into the offgas duct or for use in packed beds or "hot" transport reactors to capture sulfur pollutants and/or mercury. In the case of circulating or fluidized-bed combustors, coarse limestone particles are added to the combustor bed.

Oil shale is a naturally occurring mineral found in several prehistoric marine deposits in the United States and throughout the world. It is characterized by banded

carbonate and oxide minerals laden with a polymer organic residue called kerogen. Upon heating the kerogen depolymerizes and is devolatilized from the shale. Simultaneously, calcium and magnesium carbonate in the shale dissociate, releasing $CO_2$ gas. The volatile organic and tar can be immediately burned to produce heat or is readily condensed and recovered as an oily liquid. The residual inorganic retort is highly porous and exhibits cement properties. Thus, it can be used as a road or construction material or may be used to stabilize coal slag and fly ash solid waste.

Another potential use of the devolatilized oil shale is for pollutant sorption. Depending on the quantity and dispersion of CaO in the shale, it may react quantitatively with $SO_2$ (under fuel-lean conditions), $H_2S$ (under fuel-rich conditions), and possibly adsorb heavy metals (most importantly, mercury).

This LDRD research is focused on characterizing the physical and chemical properties and reaction mechanisms of ground and pulverized oil shale depolymerization-devolatization-calcination and subsequent sulfur and toxic metal adsorption. Previous studies indicate that the addition of appropriate amounts of oil shale to dual-fired (oil shale/coal or oil shale/ refuse-derived fuel) combustors could help make this vast domestic resource economically competitive and environmentally beneficial. From the literature review, as well as a cursory analysis of the economics of replacing limestone and other sorbents with oil shale, it was concluded that this LDRD project might indeed improve energy efficiency while reducing pollutant emissions.

The investigators' approach on this LDRD is to: 1) conduct a thorough literature review of oil shale development work to obtain oil shale properties and all possible data relevant to physical-chemical conversion mechanisms and rate measurements; 2) identify, obtain, and prepare representative oil shale material for experimental purposes; 3) set up and complete experimental tests in a drop-tube furnace to measure depolymerization-devolatilization-calcination rates for pulverized particles; 4) set up and complete experimental tests in a differential reactor to measure intrinsic kinetics and diffusion rates for sorption of $H_2S$ (fuel rich), $SO_2$ (fuel lean), $HCl/Cl_2$, and elemental mercury; 5) incorporate the kinetic rates into an appropriate particle reaction model and develop a sorbent particle reactions subroutine for a comprehensive particle-laden, reacting flow combustion code; and 6) use the combustion code to simulate possible applications in order to determine technically viable and cost-beneficial applications of co-firing oil shale with coal, MSW, and other fuel blends.

Objectives 1, 2, and 4 were completed in FY02, the first year of the project. Oil shale shown in Figure 1 was obtained from the C-A mine. Grinding and analysis tests were completed on the raw material and heated samples. The oil shale lumps were ground, sieved, and packed in nitrogen containers to preserve the fine particles for analysis and kinetic tests.

*FIGURE 1. Oil Shale obtained from the Colorado-A mine.*

Results of the chemical analysis of the ground oil shale are consistent with the literature. Approximately 25% of the oil shale is organic material, with approximately 30% of the residual substrate being CaO that is highly reactive with $SO_2$ and or $H_2S$ at the right temperature conditions. The heating value of 3,000 BTU/lbm is consistent with previous measurements of the C-A oil shale. BET surface area measurements of unreacted oil shale were in the range expected; however, BET surface areas of heated particles were less than theoretically expected.

This result has prompted the investigators to consider additional Thermogravimetric Analysis/Design Safety Criteria (TGA/DSC) analysis and even drop-tube furnace experiments to quantify kerogen release kinetics and

mechanisms as well as particle morphology. It is possible that the particles were sintered or closed by coke that formed during heat treatment to evolve the kerogen and calcine the particles. Analysis of the TGA/DSC is currently being made. It may be necessary to modify the LDRD plan in FY03 to include a series of drop-tube furnace tests to measure particle depolymerization/ devolatilization/char formation.

Recent limestone sorption tests conducted at the University of California, Berkeley (1994-96), will be used as a model for the present kinetic studies for oil shale. This will provide a credible reference for comparing oil shale sorption properties and kinetics to current technology. A differential quartz reactor and experimental test setup have been completed (Fig. 2).

A test plan and experimental procedure were completed and included in an Independent Hazards Review that was required to authorize the experimental studies. The experimental equipment and compressed gases were set up in a walk-in hood to mitigate exposure to toxic vapors. Kinetic testing is now set to begin at the start of the second year of this project, pending a decision to conduct some drop-tube furnace tests to understand virgin particle behavior during heat-up.

This LDRD research may lead to technology breakthroughs that will impact energy security and environmental quality in the U.S. If the research results prove successful, these new technologies can be deployed on existing coal-fired plants or incorporated into future coal-gasification combined-cycle configurations. An opportunity for a CRADA with private companies, and intellectual property for BBWI, DOE, and private companies is a distinct probability.

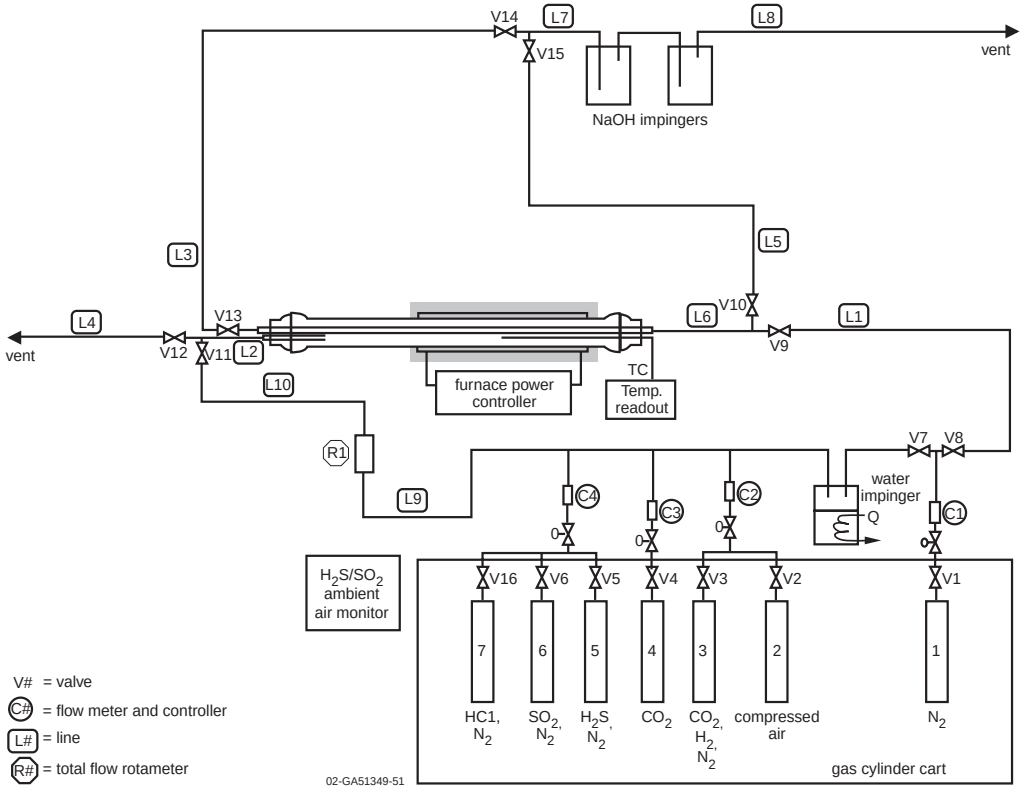


*FIGURE 2. Schematic of differential quartz reactor and test setup.*

Additionally, the LDRD is helping build research and testing capability at the INEEL. The differential reactor and drop-tube furnace experimental setups are suitable for testing other novel sorbents for pollution control. Already, tests involving activated carbon, sulfide ores, and other novel sorbents are envisioned. A mission of the INEEL Advanced Mixed Waste Solutions Strategic Initiative is to develop research capability for offgas measurements and control. If the experimental and modeling tests are successful, then a field demonstration of oil shale co-firing may be recommended.

Collaboration with a number of small companies has been established through this project, as well as DOE and several foreign countries with oil shale resources. Combustion Resources, Provo, Utah, was subcontracted to prepare and supply the research grade oil shale samples. Collaboration with Brigham Young University (BYU), Department of Chemical Engineering, for particle analysis and TGA/DSC measurements and other particle characterization was made in FY02. Additional collaboration with BYU on drop-tube furnace design and operation will be made in FY03. Collaboration with the University of California, Berkeley investigators on pulverized limestone is a possibility, as well.

Contact has been made with sorbent reaction study project principals in DOE-National Energy Technology Laboratory, Electric Power Research Institute, and private industry to ensure the relevance of the current study.

# Two-Phase Mass Flow Measurement for Geothermal Wells

*Robert P. Evans, Joe Keller*

## *Measuring two-phase flow in a single instrument*

NE108

Currently, accurate measurements of two-phase flow are not available either intrusively or non-intrusively in a single instrument. Yet, such an instrument would provide significant benefit to geothermal well sites, as well as to the oil and gas, thermal hydraulics, and nuclear industries.

This LDRD is investigating the feasibility of a low-cost, non-intrusive mass flow measurement system for single-phase and two-phase flow conditions. The technique is based on the relationship between flow noise, as measured by an accelerometer, and mass flow rate. The proposed concept of using flow noise to measure mass flow employs an approach never before used in the measurement of mass flow.

Technical objectives for fiscal year 2002:

- Conduct experimental testing to acquire flow noise data.
- Develop and validate a Large Eddy Simulation (LES)-based fluid structure interaction model.

This year's research used a two-prong approach consisting of experimental testing backed by numerical model validation. A two-phase flow loop was developed and instrumented at Idaho State University, then tested using various mass flow rates (both single- and two-phase flow conditions), test section pipe sizes, and test section materials. Data were obtained relating the standard deviation of the accelerometer signal with the mass flow rate. In addition, power spectral density plots of the accelerometer signal were obtained for various flow rates. Data also were obtained from a fast-response, flush-mounted pressure sensor under various mass flow conditions.

A series of tests were performed using test sections of different materials (stainless steel and clear polyvinyl chloride), different diameters (3-inch and 4-inch schedule 40), different void fractions, and different flow rates. Void fractions ranged from all-water (0% void) conditions to about 99% void. Mass flow rates ranged from about 300 grams per second to about 24000 grams per second.

Test results indicate a quadratic relationship between the mass flow rate and the standard deviation of the measurement signal. In addition, the pipe diameter does not seem to affect the relationship, although the pipe material and the void fraction both appear to shift the slope of the relationship. Additional testing is necessary to quantify these parameters.

The next research effort involved model development. This portion focused on the development of a numerical model that verifies the relationships between the pipe wall vibration and the physical characteristics of the turbulent flow. The model will be used to better understand the relationships identified in the experimental data. The goal is to develop a fluid structure interaction (FSI) model that couples the pipe displacement and vibration effects into the solution for the flow. The result is essentially a coupled structural and fluid solution.

The fluid portion of current state-of-the-art FSI models is based on Reynolds Averaged Navier Stokes equations and are only capable of computing statistically averaged values throughout the cross-section of the flow. These flow models are not capable of computing the instantaneous pressure fluctuations that participate in causing pipe vibration. However, a technique know as Large Eddy Simulation (LES) allows the eddies present in turbulent flow and, therefore, the changes in pressure to be modeled on the scale of the grid pattern.

The LES technique is computationally intensive and a 64-processor supercomputer has been used for these computations. The modeling of the turbulent flow using the LES approach has provided significant enhancement to current FSI models.

This past year's effort resulted in the development and validation of the LES-based fluid model. This model was verified with other models and theory. The final year of this effort will involve coupling the LES fluid solution to a structural solver such that the effects of any pipe wall deformation may be included in the final solution. In addition, the investigators plan to complete and docu-

ment the results of the flow loop testing and analyze the results to define a relationship between the mass flow rate of the fluid and the standard deviation of the measurement signal. This relationship will take into consideration pipe material and pipe diameter. The development of the FSI modeling will continue by incorporating the effects of the pipe deformation into the solution for the flow field. Efforts also will be made to locate a geothermal production facility where the information obtained can be used to measure mass flow under production conditions.

This LDRD has resulted in the award of a patent on the concept (July 2002). The research has been performed in collaboration with researchers and students at the INEEL (Joe Keller), Idaho State University, and Brigham Young University (Jonathan Blotter and Matthew Pittard). The project supports DOE energy objectives and has generated interest among the oil and gas industries as well as the thermal hydraulics and nuclear industries.

# Clean Cold Start Technology for Conventional, Electric, and Hybrid Vehicles

*Kevin L. Gering, Daryl R. Haefner*

## *Improving engine efficiency through novel heat storage and release*

NE115

Phase change materials (PCM) offer an attractive option for thermal management in hybrid electric vehicles (HEVs). The attraction in using PCMs is that they can liberate exothermic heat of fusion (crystallization) upon activation, and then absorb vehicular waste heat to become reactivated. This activation/reactivation cycle is reversible and can be repeated thousands of times for some systems.

This LDRD is applying knowledge of PCMs to the design of a thermal management system (TMS) for HEVs. The premise of the HEV application is that waste heat can be captured and stored as latent heat (heat quantity related to the reversible phase change from liquid to solid) and sensible heat, then quickly released back to key points within the automotive application to abate the effects of severe cold start conditions.

As such, well-managed PCMs within a vehicle can result in improved fuel and battery efficiencies (e.g., lithium-ion cells), longer battery lifetimes, decreased emissions, and decreased mechanical stress on the engine, particularly under harsh winter conditions.

Technical objectives for fiscal year 2002:

- Continue laboratory studies of PCM thermophysical properties.
- Complete conceptual design of TMS for HEVs.
- Submit Invention Disclosure Record covering the TMS.
- Develop computer simulator for TMS.
- Establish collaborative relationship with National Renewable Energy Laboratory (NREL).
- Begin development of heat exchanger prototype.

In follow-up work from FY01, additional candidate phase change materials with higher melting temperatures were tested in FY02 to evaluate these materials for use in vehicles under cold-start conditions. The PCMs evaluated this year have published melting temperatures in the range of 70° C to 95° C and include hydrated species of aluminum ammonium sulfate, sodium potassium tartrate, sodium pyrophosphate, and others. Properties of particular interest include the amount of supercooling, the rate of crystal growth, and the congruency of phase change with cycling. None of these higher-melting materials were found suitable in their pure form for use in the proposed application, indicating that the PCMs studied in FY01 are preferred for this application.

An Invention Disclosure Record (IDR) was submitted December 2001 (IDR B-247) and a patent application is being pursued based on the IDR and supporting optimization calculations described below. The IDR describes a unique thermal management system, using PCMs that could be incorporated in HEVs, whereupon vehicle performance would be improved and usability would be extended to more northerly latitudes. One of the novel design features in this system is a unique PCM-based heat exchanger and its use within the thermal management of the vehicle's power supply.

A computer simulation is being developed that will mimic the operation of this thermal management system within an HEV and provide guidance toward system design optimization. The simulation will track the heat flows and temperatures within the vehicle's battery cooling/heating loop as a function of ambient conditions and operating time.

Governing thermodynamic and material balance equations for the computer simulation have been developed. In addition, supporting data such as material and system-specific physical properties (heat capacities, thermal conductivities, densities, heat transfer coefficients, crystal growth rates, etc.) have been obtained as published values, estimated through published correlations, or determined through this laboratory work.

A collaborative relationship has been developed with the NREL regarding thermophysical behavior of lithium-ion cell packs foreseen as being used in next-generation HEVs. Finally, equipment and supplies have been procured for assembling a prototype heat exchanger that uses PCMs. This prototype will be tested in FY03 to fill data gaps and provide validation of computer simulations.

Domestic implementation of this technology will support U. S. energy security in addition to providing obvious consumer benefits. The primary programs at the INEEL and within DOE that will benefit from the resulting technology are those dealing with advanced

vehicle systems (e.g., conventional, hybrids, fuel cell, etc.) and those that cover thermal management of waste heat as a means toward energy conservation and energy security.

Performance data from a working TMS prototype could be used as a springboard for follow-on work through agencies such as DOE Office of Transportation Technology. In addition, upcoming completion of a patent application could act as a seed for growing an INEEL program centered on novel aspects of thermal energy storage and utilization. Potential also exists for adapting the emergent technology to military applications.

# Novel Solid Electrolyte Materials for Lithium Batteries

*Mason K. Harrup, Thomas A. Luther, John E. Wey, John R. Klaehn*

## *Improving conductivity in advanced rechargeable batteries*

NE112

The development of advanced secondary (rechargeable) lithium batteries that exhibit superior conductivity to existing technology would have nearly limitless use – from cell phones to space applications. While it is well known that polyphosphazenes with ether linkages are good ionic conductors, improvement is still needed in the solid polymer electrolyte (SPE) before widespread use of these systems can be realized.

The purpose of this LDRD is to complete the synthesis and characterization work on a new polymer family for application to advanced secondary lithium batteries. This goal is to form next-generation SPEs from polyphosphazenes by replacing specific ether linkages with thioether analogues that exhibit conductivity superior to their ether analogues. To accomplish this goal, the year's efforts were focused on employing the reliable synthetic pathway to polythiophosphazenes, developed in last year's effort, to synthesize and characterize a functioning polythiophosphazene SPE.

Technical objectives for fiscal year 2002:

- Design, synthesize, and characterize new thioether pendant groups.
- Synthesize and characterize the corresponding polymer.
- Formulate the polymers into membranes and evaluate the SPE.

Previous work at the INEEL has resulted in breakthroughs in the understanding of ion transport through phosphazenes and resulted in a superior new mechanical stabilization methodology. Unfortunately, the current materials are close, but not yet conductive enough to warrant acceptance and eventual commercialization. Modification of the polymer system is needed.

The logical approach to modifying the polymer was to replace selected ethers for their thioether analogues. The synthesis and Nuclear Magnetic Resonance (NMR) characterization of the polymer, poly[bis(2-(2-methoxyethoxy)ethanethio)phosphazene] (MEETP) has been completed. Obtaining multi-gram quantities of the pendant group (a previously unknown compound) was the longest and hardest part of the year's effort. To ensure success, the target molecule, methoxyethoxyethanethiol (MEET), was approached by two different routes simultaneously. Each of these routes was successful. However, the Mitsunobu route, while somewhat more cumbersome due to the production of multiple equivalents of side products, was the more effective route in terms of product yield. Each of the two routes to the target thiol are shown in Figure 1A and 1B (next page).

Purification of the target thiol was challenging in each route, and was accomplished through a combination of distillation and column chromatographic techniques. The principal impurity obtained in the thiourea route was the tosylated species, produced via the incomplete decomposition of the principal intermediate. This was carried through in small amounts during the distillation and had to be removed via column chromatography. This incomplete conversion in the second step of this route caused lower overall yield of the desired product.

The principal impurity in the Mitsunobu route was starting material. As each step in this reaction design was highly efficient, the total yield was much higher (82% vs. 44%) than for the thiourea route. Final purification was easily achieved through column chromatography.

Confirmation of structure and complete characterization of the MEET was accomplished through NMR analyses, using both multinuclear and multidimensional techniques. As seen in Figures 1 and 2, MEET was impurity-free and the initial assignments of both the $^{1}H$ and $^{13}C$ nuclei were accomplished. To complete the confirmation of the structure, 2-D experiments were performed. The crosspeak correlations seen in the HETCoR experiments demonstrate that the bonding relationships between the carbons and the protons and match those expected for MEET.

During the development of the synthetic route to the thiophosphazene system, the syntheses necessitated modifications from the well-established methodology for the generation of alkoxy- and aryloxy-substituted polyphosphazenes. As reported previously, the use of tetrahydrofuran as a solvent for the formation of the sodium thiolate resulted in the unexpected immediate degradation of the phosphazene backbone upon the addition of polydichlorophosphazene to the thiolate mixture.

In the effort to capitalize on the expected solubility characteristics of MEETP, further modification in the synthetic route was based on the methodology developed for poly[bis(2-(2-methoxyethoxy)ethoxy)phosphazene] (MEEP). The pendant group, MEET was reacted with sodium hydride in 1,4-dioxane to generate the sodium thiolate. Freshly sublimed hexachlorocyclotriphosphazene was heated in a sealed, evacuated glass reaction vessel at 250° C for approximately 24 hours to generate the polydichlorophosphazene. Upon cooling, the polydichlorophosphazene was dissolved in toluene and slowly added to the 1,4-dioxane solution of the sodium thiolate and monitored by $^{31}P$ NMR spectroscopy.

When the reaction was complete, the polymer was quenched by precipitation into hexanes. The crude polymer was collected and added to nanopure $H_2O$ in an attempt to redissolve and isolate using the lower critical solubility temperature (LCST) method developed for the isolation and purification of MEEP. The crude polymer would not dissolve at room temperature; however, the material did dissolve at lower temperatures. A first LCST point was found at 12° C. After redissolving in nanopure $H_2O$ the LCST point increased to 44° C. After these two precipitations, the occurrence of another LCST

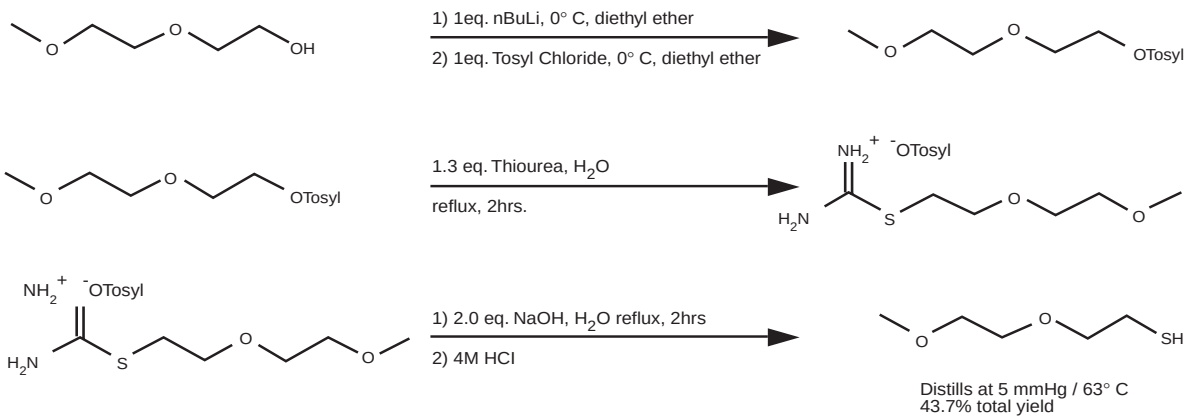


*FIGURE 1A. The thiourea route.*

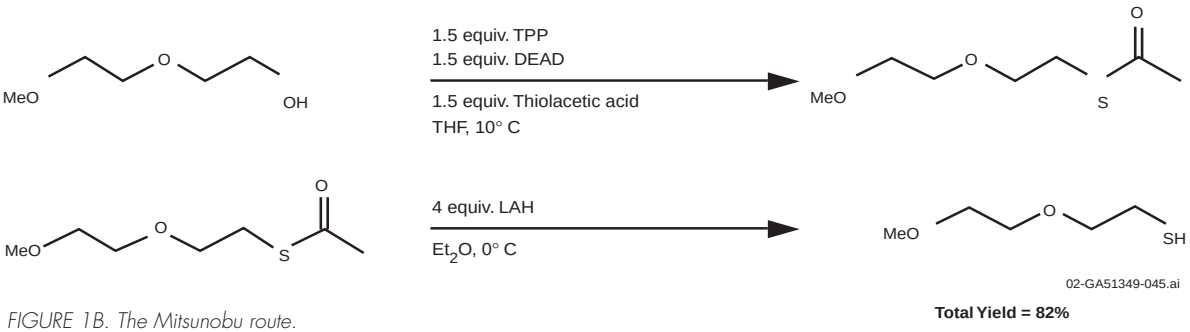


*FIGURE 1B. The Mitsunobu route.*

point for MEETP was not observed. Final purification of MEETP was performed by dialysis in nanopure $H_2O$ for one week.

Confirmation and characterization of MEETP was performed by $^{1}H$, $^{13}C$, and $^{31}P$ NMR spectroscopy. The chemical shift of the resonance in the $^{31}P$ NMR spectrum of MEETP is approximately 20 ppm downfield of the resonance observed for MEEP (Fig. 2a, b). The $^{1}H$ NMR spectra exhibit differences to the chemical shift of the resonances of the protons that are either two or three bonds removed from the sulfur that is directly bonded to the phosphorus nuclei (Fig. 2c, d).

In summary, the positive outcome of this project's efforts to-date has been the successful opening of a novel route to generating thio-substituted polyphosphazenes. The investigators have published their results in peer-reviewed literature. In addition, this work increases the INEEL's reputation in the polymer community as a leader in polyphosphazene synthesis, as demonstrated through invitations to speak at national scientific conferences.

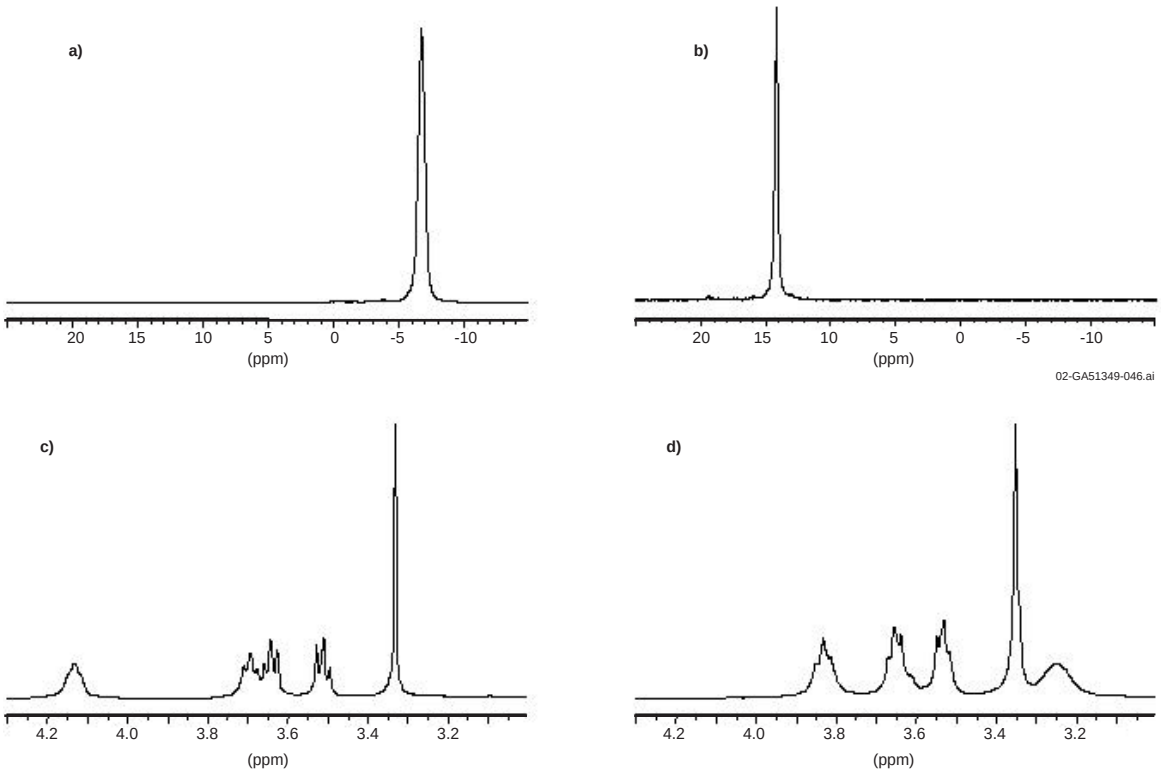


*FIGURE 2. $^{31}P$ NMR spectra of a) MEEP and b) MEETP (THF-$d_8$). $^{1}H$ NMR spectra of c) MEEP and d) MEETP (THF-$d_8$).*

# Active Neutron Spectroscopy for Neutron Capture Beam Characterization

*Jack K. Hartwell, David W. Nigg*

## *Improving cancer treatment planning*

NE117

The INEEL has had a long-standing interest in the development of neutron-based radiotherapy. Boron neutron capture therapy (BNCT), which has been of particular interest at the INEEL, is a form of neutron-based therapy that uses blood-borne boron compounds and a carefully tailored neutron energy spectrum to enhance the therapeutic dose to cancer tumors.

Cancer treatment planning for BNCT requires detailed information regarding the neutron energy spectrum of the therapy beam. The INEEL's BNCT research group is internationally recognized for its expertise in the characterization of the energy spectrum of fast and epithermal neutron therapy beams. Neutron energy spectroscopy is a challenging measurement under the best of conditions, but is even more difficult in the high neutron and gamma ray fluence environment presented in actual neutron therapy beams.

The INEEL's measurement protocol relies on the activation of threshold foils, the induced activity of which can be analyzed to determine the neutron flux profile in various energy groups. These measurements lack detail in the neutron energy region from about 50 keV to 2 MeV. This energy region is one critical to the evaluation of BNCT beam quality and dose estimation for patient treatment planning.

This LDRD research investigates techniques to provide more neutron spectral detail in this critical energy region. Through this project, the investigators have demonstrated the applicability to this task of an active detection technique using superheated drop detectors (SDD), and have successfully measured the neutron spectrum in this region at the pre-clinical BNCT beam installed at the Washington State University TRIGA reactor.

Technical objectives for fiscal year 2002:

- Develop neutron spectroscopy techniques using superheated drop detectors with the following attributes:
  - — Capable of spectrometric measurements with a neutron energy threshold of 50 to 100 keV.
  - — Reliable operation in gamma-ray fields of 20 to 40 mSv/hr.
  - — Field operation capable.
- Test the operation of the Apfel Enterprises REM SPEC SDD neutron spectrometer versus sealed neutron sources, the epithermal filtered photoneutron beam at the Idaho Accelerator Center, and the pre-clinical BNCT epithermal beam on the WSU TRIGA reactor.
- Document system performance and integrate the unit into the BNCT neutron spectral unfolding protocol.

Early in the course of this LDRD, neutron spectrometers based on the superheated drop technology became available. SDDs consist of several thousand small (approximately 100µm) drops of selected halocarbon refrigerants dispersed in a stabilizing gel matrix. The drops are dispersed at a temperature or pressure below the boiling point of the liquid, and then stabilized in a superheated state when the gel returns to ambient temperature.

When energetic neutrons interact with the superheated droplets, a bubble forms. The neutron energy required to nucleate a bubble depends on the degree of superheat, and thus is determined by the temperature of the gel media. The neutron media tubes are sufficiently insensitive to gamma radiation that they have been used to quantify the photoneutron dose to patients undergoing high-energy photon radiotherapy.

In the Apfel system (termed a REM SPEC), the media temperature is controlled by a thermal sensing and foil heater system and bubble formations are counted acoustically. In normal applications, two different media are each run at four preprogrammed temperature steps. Since each tube/temperature combination responds with a different nucleation rate versus neutron energy curve, typical neutron spectrum unfolding techniques can be used to calculate the expected spectral shape between about 50 keV to 10 MeV. Since this is the region in which the activation foil technique provides only limited information, it seemed that an SDD-based spectrometer, properly tested and developed, could provide improved neutron spectral characterization if implemented into the INEEL's beam characterization protocol. This in turn would translate into improved treatment planning for patients undergoing neutron radiation therapy.

"Few-channel" or "coarse-group" response data, like those provided by activation foils and the REM-SPEC, must be unfolded relative to known response functions and a "best guess" *a priori* spectrum to infer an incident spectrum. Spectra acquired in this research were unfolded using the manufacturer-supplied stripping code and certain more rigorous unfolding routines. These included the INEEL's least-squares direct unfolding technique used for the project's foil measurements, a maximum entropy unfolding technique (MAXED), and two iterative adjustment codes, SAND-II and GRAVEL. As their names imply, SAND-II and GRAVEL use very similar mathematical approaches, but differ slightly in the weighting factors used.

To support these unfolding techniques, a set of response functions detailing the relative detector response as a function of neutron energy, selected medium, and medium temperature was required. Since the manufacturer did not supply them, the plotted detector response curves from the users manual were digitized, and converted to an 84-Group equal-lethargy structure covering the energy range from 30 keV to 10 MeV. To allow for results normalization, the digitized response functions were compared with the cross-section versus neutron energy curves for the various foils routinely used in the foil activation protocol. The threshold (635 keV) and expected relative reaction rate of the SDD1000 (lower energy range media) at 25° C was similar to that of the $^{115}$In(n,n')$^{115m}$In reaction in the foil set. Thus, the SDD-calculated relative fluxes were normalized to this reaction when required.

The REM SPEC unit was initially tested in the INEEL laboratory versus a stainless-steel encapsulated $^{252}$Cf spontaneous fission source and a stainless-steel encapsulated $^{241}$Am-Be neutron source. The REM-SPEC measurements on isotopic neutron sources of $^{252}$Cf and AmBe were unfolded using both the MAXED and GRAVEL techniques. The *a priori* spectra were those from the literature. While the $^{252}$Cf unfolded neutron spectra showed generally good agreement with the known shape, the measured and unfolded results predicted too few neutrons in the energy region below about 4 MeV and too many above 4 MeV spectrum. This may be due to the 10 MeV upper limits of the response functions used. Results on the AmBe neutron spectrum were not good. This lack of agreement is unexplained, but may be a problem with the unfolding code input.

Measurements were performed on the filtered epithermal test beam installed on the linear electron accelerator at Idaho State University (ISU). The unit impacts 8 MeV electrons into a beryllium target, and the (γ,n)-generated neutrons are filtered through a composite filter. The output neutrons of interest have energies less than 2 MeV; consequently, only the low energy range (SDD1000) media tube was used. These data were unfolded to a two-group structure using the direct unfolding technique. The results looked reasonable, but since the beam is not well characterized no definitive conclusions could be drawn. However, this test did demonstrate that the SDD-based spectrometer could operate without interference from a gamma-ray background.

In May, the REM SPEC was tested at the pre-clinical epithermal BNCT beam installed on the TRIGA reactor at WSU. The detector head was positioned at the mid point of the beam about 5 cm forward of the source plane. Two complete measurement sets were acquired. The reactor power was 100W. The acquired data were unfolded using both the least-squares direct unfolding technique and the SAND-II iterative adjustment technique. The results of these measurements are compared with the expected spectrum in Figure 1 (next page).

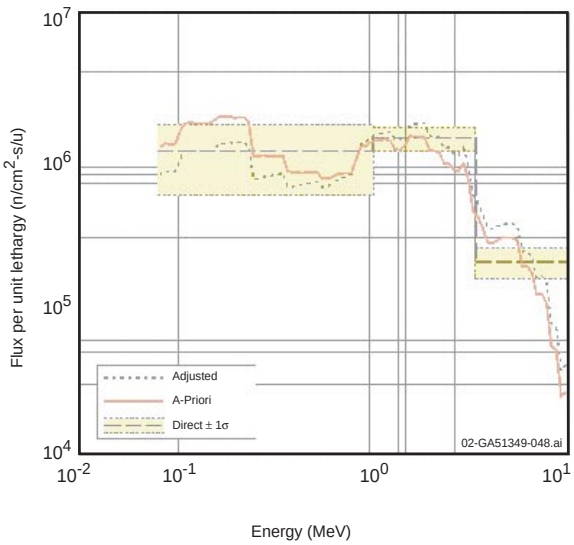


*FIGURE 1. REM SPEC results unfolded using the direct and the SAND-II iterative adjustment unfolding methods compared with the a priori calculated spectrum of the WSU free beam.*

Both techniques gave comparable results, and both techniques predict a somewhat harder neutron spectrum than that predicted from calculations and foil measurements. This is similar to the differences noted in the $^{252}$Cf tests. This somewhat harder spectral shape is also what d'Errico et. al. reported at the Essen conference for their measurement of the Studsvik epithermal beam using these detectors and a different unfolding method (Italy 2002). However, the INEEL's experience indicates that for reactor epithermal beams, the actual spectral hardness is somewhat underestimated by the transport codes, so these results may be correct.

Based on the research results, the SDD-based neutron spectrometer provides adequate detail in the neutron energy range of interest. It has the required insensitivity to gamma-ray interference, and the measured results can be adequately unfolded using standard unfolding tools. Some additional investigation into the seemingly high results at energies above 0.6 to 2 MeV seems warranted.

The INEEL is presently in its 14th year of a BNCT Research Program funded through the DOE's office of Science. Among the INEEL's contributions to this program is the capability to characterize BNCT therapy beams for those parameters important to treatment planning and dosimetry. This LDRD research will substantially augment that capability.

Successful implementation of a superheated drop detector-based spectrometer, like the REM SPEC unit under investigation in this research, into the beam characterization protocol would significantly enhance the ability to detail the neutron spectrum in the high-energy region above 100 keV. Since these high-energy neutrons contribute strongly to an undesirable dose to healthy tissue, their quantification is important for treatment planning. Such an enhancement could prolong the life of cancer patients worldwide.

# Characterization and Modeling of a Grain Combine Harvester

*J. Richard Hess, Kevin Kenney, Thomas Foust, Reed Hoskinson, John Svoboda*

## *Advancing biomass harvesting*

CE102

Large-scale displacement of petroleum as an energy resource is expected to come primarily from low-cost crop residue feedstocks. However, a lack of effective equipment and methods for harvesting, storing, and fractionating crop residues for subsequent conversion processes inhibits their utilization.

This LDRD addresses this issue by investigating approaches for implementing the unit operations of a combine harvester into a single-pass harvester for grain and crop residue. In FY01, the investigators evaluated combine harvester unit operations for biomass separation by instrumenting a harvester and creating a virtual engineering platform for visualization of the experimental data. This effort required the development of an image-based measurement system to obtain accurate numeric characterization data on the harvester biomass separation processes.

The virtual engineering platform and an image-based biomass flow measurement system are necessary tools for supporting development of a fully coupled discrete phase (Lagrangian) computational fluid dynamics model of the multi-phase biomass fractionation/flow regime. The visualization tools developed by this project will allow computational models to be linked with experimental data in a 3-D visualization system to computationally test performance of various techniques and systems.

By coupling advanced spatial sensing technologies (i.e., the imaging system) with computational and visualization technologies, researchers will be able to see the results of experimental and computational studies in the context of the combine physical-separation environment. This will enable the innate pattern-recognition skills of the expert, bringing to light key relationships that have previously been unknown, and result in breakthroughs in understanding system performance.

Technical objectives for fiscal year 2002:

- Complete development of the tools to allow users to examine experimental and computational data in a realistic interactive virtual environment.
- Determine lighting method (high-intensity strobe or laser) and associated imaging technique(s) best suited to freeze-frame rapid sequential motion of the biomass separation process.
- Develop packaging for the lighting/imaging system to allow non-intrusive installation into biomass separation machines.
- Test the selected lighting/imaging system to measure vector velocities of fluidized biomass beds.

An engineering understanding of the complex flow phenomena involving multi-phase biomass fractionation is necessary to separate biomass components. This project includes the development of new advanced spatial imaging technologies coupled with advanced computing and visualization technologies that allow researchers to see the results of computational studies in the context of the physical separation environment being studied.

For FY02, the scope of this project was reduced to complete the virtual engineering platform and development of imaging systems for discrete particle and density analysis of gas solid phase separation that might be employed in the handling and fractionation of biomass. This is important because commercially available imaging systems are designed for gas/liquid phase processes (i.e., spray nozzles) but do not work well on gas/solid phase biomass separation processes. All other originally proposed project tasks were completed in FY01 or transitioned to other funding sources.

As of December 2001, the virtual engineering platform was completed by Iowa State University (ISU) and readied for displaying fluidized bed imaging data. The data from the imaging system designed in last fiscal year was analyzed. Based on that data analysis, a redesigned imaging system (including lighting, camera, controllers and packaging) was completed and installed in a New Holland prototype combine in July 2002. The imaging system was thoroughly tested in August and September, and was proven capable of capturing image sets that could be analyzed by particle image velocimetry software. With these accomplishments, this project has achieved the deliverables promised per the modified FY02 work scope.

***Virtual Engineering Platform*** – The key functions of the virtual engineering platform are the ability to 1) examine the computational and experimental data in a realistic interactive environment, 2) compare the computational and experimental results, and 3) enable the users to ask "what-if" questions. In FY01, the initial geometric model was completed and brought into a virtual environment. Additionally, basic interaction tools were developed that enabled the user to interact and examine the geometric model.

In FY02 the foundation of the virtual engineering package was completed (Fig. 1). The foundation included expansion of the visualization software to bring two separate data sets together (e.g., computational data and experimental data.) Tools were developed and/or adapted that enable the user to review and use the data "on the fly." These interactive visualization tools include streamlines, iso-surfaces, vector planes, and search boxes. Previously completed work was updated to eliminate bugs and streamline the package.

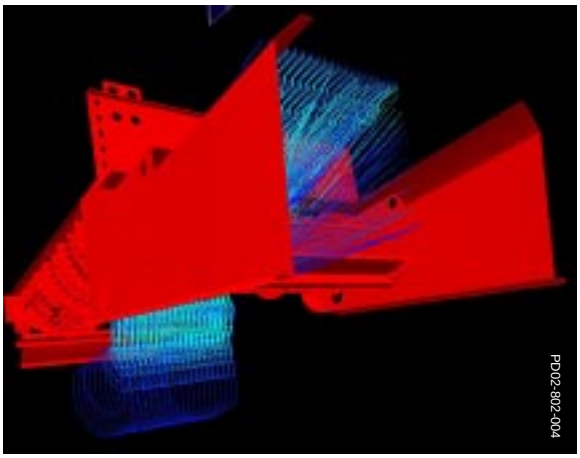


*FIGURE 1. Virtual Engineering Platform complete with the tools that enable users to examine experimental and computational data in a realistic interactive environment.*

The software being developed is based on VR-XPR, an open-source scientific visualization package being developed with project collaborator Mark Bryden at ISU. This package is transportable across all types of virtual environments from stereo walls, head-mounted displays, non-stereo screens and projectors, and large virtual rooms. Most computational platforms are supported, including IRIX, Linux, and Windows.

Additionally, work was initiated on enabling input from handheld user devices (PDAs and tablets). This will provide a more natural interface and permit the user to bring data and questions from the field into the virtual environment for broader and more comprehensive engineering analysis and investigation.

***Imaging System*** – In FY 2001, a Double Exposure Color Separation imaging system was developed. This year, the investigators began analyzing the data to determine the effectiveness of the color separation technique, and the integrated performance of the imaging system's subcomponents. It was determined that this color separation technique was inadequate for discrete identification of biomass subcomponents. The primary reason for this inadequacy was that the post-processing analysis of the double-exposed image could not identify discrete biomass particles as the image became increasingly populated with higher biomass loads.

To solve this problem, the system was redesigned to use a frame-straddling imaging technique. This technique does the first exposure at the end of the first frame, and the second exposure at the start of the next frame. The advantages of this technique include the ability to directly acquire image pairs as little as 200-microseconds apart. No post-processing is required to extract images for particle image velocimetry analysis. The technique also is affordable and easier to use as it uses white-light illumination, not color filters.

By using the strobes without filters, it was determined that laser lighting was unnecessary. This is a big advantage as lasers are more costly and not as durable as the strobes. By attaching the imaging system to a robotic positioning system, paired images of the biomass flow could be taken throughout the combine chamber (Fig. 2). From these accurately positioned images, particle-velocity data could now be calculated for every flow path across the combine separation shoe.

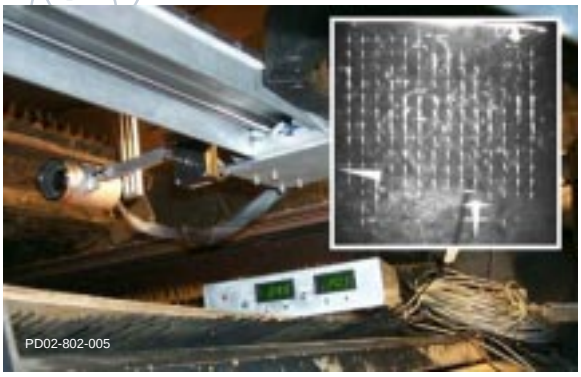


*FIGURE 2. Frame-straddling image systems installed in the separation chamber of a combine. The insert is a PIV analysis of an image set, showing the downward movement of biomass particles.*

Particle Image Velocimetry (PIV) is an experimental technique for inferring fluid velocity information from digital pictures. The insert photo in Figure 2 is taken with a digital (CCD) camera and shows the complex multi-phase fluid (air) and solids structure (straw, grain and chaff) in the chamber of the combine. The vector velocity field, represented by the white arrows, was determined after analysis with PIV. The white arrows are velocity vectors. The length of each vector is proportional to the magnitude of the local velocity. The velocity vectors indicate that the mean flow is from the top to bottom of the picture. Very few velocity vectors are located near the bottom of the picture where the straw, grain and chaff have collected. The three large velocity vectors, referred to as "outliers," are not representative of the mean fluid motion, but are indicative of shadowing effects in the picture.

The use of these experimentally derived vector velocities is important in the development and validation of numerical models solved using computational fluid dynamic (CFD) techniques. Velocity field information, such as mean velocity, vorticity and strain-rate, obtained from the PIV analyses will be used as boundary condition information in the numerical models of the combine chamber. Without some knowledge of velocity information along the boundaries of the combine chamber, the results obtained from the multi-phase numerical models would be inaccurate.

Additionally, using the virtual engineering platforms, the velocity data obtained from the PIV analyses can be compared with the numerical results obtained from multi-phase CFD models of the combine chamber in order to validate the numerical results.

As our nation presses forward with bioenergy as part of its national energy strategy, cellulosic crops, not starch, will become the feedstock of choice for biomass derived fuels and chemicals. However, current-day economics preclude any commercial scale use of cellulosic feedstocks for fuels and chemicals.

The approach to this limitation in this LDRD research has been to thresh and separate the straw crop residue on the combine. As a result of this project, CNH Global, N.V., the world's largest agriculture equipment manufacture, has partnered with INEEL to do research and development on key unit operations of combine harvesters. In addition, this project has fostered partnership with Iowa State University.

# Development of Analytical Decision-Making Tools for Energy Efficient Agricultural Biomass Production

*Reed L. Hoskinson*

## *Creating a site-specific recipe for fertilizer application*

CE110

Presently, farmers fertilize and grow wheat with the objective of producing the economically optimum crop of wheat grain. With today's growing demand for energy, however, the wheat stems are becoming a valuable bioenergy source. The farmer's ideal would be to grow an economically optimum combination of both grain and straw stems.

This LDRD investigates methods for the optimum, simultaneous production of grain and straw stems. To achieve this objective, the capability of the INEEL Decision Support System for Agriculture (DSS4Ag) is being extended to generate a spatially variable, site-specific recipe for application of fertilizers such that the economically optimum simultaneous production of both grain and biomass can be achieved.

Technical objectives for fiscal year 2002:

- Enhance the optimization function of DSS4Ag to take into consideration the costs/benefits for both grain and biomass.
- Generate a spatially variable, site-specific recipe for fertilization of the farm field.
- Fertilize the field with the above recipe in a treatment pattern suitable for statistical evaluation of results.
- Monitor site-specific production of both grain and biomass at harvest.
- Evaluate and upgrade the decision-making capability of DSS4Ag for future years.

To determine what changes growers might make to their fertilization regime when wheat straw becomes a valuable commodity, the investigators developed variable-rate fertilization recipes for two different scenarios. The fertilizer recipes were generated using the Decision Support System for Agriculture (DSS4Ag). The DSS4Ag uses advanced artificial intelligence and data mining techniques to determine the economically optimum mix of fertilizers to be applied at each point in the field.

In the first scenario, soft white spring wheat was valued at harvest at $2.80/bushel and straw stems were valued at $10/ton. In scenario two, the soft white spring wheat was valued at $2.80/bushel and straw stems were $50/ton. The two spatially variable fertilizer recipes, and a grower-specified uniform fertilizer recipe, were each clipped into 12 blocks and merged to produce the fertilization plan for a 153-acre farm field. This plan gave four replicates of each of the three treatments alternated across the field.

The field was harvested in late August 2002. The grain from each block was harvested independently. The straw was windrowed by the grain combine and baled in a later pass by a baler. The straw bales will be weighed and analyzed to determine straw stem content. All the data for grain and straw will be used to assess the economic outcome of the variable-rate treatments.

Recipes:

The grower specified a uniform fertilizer recipe of 150 units N, 40 units P and 30 units K per acre. These rates required 309 pounds of urea, 77 pounds of ammonium phosphate and 48 pounds of potash per acre.

Figure 1 shows the spatially variable fertilizer recipes for urea and ammonium phosphate for the $2.80/bushel

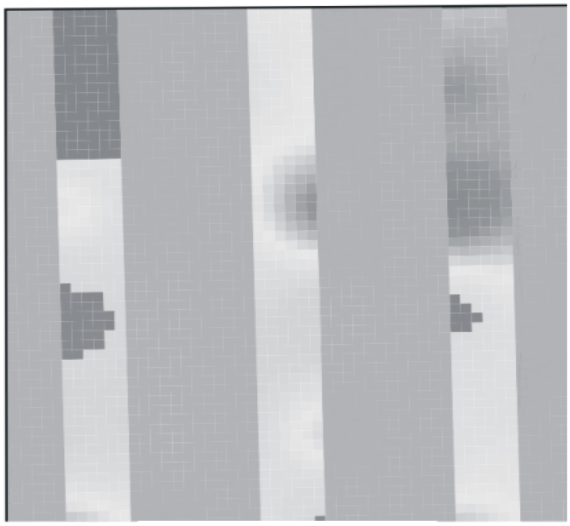

urea

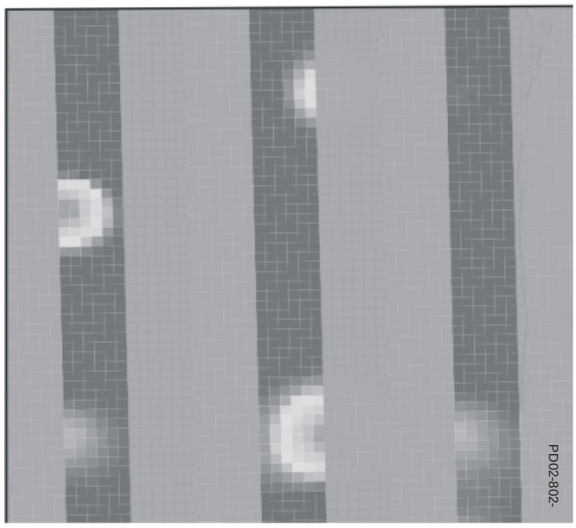


Ammonium phosphate

*FIGURE 1. DSS4Ag recipe for $2.80/bushel wheat and $10/ton straw.*

wheat and $10/ton straw treatment blocks ($10/ton straw recipe).

Figure 2 next page shows the spatially variable fertilizer recipes for urea and ammonium phosphate for the $2.80/bushel wheat and $50/ton straw treatment blocks ($50/ton straw recipe).

Table 1 shows the fertilizer requirements, in tons, for each of the three recipes for the entire 153-acre field, and the total fertilizer costs.

| Fertilizer | Grower Recipe | $10/ton Straw Recipe | $50/ton Straw Recipe |
|---|---|---|---|
| Urea | 23.6 | 13.0 | 29.2 |
| Potash | 3.7 | 0 | 0 |
| Ammonium Phosphate | 5.9 | 3.0 | 2.7 |
| | | | |
| Total Fertilizer | 33.2 | 16.0 | 31.9 |
| | | | |
| Total Fertilizer Cost | $6,750 | $3,296 | $6,378 |

02-51349-012

*TABLE 1. Fertilizer requirements, in tons, for thre three recipes.*

The DSS4Ag fertilizer decision also predicts the yield (grain and straw) at each point. The gross market value predicted for the $10/ton recipe by DSS4Ag was $52,799. For the $50/ton recipe, the gross market value was predicted at $65,836.

If the grower had presently been using a tool like DSS4Ag his fertilizer input cost would have been $3,296 and the crop's gross market value of grain and straw would have been $52,799. With the bioenergy infrastructure in place, the grower could have increased his fertilizer input cost to $6,378 and the crop's gross market value to $65,836. Thus, by increasing fertilizer cost by $20.14/acre, the farmer would have increased his crop's gross market value by $85.21/acre.

This research has benefited the INEEL and DOE Bioenergy Initiatives by demonstrating the economic

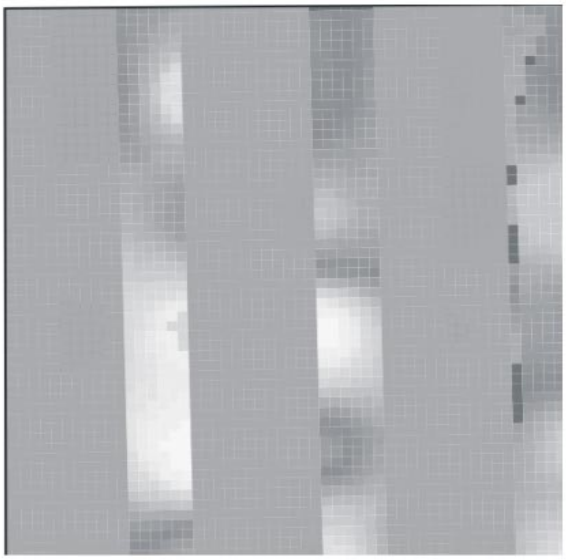

urea

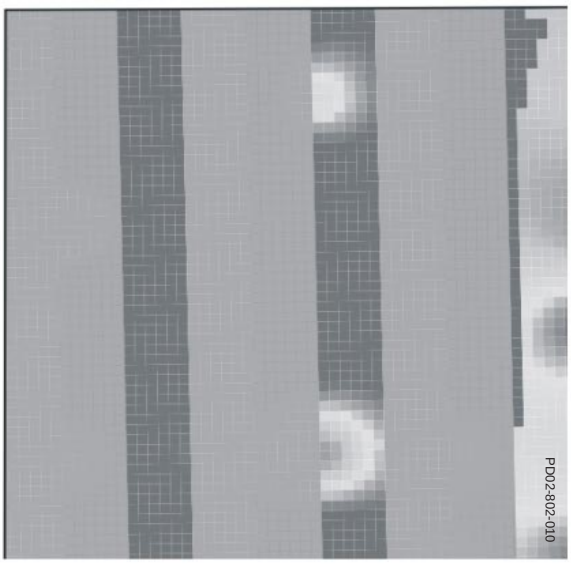


Ammonium phosphate

*FIGURE 2. DSS4Ag recipe for $2.80/bushel wheat and $50/ton straw.*

improvements the grower can achieve in support of the Bioenergy Initiatives by modifying fertilization regimes in support of Bioenergy.

It is expected that as the U.S. role in the national and international bioenergy markets grows, this DSS4Ag analytical tool for optimizing the production of the crop as well as the biomass feedstock will have significant potential. This expectation is strengthened by other INEEL research in collaboration with a major agricultural equipment manufacturer that suggests that there will be machinery available to harvest both the crop and the biomass feedstock.

# Hydrogen Technologies R&D

*Paul A. Lessing, Kendall B. Johnson*

## *Storing hydrogen in carbon*

NE125

There is a large and increasing interest in hydrogen to be used as a fuel within the United States, freeing the country from dependence on fossil fuels. Recent advances in fuel cell technology are enabling entrance into this "hydrogen economy."

Fuel cells convert hydrogen into electricity for a variety of uses, including homes, factories and transportation. However, significant advances in hydrogen storage must be realized before vehicles (cars, buses, trucks, etc.) can be propelled by fuel cells for acceptable distances without refueling.

This LDRD is exploring advanced carbon materials that can be placed within pressurized hydrogen tanks to adsorb large amounts of hydrogen, thus increasing storage capacity. Two tasks are being conducted: modification of graphite fibers and arc plasma synthesis of carbon nanotubes. The graphite fibers are being modified by propping open the layers within the graphite through the use of certain "intercalating" atoms. Initial intercalation experiments were successfully completed but hydrogen adsorption measurements have not yet been made. Carbon nanotubes have shown promise as a hydrogen storage material as well as many other applications but are presently very expensive and produced only in very small quantities. The purpose of the second task is to investigate arc plasma synthesis of carbon nanotubes, which opens the potential for cheap, high volume production. Production of soot containing carbon nanotubes was demonstrated last fiscal year. During FY02, extensive calculations were performed to improve the experimental apparatus including formation times and temperatures. Modifications to the system have been made to greatly increase the temperature and dwell time, increasing the probability of nanotube formation. Experimental data show that the needed conditions are now readily obtainable and show some evidence for nanotube production.

Technical objectives for fiscal year 2002:

- Intercalated Graphite:
  - — Design partial factorial matrix arrays of intercala tion experiments (Taguchi Method).
  - — Make glove box operational, including experimental apparatus within the box.
  - — Gain approval of modified health, safety, and environmental plans.
  - — Begin intercalation experiments.
  - — Locate commercial companies to perform high-pressure hydrogen adsorption/desorption experiments.
- Carbon Nanotubes
  - — Perform extensive calculations, including catalyst particle-formation rates for high-temperature catalyst based oncollision rates at various temperatures and pressures.
  - — Calculate reaction chamber dwell times for various volumes, gas flow rates, and temperatures.
  - — Perform extensive heat loss calculations for the reaction chambers, including conductive and radiative transfer.
  - — Make equipment improvements to include: minimizing heat-loss in reaction chamber, redesigning stainless steel injector for mixing gases, replacing copper electrode in plasma torch, and installing high-temperature thermocouple probes.
  - — Perform experimental run with modified apparatus.
  - — Obtain transmission electron microscope (TEM) images of soot samples.

***Intercalated Graphite*** – The intercalation experiments must be conducted in a glove-box (dry, inert) atmosphere because of reaction and flammability issues. To make the glove box operational, it was relocated to a new lab, after proper permitting was obtained, and re-set. New electrical and vacuum systems were installed along with vacuum piping and connectors. The glove box was then tested for gas-tightness and found to be operational.

Planning was completed for laboratory experiments of partial factorial matrix arrays (e.g., four 3-level factors) using the Taguchi method. The first set of nine individual experiments used levels of the Group IA metal elements

lithium, potassium, or cesium (into a Vycor chamber in one furnace) with one of three types of Torayca™ graphite fiber tows (into a Vycor chamber in the other furnace). The various types of graphite fibers were cut, organic sizing removed (oxidized), and samples weighed prior to loading and sealing into their Vycor reaction chambers. other experiments will involve the intercalation of both Group IA elements and other elements that will function as catalysts to the hydrogen adsorption/desorption process.

The apparatus for the intercalation experiments was assembled. This involved setting up furnace controllers, building small furnaces, and fabricating complex multi-chamber Vycor™ borosilicate glass reaction vessels. Independent Hazard Review documents were modified to accommodate loading the intercalated fibers into a special sealed container for X-ray Diffraction (XRD) characterization. These activities met the milestone to begin the intercalation experiments.

XRD data from one experiment showed a displacement of the graphite peak, a new (intercalation) peak, and a cesium hydroxide peak (due to surface contamination from trace amounts of water in the atmosphere). The graphite color changed from black to bronze also indicating that intercalation was occurring.

A commercial company was found (General Motors Research Labs, Warren, MI) that could perform the high-pressure hydrogen adsorption/desorption experiments on the intercalated graphite samples. This company became strategic partners in this research and minority-owners of the project's proposed CRADA partner (Quantum, Inc.).

***Carbon nanotubes*** – There has been great interest in graphite nanotubes since their discovery in 1991 due to the many interesting and important properties theoretically predicted for these structures. one of the properties of interest is the possibility of hydrogen storage. However, this field of research has been severely limited by the difficulty in producing high-quality samples in quantity. Many potential applications, including hydrogen storage, require kilogram to ton quantities.

Arc plasma torch synthesis of carbon nanotubes is of significant interest because the high throughputs make it scaleable to large production rates more readily than other techniques. Success in this LDRD will have significant impact on many applications for nanotubes including hydrogen storage materials.

This LDRD research can help determine the potential of using arc plasma synthesis for economical, high-volume production of carbon nanotubes for hydrogen storage and other applications. The project enhances the INEEL's research capabilities in advanced materials.

# Carbon Dioxide Sequestration in Geologic Coal Formations

*Jenn-Tai Liang, Eric P. Robertson, Shaochang Wo*

## *Reducing $CO_2$ in our atmosphere*

NE124

There is a growing consensus in the international community that $CO_2$ emissions from burning fossil fuels play an important role in global climate change. Recent efforts to reduce the carbon content in fuels and improve energy efficiency can certainly help in reducing the amount of $CO_2$ released into the atmosphere. However, large-scale carbon sequestration will definitely be required to achieve the targeted atmospheric $CO_2$ level of 550 ppm by 2025.

Of the sequestration options available, geologic sequestration of $CO_2$ in coal formations is considered one of the methods with the greatest short-term potential. Coal beds typically contain large amounts of methane-rich gas that are adsorbed onto the surface of the coal. Tests have shown that $CO_2$ is roughly twice as adsorbing on coal as methane, giving it the potential to efficiently displace methane and remain sequestered in the bed. $CO_2$ recovery of coal bed methane (CBM) has been demonstrated in limited field tests, but much more work is necessary to understand and optimize the process. Work also is needed to develop better estimates of the potential capacity of cost-effective coal bed sequestration in the United States.

This LDRD is developing mechanistic models specific to $CO_2$ sequestration in British Petroleum's (BP) Tiffany coal bed methane field. In this study, the original field model was modified to match the field performance of a 5-spot pattern in the northern part of the Tiffany Field. The model successfully matched the performance of the 5-spot pattern during the enhanced recovery period ($N_2$ injection), and predicted that the future gas injection and $CO_2$ sequestration might be restricted to only one-third of the total available pay. This suggests that the actual $CO_2$ sequestration capability of the Tiffany Field might not be as high as originally expected. The modified model also predicted early inert gas ($N_2$ plus $CO_2$) breakthrough and high inert gas cut during future gas injections. The high volume of inert gas produced could overwhelm the reprocessing capability, resulting in early termination of the project.

Results from simulations using the model indicate that the injection scenario during $CO_2$ sequestration needs to be optimized to achieve best results. The modified model was demonstrated to be an effective tool in optimizing the injection scenario.

Technical objectives for fiscal year 2002:

- Execute field model. Conduct history match and forecast field performance under injection.
- Define field performance estimates for $CO_2$ sequestration capacity and long-term integrity.
- Assess results and publish findings.
- Develop CRADA projects with industry.

To date, only one commercial demonstration of methane recovery by gas injection has been implemented. This is BP's Tiffany project in the San Juan Basin, Colorado. The Tiffany field consists of 38 producer wells and 10 injector wells. The current Tiffany field model incorporates the full geologic description, consisting of five coal layers, some of which do not extend throughout the unit. Coal continuity and thickness are greatest in the northern portion of the field.

The BP model provided good historical matches of the field performance during the primary production period. During the subsequent enhanced recovery phase, $N_2$ was injected into the field to accelerate methane recovery. The field model proved inadequate, in many respects, at accurately matching field performance during the enhanced recovery phase. Most importantly, it failed to predict nitrogen breakthrough times at the majority of the responding producers. The actual $N_2$ breakthrough times were much earlier than those predicted by the field model. With BP's proposal to supplement the nitrogen injection with the $CO_2$ captured from its gas processing plant, it is vital that the field model be modified to reflect the actual field performance during gas injection so that the reservoir's true potential for enhanced recovery and $CO_2$ sequestration can be determined.

This LDRD is focused on developing mechanistic models specific to $CO_2$ sequestration in BP's Tiffany coal bed methane field. The modeling effort to date focuses on a 5-spot pattern in the northern part of the field. The pattern area consists of one in-pattern and three off-

pattern injectors as well as four in-pattern and one off-pattern producers. The ultimate objective is to develop a full-field model for $CO_2$ sequestration in the Tiffany field.

To match the field performance during the enhanced recovery phase, the investigators assumed that the high-permeability streaks or conduits within each geologic layer contributed to the early nitrogen breakthrough. Although the high-permeability pay dominates early production response, the long-term response is in large part dictated by the amount of gas exchanged between high- and low-permeability packages. Instead of dividing each geologic layer into a fast and a slow component, the model was modified to include a high-permeability fast layer sandwiched between two low-permeability slow layers.

During history matching, layer thickness and permeability were adjusted to control gas breakthrough. Vertical transmissibility between layers was manipulated to match late time response. In FY01, it was demonstrated that the modified model matched the nitrogen breakthrough times and nitrogen cut reasonably well for all in-pattern producers. The model also did a good job matching the total gas production for all in-pattern producers. However, to match nitrogen breakthrough times and nitrogen cut, the vertical transmissibility between layers had to be set to zero. During gas injection, nitrogen was allowed to enter all three layers, not just the high-permeability fast layer. Because the permeabilities of the slow layers were low and there is no communication between the fast and the slow layers, most of the injected nitrogen entered the high-permeability fast layer. This implies that the nitrogen injection and enhanced methane recovery were restricted approximately to only one-third of the available pay. The impact of this on the sequestration capacity of the reservoir is discussed below.

The important factors that control the project lifetime and actual $CO_2$ sequestration capability are the inert gas ($CO_2$ and $N_2$) production and the inert gas cut with time. While methane production represents the income potential, it is the amount of inert gas reprocessed that actually determines the economic limit for a $CO_2$ sequestration project. In this study, three different injection scenarios were explored to study their effects on inert gas production and inert gas cut.

In the first scenario, a continuous injection of straight $CO_2$ was simulated. In the second scenario, the investigators simulated a continuous injection of a mixture of 76% $N_2$ and 24% $CO_2$ In the third scenario, the seasonal fluctuation of the nitrogen processing capability at Tiffany Field was taken into account. In this case, the injection was alternated between the $N_2$-$CO_2$ mixture (Nov. through April) and straight $CO_2$ (May through Oct.). In all three scenarios, the simulation of future injections ran from 01/01/2002 to 01/01/2020.

The modified model predicted early $CO_2$ breakthrough with high $CO_2$ cut during future gas injections. This suggests that the actual $CO_2$ sequestration capability of the Tiffany field might not be as high as originally expected. This is a direct consequence of the reduction of the available pay in the modified model. The amount of daily inert gas production that on-site facilities can handle is a limiting factor that determines the economic limit for a $CO_2$ sequestration project. The modified model predicted early inert gas ($N_2$ plus $CO_2$) breakthrough and high inert gas cut during future gas injections. The high volume of inert gas produced can overwhelm the reprocessing capability, and thus results in early termination of the project.

In this year's study, a special region feature was added to the model to quantify the $CO_2$ sequestration potential of the pattern area and to track the movement of $CO_2$ across the pattern boundary. Basically, the special region feature allows users to define a region of interest. The modified model with the special region feature can calculate the amount of $CO_2$ sequestratered in the special region and track $CO_2$ movement across the region boundary.

In addition to the injection scenarios that were used last year, a new injection scenario was added to simulate a possible actual sequestration scenario. In the new injection scenario, a continuous injection was simulated of a mixture of 76% $N_2$ and 24% $CO_2$ from 01/01/02

until 11/01/02 when the inert gas cut of the whole region reached 50%. The injection was then switched to continuous $CO_2$ to delay the increase in inert gas cut. The $CO_2$ injection was continued until 01/01/11 when the well grid pressure of an in-pattern producer (Well 7050) reached initial discovery pressure. At this point, all the producers and injectors were shut in to aviod injection above parting pressure. (Injection above parting pressure would fracture the formation and could result in uncontrolled release of $CO_2$ from the area.)

After shutting in all wells, the simulation was allowed to continue until 01/01/02 to monitor the movement of $CO_2$ across the pattern boundary. The 5-spot pattern area being used for these simulations was about 874 acres and consists of one in-pattern and three off-pattern injectors as well as four in-pattern and one off-pattern producers. The special region defined in this study was within the original pattern area and consists of one in-pattern injector and four in-pattern producers in a standard 200-acre 5-spot pattern.

For comparison, simulations were repeated using the special region for the old injection scenarios. The modified model calculates the amount of $CO_2$ moved across the region boundary by subtracting the amount of $CO_2$ produced from the amount of $CO_2$ injected and then add the amount of $CO_2$ sequestered in the region. Table 1 shows that continous $CO_2$ injection resulted in the most amount of $CO_2$ sequestered. However, a high amount of $CO_2$ moved across the boundary suggests that after the sequestration limit was reached, most of the $CO_2$ injected after that was just recycling between the injector and the producers. This indicates that the process was not very efficient.

The new injection scenario described above seems to be the most efficient one with a significant amount of $CO_2$ sequestered and yet only a relatively small amount of $CO_2$ moved across the region boundary into the region (row 3 in Table 1). These findings reveal that the injection scenario during $CO_2$ sequestration needs to be optimized to achieve best results. The modified model that was developed in this study can be used as an effective tool in optimizing the injection scenario.

Geologic sequestration of $CO_2$ and other greenhouse gases is a major focus area for the DOE. This LDRD will significantly expand INEEL capabilities to conduct geologic $CO_2$ sequestration research. As such, this effort will directly support a stated objective of the INEEL Institutional Plan within the Energy Resource area (specifically, Energy Efficiency, Renewable, and Fossil Energy). The knowledge acquired from this project will be broadly applicable to $CO_2$ sequestration in coal. It is expected that the program will continue to expand as geologic sequestration efforts grow.

With the capabilities developed in this LDRD, a CRADA agreement was signed through BP with the Carbon Capture Program JIP (composed of many of the major oil and gas companies and DOE) for a probabilistic risk assessment for $CO_2$ sequestration in coal bed methane fields. The investigators also have submitted an abstract to the 2003 International Coal Bed Methane Symposium.

| Injection Scenario | $CO_2$ Sequestered, MMscf | $CO_2$ Across Boundary into Region, MMscf |
|---|---|---|
| Continuous $CO_2$ | 13,400 | 15,612 |
| $N_2$-$CO_2$ (76%-24%)/ Pure $CO_2$/Shut in all Wells | 10,600 | 535 |
| 76%$N_2$, 24%$CO_2$ | 9,890 | 9,900 |

02-GA51349-054C

*TABLE 1. Amount of $CO_2$ sequestered and moved across pattern boundary.*

# Dependence of Coal Bed Permeability on Pore Pressure and Adsorbed Gas Content

*Jenn-Tai Liang, Eric Robertson*

## *Improving the accuracy of reservoir simulators*

PH107

Coal bed reservoirs in the U.S. contain an estimated 703 Tcf of natural gas and 141 Tcf of recoverable natural gas resources. This represents 12% of the total recoverable natural gas in the U.S., making coal beds a major contributor to the energy security of this country. Besides being reservoirs for methane, coal beds throughout the world have a huge $CO_2$ storage potential. If viewed purely as a non-commercial $CO_2$ sequestration technology, the worldwide sequestration potential for unmineable coal may be 350 billion metric tons of $CO_2$

Unlike conventional gas reservoirs, methane in coal is not stored as free gas but rather as sorbed gas, at near-liquid densities on the internal surface area of the microporous coal. In addition to methane, carbon dioxide, nitrogen, and higher molecular weight hydrocarbon gases are usually present.

Fluid movement in coal is controlled by diffusion in the coal matrix and described by Darcy flow in the fracture (cleat) system. In most coal bed methane (CBM) reservoirs, the cleat system is initially filled with water. Producing water from the cleats causes the reservoir pressure to decrease and the gas to desorb from the coal matrix at the matrix-cleat interfaces. This creates a methane concentration gradient across the coal matrix. Gas diffuses through the matrix because of the pressure gradient and is released into the cleat system where it flows to the production well and is produced.

This LDRD is investigating ways to improve the ability to model changes in coal permeability as a function of in situ stress. Permeability in coal, being dependent on cleat density and width, is not only a function of the elastic moduli of the coal matrix, but also a function of the adsorbed gas content. A current state-of-the-art coal bed permeability model based on elastic moduli and Langmuir strain-curve parameters for coal saturated with pure methane was unable to achieve a satisfactory match to field data without significantly modifying the strain data obtained in the laboratory. Because the gas adsorbed in coal beds is not pure methane, the current permeability model could be significantly improved by incorporating parameters of an extended Langmuir strain curve for gas mixtures in coal.

To obtain the gas mixture strain parameters, coal-strain measurements will be taken for a range of pressures and gases. The resulting extended Langmuir isotherm fit-parameters will be used to improve the permeability model. The permeability model will be tested and refined by comparing changes in coal permeability measured in the laboratory with calculated permeability using the improved model. The refined permeability model could be incorporated into reservoir simulators to better predict permeability decline and rebound during traditional coal bed methane production operations, but may be even more applicable during simulation of $N_2$- or $CO_2$-enhanced methane recovery from coal beds, and for $CO_2$-sequestration in coal beds.

Technical objectives for fiscal year 2002:

- Determine research approach.
- Develop equipment list necessary to accomplish work.
- Set up subcontract with Colorado School of Mines.
- Obtain and set up laboratory space at the Colorado School of Mines.

Improving the ability to model changes in coal permeability, as a function of in situ stress, will be accomplished by incorporating parameters of extended Langmuir strain curves for gas mixtures in coal into a coal-permeability model. The capacity of the coal matrix to store gas as a function of pressure is described by the Langmuir adsorption isotherm. Figure 1 (next page) compares sorption isotherms for various gases for a sample of coal from the San Juan Basin.

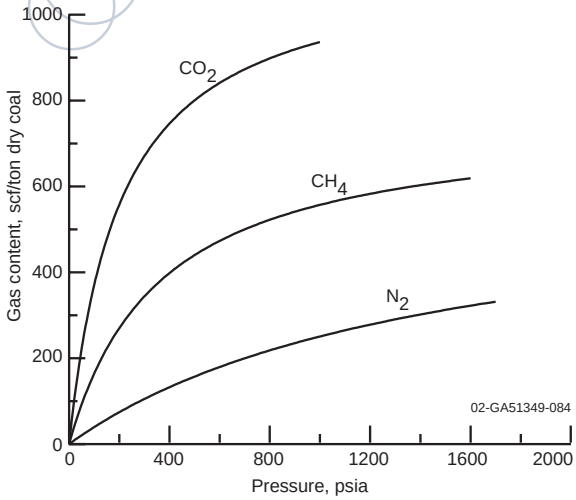


*FIGURE 1. Example of different sorption isotherms for different gases.*

Methane production from coal beds can be enhanced by injection of other gases to displace or strip the methane from the coal and accelerate production of methane at higher pressures. This process is called enhanced coal bed methane (ECBM) production. About twice the amount of $CO_2$ can be adsorbed in the microporosity of the coal matrix as $CH_4$, while $N_2$ is less adsorbing than $CH_4$. The mechanism of $N_2$-ECBM is called inert gas stripping and is primarily the result of reducing the partial pressure of $CH_4$ in the cleat system. The mechanism for $CO_2$-ECBM is called displacement desorption because the $CO_2$ is strongly adsorbed onto the coal as it is injected and displaces the methane in the matrix.

Because $CO_2$ is strongly adsorbed onto the coal matrix, coal beds throughout the world have a huge $CO_2$ storage potential. When viewed as commercial $CO_2$-ECBM projects, the total worldwide potential for $CO_2$ sequestration may be 7.1 billion metric tons while producing 68 Tcf of methane. If viewed purely as a non-commercial $CO_2$ sequestration technology, the worldwide potential may be 50 times greater.

The fluid transport mechanism in coal includes three different mechanisms: diffusion within the coal matrix, desorption from the matrix to the cleat system, and Darcy flow in the cleat system. CBM reservoirs are layered and contain orthogonal cleats perpendicular to bedding and can be conceptualized as a bundle of vertical matchsticks. Coal permeability is directly dependent on the width and frequency of the cleat system. Cleat width is dependent on the in situ stress of the coal and the gas content of the coal. These two factors affect coal permeability in opposite directions. As pore-pressure decreases, cleat-width closes and permeability reduces. At the same time, the gas content decreases and increases permeability. Figure 2 shows this effect. As pressure drops at high-cleat pressure, the dominant strain of the coal is matrix expansion and cleat-width decreases along with permeability. However, as pressure continues to drop, matrix shrinkage due to gas desorption can be the dominant coal strain, causing cleat-width to increase along with permeability.

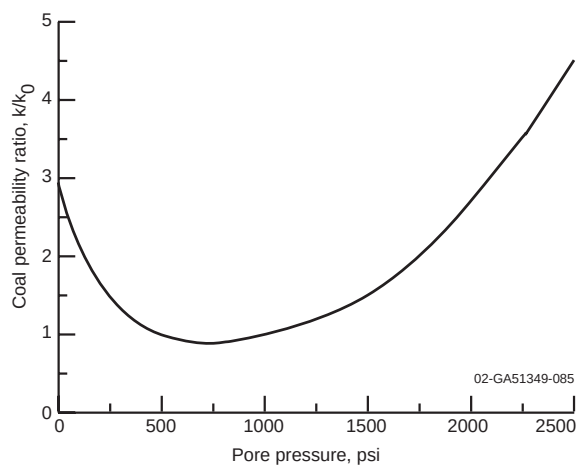


*FIGURE 2. Conceptualized behavior of permeability rebound in coal as pressure becomes small.*

Previous research has developed a simple model to account for increasing permeability at lower pressures, but was derived for pure-gas components and did not account for mixtures of gas that typically occur in coal bed methane reservoirs. The previous model, therefore, does not match actual field data and is not valuable for field simulation. As this LDRD research moves forward, equations will be developed that account for gas mixtures using extended-Langmuir strain parameters, and the permeability model will be tested based on laboratory permeability measurements using gas mixtures.

This research directly addresses the DOE Environmental Quality mission through the carbon sequestration program. To stabilize and ultimately reduce concentrations of $CO_2$) a greenhouse gas, it will be necessary to employ carbon sequestration – carbon-capture, separation and storage, or reuse. The program portfolio has six elements, two of which are addressed in this LDRD research: 1) $CO_2$-sequestration in geological formations including unmineable coal seams, and 2) models and assessments of the potential of carbon sequestration technologies.

The LDRD work will advance the understanding of how natural gas is extracted from coal beds and improve the accuracy of reservoir simulators. Understanding the mechanisms involved with natural gas extraction from coal seams will promote the development of natural gas resources from coal and help limit any disruptions in the production of natural gas. This research also provides the opportunity to add to the knowledge base about multiphase, multi-component flow in fractured porous media such as exist in contaminant flow at the INEEL site.

This research is being conducted jointly with the Colorado School of Mines, a premier engineering research institution. Future work in this and other areas is anticipated to result from this collaboration.

# Thermal Studies of Potential Increased ATR Power Margins

*Del Mecham, Scott Lucas, Steve Wagoner, Jim O'Brien*

## *Increasing power and safety margins at ATR*

NE109

This LDRD is providing the technical basis for increasing the power and safety margins at the Advanced Test Reactor (ATR) at INEEL. At issue, is the lack of a high-power heater available to use with the full-scale Critical Heat Flux (CHF) apparatus. The CHF apparatus is typical of an ATR fuel assembly and requires a large amount of power to reach critical heat flux. Commercially available heaters are not available that can reach the 40 Kilowatts or greater needed. Resolving this issue would increase the INEEL core competency in the areas of experimental and computational fluid dynamics (CFD).

Technical objectives for fiscal year 2002:

- Perform critical heat flux analysis and testing.
- Perform plume flow analysis.

This research project was conducted in collaboration with Utah State University (USU). The CHF experiments were completed for a 0.039" channel flow gap and a 0.078" flow gap by Chris Wright of USU. The latter was prototypical of the ATR. The experimental apparatus with the 0.079" flow gap was completely prototypical of ATR for plate size, channel gap and length. Prototypicality has not been preserved from past experiments.

The data indicate that a CHF limit was obtained that is larger by 70% over past experiments. The experiments were performed with both the side vents open and closed, the data being consistent for both conditions.

These results indicate that a significantly greater margin is available for CHF than was previously assumed (Fig. 1). A more representative local CHF correlation, based on the new data, would offer additional operating margins to ATR for those transients where CHF is of primary concern. In addition, the low-flow CHF data was taken under natural circulation conditions. Little to no data has been available for natural circulation CHF in narrow channel geometry. This data will prove valuable for developing additional correlations to be used in RELAP5 for predicting ATR behavior under accident conditions.

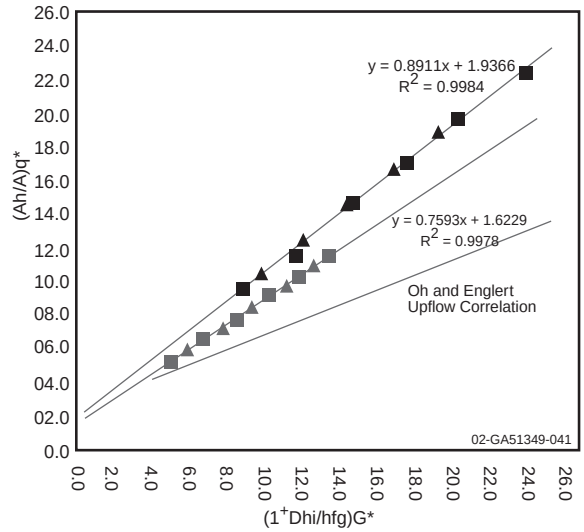


*FIGURE 1. CHF data plot and comparison.*

Richard Harrison (USU) performed single-phase plume analysis using a CFD code (Fluent) for a Complete Loss of Flow Transient in ATR. The results compare favorably and illustrate that Fluent is capable of 3-D detail for the ATR reactor vessel. Comparisons to earlier test data indicate stagnant regions and higher temperatures can develop within the vessel than predicted by RELAP (Fig. 2 next page). Fluent is not capable of representing two-phase flow and computing CHF. The results indicate a potential for future use of 3-D CFD codes to analyze events at ATR.

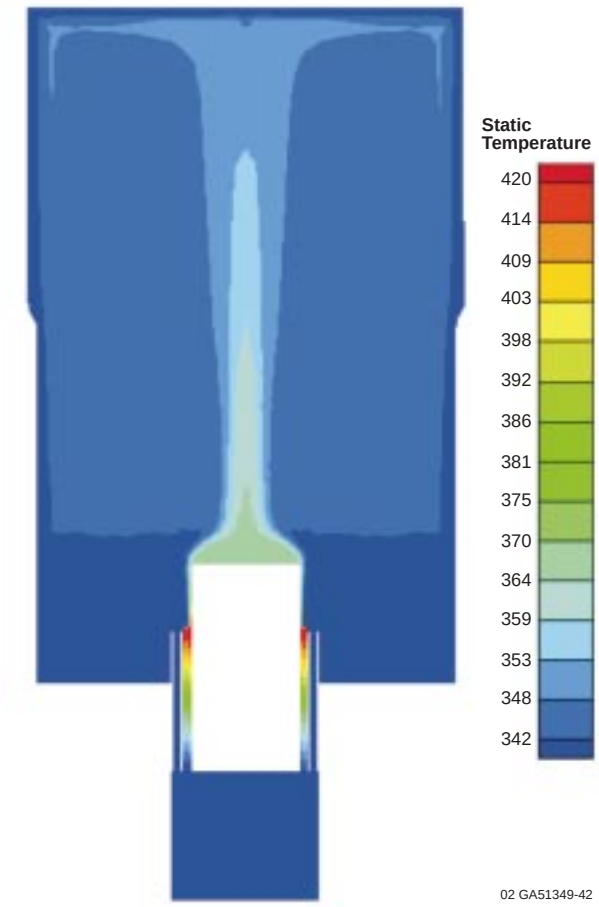


*FIGURE 2. Reactor temperature distribution.*

Planned activities include use of the data from the CHF experiments to develop a CHF correlation that can be implemented in RELAP5 or other thermal hydraulic codes. Papers on this research are being submitted to appropriate journals.

This work is increasing INEEL expertise in the area of experimental and computation fluid dynamics.

# High-Temperature Flow Measurement of Molten Salts

*James E. O'Brien*

## *Exploring non-intrusive flow measurement techniques*

NE110

Molten salts are currently under consideration as heat transfer and tritium-breeder fluids for use in high-temperature fission, fusion and solar-energy applications. Molten salts also have been proposed for use in advanced naval propulsion concepts.

The objective of this LDRD is to explore and test non-intrusive methods of flow-rate measurement that will be applicable to high-temperature molten-salt flows. During FY02, a full range of molten salt flow testing was completed at the INEEL May St. North laboratory (MSN). The assembly and instrumentation of a high-temperature molten salt transfer system also was completed at the Test Reactor Area (TRA) in collaboration with the INEEL Fusion Safety Program. Design of this salt transfer system is based on the MSN molten salt flow system.

The molten-salt flow system developed under this LDRD provides a pressure-driven flow of molten salt from a heated primary test cell to a secondary test cell and back to the primary test cell via a heat-traced fluid transfer line. The molten-salt flowmeter was located on this fluid transfer line. Flow was initiated by introducting an inert carrier gas flow to the test vessel from a compressed gas cylinder. The gas flow rate was set such that the rate of liquid displacement was sufficient to establish the liquid flow rate in the transfer line within the range of interest. Independent validation of the instantaneous molten salt volumetric flow rate was provided by simultaneous measurement of the carrier gas mass flow rate and pressure history.

Technical objectives for fiscal year 2002:

- Complete heat tracing of molten salt transfer line and flowmeter to allow for molten salt flow.
- Prepare test salt ("Heat Transfer Salt," HTS) in the eutectic composition, $NaNO_3$:$NaNO_2$:$KNO_3$, 7:40:53 for molten-salt flow testing. Verify melting point of 142° C.
- Perform a complete series of flow tests with HTS over a range of flow rates.
- Assist in development of a high-temperature molten-salt transfer system at TRA.

A schematic of the system developed for molten salt flow testing is shown in Figure 1a. along with a photograph of the actual apparatus (Figure 1b next page). The system was designed to provide a pressure-driven flow of

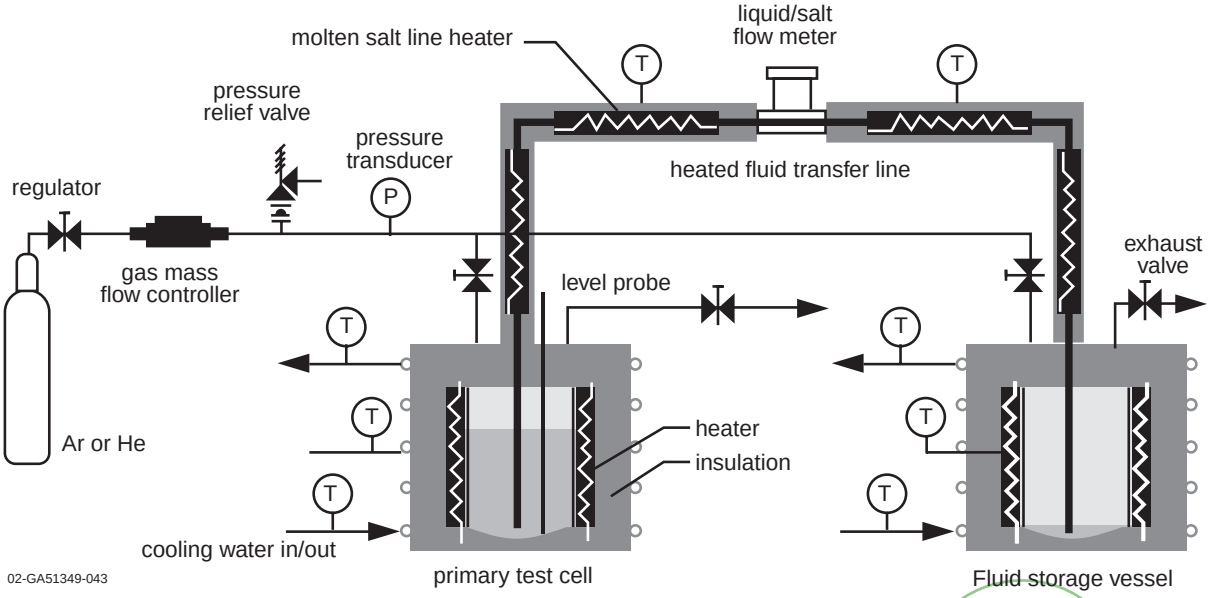


*FIGURE 1a. Molten-salt flow system.*

*FIGURE 1b. Photo of molten-salt flow system.*

molten salt from the primary test cell to the secondary test cell via a heat-traced fluid transfer line, with appropriate changes in the positions of the various valves. The system includes two water-cooled furnace assemblies, a heated fluid transfer line, molten salt flowmeter, inert gas supply, a gas mass-flow controller, and a pressure transducer on the gas supply line. Each furnace assembly houses a high-temperature ceramic-fiber heater and a stainless-steel test cylinder.

The molten salt was initially contained in the primary test cylinder in the solid phase (frozen). Prior to initiating a flow test, the test cylinders, the fluid transfer lines, and the flowmeter were heated to a temperature above the melting point of the salt (in the case of HTS, about 200° C). Flow of the test fluid through the fluid transfer line was initiated by introducing inert gas into the head space above the test fluid in the primary test cylinder at a fixed mass flow rate determined by the setting of the mass-flow controller.

Molten salt flow proceeds initially upward through the vertical portion of the fluid transfer line, then through the horizontal portion of the fluid transfer line, encountering the magnetic flowmeter at the midpoint of the horizontal line. The fluid transfer line from the top of the initial liquid level in the test cylinder to the magnetic flowmeter is initially void, resulting in a short time delay between the initiation of gas flow and the detection of salt flow by the magnetic flowmeter. During flow testing, instantaneous outputs from the liquid/salt flowmeter, the gas mass-flow controller, the pressure transducer, and the system thermocouples are recorded continuously during the flow tests at intervals of about 0.5 seconds. For this purpose, the system controller computer was interfaced to a precision modular data acquisition/instrument control chassis (National Instruments SCXI). The SCXI system was configured for the flow tests with two thermocouple/voltage analog input modules (SCXI 1102) and two analog output modules (SCXI 1124).

The flowmeter chosen for molten salt testing is a high-temperature commercial magnetic flowmeter (Yokogawa AdMag AE with ceramic liner). This flowmeter was installed on the system and initially tested with water flow. It is inherently sensitive to the average flow velocity of any electrically conductive liquid (i.e., it does not have to be highly conductive) passing through it. Accounting for the diameter of the meter flow passage, the instrument therefore provides a direct measure of volumetric flow rate. Taking the compressibility of the carrier gas into account, the actual volumetric flow of gas, Q (accm), can be determined from the measured (constant) gas mass flow from the following:

$$Q = \frac{P_{std}}{P_{act}} \frac{T_{act}}{T_{std}} Q_s - \frac{1}{P_{act}} \frac{dP_{act}}{dt} V$$

where $P_{std}$ and $T_{std}$ represent standard-state absolute pressure and temperature, $P_{act}$ and $T_{act}$ represent actual measured test pressure and temperature, $Q_s$ is the directly measured fixed mass flow rate (sccm), and V is the instantaneous system gas volume. The rate of change of system pressure, $dP_{act}/dt$, was determined numerically from the measured instantaneous system pressure. The instantaneous system gas volume, V, also was determined numerically as the sum of the known initial gas volume plus the calculated cumulative gas volume displacement.

Actual volumetric gas flow rates obtained from Eqn. (1) provide an independent measure of the liquid volume flow rate since the gas is used to displace the test liquid. Results from a representative flow test are presented in Figure 2 (next page). The upper plot in Figure 2 represents the pressure history during the flow test. The

rapid initial pressure rise is associated with the hydrostatic head required to drive the molten salt upward in the vertical portion of the fluid transfer line. The pressure reaches a peak and falls rapidly as the molten salt descends into the receiving vessel. The gas pressure then exhibits a slow linear rise associated with the hydrostatic head of the liquid in the receiving vessel.

In the lower plot, liquid volume flow rates measured directly by the magnetic flowmeter are compared to gas volume flow rates calculated from Eqn. (1). The two methods of flow rate measurement generally agree to within a few percent. The volumetric gas flow rate calculated from Eqn. (1) even captures the initial transient quite accurately.

This LDRD project was initiated in support of the Advanced Test Reactor (ATR) Applications Technology Program. It supports the Science and Technology Mission of the DOE to maintain leadership in science and technology. It also supports the DOE Fusion Energy program since molten salts are being seriously considered as heat transfer/tritium-fuel-breeding fluids for fusion reactors. Reliable non-intrusive techniques for flow-rate measurement of high-temperature molten-salt flows will be required over a wide range of flow rates and flow geometries.

In addition, this project has improved the INEEL knowledge base concerning the preparation, handling, and characterization of molten salt systems. Under the Fusion Safety Program, the INEEL has developed a unique collaboration with Japanese researchers (Jupiter II) to study the characteristics and handling of molten salts. Several Japanese researchers have visited the INEEL for extended time periods for this collaboration. The molten salt flow experiment resulting from this LDRD has been valuable in this context as well.

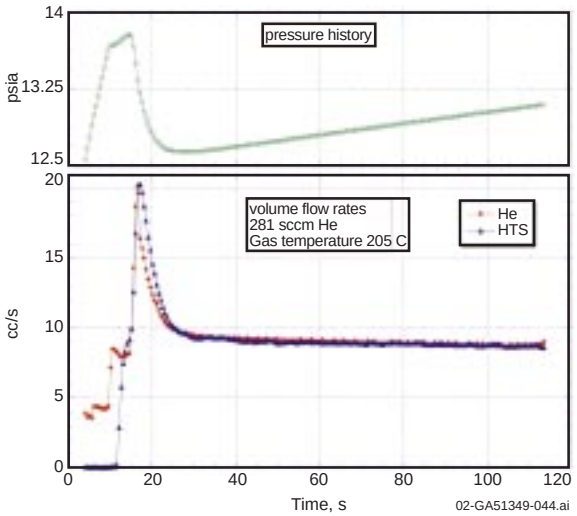


*FIGURE 2. Pressure history and volumetric flow rates of Helium carrier gas and HTS.*

# Energy Efficient Building Simulation and Technologies

*William D. Richins, Thomas K. Larson, Jeb E. Blakeley*

## *Integrating energy efficiency into the building envelope*

NE114

Conditioning air is the single largest energy cost in most buildings. This LDRD is investigating whole-building integration of energy efficiency and air infiltration in residential and DOE buildings. New technologies to detect infiltration, simulation tools, and bio-based products that improve the building envelope will be developed/investigated and tested using INEEL buildings as proof of principle. INEEL structures (Fig. 1) will be instrumented to measure continuous energy usage and air infiltration with respect to environmental conditions. Initial tests will include tracer gas monitoring, blower door fans, duct blaster leakage tests, infrared (IR) video scans, and smoke leakage testing.

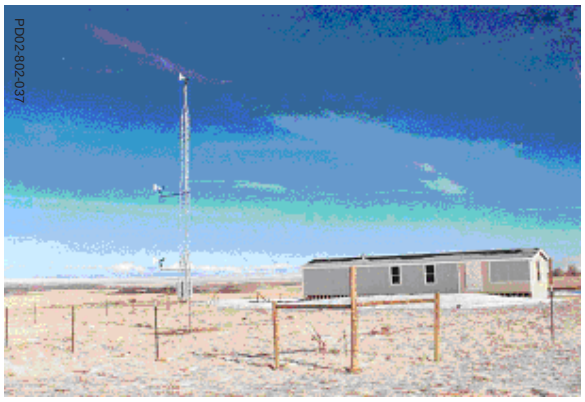


*FIGURE 1. Singlewide test home installation near Arlington, Wy.*

These data will be used to evaluate energy use, identify design and material improvements, support design and inspection guidelines, determine the effect of operable windows on infiltration, and provide data sets useful for energy analysis and air infiltration computer code verification. Data also will be collected to measure energy leaks across the mating lines of doublewide manufactured homes and to measure the effectiveness of new construction and insulation materials.

Technical objectives for fiscal year 2002:

- Investigate new air infiltration evaluation technologies.
- Develop INEEL expertise in monitoring building infiltration.
- Develop, verify, and/or improve simulation software for energy efficiency evaluation.
- Apply and test the above technologies on DOE facilities and residential housing.
- Evaluate renewable technologies and new bio-based insulating building products.

An infiltration sensor (the highest risk element of the LDRD) based on $CO_2$ concentration decay rates was developed in FY02 (Fig. 2). This procedure was automated and shown to be an effective method to measure air infiltration in windy climates. The control software developed for this system was completed and worked well. Tests showed that adequate mixing within the building is critical to achieve high quality and consistent results. An improved system with better mixing capabilities will be developed and installed in FY03. An Intellectual Property review is underway for Invention Disclosure Record "B-279 Automated tracer gas method to measure air infiltration" to investigate the potential of this prototype device.

*FIGURE 2. INEEL prototype device for air infiltratin measurement.*

To further develop expertise in monitoring building infiltration, INEEL engineers learned the procedure for and assisted in performing blower door tests. INEEL has purchased blower door testing equipment and will test the doublewide building using that equipment in FY03.

Improved simulation of energy efficiency variables in buildings will benefit the DOE buildings programs by providing a tool for optimizing energy conservation vs. investment. Progress includes an evaluation of simulation software currently available, and visits to two manufactured housing design offices to meet directly with the industry to assess needs.

A detailed model of the manufactured home's thermal characteristics has been built using DOE's EnergyPlus Version 1.0.2 software. Measured weather data and energy usage in the manufactured house was entered into EnergyPlus and its calculated temperature response was compared to measured temperatures. Calculated temperatures fluctuate over a wider range than measured temperatures and the cause is under investigation. The most likely causes are in the way the program uses the custom weather file or in the way the measured electricity and gas usage values are modeled.

*FIGURE 3. Interior of doublewide home showing instruentation and data acquisition system, September 2002.*

The extensive array of instrumentation (Figs. 3-4) for calculating thermal efficiency of the manufactured home performed well during the latter part of the winter season. Thermocouples were installed to measure vertical temperature profiles in three locations in the manufactured home: south bedroom, central room, and north bedroom. At each location, the temperatures were measured in the crawl space, belly pan, air near the floor, center of the room, near the ceiling, and in the attic. Additional temperature measurements were located at the furnace thermostat, return air plenum, the heater vent closest to the furnace, the heater vent furthest from the furnace, combustion air inlet, and flue gas exit. Electrical power consumption and propane flow completed the measurements required for monitoring thermal efficiency.

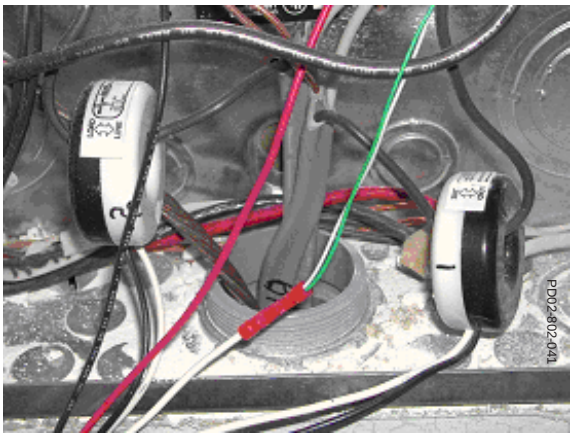


*FIGURE 4. Instrumentation for monitoring electrical usage on double-wide home.*

Three anemometers and air temperature and relative humidity measurement systems have been installed on a weather tower upwind of the manufactured home to gather local weather data. Solar insulation (Fig. 5 next page) was measured so the effects of clouds could be accurately accounted for in the energy balance. Operating furnace efficiency will be calculated also, to ensure an accurate energy balance is achieved.

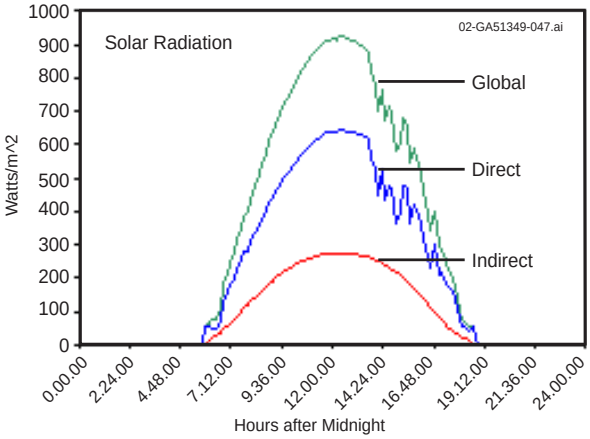


*FIGURE 5. Solar radiation, March 31, 2002, Arlington, WY test site.*

Validation of infiltration and energy efficiency measurement and modeling technologies on INEEL buildings will benefit INEEL by identifying energy-savings opportunities. Progress on this objective will begin in FY03.

Evaluation of renewable technologies was an objective scheduled for year three of the LDRD project. However, one of the industry contacts, Global Ecology Corporation, responded so enthusiastically, the investigators chose to proceed with evaluation of a bio-based insulating building material. Progress includes investigation of compression-formed masonry developed by this company. Unfortunately, the results did not indicate that the product had exceptional thermal characteristics. However, the material uses various types of industry waste products such as paper and coal combustion by-products that make it attractive as a recycled material. In addition to the bio-based material investigation, an instrumentation package was designed to assess the performance of the passive solar wall of the INEEL records storage building.

In Sept. 2002, the investigators met with researchers/builders in Alaska to discuss a joint proposal to improve the energy efficiency and indoor air quality of housing in the remote areas. The Afognak Native Corporation is working to provide good housing to these areas through their LLC, the Alaskan Manufacturing Contractors. Alaskan Manufacturing Contractors recruits residents of the remote communities to work in a plant near Anchorage to construct homes designed for shipping by barge. A white paper, "Affordable Quality Housing for Remote Alaska," will be presented to DOE in FY03.

An Intellectual Property review is underway as a result of this LDRD, for Invention Disclosure Record "B-279 Automated tracer gas method to measure air infiltration" to investigate the potential of a device for monitoring air infiltration.

Improved air infiltration evaluation techniques would benefit the DOE buildings programs by providing better measurement and modeling of building airflow. INEEL operations also would benefit through development of a portable infiltration sensor that can indicate presence or absence of negative pressure in interior spaces.

# Friction Stir Welding of Lightweight Materials

*Herschel B. Smartt*

## *Enabling unique material combinations for lightweight vehicle fabrication*

NE111

Friction Stir Welding (FSW) is a relatively new welding process that joins metals by mechanically stirring them together at elevated temperatures, but without melting. This emerging solid-state process holds promise to dramatically increase the ability to weld difficult material combinations needed in "bi-material" structures for automotive and other applications.

The purpose of this LDRD is to investigate a computer-controlled friction-welding machine and develop advanced process control algorithms to support experimental studies of FSW process physics.

Technical objectives for fiscal year 2002:

- Develop fundamental understanding of FSW process and how its parameters can be optimized for economical and practical joining of aluminum/steel interfaces used in the fabrication of cars, light trucks, etc.
- Model the FSW process using advanced techniques to determine tool and material interactions.
- Characterize selected aluminum and steel materials using Gleeble thermal mechanical testing techniques to determine tool flow stresses and material work hardening parameters at various temperatures.
- Assemble an advanced FSW machine equipped with sensors to measure critical process parameters and advanced feedback control capabilities.

During FY01, aluminum alloys were successfully friction stir welded, and welding trials were made on steel and titanium. This work was conducted initially on a small knee mill and subsequently on a much larger Computer Numerical Control (CNC) bed mill. The trials on the larger bed mill incorporated a Kistler dynamometer, a device that provides real-time measurements of the principle forces and torque on the tool. Based on this effort, the decision was made to build a dedicated FSW machine with advanced sensing and control capabilities.

In early FY02, a medium-sized conventional bed mill was obtained. This unit was converted to computer control by installing appropriate stepping motors, ball screw drive, and computer hardware (Fig. 1). A dedicated LabView graphical user interface also was specifically developed for the unit.

*FIGURE 1. FSW machine performing weld during experimental study with Vanderbilt University.*

The major advantage of this approach was that it provided a means to incorporate real-time feedback control of the machine's functions that wasn't possible using the CNC mill. The Kistler dynamometer was integrated into the computer-controlled system, as well as a Flir infrared camera for real-time measurement of tool and work-piece temperatures.

The process has been modeled using a finite element code to look at tool/work-piece interactions. The investigators were able to build-in friction heating, and have explored dynamic remeshing to handle the very large plastic strains that occur in the FSW process. Meshless methods of modeling the process also were investigated.

The solid mechanics finite element approach to modeling friction stir welding that began last year continued this fiscal year. The process was still modeled in 2-D, prohibiting the consideration of translation along the weld seam, and consequently considering only the penetration stage. In addition to vertical tool motion, "virtual spinning" of the tool is simulated by applying a radial velocity to the tool elements. Friction heating is dependent on the coefficient of friction for tool/plate contact, as well as the pressure and radial velocity. Substantial heating was generated in the vicinity of the

corner of the tool, so temperature-dependent plasticity was considered for the tool steel as well as the aluminum plate. Convection, radiation, thermal expansion and creep were not considered.

As the simulation progressed, and the tool penetrated into the aluminum plate, the plate elements near the tool became extremely distorted (Fig. 2). Both to improve accuracy and permit the simulation to continue, remeshing at intermediate stages throughout the process was required. To accomplish this, the initial mesh information generated by the I-DEAS software had to be translated to ABAQUS, and the deformed shape at the point where elements become too distorted needed to be translated back to I-DEAS.

The deformed shape was remeshed. The stress/strain and temperature data from that deformation stage were mapped onto the new mesh, and the simulation was run until the new mesh became unacceptably distorted. This year, the remeshing process was demonstrated for the friction stir weld simulation described above.

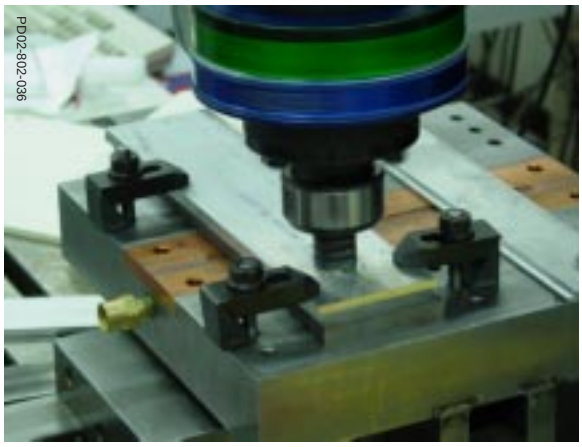


*FIGURE 2. Friction stir welding of aluminum alloy test piece.*

The major defect that occurs in FSW is formation of a continuous tunnel ("worm-hole") in the joint root, parallel to the welding direction. There is generally no visible surface indication of this type of defect. The investigators conducted an extensive experimental study of FSW with Professor George Cook of Vanderbilt University. In this study, the investigators mapped the forces, torque, and power required to perform the process as a function of both welding speed and tool rotation speed. The various welds also were examined ultrasonically to identify indications of internal discontinuities. In this study, a new flaw type was found that occurred at high welding speeds and low tool rotation speeds, resulting in extensive tearing of the fusion zone. Initial tests have been conducted for controlling the major forces during welding.

This LDRD research is providing a basis for future development and improvement of a joining process for use in critical "bi-material" structures by U.S. industry, and the DOE complex.

To explore additional opportunities and leverage the work of others in this area, the investigators joined the Friction Stir Processing Industry / University Cooperative Research Center, a consortium of the South Dakota School of Mines and Technology, University of South Carolina, Brigham Young University, and the University of Missouri, Rolla. These relationships will be explored in the future for research partnerships and joint responses to calls for proposals from DOE-office of International Trade and other government agencies.

The researchers have written a white paper describing application of this experimental capability to research on fundamental materials behavior during very high strain and strain rate plastic deformation. That paper has been submitted to DOE-Basic Energy Science for review.

# Genetic Control of Straw Stem Ultrastructure that Affects the Biomechanics of Stem Separation

*Eric D. Steffler, J. Richard Hess, Thomas H. Ulrich*

## *A genetic approach to bioproducts processing*

CE108

As our nation presses forward with bioenergy as part of its national energy strategy, cellulosic crops, not starch, will become the feedstock of choice for biomass-derived fuels and chemicals. A key, limiting factor for cellulosic feedstock utilization is the lack of equipment and methods to harvest, store, and fractionate biomass for subsequent conversion processes.

Harvesting improvements can directly address economic and environmental issues for bioproducts processing of higher value cellulosic stem while leaving behind the remaining residue to supply soil organic matter and maintain soil nutrient levels.

This LDRD is researching practical testing tools and identifying ultrastructural phenotypic and molecular markers that will be useful for selecting genotypes with improved stem component separation. The hypothesis behind this effort is that the biomechanical properties that differentiate the stem tissues of different genotypes result from functional gene expression that can be identified, characterized and used to build selection tools for breeding new varieties with improved stem separation characteristics. These new cereal genotypes would be bred to withstand field stresses, but succumb to harvesting stresses.

Technical objectives for fiscal year 2002:

- Design test equipment and quantify biomechanical differences across a significant range of wheat genotypes.
- Compare and analyze associated differences in ultrastructures at the tissue, cellular, and molecular level.
- Identify genetic information involved in developmental processes responsible for these differences.

The purpose of mechanical tests is to obtain biomechanical properties of various wheat straw varieties in both nodal and internodal regions. These data are obtained by establishing repeatable specimen preparation and test methods for specific experimental configurations.

Currently established techniques use tension and four-point bend experimental arrangements. The acquired data from mechanical testing identifies the failure points and stresses that different straw segments can withstand. These results will be used to classify the different varieties in terms of mechanical properties.

A significant portion of first year resources has been used to establish systematic processes for testing. Whole, unaltered straw stem testing in tension proved exceptionally difficult. The straw types investigated have a waxy protective surface that presented unique fixture attachment difficulties. Further experiments concluded the waxy coat prohibits straightforward bonding without elaborate surface preparation. This method resulted in various stem segment failures deemed unacceptable, and led to alternative tension test protocols.

Cross-section alteration was chosen as a secondary option for tensile testing. This was accomplished using a high-speed rotary tool to cut a smooth half circle notch out of the straw stalk. This preparation gave repeatable cross-sectional area reduction, yielding localized stress increases. While this technique requires additional care in measuring the actual cross-sectional area after failure, all failures occurred in predictable regions. This technique is successfully being used for mechanical strength approximations.

The best method for uniform stress application to cause failure involves the use of a traditional 4-pt bend fixture configuration. A small, bench scale load frame and fixture were purchased that are capable of very small load measurements (Fig. 1 next page). A modified fixture was designed and fabricated that uses generic material in 4-pt bend tension that resolves the problem of contact compression collapse. This unique fixture design is a novel approach to test hollow geometries and is a breakthrough advance in biomechanical testing.

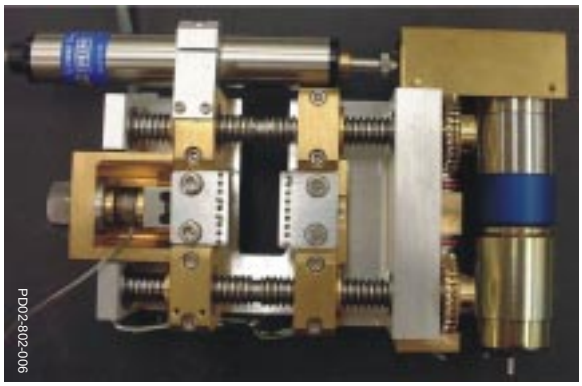


*FIGURE 1. Small load frame with fixture and transducers.*

Two primary goals were associated with the task of developing microscopy for ultrastructure analysis. The first goal was to demonstrate the ability to capture the mechanical breaking of stems during the application of stress. The second goal was to determine if high-magnification microscopy could be used to identify tissue components and the breaking lines, or points, associated with stem failure.

The capability of viewing an area suitable for capturing the breaking process was established, using a stereo-zoom microscope (Table 1).

| | x-axis | y-axis | Area | Clearance |
|---|---|---|---|---|
| Low Zoom | 13.3 mm | 18.0 mm | 240 $mm^2$ | 16 cm |
| Medium Zoom | 6.5 mm | 8.5 mm | 55 $mm^2$ | 11 cm |
| High Zoom | 2.0 mm | 2.62 mm | 5.25 $mm^2$ | 8 cm |

02-51349-010

*TABLE 1. Stereo-zoom setup of DAGE DC-330 camera captured and recorded simulated stem breaking.*

A DAGE DC-330 camera was used to capture and record simulated stem breaking via the stereo-zoom setup. By recording at video rates (60 frames/sec), individual frames could be captured and analyzed. Camera speeds and working distances can be varied to meet the spatial requirements of the load frame and associated fixtures.

Numerous specimens were surveyed and the basic tissue types in the stems were successfully imaged and identified. Untreated natural materials were examined using varying types of microscopic illumination (e.g., phase, differential interference contrast, dark field, or epi-fluorescence). Several staining procedures also were developed and tested to aid in the discrimination of tissue types.

The natural fluorescence in the Spurr's mounting media preparations provided a unique capability for identifying cellular spacing in microtome slices. This will be particularly useful in the stacking of essentially 2-D images into a 3-D volumetric reconstruction of the stem. An example of this optical capability is shown in Figure 2.

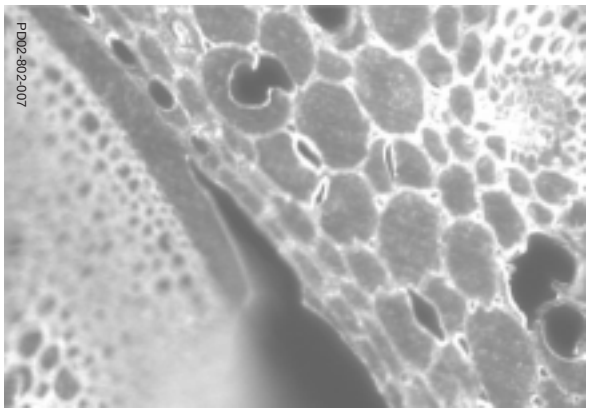


*FIGURE 2. Spurr's mounting media section, epi-fluorescence.*

Several image analysis packages were evaluated using the prepared materials under the microscope and are being adapted for this project. The examination of samples from the mechanical break tests will assess spatial differences among the various experimental preparations and stem regions that exhibit damage.

The expression of genes during development results in observed physical properties of the senesced stem. Bioinformatics is being used to help identify the types of genes influencing the desired development that leads to

mature stems with biomechanical characteristics important to the physical separation of stem components. These genes are the ones differentially expressed and associated with relevant changes occurring in different regions of the stem.

Although the biomechanical tests will be done on senesced tissues and the gene expression on green developing tissues, it is the expression of genes during earlier stages of development that ultimately contributes to the physical characteristics (e.g., strength or weakness) of the senesced stem. The goal is to understand stem growth and development as it relates to stem failure, ultimately manifested in the senesced straw. The intent is to identify useful genes that can be used as molecular markers in stem separation improvement programs.

Appropriate plant stem material for the project's biomechanical, ultrastructural, and gene expression tasks were identified. These materials were acquired by working closely with University of Idaho cereal field trial specialist Dr. Larry Robertson and National Small Grains Germplasm Research specialist Dr. An Hang. Multiple sites spanning the Snake River Valley were used to provide a range of wheat varieties. The biomass straw collection acquired in this single study is likely the largest sample set in the world. These samples will allow the investigators to test the hypothesis that the biomechanical properties of stems differ genetically among varieties, and these differences result from different genes and their expression.

Harvested and catalogued straw samples of wheat and barley collected during the summer of 2002 are a unique and valuable resource. These samples are ready for biomechanical testing for variation among varieties and are currently being stored. Insight into biomechanical variation among plant stems will help the investigators focus on the best varieties to study at the molecular level of gene expression and regulation. Fragile mutant genotypes with altered stem properties were identified. This information will be used to produce the plant materials needed to set up and prepare sequences for microarray analyses. The tasks are to develop microarray phenotyping tools and to develop and screen stem cDNA libraries.

Today as much as 30% of the cost to produce fuels and chemicals from biomass are attributed to the harvesting, handling, and transportation of the feedstock to the biorefinery. This project addresses the biological issues associated with biomass harvesting, and has contributed to the establishment of partnerships for biorefining with Cargill Dow, Iogen-Shell, University of Idaho and others. This project also has contributed to an intellectual property position regarding multi-component harvesting.

# Laser Ultrasonic Characterization of Irradiated Ceramics

*Ken Telschow, Rob Schley, John Walter, Dave Cottle*

## *Detecting key microstructural properties with lasers*

D437

The Advanced Test Reactor (ATR) at the INEEL is a unique facility in the country that allows testing of materials under high-neutron and gamma radiation flux conditions. Specimens to be tested are contained in inert gas-filled capsules inserted into the reactor. Currently, sample capsules are irradiated for a set time, removed and then measured externally in a "hot-cell" environment. This procedure is time consuming and complicated to perform safely. Research is needed to develop inspection techniques that can detect physical, microstructural and quality properties of the samples in situ, preferably in real time. Inspection must be performed in a shielded-cell environment; therefore, noncontacting and remote capabilities are essential attributes of any new inspection technology.

This LDRD investigates a new inspection technique using laser ultrasonics to detect and characterize key microstructural properties. Laser ultrasonics requires only optical access to the material surface and uses lasers for both generation and detection of ultrasonic waves. It offers a noncontacting approach to ultrasonics whenever optical access is available and has been proven in many processing environments where contacting the material surface was not possible or desired.

This research has successfully produced a complete sample positioning and laser light pipe apparatus to make laser ultrasonic measurements in a high-gamma radiation environment at the Advanced Test Reactor (ATR). Totally noncontacting remote measurements were completed using this light pipe apparatus. The success of this project has added considerable diagnostic capability to the ATR, further enhancing the unique capabilities of this important INEEL materials research facility for the country.

Technical objectives for fiscal year 2002:

- Integrate operation in a high-radiation environment with ATR personnel and establish experimental protocol.
- Update software for Resonant Ultrasound Spectroscopy (RUS) measurements and integrate with in situ measurements.
- Design optical apparatus for remote operation.
- Assess laser ultrasound measurements for flaw characterization capability.
- Validate laser ultrasonic operation and analysis software.
- Perform proof-of-principle measurements under remote operating conditions.
- Install the apparatus in the ATR gamma tube and perform high radiation measurements. (Note: An interruption in program funding caused a three-month delay. As a result, this last task was not completed in FY02 and has been rescheduled for early FY03.)

Both a mechanical light pipe tube/sample positioner and the laser generation and detection apparatus were designed and constructed for the gamma tube experiment. The plan consisted of placing a minimum of objects into the high-gamma-field environment by including only metallic mirrors and the sample with metallic positioning fixtures. Laser beams for both generation and detection of ultrasonic waves in the sample were directed into a light pipe tube from the top and traveled in a free-space manner to the bottom, ~ 20-30 feet from the laser equipment. A small curved mirror directed the source laser beam onto the sample surface. A second parabolic mirror focused the detection laser beam onto the sample (located near the bottom of the tube) and collected the scattered light. Full positioning control of the sample and all mirror orientations was designed into the top of the light pipe tube.

An interferometric detection scheme that could be used in an industrial setting was constructed using a high-speed photorefractive system to demodulate the reflected light, thereby measuring the ultrasonic displacement motion directly on the sample surface. This form of interferometer system automatically adjusts for environmental vibrations, can form interference with diffuse or multiple speckle reflection from the rough sample surface, and requires no stabilization feedback system. Provisions were made for both source and detection with contact piezoelectric transducers as well as the lasers for a redundancy on the measurement setup.

Figure 1 (next page) shows the basic setup of the light pipe tube in the gamma tube facility at ATR along with a picture of the light pipe tube fully assembled in the

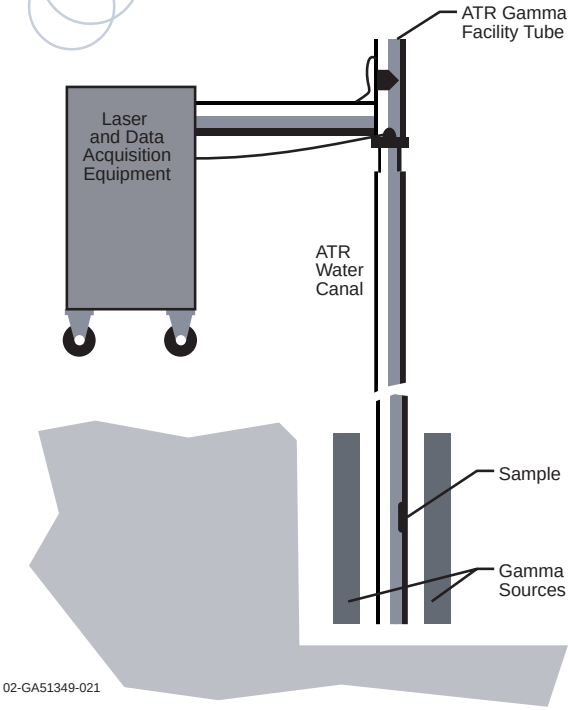

Assembled tube in full-scale laboratory test

*FIGURE 1. Schematic of the ATR gamma tube in the water canal, the laser equipment table and the light pipe/sample positioner tube for the laser resonant ultrasound measurements.*

laboratory. The complete apparatus has been set up at the IRC laboratory. Full-scale testing with both lasers was successfully performed yielding signal-to-noise ratios adequate for the measurements planned.

Several approaches were explored for laser-based generation and detection of bulk and surface elastic wave modes in ceramic/metal cylindrical and spherical specimens with and without coatings. All have proven to be successful and yield complementary information. The investigators chose to develop a laser-based form of Resonant Ultrasound Spectroscopy (RUS). Contact RUS is well established as a viable tool for materials analysis. The INEEL is implementing this technology in a totally noncontacting mode using laser ultrasonics.

This approach is very promising as it offers a means of measuring sample microstructural features and dimensional properties from the resonant vibrational mode spectrum recorded in situ to the irradiation environment. In addition, there is no need for high-precision locating and focusing of the source and detection laser beams as vibrational mode excitation and detection can be made easily at most points on the sample surface.

Excitation and detection experiments were successful in the laboratory with a standoff distance of 20-30 feet for partially diffuse reflecting objects. Laser Based Resonant Ultrasound Spectroscopy (LBRUS) spectra agreed well with the results from contact transducer measurements. The laser ultrasonic apparatus has been reconfigured in a rugged portable design using a small table with wheels. All the recording electronic equipment was installed in one rack allowing for a very compact, minimum-part-count remote apparatus.

Figure 2 (next page) shows results from a low-frequency flexural mode recorded during the full-scale laser measurement of a vibrating cylindrical sample in the light pipe tube. Recorded signal-to-noise ratios of

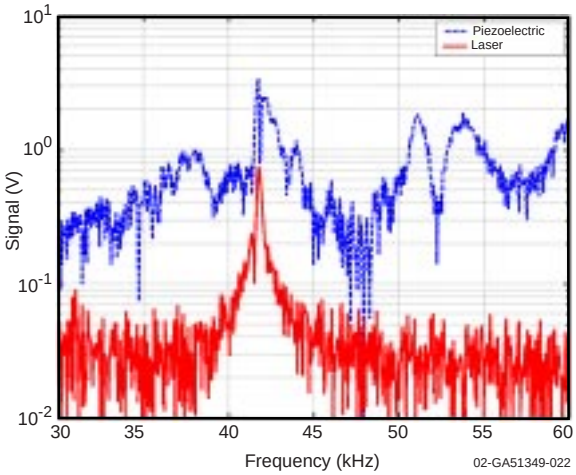


*FIGURE 2. Resonant modes of a cylindrical metallic sample recorded by both systems. Some modes were selectively excited and detected with one transducer but not the other. The laser system primarily observes flexural out-of-plane motions whereas the contact piezoelectric is very sensitive to in-plane torsional motion as well.*

better than 100 were obtained with source-pulse energy of only a couple of millijoules. Physical and mechanical properties of the sample were obtained by modeling the vibration modes recorded and varying the material properties to obtain the best fit with the experiment. This has been successfully completed for hollow cylindrical samples with and without end caps.

This work was performed to provide new diagnostic technology for inspection in high nuclear radiation environments. The results to date show that noncontact laser ultrasonic methods are promising for measurement of material properties in situ.

# Laser Ultrasonic Corrosion Monitor

*Ken Telschow, Dave Hurley*

## *Predicting corrosion in nuclear reactors*

NE118

The absence of real-time in-pile kinetic data continues to hinder the development of an accurate mechanistic model for predicting Zircaloy corrosion in nuclear reactors. A high-resolution in situ ultrasonic monitor is needed that exploits the dependence of ultrasonic propagation properties to determine Zircaloy oxide film properties.

Laser ultrasonics is a totally noncontacting approach for performing ultrasonic measurements that can resolve features such as film or coating thickness and requires only optical access to the material surface. This LDRD is researching the means for implementing these measurements first in the laboratory, then in "hot cells" and potentially in the radiation environment of the Advanced Test Reactor (ATR). This capability would add real-time in situ diagnostic capability to ATR, and significantly enhance the unique capabilities of this important INEEL materials research facility for the nation.

Several properties of the oxide film need to be measured, including film thickness, elastic constants and the presence of voids or cracks. Ultrasonics presents many different possibilities as there are many wave modes (longitudinal, shear, surface, plate, interface) that can be exploited to gain information about the corrosion film. This project investigated several methods of performing ultrasonic measurements on Zircaloy materials with laboratory techniques and will ultimately test an in situ probe.

Technical objectives for fiscal year 2002:

- Analytically model various elastic wave modes in films on Zircaloy to determine detectability.
  - — Determine the laser ultrasonic measurement precision and accuracy, and validate modeling on test samples
- Measure the properties of Zircaloy corrosion films prepared by industrial collaborators.
- Establish experimental protocol for simulated growth kinetic measurements using a laser resonant ultrasonic (RUS) approach.
- Explore laser-based RUS for interrogating sample stacks in configurations suitable for irradiation

This LDRD was interrupted during the fiscal year due to a funding shortfall. As a result of the three-month delay, work was completed only on the first two technical objectives.

Several techniques were investigated for developing in situ probes of oxidation coating thickness and microstructural properties using nanosecond laser ultrasonics for thick films (>1μm) and picosecond acoustics for thin films (<1μm). A set of samples with coatings ranging from less than 1 micron to about 30 microns was received from an industrial collaborator that formed the basis for the measurements.

The first approach investigated was the measurement of surface wave dispersion due to acoustic waveguiding. The wave speed increases with frequency for a $ZrO_2$ film on a Zr substrate forcing the higher frequency components of the wave to travel faster than the lower frequency components. An initially sharp pulse will disperse into a wide pulse, spreading its frequency components out as it travels. The shape of the dispersed acoustic pulse is a function of only the elastic constants of the material system and the film thickness.

A comparison was performed between experimental and predicted waveforms using known elastic constants for the substrate and coating. The comparison involved performing a cross-correlation between the predicted waveform and the experimental data using the film thickness as a parameter. A total of six samples were measured using this acoustic correlation method [thicknesses of 0.8, 2.3, 4.3, 7.4, 25.4 and 35.6μm (from weight gain measurements)]. The predicted film thickness for which the simulated and experimental data were most similar was 4.0μm for #3 (4.3μm), 5.8μm for #4 (7.4μm), 29.1μm for #5 (25.4μm); data on the other samples did not allow an unambiguous comparison.

The graphs in Figure 1 (next Page) compare the correlation of the simulated signal using the predicted

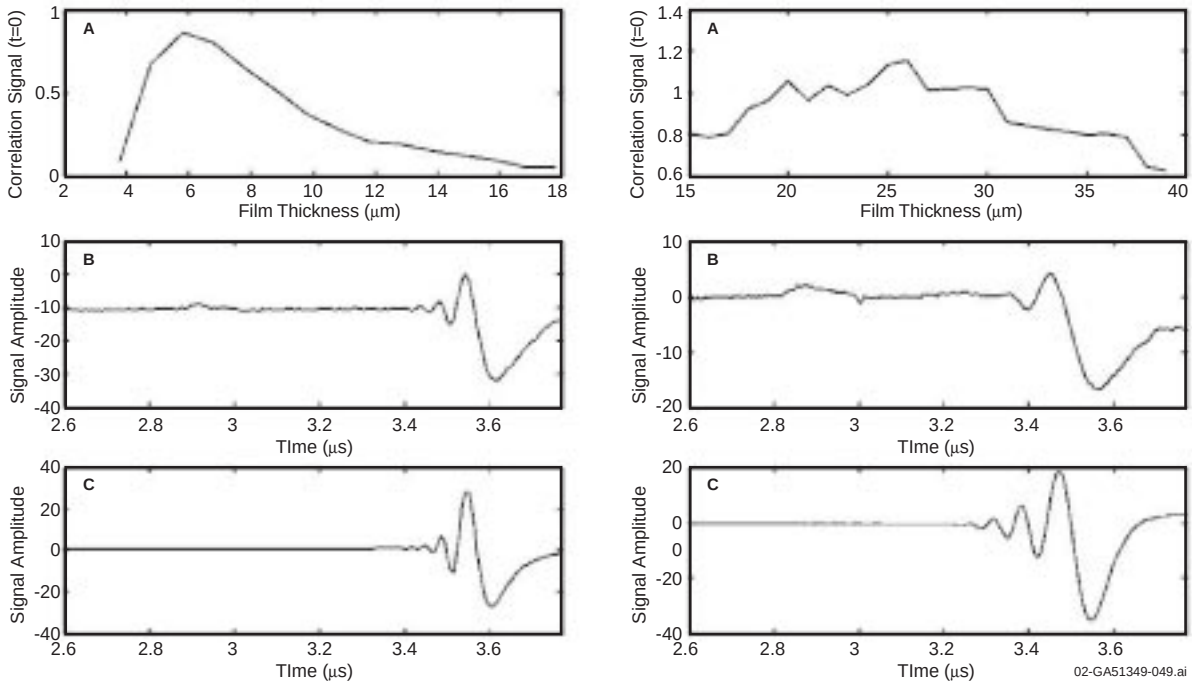


*FIGURE 1. Comparison of the correlation (top graphs), measured waveform (middle graphs) and predicted waveform (bottom graphs) for (left) sample #3 (4.3μm) and (right) sample #5 (24.8μm).*

value of the film thickness to the experimental data for a thin film, #3 (left), and a thick film, #5 (right). In contrast to sample #3, the acoustic correlation signal exhibited a broad peak for #5, complicating the film thickness determination. The lower frequency components of the waveforms appear to be in close agreement. However the higher frequency components, present in the simulated signal, are not present in the experimental data. Large attenuation of the high frequency acoustic wave components caused by the heterogeneity of coating properties present in the thicker samples may account for the discrepancy.

From the picosecond measurements, the films appear to be heterogeneous and nonuniform in thickness and microstructural features or flaws. The oxide coating appeared to be semitransparent resulting in significant penetration of the pump and probe beams to show a variety of generation and detection mechanisms at work. Two thin film (~220nm) artificially coated samples were obtained from opticoat Inc. with optical-quality $ZrO_2$ films deposited on Si and Al substrates. These high quality samples were examined to serve as a baseline for understanding measurements performed on $ZrO_2$/Zr film/substrate samples. The baseline results showed very reproducible results with predictable optical responses and, in the case of the Al sample, generation of high frequency longitudinal waves from the surface that reverberated within the film. Time-of-flight measurements of these echoes agreed well with those measurements predicted for the known film thickness.

In sharp contrast to the artificially coated samples, results for the corrosion samples varied markedly with

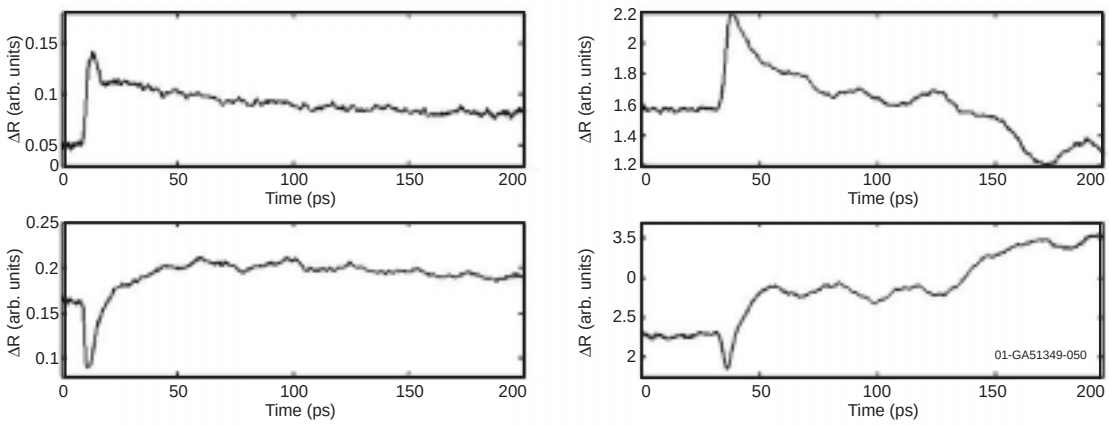


*FIGURE 2. Picosecond acoustic waveforms for two different locations on the sample surface for (left) the thick sample #5 and (right) the thin sample #1.*

location along the surface. Figure 2 shows results from two different locations on sample #5 (left) and #1 (right). For the thick-film sample, the signal is not complicated by the presence of acoustic echoes since the sound transit time across the thickness of the film is much larger than the time of observation. The change in signal polarity as a function position indicates that the thermooptic constants are spatially inhomogeneous.

In contrast to the thicker film, the results for the thin film revealed the presence of acoustic waves. For the thin-film data, two mechanisms for acoustic wave detection may be present, which complicates the film thickness determination directly from the data. One interpretation consistent with these waveforms results in a film thickness estimate of between 630-730nm. Work is ongoing to fully explain these results. Variation in film thickness caused by heterogeneity and surface roughness is one possible explanation for these observations.

This work was performed to provide new diagnostic technology for inspection in high nuclear radiation environments. The results to date show that noncontact laser ultrasonic methods are promising for investigation of corrosion processes in situ. Further work shall delineate capability for in situ measurements and demonstrate real-time measurements during the corrosion process. Strong collaboration has been developed between researchers at the INEEL and customers of the ATR.

# Removal of Minerals from Wheat Straw for Increased Straw Utilization for Bioenergy and Bioproducts

*David N. Thompson, Francisco F. Roberto*

## *Turning straw into a renewable resource*

CE101

Agricultural crop residues are a valuable renewable resource for producing bio-based products. In 1999, American farmers harvested 53,909,000 acres of wheat. The straw from this acreage represents over 100 million tons annually. Currently, some of the straw is harvested (baled) for use as livestock bedding or low-grade animal feed. These low-value uses provide only a minimal return. Nationally, only about 3.2% of the economic return on wheat is from straw.

Producers have long recognized the potential economic and environmental benefits in producing bioenergy and bioproducts from excess wheat straw residue. However, the silica and alkali metals in wheat straw limit its use for bioenergy and gasification. This LDRD explores the feasibility of removing or degrading these minerals from straw residue to create a next-generation bioproduct that offers a renewable energy resource.

Slag deposits occur via the eutectic melting of $SiO_2$ with $K_2O$, trapping chlorides at surfaces and causing corrosion. A minimum melting point of 950° C is desirable, corresponding to a $SiO_2$:$K_2O$ weight ratio of about 3:1. In this year's research, mild chemical treatments were used to reduce Si, K, Cl, and hemicellulose, while varying temperature, concentration, %-solids, and time. Dilute acid was effective at removing K, Cl, and hemicellulose, while dilute alkali was more effective for Si. Treatment of straw in this manner may prove economical for increasing use of the straw for combustion or gasification.

Technical objectives for fiscal year 2002:

- Use dilute chemical washes to demonstrate removal of potassium, chlorine, and /or silica to levels acceptable for combustion in boilers.
- Prove the principle of removing straw cuticle using cutinase or lipase enzymes.
- Prove the principle of degrading polyphenols in the epidermal cell wall using peroxidase enzymes.
- Devise an integrated process for debarking of straw.

The first year of this project, as well as the first three-quarters of the second year, focused on wash methods for removing silica and alkali minerals from wheat straw stems. The organic and ash compositions of the untreated baled straw and untreated mechanically separated straw stem fraction are shown in Table 1. Mechanical separation reduced the total ash and $SiO_2$ concentrations of the harvested fraction by 23% and 44%, respectively, thereby reducing overall slagging potential. However, mechanical separation concentrated the alkali metals relative to $SiO_2$, reducing the $SiO_2/K_2O$ and $SiO_2$/KCl ratios. Although reduction of total $SiO_2$ is important for overall reduction of potential slag formation, removal of $SiO_2$ without at least proportional removal of K is detrimental since it decreases the $SiO_2/K_2O$ ratio.

| Component | Wt% of Component[a] in Westbred 936 whole straw | Wt% of Component[a] in Westbred 936 stem fraction |
|---|---|---|
| Glucan | 32.1 | 37.2 |
| Xylan | 19.3 | 19.4 |
| Galactan | 1.0 | 0.9 |
| Mannan | 4.5 | 3.0 |
| Arabinan | 2.1 | 1.6 |
| Lignin with Extractives | 20.3 | 18.9 |
| Other Organics[c] | 9.5 | 10.3 |
| Ash[b] wt% | 11.2 | 8.7 |
| $SiO_2$ | 2.6 | 1.3 |
| $K_2O$[d] | 1.7 | 1.2 |
| KCl[d] | 5.2 | 5.2 |
| Other Minerals | 1.6 | 0.9 |
| SUM | 100 | 100 |

02-51349-006

a. Based on 100% dry weight of material

b. Oxide contents estimated by mass balance from elemental composition as determined by Energy Dispersive Spectrometry

c. Other organics are attributed to uronic acid, protein, etc. contents and to recovery errors in carbohydrate analysis technique

d. Potassium assumed to first combine with available chlorine, and then apportioned as oxide

*TABLE 1. Composition of whole Westbred 936 straw and the mechanically separated straw stem fraction.*

Washing straw with aqueous liquids removed both organic and mineral matter. Most of the removal occurred in the first 4 h. The ratios of organic to inorganic losses were similar with water, dilute $H_2SO_4$, and

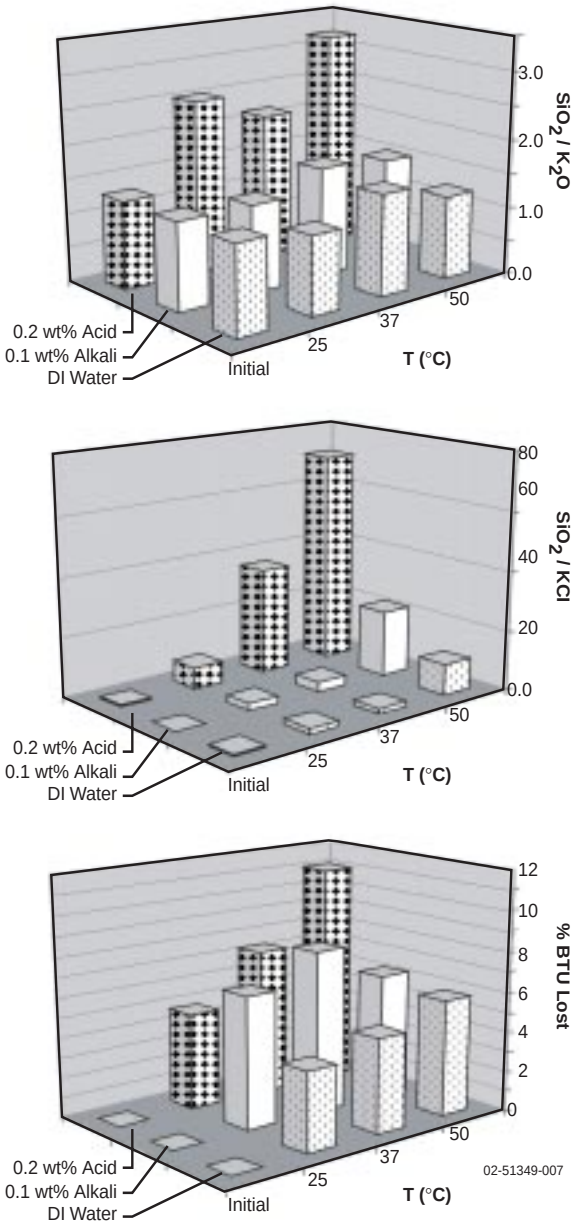


*FIGURE 1. From left to right, the effect of washes on silica to potassium oxide ratios, silica to potassium chloride ratios, and on BTU losses for selected samples.*

dilute NaOH, with similar selectivities for organics versus minerals. The minerals appeared to be released along with organic material, such that very short or very long washes released approximately the same ratio of organic and inorganic components of the straw. General comparisons of the effects of these washes on $SiO_2/K_2O$, $SiO_2$/KCl, and the loss of heating value, at 25, 37, and 50° C are shown in Figure 1. Acid washing dissolved most of the potassium, and gave the highest $SiO_2/K_2O$ ratios. Some acid washes removed sufficient potassium to raise the $SiO_2/K_2O$ ratio above the desired minimum ratio of 3.0. The highest removal of K and Cl in straw stems occurred with a 0.2 wt% acid wash at 50° C. This acid wash increased the $SiO_2/K_2O$ ratio from 0.9 to 3.2, and increased the $SiO_2$/KCl ratio, though other mass was lost. Thus, both water and acid removed some $Sio_2$ but its removal was offset by the removal of organic matter, and the concentration in the washed stems remained the same.

Alkaline washing dissolved up to 20% of the $SiO_2$ and slightly lowered the final $SiO_2$ concentration in the straw. However, the $SiO_2/K_2O$ ratio was lowered because a less-than-proportional amount of potassium was removed. To estimate the losses of heating value, all components of the organic matter were assumed to be of equal heating value per unit weight.

In general, higher wash temperatures resulted in greater loss of mass in acid washes, with smaller increases in the base and water washes. Increases in acid concentration increased the amount of mineral removed, but did so at the expense of BTU content since organic matter also was removed. About 80% of the mass removed in the acid washes was organic (not shown).

Thus, there are trade-offs between the cost of the lost heating value and the benefits of reducing minerals through use of the treatment. The trade-offs will depend on a number of factors, including the boiler/gasifier design, the operating conditions, the feedstock, and the cost of down-time required to remove slag from the heat transfer surfaces; these will vary significantly among power generation and gasification facilities.

The differences between mineral removal at 37° C and 50° C (not shown) were not as great at higher mass

loadings, since solubility limited the amount of material that could be dissolved, and offset the more aggressive solvent characteristics at the higher temperature. A continuous wash that lowers the effective "loading" even further would overcome the solubility limitations and likely result in higher mineral removal than experienced in these batch experiments.

Generally cellulose and hemicellulose concentrations were not significantly affected by dilute acid washes up to 0.4% acid. However, 1% acid caused significant loss of hemicellulose. A 5% acid wash completely converted both cellulose and hemicellulose to an acid insoluble fraction due to concentration of residual $H_2SO_4$ during the 105° C drying step. If the acid-insoluble organic matter was still combustible, the total BTU content may not be significantly affected. Hence, it is clear that acid concentrations of 1 wt% and higher should not be used if recovery of intact carbohydrates is desired.

This study indicates that in batch washing, acid is preferred as a wash solution for removal of alkali minerals from straw for use in fluidized bed combustors, gasifiers or boilers. Future work should include testing acid-washed whole straw and physically separated straw stems in a fluidized bed combustor and/or gasifier to determine the slagging properties of the washed straw.

In addition, the effect of adding CaO or MgO after washing to modify the eutectic composition and thereby further increase the ash fusion temperature should be investigated. Data from these tests, and estimation of eutectic compositions and ash fusion temperatures, will help in the application of these separations to fluidized bed combustion, gasification of biomass and combustion in boilers. The acid-washed straw also should be tested for ease of drying and densification as part of a distributed bioenergy system.

In the last quarter of FY02, acid treatment tests were conducted on physically separated wheat straw stems previously treated for 12 weeks with *Pleurotus Ostreatus*. This was done to investigate whether acid treatment severity could be reduced if the straw stems were treated in a distributed manner using a white rot fungus.

Fungal-treated stems available from another INEEL Bioenergy Initiative project were treated using similar acid treatments to those above, except at higher temperatures (90° C, 112° C, and 121° C). Pretreatments were performed at 5 wt% solids in 2 wt% $H_2SO_4$ for six hours at the three temperatures, in a shaker bath or in an autoclave depending on the treatment temperature. These pretreatments are by no means efficient acid pretreatments, since temperatures of 150° C -230° C are required, along with rapid decompression/cooling, for near-complete enzymatic conversion of the pretreated cellulose to glucose. Rather, the aim was to compare the relative efficiencies of glucose recovery from the initial straw stems (no fungal treatment).

The results are shown in Table 2 with the fungal inoculum sizes and moisture levels used in the fungal treatments.

In the fungal treatments, significant amounts of cellulose were consumed by the fungus and indigenous microbes (the initial straw was not sterilized before treatment to reduce the cost if in a distributed system).

| ***P. ostreatus* inoculum size (mg / g straw)** | **% moisture (g $H_2O$ / g straw)** | **% of Original Glucose Recovered** | | | |
|---|---|---|---|---|---|
| | | **No Acid Treatment** | **90°C** | **112°C** | **121°C** |
| 0 | - - - | 9.3 | 11.0 | 14.7 | 14.9 |
| 44.0 | 160 | 2.1 | 2.1 | 6.4 | 11.2 |
| 70.0 | 110 | 1.0 | 1.7 | 6.6 | 12.0 |
| 105 | 120 | 0.1 | 4.5 | 8.6 | 9.2 |

02-51349-008

*TABLE 2: Recovery of cellulose as glucose from untreated and fungal-treated straw stems.*

This amounted to 37.4%, 32.6%, and 43.6% of the cellulose in the straw stems. Recovery of glucose after fungal treatment was thus very poor for subsequent acid pretreatments at lower temperatures followed by enzymatic hydrolysis. The best recovery of glucose was at 121° C, where the glucose recovery approached the control (no fungal treatment) even after taking into account fungal glucose consumption. Thus, a higher fraction of the remaining cellulose in the fungal-treated stems was convertible to glucose using cellulase enzymes.

To fully address the potential benefits of a distributed fungal pretreatment it would be necessary to use the more efficient acid pretreatment methods described above, at lower temperatures than commonly used (150° C -230° C). Based on these results, a lower temperature acid pretreatment is probably attainable for the fungal-treated straw stems. However, it is likely that any benefit of increased cellulolytic digestibility would be more than offset by cellulose yield losses unless a fungus is used that degrades far less cellulose.

Results indicate that water and acid washes would work in an appropriately designed system to reduce K loads and the $SiO_2/K_2O$ ratio for combustion or gasification in fluidized beds. Alkali washes remove some $SiO_2$ but less K than water or acid, and thus do not achieve the desired reductions in $SiO_2/K_2O$. An Invention Disclosure Record was filed on the debarking strategy, including both chemical and enzymatic methods. The results of this research also have been disseminated to peer groups and presented at international conferences.

The Committee on Biobased Industrial Products of the National Research Council recently recommended several research priorities for conversion of biomass to bioenergy and bioproducts. These priorities included equipment and methods to fractionate biomass for subsequent conversion processes, and methods to increase the efficiency and reduce the costs of conversion of biomass to bioenergy and bioproducts. This LDRD research fits well into both of these priority areas.

Biomass is an important area for DOE and the nation, with applications spanning energy security, environmental stewardship, and the energy economy. This project enhances the INEEL Bioenergy Initiative's ability to address these needs. This LDRD supports future DOE missions by addressing specific BioEnergy and BioProducts research goals.

# Computational Fluid Dynamics Model Based Control of Two-Phase Flow

*Charles R. Tolle, Herschel B. Smartt, Tim R. McJunkin*

## *Controlling fluid dynamic processes for improved energy production*

CE109

Computational fluid dynamics (CFD) based techniques have made great progress over the last 20 years with increased understanding of the physics that drive the fluid motion as well as ever increasing computational capability. This is especially true for multi-material flows such as solid particles entrained in an air or other gas stream. These types of flows are very complex and provide some unique challenges to CFD modelers trying to simulate and predict the behavior of these flows with a reasonable degree of accuracy. Simulation is further complicated when active control surfaces need to be modeled within real-time computational demands.

This LDRD explores methods of CFD modeling techniques that can be used within open-loop and close-open control systems for multiphase processes. This year's efforts centered on the development of compact CFD model code that could be used as the basis for an embeddable real-time controller using low-cost U1-server clusters and/or field programmable gate array (FPGA) hardware.

Technical objectives for fiscal year 2002:

- Employ a discrete phase modeling approach on the transport equations for the continuous (air) solved in the Eulerian reference frame for two different density particle phases in a Lagrangian frame of reference.
- Develop a two-phase hydrodynamic model that treats the fluids and solids as two interpenetrating continua to describe phenomena such as particle segregation and elutiation, which offers a more accurate simulation without additional computational resources.
- Convert SPH-Riemann Hybrid Lagrangian Particle (SPH-RHLP) modeling code, which is a gridless method that allows for easy movement of active control surfaces without the time consuming remeshing, from its original Fortran into C.
- Design a new parallelizable, grid-based neighborhood-tracking scheme to avoid an N log N search algorithm.
- Marry the SPH-RHLP C based code to the grid-based neighbor-tracking scheme. Implement in a parallel-superset language of C called Cilk.
- Test SPH-RHLP parallel implementation for scalability.

Fluid dynamic processes are fundamental to energy and bioenergy production processes such as feedstock separation and mixing operations within bioreactors/fermenters. Moreover, these types of fluid dynamic processes are not amenable to lump-sum parameter models; thereby, severely limiting the applicability of classical control theory (i.e., linear theory) to control optimum production rates as well as robust disturbance rejection. Due to these limitations, many of these processes have only gained simple regulation-based controllers (e.g., PID set-point controllers) that are based on indirect process measurements instead of primary physics-based measures.

Simple regulators using indirect process measurement perform a useful first level of control; however, their efficiency is generally reduced resulting in costly, increased energy and reduced production quality. The most pressing need that prevents application of advanced optimal controls to these processes is the lack of real-time, physics-based models that can handle active control surfaces and rate changes. Based on detailed analysis and literature review of CFD modeling techniques, it was decided to evaluate four alternative modeling approaches:

***Discrete phase modeling*** – In this approach the transport equations for the continuous (air) are solved in the Eulerian reference frame. The two different density particle phases are treated as discrete secondary phases in a Lagrangian frame of reference. A coupled approach is being used so that the effect of the continuous phase on the discrete phases is accounted for, and vice-versa. Statistical methods are being used to trace the turbulent dispersion of particles about a mean trajectory. For this effort, the commercial CFD code FLUENT is being used.

***Two-phase hydrodynamic model*** – This model treats the fluids and solids as two interpenetrating continua. In this approach all of the particles are considered to be identical, characterized by an effective diameter and identical material properties. To describe phenomena such as particle segregation and elutiation, the model must account for the two types of particles, characterizing each particle type by its unique density. This is accomplished by treating the two classes of particles as distinct continuous phases, each with its own set of

governing hydrodynamic equations. This negates the need for statistical methods potentially offering a more accurate simulation at the expense of more computational resources. This approach is using a national laboratory code Multiphase Flow with Interphase eXchanges (MFIX) coupled with a commercial multiphase CFD code CFX-4.

***SPH-Riemann Hybrid Lagrangian Particle Method*** - This method characterizes each particle by an effective diameter and identical material properties for computation purposes, while allowing for additional properties to be attached to the particle to reflect contaminants or chemical makeup interactions. Because this method is gridless, it allows for easy implementation and movement of control surfaces without the time consuming remeshing.

To evaluate these alternative modeling approaches and their ease of coding implementation, two simple experiments have been outlined as a comparison benchmark. To date, a license for the commercial CFD code FLUENT has been secured, as well as a Fortran implementation of the SPH-Riemann Hybrid Lagrangian Particle Method. The latter code was ported to C from Fortran. Parallel redesign of the SPH-RHLP algorithm began with the design of a new grid-based neighborhood-tracking scheme for particles that avoid an N log N neighbor search algorithm within traditional SPH algorithms.

The SPH-RHLP C-based physics algorithms were redesigned to allow for parallel-particle-to-particle-interaction calculations to be made. These new algorithms were then married together in a new code implementation using Cilk.

This new, highly parallel SPH-RHLP code base was tested for scalability given a variety of decreasing parallel implementations on INEEL's 64-processor SIG origin Computer (Fig. 1). It was learned that the code's scalability is highly sensitive to both problem size as well as neighborhood size.

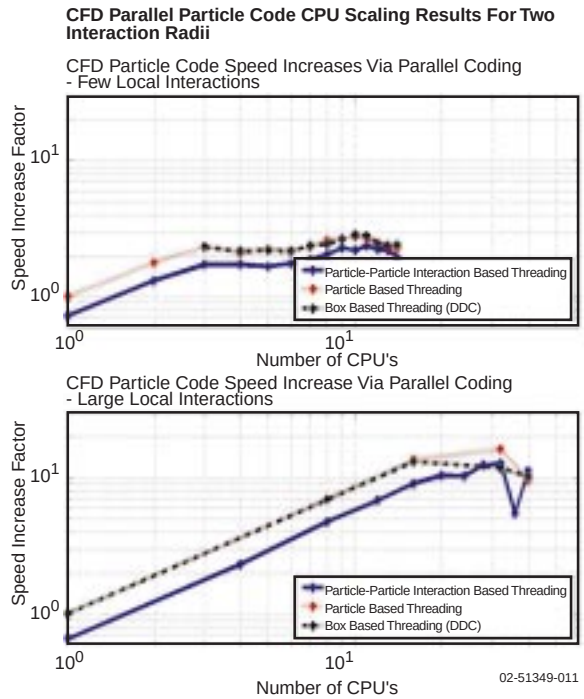


*FIGURE 1. SPH-RHLP parallel scaling study for three levels of parallelism and two neighborhood sizes; i.e., top graph's neighborhood is 1/10th that of the bottom graph's.*

The new code base was designed for simple extension to 3-D CFD modeling, to be implemented next year. Further, the current single-phase code was designed to handle N dimensional particle types, given that the appropriate physics models have been added to the code. This new code is highly modular and extendable for this exact propose. Likewise, this new code base serves as a stepping-stone toward possible FPGA parallel implementation.

Due to its implementation within Cilk, one can easily estimate the optimal number of CPU's needed within a cluster to maximize the cost/speed increase needed within industrial operations (using Cilk's critical path and total work profiling tools). Finally, in conjunction

with this new SPH-RHLP code, development began on a new GUI based particle setup program (Fig. 2). This GUI application will allow easy design of CFD problems to be run using the new CFD SPH-RHLP engine. In the year that follows, particle sources and sinks will be added long with active control surfaces.

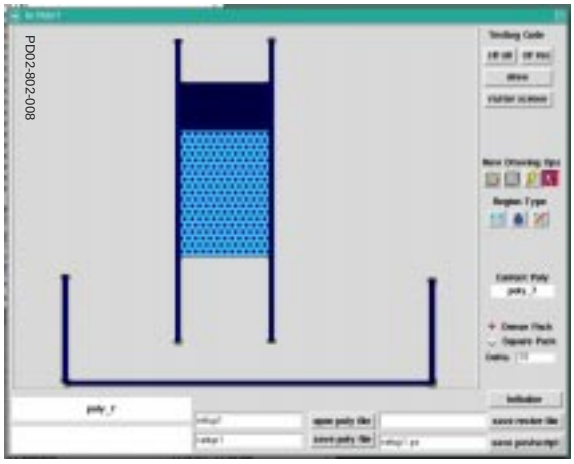


*FIGURE 2. Model of a GUI-based particle setup program being developed for use with the SPH-Riemann Hybrid Lagrangian Particle code.*

The control of fluid dynamic processes is fundamental to the production of energy and bioenergy in an efficient, environmentally sound manner. Although simple regulators using indirect process measurement perform a useful first level of control, their indirect nature leads to inefficiency, which directly leads to costly increases in energy usage as well as reduced quality in end products. This LDRD is supporting DOE interests in new approaches to improved energy production.

# Acidophilic Bioprocess for Production of Organic Acids from Biomass

*Thomas E. Ward, Will Keener*

## *Reducing dependence on non-renewable petroleum resources*

CE105

Most organic acids are currently produced from non-renewable petroleum feedstocks. Replacement of petroleum-based processes with those that are biologically based offers several potential advantages that include: reduced use of petroleum resources, reduced consumption of energy in the manufacture of chemicals, and decreased production of wastes due to the high specificity of biochemical processes. For these reasons, several programs in the DOE Office of Energy Efficiency and Renewable Energy support development of biologically based processes for production of chemicals and fuels.

This LDRD is exploring a novel bioprocess for production of organic acids from a variety of biomass feedstocks, including several now treated as waste, using acidophilic (acid tolerant) bacteria. The project focuses on production and characterization of acidophilic bacteria capable of synthesizing significant amounts of an organic acid.

A low pH process for production of organic acids offers several potential advantages over the current neutral fermentation processes in use. For example, base would not have to be continuously added to prevent the pH from falling to inhibitory levels, saving the cost of the base and the cost of disposal associated with the large amounts of waste salt produced. At low pH the product would be extractable into an organic phase as the first step of concentration and purification. In a two-phase reactor, such an organic phase could permit continuous operation (increasing efficiency), and prevent buildup of inhibitory levels of the product.

Technical objectives for fiscal year 2002:

- Introduce specific plasmids containing a cloned lactate dehydrogenase (LDH) gene into acidophilic bacteria.
- Assay LDH activity and lactic acid production in transformed acidophilic bacteria.
- Develop bioprocess using the genetically engineered bacteria to produce lactic acid.

The gene coding for the soluble LDH of *E. coli* was previously amplified from genomic DNA and cloned into pMMB277, an IncQ, broad-host-range vector containing a gene for chloramphenicol resistance. This vector allows maintenance and expression of the LDH gene in the acidophilic bacterial cells that are the focus of this LDRD.

After confirming that a DNA fragment of the correct size had been cloned, and that high levels of LDH enzymatic activity were present in *E. coli* cells carrying this plasmid, the plasmid was introduced into acidophilic strain PW1 using electroporation. A number of candidate transformants (chloramphenicol resistant) were analyzed for the presence of plasmid, and several contained the starting plasmid but, surprisingly, at distinctly different levels.

Two of these plasmid-containing acidophilic strains were grown on glucose in the presence and absence of the inducer IPTG. The cells were harvested, broken open, and assayed for LDH enzymatic activity. Both strains showed significantly increased levels of this enzyme compared to the non-transformed parent strain. However, when the culture medium from these cells was analyzed for organic acids using HPLC, nothing above background was observed. The broken cells also were assayed for organic acids. Although low levels of some acids were present, essentially no lactic acid was observed. This result was completely unexpected, as this strategy of increasing LDH activity has successfully resulted in production of lactic acid in a number of other bacterial species.

It is known that bacteria have a variety of pathways for metabolizing sugars, but all known pathways result in the production of pyruvic acid, the direct precursor of lactic acid. The results observed could be due to the fact that these cells produce very little pyruvate, thus restricting the amount of lactate that can be produced. An alternative explanation is that lactate was produced but was further metabolized.

To determine whether these acidophilic cells are likely to produce significant amounts of pyruvic acid, they were assayed for pyruvate kinase, the enzyme responsible for synthesizing pyruvic acid. The cells appeared to possess this activity and thus should be able to produce moderate levels of pyruvic acid.

To determine whether there might be something wrong with the experimental design, the investigators grew the *E. coli* cells containing the various plasmids on glucose

under inducing and non-inducing conditions. The supernatants were assayed and contained significant amounts of lactic acid, especially under the inducing conditions, so this assay approach appears to be valid.

It was then decided to transform additional acidophilic strains in case there was something peculiar about the first strain selected. Three additional strains were chosen for this series of experiments: CM3A, CM1 and CM4. The previously used plasmid was electroporated into these three strains, and the cells were inoculated onto chloramphenicol containing plates. Chloramphenicol resistant colonies were grown, broken open, and assayed for LDH activity.

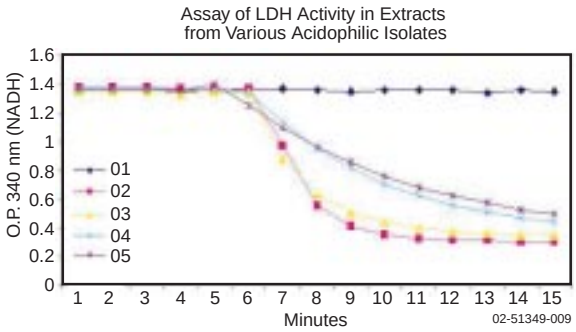


*FIGURE 1. Assay of LDH activity in extracts from various acidophilic isolates transformed with a plasmid containing an* E. coli *LDH gene. 1) No added extract, 2) Strain CM1, isolate #1, 3) Strain CM1 isolate #2, 4) Strain CM4, isolate #4, 5) Strain CM4, isolate #9.*

The single chloramphenicol resistant colony of strain CM3A had no measurable LDH activity. Two of the three chloramphenicol resistant colonies of strain CM4 assayed had fairly high levels of LDH activity, and both chloramphenicol resistant colonies of strain CM1 assayed had very high levels of LDH activity (Fig. 1). The project ended before supernatants from these (positive) cells, growing in glucose, could be assayed for the presence of lactic acid.

This LDRD will potentially provide a much-improved technology for production of organic acids from biomass, resulting in savings of petroleum feedstock resources and process energy, as well as significantly reduced waste production. The project supports the INEEL Bioenergy Clean Energy Initiative and brings enhanced capabilities to INEEL. These enhancements include added expertise in and new technology for microbiological production of chemicals from biomass resources, which addresses major goals of the DOE-EE Biomass Program and the Plant/Crop Based Renewable Resources 2020 Vision Document; increased expertise in genetic engineering of acidophilic bacteria; and additional capabilities in developing and optimizing fermentative bioprocesses using acidophilic bacteria (genetically engineered or not).

# An Innovative Gas-Cooled Fast Reactor

*Kevan D. Weaver, James Sterbentz, Jacopo Buongiorno, Cliff Davis*

## *Meeting criteria for economical, safe reactor design*

NE122

The fourth generation of nuclear power reactors will have to compete economically with coal and natural gas-fired power plants, while maintaining safety, increasing proliferation resistance, and minimizing waste. The goal of this LDRD is to identify, analyze, and resolve the key technical issues associated with the development of this reactor concept to meet these criteria.

The major issues involved with this fourth-generation concept are loss-of-coolant/loss-of-flow accidents, long-life core/fuel designs, and materials compatibility at high temperatures and pressures. This research is investigating various fuel, core, coolant, plant, and material designs of gas-cooled fast reactors (GCFR) to meet these criteria while producing low-cost electricity and consuming actinides to reduce waste, increase proliferation resistance, and retain high safety margins.

The specific tasks used to accomplish these goals are: 1) reactor physics and core design, where long-life cores (including fuels) are being studied to optimize the transuranic destruction rate, minimize waste production, and maintain a low lifetime reactivity swing; 2) plant engineering design, where both high-temperature helium and supercritical pressure and temperature $CO_2$ coolants are being studied; and 3) high temperature material studies, including $CO_2$ steady-state and air ingress experiments of candidate cladding and structural materials.

Technical objectives for fiscal year 2002:

- Evaluate reactor physics and core design.
- Evaluate plant-engineering design.
- Perform materials studies.
- Characterize waste forms.
- Perform qualitative economic analysis.

The steady-state and transient temperature limits were estimated for the metal pebble fuel and cladding. It was found that a steady-state cladding temperature of 580° C to 600° C would allow for 15-20% at burnup. On the other hand, the transient cladding limit was identified at 725° C. Finally, the fuel temperature limit was identified at 1000° C for both steady state and transient conditions (Fig.1).

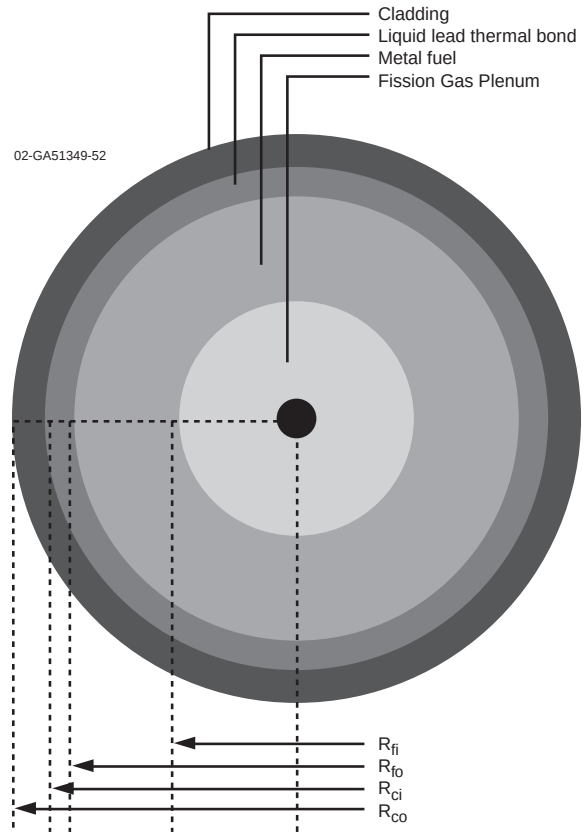


*FIGURE 1. The pebble fuel geometry.*

***Neutronics of Pebble Fuel*** – Two infinite lattice models were constructed. One model was based on a unit cell with a face-centered cubic (fcc) array of pebbles, heterogeneous model, and the other a simple homogenized unit cell model of like dimensions. The fcc model had a theoretical packing fraction of 0.74, whereas the project pebble-bed is assumed to have a 0.68 packing fraction. Both unit cell models had reflective boundary conditions applied to each of the six unit cell faces so as to create the transport effect of an infinite lattice of identical unit cells.

The calculated k-infinities associated with the two unit cell models were 1.466848 ± 0.000733 (heterogeneous), and 1.460812 ± 0.000584 (homogeneous). The two k-infinity values were not identical as expected, however, they were sufficiently close in magnitude that the homogeneous model could be used in place of the heterogeneous model with reasonable confidence. Based on the calculated results, a core size of approximately 1.83-m diameter and 1.83-m height would be reasonable.

To boost core reactivity and reduce neutron leakage, a neutron reflector is an important aspect of the core design. Of the three reflector materials evaluated, the lead (Pb) reflector gave the best reactivity boost to the core. However, upon a loss-of-coolant (LOCA), the worth of the lost $CO_2$ injected a positive 1,114 pcm of reactivity into the core, whereas, the nickel reflector injected only +877 pcm. A preliminary core depletion calculation was performed to determine how long a plutonium-fueled core could remain critical. For an assumed total core thermal power output of 400 MW(th), the core remained critical for approximately five years.

***Metal Matrix Fuel*** – To ensure that no innovative option escaped scrutiny it was decided to carry out a set of very fundamental studies. The first of these studies merely involved calculation, using the Monte Carlo N-Particle transport code (MCNP), of the spectrum average microscopic absorption cross-section of all of the elements in the periodic table in a representative GCFR spectrum. While few could satisfy other practical requirements, some elements like the alkaline earth metals might be put to useful service. As expected, lead and bismuth were superior performers, as befits their use in LBE cooled fast reactors.

Next a simple matrix-type core was defined containing a large volume fraction diluent. Select elements were then substituted in turn. Aspects compared were beginning of life multiplication factor, k, coolant void coefficient, macroscopic absorption cross-section, and $B_1 = (k-1) / (\Delta k / \Delta B)$, the linearly extrapolated burnup potential. For example, of the common "practical" materials for nuclear service zirconium was the best, but only a fair performer; sulfur and phosphorus (e.g. as US and UP fuel) might be worth looking into; moderation by the common ceramic anions C, N, O seriously degraded performance and the intermetallic oddball $Sr_2Pb$ (melting point = 1155° C) might be a useful in-core energy-storage medium.

Some intriguing possibilities were evident, both metallic and ceramic. Nevertheless, if one refers to the "perfect mirror" case, it is evident that fast neutron reflector materials are significantly less effective than are the reflectors available for thermal reactors.

***Plant Design Studies*** – This task focused on the overriding issue of post-LOCA decay heat removal. A review of the significant worldwide effort on the first generation of GCFR designs in the 1970s has identified this as the principal area of concern by far. A preliminary performance analysis was performed of a generic decay heat removal system that is capable of both passive (natural convection) and active (blower-forced convection) operation. Principal findings were as follows:

- Cooling by natural convection alone is only feasible if post-LOCA pressures of more than several atmospheres of $CO_2$ can be maintained.
- Helium is significantly inferior to $CO_2$ (factor of 5-10), which virtually dictates reliance on forced convection if this gas is used in the power cycle.
- Significant reliance on natural convection restricts the designer to modest fuel specific powers – on the order of 25 KW/kg HM, which has a negative impact on fuel economy.

***Supercritical $CO_2$ Power Plant*** – The indirect-cycle, supercritical $CO_2$ (S-$CO_2$) power plant devised last year for the INEEL /Massachusetts Institute of Technology (MIT) LDRD project on PbBi cooled fast reactors was transformed into a direct-cycle plant for GCFRs. A cycle

efficiency of approximately 44% at the modest $CO_2$ core outlet temperature of 550° C was achieved. Figure 2 compares the relative size of steam, helium and $CO_2$ turbines, which presages the likelihood that the S-$CO_2$ plant will be very compact and correspondingly inexpensive.

Attention is now being turned to the key issue of cycle control, which may differ significantly from that of helium Brayton cycles because the S-$CO_2$ compressor operates so close to the critical point.

***Incorporation of $CO_2$ Properties into ATHENA*** – Carbon dioxide fluid properties were successfully implemented in ATHENA. Only minimal changes were required within the NIST database. The transport properties of thermal conductivity and viscosity were successfully implemented through the use of tables that cover wide ranges of pressure and temperature.

The implementation of the thermodynamic properties was validated by comparisons of fluid density and specific enthalpy from an independent source of data as a function of pressure and temperature. The results of the validation calculations were typically within 1% of the reported values. The validation concentrated on the subcritical gas and supercritical regions, which are the most important regions for analysis of gas-cooled fast reactors. The subcooled liquid and two-phase regions have not been tested thoroughly.

***Dissociation of $CO_2$*** – An important issue associated with using $CO_2$ as the working fluid is dissociation at higher temperatures. The potential for corrosion (oxidation) would be greater in this case, and a simple calculation was performed to verify what amount of oxygen would be found in the system, given a particular temperature. Thus at 600° C, dissociation is minimal (about 1 ppb) and should not present a problem for this concept.

This LDRD supports the Generation IV initiative in advanced reactor design, which has become a prominent focus of the INEEL. In addition, this project has already become important in evaluating the feasibility of the Generation IV gas-cooled fast reactor, which is a high priority concept for the U.S.

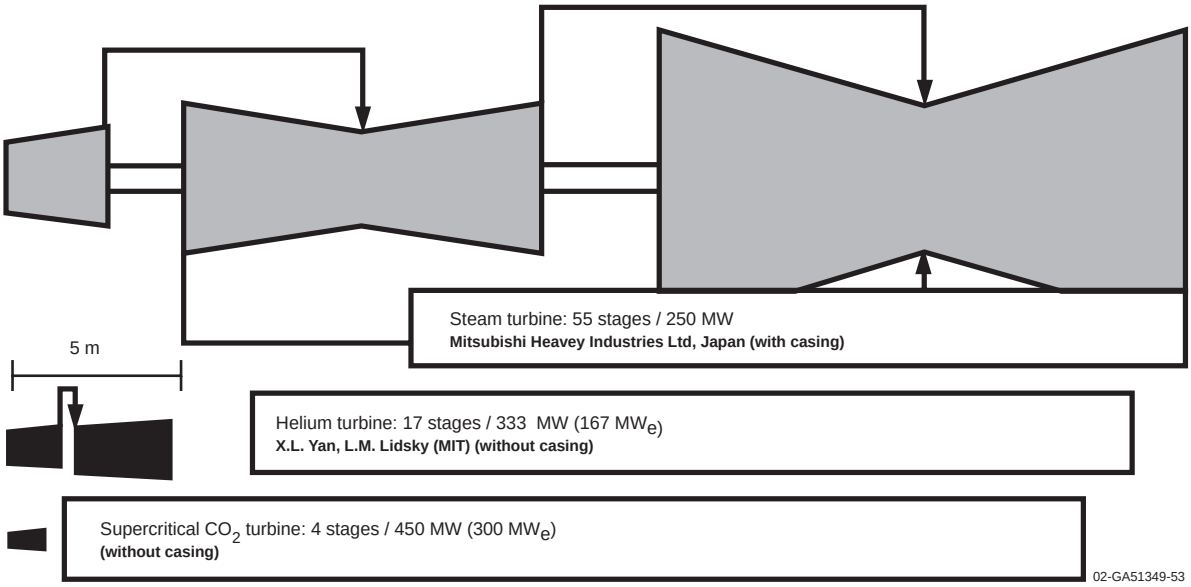


*FIGURE 2. Comparison of turbine sizes.*

# Characterization of Methane Hydrate Deposits

*David M. Weinberg, Dennis C. Kunerth, Rick S. Colwell, Kevin L. Gering*

## *Supporting development of new energy resources*

NE123

Exploiting natural gas hydrates as a resource, and mitigating the hazards of drilling operations and location of petroleum or gas production infrastructure on hydrate-containing sediments, requires additional knowledge and new tools. Current seismic technologies can sense the presence of hydrate formations, but cannot characterize the quality or morphology of the hydrate within the formation. Nor can any current technology monitor the integrity of a hydrate structure with time, as its environment changes due to drilling, production or mechanical loading.

This LDRD is exploring acoustic, in situ characterization/monitoring technologies to address this need. To date, the work performed has used a 1-D approach to acquire P- and S-wave responses as hydrate surrogate forms/dissociates in simulated sediments. Although successful, the work demonstrated the difficulty in generating and propagating S-waves in unconsolidated sediment; i.e., S-wave data was obtained only after a residual water phase froze to fully rigidize the sediment bed.

Vital to determining effective material properties, thereby allowing phase, morphology, and mechanical properties within the geologic matrix to be deduced, is the need to reliably obtain both P- and S-wave acoustic data. A means to potentially overcome this experimental difficulty is to use a 2-D approach similar to that used in the field by offsetting measurements to obtain mode conversion of P-waves to S-waves at an interface. A 2-D reactor was built in this LDRD to validate this approach.

Technical objectives for fiscal year 2002:

- Complete 1-D experiments using THF gas hydrate surrogate.
- Design and build 2-D experimental system to improve data collection.
- Generate and present technical papers summarizing work performed in FY01 and FY02.

Standardized techniques to determine the physical characteristics of natural gas hydrates do not exist. Although existing seismic technologies using velocity measurements can generally sense the presence of hydrate formations, they are unable to characterize the hydrate in any useful quantitative way – an absolute requirement if methane hydrates are to be looked at as a potential energy resource.

The investigators demonstrated the feasibility of such measurements. A 1-D experimental system was developed to collect acoustic measurements during the formation and dissociation of a THF•17$H_2O$ hydrate in simulated unconsolidated sediment (sand). First-of-a-kind measurements made during the formation/dissociation processes demonstrated that these processes can be monitored with time and data on acoustic material properties and thermal characteristics can be obtained. The experimental system and typical data are shown in Figure 1.

When the temperature at the chill plate reached approximately 4° C during the experiment, the THF hydrate nucleated and started to grow. At that point, there was an exothermic spike in the temperature profile and the compressional (P) wave detected the formation of a hydrate front/interface that began moving upward. No change was detected in the shear (S) wave measurements. When the temperature reached approximately -1° C at the chill plate (about 15 minutes later,) a second exothermic spike was observed. At that time, a weak front/interface following the hydrate front was detected by both the S-wave and P-wave. This second front was formed by a residual water phase that froze within the solidified hydrate/sediment. The residual water phase occurred because the THF/water mixture did not have perfect stoichiometry. Volatility of the THF and the use of a reagent-grade material resulted in an excess-water-to-THF mixture. These results indicate that, for the THF system, the hydrate formed in the pore spaces but did not fully consolidate the sediment bed. Therefore, there was insufficient shear modulus to support S-wave propagation.

Only after the water phase froze did sufficient shear modulus exist to support S-wave propagation. Simply put, it is the freezing of the residual water that imparts sufficient stiffness to the material to support S-wave transmission. Further, it can be implied that the onset of P-wave velocity changes must be caused by a change in the system's bulk modulus, with essentially no change in shear modulus.

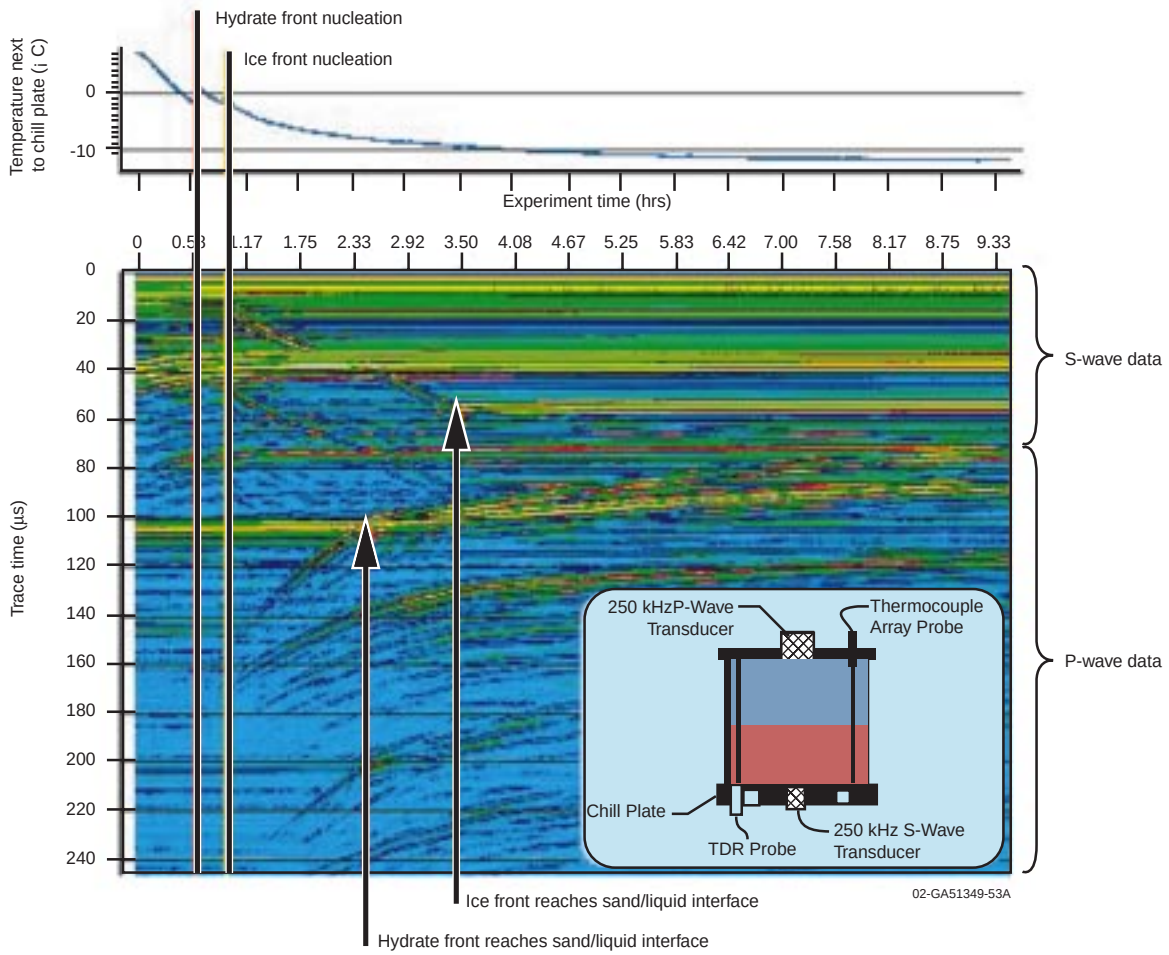


*FIGURE 1. Data obtained during the formation of THF hydrate. The reactor is cooled from the bottom, creating a THF hydrate front that propagates upward. (The sides of the reactor are insulted to minimize radial heat loss.) The S-wave transducer is mounted in the bottom plate to provide direct coupling to the solid hydrates/sediment structure (S-waves are not supported by the liquids or materials having a very low shear modulus). The P-wave transducer is mounted at the top; as a result, the S-waves propogate in the opposite direction to the P-waves.*

The inescapable conclusion is that the residual ice is forming primarily in the pore throats, while the THF hydrate is crystallizing in the pore spaces. The time lag between the start of the two fronts and their arrival at the sediment/liquid interface increases with time, which provides information regarding thermal diffusivity of the system through time, a requirement for a hydrate formation/dissociation monitoring device.

It was concluded that this experimental approach could collect data on effective acoustic material properties

(effective refers to measured property resulting from a combination of individual components), process kinetics, and thermal characteristics.

The key to continued experimental progress was the development of techniques to reliably obtain both P- and S-wave acoustic data. A means to potentially overcome the experimental difficulties encountered in the 1-D work with the generation and propagation of S-waves was to implement the use of 2-D approach similar to that used in the field. The term “2-D” refers to the use of offset measurements to obtain mode conversion of P-waves to S-waves at an interface. A simplistic illustration of the concept is provided in Figure 2. A reactor system has been successfully built and designed by the investigators to evaluate and use the 2-D approach.

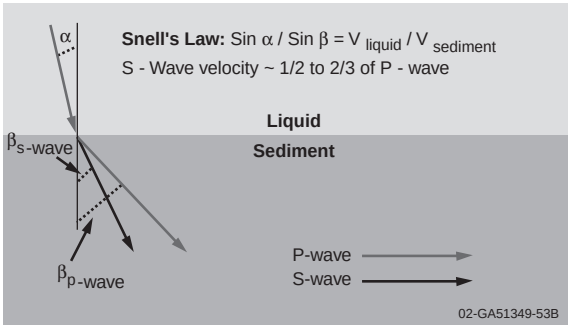


*FIGURE 2. An incident P-wave beam striking an interface at an angle will result in the transmission of both a P-wave and a mode-converted S-wave as described by Snell’s law.*

In summary, this LDRD successfully conducted experiments to characterize the acoustic response to hydrate formation and dissociation processes in unconsolidated sediment beds, and designed and built an experimental system to implement a 2-D approach to generate and detect P- and mode-converted S-waves in simulated sediment beds. A total of six papers have been generated from this research and submitted to publication and/or presented at national meetings.

The research performed in this LDRD provides data that can be used to develop better seismic processing algorithms, and forms the basis for field technologies that can characterize physical hydrate properties and monitor them with time. This work is supporting national energy security needs by contributing to the knowledge required to develop natural gas hydrates as a potential energy resource.

# Environmental

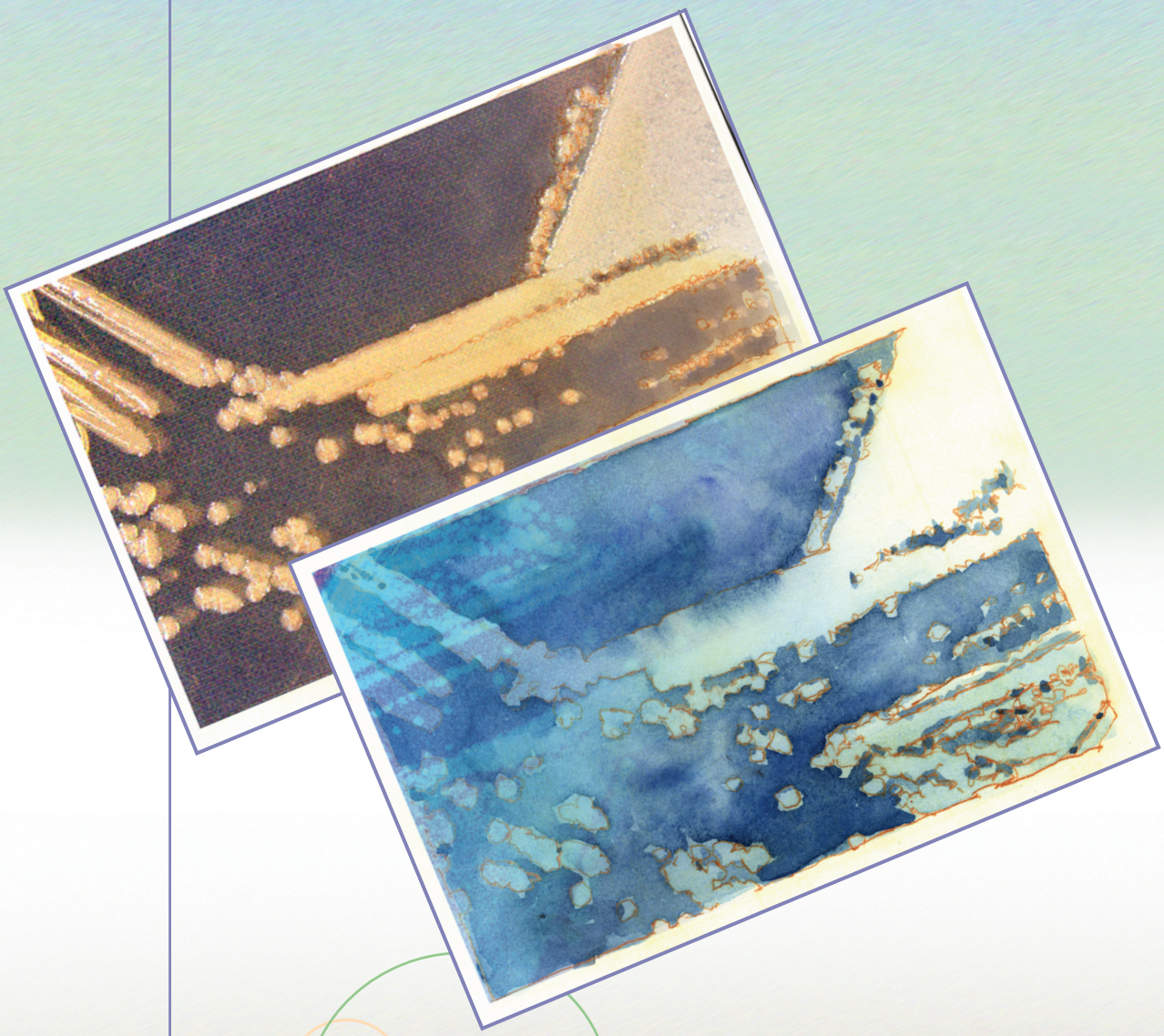

## LDRD Annual Report for FY-2002

Idaho National Engineering & Environmental Laboratory

# Elemental Tracers and Multi-Variate Receptor Modeling Methods in Assessing Air Pollution

*Michael L. Abbott, Jeffrey J. Einerson*

## *Predicting area contributions to regional pollution*

ET110

Regulatory permitting and stakeholder acceptance of important waste treatment projects at the INEEL (e.g., Advanced Mixed Waste Treatment Project (AMWTP) incinerator, New Waste Calciner Facility (NWCF) calciner) and other DOE and commercial sites have been impacted in the past by the inability to provide accurate predictions of long-range atmospheric transport of pollutants and by a general lack of scientific understanding of air pathway transport.

This LDRD is researching a new approach to characterize and source-apportion air pollutant fallout on a region-wide scale to enhance the INEEL's ability to meet regulatory permitting requirements for existing and future EM-waste treatment facilities. The research is: 1) developing a comprehensive, database of trace element and ion constituents in air pollutant fallout on a regional scale, 2) identifying multivariate correlations of these constituents that provide unique chemical fingerprints for the major source areas (e.g., cities, INEEL facilities), and 3) calculating the source-specific contributions to total fallout at downwind mixing sites, using multivariate mixture models (classical and alternating least squares).

This research is enhancing scientific understanding of the relative influence of major emission source areas in the region, which is critical for development and application of proper emission control strategies (are we controlling the right sources?) and for stakeholder understanding of DOE facility impacts relative to other sources.

In FY02, 135 snow samples were collected on the INEEL property and surrounding region, and analyzed in triplicate using inductively coupled plasma mass spectrometry (ICP-MS) and ion chromatography (IC). Twenty-seven trace elements and six common ions were measured in most samples. A classical least squares (CLS) mixture model was developed using the chemometrics software, Pirouette® (Infometrix). The model was used to predict source contributions to fallout at four downwind locations where plumes from several source areas mixed.

For the FY02 sampling data, the CLS model predicted from 36%-58% of the total measured fallout. Refinement of the sampling design (planned for FY03) will improve this prediction.

Technical objectives for fiscal year 2002:

- Analyze remaining FY01 sampling data and perform additional snow sampling.
- Develop proficiency in advanced pattern recognition software (Pirouette®).
- Develop and test a multivariate (CLS) source apportionment model.
- Publish or present results.

*Sampling and Analysis* – Over 385 snow samples were collected over two winters and analyzed for a broad suite of trace elements using inductively coupled plasma mass spectrometry (ICP-MS) and common ions. Laboratory analysis was done by the U.S. Geological Survey (USGS) National Research Program lab in Boulder, CO.

In FY01, 39 trace elements and nine ions were measured that provided the first comprehensive database of the constituents and the spatial and temporal trends in regional fallout. In FY02, the sampling design was modified to facilitate development and testing of a CLS source apportionment model. "Source profile" sampling site locations (upwind and downwind of major regional source areas) were determined using a real-time National Oceanic and Atmospheric Administration (NOAA) trajectory model (INELVIS). These sites were used to build the CLS model.

"Mixing" site locations (where plumes from two or more source areas likely mixed) also were sampled after a different snowfall event. The data from these sites were used for prediction by the CLS model.

***Pattern Recognition*** – The data were analyzed for spatial and chemical patterns using regional isopleth plots, bivariate multi-plots, and principal component analysis (PCA).

Results from FY01 showed that the highest concentrations occurred near the two largest cities in the region (Pocatello and Idaho Falls) while the lowest results occurred on the INEEL. Pocatello had very high concentrations of V, Cd, Fl-, U, Mo, and Tl. PCA showed clear clustering only at the Pocatello site and a shift in the principal component (PC) scores over time.

The chemical loadings for PC 1 were rare earth elements and Al, and were attributed to a combination of fugitive emissions from the phosphorus industry in Pocatello and crustal (blowing dust) input. PC 2 was loaded with Tl, Cd, Zn, V, and Ni, which were attributed to the Pocatello phosphorus industry and oil combustion. The source profile sampling done in 2002 showed maximum concentrations at Pocatello to be 1-3 orders of magnitude higher than those observed at any of the other source areas for all constituents except $NO_3^-$.

***Source Apportionment*** – Source area inputs, calculated as the difference between the downwind and upwind constituent concentrations, and background inputs (upwind concentrations) were used to "build" a multivariate CLS model in Pirouette®. The CLS model was used to predict source contributions at four downwind test sites where plumes from several source areas mixed (based on INELVIS model predictions). The results for these three test cases showed reasonable results – 15%-27% of the fallout was from a source area (Rexburg) that, based on model plume projections, would likely have had some impact at the sites with the remaining due to non-regional background input (Fig. 1 and Table 1).

*FIGURE 1. Mixing zone sampling locations (where emissions from two or more sources might mix) were determined using INELVIZ modeling of air masses during a 2/19/02 snowfall event.*

| | Percent (%) contribution at mixing site: | | | |
|---|---|---|---|---|
| Source[a] | RXBM1 | RXBM2 | RXBM3 | IDAM1 |
| HELS2 | 0 | 0 | 0 | 0 |
| BLAS1 | 44 | 39 | 39 | 45 |
| BLAS2 | 2 | 1 | 0 | 1 |
| IDAS1 | 0 | 0 | 0 | 0 |
| IDAS2 | 0 | 0 | 0 | 0 |
| RXBS1 | 0 | 0 | 0 | 0 |
| RXBS2 | 15 | 23 | 27 | 19 |
| POCS1 | 0 | 1 | 3 | 0 |
| POCS2 | 0 | 0 | 0 | 0 |
| CPPS1 | 38 | 36 | 31 | 35 |
| CPPS2 | 0 | 0 | 0 | 0 |

[a]S1 = background (upwind of source area);
S2 = source area (downwind-upwind).

02-GA51349-030

*TABLE 1. CLS model predictions of source contributions at the four mixing sites.*

Just as important in the CLS model predictions are the sources that are not contributing to fallout at the mixing sites (e.g., INEEL). Simple air dispersion models will predict some input at these sites. When totaled across all contributing sources, CLS predicted from 36%-58% of the total fallout measured at the mixing sites. Improvements in sampling design (e.g., transects downwind from source areas, assessment of additional source areas, source profile and mixing site sampling after the same snowfall event) are being planned in FY03 to increase the percentage of predicted source contributions accounted for in measured fallout and to refine the method.

Understanding who is responsible for what at sensitive downwind locations (e.g., communities, parks, sensitive ecosystems) will: 1) enhance stakeholder understanding

of the relative source impacts in the region, 2) facilitate stakeholder acceptance and regulatory permitting of DOE facilities, 3) ensure cost effective and sound emission control strategies, and 4) contribute to waste treatment technology path forward decisions. This LDRD research will contribute to DOE's long-term stewardship efforts by providing information on INEEL source contributions to region-wide surface buildup of contaminants.

A paper on the research results was presented at the International Conference on Air Quality III – Mercury, Trace Elements, and Particulate Matter (September 2002). The conference was co-sponsored by the DOE National Energy Technology Laboratory that is doing similar types of source apportionment studies in the eastern U.S. and expressed interest in this LDRD.

# Improving Stakeholders Interactions: A Stakeholder-Based Research Methodology for Reaching Decisions on Polarized Issues

*R. Sam Alessi, Michael Mayhew*

## *A relationship-oriented approach to problem solving*

ET108

The political and emotional charge of DOE issues, historical distrust of the government, and expensive solutions that negate the interests of the community, have typically been barriers to achieving DOE's established policy of public participation. This LDRD is analyzing the interactions between DOE and stakeholders, and producing scientific data that can be used to strengthen sustainable relationships between these diverse groups. Failure to intervene and foster positive discussions can deadlock projects and create a deep regional impact because unpopular decisions are mandated without considering the values or interests of the local community. Approaches are needed that will fortify the community by building trust while striving to achieve common goals.

This research applies human systems science to show how stakeholders organize their thinking around complex problematic issues. Our thesis is that it is necessary and prudent to understand the characteristics of stakeholder beliefs and rationalizations prior to invoking any decision-making method. An approach has been created that incorporates elements from anthropology, systems design, and systems therapy. This innovative approach produces a deep, fundamental understanding of stakeholder concerns. The knowledge gained can be used to balance meaningful human needs with technological advancements that will benefit all parties.

A pilot project was established with current and future stakeholders: Eastern Idaho high school students, and a regional group of adult INEEL stakeholders. High schools students discussed their concerns about the growth of Idaho Falls, the risks created by increased population, and their feelings of helplessness to control the future. The INEEL regional stakeholder group felt that the "messiness" of the democratic process coupled with the "human nature" of citizens to not become involved, created a hopeless view about the future of the INEEL.

A survey instrument was developed and tested to determine the extent of the fatalistic belief held by both regional youth and adults.. Results show approximately 18% to 32% of respondents with fatalistic belief tendencies. The approach holds promise for helping diverse groups communicate at a more fundamental level and explore ways to overcome beliefs that limit creativity and opportunity.

Technical objectives for fiscal year 2002:

- Gain a deeper understanding of the initial viewpoints of stakeholders involved in the long-term future of the INEEL.
- Investigate how fatalistic beliefs and attitudes in youth and adults affect their ability to make good decisions and become effective future citizens.

This work supports the objectives of the Department of Energy's Public Participation Policy that states:

> *"The Department recognizes the many benefits to be derived from public participation, for both stakeholders and DOE. Public participation provides a means for the Department to gather the most diverse collection of opinions, perspectives, and values from the broadest spectrum of the public, enabling the Department to make better, more informed decisions. Public participation benefits stakeholders by creating an opportunity to provide input and influence decisions…. This early involvement enables the Department to make more informed decisions, improve quality through collaborative efforts, and build mutual understanding and trust between the Department and the public it serves."*

The methodology of this LDRD integrates approaches from science and engineering disciplines, including anthropology, therapy, and systems design, to focus on the task of social and technical problem solving. First, anthropological methods are used to describe communication patterns and underlying assumptions among stakeholders. Next, therapeutic concepts are used to interrupt divisive communication patterns between participants and to assist the members in acknowledging and respecting the views of the others. Stakeholders participate in creating a new communication pattern, underlying assumptions, and physical solutions. The beliefs and perceptions of the stakeholders become intrinsically incorporated into the model and are a template of critical stakeholder requirements.

***Eastern Idaho Adult Stakeholders*** — Adult stakeholders were selected for greatest diversity possible and then trimmed to 10 members through a ranking process that involved stakeholders both external and internal to the INEEL. Stakeholder affiliations included, preservationist, professor, activist, DOE Citizen Advisory Member, local governance, media, Native American, environmentalist, and governmental regulator. Two separate two-hour sessions were convened and audio taped. The recording was transcribed literally and the only editing of the text was the removal of any identifiable information about the participants.

Initial findings are published in a report that was checked with stakeholders for accuracy and intent. Additionally, the results have been presented to the American Nuclear Society (Alessi et al., 2002). The emergent themes were identified from the actual language of the stakeholders, thus any quotes are literal and left in the form in which they were spoken.

The focus group began with a very broad opening question:

"Since the end of the cold war, it's been hoped that sites could be cleaned up and returned to the public. For a variety of reasons, DOE feels that they cannot completely clean up sites, but need to leave some waste in place, but in a safe manner. My question to you is, in response, what would you like to input into that? What would you say in response to that? [Pause] So if you had decision-makers here and policyholders or someone like that here, and with that set before them, what would you like to say?"

The purpose of this question was to focus the discussion on the issue of long-term stewardship of INEEL waste. To do this the investigators chose to state this issue in its narrowest sense even though not all sites will leave waste in place or attempt to transfer land to the public.

The main topics and issues discussed included concerns about the process for making decisions, including the need for public involvement, full disclosure of information, respect for the public, the honest assessment of the situation, and inclusion of community values. Public involvement was discussed more fully, including public attitudes on involvement and needs associated with public involvement. Additionally, science associated with waste management was discussed in terms of its complexity and whether that complexity is fundamentally social or technical. The narrative also was analyzed for the "impact on stakeholders" that affects the apparent lack of public involvement, unclear INEEL plans, and the overall influence of what was called *messy* government by stakeholders.

Overall, the results indicate a rather gloomy future. Uncertainty and confusion have led these stakeholders to fatalistic and cynical viewpoints that anything can be different. This negative view saps creativity about a positive future. Some stakeholders feel that decisions are made in a way that begs a fight. ("Here's the decision, now come up and fight it if you want to fight it.")

This research uncovered a number of paradoxes among the stakeholders that crippled the ability to create a beneficial future. Fatalistic beliefs and behavior were mirrored against a fundamental desire to help and not hurt. Beliefs that the future cannot be different were contrasted with some successes (e.g., KYNF stoppage of the INEEL incinerator), though the successes were negative. No "courageous" leadership could be identified by the group, yet stakeholders had a desire to be led and articulated a clear description of the needed leader. Overall, creative thinking was subsumed by dialogue that was saturated in the problem. Any passion to create a better future was eclipsed by the overarching fatalism.

Stakeholders did finally identify a solution that could lead to better stakeholder relationships and a more creative future for Eastern Idaho. They expressed a desire for monthly dialogue and, as stated by one stakeholder: "…for discussions to exist, there has to be a forum. I don't think we'll necessarily resolve anything or there's going to be some panacea as a result of that. But right now it's discussions through third and fourth parties, and…we know that model doesn't work…."

This desire for a new way to interact promotes the possibility for cooperation, rather than condemning stakeholders to more long years of contention and near-gridlock for projects that appear threatening to some.

Forming a direct dialogue and redirecting the issues discussed, can create a path to a more productive future in which stakeholders accept and even assist development, while using their influence and innovative ideas to provide new possibilities and directions.

***Eastern Idaho Teen Stakeholders*** — An emergent finding from the 2001 INEEL qualitative study with regional youth (Hill-Molder et al., 2001) was the indication that teenagers in Eastern Idaho have a fatalistic outlook that influences their ability to plan for the future. Literature research indicates growing fatalism worldwide. This LDRD hypothesizes that fatalism will negatively impact levels of trust and interfere with sound, positive decision-making skills in both the personal and public domains.

Since findings from adults also indicated fatalistic beliefs, a survey instrument was constructed to determine the level of fatalism existing in Eastern Idaho. Causes of fatalism (locus of control, explanatory style, and religious dogmatism), and how fatalism affects the level of trust toward nuclear weapons, nuclear power and the storage of nuclear waste were included. Trust in self, the INEEL, and the federal government also will be studied and compared with demographic variables like age, sex, level of community involvement and parent's occupations. Finally, decision-making skills and how they are affected by fatalistic attitudes were added items to the survey.

The survey instrument was pilot-tested with an opportunistic sample of 55 participants from Eastern Idaho. They represented teenagers age 13 through 19 from three separate counties in Eastern Idaho: Bonneville, Bingham and Jefferson. The pilot test results showed that 18% to 32% of the test population were somewhat to very fatalistic. A portion of that population also showed lower levels of trust and did not believe their choices could make a difference. If the results of a larger study support the test population results, it is advised that some intervention be taken to reduce the negative implications. This project's investigators plan to administer the full survey in the fall of 2002.

Direct benefits from this research are that the INEEL, regional stakeholders and the DOE can gain a better understanding of different viewpoints that influence the progress of projects at the INEEL. Additionally, INEEL plans can benefit from clearer knowledge of stakeholder needs. Design engineers benefit by being able to create technology that will not raise stakeholder concerns.

INEEL's capability to work with stakeholders to understand fundamental needs and to include this information in the construction of plans and in technology designs is a national asset. Since many investigations into failures of large-scale complex technologies are traceable to faulty requirements and misunderstood stakeholder needs, this research will put the INEEL on the cutting edge of advanced planning and engineering design.

The DOE is committed to encouraging public participation and fostering a viable relationship with stakeholders. The approach described in this research facilitates the interaction between agencies, entities, and stakeholders to develop trust and enrich decisions that will impact future generations.

# Biologically Based Catalysts for Processing and Detection in Harsh Service Conditions

*William A. Apel, Frank Roberto, Vicki Thompson*

## *Detecting heavy metals with microbes*

ET105

Extremophilic microbes live at life's extremes; i.e., very high and very low pHs, high and low temperatures, high osmotic pressures, high barometric pressures, etc. Enzymes from extremophilic microbes often share the microbes' resistance to extremes and can potentially be used to create biosensors and biocatalysts that have the high degree of specificity normally associated with enzymes, while being stable under a variety of environmental extremes that would typically inactivate enzymes.

This LDRD is investigating enzymes from extremophilic microbes for use as biosensors to detect and monitor environmental contaminants such as toxic metals and, in the longer term, for use as bio-catalyses for industrial, energy and national security applications. As an initial thrust in this project, the investigators have determined two tasks: 1) characterization and evaluation of different classes of extremophilic enzymes for use in biosensors to detect heavy metals in the environment; and, 2) development of genomic information to allow improved extremophilic enzyme stability through structural modification using molecular techniques.

The enzymatic biosensors developed from this work could ultimately provide a low-cost, selective and stable method for making real-time, in situ, quantitative metal measurements in a number of environments including the subsurface. This capability will effectively support not only environmental initiatives, but also initiatives directed toward the development of clean energy and chemicals from renewable resources.

Technical objectives for fiscal year 2002:

- Characterize enzyme and compare to commercially available catalases.
- Conduct large-scale purification of a thermostable catalase enzyme from *Thermus brockianus*.
- Continue elucidation of the *Halomonas campisalis* genome.

The work on this LDRD is specifically directed toward development of sensors for detection of toxic metals in the environment using extremophilic enzymes. While this is a nationally important topic and is key to the cleanup of many metal contaminated sites, this work contributes to the national good far beyond environmental cleanup, since it contributes to the technical bases for the ultimate understanding and development of extremophiles and their enzymes for a host of applications of national importance. These applications include, but are not limited to: national defense (e.g., use of extremophiles for surface cleaning after "dirty bomb" explosions, use of extremophilic enzymes to make personal protective equipment to degrade neurological toxic agents, etc.); energy independence (e.g., understanding of gas hydrates formation on the ocean floor within U.S. territorial waters and in Alaskan tundra, production of fuels from agricultural byproducts, etc.); and, advanced manufacturing processes (e.g., production of drugs in racemically pure forms, production of commodity and specialty chemicals from renewable, agricultural bioproducts, etc.).

For the biochemical characterization task in this LDRD, a large-scale procedure for purification of a thermostable catalase from *Thermus brockianus* was completed. The Utah State University Biotechnology Center was contracted to culture *Thermus brockianus* in their 100-L fermentor. They also ruptured the cells, providing the cell extract as the final product.

The large-scale purification procedure was scaled up from a small-scale procedure with the aid of the Applied Biosystem Vision protein purification system obtained during FY01. The procedure consisted of an ion exchange step, a hydrophobic interaction step, and a gel filtration step. This resulted in a 65-fold purification of the catalase enzyme with a specific activity of 5300 U/mg. The enzyme was purified to homogeneity as evidenced by the presence of a single band on a SDS-PAGE gel.

Comparison with molecular weight standards on the SDS-PAGE gel gave a catalase subunit size of 42 kDa. Results from the gel filtration step gave a native protein molecular weight of 178 kDa implying that each catalase molecule has four subunits. The catalase was active over a temperature range from 30° C-94° C and a pH range from 6-10 with optimum activity occurring at 90° C and pH 8.0. The enzyme was extremely stable at elevated temperatures with half-lives of 330 hours at 80° C and 6.5 hours at 90° C. Analysis of the kinetics properties of the enzyme resulted in a $K_m$ of 35.5 mM and a $V_{max}$ of 27 mM/min for hydrogen peroxide.

The enzyme also was not inhibited by hydrogen peroxide at concentrations up to 450 mM. This tolerance to hydrogen peroxide was unusual compared to other catalases in the literature that typically show inhibition at hydrogen peroxide levels above 30 mM.

The enzyme was strongly inhibited by cyanide and the traditional catalase inhibitor, 3-amino-1,2,4-triazole as is typical of most reported catalases. The catalase enzyme did not show any peroxidase activity with peroxidase substrates o-dianisidine and 2,2'-azino-bis(3-ethylbenzothiazoline-6-sulfonic acid) suggesting that this catalase was a typical monofunctional catalase. Spectral analysis of the enzyme showed a strong Soret peak at 410 nm, typical of heme enzymes. Dithionite easily reduced the enzyme resulting in a shift in the Soret peak to 419 nm that is unusual for a monofunctional catalase. Addition of cyanide to the enzyme did not result in a spectral shift. This is also unusual behavior for a heme enzyme since cyanide forms a complex with the heme and results in a red shifting of the Soret peak.

The amount and type of heme present was determined through formation of a pyridine hemochrome. This analysis showed that the catalase contained 5.5 molecules of protoheme IX per catalase molecule. This value is high compared to commonly reported literature values of 2-4 molecules of protoheme IX per catalase molecule.

The *T. brockianus* catalase was compared to two commercially available enzymes obtained from beef liver and *Aspergillus niger*. The temperature optima for the beef liver and *A. niger* catalases were much lower at 40° C and 50° C, respectively, than the *T. brockianus* optimum of 90° C. Both the beef liver and *A. niger* catalases were active over a broad pH range of 5-11 and 3-12, respectively.

These ranges are somewhat larger than the *T. brockianus* catalase that was active over the range 6-10. However, the stability of the *T. brockianus* catalase was superior to those of *A. niger* and beef liver catalases. Incubation of the respective enzymes at 75° C showed that the beef liver catalase completely lost activity after two minutes and the *A. niger* catalase lost activity after two hours, while the *T. brockianus* catalase maintained activity over 330 hours. Similarly, the *T. brockianus* catalase had better stability at elevated pH compared to the commercial enzymes.

Beef liver catalase lost all activity after 24 hours at pH 10. The *A. niger* catalase lost 40% of its initial activity at 24 hours. *T. brockianus* catalase still had 100% of its initial activity after 24 hours at pH 10.

These properties indicate that the *T. brockianus* catalase has potential for industrial use in hydrogen peroxide bleaching processes. Hydrogen peroxide use in industry is increasing, particularly in textiles, as an alternative to chlorine bleaching. Bleaching with hydrogen peroxide occurs at pHs above 9 and at temperatures above 60° C.

After the bleaching step, it is necessary to remove residual hydrogen peroxide due to interferences with subsequent dyeing steps. Since commercially available enzymes are rapidly inactivated under those conditions, it is necessary to neutralize and cool the bleach baths prior to treatment with catalase. This increases process cost since subsequent steps occur at elevated pH and temperature. Use of *T. brockianus* catalase would eliminate the need for the neutralization/cool down step.

The cumulative effect of budget cuts this fiscal year resulted in a reduction in work scope for this LDRD, eliminating any further attempt in FY02 to pursue genetic manipulation of urease through molecular breeding strategies. Analysis of sequence information generated for *Halomonas campisalis* has also been impacted since this requires significant labor, as opposed to the actual sequencing process, which is largely automated now.

This year, the investigators resolved the remaining lab automation issues associated with the use of the MWG Robosmart-384 for plasmid isolation, sequencing reaction preparation, cycle sequencing, and dye terminator removal. MWG and Millipore technical service staff installed a mixing station on the deck that permits mixing and re-suspension steps to be performed more quickly and reliably. Recent runs (as assessed by sequencing quality on the ABI Prism 3700 DNA sequencer) indicate quality scores equivalent to those obtained by manual processing, and with substantial reduction in staff labor.

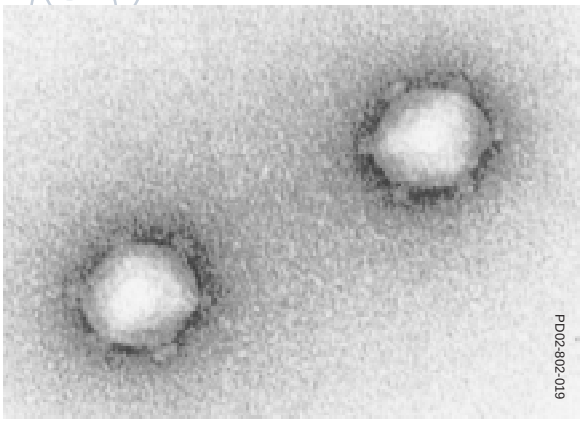


*Figure 1. Electron micrograph of a novel thermophilic virus isolated from Sulfolobus enrichments obtained in Yellowstone National Park (sequencing of this viral genome performed at INEEL). Approximate diameter 0.5 um.*

An additional 800 clones have been sequenced since the Robosmart-384 modifications were made. No attempt has been made to analyze the raw sequence information yet, but all data is archived awaiting the start of the new fiscal year.

A new version of system software for the ABI Prism 3700 DNA sequencer was installed that streamlines data handling and movement to the bioinformatics software packages and archival storage at INEEL. A commitment was obtained to support maintenance and improvement of bioinformatics resources established through this LDRD.

This work represents results from year two of a three-year project. From this work, a patent, "Method for Heavy Metal Analysis and Speciation and Biosensor for Affecting the Method" was filed in July 2002. The investigators also have signed a Memorandum of Understanding with Washington State University and Concurrent Technologies Corporation to form the Consortium for Extremophile Research (CER). The goal of CER is to further, in a collaborative manner, extremophile research conducted by the member institutions and benefit the nation and DOE by developing advanced, environmentally friendly, economical processes based on extremophilic microbes and/or their enzymes. An example of the novel viruses being recovered is shown in Figure 1.

In addition, the investigators have begun discussions with a major supplier of hydrogen peroxide for industrial uses who has indicated interest in working with the INEEL to further develop the *T. brockianus* catalase. Two presentations and one publication resulted from this research in FY02.

# New Ion Injection Technologies for Ion Trap Secondary Ion Mass Spectrometry

*Anthony D. Appelhans*

## *Using mass spectrometry to find trace toxins in our environment*

S028

Ion trap secondary ion mass spectrometry (IT-SIMS) is a unique method for studying the chemistry of surfaces and detecting trace levels of hazardous and toxic materials on environmental samples such as soil and minerals. The general technique and the associated technology have been developed at the INEEL, and six IT-SIMS instruments are currently used in applied chemistry research programs at the INEEL and other government laboratories. The laboratory's experience and knowledge in this area have led INEEL researchers to conclude that the ion injection function within this technology offers a unique opportunity to make a major technical advance; it is poorly understood, far from optimized, and little studied because of the complexity of the issues involved.

Current practice for external ion injection throughout the ion trap mass spectrometry community is based on empirically determined methods, with limited understanding of the underlying mechanisms and how they interrelate. In this LDRD, the investigators are applying a combination of computer simulations and experiments to elucidate the mechanisms, identify how the mechanisms interrelate, and develop strategies for optimizing ion injection efficiency.

In comparing simulations with experiments, the research demonstrated that a relatively simple model for ion collision dynamics sufficiently predicts the observed behavior. The model is being used to investigate alternative injection strategies. Enabling the injection of externally produced ions opens up new areas of research and application for SIMS, particularly for those cases where hazardous materials are involved. Development of this technology will support new research initiatives focused on understanding chemical speciation and fate and transport, and further development of field transportable ion trap SIMS for environmental and defense-related applications.

Technical objectives for fiscal year 2002:

- Investigate the injection and trapping process analytically using the SIMION ion optics simulation program.
- Develop and test full 3-D SIMION models that include mass/angle dependent collisional energy transfer.
- Modify an existing ion trap mass spectrometer (ITMS) to include an external ion source in which the ion kinetic energy can be varied, and that can produce ions over a broad mass range.
- Conduct experiments using the modified ITMS to calibrate the ion focusing, beam profile and collisional physics of the SIMION model.
- Measure the effect of collision gas mass and structure, and analyte mass and ion structure, on collisional losses and trapping.
- Apply the model and evaluate new ion injection optics.
- Publish results in scientific journal.

Secondary Ion Mass Spectrometry is a conceptually straightforward technique: a surface (the sample) is bombarded with energetic ions (~ 10 keV) that knock molecules and atoms off of the surface (referred to as sputtering). Some of the sputtered molecules and atoms are ionized in the process. These "secondary" ions are injected into a mass spectrometer for detection and to determine their composition.

The application of the ion trap mass spectrometer for SIMS, and the application of SIMS to environmental measurements, has been pioneered at the INEEL. A diagram of an ion trap SIMS is shown in Figure 1.

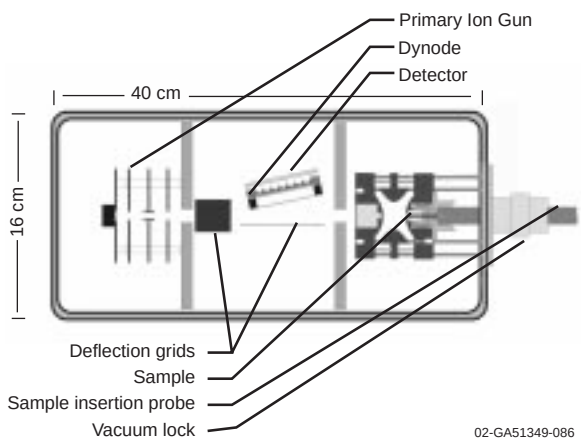


*FIGURE 1. Typical configuration of an ion trap secondary ion mass spectrometer with a sample insertion probe.*

The ion trap mass spectrometer has some unique attributes that make it particularly useful for environmental measurements. It can selectively trap ions within a one mass/charge (m/z) ratio window, enabling the "signal" to be integrated in time and space for increased sensitivity. Additionally, because the ions are trapped, they can be collisionally dissociated and their fragments collected in the trap, enabling the original ion composition to be determined with high specificity. Once in the trap, the ions or their fragments also can be reacted with other ions or neutrals, enabling the study of reaction chemistry pathways and rates. The key, then, is getting the ions into the ion trap.

An ion trap mass spectrometer has been modified to measure ion injection efficiency. Modifications included development of a split Faraday cup electron multiplier detector assembly for measuring absolute (as opposed to relative) ion collision losses and ion trapping efficiency, and development of a low-energy ion source beam line capable of producing low-energy (5 eV) ion beams for injection experiments. The instrument has been used to quantify the effect of collision gas mass and structure and analyte mass and ion structure on collisional losses and trapping.

Concurrent with the experimental effort, a detailed analytical model of the system has been developed using the ion optics program SIMION. The model includes a complete geometrical description of the ion source beam line, ion trap mass spectrometer, and the split detector assembly. Also included is a gas collision model that accounts for gas and ion physical properties, and uses a Monte Carlo approach for modeling collision probability and scattering. The model has been tested against the experimental results for a variety of ion energies, masses, and collision/buffer gases in order to establish its quantitative predictive ability. An article titled "Measurement of external ion injection and trapping efficiency in the ion trap mass spectrometer and comparison with a predictive model" was published in the International Journal of Mass Spectrometry.

The parameters that control the trapping efficiency include the energy and mass of the injected ion, the concentration (pressure) and mass of the buffer gas, and the characteristics of the ion trajectory (angle) as it enters the ion trap coupled with the amplitude and phasing of the ion trap RF voltage. Measured and calculated collisional losses (due to scattering of the ion beam by collisions with the buffer gas) using potassium and cesium ions in helium and nitrogen buffer gas were compared to establish the validity of the gas collision model used in the simulations. The results indicated that the necessary physics were included in the collision model and that the physical geometry was modeled at an appropriate resolution. This provided confidence that the model could now be used to predict performance.

Experiments and simulations were conducted to measure/predict the trapping of ions for a range of injection energies from 5 eV to 24 eV with Cs and K ions using helium buffer gas. The agreement between the experiments and the simulation was very good and provided confidence that the model can be used in a predictive manner for exploring alternative geometries.

The trapping efficiency also is dependent on the amplitude of the RF voltage, which is proportional to q (a dimensionless quantity describing the operating conditions of the ion trap). Predicting the q dependency is a very stringent test of the quality of the model because the resonance displayed in the efficiency curve is dependent on higher order fields within the ion trap, and the purity and magnitude of these fields are critically dependent on the trap geometry. Comparison of the simulations with experiments showed that the geometrical model is very representative of the actual system and is able to predict the peak in the resonance for a wide range of ion energies.

The model was used to test an alternative injection method using a large diameter aperture in the ion trap entrance covered with a fine-wire grid. Modeling indicated that if the angle of the incoming ion's trajectory was steep or could be diffracted by the grid wires, there was a higher probability of trapping. Experiments confirmed this result, demonstrating increases in trapping efficiency of up to 50% as the insertion angle increased.

The gridded end-cap design was implemented on one of the INEEL ion trap mass spectrometers in conjunction

with an electron gun for use in sample charge compensation. This combination permitted optimum ion injection efficiency while enabling control over sample charging using the electron beam. This combination has increased the ion injection efficiency by a factor of 10 for those sample types that suffered from severe charging. Figure 2 shows the mass spectra of a detergent film on stainless steel with and without the electron flood charge compensation. An article describing the electron gun and associated ion optics has been accepted for publication in the International Journal of Mass Spectrometry.

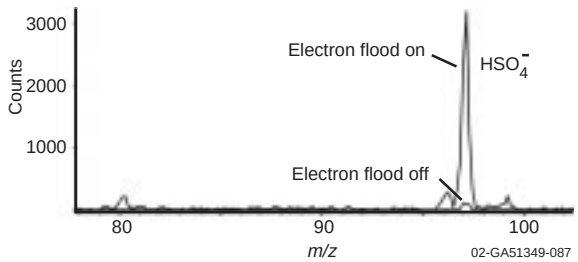


*FIGURE 2. Negative ion mass spectra of a detergent film on stainless steel taken with and without electron flood charge compensation. Signal levels were increased an order of magnitude.*

As a result of this research, the electron flood gun and associated ion optics design are being implemented in an ion trap mass spectrometer for use by the U.S. Army to detect chemical warfare agents. The modeling and design capabilities also will be applied in a program recently proposed to the Technical Services Working Group "The Rapid Identification of Terrorists, Involved with Weapons of Mass Destruction, Using Ion Trap-Secondary Ion Mass Spectrometry." The ion-molecule collision modeling capability developed and validated in this LDRD is being applied in the analysis of uranium speciation as part of the Environmental Science Research.

# Ion Mobility Spectrometry

*David A. Atkinson, Robert G. Ewing, Carla J. Miller, Keith A. Daum*

## *Expanding applications for IMS*

SC105

Ion mobility spectrometry (IMS) has become an important analytical tool for trace organic detection. With the current paradigm shift of moving analytical measurements from the laboratory to the field, IMS is leading the way with highly sensitive, handheld instrumentation that can provide real-time data. However, a lack of understanding concerning the fundamental chemical and physical processes involved in IMS has historically slowed its development.

This LDRD encompasses fundamental science experimentation involving IMS that will enhance the basic understanding of the instrument's operation. The focus of the work is to explore gas phase ion/molecule reactions and ionization mechanisms that are the core of IMS performance. An understanding of the fundamental science behind IMS allows new applications in the INEEL/DOE mission areas to be developed. This work builds upon INEEL expertise and augments IMS understanding, enabling the INEEL to develop and expand its IMS capabilities and cultivate an international reputation in IMS research.

Technical objectives for fiscal year 2002:

- Augment the current gas phase ion-molecule reaction knowledge base to provide a better understanding of the mechanisms behind IMS operation.
- Use the increased knowledge in gas phase ion chemistry to apply IMS for solutions to critical analytical detection issues.
- Provide an enhanced portable detection capability to solve problems in environmental monitoring and national security.
- Continue to nurture fruitful university ties.

IMS provides some impressive advantages in sensitivity, selectivity, portability, and response time when compared to other field analytical techniques. In spite of this, IMS is not as widely used as it could be. The amount of published literature on IMS is diminutive compared to most laboratory techniques such as mass spectrometry and infrared spectroscopy. This suggests that operational behaviors and mechanisms of IMS are not well understood. Therefore, further detailed study of the fundamental processes behind the instrument is needed to enhance the utility of IMS.

There is also a large body of untapped potential applications to which IMS would be an ideal detector, especially as field measurements become more prevalent and important. Besides being a highly useful analytical chemistry technique, IMS is finding new uses as a physical chemistry experimental tool. Gas phase ion-molecule reaction and cluster energies, as well as reaction kinetics can be studied using IMS. This knowledge is enhancing not only fundamental science understanding of gas phase thermochemistry, but also providing positive feedback into new IMS instrument designs. IMS is also finding new uses in the biological arena, both as a detection device and a macromolecular characterization tool. Gas phase conformation differences between similar biomolecules (such as stereoisomers) can be studied using IMS. It should be obvious that IMS is a high performance, multi-use, portable technology that serves as a versatile analytical and physical chemistry tool with much unexploited potential.

However, IMS does have some limitations. Notable problems have been resolution of similar analytes, masking by interfering compounds, and unpredictable responses. These limitations have generally been associated with a lack of understanding of the chemical ionization mechanisms at the atmospheric pressure conditions that determine IMS responses.

This research uncovered a number of key findings concerning the fundamental ion-molecule chemistry in IMS. First of all, the formation of reactant ions in IMS can be manipulated to allow a choice of product ions, thereby reducing the potential of interference or masking of the target chemicals. This finding is important in trying to reduce false alarm rates when using the instrument and increase the confidence level of detection.

Furthermore, through the judicious choice of reagent chemicals with certain thermochemical properties, reactant ions with a desired gas phase acidity or electron affinity can be formed that can preferentially ionize an analyte. Reagent chemicals also can be selected to promote adduct formation reactions in some analytes in order to form detectable analyte ions that can be resolved from interfering compounds. The choice of chemical to form reactant ions is important. Each chemical has a different potential for clustering with a reactant ion and clustering leads to loss of reactant ion effectiveness in product ion formation. The formation of product ions in the analysis of explosives has been studied in great detail at the INEEL, and this broad knowledge has been recently disseminated to the scientific community.

A major discovery in this work was that the ionization mechanism for TNT was found to proceed through a previously unidentified pathway. This finding is highly significant in that it allows for the detection of TNT through alternative chemical reactions, which may prove to be more sensitive or selective than the currently used methodologies. If properly controlled, drift tube reactions have the potential to drastically improve or degrade an analysis. Control of the gas flows in an IMS can be used to independently evaluate the mechanisms leading to ion formation and the influence of drift tube reactions.

Another major discovery of this work relates to the position of the hydrogen atom on TNT that undergoes abstraction during chloride or oxygen reactant ion based ionization. Work using deuterated TNT revealed that the methyl hydrogens are the only ones involved in gas phase abstraction. The position of the abstracted hydrogen has been debated in the IMS community for years. This study is the first to experimentally establish the answer.

Another debate in the IMS community concerns the separation of the TNT proton abstracted species and the TNT electron attached species. The debate has centered on the small difference in Ω (collisional cross sectional area) between the two species, since TNT is a fairly rigid molecule and should not undergo a large conformational deformation after abstraction. This argument is backed by the fact that many ions do not show a change in mobility with a change in water cluster number. A study in this LDRD was able to experimentally determine that the difference in mobility of the two TNT ionic species is not due to a difference in Ω, but instead a difference in the dipole interaction taking place in collisions with the drift gas.

To further study ion-molecule reaction chemistry, an in-house-built IMS was coupled to a PE-Sciex mass spectrometer. The coupled instrument was custom designed to provide the ultimate in performance and flexibility. The IMS module was developed as an interchangeable source, such as the electrospray and corona discharge sources that were purchased as part of the mass spectrometer system. This setup allows for fast (five minute) changes between the front-end systems. The system was intended to study gas phase ion-molecule reactions that occur in IMS and provide mass identification of IMS peaks. Thus, the IMS was designed completely around this concept, with a custom gate driver, a novel corona discharge source, and a large volume drift tube implemented to allow for optimal conditions to study the reaction chemistry. This custom designed instrument was key in collecting the data for some of the publications resulting from this project (Fig. 1).

Applications and deployment have also played a role in this research. One major application studied concerned the detection of nitrocellulose using IMS. The use of gunpowders in the manufacturing of pipe bombs has always been a concern to police departments throughout the country. Gunpowders typically consist of nitrocellulose, nitroglycerin, and dinitrotoluene. All three of these components are difficult to detect with common trace explosive detectors due to the degradation temperature. Terrorists also have begun making their own nitrocellulose since it can be carried onboard aircraft without being detected by x-ray systems or trace explosive detectors.

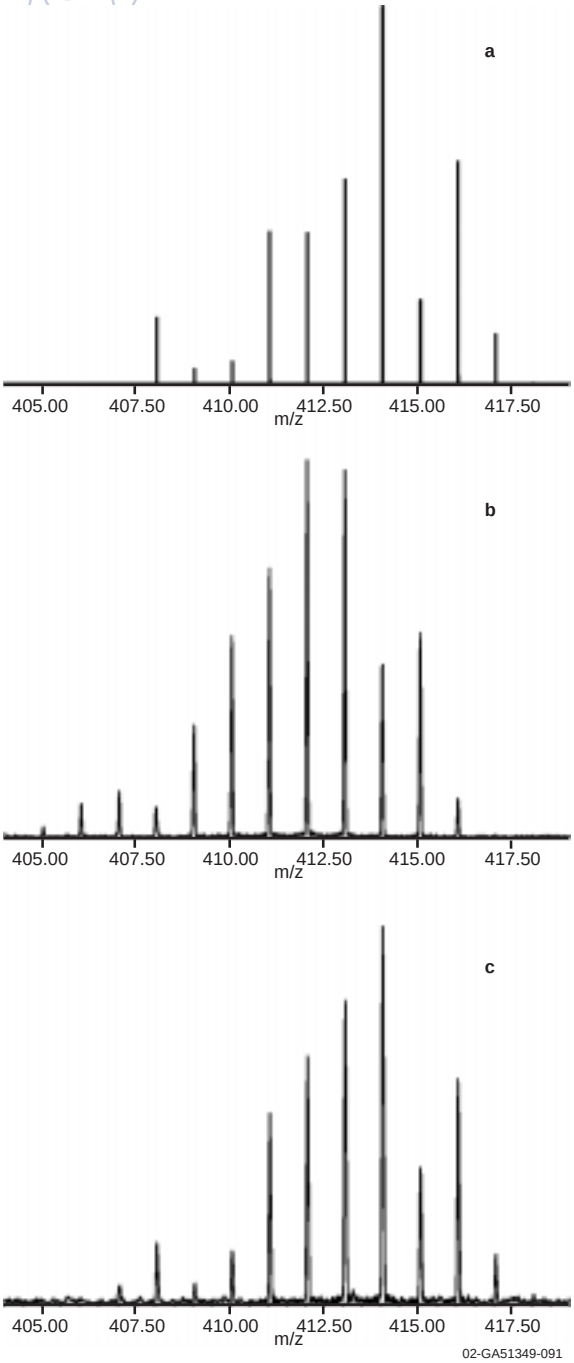


*FIGURE 1. Atmospheric pressure ionization mass spectrometry of chlorinated ethanes illustrating pseudo-molecular ion formation.*

A technique has been developed (a patent application has been filed), for the detection of nitrocellulose using ion mobility spectrometry. The currently marketed ion mobility spectrometry (IMS) instruments cannot readily identify nitrocellulose. If IMS provides any signal at all, it is typically just a nitrate peak. This is not enough to uniquely identify nitrocellulose from the host of other chemicals and materials that may provide a nitrate background peak (such as cured meats). The nitrate peak appears as a shoulder on the chloride reactant ion peak, making it difficult to discern the two peaks in many cases. The novel technique developed allows for the detection of the nitrocellulose using a discrete peak located to the right of both the nitrate and chloride peaks in the spectrum. The technique is easily adapted to commercially available instruments, greatly enhancing instrument detection capabilities.

Another study looked at vapor detection, rather than the typical particle-based detection of plastic explosives. The vapor detection of plastic explosives is difficult due to the low-vapor pressures of explosive components (e.g., RDX and PETN) present in the complex elastomeric matrix. To facilitate vapor detection of plastic explosives, detection agents (taggants) with higher vapor pressures can be added to bulk explosives during manufacture. This task investigated the detection of two of these taggants, ethylene glycol dinitrate (EGDN) and 2,3-dimethyl-2,3-dinitrobutane (DMNB), using a hand held ion mobility spectrometer. The two taggants were detected both from neat vapor sources as well as from bulk explosives (NG-dynamite and C-4 tagged with DMNB). EGDN was detected from NG-dynamite as $EGDN.NO_3^-$ at a reduced mobility value of 1.45 $cm^2V^{-1}s^{-1}$ with detection limits estimated to be about 10 $ppb_v$. DMNB was identified from tagged C-4 as both negative and positive ions with reduced mobility values of 1.33 $cm^2V^{-1}s^{-1}$ for $DMNB.NO_2^-$ and 1.44 $cm^2V^{-1}s^{-1}$ for $DMNB.NH_4^+$. Positive ions for cyclohexanone were also apparent in the spectra from tagged C-4 producing three additional peaks.

A main goal of the IMS project at the INEEL has been to enhance capabilities through close collaboration with university partners. Ties with university collaborators continued through this research, as Washington State University and Montana State University made significant contributions to manuscripts in preparation for publication. A highlight of FY02 university collaborations was having Professor Peter Harrington from Ohio University take a faculty sabbatical and spend a year at the INEEL working closely with chemistry department personnel. This project benefited greatly with enhancements in IMS data interpretation and chemometrics skills in the IMS group. Professor Harrington was also invaluable in collaborating on IMS application projects.

IMS is becoming more widely used all the time yet the fundamental understanding of the technique is weak. This presents a tremendous opportunity to not only push the envelope of understanding, resulting in scientific publications, but to move this understanding into new application areas, resulting in intellectual property and new business. Sensitive, field-deployable chemical detectors are the wave of the future for environmental and national security needs. IMS fills the bill, but a greater understanding of the technique is needed to use it effectively and to its full potential. Fundamental science studies, such as those performed in this project are necessary to maintain the viability of technique to respond to new application challenges in INEEL and DOE mission areas.

# Advanced Control Architectures for Human-Robot Synergy in Complex Domains

*David Bruemmer*

## *Robot "autonomy" offers peer-peer interaction*

ET116

Intelligent robots provide the potential of reducing operator workload and error while promoting safety and efficiency for remote tasks in a variety of environmental, military and industrial applications. As robotic systems move toward cooperative, integrated and autonomous functioning, it is expected they will be able to duplicate and extend human dexterity, perception, and overall work efficiency.

This LDRD effort is investigating a remote characterization robotic system that can adjust its level of autonomy during a task, leveraging its own intrinsic intelligence to meet whatever level of control is handed down from the user. This research can pave the way for a new class of mixed-initiative robots that work with humans as well as for them, accepting high-level tasks with minimal demands on the user. Some of these tasks include enabling remote sensor deployment (already relevant to ongoing site operations) to be accomplished in days rather than months. A fieldable robotic system, including software control architecture, interface systems, robotic hardware and sensor suite, also can accomplish a host of challenging remote characterization tasks.

Technical objectives for fiscal year 2002:

- Implement sliding autonomy to support changing communication, cognitive, perceptual and action capabilities of the user and robot.
- Develop self-monitoring capabilities and continuous assessment of perception and behavior performance.
- Develop an innovative, customized communications protocol to support adjustable autonomy interactions over long distances and through cluttered environments.
- Develop simultaneous localization and mapping techniques that capture an abstracted representation of the robot's experience vis-à-vis the task and environment.
- Develop sensor-suites and fusion algorithms to enhance perception capabilities for sensing, interpreting, and "understanding" environmental features and humans, including thermal imaging sensor, scanning laser, sonar and infrared (IR).
- Develop a novel graphical interface for mixed-initiative interaction between robots and humans.

Research to date (Fig.1 next page) has resulted in development of a control architecture, supporting the following modes of remote intervention:
1) Teleoperation, 2) Safe Mode, 3) Shared Control and 4) Full Autonomy.

***Teleoperation*** — The interaction substrate used in previous INEEL teleoperated robotic systems was revamped based on feedback from people who have deployed such systems. Within teleoperation mode, the user has full, continuous control of the robot at a low level. The robot takes no initiative except to stop, once it recognizes that communications have failed.

***Safe Mode*** — Within safe mode, the user directs the movements of the robot, but the robot takes initiative to protect itself. In so doing, this mode allows the user to issue motion commands with impunity, greatly accelerating the speed and confidence with which the user can accomplish remote tasks. The robot assesses its own status and surrounding environment to decide whether commands are safe.

***Shared Control*** — The robot takes the initiative to choose its own path, responds autonomously to the environment, and works to accomplish local objectives. The robot responds to its local (~ 6-10 meter radius), sensed environment and handles low-level navigation and obstacle avoidance. The user supplies intermittent input, often at the robot's request, to guide the robot in general directions. The problem of deciding how and when the robot should ask for help has been a major line of inquiry and will be a major issue in upcoming human subject experiments.

***Full Autonomy*** — The robot performs global path planning to select its own routes, requiring no user input except high-level tasking such as "follow that target." The robot can operate for long periods of time in this mode with no human intervention and has the ability to make decisions about the task and respond to changes in the environment.

*FIGURE 1. Intelligent robot is part of teleoperated robotic system.*

*FIGURE 2. Specialized interface on a touch-screen tablet PC.*

For each of these levels of autonomy, perceptual data is fused into a specialized interface that provides the user with abstracted auditory, graphical and textual representations of the environment and task that are appropriate for the current mode. Currently, this interface is used on a touch-screen tablet PC (Fujitsu Corp.).

Within this interface (Fig. 2), blockages are shown as red ovals and resistance to motion is shown as arcs emanating from the wheels. The robot relays a great deal of synthesized, high-level information (including suggestions and requests for help) to the user in a textual form, using the feedback textbox within the image window. The robot also provides textual reports on environmental features at the bottom of the map window and reports on communications status at the bottom of the robot status window. The robot status window provides a variety of information about the robot including pitch and roll, power, heading, and speed, as well as a fusion of this information into a single measurement of "health." The user can move the robot by touching the arrows or a joystick. It is possible to pan and tilt the camera automatically by touching regions of the visual image.

Integration of real-time localization and mapping was also accomplished in FY02. As the robot travels through its environment, it builds a map "on the fly." As this task is further developed, the interface will allow a number of autonomous tasks (e.g., searching a specified region or going to a goal location) to be issued by interacting with the map itself.

These levels of operator intervention can greatly improve on the options provided with a strictly teleoperated system such as those currently used for urban search and rescue, military operations and remote characterizations of hazardous DOE environments. The human user can switch between these modes to cope with different components of the task. For instance, when a user wishes to move into a new room he/she simply points the robot at a door and then allows the robot to guide itself through the doorway – a task that requires today's robot operators many minutes of trial and error.

The control architecture was "taken to task" by having real robotics operators from different domains, including search and rescue, military, and nuclear industry, to actually drive the system and evaluate it. With no exceptions, operators have declared the interface and, in particular the ability to switch levels of control, to be a great asset. In the words of a chief of search and rescue operations at the world trade center: "Before using the INEEL system, I believed there was no place for

autonomous systems within a search and rescue environment. After using their system, I believe that the 'autopilot' capabilities will be a great asset."

The latest development, and perhaps the most innovative aspect of this LDRD project to date, is that a "theory of human behavior" has been imparted within the robot's intrinsic intelligence, enabling the robot to assess human performance. The "theory of human behavior" allows the robot to switch modes when communications has been interrupted or when the robot recognizes that the human is performing poorly. For example, the robot might switch modes when the human has repeatedly placed the robot or the environment in danger, or when the human has been unsuccessful in extricating a robot from a cluttered area. Although the human can ultimately override this capability, it provides a means for true peer-peer interaction.

This LDRD research has already spurred significant interest among government agencies and private industry. The U.S. Army is having the control architecture transitioned onto a number of its robots. In addition, demonstrations at Ft. Leonard Wood have led to INEEL inclusion in the development of countermine behaviors for autonomous army robots. Several major robotics companies, including iRobot, Remotech and RTI have expressed interest in this technology.

# Detection of Buried Objects Using Imaging Laser Acoustics

*Vance A. Deason, Kenneth L. Telschow, Scott Watson*

## *Unearthing land mines with full-field, real-time imaging*

SC113

Acoustic waves have long been used for seismic exploration within the depths of the earth. However, locating buried objects near the surface requires very high spatial resolution due to the need for higher acoustic frequencies that are appropriate for small objects in the near field. Heterogeneity, porosity and multiphase composition significantly complicate the acoustic wave propagation and depth of penetration. Nevertheless, acoustic techniques and particularly laser-based single-point measurement techniques, have been shown to successfully detect and locate buried objects such as land mines.

This LDRD project extends this approach to full-field real-time imaging for simultaneous detection and location of buried objects in the near surface terrestrial environment. Specifically, the goal is to demonstrate the use of the INEEL Laser Ultrasonic Camera for locating buried objects using ultrasonic imaging techniques developed at the INEEL. Improvements in these techniques will benefit U.S. interests in humanitarian and military de-mining, and in the environment.

Technical objectives for fiscal year 2002:

- Demonstrate low frequency (~ 15 kHz) acoustic imaging operation.
- Determine large-area operation limitations using available laser equipment.
- Capture images of acoustic waves propagating in sand.
- Capture images of acoustic waves interacting with buried objects.

The INEEL Laser Ultrasonic Camera is used to directly image, without scanning, acoustic or ultrasonic waves on the surface of any object. Real-time video images show the location (relative phase) and magnitude of the waves and how they interact with defects, cavities, and internal geometry, or changes in material composition. This interaction may involve absorption, reflection, scattering, diffraction, refraction and interference effects as the waves contact the buried object or feature. Figure 1 shows an image of acoustic waves reflecting from a buried object and then interfering with the main wave, using the INEEL Laser Ultrasonic Camera. By analyzing such effects, one can gain information about the properties of a hidden object.

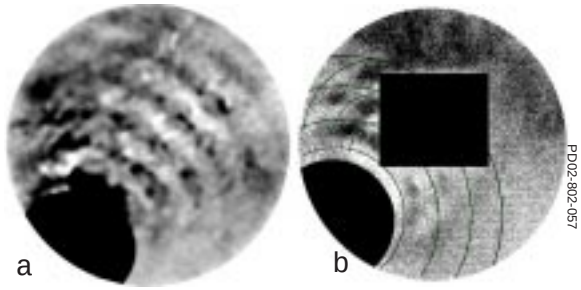


*FIGURE 1. INEEL Laser Ultrasonic Camera image of acoustic waves in sand: circular object is sound source. The left image shows waves with no buried object, while the right image shows waves reflecting from a buried rectangular object. Circular lines have been superimposed to help in visualizing the wave fronts.*

While loose material such as sand or soil are not ideal media for propagation of acoustic waves, it has been amply demonstrated that acoustic detection of buried land mines is both feasible and practical. Figure 2 (next age) summarizes some of these data. Figure 2a shows a theoretical model of acoustic wave interaction with a buried land mine. Figure 2b shows actual data taken on three buried objects by a scanning acoustic detector. Such scanned images are typical of conventional acoustics and slow to acquire. They also have poor resolution. The INEEL Laser Ultrasonic Camera promises to offer a better way.

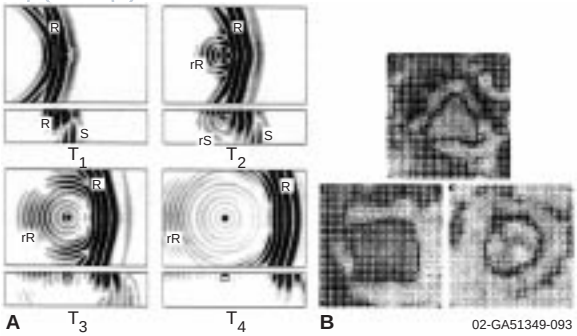


*FIGURE 2. Supporting data from other sources. A) Theoretical simulation of the interaction of surface waves with a buried land mine showing the ringing produced by acoustic excitation of the object. B) Images made by scanning a point detector over the area. Buried triangular, square and round objects are shown. (Images taken from Detection and Remediation Technologies for Mines and Minelike Targets V [2000]: "Three-dimensional FDTD model to study the elastic-wave interaction with buried land mines" [Schroder and Scott], and "Shape discrimination of buried objects using an acoustic land mine detection system" [Lafleur, Sabatier, et. al.], respectively).*

***Experimental Data*** — A large container was partially filled with construction sand to provide a test bed for efforts to develop excitation and detection methods. The sand was a light brown color and rather coarse. After trying a number of excitation techniques, a simple acoustic speaker with a metal throat was found to provide the best excitation transducer. The metal exit port of this speaker was placed in direct contact with the sand and angled to emit sound waves in the general direction of the observation area. This area was originally about 45 cm across, but was reduced to 20 cm to better focus on the limited area excited by the speaker. A laser illuminated this area with an intensity of about 6 mW/cm$^2$. The reflected light was collected by a lens about one meter away so as to form an image of the target area. This reflected light picked up information about the vibrations present everywhere on the observation area. The INEEL camera demodulated this signal to provide a real-time, full-field image of the vibrational wavefront amplitude and distribution on the surface of the sand.

The images produced by the INEEL camera were recorded by a digital video camera and stored on a computer for display and further processing. Figure 2 shows a typical image of the distribution of wavefronts. The waves have amplitudes of only a few nanometers, and the image is composed of as many as 1,000,000 independent pixels (simultaneous independent measurement points). It is extremely difficult to make such sensitive measurements without isolating the object on a special table that prevents floor vibrations from overwhelming the results. However, the INEEL camera was able to record such nanometer waves even though the sand box sat directly on the lab floor. The investigators believe there are several enhancements that could further improve the rejection of environmental noise that is usually far larger than the desired data.

***Data*** — The image in Figure 1a, taken by the INEEL Laser Ultrasonic Camera on sand, shows 16 kHz waves traveling out from a source (black circle) and interacting with a buried square object (Fig. 1b), whose location is also marked in black. While this preliminary result is very encouraging, several areas need further improvement before this method can become a useful field technique.

Others have demonstrated similar results using more conventional techniques based on scanning point measurements. Figure 2a shows a simulation of acoustic wave interaction with buried mines, where resonant vibration of the mine is visible long after the excitation wave passes. The images also show that resonances of typical land mines can be distinguished from those of buried rocks and sticks. Figure 2b shows actual data taken of acoustic wave interactions by scanning over buried objects of different geometries (triangular, square and circular plates).

These results are significant in that this project has demonstrated a new method for detection of acoustic vibrations as images, and specifically on coarse sand or soil. Compared to other techniques, this method has far

higher spatial resolution (number of pixels), excellent sensitivity to acoustic vibration, and good rejection of environmental noise. It is also potentially much faster. All other techniques require a laborious point-by-point scanning by a detector to slowly build up an image. Because of the time required, such competing methods rarely produce images with more than a few dozen or a few hundred points, producing a very coarse image.

The technique demonstrated in this project provides full digital imaging resolutions limited only by the resolution of the camera (currently several million, but commercially available camera resolution is increasing rapidly). Each pixel is an independent measurement of the acoustic amplitude at the corresponding point on the original object surface. This method promises to provide improved functionality for military and humanitarian de-mining efforts, and for near-surface probing for a variety of industrial and environmental purposes.

As a result of this year's work, the investigators have identified the following needed improvements:

- Improved utilization of light to decrease laser size.
- Reduced sensitivity to environmental noise.
- Improved excitation method.
- Test data on realistic mine models.

National Security, DOE, Defense Department (Army, Navy, DARPA) and international de-mining efforts all have strong interest in and have funded conventional mine detection efforts. The method presented in this LDRD is both novel and powerful enough to gain external funding, if sufficient success can be demonstrated to overcome the prejudice for orthodox solutions to this problem.

Collaboration was initiated in late FY02 with the CenSSIS consortium at Northeastern and Boston Universities, and with Pacific Northwest National Laboratory to work on data analysis and interpretation.

# Behavioral and Control Modeling for Large-Scale Micro-Robot Systems

*Don D. Dudenhoeffer*

## *Getting robots to work together*

H062

Development of autonomous vehicles to support and supplement human operations is a critical area of research for DOE and DOD. The DOE has identified the potential for distributed robots to play a role in reducing cost, improving worker health and safety, augmenting product quality and increasing overall productivity. Additionally, the U.S. Army's Future Combat Systems (FCS) initiative calls for the integration of unmanned autonomous forces with human soldiers.

The area of robotics is vast. This LDRD is exploring the challenging area of large-number deployments of small robotic elements. The objective is to evaluate command and control (C2) architectures that permit deployment and operational tasking of many small to mid-sized robots. The problem of creating coordinated social behavior from simple, reactive behavior sets is not easily solved. In previous work, the INEEL has developed and tested C2 architectures using computer simulation. Now the goal is to port the resulting C2 architecture onto a collective of cost-effective, small, mobile robots to address real-world issues surrounding deployment and tasking.

For large numbers of robots to be deployed as a viable force, human users must be able to interact with functional units – strategic groupings of robots – rather than issue commands to each individual robot. Instead of the user exerting global, centralized control from above, this project is evaluating individual robot behaviors that can promote the emergence of "swarm intelligence," as seen in a colony of ants or swarm of bees.

While the focus of the project is on collective performance, each individual robot acts in a fully distributed, autonomous fashion using highly robust suites of sensors and behaviors. To enable useful group behavior, the investigators have developed an innovative, multi-modal communication architecture consisting of acoustical chirping, and infrared and radio frequency (RF) communications.

Technical objectives for fiscal year 2002:

- Determine command and control architecture to communicate human intent to the collective, including the ability to reposition and reshape the collective.
- Create an operator interface structure for visualizing the collective behavior and issuing real-time commands.
- Demonstrate the command and control architecture and operator control unit supporting a human operator in working with a team of robots.
- Explore integration opportunities into INEEL site operations.
- Present research in technical papers and expose to peer groups for review and discussion.

For FY02, the project had two thrust areas. The first focus was the development of emergent behaviors and the command and control system that supports the deployment of heterogeneous teams of robots. The second thrust centered on the integration of heterogeneous robotic platforms together to perform INEEL operations-relevant tasking.

Using a team of small, sensor-rich robots and a larger, Parent robot, the investigators explored the problem of how to enable flexible, adjustable autonomy control for a multi-robot remote characterization task. To accomplish the task, the robot team must autonomously deploy into a building, efficiently search through corridors and rooms to locate a spill, and then cooperatively form a perimeter around the chemical spill, once found. The system should be able to accomplish these objectives with human input varying from complete to none at all.

Social potential fields were implemented on a collection of 12 robots using a combination of infrared obstacle avoidance, light sensing and audible chirping. The effect is that each robot exerts both an attractive and repulsive force field. The attractive field, based primarily on sound, can either discourage robots from moving too far away (an essential aspect of stable swarming behavior) or can actively pull other robots toward it as in the case of the "come hither" chirp emitted by a robot that has found an area of interest, such as a spill. The repulsive field discourages robots from coming too close and is comprised of sound (robots avoid chirps above a certain volume) and the various obstacle-avoidance sensors, which include infrared, light sensing, and bump sensing as a last resort.

Social potential fields provide a basis for online adaptation. By adjusting these fields based on bumps and

turn frequency, the robots can automatically adapt themselves to various environments and changing swarm densities. The investigators believe such an approach is uniquely appropriate for distributed systems, especially as systems are scaled toward large numbers of very small-scale, resource-constrained robots. For one thing, the sensors involved make minimal demands of cost, size, and processing power. In addition, this intrinsic means of behavior modulation system permits a user to control swarming behavior at a high, abstract level. Most importantly, it provides the swarm with a means to automatically regulate itself.

To support human-robot interaction, a graphical user interface (GUI) was developed that allows hierarchical tasking for groups of robots. This software was married to individual robot behaviors and a multi-modal communication architecture comprised of radio, infrared, and audible chirping. The ability for the robots to chirp and respond to chirps is the basis for the implementation of social potential fields – attractive and repulsive forces that can promote grouping behaviors between adjacent entities such as might be seen in a flock of birds or a school of fish.

Through coverage experiments in a test-bed environment, it was found that social potential fields provide a means to control a variety of emergent swarm effects including swarm size, swarm density, and swarm translation. Figure 1 represents a group of the robots after having found and surrounded a mock hazardous spill using the chirping behavior.

The second thrust this year centered on the integration of heterogeneous robotic platforms to accomplish INEEL operations-relevant tasking. An appropriate operations-relevant task was found at the INEEL Power Burst Facility (PBF). Shawn Parkinson who works in Mixed/Hazardous Waste Management at PBF described a need for a small robotic vacuum cleaner that would randomly and constantly operate in one of the waste storage facilities. While this application represented the development of an individual unit, it also represented an opportunity to explore the paradigm of robotic team

*FIGURE 1. Five robots form a perimeter around a water spill.*

coordination. In previous work, the use of small disposable robots was evaluated to find a hazardous spill. This new application represented the next step; that is, teaming the small robots with a larger robot to clean up the spill.

To this end, a robotic vacuum named HARV (Hepa-filtered Autonomous Robotic Vacuum) was developed (Fig. 2). The concept is to allow tele-operation of HARV and support integration of HARV with a team of smaller robots. In this scenario, the smaller robots enter a room to conduct a characterization and mark any contaminated areas. HARV then enters the scene and is directed by the smaller robots to the priority areas for cleanup.

*FIGURE 2. Robotic vacuum named HARV.*

The HARV chassis is built on an existing platform developed several years ago to demonstrate the operability of articulated axle/wheels for improved mobility over obstacles. The chassis was resurrected for this project. The micro controller is based on an Onset Computer's Motorola 68332. The robot control and communications interface board was designed at the INEEL for the micro-UAV project and is being tested for other applications. A sonar sensor system has been integrated for detecting objects and to assist in navigation. The investigators also have the ability to integrate a camera system on HARV to allow the operator to direct motion and assess the hazards in the area. HARV has teleoperation capabilities, but also has autonomous behaviors.

This project has been essential for the INEEL's involvement in the "Swarm" robotics community. The research has laid the foundation for past, current, and future projects in a research area, which previously did not exist at the INEEL. Of specific note are the opportunities this research has opened with the Defense Advanced Research Projects Agency (DARPA), by providing the research foundation to position INEEL for future projects. The development of HARV also presents an opportunity to support operations at the INEEL if developed beyond the prototype unit.

This LDRD has developed experience and national recognition for this type of research and resulted in one new hire at INEEL.

# Characterization of Legacy Risk

*Steven A. Eide, Robert L. Nitschke*

## *Improving long-term risk information and performance indicators*

PH102

A key issue related to the INEEL strategic thrust in environmental management (EM) is the evaluation of risk from environmental waste in its present state or in its end state for long-term stewardship. The purpose of this LDRD project is to comprehensively characterize the legacy, or long-term, risk burden from environmental waste. This work includes the development of a strong foundation for the concept of legacy risk for hazardous waste materials and applying it to the INEEL EM program.

Appropriate characterization of legacy risk allows a variety of risk comparisons to be performed. These include prioritization of site and DOE complex environmental wastes, evaluation of the risk effectiveness of waste management programs, site and DOE complex risk reduction (by year) as waste management programs progress, and the evaluation of risks of various proposed end states. Such risk information is an essential input to complex environmental decision-making. This information also helps explain DOE EM programs to stakeholders, and provides risk-based performance indicators to monitor DOE EM progress in the cleanup area.

Technical objectives for fiscal year 2002:

- Develop a comprehensive risk framework concept for EM program analyses that enables a variety of risk analyses and comparisons.
- Complete development of the Environment, Safety, and Health Risk Assessment Program (ESHRAP) technical models and software to support the risk framework.
- Present papers on the ESHRAP software, the comprehensive risk framework concept, and the legacy risk concept at technical workshops and conferences.
- Apply the risk framework and legacy risk concepts and ESHRAP software to support the identification and evaluation of alternatives considered by the INEEL in its plan to accelerate cleanup and reduce risk (the “2012 top to bottom” review).
- Apply the risk framework concept and ESHRAP software to support risk-ranking of facilities at INEEL that will undergo decommissioning (D&D), including development of D&D models for ESHRAP.

This LDRD identifies and evaluates ways to measure legacy risk of environmental waste. Legacy risk measure provides a means to estimate the long-term risk from environmental waste at any point in its life cycle. The potential benefits of such a risk measure include the ability to prioritize environmental wastes (as they presently exist) with respect to ES&H risk, and to measure the reduction in site risk resulting from EM activities. When combined with estimates of the risk from such activities (using a code such as ESHRAP), the risk benefit versus risk cost can be evaluated for any activity or entire programs. In addition, the comprehensive risk information contained in the legacy risk measure and ESHRAP analyses of EM programs provides valuable input to complex decision-making. These risk applications can be applied at a single DOE site or to the entire DOE complex.

Technical tasks for this research include: refinement of the legacy risk concept; assurance of completeness in long-term risk scenarios; issue identification and evaluation; trial application at the INEEL; consideration of uncertainty and sensitivity; and, path forward. Work during FY02 focused on three main efforts: completion of the ESHRAP technical models and software to support legacy risk analyses; addition of D&D and long-term stewardship models; and, initial support to INEEL projects.

To guide the completion of the ESHRAP technical models, acceptance criteria were developed. The vadose zone and groundwater simplified models were refined and expanded to include multiple indicator radionuclides. The investigators expanded legacy risk intruder modeling to include a variety of types of intrusions – scavenger, residential, and drilling crew – with multiple options for frequencies, durations, and numbers of individuals involved. Models also were reviewed for opportunities to reduce conservatism to more closely approach best estimate. As part of this effort, recent DOE data were statistically analyzed to obtain up-to-date injury, death, and radiological exposure rates. Finally, documentation was begun of the technical models and software implementation.

Another major effort in FY02 was the development of D&D models for ESHRAP. As part of this effort, a Master of Science candidate collected and analyzed personnel and exposure data from DOE D&D projects. These data were used to develop the D&D models for ESHRAP.

For the third main effort, the legacy risk concept and the ESHRAP software were used to support two major INEEL planning activities. The first application supported the identification and evaluation of alternatives considered by the INEEL in its planning to accelerate cleanup and reduce risk (the "2012 top to bottom" review). Sample results are presented in Figures 1 and 2. Without the use of the legacy risk concept, neither of these types of risk comparisons would be possible. The legacy risk concept and ESHRAP software were applied to support the risk ranking of facilities at the INEEL that will undergo D&D.

This LDRD provided support to both a Ph.D. student (the principle investigator) and an M.S. student. Their thesis work included further development of the legacy risk concept and the ESHRAP code, and the development of D&D models for ESHRAP.

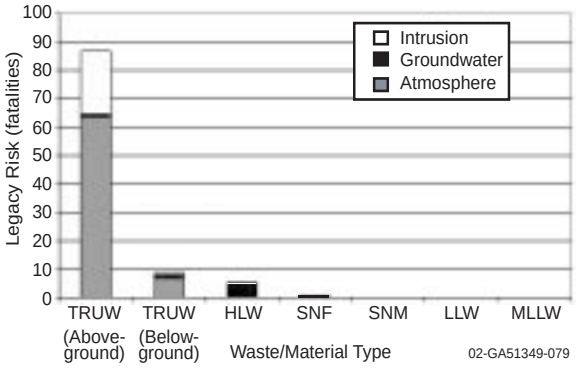


*FIGURE 1. INEEL waste material legacy risk ranking.*

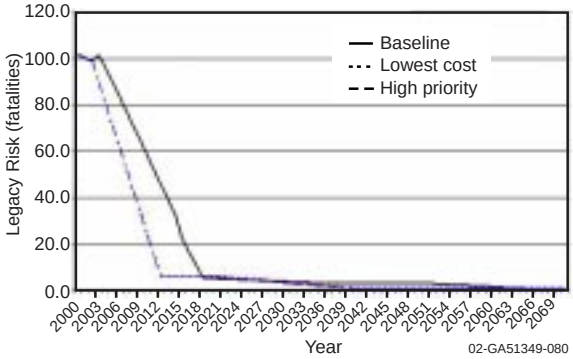


*FIGURE 2. INEEL legacy risk reduction with time for various program alternatives.*

Insights from this year's work confirmed that the comprehensive risk picture approach using the ESHRAP software is on the right track. The approach incorporates (or will incorporate) all of the risk characteristics identified by stakeholders. It also was found that no other DOE site presently has the capability to develop the comprehensive risk picture envisioned for the INEEL.

Work in FY03 will include a quality assurance of the technical models and ESHRAP software implementation, completion of the ESHRAP documentation, consideration of uncertainty and sensitivity analyses, and a sample application to an INEEL program such as the 3100 $m^3$ program to characterize and ship transuranic waste to the Waste Isolation Pilot Plant. This program will be completed in 2003. Thus, the application will include both prediction of ES&H risk from the program and comparison of results with actual data.

This LDRD is supporting DOE EM efforts by developing risk-based performance information for better decision-making, and performance indicators for tracking cleanup progress.

# Controlled Growth of Nanowires

*James R. Fincke, Tim Hyde*

## *An important building block of next-generation devices*

NC102

Nanowires with controlled nanostructure are the building blocks and interconnects from which true nanosized electronics, sensors, mechanical devices, and nano electro-optical devices will ultimately be constructed. This LDRD focuses on the controlled synthesis of 1-D nanostructures, nanowires and nanotubes, using plasma-assisted chemical vapor deposition (PACVD).

Technical objectives for fiscal year 2002:

- Demonstrate growth of metallic nanowires.
- Measure electrical characteristics of metallic nanowires
- Demonstrate prototypical nanowire sensor configuration

This LDRD successfully grew silicon nanowires using the PACVD system developed for this program. The PACVD system was based on a microwave-generated plasma. Figure 1 shows the silicon nanowires that were grown on a silicon substrate coated with an iron catalyst. Tetramethyl Silane was disassociated in the plasma to form the silicon ions that were used as the building blocks for the nanowires.

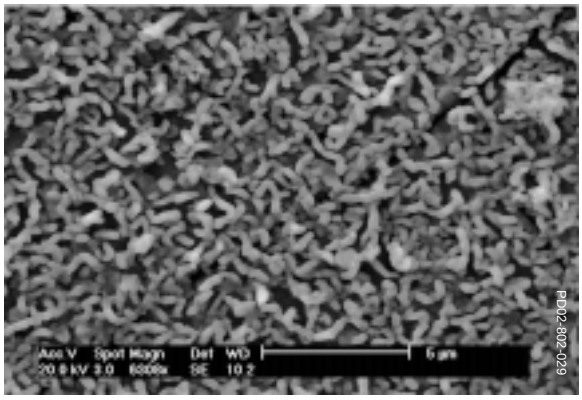


*FIGURE 1. Silicon nanowires formed using a microwave plasma-assisted chemical vapor deposition process.*

Significant effort was expended in attempting to grow Tin (Sn) nanowires. This effort involved Bismuth (Bi) coatings as the catalyst and then disassociating Tetramethyl tin. Although tin structures were formed, no nanowires were produced. The attempt was made to form tin wires that could then be oxidized to form tin oxide ($SnO_2$) that in turn, could be used to form CO sensors and doped to make sensors for other gases.

This LDRD also attempted to develop a process that would grow nanowires to be incorporated into a nano circuit. Figure 2 shows several carbon nanotubes that were grown on electrically insulating silicon oxide from a Nickel catalyst base. The concept was to use a combination of masking and metal deposition to form electrical connections on either end of the tube(s). The electrical properties of the tube could then be measured under various conditions. Time, funding and the technical complexity of forming nano circuits prevented this task from being completed.

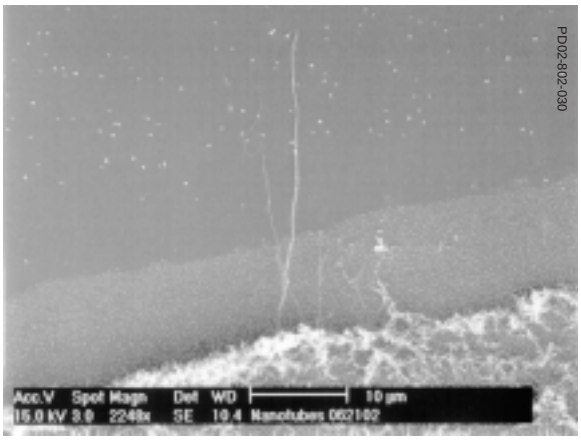


*FIGURE 2. Carbon nanotubes on silicon oxide substrate, originating from Ni catalyst particles.*

This project resulted in the construction of a laser ablation system and a microwave plasma system. In addition, a radio frequency (RF) plasma chamber was largely completed. The work was expected to continue in FY03. However, since the principal investigator, Jim Fincke, a Science Fellow, left the company, funding was not continued for FY03. The equipment built/reassembled for this project will be retained and evaluated for usefulness in other projects and programs.

# Use of Engineered Nano-Particles for Nutrient Delivery and Bioremediation in Subsurface Environments

*Yoshiko Fujita, George Redden, Glenn Moore*

## *Delivering food to microbes for bioremediation*

ET114

Effective subsurface bioremediation requires the simultaneous co-localization of contaminants, capable microorganisms, and nutrients for microbial stimulation. The objective of this LDRD is to demonstrate that synthetic colloids can be used to deliver nutrients in porous media for in situ bioremediation.

This project addresses the need to prevent biofouling caused by nutrient use at an injection point, and the need for more effective nutrient delivery to contaminated zones. The investigators are focusing on the development and application of particles that can transport and release nutrients in a delayed or time-release fashion. The project includes colloid synthesis, evaluation of colloid and nutrient transport, verification of nutrient utilization and microbial growth, and development of a model to describe the delivery process.

Demonstrating the application of synthetic colloids for targeted nutrient delivery will be a significant contribution to in situ bioremediation, a technology of great interest to DOE with its legacy of subsurface contamination. This project is an integral part of an active and growing INEEL research program focused on environmental colloid science. Other program elements include LDRD projects to explore mass transfer of surface-active species on and off of colloid surfaces, and to characterize natural colloids in the Snake River Plain Aquifer system. These projects operate synergistically, and together benefit DOE with respect to the development of new, potentially cost-saving remediation techniques as well as increased understanding of the role of colloidal particles in contaminant transport.

Technical objectives for fiscal year 2002:

- Evaluate colloid synthesis and phenol incorporation techniques.
- Develop capability to assay microbial cells for phenol exposure.
- Design and construct prototype columns for transport experiments.
- Evaluate models for colloid transport and release of substrate.

Colloid synthesis activity in support of this project initially focused on processing of mesoporous silica colloids using the sol-gel process. In this process, a silicon ethoxide was hydrolyzed and then condensed in the presence of either an ionic or nonionic surfactant. A variety of formulations were prepared, based on the published literature.

Several problems were encountered with this process. Namely, narrow size distributions were not obtained in the submicron regime, and the pyrolysis step used to remove the templating agent created significant agglomeration or sintering of the colloidal particles. It also was established that the two nutrients tested for this project, phenol and sodium lactate, were too quickly released from the 20-30 nm pores of the silica colloids. Thus, the desired time-release characteristics were not realized.

In the second half of FY02, polymeric colloidal synthesis approaches were investigated. It was determined that the poly (propylene carbonate) QPAC40 (Empower Materials, Newark, DE), a water insoluble polymer, could be dissolved in acetone and subsequently mixed with water to form 200-600 nm colloids. The colloidal particle formation occurred as a consequence of rapid acetone dilution in the system, causing condensation or precipitation of polymer. The acetone was removed by evaporation and dialysis.

The resulting aqueous colloidal suspensions were found to be stable for several months. Electrophoretic measurements determined that the QPAC colloids had a zeta potential in simulated groundwater of -17 to -20 mV, very close to that of natural colloids found in Spreading Area B soil samples (-15 mV). Efforts subsequently were made to incorporate phenol into the colloids as they formed.

Unfortunately, given the synthesis technique employed and the properties of the polymer, it was determined that an insignificant amount of phenol was incorporated into the particle. However, the particles were useful for development of protocols for column transport studies.

Most recently, the investigators have been examining other polymer systems, most notably the polyphosphazenes. Polyphosphazenes have been used for years in chemically resistant applications such as o-rings, semipermeable membranes, and biomedical applications such as dental implants. Three

polyphosphazene polymers are being evaluated for this application: poly (bis phenoxy) phosphazene, poly [diacetone D-glucofuranose- (protected sugar), trifluoroethoxy-] phosphazene, and poly (α-D-glucofuranose- (deprotected sugar), o-allyl phenol-, t-butylphenol-) phosphazene.

As a first test for colloid formation, the three polymers were dissolved in tetrahydrofuran (THF; 0.6 g of polymer in 15 ml THF) and then a few drops of the solution were dispensed into a vial of water and shaken vigorously. Precipitation of the polymers resulted in particle size distributions with mean diameters in the 175 to 240 nm range. Figure 1 is a scanning electron micrograph of the poly (bis phenoxy) phosphazene colloids.

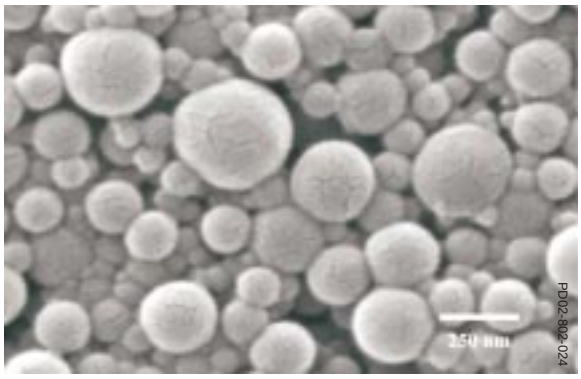


*FIGURE 1. Scanning electron micrograph of colloids synthesized from poly (bis phenoxy) phosphazene.*

The next step will be to determine whether phenol can be incorporated into the particles during synthesis. Initial tests with poly (bisphenoxyphosphazene) and 5% by weight phenol, showed that when the mixture is cast as a thin film and then submerged in water, gradual diffusion of phenol out of the film occurs over the course of several days. These results are encouraging with respect to the potential for synthesis of polyphosphazene nanoparticles that can carry phenol and deliver it in a time-release manner.

Synthesis of polylactide (PLA) nanoparticles also is being investigated using the supercritical anti-solvent process (SAS). A 0.5 wt% PLA solution (molecular weight 2000) in dichloromethane was sprayed through an orifice nozzle at 2 ml/min into a chamber containing carbon dioxide at 75° C and 1100 psi. Pure carbon dioxide also was pumped into the spray chamber at a flow rate of 20 ml liquid $CO_2$ per minute. A PLA solution (18 ml) was pumped into the spray chamber, which was then thoroughly flushed with $CO_2$ to remove any residual solvent.

The dry PLA powder was dispersed in water. The resulting suspension settled after ~1 day, indicating particle size in the micron range. PLA concentration and solution flow rates will need to be adjusted to produce particles in the nanometer size range. In addition, modifications will have to be made to incorporate phenol into the particles.

Because in the column experiments it is important to demonstrate that the nutrient carried by the colloids (phenol) has been effectively delivered to cells in the far reaches of the column, a capability for detecting the exposure of microbial cells to phenol is being developed. For this purpose, the investigators are working with the bacterium *Burkholderia cepacia* G4 (ATCC 53617), a common rhizosphere organism that can cometabolically oxidize the pollutant trichloroethene (TCE) through the action of the enzyme toluene-2-monooxygenase.

G4 and other *B. cepacia* strains closely related to G4 have been investigated for use in bioaugmentation strategies to remediate TCE. The toluene-2-monooxygenase activity in the cell can be observed by the production of a fluorescent product from the enzymatic substrate 3-hydroxyphenylacetylene. The investigators have demonstrated that they can assay the activity of the toluene-2-monooxygenase from the bacterium *B. cepacia* G4 when cells are induced by toluene or phenol using the fluorescent probe 3-HPA. Conditions for maximal 3-HPA oxidation (formation of fluorescent

product) have been determined. With epifluorescence microscopy, 3-HPA activity can be observed in as few as $10^5$-$10^6$ cells exposed to phenol.

Procedures have been developed and are being refined for consistent expression of the toluene-2-monooxygenase in G4 cells that have been exposed to phenol. The investigators also have been testing the growth of G4 in the presence of the polymers gused for colloid synthesis to verify that the carrier material itself is not inhibitory to the organisms. Thus far, none of the tested materials appears to be inhibitory. In fact, cells incubated with poly [diacetone D-glucofuranose-(protected sugar), trifluoroethoxy-] phosphazene maintained cellular size and RNA production, suggesting that this compound may, in fact, enhance growth.

During FY02, bench-scale columns were constructed for transport studies with the synthetic colloids, using saturated and unsaturated conditions. Preliminary experiments using a three-inch-long, packed sand column and saturated conditions were used to optimize and validate protocols for detection of colloids in the effluent. The QPAC40 colloids were detected using a Coulter N4 submicron particle size analyzer. Future experiments also will use either a UV/VIS or Fluorescence HPLC detector, configured in an in-line fashion. These detectors should allow tracking of the phenol concentration in the effluent of the column.

Modeling for this project must include both transport of the colloid in porous media, and release of the carried substrate from the particle. A literature survey was conducted of currently available models for colloid transport. All models are based on filtration theory in a continuum. Recent advances appropriate for this project have been identified. Although these models do not address colloid behavior in heterogeneous or unsaturated media, they will be suitable for predicting and simulating colloid behavior.

Predictions will be used to help design the transport experiments for this project. With respect to this particular project application, the deficiency of the available models for colloid transport is the lack of a kinetic term that will permit modeling slow diffusion of solutes from a mobile source (colloid). Some modification may be required that will be based on the modeling of solute diffusion from a spherical particle (based on Fick's law), which is already well established in the literature. These Fickian diffusion models can be used alone to evaluate candidate particles for release of solutes prior to column transport studies. For a coupled model, assistance with programming, if necessary, will be sought from the appropriate individuals within the INEEL.

This research could ultimately lead to significant cost savings to DOE by providing a more efficient means of delivering nutrients to a subsurface contaminated zone undergoing bioremediation. The LDRD is part of a "stable" of INEEL colloid science-related projects that are developing base capability in this area at the INEEL. Investigators at Inland Northwest Research Alliance (INRA) and other universities have openly expressed interest in this project, suggesting opportunities for future collaboration.

# High Intensity Perrhenate Ion Gun for Use as a Primary Ion Beam in SIMS (Secondary Ion Mass Spectroscopy)

*Kendall B. Johnson*

## *Expanding SIMS applications*

SC114

The perrhenate anion ($ReO_4^-$) has been shown to be a highly effective projectile for use in primary ion beams in Secondary Ion Mass Spectrometry (SIMS). It produces more molecular secondary ions than other projectiles, preserving more molecular information, and it greatly reduces charging when interrogating insulating surfaces. However, in the past the $ReO_4^-$ emitters have suffered from low currents (typically 0.2nA, maximum 0.5 to 1.0 nA) and non-uniform emitting surfaces. This low output limits their use to static SIMS and precludes use in dynamic SIMS or depth profiling. The non-uniform emission across the face of the emitter complicates focusing and results in non-uniform bombardment of a sample surface.

This LDRD is investigating a greatly improved perrhenate anion ($ReO_4^-$) emitter for use in primary ion beams in SIMS. Using Barium Sulfate ($BaSO_4$) as an oxidizing agent, the investigators have produced high-output $ReO_4^-$ emitters with much more uniform emitting surfaces. Sustained ion currents have been produced up to several hundred nano-Amps (nA), three orders of magnitude over previous emitters. In addition, the surface emits much more uniformly, allowing better focus and more uniform bombardment of the sample. With the development of this state-of-the-art emitter, the $ReO_4^-$ anion might become the projectile of choice as a primary ion beam in SIMS for many applications.

Technical objectives for fiscal year 2002:

- Design and test various mechanical/chemical designs for perrhenate ion ($ReO_4^-$) emitters for use in ion guns including:
  - Re (rhenium) rod in Pt (platinum) tubes with the space in between packed with $BaSO_4$ (barium sulfate) oxidizer, and
  - Re powder mixed with $BaSO_4$ at various concentrations (4.7, 15, 30, 50 atomic percent) packed in the end of Pt tubes of various sizes.
- Prepare journal article on research findings.

There is growing interest in the use of molecular ions for sputtering surfaces when conducting analyses by SIMS or for depth profiling. This interest is due to increased sputtering yields that are attained when high-energy molecular ions are used to bombard a surface. A variety of molecular sources have been used, including $SF_6$ (neutral), $SF_6^-$, $SF_5^+$, $ReO_4^-$, gold clusters, and a variety of other species.

For many years the INEEL has had a strong and active SIMS group that has made substantial contributions to the field. Perrhenate anion ($ReO_4^-$) emitters developed at the INEEL have been used since 1990 in all the SIMS instruments in the SIMS group. These emitters have proven to be long lived and relatively trouble free. Most importantly, when used to bombard a sample they are effective for desorbing intact ions of molecular species adsorbed on the surface of that sample. This large heavy anion spreads its impact energy over a larger area than smaller lighter ions and does not penetrate as far into the surface. In effect, this gently lifts secondary ions from the surface with greater efficiency and breaks fewer chemical bonds, thus preserving more chemical information (i.e., rather than only giving atomic information). Further, it has been shown experimentally that when looking at insulating surfaces, the usual charging problem is greatly reduced when using the perrhenate anion as a primary beam as opposed to a positive ion.

Thus this projectile has proven highly effective for the desorption of secondary ions from complex and electrically insulating surfaces and has been a resounding success in the application of SIMS for the analysis of contaminants adsorbed onto soil, rocks and other materials. This application is of particular interest for studying contamination of soils and the subsurface, in addition to detecting chemical warfare agents and biological specimens — both applications of great interest to the INEEL and the nation. While these guns have been a success, they have substantial limitations associated with the emitters. These limitations include low ion output current, non-uniform emission across the face of the emitter, a propensity to be poisoned when exposed to certain vapors, and insufficient robustness. This LDRD research has greatly improved emitters.

The perrhenate ion guns used in the past are composed of an ion emitter and the associated ion optics to accelerate and focus the ion beam. The perrhenate ion emitter consists of a short, small-diameter rhenium tube

(0.042" ID x 0.060" OD x 0.15"long) packed with a mixture of powdered europium oxide and barium perrhenate. One end face of this tube, with the powder packed flush with the tube end, is the emitting surface. The tube is supported at the back by two rhenium ribbon filaments (.001" thick x 1mm wide x ~5 mm long) that also serve as resistive heating elements. When heated to between 800° C and 900° C perrhenate anions are emitted.

These emitters are not readily scaleable to the higher intensities needed for dynamic SIMS; i.e., depth profiling, limiting their use to the analysis of the top few monolayers of a surface. They are limited to intensities of 0.5 to 1.0 nA and typically operate at around 0.2 nA. When the temperature is increased to give currents of 1 nA or more, the lifetime can be reduced to a week or less. If the temperature is pushed to excessive levels the emitter is permanently damaged and requires replacement.

Non-uniform emission across the face of the emitter complicates focusing and results in non-uniform bombardment of a sample surface. This limits the applications to the irradiation of broad areas and forbids its use in a SIMS imaging system or for probing small areas. Further, non-uniform emission can produce background signals due to the primary ion gun beam striking surfaces beyond the sample of interest. The large, non-uniform emitting surface is due to the fact that within a short time (several days) the ion emission moves from the packed powdered material in the center of the tube end face, as intended, to the edge of the rhenium tube itself. (These emitters are often used for several years.) This creates a donut-shaped emitting surface. Furthermore the emission is non-uniform and often varies substantially with time and often even scintillates. The background oxygen pressure in the system also affects the ion output and the emitters can be poisoned when exposed to certain vapors.

These emitters are not as rugged as desired. The thin rhenium ribbon filaments used to support and resistively heat the emitter become weak and sag in time when heated hot enough to raise the emitter to the desired temperature. When used within appropriate limits, these emitters have lasted for up to eight years. However, there have been occasions where analysis has been limited by one or more of the above-mentioned issues.

In considering how to increase the ion output current of these emitters, an activating agent was sought with more refractive properties. The objective was to operate at higher temperatures hoping to increase the reaction kinetics. Barium Sulfate ($BaSO_4$) was chosen as a likely candidate. It contains Barium or Strontium, which seem to be important, and has a considerably higher melting point (1350° C) than other known activating agents. $BaSO_4$ also contains a complex anion with many oxygen atoms, which are necessary for the oxidation of Rhenium to Perrhenate.

The use of $BaSO_4$ as an activating agent has been a great success. It has resulted in perrhenate anion output currents up to three orders of magnitude higher than the previous systems. This discovery has enabled design and testing of an emitter with greatly improved properties for use in the INEEL perrhenate guns. Several configurations have been investigated. While these investigations have been far from exhaustive at this point, they have been sufficient to obtain a greatly improved emitter.

Initial tests consisted of putting a slurry of $BaSO_4$ directly on a Re ribbon. This activated the Re and resulted in high perrhenate anion current output but produced very non-uniform emission across the face of the emitter, including scintillating bright points. Activation with $BaSO_4$ did not produce $ReO_4^-$ anions until over 900° C and produced the largest currents between 1100° C and 1300° C as measured with an optical pyrometer. These operating conditions for $BaSO_4$ activation are several hundred degrees higher than the previous systems

The investigator's first attempt was to try to activate the end of a Re rod. This was done using a Re rod (0.020" OD) mounted inside and concentric with a Pt tube (nominal 0.033" ID x 0.050" OD). The concentric space between the rod and the tube was packed with $BaSO_4$, being held in place by the inert Pt tube. This configuration produced high ion currents (1 – 30 nA) but

produced very non-uniform emission, with most of the emission coming from the sides of the rod rather than the end face. Furthermore, it developed large sensitivities to $O_2$ levels in the vacuum over time.

Powdered Re (635 mesh) mixed with various amounts of $BaSO_4$ packed in the end of a Pt tube, was tried in an attempt to disperse the $BaSO_4$ more uniformly in the Re metal and obtain a large exposed Re surface area (Fig. 1). This arrangement was very successful. Various concentrations of $BaSO_4$ were used in the following atomic percentages, 4.7, 15 30 50 (at %). All worked well to produce large perrhenate ion currents except the 50 at % mix, which had such a high volume percentage of $BaSO_4$ that it did not pack well in the tubes. The 30 at % was perhaps the best giving the high outputs (100+ nA) for the longest period of time. Pt tubes with IDs of 0.016", 0.033, and 1.32mm were all used successfully.

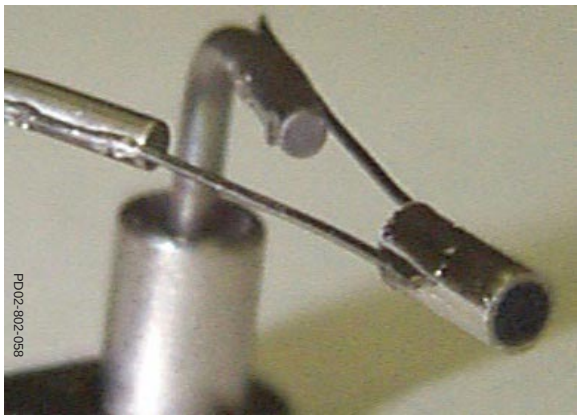


*FIGURE 1. New emitter, Re powder/BaSO4 in 1.32 mm ID Pt tube.*

Perrhenate anion currents of over 100 nA have been easily obtained and sustained for over one week of continuous output followed by several continuous weeks at around 10 nA. The highest output obtained was over 500 nA, which dropped gradually over several days to 200 nA. This output is three orders of magnitude higher than the previous emitters. The total measured output is a function of emitting surface area and the ion optics. When used intermittently, as is usually done in practice, these emitters should last for years.

The emitters show greatly improved uniformity of the emitting surface. Imaging the emitter surface shows that for these high currents, the emission is nearly all from the packed powder region inside the Pt tube. This allows better focusing on smaller spot sizes. In general, the ion currents from these sources are much more constant than previous ones. The earlier emitters often had fluctuations of 20%. These emitters are usually below the measurable limit of 0.01%. Furthermore, they have much less sensitivity to background $O_2$ levels in the vacuum system.

The Re ribbon support/heating legs of the previous emitters were replaced with Re wires. Calculations were performed to select the appropriate wire diameter to match its resistivity to the power supplies for highest heat input. The Re wire diameter selected was 0.010". This wire size decreased the surface area and increased the cross-sectional area of the support/heater legs, decreasing the radiant heat losses and increasing the thermal conductivity to the emitter. Not only did this improve the thermal properties of the system but also its mechanical robustness. The support legs are considerably larger and don't have to be heated as much, providing superior support.

The INEEL currently has a variety of programs that rely upon the SIMS developed at the INEEL. The programs that will benefit from this work are: the BES program Surface Ionization Mass Spectrometry; the ESR programs for chemical speciation, of which there are two, one using sputtered ions and the other sputtered neutrals; the ESR program for the typing of bugs by the signature ions sputtered from their lipid layer; the DOD program with defense threat reduction agency (DTRA) for chemical weapons detection; the non-stockpile

program with the Army for chemical weapons detection; and, a program from Dugway Proving Ground for the measurement of chemical weapons degradation pathways. These programs are multidisciplinary and are significant in DOE and INEEL mission areas including environmental quality, national security and science and technology.

This type of ion gun will open up a wide range of potential new application areas that require high sputter rates. With the ions being produced from a relatively small area in the exact center of the assembly, the beam diameter can be significantly reduced in size and is more symmetrical and even in intensity across the impact area. This design provides a superior ion beam for application to the SIMS and sputtered neutral instruments for which it will be applied. The concept also opens up the possibility of developing a SIMS imaging system using the perrhenate ion as the primary beam. A further benefit of the new ion gun is its rugged design. This ruggedness will be beneficial for use in portable instruments under development for military applications, although once fully developed, these instruments will apply to a much broader range of applications than Chem-Bio detection.

# Enhanced Transport in Nano-Crystalline Ceramic Films

*Paul A. Lessing, Gary Huestis*

## *Improving ionic conductivity*

NC103

Some ceramic oxides have the potential for enhanced ionic transport due to nano-crystalline grain boundaries. This enhancement could bring orders of magnitude improvements to a number of applications.

The goal of this LDRD is to explore organometallic precursor methods to fabricate ceramic films that could exhibit greatly enhanced transport (e.g., 1000X faster) of ions (protons) due to nano-crystalline grain boundaries. Proton transport is important to DOE because of its many energy-related applications, including: fuel cells, sensors, batteries, and hydrogen-conducting membranes (e.g., hydrogen removal from spent nuclear fuel canisters). Good progress is being made on this project and very thin ceramic films consisting of nano-sized crystals have been fabricated at INEEL.

Technical objectives for fiscal year 2002:

- Develop polymeric precursor chemistry (suitable for spin casting) for two different NASICON-type ceramic compositions.
- Spin-cast thin films of the polymeric precursors.
- Develop techniques to convert the polymeric films into nano-crystalline ceramic films.

Two different NASICON compositions have been fabricated: 1) $NaZr_2 Si_x P_{3-x} O_{12}$, and 2) $Na_{1+x} Sn_{2-x} In_x P_3 O_{12}$. Thus far, much more success has been found with the tin (Sn) composition. The zirconium (Zr) compositions have proven difficult to work with due to complexities in the Zr chemistry that led to extremely fine precipitates of compounds such as zirconium phosphate. (Work is ongoing to solve this problem.)

The flow diagram for the process being developed at INEEL is shown in Figure 1. Various metal cations (e.g. Zr, P, Si, Na, etc.) are chelated (onto a reactive polymer) from a water-solubilized salt, while the polymers concurrently undergo polymerization and cross-linking reactions. Good chelation helps prevent mixed-cation precipitation during heating. Polymerization increases the viscosity and allows for adjustment of the film thickness during spin coating. Too much cross-linking can cause cracking of the coating during calcination. The proper viscosity is necessary for thin films to be formed using spin casting.

These films are then heat-treated (calcined in oxidizing atmospheres using various heat-treating schedules) to create ceramic films. The ceramic films were characterized with regard to their morphological, microstructural, and crystallinity properties. This work has successfully demonstrated the ability to produce thin ceramic films with an extremely fine (nano-crystalline) microstructure.

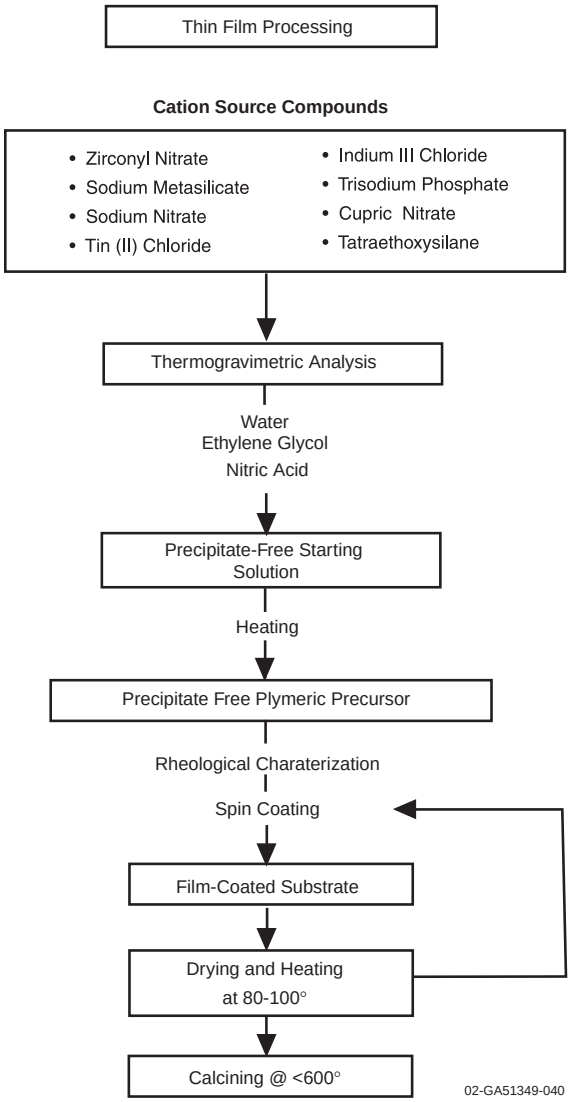


*FIGURE 1. Process developed to fabricate thin-film ceramics.*

A TEM micrograph of a recently produced sodium-NASICON thin film (fabricated at INEEL) is shown in Figure 2. A Selected Area Diffraction Pattern is shown verifying the film is polycrystalline. Note that both the film thickness and crystallite size are extremely fine. Increasing the film thickness can be achieved by increasing the viscosity of the polymeric precursor, spinning at lower speeds, or multiple coatings. However, films thicker than about 0.2 microns (200 nanometers) made as a single coating have been found to crack, due to shrinkage stresses during calcination.

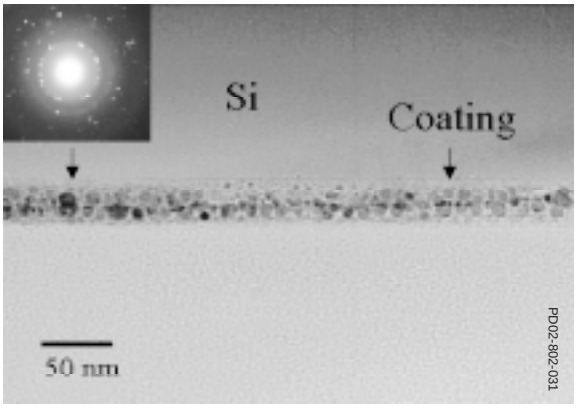


*FIGURE 2. Transmission Electron Micrograph of a nano-crystalline thin film coating of Na-"NASICON" on a smooth Si wafer.*

A paper is currently being written on the results of this study for submittal to a scientific journal, covering the details of the chemistry, casting process, and characterization of the ceramic films (TEM, SEM, XRD, etc.).

In future work, the investigators plan to ion exchange (electrochemically) the sodium ions out of the ceramic films and replace them with protons (from a mineral acid). Special substrates that are permeable to hydrogen will be developed to support the thin films on special metallic thin-film electrodes. These developments will enable the fabrication of various test cells and practical devices.

This LDRD supports INEEL's Nanotechnology Initiative and will result in future proposals in response to DOE (e.g., Basic Energy Science) needs. The project has resulted in collaboration with Argonne National Laboratory-West. Discussions also are underway for collaboration with Sandia National Laboratory regarding the characterization of this project's ceramic films.

# Making Sustainable Decisions Using the *KONVERGENCE* Framework

*Steven J. Piet*

## *A new framework for better science-based decisions*

ET106

Hundreds of used nuclear facilities and contaminated sites must be cleaned up. "Cleanup" includes decommissioning, environmental restoration, and waste management. Cleanup can be complex, expensive, risky, and time consuming. Decisions can stall, are often controversial, can be blocked, and are sometimes redone – some before implementation, some decades later.

The goal of this LDRD is to make cleanup decisions easier to make and more robust, transparent, consistent, and sustainable by a holistic framework that emphasizes relevant time scales. Sustainability, in this context, means decisions that work better over the entire time period — from when a decision is made, implemented, and continued until the hazards are destroyed or decay to levels that society wishes to ignore.

In this research, experiences and analyses are being melded with ideas from decision science, action science, sociology, psychology, political science, ethics, history, "hard" sciences, risk assessment, and many engineering disciplines. The *KONVERGENCE* framework combines new ideas, modifications of others' ideas, and existing ideas. The framework includes the *KONVERGENCE* mental model describing the underlying decision dynamics that require cleanup alternatives to be (and to remain) *konvergent* with *knowledge* of the problem and alternatives, *values* of those impacted by the decision, and *resources* needed to implement alternatives so that the decision works over time.

Another key framework element is proper framing of the decision, including the need to consider the adaptability of alternatives to reduce the resistance to making decisions and increase the sustainability of decisions once made. The framework also is built on general *values* and principles to guide both process and result.

Technical objectives for fiscal year 2002:

- Improve and begin to validate the decision-support framework/guidebook by test cases.
- Build on the framework started in FY01 by developing quantitative tools.
- Begin to transfer knowledge via presentations to the INEEL Citizen Advisory Board (CAB), publications, interaction with operations/cleanup personnel, etc.

In FY02, the guidebook was completed and distributed in draft form. Three papers also were presented at the Spectrum 2002 Conference.

There has been limited internal team testing and very helpful suggestions from individual volunteer members of the INEEL Citizen's Advisory Board. More feedback and testing are planned next year, the third year of this three-year R&D project.

The inadequacy of current approaches to cleanup decision-making is illustrated by the high controversy and resultant stalling of some decisions, as well as remaking of past decisions. This is described by the National Research Council's Long-Term Institutional Management of DOE Legacy Waste Sites, Committee on the Remediation of Buried and Tank Wastes, 2000:

"Because uncertainty is inherent in many of these areas, and because DOE's preferred solutions – reliance on engineered barriers and institutional controls – are inherently failure prone, step-wise planning for DOE legacy sites must be *systematic*, *integrative*, *comprehensive*, and *iterative* in its execution through time, *adaptive* in the face of uncertainty, and *active* in the search for new and different solutions. Planning for long-term institutional management should commence while remediation is underway."

The comprehensive *KONVERGENCE* framework (Fig. 1) includes:

- A mental model, *KONVERGENCE*, that describes some of the underlying decision dynamics that require cleanup alternatives to be (and remain) *konvergent* with *knowledge*, *values*, and *resources* so that the decision works over time.
- Strategic improvements to reframe the problem and expand the spectrum of alternatives to include adaptable alternatives and decision networks.
- Tactical improvements such as processes and analytical tools derived from experience, values/principles, and relevant literature.

- Initial extensions of existing risk and cost estimation tools to provide earlier and more comprehensive inputs to decision-making.
- Some implications for R&D into possible solutions that may increase adaptability while still reducing risk of residual hazards.

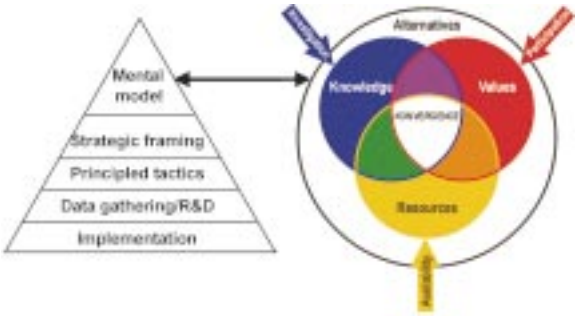


*FIGURE 1. The KONVERGENCE Framework (left) is an integrated package that will improve the odds to make and keep cleanup decisions. It is built on the KONVERGENCE model (right) that posits the need to keep konvergence among* Knowledge, Values, *and* Resources.

The framework models regulations as an imperfect overlay or "snapshot" of *values*. The fact that regulations can never totally substitute for *values* is one of the underlying challenges.

Also, the number of participants in a decision is always less than the full set of stakeholders, everyone potentially impacted by a decision. The framework suggests more effective, appropriate, and timely involvement and analysis to improve the validity of the *values* considered. An improved *values* component should make the decision more robust against "late entry" players.

The framework includes a generic set of values and 20 principles that are a starting point for establishing "common ground" on both the process and objectives to select among alternatives. As an example, the generic 20 principles include two Precautionary Principles.

- Precautionary Principle 1– "Actions that pose a realistic threat of irreversible harm or catastrophic consequences should not be pursued unless there is some compelling countervailing need to benefit either current or future generations." -National Academy of Public Administration (1997)
- Precautionary Principle 2 – "Where there are threats of serious or irreversible damage, scientific uncertainty shall not be used to postpone cost-effective measures to prevent environmental degradation." -1992 Rio Summit.

These principles advocate caution in differing ways. The first principle cautions against *taking actions* prematurely if the actions pose threat of irreversible harm. The second principle cautions against *not taking action* to protect against the threat of irreversible harm.

Some cleanup problems can encompass risk of both types. Consider the case of a long-lived hazard that, if left alone, will eventually degrade, increase in risk, and become more difficult to cleanup. Precautionary Principle 2 would argue to take cost-effective measures now! But which measures? Precautionary Principle 1 would argue against taking an irreversible action that might not be wise from the long-term view. In such situations, how can we proceed? No action is dangerous; taking a wrong action is dangerous. The concept of adaptable alternatives (managed risk) can offer a way out.

Some past waste decisions have already drifted out of *konvergence*. Thus, the degree of *adaptability* (i.e., solutions that are repairable or reversible) is a factor in reducing the resistance to making decisions and increasing decision sustainability.

As alternatives are developed, diagnosis of opposition needs to be probed more deeply to provide a better basis for refinements, prior to spending millions of dollars on detailed engineering, while recognizing the limited potential to solve *values* problems with increased *knowledge*, etc. Finally, decision makers must recognize that *knowledge*, *values* and *resources* interact dynamically and change over time.

This LDRD is pursuing a science-based decision framework for decommissioning-stewardship-waste decisions. This effort will support EM Operations and better decision-making operations at the INEEL, within the DOE Complex, and elsewhere.

# Nucleation and Growth of Nanoparticle Materials in Supercritical Fluid Processes

*Harry Rollins*

## *New, versatile methods to control particle properties*

NC104

Materials with dimensions on the nanometer scale have interesting optical, electronic, magnetic, catalytic, and even mechanical properties that are significantly different than those of individual molecules and bulk materials. The properties of these materials are highly dependent on the particle size, and thus size distribution. Due to the many potential applications of nanomaterials, it is highly desirable to have a versatile and reliable method for their production that allows control of the particle size, morphology and crystallinity.

This LDRD is investigating such a technique. To accomplish this objective, a variety of nanoscale materials are being prepared using supercritical fluid processing techniques, and the effects of the preparation conditions on particle properties are being evaluated.

Technical objectives for fiscal year 2002:

- Prepare and characterize metal nanoparticles (silver).
- Prepare and characterize semiconductor nanoparticles (silver sulfide).
- Evaluate effects of processing conditions on particle properties.
- Present results at national conference.

Metallic silver nanoparticles were prepared using a novel reactive spray processing method. A solution of silver triflate in liquid carbon dioxide was prepared using tributyl phosphate (TBP) as a co-solvent. TBP is a charge-neutral species that forms complexes with many metal salts that are soluble in non-polar solvents, such as carbon dioxide. The silver triflate solution in carbon dioxide was pressurized and heated to supercritical conditions (104° C, 3500 psi) and then sprayed through a capillary nozzle into a solution of sodium borohydride in ethanol at room temperature. Figure 1 shows a transmission electron microscope (TEM) image of metallic silver nanoparticles prepared using these conditions. The average particle diameter was 12.91 ± 2.23 nanometers.

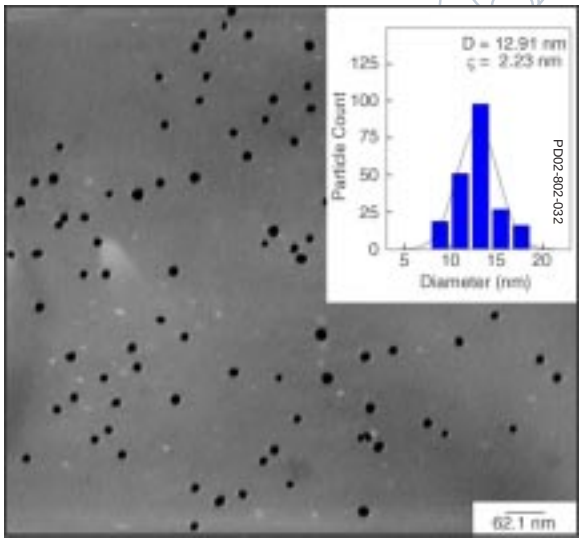


*FIGURE 1. TEM image and particle size distribution of silver nanoparticles prepared by reactive spray processing using supercritical carbon dioxide solutions. (T = 104° C, P = 3500 psi, 1.41 wt% TBP in $CO_2$ [$NaBH_4$]/[Ag+] = 5.7, [TBP]/[Ag+] = 106.)*

Silver nanoparticles also were characterized using UV-visible absorption spectroscopy and exhibited a plasmon absorption band at ~ 400 nm, characteristic of silver nanoparticles. In addition, the silver nanoparticles were characterized using powder X-ray diffraction. Preliminary results indicate that particle size and size distribution are influenced by the processing temperature, the concentration of TBP, and the concentration of silver triflate.

Silver sulfide nanoparticles were prepared using similar processing conditions. A solution of silver triflate in supercritical carbon dioxide (with TBP co-solvent) was sprayed into a room-temperature solution of sodium sulfide. Figure 2 shows a TEM image and particle size distribution for silver sulfide nanoparticles prepared using a possessing temperature of 110° C and 1.38 wt% TBP.

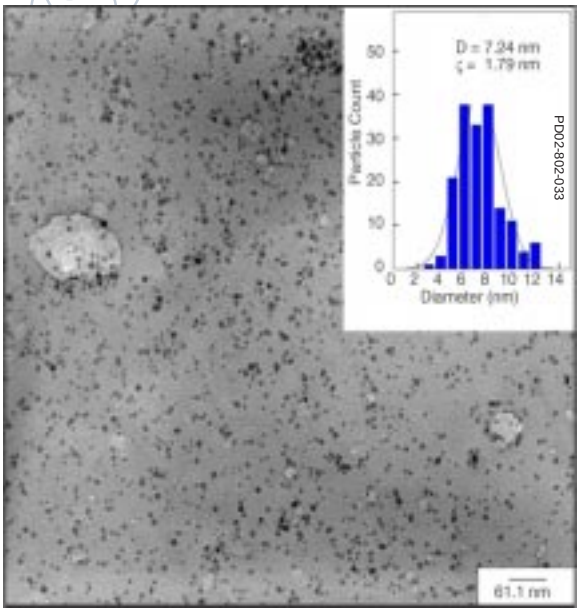


*FIGURE 2. TEM image and particle size distribution of silver sulfide nanoparticles prepared by reactive spray processing using supercritical carbon dioxide solutions. (T = 110° C, P = 3500 psi, 1.38 wt% TBP in $CO_2$, $[S^{2-}]/[Ag+] = 8.2$, $[TBP]/[Ag+] = 106$).*

The nanoparticles had an average diameter of 7.24 ± 1.79 nanometers. Silver sulfide nanoparticles prepared using lower processing temperatures (50° C and 70° C) and lower TBP concentrations (0.22 wt%) had particle diameters of ~ 3 nm with particle size distributions of ~ 1 nm. The silver sulfide nanoparticles were characterized using UV-visible absorption spectroscopy and exhibited quantum confinement effects. The absorption onset was at ~ 1200 nm for the 7.24 nm particles and ~ 900 nm for the 3 nm diameter particles, indicating a shift in the band gap to higher energy with decreasing particle size.

Results on the preparation and characterization of silver and silver sulfide nanoparticles were presented at the American Chemical Society National Meeting on August 19, 2002. The project also supported the publication of two peer-reviewed articles.

The effects of processing temperature, the concentration of TBP and the concentration of silver triflate on particle size and size distribution continue to be investigated. This method will be applied to the preparation of other metal and metal sulfide nanoparticles.

The proposals, publications, and presentations resulting from this LDRD enhance the reputation and recognition of the INEEL in the scientific community, and demonstrate that the INEEL is actively involved in basic and applied research and development. The capabilities of the INEEL in the preparation and characterization of nanomaterials was greatly enhanced through this project.

# Elucidating the Photo-Physics of Complex Metal Ions Trapped in a Fourier Transform Mass Spectrometer

*Jill R. Scott, Paul L. Tremblay*

***Leading to new energy technologies***

SC111

A better understanding of electron- and energy-transfer modalities could lead to the development of new energy technologies such as improved energy collection, conversion and storage devices.

The primary focus of this LDRD is investigation of sensitive techniques for the measurement of ground and excited-state energies from a number of complexes that have properties suitable for the conversion of light energy to chemical or electrical energy. The technical capabilities that will be developed at the INEEL are the integration of a sensitive optical detection system with a Fourier transform mass spectrometer (FTMS) for the study of chemical complexes with narrow absorption and emission bands in a solvent-free environment. The investigators have chosen fluorescence as their first emphasis because the sensitivity of fluorescence > absorption > infrared ≈ Raman.

While gas-phase data for atomic ions and a few small molecular ions exist, virtually no information exists about spectroscopic characteristics for large, non-volatile gas-phase ions. For example, extinction coefficients and quantum efficiencies are not available in the literature. The study of the optical properties of large ions in the gas phase is at an embryonic stage similar to condensed-phase spectroscopic studies in the early 1900s.

Another complication is that the ions produced in the gas phase may not resemble those in solution, or their behavior may be significantly different without the presence of solvent. The investigators observed gas-phase fluorescence behavior of $Ru(bpy)_3^{+1}$ that has not been reported for this complex in solution. Additionally, mechanisms of ion production play an important role in the structure of metal-bipyridine complexes that would be difficult to see without the high resolution and mass accuracy of the FTMS.

Technical objectives for fiscal year 2002:

- Integrate fluorescence spectra gathering with fluorescence life-time apparatus.
- Optimize signal-to-noise ratio.
- Investigate ion production and stability for compounds of interest.
- Explore magnetic field effects on fluorescence lifetimes and spectra.
- Publish and present research.

In work conducted this fiscal year, fluorescence spectra of $[Ru(bpy)_3]^{+1}$ showed bi-exponential decay ($k_1 = 3 \times 10^7$ s and $k_2 = 2 \times 10^6$ s), suggesting the presence of two species, while mass spectrometry of the ions suggested there was still only one species present. Photodecomposition studies exposing the ions to more intense laser power revealed a mixture of loss of a bipyridine ligand with and without additional loss of a hydrogen (H). It is possible that the second species present in the gas-phase fluorescence studies has the same composition as $[Ru(bpy)_3]^{+1}$, but is a transition state for the photo-decomposition reaction.

The apparent instability of $[Ru(bpy)_3]^{+1}$ and other metal-bipyridines was observed to depend on the ion generation method. Currently, direct laser desorption (LD) and matrix-assisted laser desorption/ionization (MALDI) are available. Close examination of the mass spectra of $Ru(bpy)_3^{+1}$ revealed that H loss could also occur depending on the ionization conditions. This loss is not noticeable without the high resolution and mass accuracy of FTMS.

Loss of H was observed for both $[Ru(bpy)_3]^{1+}$ and the major fragment peak $[Ru(bpy)_2]^{1+}$. If the isotopic distributions of the ion clusters are closely evaluated as in Figure 1 for $[Ru(bpy)_2]^{1+}$, the pattern for the LD spectrum (Fig. 1b) does not match the theoretical spectrum in Figure 1a. The observed isotopic peak pattern can be explained by a linear combination of abundances derived form a series of H losses producing $[Ru(bpy)_2\text{-}H]^{1+}$, $[Ru(bpy)_2\text{-}2H]^{1+}$, and $[Ru(bpy)_2\text{-}3H]^{1+}$. A linear combination of abundances of these peaks corresponding to 49%, 41%, and 10%, respectively, gives an isotopic pattern similar to the experimental distribution. Addition of these ions to the isotopic cluster accounts for the extra peaks observed at m/a 405, 406, and 407 as well as the apparent shift in the location of the mono-isotopic peak to a lower m/z value. The percentage of $[Ru(bpy)_2]^{1+}$ contributing to the isotopic pattern is <1%.

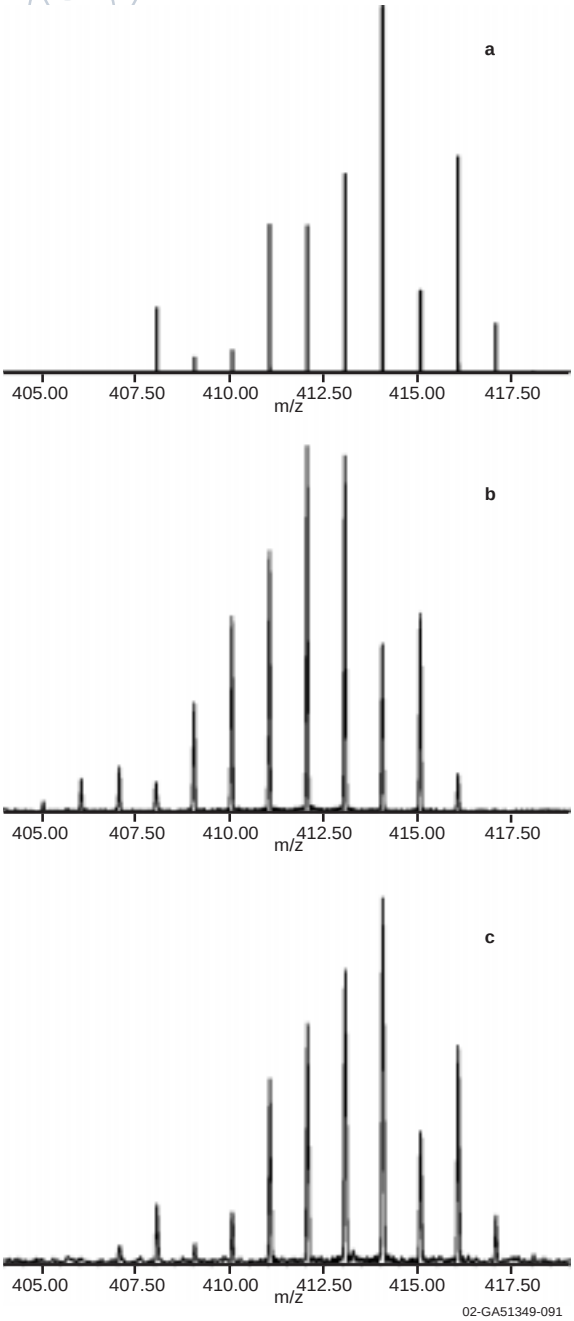


*FIGURE 1. Isotopic patterns for peak cluster at m/z 414 derived from $[Ru(bpy)_3]CL_2$; a) theoretical distribution for $[Ru(bpy)_2]^{1+}$, b) experimental LD spectrum, and c) experimental MALDI spectrum using sinapinic acid as matrix.*

The choice of matrix is an integral step in correctly characterizing these species by MALDI mass spectrometry. Figure 1c shows the isotopic distribution of the ($[Ru(bpy)_2]^{1+}$) ion from the MALDI spectrum of $[Ru(bpy)_3]Cl_2$ using sinapinic acid as the matrix. A slight shift in the isotopic peaks compared to the theoretical distribution (Fig. 1a) is observed however, not to the extent seen in the LD spectra (Fig. 1b). Further studies using 2,5-dihydroxybenzoic acid (DHB) as the matrix revealed poorer results by the presence of a greater number matrix adducts and additional losses of H similar to that observed in the LD spectra.

These results are consistent with a reaction scheme (Fig. 2) for hydrogen loss involving the breaking of the metal-nitrogen bond, rotation of a pyridine ring, and reformation of an ortho-metallated complex by a metal-C bond. The results demonstrate the importance of sample preparation and the utility of FTMS for correct characterization of metal poly(pyridyl) complexes.

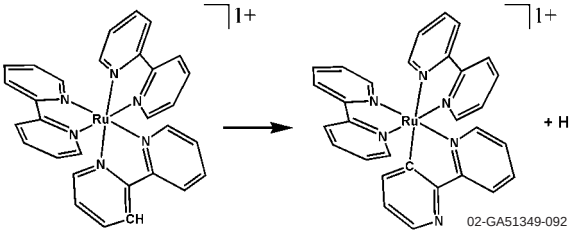


*FIGURE 2. Scheme for loss of H from $[Ru(bpy)_2]^{1+}$ .*

The advent of ionization techniques such as electrospray (ESI) and matrix-assisted laser desorption/ionization (MALDI) for large molecules and development of trapping mass spectrometers have laid the foundation for the spectroscopic study of molecular ions. Initial investigations with ESI show that it is a softer ionization method that does not produce losses of H. Additionally, ESI will allow production of $Ru(bpy)_3^{+2}$ for more direct comparison to solution species. Because the FTMS is part of the laser-based optical and chemical imager (LOCI) for surface analysis, incorporating ESI

into the instrument used in this project will require an innovative approach to be compatible with the current instrument configuration.

Ideally, fluorescence spectra (both excitation and emission) as well as fluorescence lifetime data are necessary to thoroughly characterize a chemical species. This LDRD's initial focus has been on lifetime studies because fluorescence lifetime is extremely sensitive to the chemical environment. Therefore, fluorescence lifetimes in the gas phase should be very different than those in solution. This factor should be especially true for complexes such as ruthenium polypyridines because the solvent couples to the vibrational and rotational mode, affecting the fluorescence decay. Therefore, the investigators have obtained access to a high quality spectrograph with an intensified charge-coupled device (ICCD) camera for obtaining the emission spectra. The emission spectra should provide information that will allow investigation of the electronic nature of the different metal-bipyridine complexes observed in the gas phase.

This LDRD addresses the intrinsic characteristics and reactivity of molecular ions in the absence of solvent, fundamental knowledge that is not currently available to DOE. A primary DOE mission is development of new energy technologies. This work will facilitate understanding of electron- and energy-transfer modalities that could lead to development of improved energy collection, conversion, and storage devices.

Because many surface analysis techniques rely on mass spectrometers, including those at the INEEL, it is necessary to understand how the gas-phase ions generated during such analyses relate to the surfaces from which they are derived. Mass spectrometers cannot provide direct information about structural characteristics; therefore, it is necessary to incorporate the technology to directly measure the electronic and vibrational characteristics of gas-phase ions.

Ultimately, it is expected that publications generated by this project will enhance the INEEL's success in supporting DOE programs.

# Recombinant Adhesive Protein Production and Investigation into Alternate Natural Adhesive Systems in Marine Mussels

*Heather Silverman, Frank Roberto*

## *Super adhesives from marine mussels*

ET107

Marine mussels, like the edible blue mussel, *Mytilus edulis*, attach to a variety of surfaces in an aqueous environment using a natural protein adhesive that is incredibly strong and durable. There are no conventional glues that can rival the unique underwater adhesion of these mussels.

Other researchers have shown that at least six different proteins are involved in the formation of the structure (termed the byssus) used by the blue mussel for attachment. However, the interactions of the proteins with each other and with surfaces are not well understood because of the difficulty in obtaining appreciable quantities of the proteins for testing. A deep-sea species, referred to as *Bathymodiolus childressi* (formerly Seep Mussel Ia), has been shown to produce adhesive structures that have survived centuries in a natural gas (methane) and high-saline environment.

The objectives of this LDRD research are 1) identification and confirmation of gene sequences for the six known adhesive-related proteins from *M. edulis*, 2) large-scale recombinant protein production of adhesive-related proteins, 3) comparative analysis of adhesive-related genes from *M. edulis* with *B. childressi*, and 4) genomic screening of a methanotrophic bacterial endosymbiont from *B. childressi* for enzymes with industrial capabilities. Exploitation of the natural adhesive systems in marine mussels can provide biomimetic glue products that are water-impervious, inexpensive alternatives to conventional adhesives available today. Solutions to combat biofouling as well as identification of enzymes for industrial uses also may result from this research.

Technical objectives for fiscal year 2002:

- Identify and confirm at least six adhesive-related genes for *Mytilus edulis*: foot protein-1, -2, and –3; nongradient byssal precursor, Precollagen-D and –P. Putatively identify multiple genes for Mefp-2 and Precollagen-P families.
- Initiate small- and large-scale production of recombinant adhesive-related proteins from *M. edulis*.
- Obtain *Bathymodiolus childressi* deep-sea mussels.
- Isolate RNA for construction of a foot organ cDNA library to identify adhesive-related genes from *B. childressi*.
- Initiate growth and screening of a methanotrophic endosymbiont from *B. childressi*.

The budget for this LDRD was cut 17% in FY02. Thus, the original milestones were revised as follows: conduct a less-extensive exploration of an alternative deep-sea mussel species, and perform minimal or no atomic force microscopy (AFM) analysis.

The successful transformation of *M. edulis* adhesive-related clones into a microbial host was verified using modified plasmid purification techniques and the polymerase chain reaction (PCR). Heterologous expression of recombinant proteins (designation "r") depends on the maintenance of the plasmids containing the adhesive genes of interest in a host. Small-scale recombinant protein production (100-500 mL) was initiated for these clones as well as a control recombinant beta-galactosidase protein. Results from 26-hour induction and 96-hour fed-batch induction experiments revealed recombinant beta-galactosidase protein production at 8.4% and 12% of total protein production, respectively (Fig. 1). Production of adhesive-related proteins was not identified using these small-scale volumes.

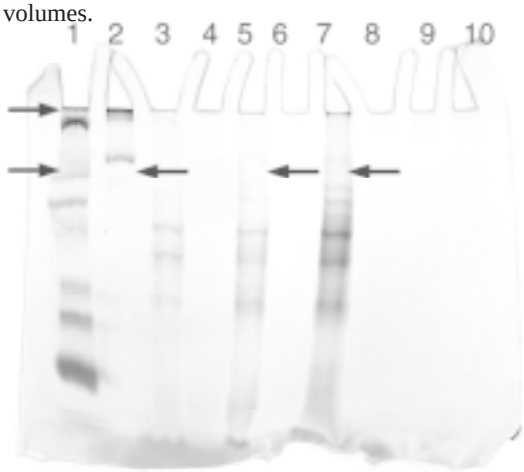


PD02-802-021

*FIGURE 1. Control recombinant beta-galactosidase protein production. Lane 1 represents a protein ladder: the top arrow corresponds to 250 kDa, the bottom arrow corresponds to 98 kDa. Beta-galactosidase appears at ~123-130 kDa. Lane 2 represents purified beta-galactosidase (positive control). Lane 5 represents recombinant beta-galactosidase following 26-hour induction. Lane 7 represents recombinant beta-galactosidase following 96-hour fed-batch induction. Recombinant beta-galactosidase protein production was estimated at 8.4% and 12% of total protein production, respectively, by enzymatic assay procedures.*

Technical efforts focused primarily on methodologies for the production, purification, and identification of rMefp-1due to potential applications. Numerous strategies for protein induction, cell lysis, and protein solubilization and concentration were tested. Larger-scale induction experiments (up to 2 L) were performed to aid in obtaining measurable quantities of rMefp-1. Results indicated a protein corresponding to the size expected for rMefp-1 (~130 kDa). However, confirmation of rMefp-1 requires additional purification procedures that will be performed in FY03. The difficulty in purification of adhesive-related proteins from *M. edulis* stems from their solubility at low pH (acidic conditions). The host used for recombinant protein production also produces proteins that are acid soluble.

Screening of a new cDNA library (constructed from the foot organ of *M. edulis* in FY01; pGEM T-Easy vector, Promega, Madison, WI) was completed. No new adhesive-related genes were identified. However, DNA information for an aromatic dioxygenase was obtained and could be useful in identifying the catechol oxidase enzyme important in the underwater adhesion of the blue mussel.

Twenty-one deep-sea mussels (*Bathymodiolus childressi*) were obtained from an outside researcher following an exploration to the Gulf of Mexico. The animals were recovered from a water depth of about 550 meters, with a water temperature of ~7°C and methane concentrations of ~1.6 ppm. Total RNA was isolated from excised foot organs for use in identifying adhesive-related genes and performing a comparison with genes from *M. edulis*.

Homogenized gill tissue from *Bathymodiolus childressi* deep-sea mussels was processed for culturing of a methanotrophic endosymbiont. Results from microscopic images suggest successful growth of the previously reported unculturable methanotrophic endosymbiont (Fig. 2). Enzymatic assays are underway to determine the methane-oxidizing potential of the microbe. Experiments in FY03 also will focus on enrichment of the specific methanotroph and subsequent genomic screening.

*FIGURE 2. Putative methanotrophic endosymbiont cultured from homogenized gill tissue of the deep-sea mussel* Bathymodiolus childressi. *The bacterial endosymbionts are found in vacuoles within animal cells near the gill surface. The coccoid-shaped methanotrophs are about 1 μm in diameter and clustered together in high numbers. Microscopic image obtained from DAPI-stained cultures at ~1,000x magnification.*

INEEL Biotechnology capabilities in the areas of protein structure/function relationships, large-scale production of recombinant protein, genomics of extreme environments (deep marine), and novel atomic force microscopy techniques will be gained from this continued research. DOE missions benefiting from this work include the areas of Environmental Quality (less toxic and hazardous adhesives, combating marine and freshwater biofouling), Science and Technology (natural adhesives for biomedical, electronics, aviation, automotive, plastics, forest, pulp and paper industries) and National Security (underwater adhesives for special operations).

# Integrated Experimental and Mathematical Analysis of Complex Chemical and Biological Systems

*Daphne Stoner, Charles Tolle, Timothy McJunkin, John Walter, Randall LaViolette*

## *Mapping complex environmental systems*

S472

The ability to numerically quantify the visual "look" of measured data sets through mathematics is useful in characterizing complex systems. It is thought that by considering changes in these quantities over time, new biological models can be developed that lead to a better understanding of community interaction. This understanding is of significance because of the importance of microorganisms in water resources, materials transport and the potential use of microorganisms for in situ processes such as mineral dissolution and recovery, enhanced oil recovery and remediation technologies.

The goal of this LDRD is to provide "first of its kind" capability to describe in a mathematical way the heterogeneous, spatially complex systems relating to energy use, energy conservation and the environment. The investigators have developed a software application for generating synthetic biofilm images and another to process image data and perform the spatial analysis procedures. Biofilm images were acquired, and fractal and lacunarity analysis procedures were developed that can be used to describe, in analytical terms, the patterns formed by biofilm formation.

This mathematical description (i.e., lacunarity) of the spatial characteristics of biofilms and other biological and chemical systems has application to: subsurface biogeochemical systems; corrosion and biofouling in nuclear/conventional power systems and industrial processes; and biological materials, processes, and structures. The selected model system, the colonization of hematite surfaces by the bacterium *Shewanella* sp., is relevant to biogeochemical iron cycling, the natural attenuation of chlorinated solvents and the fate and transport of radioactive materials in subsurface environments.

Technical objectives for fiscal year 2002:

- Complete exploratory development of lacunarity algorithms for ramified data.
- Refine software for obtaining simulated biofilm images.
- Develop initial lacunarity algorithms for dense data sets and apply to simulated and experimental biofilm images.
- Improve fractal dimension estimate algorithm.
- Acquire time-lapse images of *Shewanella* biofilms grown on hematite in a flow cell system.
- Prepare and submit technical articles and make technical presentations based on research findings.

This LDRD is developing algorithms that can be used to numerically quantify the visual "look" of measured data sets. A number of mathematical approaches are used to quantify a data set's look; these include fractal dimension, lacunarity, and connectivity. This project focuses on using fractal dimension in conjunction with lacunarity calculations to quantitatively describe biofilm structure.

Fractal dimension alone does not fully describe the visual look or texture; i.e., the space-filling characteristics of a data set. The investigators developed an algorithm for calculating the lacunarity of ramified data sets. A graphical user interface (GUI) also was developed for generating synthetic textures with an adjustable fractal dimension and lacunarities that better conforms to this new definition of lacunarity and is independent of the fractal dimension adjustment. The Tool Command Language (Tcl) interface was rewritten to make it substantially easier to use; i.e., file selection allows for browsing, and the built-in help is fairly thorough. The latest version is 1.58, and runs on both UNIX/LINIX and Windows.

The simulation code has been freed of direct tie to the interface, so that it is more readily modified or improved without knowledge of Tcl coding. This also eliminated the system dependent code (for UNIX or Windows) so that there is only one, system-independent, C-code for the simulation program. This code can be compiled for either UNIX or Windows. While some changes in the simulation program could require changes in the interface program, the two are separate. In other words, changes in the Tcl code do not require understanding of C and changes in the C code do not require knowledge of Tcl.

To facilitate the use of the lacunarity and fractal dimension estimation algorithms being developed in this project, an additional GUI-based software package was developed, named Mapper. This package brings the power of massively parallel computations on a Beowulf Unix cluster to the novice computer researcher's hands.

Mapper enables researchers to quickly topologically reduce an image data set into a simpler fractal dimension and/or lacunarity region map that can then more easily be correlated with other known maps of bio-diversity within the spatial-distributed system of interest. It is these correlations that can lead to new models that will predict biofilm growth as well as health for use within future control systems.

Finally, a new method for estimating lacunarity on dense data sets was developed this year. The results for the application of this new method to synthetic biofilm images are shown in Figure 1. Work continues on the refinement on the dense lacunarity definition and estimation algorithm.

One manuscript was submitted for peer review, a poster was presented, and two manuscripts are in preparation. Technical articles and meeting presentations will demonstrate and enhance the INEEL's international reputation in advanced computational methods. This is the final year of the project. No further activities are planned.

The new method developed in this LDRD for calculating lacunarity for both ramified and dense data provides a basis for developing cross-cutting technology that will be used by both the DOE and DOD in many modeling and detection applications. Accordingly, the research will support interests of the DOE Basic Energy Sciences, Fossil Energy, Environmental Research, and Environmental Management programs. Initial inquiries have been made with the DOD, namely TARDEC-TACOM in Warren, MI. DOD is interested in more fully quantifying cluttered image textures for use in vehicle and target detection applications. One such application is to use the new lacunarity estimator as a rough-cut parser for object recognition and target detection algorithms.

*FIGURE 1. The results of analysis of a simulated biofilm image: A) image, B) lacunarity, C) composite of Ltot, Lac, and fractal dimension, D) lacunarity tot; E) fractal.*

# Nanostructure Characterization for Sensing

*Ken Telschow, Napoleon Thantu, Dave Hurley*

## *Improving key properties for new sensor devices*

NC101

Fundamental understanding of optic, electronic, and elastic processes within nanostructured materials provides a basis for developing novel high-performance photonic, optoelectronic and electronic devices with unparalleled capabilities. This LDRD seeks to investigate both photon and phonon dynamics in the confined state of nanostructured materials, prepared by INEEL collaborators and others, for enhanced sensing properties.

Technical objectives for fiscal year 2002:

- Demonstrate the utility of ultrafast optical techniques for characterizing and understanding the dynamics of charge carriers in nanostructured materials.
- Research the potential of these materials for developing new sensor methodologies and devices for performing environmental sensing and monitoring, storing energy efficiently, detecting biological agents, and tagging and identifying objects of interest.

***Nanoscale Photon Dynamics*** — Novel behavior in wide-bandgap inorganic semiconductor quantum dots was explored. Work focused on the enhanced nonlinear optical characteristics due to the reduced spatial dimensionality that elementary charged carriers, such as electrons encounter in these systems.

In the past year, the investigators continued to research CuCl, CuBr, and ZnSe semiconductor quantum dots embedded in borosilicate glass and $Cu^+$- and ZnS-doped Corning Vycor glasses. The Vycor glasses have nanopores infiltrated with $Cu^+$ and ZnS. A new fabrication procedure was devised for the ZnSe-doped glasses, whereas CuCl and CuBr glass melts were first produced at Corning and later given heat treatments at INEEL to initiate nucleation of CuCl and CuBr nanocrystals. $Cu^+$- and ZnS-doped glasses were obtained from the Naval Research Laboratory.

Tunable second harmonic generation (SHG) in the UV-visible was observed from all of the above quantum dots. The size of the nanocrystals was ~5 nm, measured by transmission electron microscopy and low-temperature absorption spectroscopy. The measured efficiencies for 2-mm thick samples were ~$10^{-8}$–$10^{-10}$ at 758–855 nm.

The second harmonic was virtually nonexistent when glass samples did not contain the semiconductor nanocrystals. Evidence was found for second harmonic scattering at 266 nm from the $Cu^+$-doped Vycor sample when a 532 nm fundamental was employed. Measurements of ZnSe samples showed two-photon luminescence upconversion, in addition to the second harmonic generation. The measured nonlinear optical characteristics were abnormally large. These measurements showed that SHG could originate in the nonplanar interfaces between the glass host and particles as small as a few nanometers.

Time-resolved luminescence measurements showed optical energy transfer in real time among shallow traps lying near the conduction band of the ZnSe and CuCl semiconductor nanocrystals. Figure 1 (next page) shows time-resolved luminescence measurements as a function of the second harmonic wavelength in ZnSe quantum dots. The fast component contains contributions due to SHG and two-photon luminescence upconversion. The complex multi-exponential decay on the order of several nanoseconds to hundreds of nanoseconds pertains to relaxation to shallow traps. This is believed to be the first demonstration of shallow trap dynamics in glasses doped with CuCl and ZnSe quantum dots.

***Nanoscale Phonon Dynamics*** — Work also focused on methods to create quantum-confinement using picosecond surface acoustic waves (SAW). Acoustically induced confinement is very appealing because the parameters that dictate the material properties of a confined system (i.e., confinement boundary conditions) can be easily controlled in situ by changing the parameters of the acoustic wave, such as wavelength and wave amplitude.

Laser generation of picosecond SAWs was achieved by spatially modulating the optical refractive index at the sample surface on a nanometer length scale. This was accomplished by using electron beam lithography to deposit a periodic series of metallic bars forming an absorption grating on semitransparent substrates. For SAW generation, the absorbed laser energy was converted into a SAW having the same spatial period as the grating and a propagation direction that was perpendicular to the bar/grating axis.

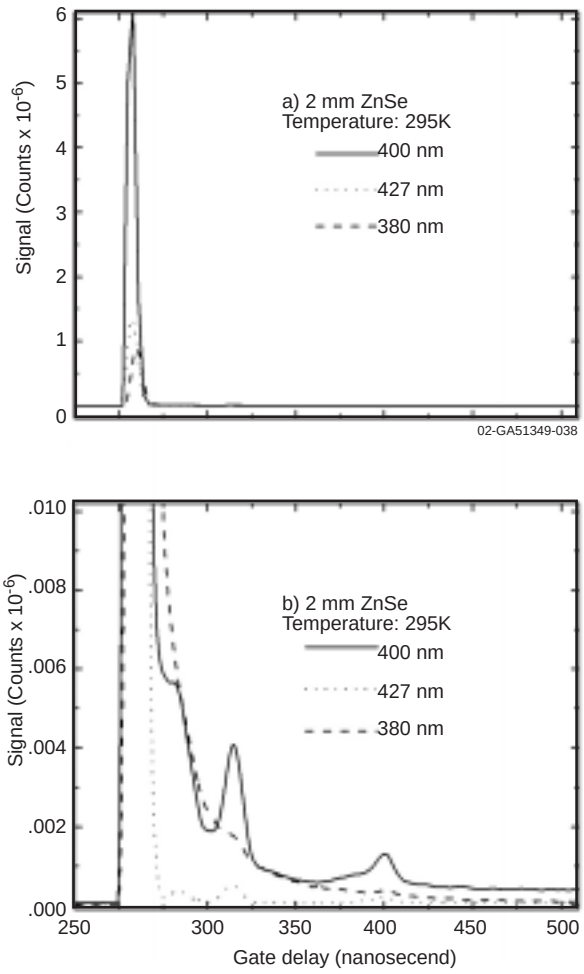


*FIGURE 1. (Top) time-resolved SHG, (bottom) magnification showing the multi-exponential decay.*

Two samples were prepared using electron beam lithography consisting of 5mm long bars periodically deposited on (100) Si, and (100) GaAs substrates. Figure 2 shows the results for the Si and GaAs samples, with center frequencies of 23 GHz and 13 GHz, respectively. These frequencies correspond to those predicted for a surface wave on the substrate material of wavelength

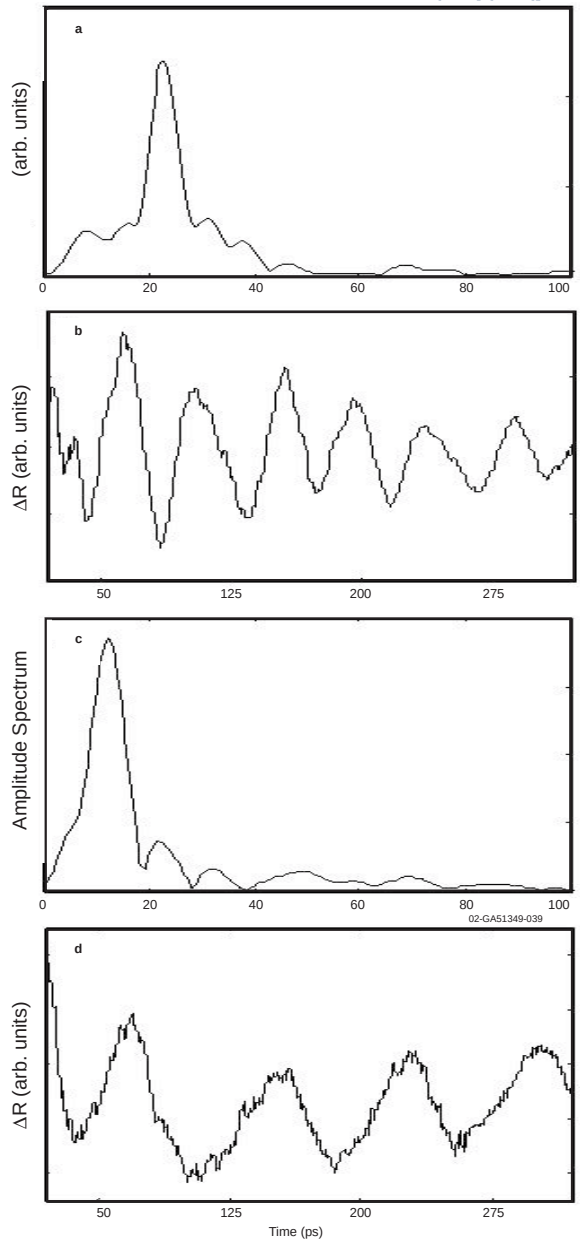


*FIGURE 2. (a and c): Magnitude of the Fourier transform of the change in reflectivity for Si and GaAs, respectively. (b and d): Change in reflectivity for Si and GaAs, respectively.*

equal to the grating period (22.4 GHz-Si and 12.4 GHz-GaAs). The influence of mechanical loading on the SAW velocity has been qualitatively explored and found to be negligible for an aluminum grating on Si and GaAs substrates. In the coming year, this work will be built upon to produce and experimentally verify acoustic confinement. These studies demonstrated, for the first time, the ability to optically generate and detect picosecond surface acoustic waves in GaAs with suboptical wavelengths.

This research has resulted in collaborations with Naval Research Laboratory, Argonne, Sandia, University of Chicago, Corning Glass, Schott Glass, University of California, Berkeley and University of Utah. In addition, the work has resulted in three published articles in peer-reviewed journals and three presentations at conferences, as well as additional proposals.

# Trace Chemical Species Detection and Analysis Using Femtosecond OHD-RIKES

*Napoleon Thantu, Robert S. Schley*

## *A better understanding of chemical transformations*

SC104

Environmental science research encompasses more than just detection and identification of chemical species in the subsurface and elsewhere. There is a need to understand the fundamental dynamic processes and chemical reactions that determine the fate of chemical species and their transformations. Since many chemical processes are mediated at surfaces and interfaces, measurement tools that can selectively probe interfacial phenomena under naturally occurring conditions offer much utility. Ultrafast nonlinear optical techniques appear to be most appropriate for performing such measurements. They rely on optical excitation pathways that are highly restrictive and selective. However, these optical excitation pathways are inaccessible with linear optical techniques. Under certain conditions, the photons that traverse these pathways only interact with interfacial species, permitting a selective probe of interfacial chemical dynamics without interference from bulk chemical species.

This project focuses on the utility of ultrafast nonlinear optical techniques that recently have been implemented at the INEEL for the investigation and analysis of environmental and chemical systems. In particular, the research stresses the sensitivity, interfacial selectivity, and potential for compact instrumentation of coherent Raman and frequency up-conversion experimental measurement tools that rely on ultra-short optical pulses as the excitation source. Ultrafast nonlinear optical experimental approaches can time-resolve chemical reaction dynamics on a subpicosecond time scale, providing information on transient species. Since ultrashort pulses with large coherence bandwidths provide the excitation photons, single-shot spectroscopy is possible.

Technical objectives for fiscal year 2002.

- Determine theoretical description of fundamental ultrafast dynamics in liquids involving simultaneous absorption of two photons in the third-order ultrafast spectroscopy.
- Determine TCE detection limit in $H_2O$ and $CS_2$.
- Prepare manuscripts for publication and make presentations on research findings.

Coherent light scattering techniques such as CARS (coherent anti-Stokes Raman scattering) are especially useful in probing adverse environments such as flames and plasmas. Phase matching requirements lead to a coherent signal output that is highly directional, permitting spatial filtering of the signal from background radiation. Use of single frequency lasers requires a second laser to scan the Raman-active vibrational spectrum of the material of interest, and can lead to a complex and spatially non-compact instrumentation for fieldwork. On the other hand, a complete Raman spectrum can be potentially obtained in a single laser shot by use of a broadband laser source.

The investigators in this LDRD employ a time-domain approach that relies on a broadband, femtosecond laser source that is sensitive to weak depolarized intermolecular and intramolecular Raman modes. These transitions can be used as signatures to distinguish chemical species. This so-called femtosecond optical heterodyne detected Raman induced Kerr effect spectroscopy (OHD-RIKES) in one form or another has been employed by many ultrafast laser laboratories in their studies on ultrafast dynamics in condensed phases. Although femtosecond OHD-RIKES and traditional frequency-domain depolarized light scattering experiments extract the same information, OHD-RIKES more reliably reveals the very low frequency information of the intermolecular Raman spectrum. This low frequency region is sensitive to inhomogeneities of the intermolecular environment, temperature, and molecular symmetry.

In the past year the investigation of environmentally significant molecular liquids was continued. These molecular liquids included aniline, trichloroethylene and carbon tetrachloride. The ultrafast dynamics in aniline was investigated with emphasis on instantaneous electronic contribution. Aniline, a normally colorless and transparent liquid, undergoes photodegradation when exposed to ambient light. This photodegradation produces diazo dye impurities that exhibit absorption near 400 nm.

In this year's experiments employing 800 nm probe photons, the aniline liquid showed simultaneous

absorption of two 800 nm photons due to these impurities. It was observed that this coherent two-photon absorption led to a dip in the instantaneous electronic contribution near the time origin in the OHD-RIKES transient. The electronic two-photon absorption has important ramifications for local potential that each liquid molecule feels. A theoretical description was developed based on a detailed four-wave mixing analysis, of this phenomenon in the manuscript titled "Coherent Two-Photon Absorption in the Third-Order Ultrafast Spectroscopy of Aniline," to be submitted to *Chemical Physics Letters*.

Figures 1a and 1b show the OHD-RIKES transients of aniline taken at two different wavelengths. One wavelength at 788 nm is resonant with the two-photon

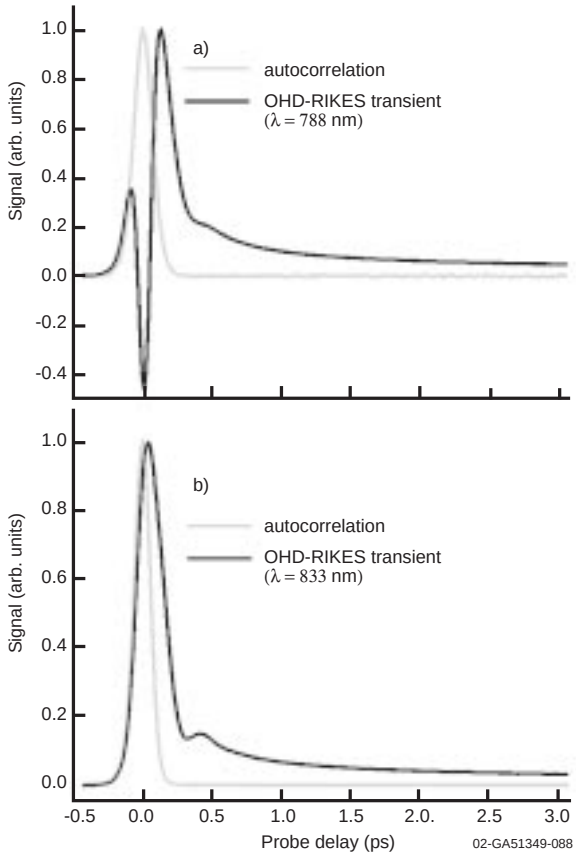


*FIGURE 1. Wavelength-dependent OHD-RIKES of aniline.*

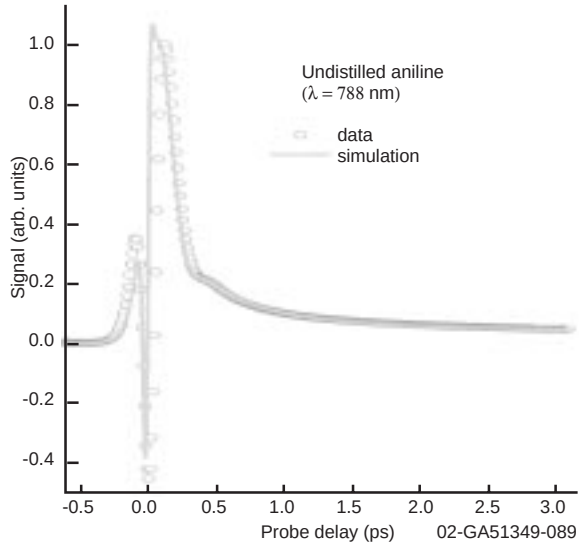


*FIGURE 2. Theoretical simulation of two-photon absorption in aniline.*

energy at 400 nm, while the second wavelength at 833 nm is not. The dip due to two-photon absorption is present in the data of Figure 1a. Figure 2 shows the theoretical simulation of two-photon absorption and compares it to the data in Figure 1a.

The detection limit of TCE diluted with water and carbon disulfide was investigated. The detection of TCE was made by low-frequency Raman-active intramolecular vibrations that were observed in the Fourier transform of the OHD-RIKES transient. The current detection limit was ~ less than 0.1% by volume. The OHD-RIKES signal scales with square of the pump laser intensity. This limit might be substantially lowered if higher laser pulse energies were used. Since the pulse energies were ~ 5 nanojoules, the detection limit, in principle, could be lowered by more than six orders of magnitude with higher pulse energies on the order of microjoules - millijoules available with commercial lasers.

This LDRD has resulted in a number of collaborations with other national laboratories and Boise State University.

# Mechanical and Flow Properties of Dry Granular Media

*Clinton Van Siclen*

## *The role of granular disorder*

SC112

Granular materials are ubiquitous in U. S. industry (e.g., pharmaceutical, food processing, construction). At the same time, their static and dynamic properties are so poorly understood that granular media remain a subject of great scientific interest. Indeed, these materials were singled out in a recent compilation of basic science needs prepared by the National Research Council. DOE in particular has a natural interest in this research area, as the handling and transport of granular material, which itself may literally be dirt cheap, is highly energy intensive.

To initiate research in this area at the INEEL, this LDRD project looks specifically at the role of granular disorder in producing the observed static and dynamic properties. In the case of a metastable configuration of grains (i.e., in a pile or container), the heterogeneity gives rise to "stress chains" (linear clusters of contacting grains at which stress is concentrated) that produce or influence the static properties. To relate these stress chains to the structure of the granular medium, a novel stochastic method for calculating the contact forces in a *frictionless* pile has been developed. The use of frictionless assemblages ensures that 1) forces can be calculated given only the positions of the grains, and 2) a variety of granular structures can be constructed. Preliminary results for simulated, frictionless sand piles built by adding grains at the apex of the pile indicate that stress chains tend to divert the weight away from the middle of the pile, in agreement with experiments on real sand piles conducted elsewhere.

Technical objectives for fiscal year 2002:

- Develop method to calculate the contact forces in frictionless granular assemblages.
- Develop computer code to create frictionless sand piles.
- Obtain preliminary results (e.g., observation of force chains) to compare with experiment.

The properties of granular materials are very difficult to predict. This is at first thought surprising, since surely a statistical or mean-field approach can be taken for a system comprised of a very large number of nominally identical particles. But in fact this is not the case due to local force fluctuations and structural heterogeneities that strongly influence the macroscopic properties. A classic example is the existence of "force chains" in sand piles. These are evidently related to the experimentally observed stress minimum at the substrate directly under the apex of the pile.

To better understand the production of macroscopic, static properties, the example of the sand pile was developed in some detail. It is not immediately obvious how to construct a useful model. Because the number of (normal and transverse) forces at the intergranular contact points exceeds the number of force-balance equations, the forces cannot be calculated given only the locations of the grains. This problem is overcome in studies of random assemblages by quenching an energetic system of interacting particles, where the forces between particles are calculated at each time step as the dynamics simulation proceeds. But this approach cannot be taken for sand piles, as those have an internal structure that reflects their particular growth mechanism.

The indeterminate force problem is avoided in the case of "ideal" sand piles. Several researchers have considered 2-D piles of identical disks in a regular arrangement forming a pyramid. All contact forces are normal (i.e., directed along the line connecting the centers of two contacting disks), so those may be calculated. In fact, the symmetry of the pile permits an analytic treatment. Interestingly, the force on the substrate was found to be uniform under the pile, rather than peaked under the apex of the pile as might be intuitively expected. The same result was obtained for regular 3-D ("cannonball") piles. Similar calculations were performed for regular 2-D piles where grains were selectively removed to simulate void defects and the resultant arches as occur in real sand piles. The vacancies were arranged in a periodic manner so that all contact forces between grains were normal. Again, the force on the substrate was found to be uniform under the pile.

These results motivated further consideration of frictionless piles. (A zero value for the coefficient of friction $\mu$ disallows torques, so all contact forces are normal.) A very useful form of the force equations for a single grain was derived that suggested a novel, stochastic method of solving the set of force equations for an assemblage of grains. It further showed that a necessary requirement for a frictionless pile is that each grain be exactly supported by *d* grains, where *d* is the dimension of the system. This stochastic method was checked by reproducing, both by inspection and numerically via computer code, the results for idealized sand piles available in the literature. Some new, analytical results for regular piles with a single vacancy were obtained as well. These show that the diversion of forces, or "arching," due to the vacancy is sufficient to produce a significant stress minimum at the substrate under the apex.

Of greater interest are the force distributions within and under more realistic sand piles. Simulated, 2-D sand piles were created by dropping grains (disks), one at a time, at the specified apex of the pile, and allowing them to roll down the sides of the pile. A grain *i* would come to rest where it could be supported by two grains *j* and *k* (bounds can be placed on the allowed values of the angles $\phi_{ij}$ and $\phi_{ik}$ to adjust the degree of granular ordering and to influence the sand pile angle of repose). One local growth configuration must be forbidden however, that where the new grain lodges in a "wedge" position between two grains such that it lies at a lower elevation than one of those two supporting grains (say, grain *j*). Clearly that position requires friction for the local grain configuration to be stable. Furthermore, grain *j* would thereby acquire a third "supporting" grain, which is not allowed in a frictionless assemblage. To remove the offending configuration, it is effectively swept away in an avalanche. The intent of these growth rules is to produce an internal pile structure that resembles that of real sand piles. An example of a simulated, 200-grain frictionless sand pile is shown in Figure 1.

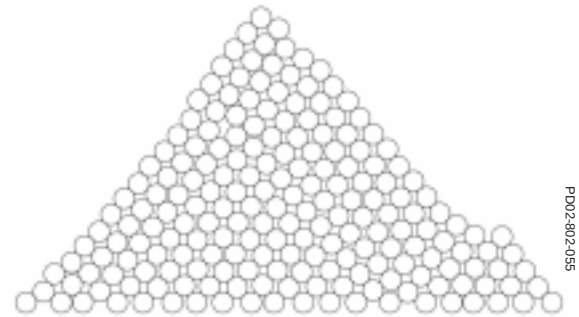


*FIGURE 1. Two-dimensional, frictionless sand pile created by dropping a grain at a time from a fixed location above the pile.*

Figure 2 presents the nodal network corresponding to the same sand pile, where the widths of the bonds indicate the relative magnitudes of the contact forces between grains. The red bonds identify contact forces that are tensile. These of course are nonphysical for a cohesion-less sand pile. As the tensile forces originate at those grains that produce a convex "knee" at the pile surface, they will presumably disappear (i.e., those forces will become slightly compressive) for simulated sand piles having a much smaller angle of repose as typical of real sand piles.

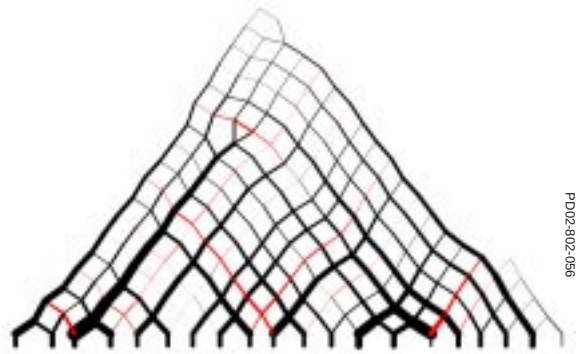


*FIGURE 2. Nodal network corresponding to the sand pile in Figure 1. The width of a bond connecting two nodes indicates the magnitude of the contact force between the two corresponding grains. The heavy black lines identify "force chains" that tend to direct the weight of the pile towards the wings.*

The black "force chains" are the dominant feature in Figure 2. They tend to divert the weight away from the middle of the pile while the red "low-stress" chains, which run to the center of the pile, tend to effectively decompress the middle of the pile. This mechanism for producing the celebrated "stress minimum" beneath the apex of a sand pile will be studied in detail in FY03.

This treatment of frictionless piles enables many interesting research issues to be considered. For example, recent experiments show that the stress minimum is *not* present in the case of sand piles built a layer at a time. Simulated, frictionless sand piles can certainly be constructed in this manner, and the internal force structure calculated as above. The force structure in a granular assemblage confined in a silo is also of interest, since the walls of the silo carry part of the weight of the granular material. Other research conducted under this LDRD includes a "thermodynamic" derivation of the expected weight distribution in non-cohesive granular media. This distribution has been obtained previously, but the new derivation makes use of only the single assumption that force chains are spatially uncorrelated. The validity of this assumption can now be assessed for frictionless piles.

Based on this research, DOE-Basic Energy Science has solicited a proposal from the principal investigator. Contact has been made with prominent researchers at Argonne National Laboratory, Los Alamos National Laboratory, and the University of New South Wales (Australia) who are potential collaborators in future work. In addition, the expertise gained through this LDRD project may find application in applied research at the INEEL. For example, the collection of "pebbles" in pebble-bed nuclear reactors constitutes a confined granular medium whose properties are of current interest.

# Carbon Fractionation Potential of Soils Via $CO_2$/ Water Gradient Fractionation

*Gregory J. White, Harry W. Rollins, David A. Atkinson*

## *Measuring carbon storage in soils*

ET115

Various strategies have been proposed to reduce atmospheric $CO_2$ by transferring carbon to soil organic matter for long-term sequestration. Traditional methods for measuring soil carbon focus on total organic carbon without considering the tremendous inherent heterogeneity. Methods are needed for quantifying different carbon compounds based on their longevity in the soil. Recent research has focused on the application of nuclear magnetic resonance (NMR) for this purpose. However, NMR has low resolution, high cost, and is not field portable.

The research conducted in this LDRD investigates the development of an alternative technique for quantifying carbon fractionation in soils using high-temperature, high-pressure, $CO_2$/water supercritical fluids extraction. Extracts have been recovered from several different soil types, and efforts were made to identify the compounds in the extracts. Field tests with additional soils collected from a well-characterized ecological research site also were conducted. Although considerable additional research is necessary, the technique shows some promise in advancing measurement of carbon in soils by enabling a method of rapid, tunable analysis of soil carbon fractions that is both more sensitive and more cost effective than current techniques. In turn, this could help refine models of subsurface contaminant transport.

Technical objectives for fiscal year 2002:

- Complete construction of the extraction system.
- Continue to test and tune the extraction system to maximize organic extracts from representative soils.
- Develop a technique for identifying key organic compounds.
- Test the system with a suite of soil samples collected from a well-characterized ecological research site.

The objective of this research is to develop an analytical technique for assessing carbon in soils by various key carbon fractions. Accurate prediction of carbon cycling in soils is difficult because soil organic matter consists of a complex array of carbon compounds ranging from highly labile water-soluble compounds (e.g., simple sugars, amino acids and aliphatic acids) to less labile carbohydrates (e.g., cellulose and hemicellulose) to highly refractory materials (e.g., lignin and “humus”). Humus is a generic term for a range of largely unidentified and variable polymeric compounds that are highly aromatic and aliphatic in composition. The accumulation and distribution of soil organic matter is dependant on the quantity and distribution of organic inputs, rates of decay, and the ability of the soil to protect soil organic matter. Since different carbon fractions possess dramatically different residence times in soil, this will allow for better assessment of the actual carbon storage capacity for a soil.

During FY02, a variety of soils were extracted using water at a series of temperatures up to 350° C. These included soils from a wide variety of sites collected the previous year (garden, lawn, and fallow agricultural soils from the Idaho Falls area; soils from quaking aspen and lodgepole pine forests in eastern Idaho; a sample from a saltwater marsh in South Carolina, and soils from redwood and live oak forests in California). The carbon from these various soils was expected to yield distinctly different carbon profiles. Additional samples were collected from the Cedar Creek Long-Term Ecological Research Site in Minnesota during FY02. These samples represented soils of the same type, but which differed in terms of management history. They included samples from abandoned agricultural sites (ranging from 20 to 80 years since abandonment), along with adjacent forest and savanna locations. For the Cedar Creek samples, similar carbon profiles were expected, showing differences in the range necessary for the technique to be broadly applicable.

The soil extracts were characterized using a wide variety of analytical methods including UV-visible absorption spectroscopy, FT-IR absorption spectroscopy, and NMR spectrometry. Figure 1 (next page) shows FT-IR spectra of extracts of a typical soil sample obtained at temperatures of 50° C, 100° C, and 150° C. The efficiency of extraction was determined gravimetrically for a series of samples and found to increase with increasing temperature and to vary with soil type (see Table 1 next page). The more efficient extraction at higher temperatures was reflected in the strength of the transitions in the FT-IR spectra. At lower temperatures a variety of oxygen-containing compounds were readily extracted. Increasing the extraction temperature to

150° C resulted in a large increase in the relative proportion of aliphatic carbon material that was extracted. This is seen in the large increase in the intensity of the band that is at ~ 1400 –1450 $cm^{-1}$. UV-visible absorption spectroscopy was also used to determine the effects of temperature on the extract properties. The ratio of absorbance at 465 nm to 665 nm (E4/E6) has been shown to correlate with the molecular weight of humic and fulvic acids, with smaller values corresponding to larger molecular weights.

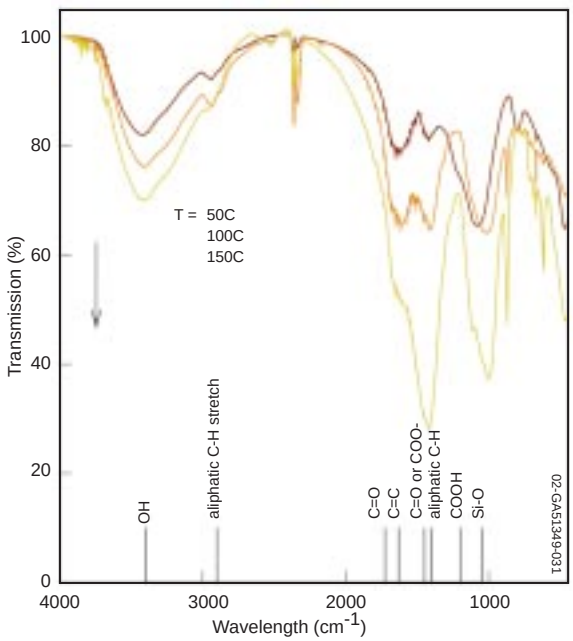


*FIGURE 1. Effect of temperature on the properties of extracts. Transitions for various functional groups are shown for comparison.*

| SOIL | E4/E6 100 | E4/E6 150 | Efficiency (wt%) 150 |
|---|---|---|---|
| Old Field 29 | 8.59 | 6.06 | 2.73 |
| Savanna | 8.21 | 5.74 | 0.25 |
| Forest | 7.10 | 5.46 | 0.89 |
| Old Field 22 | 6.30 | 5.28 | 1.84 |
| Old Field 69 | 6.43 | 5.21 | 1.05 |

02-GA51349-032

*TABLE 1. Efficiency of extraction for a series of samples at different temperatures.*

The E4/E6 ratio for a series of soil samples obtained from the Cedar Creek Long-Term Ecological Research site was determined for extraction temperatures of 100° C and 150° C. For all of the soil samples, the E4/E6 ratio for the extracts obtained at 150° C was higher than for those obtained using an extraction temperature of 100° C. This data agrees well with the FT-IR results indicating the extraction of higher molecular weight material at higher temperatures. This is also consistent with the decreasing polarity of water with increasing temperature. The previously cultivated soils (#22, #29, and #69) contained a larger quantity of extractable material than the uncultivated soils. The savanna soil (which had been burned fairly regularly) had the least extractable quantity of material. $^{13}C$ and $^{1}H$ nuclear magnetic spectroscopy also was used to characterize the extracts. NMR spectra for all the samples were similar and showed several broad peaks in the alkyl region with little or no signal in the aromatic regions.

All of the extracts contain a mixture of a large number of different chemical species. To quantify the various species more precisely, several separation strategies were employed. Due to the low volatility of the components, the extracts were derivatized to the corresponding ester and analyzed using GC-MS. Volatility of the samples was still low making the gas chromatography problematic. The soil extracts were then separated using size

exclusion chromatography, which separates samples based on molecular weight. Chromatograms of different extracts all showed similar features and had a broad distribution of molecular weights. Molecular weight distributions for the extracts were not determined due to a lack of suitable standards and interactions of the extract materials with the solid phase of the size exclusion chromatography column.

Although the driving need for the analytical capability investigated in this LDRD is to improve measurement and predictability of carbon storage in soils relating to global climate change, the technique may also substantially enhance the predictive ability of models of subsurface transport of contaminants, and therefore is applicable to the Subsurface Science Initiative and Long-Term Stewardship issues.

According to the recent U.S. DOE document "Carbon Sequestration – State of the Science," research is needed in the area of terrestrial carbon sequestration *"…that will lead to an ability to understand, predict, assess, measure, and implement substantially increased sequestration of carbon in soil and vegetation systems."* Current efforts to quantify, predict, and verify the capacity of soils to store C are hampered by (1) the complexity of soil organic matter; (2) difficulties in predicting C turnover times; and (3) the lack of accurate, cost-effective, field-portable analytical tools for measuring different C compounds or classes of compounds in the soil. Methods are needed that will allow for the accurate assessment of carbon storage or sequestration in soils. The research conducted under this LDRD will develop such a technique that, if successful, can lead to dramatic improvements in the measurement and prediction of carbon sequestration in soils.

To date, this LDRD has resulted in collaborations with researchers at Idaho State University and the University of Maine. In the future, collaborations with researchers involved with the Free Air $CO_2$ Enrichment (FACE) and the AmeriFlux programs, both of which are sponsored in part by DOE, also will be pursued.

# National Defense

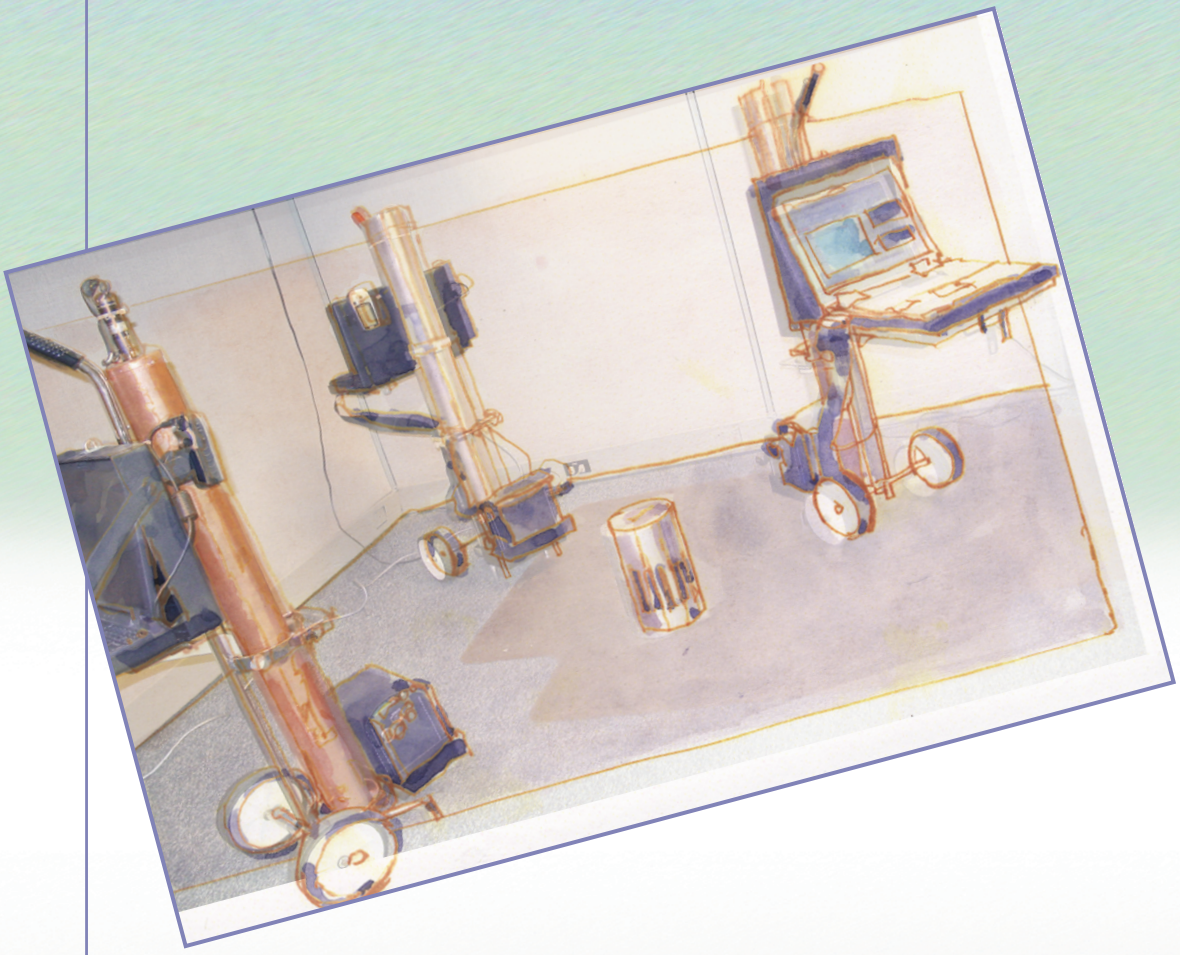

# LDRD Annual Report for FY-2002

Idaho National Engineering & Environmental Laboratory

# Second Generation Neutron/Gamma Sensor

*Rahmat Aryaeinejad, Edward Reber, Dave Spencer*

## *Increasing border security with a handheld detector*

NS109

A small battery-operated sensor that can detect gamma rays and fast neutrons would be extremely useful in applications such as U.S. Customs inspection, border security, environmental radiation monitoring and more.

This LDRD project investigates development of a handheld device to measure fast neutrons and gamma rays using a single detector. The device will operate one rechargeable Li ion battery and be able to detect both gamma rays and neutrons. Since this detector is sensitive to fast neutrons, there will be no need for a moderator around the detector. Consequently, a smaller and lighter detection system can be fabricated.

The handheld detection system uses a single 12.7 mm (diameter) by 12.7 mm (long) liquid scintillator detector (BC501). The use of only one detector requires that the neutrons and gamma rays be distinguished by the shape of their pulses in the detector. Two methods of pulse shape discrimination (PSD) are evaluated in this work: charge integration and zero crossing. Figures of merit were calculated for both methods for a threshold energy range of 50 to 600 keV. Results show that the zero crossing method gives much better PSD for 100 keV and lower, whereas the charge integration method leads to better separation above 100 keV. However, the neutrons and gamma rays are totally separated for energies of 100 keV and above in both techniques. The investigators are currently designing a miniaturized electronic system to be incorporated into the handheld device.

Technical objectives for fiscal year 2002:

- Design and develop digital signal processing and time integration for the best neutron/gamma separation.
- Develop software for manipulating 2-D data to separate neutrons from gammas and to display the results online.
- Perform measurements at different threshold settings to determine the optimum performance.
- Compare the results of the two PSD techniques to decide which method leads to better performance and easier miniaturization of the electronics.
- Fabricate two different sizes of fast-neutron detectors in collaboration with Bicron Inc.
- Design and develop electronic breadboard system, tests and performance measurements using simulated neutron and gamma ray signals.
- Complete the design of a prototype high-voltage board.
- Present findings at conferences and in technical journals.

An earlier neutron/gamma detection system developed at the INEEL used a combination of two Li-6/Li-7 glass scintillators. Because Li-6 is only sensitive to thermal neutrons, these detectors needed to be inside a polyethylene block. This made the detection system slightly bigger and heavier than what was required for some applications. Other detectors like a boron-loaded plastic scintillator can be used to detect both thermal and fast neutrons, although, the discrimination between gamma rays and fast neutrons is not as good as with liquid scintillators.

Using a xylene liquid scintillator detector (BC501 manufactured by Bicron) and pulse shape discrimination techniques, the investigators in this LDRD are creating a single detector capable of both neutron and gamma ray detection. Two different methods of pulse shape discrimination, "Charge Integration" and "Zero Crossing," were used to separate gamma rays from neutrons. To quantify the separation of the peaks corresponding to the neutrons and gamma rays, a figure of merit (FOM) was used:

$$FOM = \frac{peak_seperation}{FWHM_{\gamma} + FWHM_{n}}$$

Where peak_separation is the number of channels between the gamma ray peak and neutron peak, centroids and the FWHM$\gamma$,*n* are the full width at half maximum (channels) of the gamma and neutron peaks, respectively. This figure of merit was used to compare the results of the two methods. Table 1 summarizes the results of the

| Threshold (keV) | Zero Crossing (FOM) | Integration (FOM) |
|---|---|---|
| 50 | 1.197 | 0.850 |
| 75 | 1.221 | 1.009 |
| 100 | 1.302 | 1.189 |
| 300 | 1.454 | 2.319 |
| 500 | 1.526 | 2.829 |
| 600 | 1.655 | 3.156 |

02-GA51349-058

*TABLE 1. Comparison between charge integration and zero crossing (Z/C) methods vs. threshold energy.*

two PSD methods. At first glance one can see that the zero crossing method is better for threshold values of 100 keV and lower. On the other hand, the charge integration method seems to be better for higher thresholds (>100 keV). Wolski et al. have reported similar results except they used the traditional method of charge integration and were unable to resolve the $\gamma/n$ below 300 keV without raising the gain of the photomultiplier. The method explored in this research can separate gammas and neutrons down to 50 keV without any need for raising the photomultiplier gain.

When the FOM is about 1.3 or higher, the neutron and gamma ray peaks are well separated and there is no need for more separation. Since the neutron and gamma ray peaks are well separated in both methods above 100 keV, the focus must be on the separation below 100 keV to determine which method is the best overall. The zero crossing method for separation performs best in this lower region, and therefore is the best method to discriminate between neutrons and gamma rays over the entire range of thresholds. The complete results of these tests were published this year in the peer-reviewed *IEEE Transactions on Nuclear Science* (August 2002).

Figure 1a shows the 12.7 mm x 12.7 mm liquid scintillator detector that will be used in the prototype system. The miniaturized electronic system (Fig. 1b) is currently under development at the INEEL. The output from a photomultiplier tube is amplified, inverted, and RC shaped. A comparator provides a discrimination level to eliminate low-level and noisy input signals. The comparator output's leading edge starts a one-shot. The one-shot pulse time is set to be greater than the comparator pulse time of a gamma signal, but shorter than the pulse time of a neutron signal. The comparator output (gamma or neutron pulse) also is sent to the input of a latch. The latch clocks the input on the one-shot trailing edge. The output level of the latch will determine if the event is gamma (high) or neutron (low).

The proof-of-concept for this electronic system was already established on the simulated neutron and gamma-ray signals. The investigators also have completed and successfully tested a prototype surface mount Cockroft-Walton (CW) high-voltage board. These results were

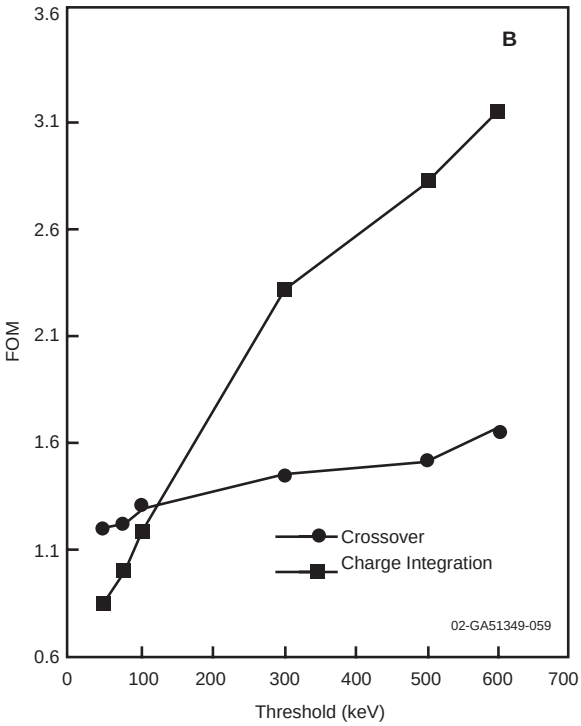


*FIGURE 1. (a) Photo of the 12.7 mm x 12.7 liquid scintillator (BC501A), and (b) the electronics diagram.*

published in the peer-reviewed *IEEE Transactions on Nuclear Science* (June 2002). The size of this board is approximately 1" x 3.5", which includes sockets for two photomultipliers. The whole system, when attached to the detector, draws less than 15 mA current. This is lower than commercially available high-voltage units by a factor of 10, which means the batteries will last 10 times longer. This CW board is already incorporated into the previous neutron/gamma pager based on Li-6/Li-7 sensors.

The tragic events of September 11, 2001 demonstrate the vulnerability of the United States to catastrophic attack, especially by nuclear and radiological weapons. This sensor is ideally suited for detecting smuggled special nuclear materials, and therefore has been designed to be used by law enforcement agencies, customs agents, Special Forces, armed forces, and both private and public industry/government security personnel to interdict and prevent a nuclear or radiological attack on the United States or its interests or citizens abroad. The combination of a smaller size, lower cost, and more sensitive sensor will significantly support other INEEL programs as well, in particular the environmental, nuclear, subsurface, and especially national security divisions of the laboratory. In addition, this project has a commercial potential that could lead to a CRADA agreement or licensing with Imaging and Sensor Technologies Company for developing a prototype system.

# Multipath Propagation Analysis, Simulation, and Prediction in Wireless Environments

*Scott G. Bauer, Allan A. Anderson, J. Hope Forsmann, Lynda Brighton*

## *Wireless devices as geographic locators*

NS123

Understanding multipath propagation for digital high-speed wireless environments is important to the development of mitigation strategies to enhance the quality of service (QoS) to users. Multipath occurs when a wave propagates to a point in space via different paths. The multipath in wireless environments is caused by the direct reflection and/or refraction of electromagnetic waves off objects such as buildings, hills, water, towers, and indoor environments. Multipath fading occurs when one or more reflected signal is delayed because its indirect path combines with the direct transmission. Depending upon the phase relationship an additive or subtractive effect occurs at the handset and is seen by the user as multipath fading or in digital networks as inter-symbol interference.

Multipath is common in all urban and enterprise environments, it is quantifiable, and can be characterized. The focus of this LDRD research is to investigate current modeling techniques used by the industry to predict multipath propagation. Strategies have been developed to collect and characterize data specific to digital high-speed cellular and wireless local-area network (WLAN) environments. Significant findings have shown that multipath can be a unique identifier as a geographic location method in non-traditional environments. Multipath radio frequency (RF) signatures may provide potential unconventional methods of detecting security breaches, network intrusion, or asset location for WLAN environments. From exploration with directional RF antennas, a case has been built for the use of "Smart Antenna" technologies, potentially providing increased spectral efficiency, the suppression of interference, and the increase of dynamic range.

Technical objectives for fiscal year 2002:

- Deploy 802.11b WLAN network with multiple access points and multi-user support.
- Evaluate and obtain network and WLAN measurement tools. Develop physical measurement strategies for the collection of multipath data in a lab and indoor office facility.
- Conduct multipath measurements to better understanding the performance characteristics of a WLAN system.
- Develop technique to exploit multipath to geo-locate a client of the WLAN system.
- Explore novel techniques that would allow intrusion detection by exploiting multipath characteristics.
- Evaluate how a directional narrow beam antenna affects WLAN performance to support or dismiss the potential promise of Smart Antenna technologies.

Geo-location and security enhancement methods were hypothesized that use the frequency-selective multipath fading characteristics of WLAN and WLAN sensitivity to changes in surroundings. For the proposed technology, these characteristics are useful. Therefore, high-multipath and RF-reflective environments are considered RF friendly as opposed to conventional geo-location technologies that consider these environments difficult, complex, and prohibitive. Image Change Detection (ICD), or similar software, was evaluated for these applications. Actual WLAN systems were used along with the ICD software to demonstrate a physical change in the environment.

WLAN 2.4GHz ISM band spread spectrum methods of RF communication rely upon a pseudo, randomly changing carrier frequency with a maximum frequency deviation range, in this case approximately 20 MHz. In this effort, the ability to measure unique fingerprints at various locations inside a building using the 2.4 GHz band was demonstrated. Directional data was collected from a single receive antenna that was rotated a total of 360 degrees while collecting RF amplitude data at discrete angles. The antenna was positioned at various locations inside an office laboratory facility. The signal was transmitted from another point in the same building and had spectral characteristics similar to that of a WLAN signal. Image Change Detection software written at the INEEL was used to provide a quantitative value representing the degree of correlation between fingerprints.

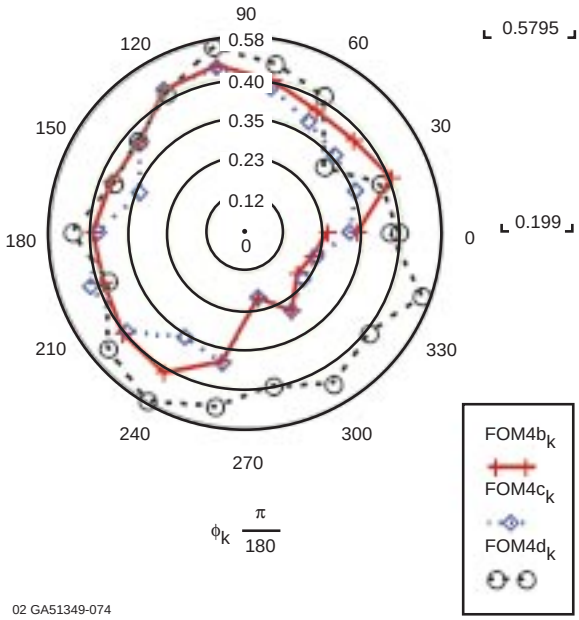


*FIGURE 1. Polar plot of correlation figure-of-merit data showing effects of opening a walk-in metal door in a hallway. The three RF frequency spectra were centered at 2.457GHz with a frequency span of 20MHz. The dashed trace identified by FOM4d was collected while the door was closed. The correlation data FOM4b and FOM4c were collected while the door was open*

The processed data collected representing correlation fingerprints is shown in a polar plot in Figure 1. The distortion in the polar curves between 240 degrees and 25 degrees can be seen, due to a change in the multipath environment. The decrease in correlation magnitude seen in this region is a direct result of the open or closed position of the door.

Similar effects on the degree of correlation can be observed in a WLAN system of multiple clients when one of the clients has either been activated or deactivated. Other possible conditions that might result in similar effects include: modifications to client antennas or antenna type, antenna movement in orientation or position, changes in spectral characteristics, and modification to building structure. The sensitivity to such conditions could allow this technology to be useful in geo-location applications, detection for specific security breaches, location of users, tampering and covert activity detection, and denial of service of unwanted omni antenna emissions.

With the advent of wireless local area networks and the ubiquitous use of cellular phones, a technique for improved wireless performance is essential. Through spatial filtering, smart antenna systems might allow frequency reuse within a small area and in essence, double an access points capacity (for WLAN) or a cell's capacity (for cellular). Smart antenna systems also have the potential to extend the range of the access point (cell) by steering the beam to the user's signal, and reduce interference by steering the nulls towards the unwanted signal. Smart antenna systems consist of a multi-element antenna array, electronics (receiver, DSP, etc.) and software that control the amplitude and phase of each of the antenna array elements as well as implement time-delay equalization.

During the research effort, WLAN performance data was collected with a stationary access point configured with an omni directional antenna and a roving laptop (client) configured with a directional antenna that could be rotated 360 degrees. As shown in Figure 2a and 2b, (next page) the number of packets lost increases significantly at certain rotational angles, while at others, it is in an acceptable range.

As the laptop is moved to other locations, the angular direction at which packets are lost, as well as the quantity of packets lost, changes as can be seen in Figure 2b. With the use of a smart antenna system, the number of packets

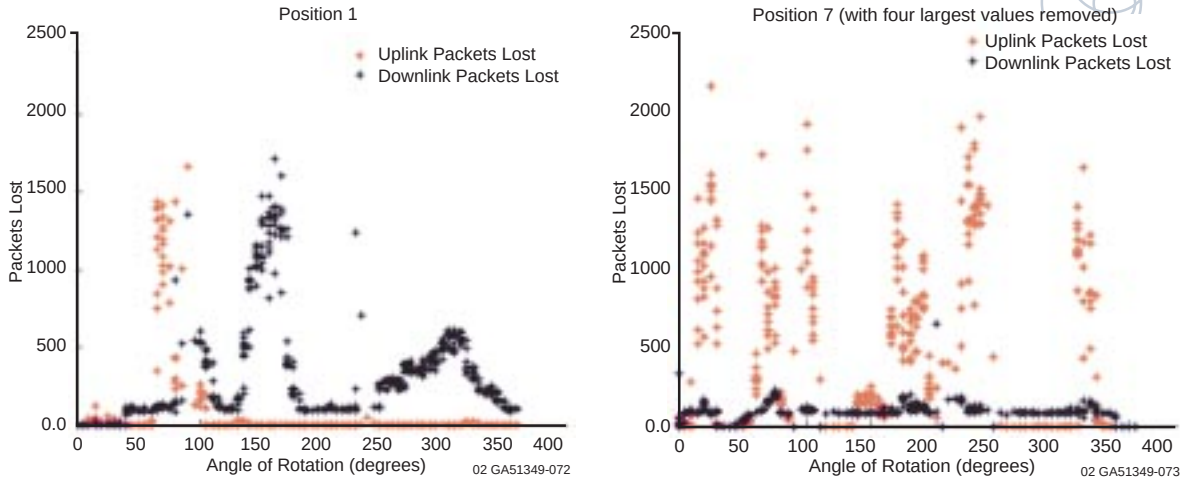


*FIGURE 2. WLAN packet-loss performance data at position 1 and position 7. Orinoco Access Point with a fixed Omni directional antenna. Client with directional antenna (BW= 17 degrees, gain = 15 dB). Horizontal axis is the angular position of this directive antenna. Vertical axis is a measurement of the number of packets lost. Blue indicates data transmitted from the access point. Red indicates data received by the access point (transmitted by the client).*

lost should be minimized for most angles relative to the client (laptop) and/or access point. Significant performance benefits can be achieved.

During this research an effort was conducted in finding an existing antenna array that would support a WLAN smart antenna system. None were found that met the requirements put forward: 1) multi-beam antenna, 2) electronic scanning over 360 degrees, 3) simultaneous control over all antenna beams, 4) operational at 802.11b frequencies. Companies that are attempting to market and develop smart and adaptive antennas should be sought for future research efforts.

# Selected Release of Polymer Degradation Agents by Photoinitiation

*Michael T. Benson, Eric S. Peterson*

## *Time-release delivery of specific agents*

NS102

Photo-initiated degradation of polymers is finding applications in a variety of fields, such as the controlled delivery of drugs. The obvious advantage of light initiated degradation over chemical initiation is the absence of waste solvents and chemicals.

This LDRD research is investigating the photo-initiated degradation of terpene-containing microspheres. Previous studies at the INEEL have shown that the slow release of terpene is possible using gelatin/acacia microspheres. Although the release rate is controllable through crosslinking density and microsphere wall thickness, choosing the time for terpene release has not been possible to date. One approach allowing controlled terpene release is to use an impermeable microcapsule that is degraded, releasing the terpene all at once when it is needed. This is possible using a polymer crosslinking agent that undergoes photooxidation upon exposure to high intensity UV radiation.

The two types of crosslinking agents investigated in this study were isocyanate and melamine. Crosslinked poly(vinyl alcohol) (PVA) and polyacrylate (PAA) were determined, through testing by pervaporation of terpene through a thin film of the polymer, to be the best polymer candidates. Dynamic Mechanical Analysis (DMA) was conducted on the crosslinked PAA to predict the behavior of the film over an extended period of time (years to decades). A method to form microspheres has been initiated and is in progress. A computational study of the crosslinking mechanism is in progress, to gain a better understanding of the crosslinking process and the degradation process.

Technical objectives for fiscal year 2002:

- Review literature to identify additional crosslinking agents and polymers.
- Crosslink promising polymers.
- Test permeability of terpenes through crosslinked polymers.
- Choose one polymer system to study.
- Find suitable encapsulation methods for the chosen polymer/crosslinking agent.

It has been shown in INEEL lab studies that the slow release of terpenes, dipentene or α-pinene, is possible through microencapsulation. The terpene slowly diffuses through gelatin/gum arabic microcapsules. The diffusing terpene has been used to degrade an adhesive over several days or weeks, depending on the microcapsule loading. The holding time is the time required for adhesive failure. *As the loading is increased, there is a very clear trend in the data: the time required for catastrophic failure decreases.* The holding time with 5 grams of microcapsules is less than half the holding time without microcapsules. The release of terpene slowly degrades the adhesive to the point of failure. Before this technology can be used industrially, one important issue needs to be addressed: more precise control of the terpene release.

Better control is possible by not allowing the terpene to escape until the microcapsule is "activated." In this context, activation is the photo-initiated degradation of the microcapsule, allowing the terpene to escape.

Two classes of crosslinking agents have been identified for use in this project. Both melamines and isocyanates photodegrade upon exposure to high intensity UV radiation. Two melamine crosslinking agents have been synthesized. Hexamethylol melamine was reacted with both methanol and ethanol, producing the methoxylated and ethoxylated crosslinking agents. With a terminal ether group that can be changed, the solubility and handling properties of the crosslinking agent can be modified. The biuret of 1,6-diisocyanohexane has been synthesized, and is the only isocyanate type crosslinking agent investigated.

Two polymers, polyacrylic acid and poly(vinyl alcohol) (PVA), have been crosslinked with the fully (MF-6), and the partially (MF-3) substituted melamine. These polymers have been the most promising due to their impermeability to terpene when crosslinked, as determined from pervaporation studies. Figure 1 (next page) shows the reaction between PVA and the methoxylated melamine. A method to form microspheres from PVA has not been found, though literature methods exist to form PAA microspheres. Consequently, PAA has been more fully investigated and characterized, specifically through dynamic mechanical analysis. DMA can be used to determine physical characteristics of a polymer, such as storage modulus and loss modulus. From these properties, it might be possible to investigate the physical properties of the polymer in the long term (months to years).

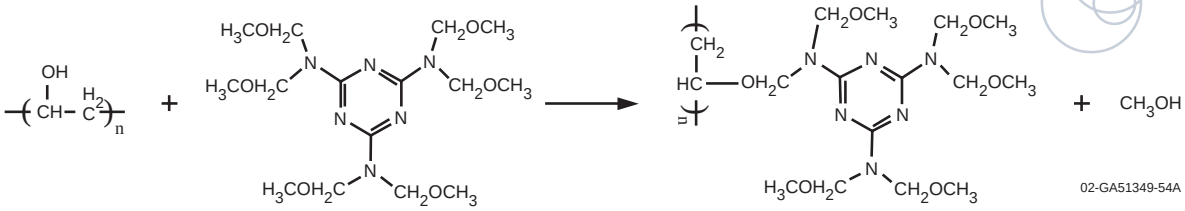


*FIGURE 1. PVA reacting with methoxylated melamine.*

The mechanical property results for a crosslinked PAA are shown in Figure 2. The temperature/frequency dependencies on the dynamic mechanical properties were investigated. The storage modulus of one sample (analyzed twice under exact DMA-TTS conditions) versus temperature are plotted in Figure 2a, showing the results from three of the frequency scans acquired during the DMA-TTS analysis. Scans at other frequencies were omitted for clarity.

The storage modulus, which is related to the stiffness of the sample, increases from 30° C to 70° C, in what is generally considered the glassy polymeric region. The rise in storage modulus in this region eliminates the possibility of a β transition generally associated with the crankshaft mechanism, due to increased mobility of short branching side groups or the $(CH_2)_n$ backbone. The

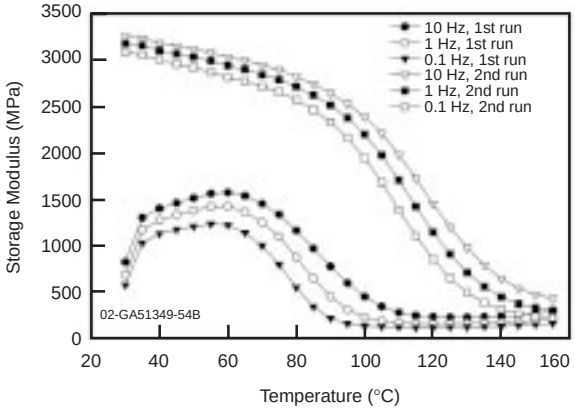


*FIGURE 2. Storage modulus vs. temperature at multiple frequencies (two consecutive runs) for PAA/MF-3.*

DMA-TTS scan covers the full range of polymer behavior from a glassy polymer region (left) through a relaxation process (center) and just about encompasses the rubbery plateau region (right).

The storage modulus of the first DMA-TTS run sample shows that the material is "relatively stiff" for a lightly crosslinked material throughout the glassy region. However, the storage modulus drops considerably while transposing through the a relaxation, the glass transition process. By the time the sample reached 100° C, the storage modulus dropped two-fold. Due to the observation that the material may still be crosslinking in the oven, the same sample was again subjected to the exact DMA-TTS conditions and re-analyzed (second run), also shown in Figure 2. The storage modulus of the sample increased by over four-fold at the 30° C starting temperature from the first run. The storage modulus decreased throughout the second run, indicating the material was completely crosslinked.

Crosslink densities were calculated at 10 Hz for both runs. Run 1 has a crosslink density of 2.27 x $10^4$ moles/$m^3$. Run 2 has a crosslink density of 4.03 x $10^4$ moles/$m^3$. The crosslink density has roughly doubled after the first DMA-TTS run, even after crosslinking at 110° C for 30 minutes. Based on literature values, PAA/MF-3 is a highly crosslinked film.

It would be very useful to use the time-temperature data to predict physical properties, such as molecular weight or aging. Attempts to generate a time-temperature superposition master curve from the time-temperature data were not successful (standard error >250). It would appear that PAA crosslinked with MF-3 is not a rheologically simple material.

To better understand the degradation process, a computational modeling study was performed on the reaction shown in Figure 1, with a fully methoxylated melamine crosslinking agent and a partially methoxylated melamine crosslinking agent. The degree of methoxylation on the crosslinking agent determines the operative crosslinking mechanism, either specific acid catalysis or general acid catalysis. The partially methoxylated melamine investigation has been completed, while the fully methoxylated melamine study is still underway. For simplicity, PVA was used and not PAA. While this may make a small difference in the addition of the polymer to the crosslinking agent, the initial steps of the mechanism will not change. The computational studies can be expanded to investigate differences in the reaction due to the different polymers.

In the partially methoxylated melamine, the initial steps in the mechanism are protonation of the melamine followed by liberation of methanol. The reverse, addition of methanol, is exothermic with a downhill transition state although the elevated cure temperatures required will remove methanol from the reaction medium, driving the reaction to completion. After liberation of methanol, the addition of the polymer can follow an acid catalyzed or non-catalyzed mechanism, depending on acid strength. Energetically, following the acid catalyzed mechanism appears to be an easier mechanism, although the proton has to be abstracted to obtain the neutral product. In the non-catalyzed mechanism, a barrier of 33.9 kcal/mol has to be overcome to add the polymer. The protonated polymer product has a lower proton affinity (222.3 kcal/mol) than the protonated Schiff-base (228.8 kcal/mol), making proton abstraction easier after polymer addition. This suggests polymer addition will proceed through the acid catalyzed mechanism, the same as the fully substituted melamine. This is not the case experimentally, though, where the reverse reactions dominate the cure response behavior. In a highly acidic environment, the amount of energy required to break the polymer-crosslinker bond is considerably less (by 32 kcal/mol) than a non-acidic environment.

Of the technical objectives described for FY02, all have been completed except for the last objective of finding suitable encapsulation methods for the chosen polymer/crosslinking agent. This final task is ongoing.

One article on the computational modeling of a partially methoxylated melamine crosslinking agent (MF-3) crosslinking PVA has completed peer review with publication expected in early 2003. A second article, on the computational modeling of a fully methoxylated melamine crosslinking agent (MF-6) crosslinking PVA, is nearly complete. Two presentations at a national American Chemical Society meeting resulted from this work.

This LDRD supports the National Security Program. The project has supported development of materials approaches to controlled degradation of materials under specific conditions. The customers for this technology have been made aware of this progress and are very interested in seeing its continued development. This LDRD work is featured in several pending proposals with various government agencies and has continued to enhance the INEEL's reputation in the materials degradation arena.

# Information Visualization by Query

*Kurt Derr, Kenneth Rohde*

## *Stitching together information at the desktop*

NS104

Bringing disparate information together in the same visualization allows relationships to be realized that might otherwise be difficult to see in traditional information/stove-piped software systems. The purpose of this LDRD is to investigate the feasibility of a software prototype, Information Visualization by Query (IVBQ), that would give office workers (non-technical users) the ability to retrieve information from many data sources and visualize that information in many forms, *with no user programming required*. The data sources may be files or relational databases somewhere on the network, real-time feeds from a network connection or data files in XML (eXtensible Markup Language) format. The visualizations may be bar or pie charts, x-y plots, tables, hierarchical charts, 2-D maps, or 3-D.

Technical objectives for fiscal year 2002:

- Enhance IVBQ to make the program a working prototype.
- Demonstrate the IVBQ prototype at a software conference.
- Incorporate geographical information system (GIS) capabilities.
- Incorporate the ability to connect applications to data sources and visualizations.
- Enable IVBQ to read XML data and export data from any source in XML format.
- Produce a demonstration CD of a prototype version of IVBQ.

A working software prototype, IVBQ, has been developed for integrating and visualizing information. IVBQ is a client-server application written in the Java computer language that can run on any computer with a Java 2 virtual machine, such as Microsoft Windows, Solaris, or Linux.

IVBQ provides the following capabilities and features:

- Retrieve, visualize, and integrate information from disparate sources.
- Monitor data sources, or enterprise systems, for user-specified events, which in turn signal user-specified tasks.
- Discover the content of existing corporate relational databases.
- Connect applications to data sources and visualizations.
- Read and write XML data.

IVBQ is a client-server application that enables an enterprise to retrieve information from disparate sources and present and manipulate it in numerous visualizations. Bringing disparate information together in the same visualization allows relationships to be realized that might otherwise be difficult to see in traditional information/stove-piped systems.

IVBQ ties together data from many applications or domains into one cohesive integrated solution. IVBQ enables the user to integrate information at the desktop level. For example, a user may select rows from multiple table views and merge the rows of data into a new table view. This data can then be viewed in other 2-D visualizations.

Information such as imagery, organizational information, and logistical information can be acquired from many different sources, such as relational databases, files, live network connections, GIS sources (ESRI MapObjects and ArcView IMS servers), XML sources, intelligent devices monitoring equipment, etc.

A broad range of advanced visualizations allows users to view and interact with their data and conduct “what if” scenarios. Some of the visualizations provided by IVBQ include 2-D (charts such as pie, line, scatter, bar, Gantt, tables, time plots), 3-D, tables, trees, and maps. A very intuitive graphical user interface allows users to simply drag and drop data sources and visualization views onto a connecting pane and then connect these elements together to visualize the information.

IVBQ is not tied to any particular data source or database system, and the database(s) does not need to be on the same physical computer. IVBQ automatically discovers the contents of any relational database and allows a user to visualize the information from the database in a 2-D or 3-D format. The database metadata is dynamically generated and used to visualize the information. IVBQ requires metadata information from every data source.

IVBQ can import and export data from/to other applications using the XML. Any data imported from an XML file can be visualized in an applicable 2-D or 3-D form. Table visualizations created in IVBQ can be exported to an XML file.

Business users typically need to access myriad data sources, monitor the state of the data vital for real-time decision-making, and then take specific actions based on the state of the data. IVBQ lets users create agents that monitor data for specific conditions to automate routine decision-making. When these conditions are met, an agent can initiate several responses, such as sending email, notifying the user with a pop-up message, running an application, or printing or saving the information. For example, a user could create agents that monitor inventories and supplies for building products. When inventories fall below certain levels, an agent sends email notifying the user that the product supplies need to be ordered along with the name of the cheapest supplier. Alternatively, instead of notifying the user, the order could automatically be placed with the supplier.

Users can connect applications to data sources and visualizations through the drag-and-drop graphical user interface. For example, a Java application could receive data from a relational database, process the data, and then have the data visualized in a 2-D IVBQ plot. Alternatively, the Java application could filter the data it receives from a relational database, pass the filtered data to another application that does some analytical processing, and then pass on the processed data to an IVBQ bar chart.

The main graphical user interface for IVBQ is shown in Figure 1. The user interface is split into two panes – a tool pane on the left and an information pane on the right. The tool pane represents generic data sources, visualizations, and action entities. The information pane represents specific data sources, how those data sources are being visualized, user-specified actions for the data sources, and query results from one or more data sources. The visualization entities from left to right and top to bottom are bar chart, pie chart, XY plot, table, 2-D map, hierarchical chart, and query table. The data source entities are file, network, relational database, relational database table, and XML sources. The action entities are email, run application, and desktop user notification.

A user visualizes information by dragging and dropping both data source and visualization entities from the tool pane to the information pane. The user can specify particular data source information by double-clicking on the data source entity. A context menu enables a user to connect the data source to the visualization and to view the information. A user can visualize a data source in multiple ways, or take multiple actions based on the state of the data by connecting action entities to the data sources.

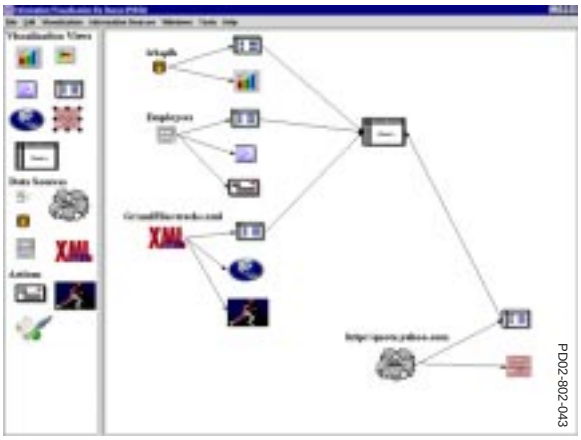


*FIGURE 1. An example of the use of IVBQ.*

The following data source-to-visualization connections are shown on the information pane in Figure 1 (Note that the actual visualizations are in separate displays not shown on this diagram.):

- A relational database data source, ivbqdb, being visualized in a table and a bar chart.
- The relational database table data source, Employees, is visualized in both a table and a plot. An email notification will be sent based on the state of the data in this table.
- An XML file data source, tracks.xml, is visualized as a table and a 2-D map, and an application is run based on the state of the XML data.

- A network data source, http://quote.yahoo.com, is connected to the Yahoo Web site and is retrieving information that is being displayed in a table and in a hierarchical chart.
- A query table is created based on the results of a query across the relational database, relational database table, XML, and network data sources.

The prototype evaluated under this LDRD is using the Extensible Information System (XIS) Java toolkit (Polexis Corp.). Polexis developed XIS through five years of DARPA funding and it is available to the INEEL and other government agencies at no charge. XIS enables a developer to produce applications and e-commerce solutions that can use and share information simultaneously from a wide range of data sources. XIS is a core technology for the Defense Information Infrastructure Common Operating Environment (DII COE). The use of XIS in this software design positions the INEEL to support government agencies currently using XIS, and future organizations as they begin to use this technology.

# A Compton-Backscatter Photon Source for Tunable, Monoenergetic, Hard X-rays

*James L. Jones, Greg D. Lancaster*

***Expanding regional capabilities***

NS122

There is strong scientific and industrial interest in bright monochromatic and tunable x-ray sources. These sources are being widely used in various scientific research fields as well as in medical, technology and industrial research applications. This LDRD is developing INEEL capability in tunable x-ray sources to directly support advanced research in these areas. Specifically, this added expertise is expected to benefit: 1) investigations of sub-micron and sub-nanometer structures on silicon (wafer) surfaces, 2) imaging for material probing, 3) chemical identification, 4) spatial element identification and mapping in stressed and unstressed materials (e.g., NDE/NDA), and 5) medical radiation therapy using very focused, tunable photon energies resulting in the most favorable dose distributions to the patient.

Technical objectives for fiscal year 2002:

- Modify the laser for optimal injection into the electron beam.
- Design optimal laser pulse and electron beam injection synchronization.
- Optimize electron beam and laser focusing scheme.
- Demonstrate optimal system operation.
- Investigate x-ray beam properties vs. laser beam and electron beam parameters.
- Measure x-ray beam flux and energy and compare to theoretical predictions.
- Measure x-ray polarization and compare to theoretical values.
- Prepare scientific papers.

In collaboration with Idaho State University researchers F.H. Harmon, D. Wells and K. Chouffani, Laser-Compton Scattering (LCS) experiments are being performed. During experiments, sharp monochromatic x-ray lines have been observed. These unique x-rays are produced using the so-called inverse Compton effect, whereby optical laser photons are collided with a relativistic electron beam. Work this year has demonstrated these beams using a 20-MeV electron beam in a head-on collision with a 100-MW, 7-ns Nd:YAG laser. The LCS x-ray energy lines and energy deviations were measured as a function of the electron beam energy and energy-spread, respectively. The results showed good agreement with the predicted values.

Figure 1 (next page) shows the developed experimental and optical configuration. The figure also includes an illustration of the LCS process.

The LCS optical system is driven by a Nd:YAG laser. The 9-mm diameter laser beam is first expanded to a 45-mm diameter beam and then focused by a 5-m focal length lens. The lens' focal point coincides with the center of the laser/electron interaction chamber. An off-axis 45° broadband mirror, whose center is located 2.4 cm from the beam line axis, steers the laser beam toward the center of the interaction chamber.

A 1.3-GHz RF linear accelerator (LINAC) is used as the 20-25 MeV, short-pulsed, electron beam source. The LINAC's pulsing signal also externally triggers the laser. Multiple high precision digital delay generators are used to trigger the laser such that the 7-ns laser pulse arrives at the interaction chamber coincidently with the 5-20 ns electron pulses. As predicted, interaction with the 20-MeV electron beam and the 1064- and 532-nm laser pulses generate two x-ray lines at 7.5 and 15 keV, respectively, along the direction of electron beam. Figure 2 illustrates the resulting 7.5 and 15 keV x-ray emission lines.

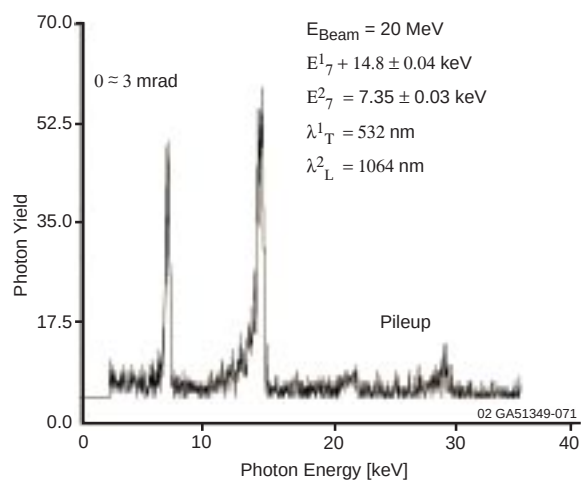


*FIGURE 2. LCS spectrum from the interaction of electron beam and laser fundamental and 2nd harmonic lines.*

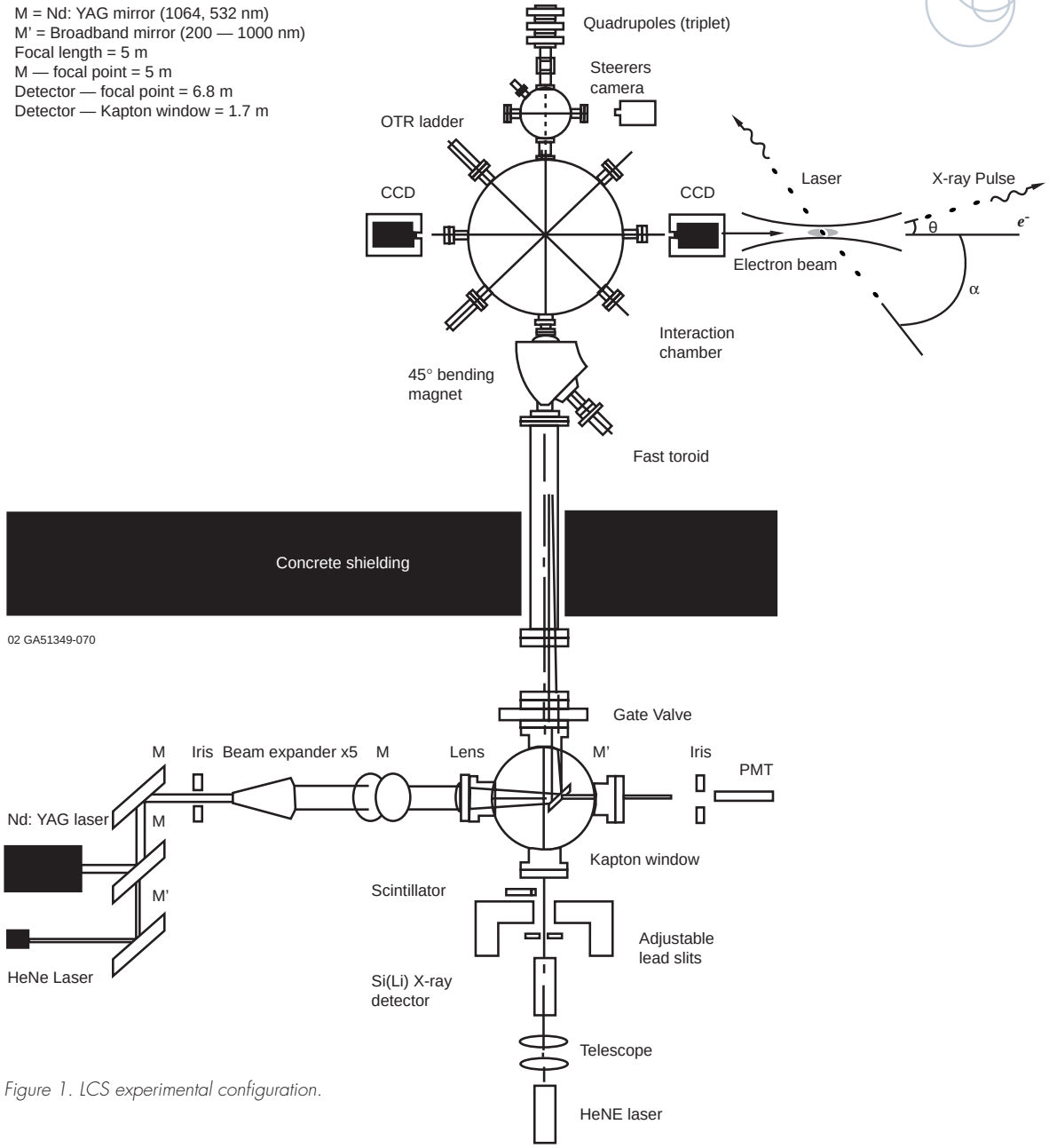


*Figure 1. LCS experimental configuration.*

The spectra show clear sharp distinct monochromatic x-ray peaks on top of a low background. The additional higher energy peaks are due to pile up from the first two major lines. There is good agreement between the data collected and the theoretical predictions for photon energies as a function of the electron beam energy.

The angular distribution of the LCS was measured by translating a Si-PIN photodiode x-ray detector along both the horizontal and vertical axes. A fit to the data showed that electron beam energy was equal to 22.087 MeV and that the laser/electron interaction point was located about 7.34 m from the x-ray detector. This electron beam energy result was consistent with predicted values.

The maximum x-ray yield registered to date at the LCS facility is equal to $3 \times 10^5$ photons/bunch. The latter yield corresponds to an intensity of $5.6 \times 10^{13}$ photon/s and, therefore, a brilliance equal to $2 \times 10^{11}$ photons/(mm$^2$-mrad$^2$-1% bandwidth), when colliding a Nd:YAG laser with a 20-22 MeV electron beam. This intensity is three orders of magnitude higher than the highest yield obtained from planar channeling radiation, which has been considered the brightest x-ray source generated by medium electron energy LINACS.

Several scientific papers have been prepared for conference presentation and journal publication as a result of this LDRD, enhancing the reputation of the INEEL in this advanced research area.

# Mechanical, Physical and Metallurgical Factors Affecting Liquid-Metal Embrittlement of Steels

*Kevin L. Kenney, Eric D. Steffler, Ben Perrenoud*

***Turning metals "failure" into success***

NS129

This project is classified. For additional information, please contact the principal investigator. Appropriate clearance, and need to know is necessary.

# Cermet Filters for Hazardous Material, Chemical, and Biological Weapon Agent Destruction

*Peter C. Kong, Larry D. Zuck, Arnold W. Erickson*

## *Extending high-temperature cermet filters applications*

ES101

In the aftermath of 9/11 and the subsequent anthrax attack on America in 2001, the nation is propelled to develop new technologies for critical infrastructure protection, environmental security, and national security. The U.S. military, fighting against unconventional enemies, needs the utmost protection against weapons of mass destruction.

Functional high-temperature cermet filters have potential application in hazardous chemical and biological agent destruction. This technology is adaptable for command structures and combat equipment protection on battlefields. Therefore, the research and development of the cermet filter technology for large- and small-scale protection of the nation and its fighting forces takes on a new urgency.

This LDRD researches functional high-temperature cermet filters for application in hazardous chemical and biological weapon agent destruction. A single-step combustion synthesis process manufactures the cermet filter. Metal and ceramic powders are mixed with sacrificial fillers to form a green compact. The compact is fired at high temperatures to initiate the combustion synthesis process. The synthesis is complete when all metal components are reacted forming a net shape structure. The cermet filter can be brazed to metal or ceramic housing structures during synthesis. Material properties include inexpensive starting materials, high melting temperatures, high-heat capacity, good thermal-shock resistance, low thermal-expansion coefficient, electrically resistive heating, lightweight strength, flameless oxidizer for CO, $H_2$ and hydrocarbons (producing ammonia and hydrocarbon gases for $NO_x$ reduction), and high particulate-removal efficiency. Limited bench-scale testing of the technology this fiscal year for the destruction of tributyl phosphate (TBP), a simulant of chemical weapon agent VX, has demonstrated complete success.

Technical objectives for fiscal year 2002:

- Continue research and development of cermet filter materials and systems.
- Perform bench-scale cermet filter destruction of chemical weapon agent simulants.
- Plan Phase III field test of the cermet filter systems for chemical and biological weapon agent destruction.

Because of a $100K funding reduction from the original FY02 request, the planning of the Phase III field test of the technology was eliminated from this year's work scope. The accomplishments in FY02 centered on technical tasks such as combustion synthesis and porosity engineering, cermet filter bonding to housing development, and chemical weapon agent surrogate destruction testing.

***Cermet Filter Combustion Synthesis and Porosity Engineering –*** The research and development of combustion synthesis for cermet filters achieved a significant level of success. This task centered on the aluminum combustion synthesis process:

$$Ni + Al + Al_2O_3 \rightarrow NiAl + Al_2O_3$$

The starting materials Ni, Al, and $Al_2O_3$ powders with sacrificial fillers were well ground and mixed with a mortar and pestle. The powders were dry-pressed at 20,000, 10,000 or 5,000 psi in a graphite sleeve lined mold. The two compacting pressures used in making the green compacts were for percent porosity development assessment. The green compact was fired in the mold at 850° C to initiate the combustion synthesis. The furnace was brought to a holding temperature in four hours and then held for four additional hours for the reaction to complete. At 660° C Al started melting. Molten Al is extremely reactive and will react with another metal to form metal aluminides by solid-state combustion reaction. In an Al thermite reaction, molten Al reacts with a less stable oxide (compared to alumina) such as NiO to form metal aluminides and alumina. The heat released by the solid-state combustion synthesis was tremendous and partially fused the compact together to form a net-shape product.

Sugar and hair sacrificial fillers were used for porosity engineering. The percent porosity produced in the final product was related to the volume per cent of the filler materials and the applied compacting pressure during powder consolidations. In general, low powder consolidating pressures (5,000 psi) with a fixed volume fraction of filler materials produced cermet filters with higher porosity than the same material compacted at higher pressures (10,000 and 20,000 psi). The porosity produced by sugar fillers was irregular in shapes and sizes. When human hair was used as filler materials, more controlled

porosity morphology evolved in the cermet filters. The pores were round and the average size was 60 µm. The average pore channel was in the order of hundred microns.

In general, the human hair filler produced much more uniform pore morphologies than sugar fillers. Animal hair fillers (e.g., horse mane and tail) are suitable filler materials also. These types of hair are thicker and will produce different pore morphologies than human hair. Horse mane fillers had been used to fabricate a large cylindrical (5" x 4" x 0.25") thin shell cermet filter destruction reactor; however, the attempt was unsuccessful. The thin shell cermet filter partially crumbled after the combustion synthesis step. The powder consolidation step may have contributed to the failure of making the thin shell. This problem will be investigated and solved in FY03. In theory, it is perceivable that by manipulating the volume fractions, the types of filler materials, and the powder compacting pressures, a net-shape cermet filter with desirable pore morphologies and very low pressure-drop could be achieved. This development will be completed in FY03.

***Cermet Filter Bonding to Housing Development*** – One of key elements of the destruction reactor research and development is the bonding of the cermet filter to the reactor housing. An early approach synthesized the cermet filter first and then bonded the cermet filter to the reactor housing. In the early bonding process, a thin layer of nickel and aluminum powder was painted either on the inside wall of a short stainless steel collar or on the edge of the cermet filter disc. The cermet filter disc was then pushed into place. The system was fired again in the furnace at 800$^{o}$C to initiate the combustion synthesis process. During combustion nickel and aluminum reacted to form the aluminide, and intense heat "welded" the cermet filter disc to the stainless steel collar. This approach was not ideal. During insertion of the cermet filter disc into the collar, a significant amount of the bonding agent was pushed out from the wall, leaving some areas on the collar devoid of bonding agent. The result was partial separation of the cermet filter disc from the collar wall.

A different approach was developed. Before powder consolidation, the collar internal wall was painted with the nickel and aluminum bonding powder. The green cermet powder was than loaded into the collar and pressed at desirable pressures. The collar and the green powder were fired together in the furnace to initiate the combustion synthesis process. With this method, no separation between the cermet filter disc and the collar wall was observed. The cermet filter disc was permanently bonded to the collar. Upon SEM analysis, a distinct reaction product (nickel aluminide) zone was created at the interface between the collar wall and the cermet filter disc. By exploiting the material and the combustion synthesis process characteristics a single-step method was successfully invented to fabricate a complete cermet filter reactor.

***Cermet Filter Reactor Development*** – The successful method above was applied to fabricate a long cylindrical cermet filter reactor for the destruction of chemical weapon agent simulant. The cermet filter reactor is 5" long and 1.5" in diameter. The cermet filter is 3" long and is fabricated in the mid section of the reactor housing. The stainless steel housing was painted with a layer of Ni and Al powder. Well-mixed cermet green powder was then loaded into the mid section of the reactor housing and compacted at desirable pressures. The reactor system was fired in the furnace to carry out the combustion synthesis process. The destruction reactor was successfully made in a single step. A quartz window at one end of the reactor provided observation access. Figure 1 shows the cermet filter reactor for chemical weapon simulants destruction tests.

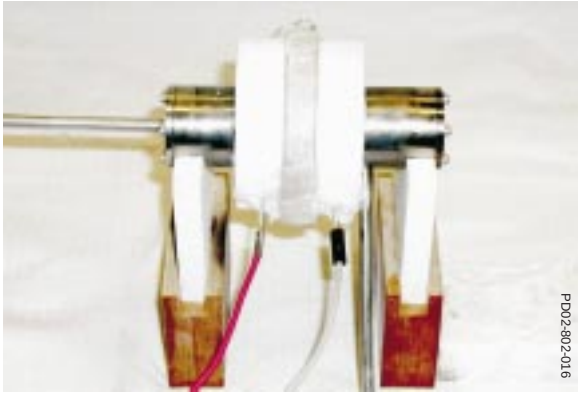


*FIGURE 1. Cermet filter reactor.*

***Chemical Weapon Agent Simulant Destruction Test*** – Several agents and their simulants were identified for eventual destruction tests. These agents included mustard gas, sarin, and VX. Among these agents, VX has a nontoxic simulant, Tributyl phosphate (TBP) that closely resembles the real agent. TBP has a molecular weight and structure extremely close to VX. If the cermet filter can destroy the TBP, it very likely can destroy VX and other highly toxic agents.

VX is highly toxic. The molecular composition of VX is $[(CH_3)_2CH_2]_3(CH)_2NSPO_2$ and with a molecular weight of 267. The nontoxic simulant, TBP, has a molecular composition of $[CH_3(CH_2)_3]_3(CH)_2PO_4$ and a molecular weight of 266. TBP is a sticky oily substance and has a fairly high boiling temperature. During the tests, TBP was injected at a rate of 0.01 cc/min into the heated cermet filter reactor. Air was the oxidant and the flow rate was set at 500 cc/min. The destruction product was captured in cold traps using liquid-nitrogen-cooled ethylene glycol as coolant. The coolant temperature could reach below –80° C. The destruction product was then analyzed by gas chromatograph (GC) for residue TBP. The GC detection limit was 1 ppm. All the results showed that residue TBP was either below the GC detection limit or non-existent. Figure 2 shows the GC data of the TBP before and after destruction.

The application of the cermet filter technology in this LDRD has been extended to address the emission problems ($NO_x$, $SO_x$, carbon particulate, and hydrocarbons) associated with diesel exhaust. The DOE Office of Heavy Vehicle Technology (OHVT) has shown interest in this technology for after-treatment of diesel engine exhaust and directed the INEEL to Cummins Inc. for technology assessment. Recently, the INEEL initiated contact with Cummins for potential partnerships with Houston Public Works Department, the Seattle Port Authority, and the DOE OHVT to develop and demonstrate the cermet filter technology for diesel engine exhaust treatment.

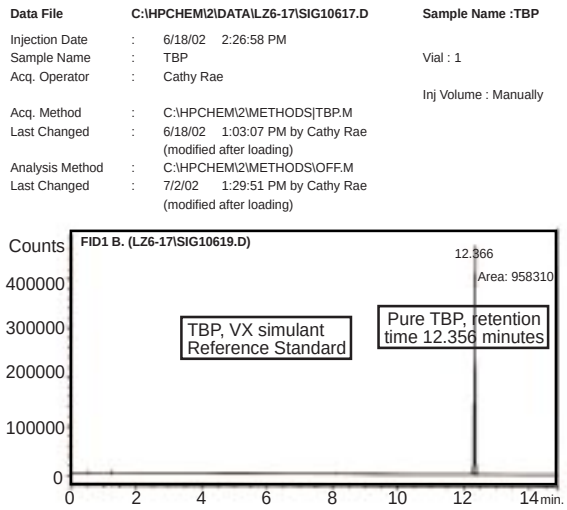


*FIGURE 2a. GC data for TBP reference standard.*

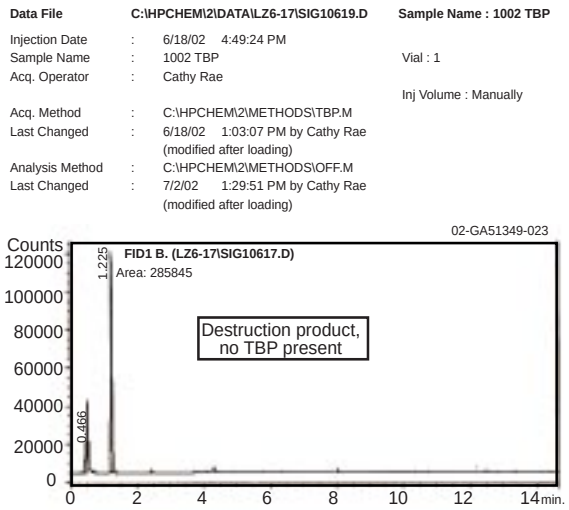


*FIGURE 2b. GC data for TBP destruction product.*

# Distant Neutron Source Detection and Location

*Dale Kotter*

## *Detecting nuclear materials on the move*

NS119

The need for an unattended mobile nuclear sensor system that can detect nuclear weapons or so-called dirty bombs has become a priority among several government agencies. Current technologies rely on small-area and fixed-point-of-view detectors. This reduces the probability of seeing a strategically placed or moving target. In addition, these detectors often require long sampling periods, limiting real-time applications such as deployment in a moving vehicle.

This LDRD is investigating technology that addresses these limitations by developing a prototype Radiation Detection Tracking System (RDTS) to detect and locate Special Nuclear Material (SNM) in environmental restoration and national security applications. The prototype system has demonstrated the potential for a major improvement in sensitivity, range and field-ability of radiation detectors. This improvement is realized through intelligent data analysis methods and the fusion of data from multiple small-area detection systems.

The system uses a custom-configured Helium-3 neutron detector. A data acquisition/analysis system with associated software offers real-time operation, and a satellite-based global positioning system (GPS) supports methods to locate SNM. Remote communications and networking capabilities also have been developed. These features allow an array of RDTSs to be networked together as a single virtual instrument with the ability to acquire radiation profile data from various points of reference and provide wide-area coverage. Because the technology is capable of operating in real time, it allows deployment on moving vehicle-based platforms. As a result, this new technology increases the probability of detecting items that may be concealed, shielded and mobile.

Technical objectives for fiscal year 2002:

- Design, build, and test a network of neutron Radiation Detection Tracking Systems.
- Package the system to be field portable.
- Implement remote communications and networking capabilities for wide-area monitoring.
- Demonstrate ability to fuse data from multiple detectors to locate SNM.

Several facts of physics inhibit the ability to track and locate SNM. When the SNM is shielded in a radiation-blocking material, like lead, it is undetectable. Earth's natural radiation can easily mask a distant radiation source's signal. And sufficient dwell time to integrate counts and discriminate from background levels is not easily achievable on a fast-moving source and a fixed detector. No existing methods fully address these limitations. It is not sufficient just to deploy arrays of permanent nuclear detectors in strategic locations. The value of road-based, mobile detectors that can get a close look at SNM in transit is apparent.

Through this LDRD, the INEEL has developed and demonstrated a Radiation Detection Tracking System for the standoff detection and location of SNM, which can operate in a mobile and networked mode. The system (Figure 1) provides a real-time means of screening large urban areas and is easily deployed on existing vehicles/infrastructure. At a border checkpoint or port of entry, the system can be configured and deployed on multiple platforms to conduct random search patterns of vehicles, containers, and storage areas. The system also can be used to detect a moving SNM target. Major improvements this system provides over existing technology include:

- Sensitivity – customized HE-3 detectors.
- Range – variable wide-area coverage by fusing results of multiple platforms, each with range of 30-50 meters.
- Field-ability and deployment – portable, mobile detector platforms.

The detectors, each on a mobile platform, are networked to function as a single virtual instrument with the ability to acquire radiation profile data from all points through which the sensors are transported. Multi-detector spectrums are concurrently analyzed to enhance the range and sensitivity of the detectors. Several RDTS systems can be deployed in parallel to increase the region of surveillance.

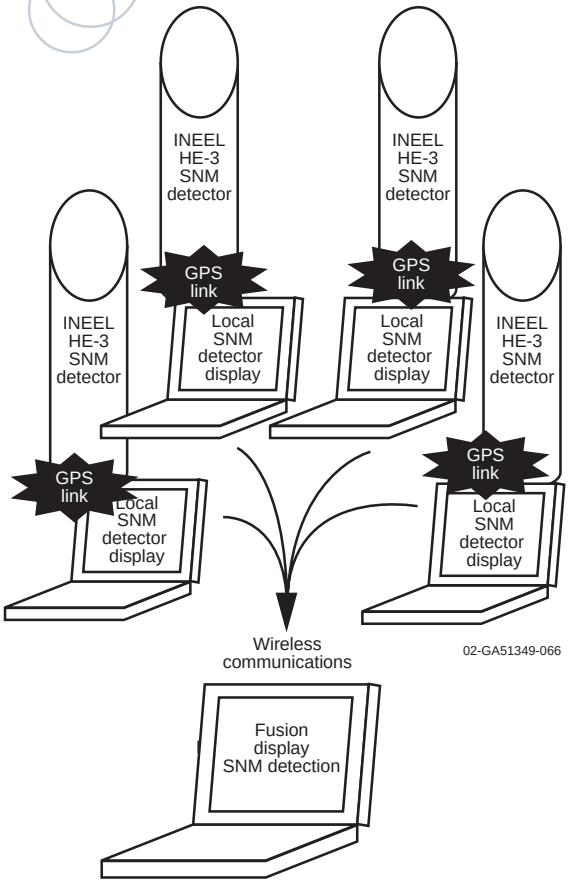


*Figure 1. Schematic of INEEL's Integrated Mobile System for Standoff Detection and Location of Special Nuclear Materials.*

The scope of the INEEL research was to design, build and test a network of three Radiation Detection Tracking Systems. The systems were integrated onto mobile platforms with a global positioning system, remote data acquisition/analysis system, and cooperative communication network for fusion of sensor data (Fig. 2). During operation a position-dependent detector response is acquired. The response is a function of neutron counts/sec. Each individual detector response is correlated with other remote detector data to obtain overall "counting" statistics. Specialized algorithms predict the "smart" movement/relocation of the detectors based on relative neutron counts, platform positioning, and trilateration techniques. The suspected detection of a SNM target is analyzed in a post-processing utility, using neural network classification methods.

*FIGURE 2. Networked Radiation Detection Tracking Systems (RDTS).*

The prototype systems use helium-3 type detectors for acquisition of a neutron radiation signature. A commercial off-the-shelf HE-3 detector was custom-configured to optimize signal-to-noise performance, reduce neutron backscatter effects, and eliminate electromagnetic interference. Field-based data acquisition is performed using a laptop computer and commercial data acquisition modules. A wireless communication network is used for fusion of sensor data from multiple field systems. A differential global positioning system tags each detector response with real-time location coordinate data and provides tracking of all the mobile neutron detector platforms. Specialized software was developed to acquire detector data, support remote data acquisition and support concurrent acquisition of data from multiple sensor platforms. A host computer provides oversight of all detector platforms deployed in the field.

Extensive work has been done on a "target identification and location algorithm." This is a method to acquire a "suspect target" signature from multiple detectors, each with a different field of view. Advanced statistical methods are used to differentiate suspect targets from

background clutter and calculate the probability that the data set represents SNM. A trilateration algorithm is used to estimate the location of the SNM.

Field tests disclosed several variables that distort identification of SNM such as barometric effects, moderating effects of the structure/surroundings, cosmic effects, changes in source signatures from shielding/packaging methods, and dynamic conditions such as moving sources. The current algorithms are unable to compensate for changing background conditions. It is believed that further work can benefit from the ability of neural networks to learn 'nonlinear' events to compensate for environmental factors.

The system was scheduled to be field-tested with actual SNM in-transit conditions at the Nevada Test Site Detector Rodeo, however the event was canceled. An alternative demonstration was performed under controlled laboratory conditions with a stationary calibration radiological source. The concept of locating a source based on simultaneous acquisition of neutron radiation from several networked detectors, each with a different field of view, was demonstrated.

Application for an unattended mobile nuclear sensor system is a priority among several agencies. Since Sept. 11, the federal government has sharply increased support for research into advanced sensors that could detect nuclear weapons or so-called dirty bombs if they fall into the hands of terrorists in the United States. Several government agencies have been briefed on the technology involved in this LDRD, with proposals submitted to continue product development.

# Microantenna Infrared Tags

*Dale Kotter*

## *Identifying "assets" with unique infrared patterns*

NS124

In national security and military operations there is a continuing need to tag, track, and locate "assets" from standoff and remote distances. One such means is through the measurement of the unique thermal infrared (IR) emissions from the asset. The INEEL has demonstrated the fabrication of microstructures that behave like antennas in the IR region of the electromagnetic spectrum.

This LDRD is researching microantenna-array technology to enhance infrared signatures of controlled assets. The antennas were structured in an array and tailored to radiate a unique infrared spectral pattern or tag. When fully developed the tag could be applied to the exterior surface of a controlled item to enhance that object's IR emission so that it can be remotely monitored using standard imaging (e.g., thermal imager) that has been configured for that purpose.

The technology is easily adaptable to covert deployment and can operate without external power. It is excited by natural solar radiation or by a standoff infrared source. The tag can be remotely monitored using standard FTIR technology. Key features include the ability to discriminate friend from foe, and the tailoring of the thermal profile to enhance long-distance standoff monitoring.

Thermal signatures of assets can be masked or distorted by environmental noise and high background interference, resulting in false detection. Other applications require high-resolution thermal imagery to discriminate a single asset from a common group. Current technologies have unacceptable infrared signature discrimination at standoff distances. In life-critical friend-or-foe identification and monitoring applications, tag errors are not acceptable. This technology addresses current limitations. Preliminary results have demonstrated unique tag signatures that are immune to deception and that greatly reduce tag errors.

Technical objectives for fiscal year 2002:

- Design an antenna-array structure that can be integrated into macroscopic surfaces.
- Fabricate a prototype of a microstructured surface capable of infrared signature modification.
- Fabricate an array of microantennas with resonant absorption in the 8-12um bands.
- Demonstrate the adaptability of the technology to covert deployment and operation without external power.
- Perform optical characterization tests.
- Demonstrate remote monitoring of the tag using standard thermal imagery and the ability of the tag to discriminate friend from foe.
- Demonstrate the concept that the thermal profile can be tailored to enhance long-distance standoff monitoring.

The INEEL, in conjunction with the University of Central Florida, has been at the forefront in the research of micro-sized planar lithographic antennas. Several prototype antenna structures have been designed and experimentally tested. It has been demonstrated that infrared signature tagging is possible using microstructured surface treatments, such as a cross-dipole-array frequency selective surface (FSS) as seen in Figure 1. Preliminary results have demonstrated that unique diffraction patterns can be generated that provide the means for positive identification of the tagged item. It also has been demonstrated that the infrared response is a direct function of the physical antenna geometry. The mechanism for tailoring the microantenna tag for infinite IR barcode configurations has been defined.

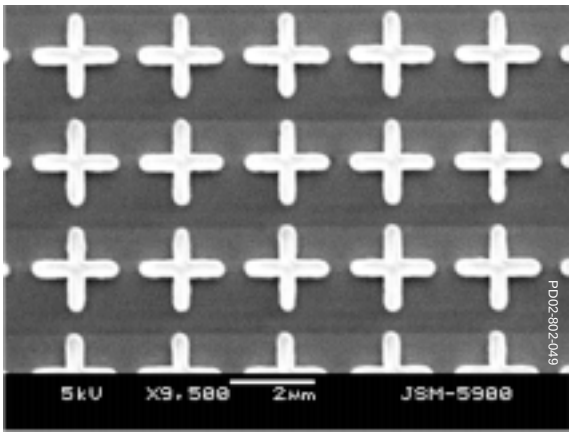


*FIGURE 1. IR FSS, fabricated as Al-on-Si cross-dipole array.*

Presently, electron-beam lithography is used for fabrication of arrays of metallic structures on dielectric and semiconductor substrates. At this stage of the research, e-beam lithography provides a convenient way to systematically investigate dimensional, spacing, and geometrical effects in a controlled manner. This approach allows for systematic trade studies.

The microantenna array tag requires no power or external electronics and acts as a receptor of IR energy. The antenna structure is "tuned" to resonate at a specific infrared frequency. The antenna structure acts as a diachronic filter of infrared emissions, independent of whether it is excited by broadband sunlight or an external source. The antenna has an inherit gain and generates current waves at the excitation frequency. This results in a distinct and enhanced IR signature that should be more readily detected with standoff instrumentation.

In the next phase of the research the ability to tag several controlled items with a unique identifier will be demonstrated. Different antenna geometry's will be applied to a series of controlled items to achieve a unique thermal signature, in effect a distinct IR frequency spectrum. This spectrum acts as an electronic infrared serial number that can be read remotely.

When fully developed the tag can be imbedded into the surface of the object, and will have no discernable visible signature. When viewed in the infrared regions, the tag would clearly identify the object of interest.

FY02 research has validated the fundamental design approach. A prototype microantenna tag has been configured and tested. It has been experimentally demonstrated that the microantenna arrays exhibited a resonance response within the mid-infrared bands. It appears feasible to exploit antenna sub-band and polarization features to implement tagging that isn't easily defeated. Studies have demonstrated that the array of antennas exhibited a unique diffraction pattern. This is the phenomenon exhibited by an infrared wave front that when passing by the antenna array is modulated, thereby causing a redistribution of energy within the wave front. This results in a unique infrared optical spectrum – like a fingerprint (Fig. 2).

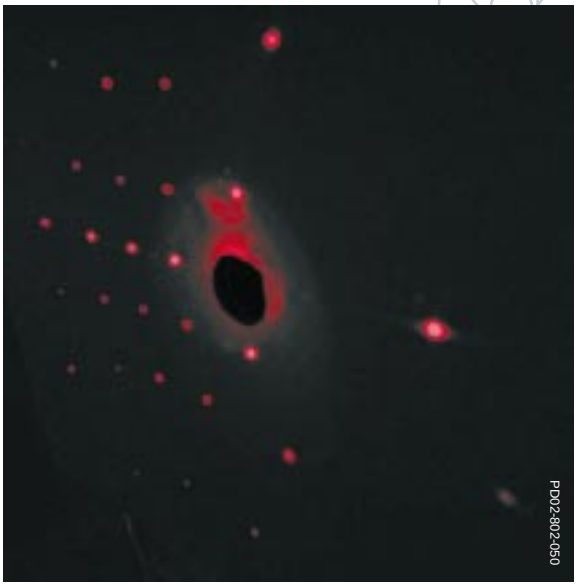


*FIGURE 2. Diffracted response of IR microantenna tag.*

The ability to remotely read the infrared fingerprint was demonstrated by using a laser to excite a tag response and measuring a single-order diffraction pattern using a standoff thermal imager. The diffraction pattern was processed and reconstructed into the original tag pattern. Proof of concept has been demonstrated.

This technology addresses several National and Homeland Security applications. The infrared tag could provide means for item-level tracking using standoff or space-based assets. The technology has been briefed to several agencies, with an invited presentation to the JASON committee.

# Ultrasonic Detection and Characterization of Buried Objects: Air-Coupled Techniques

*Dennis C. Kunerth, Alan Porter*

## *Finding and imaging unexploded ordinance*

NS110

The detection and characterization of unexploded ordinance (including land mines) are not being fully addressed by current technologies. Problems encountered include large numbers of false indications, limited spatial resolution, and ground conditions that make detection ineffectual. Ground penetrating radar (GPR) is a good example of a capable technology that is rendered ineffective by soil conditions such as high moisture content. As moisture content increases, penetration decreases. Moisture content also affects resolution by increasing image clutter and forcing the use of lower frequencies (i.e., longer wavelengths) to maintain penetration.

Recent developments in the field of air-coupled ultrasound provide the potential for imaging and evaluating buried metallic and nonmetallic objects such as unexploded ordinance, chemical weapons materials, and radioactive waste containers beneath the surface of unconsolidated materials (soil). Unlike GPR, moisture in the soil enhances ultrasonic transmission, thereby making ultrasonic techniques a natural complement to GPR. Previous use of air-coupled ultrasound was limited by excessive acoustic impedance mismatch between air and the test media, and the extreme attenuation of air at higher frequencies (>200kHz). The development of high efficiency piezoelectric transducers and pulse-compression and processing techniques developed for the radar industry have provided the necessary enhancements such that air-coupled ultrasound can now be used in applications not previously feasible. As a result, additional capability has been established at the INEEL in the form of air-coupled, non-contacting ultrasound (NCU).

This LDRD is investigating use of this new capability to determine critical acoustic properties of unconsolidated materials and to confirm its feasibility in imaging buried objects.

Technical objectives for fiscal year 2002:

- Investigate methods for increasing the area/volume being interrogated using air-coupled techniques.
- Evaluate the use of surface acoustic waves combined with air-coupled ultrasonic transducers to detect buried objects.

Prior work demonstrated the ability of pitch-catch air-coupled ultrasonic techniques to propagate through unconsolidated sediment; for example, objects have been detected 40 mm below a water-saturated sand surface at 65 kHz. However, this approach requires the use of aligned transducer pairs. The fixed alignment results in an effective acoustic focal depth that limits the detection of objects to a narrow vertical band in the matrix. Surface acoustic waves potentially can be used to improve near-surface detection capabilities as well as increase the volume of material being interrogated. They are sensitive to objects ~ 1/2 wavelength into the test material. Note that a receive transducer or an array will still be required to sense the signal and scan an area. The basic concept of how surface waves can be used is illustrated in Figure 1.

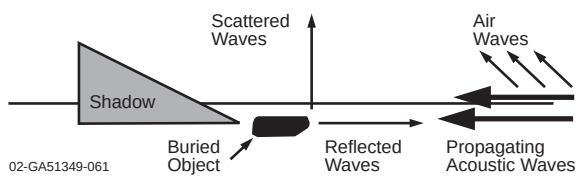


*FIGURE 1. Propagating acoustic surface waves will interact with subsurface objects to produce characteristic responses that can be detected via air-coupled acoustic transducers; i.e., detection of scattered waves or loss of airwaves resulting in a shadow.*

Figure 2 is an image obtained using an air-coupled transducer to sense airwaves generated by a propagating 1 MHz acoustic surface wave. Observed in the image is a shadow (lack of detectable air waves) produced when a 4 mm subsurface defect disrupts a surface wave traveling from left to right in a metallic test piece. The 4 mm defect is 0.5 mm below the surface of the sample.

Although the concept is simple, experiments in the laboratory emphasize the technical difficulties associated with evaluating this approach. The difficulties encountered include implementing a source compatible with air-coupled techniques, using test frequencies that have significant propagation and resolution in unconsolidated materials, and using lab samples whose size limits test frequency range. Implementation of a suitable source may present the most significant problem to implementing an air-coupled technique. Use of noncontacting sources such as a sparker or speaker source result in high amplitude air-born noise signals that mask the signal of interest. Increased source to sensor distance may improve this situation but this is difficult to simulate in the laboratory. Contacting sources such as piezoelectric or mechanical vibration sources minimize the air-born noise signal but provide a weak source signal (mid to upper kHz range), limiting both propagation distances and detectability.

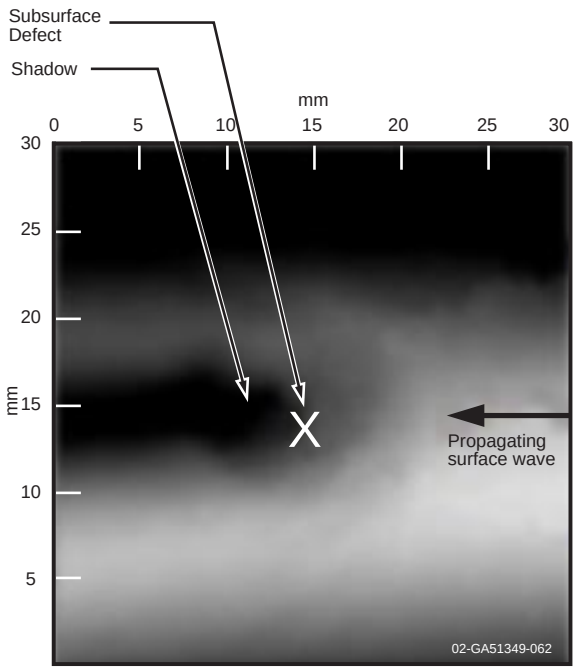


*FIGURE 2. Scan over a 4 mm subsurface defect in a metallic test sample using a 1 MHz air-coupled transducer. A defect-free area yields a relatively uniform response across the image. A contact comb transducer was used as the source for this image.*

Suitable test frequencies are a compromise between wavelength and propagation distances. Higher frequencies produce shorter wavelengths that improve spatial resolution but limit depth of interrogation as well as propagation distances. Longer wavelengths (lower test frequencies) improve propagation but limit the size of detectable objects. The issue of wavelength also influences the signals generated for lab-scale samples. The longer wavelengths that provide good propagation interact with the boundaries of the lab-scale samples to produce complex signals difficult to interpret. In other words, only limited success has been achieved in the laboratory to demonstrate feasibility. Low amplitude surface waves have been generated and their associated signals recorded using air-coupled techniques but no buried objects have been reliably detected. It is believed field experiments will be required to fully test and demonstrate the technique.

The detection and characterization of subsurface objects is important to the DOE and a number of industries. Air-coupled ultrasonics and/or the associated data processing techniques have the potential to address specific technology gaps. Successful demonstration of feasibility will position the INEEL as a leader in the development and implementation of this technology for detection of subsurface objects.

# Novel Cyclodextrin-Based Sorbent Materials for EM Waste Separation Needs

*Glenn Moore*

## *Remediating waste from underground storage tanks*

ES102

Within the DOE Complex, there are approximately 335 underground tanks stored with over 90 million gallons of high-level and low-level radioactive waste. Most of these tanks contain highly acidic or basic aqueous solutions, dissolved contaminants, suspended solids, and sediment. Efficient and cost-effective technologies are needed to separate suspended particulates prior to removing the dissolved radionuclides via ion exchange or other processes. Rotational ultrafiltration is a promising separation technology that has not been adequately evaluated for such applications.

This LDRD project investigates the use of novel Russian-made ceramic-coated stainless steel filtration membranes in a laboratory-scale rotational ultrafiltration system to address this environmental remediation need. The research was funded through the INEEL's National Security Directorate as a means of fostering collaboration with Russian technologists in nuclear waste management.

Technical objectives for fiscal year 2002:

- Evaluate Russian-made Trumem® ceramic membranes using rotational ultrafiltration system.

Crossflow ultrafiltration (CU) is DOE's baseline technology for suspension filtration. Crossflow filtration is an established industrial technology that typically employs an array of porous metallic tubes. Dewatering takes place when a suspension is passed through the inner bore of the tubes under pressure, forcing permeate through the tube's porous cross section. The retentate is either collected or returned to the inlet side of the system for further concentration.

One advantage of CU systems is the robustness of the tubular filter elements, typically sintered metal that can be chemically cleaned and/or back-pulsed under pressure to remove fouling deposits. Fouling deposits reduce permeate flux and are often the limiting factor in CU system performance. This problem arises as a consequence of reduced hydraulic turbulence at the membrane surface with increasing feed concentration.

The rotational ultrafiltration or high-shear rotary ultrafiltration (HSRUF) process makes use of fluid turbulence at the surface of a rotating filtration-disk in order to prevent the formation of fouling deposits. The filtration disks are typically rotated at several hundred rpm in close proximity to turbulence inducers "wagon wheels" at each face. Additional advantages of a rotating-disk system include a small footprint that can be realized with a stacked-disk configuration and the ability to use thin filtration membranes that afford high permeate fluxes. One drawback of rotational ultrafiltration systems is the mechanical complexity associated with having rotating components operating inside a pressurized fluid reservoir.

The ceramic membranes evaluated as part of this project are a commercial product of Membrane Technology Company in Russia and were procured from Trumem International of Bellingham, WA. The Trumem® membranes consist of a 15µm-thick ceramic coating applied to a 185µm-thick stainless steel substrate that has a nominal pore diameter of 1.5µm.

The ceramic coating material is composed of titanium dioxide ($TiO_2$), or $TiO_2$/zirconia ($ZrO_2$), or $TiO_2$/alumina ($Al_2O_3$)/silica ($SiO_2$). Membrane Technology's patented fabrication process affords variation of membrane pore size and composition, making these membranes suitable for a wide range of filtration applications. For this project, membranes having nominal porosity in the range of 0.05-0.8µm were evaluated. The membranes were obtained in bulk sheet form (11.2" x 11.2"), 25mm and 76mm disks, in the annular geometry needed for the rotational ultrafiltration system.

A laboratory-scale rotational ultrafiltration system manufactured by SpinTek Filtration, Los Alamitos, CA, was used for this investigation (Fig. 1 next page). The Spintek Speedy™ system was configured with a single rotating disk. The filtration disk consists of an 11-inch diameter Ryton platen with a ceramic membrane and an underlying polymer mesh affixed to each face. The disk provides 1.0ft$^2$ of effective membrane area. The system as received from the manufacturer was configured with a single-speed 1170-rpm motor. For this project the Speedy unit was modified for use with an off-the-shelf variable-speed motor of ~50-1500 rpm.

*FIGURE 1. The Spintek Speedy™ rotational ultrafiltration system used in this investigation.*

To accommodate the motor retrofit, a modified filtrate/permeate collection coupling was designed and fabricated at the INEEL (Fig. 2). This design improvement eliminated the need for a continuous hollow shaft running from the filter housing through the whole length of the motor. The system improvement task was performed keeping in mind the challenges involved with remote maintenance and operation of processing equipment in isolated radiological containment areas.

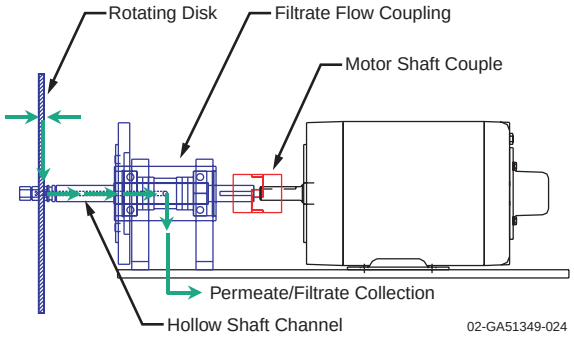


*FIGURE 2. Drawing of design modification that allowed the use of an off-the-shelf variable speed motor. The pressure vessel assembly is not shown.*

The system modification resulted in enhanced capability and a simplified, modularized design. The modified system could be deployed in a containment area via: 1) passing the motors' shaft through a sealed penetration into a containment area, or 2) by incorporating a magnetically coupled motor drive. These options allow the motor to remain outside the containment area, which is advantageous from a maintenance point of view.

The modified Spintek RU system and the Trumem membranes evaluated in this project provide a good starting point for waste separation development activities at the INEEL. A DOE external report is being prepared so that the experimental results of this project can be adequately presented and discussed. In summary, this project was successful in establishing a versatile rotational ultrafiltration capability at the INEEL. The filtration system and complementary resources (e.g., particle size analysis, materials characterization, etc.) stand ready to address DOE separation technology investigations.

Good working relationships with Trumem International and an associated company, ASPECT USA, have resulted from this LDRD research. ASPECT USA is interested in building upon and using these filtration capabilities to conduct technology demonstrations in support of the DOE Hanford Site. It is anticipated that the INEEL's enhanced capabilities base will foster additional institutional and industrial inquiries.

# Probalistic Risk Monitoring Software for SAPHIRE

*Steven D. Novack, Scott Hartley*

## *Managing risk over the lifetime of complex systems*

ES106

The DOE has approved the use of INEEL risk assessment software, System's Analysis Programs for Hands-on Integrated Reliability Evaluation (SAPHIRE), for use in Russian nuclear power plants (NPPs). SAPHIRE is used to quantitatively model the safety systems and associated support systems that mitigate accident sequences from occurring in a nuclear power plant. These logic models (e.g., fault trees and event trees) identify weaknesses, vulnerabilities, and the risk of damage to the NPP core. Traditional risk assessment software provides a static look at plant/system risk and does not allow for daily or planning updates to these models. Due to the prohibitive cost of commercial risk assessment software, Russian-managed NPPs prefer SAPHIRE, which is free. A risk monitor for SAPHIRE would provide a manner to modify and view daily future risk concerns either due to equipment failures or planned maintenance activities, adding significant value to this software.

This LDRD focuses on providing a SAPHIRE-based risk monitor for supervisors and operators of complex systems to manage risk of operating systems over the lifetime of the system. Specifically, this tool was focused on the Russian-designed nuclear power plants to aid in preventing catastrophic accidents. The INEEL risk monitor provides advanced assessment capabilities that include: increased speed for risk calculations of core damage scenarios, more accurate estimations on common cause failures (CCFs), distributed system architecture, and a visualization interface that is more easily understood by operators rather than risk analysts. This tool incorporates INEEL research in advanced techniques for CCF estimation using the Alpha methodology and from the Virtual Reality Reliability, Availability, Maintainability (VRAM) software and modeling advancements.

Technical objectives for fiscal year 2002:

- Finalize risk monitor: user interface, and mapping and quantification routines.
- Test risk monitor.
- Install and distribute; train operators.

Success in meeting the above tactical objectives in FY02 was moderate due to a decrease in this LDRD budget. The first technical objective was completed, resulting in a finalized user interface, and mapping and quantification routines on the risk monitor. Finalizing this objective took increased time due to testing and modification of the SAPHIRE API Dynamic Link Libraries, which had not been tested prior to this LDRD. Although testing was not comprehensive, the product works as a demonstration with two NUREG-1150 U.S. nuclear power plant models.

The risk monitor user-interface was modified into three areas. These areas correspond to risk analysis, management, and reporting (Fig. 1 next page).

A more robust model management module has been added to be able to simulate risk for multiple plant states (e.g., at power, shutdown, cold standby) (Fig. 2 next page).

Diagnostic tools have been added for the user to enhance the ability to identify changes in updated models used in the risk monitor (Fig. 3 next page).

An Interval View was added to aid the user in setting components out-of-service. During testing it was found to be more difficult to provide this ability via the calendar view (Fig. 4 next page).

This work has enabled the INEEL to use the extensive static risk models developed in SAPHIRE to monitor risk on a changing plant or system. Nationally, this LDRD has made it possible for standardized risk models developed in SAPHIRE to be incorporated into a risk-monitoring program for the nuclear industry under the umbrella of the Nuclear Regulatory Commission (NRC). The project also has opened doors for international collaborative work with such prestigious research facilities such as the RRC Kurchatov Institute. The addition of a risk monitor for SAPHIRE will greatly benefit the INEEL in its goal of establishing expertise and tools to perform risk assessment.

This project supports ongoing INEEL work with the NRC and the SAPHIRE code, collaborative work with universities and foreign research centers, and the need

for advanced tools for future situation and awareness need. The risk monitor also aids the INEEL Initiatives: Critical Infrastructure and Non-Proliferation Initiative and Generation IV Reactor.

Contacts have been established through this LDRD at NASA with Michael Stamatolatos in Washington, D.C. and with Johnson Space Center (JSC) in Houston. This work involved monitoring situational risk for the International Space Station (ISS) and the Space Shuttle. RRC Kurchatov Institute and Utah State University have participated in this program. In addition, the International Atomic Energy Association (IAEA) has expressed interest in the risk monitor and SAPHIRE for placing it in future Nuclear Safety Centers for Eastern Europe.

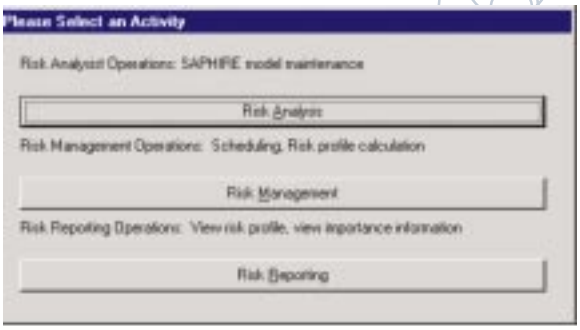


*FIGURE 1. Open risk monitor screen.*

*FIGURE 2. Multiple plant and plant state model form.*

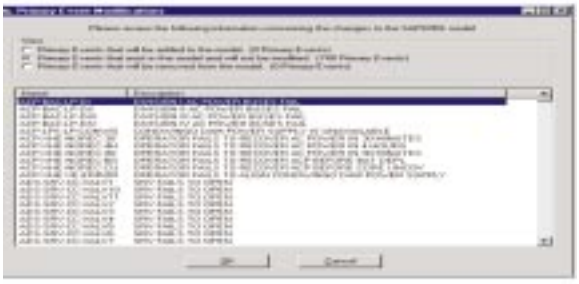

*FIGURE 3. Diagnostic view of model differences.*

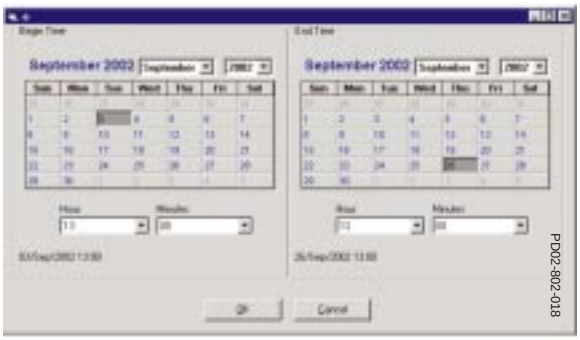


*FIGURE 4. Internal View.*

# Technical Advancement for the INEEL CIP SCADA Test Bed

*Steven D. Novack*

NS131

This project is classified. For additional information, please contact the principal investigator. Appropriate clearance, and need to know is necessary.

# Cutting of Structural Materials using Energetic Materials

*Michael H. O'Brien*

## *Next-generation cutting materials offer better efficiencies and control*

NS127

Cutters using energetic materials mixtures are already in commercial and military use for Explosive Ordnance Disposal (EOD) and related applications. However, current devices use obsolete technology and are large, heavy and inefficient. The user community needs a tool kit to allow operators to select the energetic load, composition of energetic material, and nozzle combination to provide the desired cut shape and depth.

The INEEL is a leader in several areas of high-efficiency cutting. Over the past several years, the INEEL energetic materials team has been developing high-efficiency thermitic cutting compositions. These new materials are capable of cutting eight to 10 times more target material per gram of reactant mixture than other compositions currently in use. These dramatic improvements in cutting efficiency offer the opportunity to develop a new generation of tools for EOD and other activities with similar cutting needs. Experts also have communicated the need for very close control of hole depth and shape. The currently available generation of cutters does not offer such control.

The purpose of this LDRD project is to demonstrate the feasibility of an advanced cutting kit. The project will develop combinations of cutting compositions and containers, and demonstrate a range of finely controlled cuts. To ensure that useful controls and systems are generated, external EOD user community representatives will be used as advisors and progress reviewers. These external experts will ensure that device systems and methods are relevant to community needs and that demonstration materials are convincing.

Technical objectives for fiscal year 2002:

- Coordinate with outside experts (EOD and others) to define feasibility demonstrations.
- Design and fabricate reaction chambers.
- Design, mix, and consolidate energetic parts.
- Test matrix of materials and select demo candidates.
- Conduct materials demonstrations.

The project scope for this LDRD was dramatically reduced for several reasons. As a result, only a minor portion of the original funding was expended and only a portion of the year's technical objectives was accomplished.

In FY02, initial contact was made with external experts to guide the research and development effort. The project was discontinued before any meetings or significant exchange of information was accomplished. However, these external experts are still willing to participate in this work if it should continue in the future.

A minor amount of new experimental and analytical data was acquired. Some new reaction chambers and energetic parts were designed and fabricated. This equipment was used in cutting tests on a few new structural materials prior to work discontinuation. These early results were encouraging, though very limited in scope.

The essential next step is to do the work described in the original scope and provide a feasibility demonstration for potential customers. Once complete, this effort would likely provide a variety of external funding opportunities, patent possibilities, and collaborations.

DOD and other government agency customers have been briefed on the potential for improved tools in the cutting family. With the world's current emphasis on disposal of a wide variety of ordinance, the market is large and ready for a dramatically improved kit of cutting materials.

# Novel Selective Matrix for Collection and Identification of Priority Pathogens

*Frank Roberto, Vance Deason, Heather Silverman, Amber Miller, Scott Watson*

## *Detecting bioterrorism agents with nanosensors*

NS118

New, reliable and sensitive methods of detecting pathogens, especially those that might be used by bioterrorists, are sorely needed, as was demonstrated last fall as our nation attempted to deal with anthrax spores dispersed through the U.S. Postal Service and federal and private mail facilities. The focus of this LDRD research is to develop a nano-pattern recognition strategy (nanosensor) based on the derivatization of selective matrices for the detection of pathogenic microorganisms or toxins.

Organically modified sol-gels, commonly referred to as ormogels, are polymers containing both organic and inorganic moieties that can be polymerized using laser holography to produce 3-D structures with geometric and chemical matches or affinities; e.g., for particular bacterial cells or proteins. The silica backbone of ormogels provides mechanical strength, while the organic components consist of organic monomers that can be polymerized to provide reactive groups to which antibodies and fluorescent or other sensing and reporting mechanisms can be attached covalently. Polymerized composite ormogel material has a high degree of optical transparency, enabling the use of conventional light-based detection strategies.

Holographic structures complementary to a microorganism or protein of interest can be written into ormogels using a UV laser. The resulting size of the pathogen-specific pattern within the ormogel is very small, approximately 200 nanometers. The fabrication of an inorganic/organic hybrid composite material (hybrid glass) with antibodies or other ligands to produce a stable polymeric matrix, or "nanotrap", provides a means of both identifying and capturing relatively small numbers of pathogenic toxins and microorganisms. In addition to serving as a novel strategy for detecting bioterrorism agents, other uses for the holographic imprinting technique could include the detection or remediation of environmental contaminants.

Technical objectives for fiscal year 2002:

- Establish prepolymer formulations for sol-gels with Dr. Anna Wojcik (Hybrid Glass Technologies, Inc.; Rutgers University Department of Ceramic and Materials Engineering).
- Obtain sol-gel film samples.
- Identify optimal binding conditions for a pathogenic bacterial strain of *Escherichia coli* with specific cell antibodies ($IgG_1$ and $IgG_2$).
- Perform enzyme-linked immunosorbent assays (ELISAs) using various antibody-modified model matrices.
- Modify select antibody-modified matrices and sol-gel film samples with protein components (Protein A and Protein G).
- Develop a visualization and enumeration strategy for binding of pathogenic *E. coli* to antibody-modified and sol-gel film samples (colorimetric properties, direct cell counts, imaging).

ELISA experiments using $IgG_1$ and $IgG_2$ (two types of immunoglobulin molecules) and two pathogenic strains of *E. coli* (#12793 and #13736, ATCC, Manassas, Va.) were performed to determine the optimal binding conditions for IgG subclasses and *E. coli* strains. Standard polystyrene microplates (used in medical-based ELISA research) served as the solid matrix for the binding of immunoglobulins and bacteria. Results from these initial ELISAs reveal maximum *E. coli* detection with strain #12793 and immunoglobulin subclass $IgG_2$.

Subsequent ELISA experiments tested the binding of immunoglobulins and pathogenic bacteria with the addition of Protein A and Protein G on solid matrices. Protein A and Protein G have the ability to specifically bind the Fc region of IgGs, thereby orienting the Fab region (antigen binding portion) for binding to bacterial cell surface proteins. Protein A and Protein G were bound to microplates by either passive absorption or activation with the homobifunctional cross-linker dissuccinimidyl suberate (DSS). Binding of *E. coli* strain #12793 to IgG subclasses on standard polystyrene microplates or microplates grafted with amine functional groups (MaxiSorb and CovaLink NH, respectively; Nalge Nunc International, Naperville, IL) was tested with the addition of Protein A and Protein G. Results indicate an increased colorimetric signal detected with DSS-activated Protein

| Prepolymer Film Formulations | | Covalink NH Microplate Module | | | |
|---|---|---|---|---|---|
| Designation/Reactive Group | Result | Protein A | Protein A/DDS | Protein G | Protein G/DDS |
| F2/urethane and amine | YES | 0.883 | 0.995 | 0.580 | 0.869 |
| F3/amine | YES | | | | |
| F4/amine | YES | | | | |

02-GA51349-065

*TABLE 1. Colorimetric detection of prepolymer film formulations and CovaLink NH microplate modules. Optical densities were measured on a BioRad 450 Microplate Reader at 495 nm. For prepolymer film formulations, YES indicates colorimetric detection. For CovaLink NH microplate modules mean optical density is indicated.*

A and Protein G on the CovaLink NH modules (Table 1). Reactive chemistries to Protein A and Protein G show enhanced detection potential of pathogenic bacteria.

Prepolymer formulations for sol-gels containing the organic monomers urethane and amine groups or amine groups were prepared as films on glass slides by university/industry collaborators. Protein A and G were covalently bound to three film formulations with DSS. Preliminary results indicate successful binding of Protein A and Protein G to the prepolymer formulations.

An enumeration strategy for detection of the number of bacterial cells bound by the prepolymer films (or in microplates) was developed. Only through precise bound-cell counts could the sensitivity of the nanosensor be evaluated. Future work in FY03 will focus on optimizing and enumerating cell binding to prepolymer films with subsequent fabrication of a 3-D ormogel specific for the bacterial cells of interest.

Optical techniques to produce appropriate regular mesh structures with pore spaces on the order of 1 µm were developed and a suitable sol-gel monomer (designated M3) was obtained from a project collaborator. An example of the regular structure obtained is depicted in Figure 1.

This LDRD seeks to develop materials that can selectively capture and detect pathogenic microorganisms. In the defense and national security arena these materials could serve as “monitoring sentinels” detecting pathogens that might be used in bioterrorism, supporting National Security missions.

PD02-802-046

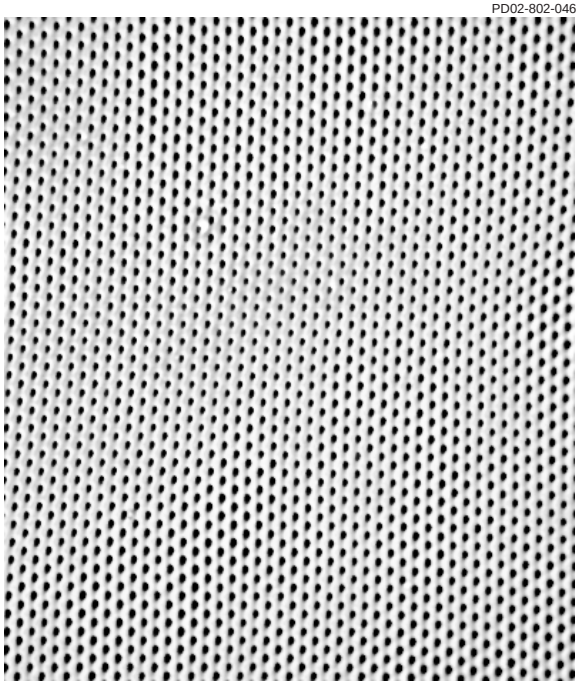

*FIGURE 1. Regular microstructure pattern obtained with sol-gel monomer M3.*

# Imaging Applications of Photon Beams Produced with Compton Backscatter of Laser Beams

*Tim Roney, Tim White, Greg Lancaster*

## *Supporting non-intrusive, nondestructive inspection*

NS121

The ability to generate intense sources of tunable, near-monochromatic, pulsed x-rays creates numerous opportunities for development of material, biological and surface science experiments. In the past, the only places where such x-ray beams could be generated was at synchrotron facilities that are difficult to access. This LDRD is bringing this important capability to the INEEL where it will help develop new customers and support non-intrusive and nondestructive inspection of transuranic, mixed and remote-handled wastes.

The source of pulsed x-rays arises from the interaction of a pulsed relativistic electron beam and a pulsed laser beam, known as Compton Backscatter (CBS). Low-energy optical photons are scattered by the electrons resulting in a pulsed beam of higher energy (x-ray) photons propagating in nearly the same direction as the electron beam. To prepare for these experiments, x-ray detection and imaging systems are needed that satisfy conditions created by the x-ray generation process, the x-ray beam and particular applications. This LDRD is directed toward characterizing the x-ray beam and developing x-ray-imaging systems consistent with the photon beam generation capabilities of the test facility.

In the first year of this LDRD, x-ray beam characterization and imaging experiments were performed. Beam characterization demonstrated expected small variations in x-ray energy and intensity as a function of beam angle. For imaging, the output of the x-ray beam does not yet supply sufficient flux for imaging with conventional 2-D x-ray imaging components, thus the initial experiments were used to characterize background radiation. In the second year of the project, the output flux will be increased by a factor of roughly 100 through electron beam stabilization, improved alignment, and a higher repetition rate laser.

Technical objectives for fiscal year 2002:

- Characterize pulsed Compton Backscatter x-ray source with respect to imaging applications.
- Determine optimum detector(s) for pulsed x-ray beam.
- Design and build laboratory prototype x-ray imaging system for small objects.
- Develop data acquisition protocol and imaging algorithms for pulsed x-ray beam.
- Demonstrate imaging system on test object.

In FY02, investigators collaborated with Idaho State University to characterize the pulsed x-ray beam from Compton Backscatter and began x-ray imaging experiments. The angular characteristics of the x-ray beam were measured. Figure 1 shows the results of the characterization runs. Note that the x-ray beam energy and intensity both vary with angle away from the central beam. This information is critical for imaging, as both beam energy and intensity corrections will need to be performed. Alternatively, the beam energy variation with angle may be used to design an energy-dependent scanning system that would allow for material identification. The components used in the imaging experiments were placed at the location of the Si(LI) detector shown in Figure 1 (next page).

The first imaging experiment was to determine the possibility of implementing a real-time imaging capability using a phosphor screen and a digital video camera coupled to an optical image intensifier. The video camera limits the exposure of each frame to 1/30 second and integration was attempted over multiple frames. The combination of a low x-ray flux and the readout rate was not sufficient to overcome the noise. In the second experiment, the video camera was replaced with a high dynamic range, slow-scan (indefinite integration time),

*FIGURE 1. Geometry for CBS imaging experiment (top) and results of characterizing beam energy and intensity with respect to angle. The Si(Li) x-ray detector was used for the energy/intensity profiles. Imaging components replaced the Si(Li) detector when imaging was performed. The graph on the bottom left shows x-ray energy as a function of vertical observation angle. The graph on the bottom right shows intensity as a function of observation.*

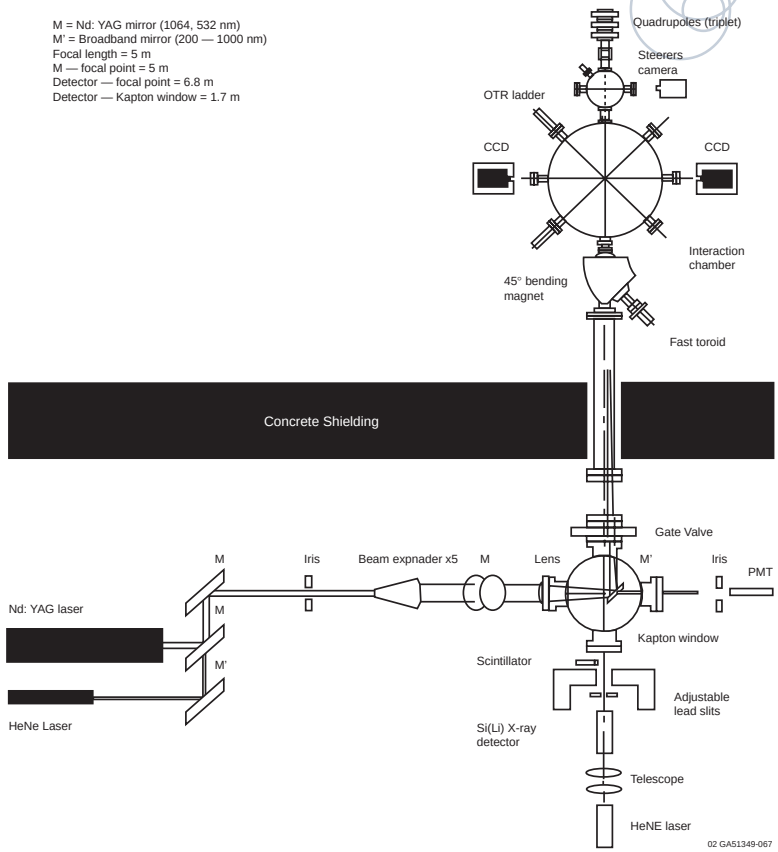


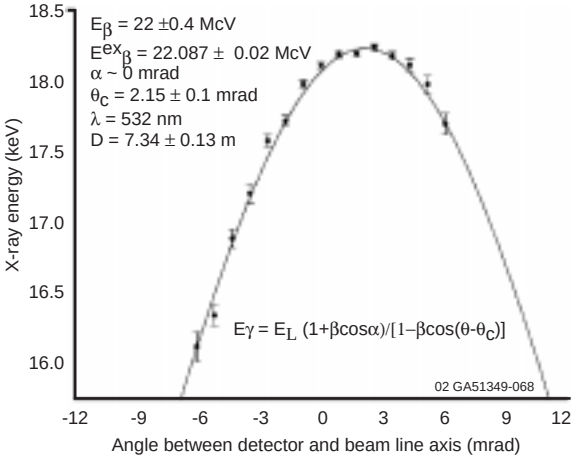


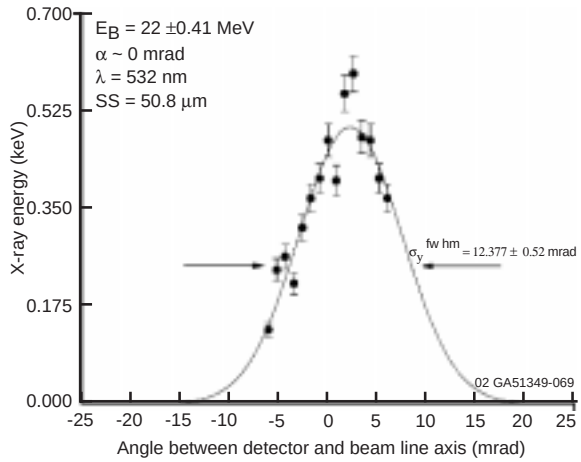

PD02-802-048

*FIGURE 2. (Top) Bremstrahlung image in Compton Backscatter geometry. The image was collected with a cooled CCD camera, lens-coupled to a glass scintillator with the laser beam off. The Bremstrahlung x-rays that are imaged are produced by dropping a phosphor "flag" into the electron beam within the interaction chamber. The square region is the extent of the scintillator. The dark circular region on the left side of the image is the 45° bending mirror for the laser beam. The vertical bright region is the exit window – the rest of the exit window is occluded by a stainless-steel cover. The large bright blobs may be imperfections in the scintillator. The smaller white blobs are probably direct x-ray interactions on the CCD.*
*(Bottom) Compton Backscatter image. Same configuration as above except the laser has been turned on and the detected photons should be low-energy Compton from the backscatter interaction of the laser and electron beams. The large blobs may be imperfections in the glass scintillator that are excited by the Bremstrahlung radiation generated by stray electrons striking the edges of the accelerator. The small bright "speckles" are probably direct detection of those Bremstrahlung x-rays by the CCD.*

scientific-grade CCD camera. Using this arrangement the investigators were able to record a photon flux from the Bremstrahlung radiation produced by the accelerator (Fig. 2) but were still unable to detect x-ray photons sufficient to record an image.

Successful imaging with CBS x-rays will depend on a 10X flux increase from beam stabilization and hardware/alignment in FY03. An additional gain (10X) in the short term will come from a higher repetition rate laser. Thus a 100X improvement factor in x-ray flux is expected in FY03. A scanning point detector and a more sensitive 2-D imaging detector will be employed.

Development of imaging systems to be used in conjunction with accelerator-based sources of radiation provides an important new capability in the region that will directly benefit the INEEL and its customers.

# Classified Cluster Computing

*Andrew Shewmaker, L. Eric Greenwade, Tom K. Larson*

## *Increasing security, inexpensively and without loss of performance, on cluster computers*

NS128

Scientists around the world use Beowulf clusters, a class of inexpensive supercomputers, to supply their computing needs for a variety of problems (Fig. 1). Some of these computational problems require that the cluster designer, administrator, and user take stringent security precautions. For example, a designer must guarantee that each user, and his or her data, is isolated from other users and their data. This requirement means that each user or project requires a separate storage device. While swapping the hard disks on a single workstation is easy, swapping the hard disks on the several dozen machines that make up a cluster is not desirable. One possible solution that a cluster designer might pursue is to run the cluster machines diskless. If the only storage for the cluster resides on the head machine, the system through which the entire cluster is controlled, then user isolation becomes simple again. However, isolating storage could worsen the bottleneck in the cluster's network and hinder performance. Thus, increasing security on a cluster creates a whole array of conflicts with performance and usability that must be addressed to do work securely and efficiently.

*FIGURE 1. A rack of cluster nodes.*

This LDRD is investigating the feasibility of creating a secure Beowulf cluster that can provide relatively inexpensive high-performance computing (HPC) for classified projects. Resolving the security issue without negatively impacting performance and usability will allow the INEEL to take on new national security roles within DOE missions and better address the computational needs of existing INEEL classified programs. Example applications that would require this type of resource are ballistic penetration simulation, information protection research, and critical infrastructure analysis and simulation.

Technical objectives for fiscal year 2002:

- Acquire cluster hardware.
- Assemble cluster.
- Test and benchmark cluster.
- Write classified cluster "how to" document.

Due to unforeseen difficulties, not all of the technical objectives for this year were fulfilled. The first problem encountered was the ongoing process of getting a security clearance for the principal investigator, Andrew Shewmaker. It was decided to wait to submit the security plan until the clearance came through. The second difficulty was a hardware failure in the head system of the cluster. The head system is a single point of failure in the cluster for many reasons. As a result, the cluster is currently unusable. The head system is under a three-year warranty and has been sent in for repairs. A duplicate head system has been received and is ready to take its place immediately.

Even though this project is behind schedule on achieving some of its objectives, these setbacks provide important information from which to learn. Through this project the INEEL has acquired additional expertise in secure, high-performance computing environments.

From the work done to date, it became apparent that the original cluster design was too fragile. The design needs more redundancy because the most important part of the system was a single point of failure. When the head system of the cluster died, the entire cluster was useless. The head system is now being repaired and a duplicate system has arrived. The investigators plan to use the second head system as a hot spare, replacing the original system as needed by swapping hard drives. These hard drives are held in by a lever and accessible from the front of the tower cases. Another option under consideration is to run the secondary head system side-by-side with the original in high-availability mode. The first option is much less expensive to implement because the software configuration is simple.

When the classified cluster computer at the INEEL is completely set up with a hot spare head system and an approved security plan, it will provide a good foundation for applications with security and high-performance computing requirements. At that point the cost of setting up this kind of environment will be known, but the total cost of ownership will not.

A second proposal has been submitted to address the need to comprehensively examine the classified cluster and its security protocols with two users. The first user will be simulating and visualizing projectile fire damage on armored vehicles. The second user will be simulating and visualizing radar and radar "jammers." These experiments will assess and address the cluster's hardware, software and security protocol inefficiencies.

# Plasma Spray Processing Development for Energetic Materials

Dave Swank, Mike O'Brien

## *Turning energetic compositions into complex shapes*

NS107

The thermal spray coating process has a variety of applications in the aerospace, paper, mining, and automotive industries. Applications in the automotive manufacturing industry, in particular, are rapidly expanding. Currently these applications include, but are not limited to, thermal barrier and wear resistant coatings for oxygen sensors, cylinder bores, exhaust valves and alternators. The process consists of introducing a metallic or ceramic particulate material into a hot gas jet that is generated by either electric arc discharge (plasma) or oxygen-fuel combustion. The particles are heated and accelerated by the gas jet to be deposited on the substrate to form a coating.

A small amount of pioneering plasma spray of energetic compositions was done at the DOE Mound facility in the early 1990s prior to the shutdown of R&D activities there. The INEEL has acquired the specialized equipment formerly used at Mound and is preparing to carry on those studies. As part of that effort, this LDRD project is investigating initial operating conditions on simulated inert compositions using instrumented plasma equipment then validating these conditions using the energetic material plasma spray apparatus being installed in the new materials science laboratory.

This project is developing the capability to coat substrates with reactive energetic material mixtures using the plasma spray coating processes. The objective is to investigate process parameters for plasma spray of energetic materials including thermite and intermetallic compositions. This unique technology offers a significant leap forward in rapid forming of complex shapes and represents a critical enabling technology applicable to several valuable national security program interests.

Technical objectives for fiscal year 2002:

- Develop initial plasma spray operating conditions for fabricating unique energetic materials.
- Install and make operational unique plasma spray equipment in the Material Science Support Laboratory (MSSL).
- Validate plasma spray operating conditions at MSSL.

Initially surrogate non-reacting materials were used to develop an understanding of the plasma spray process operating parameter windows for energetic materials. Measurements of sprayed alumina and aluminum particle velocity and temperature were made for torch input parameters of total gas flow, gas mixture, carrier gas flow, torch current, and powder mass flow. These measurements will be used to guide the application of energetic materials.

As an illustration, Figure 1 shows plots of aluminum particle velocity and temperature as functions of total gas flow and torch current. If, for example, an unacceptable level of aluminum is oxidized during the spraying

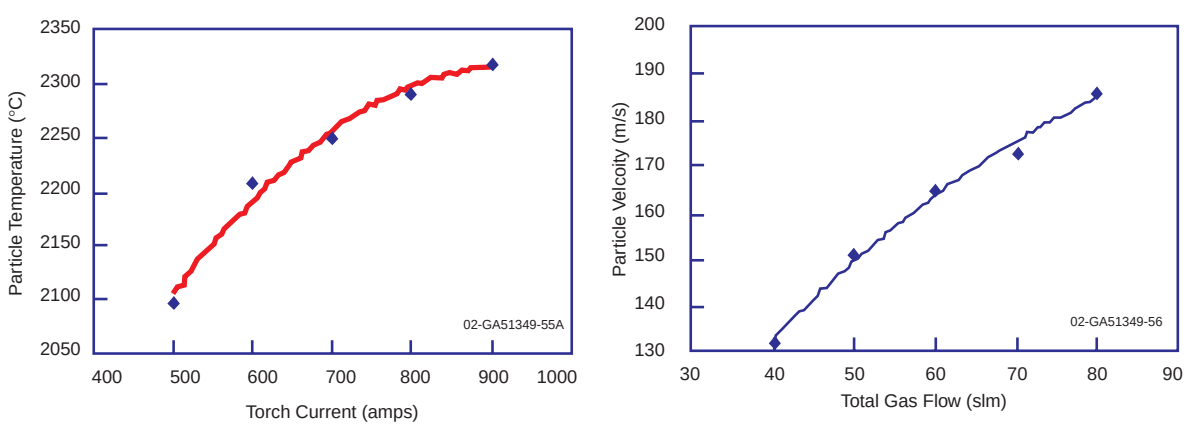


*FIGURE 1. Average particle temperature and velocity as a function of torch current and total gas flow rate.*

process, these plots indicate it is possible to lower the sprayed particle temperature and increase its velocity by decreasing the torch current and increasing the total gas flow. This will reduce the sprayed particle residence time and temperature in the entrained air atmosphere, reducing its chance to oxidize.

Trial coatings of alumina and aluminum as surrogate fuel and oxidizer were fabricated with the SG-100 plasma spray torch. The coating cross section micrograph in Figure 2 shows that good dispersion of the aluminum (light color material) in the alumina (dark color material) was achievable. As expected the deposition efficiencies of alumina and aluminum were different due to their differences in melting point. To fabricate a thermite coating of a particular stoichiometric mixture it is important to have a quantitative understanding of these relative deposition efficiencies. The result of an experiment to determine relative deposition efficiencies is shown in Figure 2 as the percent by volume of aluminum deposited in the coating, with the balance being alumina, as a function of the percent of aluminum fed to the spray torch. With this information, it is now possible to customize the mixture ratio of fuel to oxidizer in the energetic coating.

Nearly all industrial plasma spray equipment uses ball and tube-type flowmeters to monitor the torch and carrier gas flow rates. The equipment from the DOE Mound facility is no exception. Thus far, the experimental work has been performed in the thermal spray laboratory using much more accurate mass flow controllers to control the torch and powder carrier gas flow rates. To be successful at translating the information and process operating parameters from this lab to the MSSL, where actual energetic coatings are to be fabricated, it will be necessary to replace the ball and tube flowmeters of the MSSL system with a more accurate gas flow control system. To this end a matching gas control system for MSSL has been built and installed that is computer operated with Labview software.

The plasma spray equipment acquired from the DOE Mound facility has been installed in the MSSL plasma spray bay. This is a complete system that has been augmented with an automated torch gas control w/ computer, dual powder feed systems with scales, automated sample translation system w/computer,

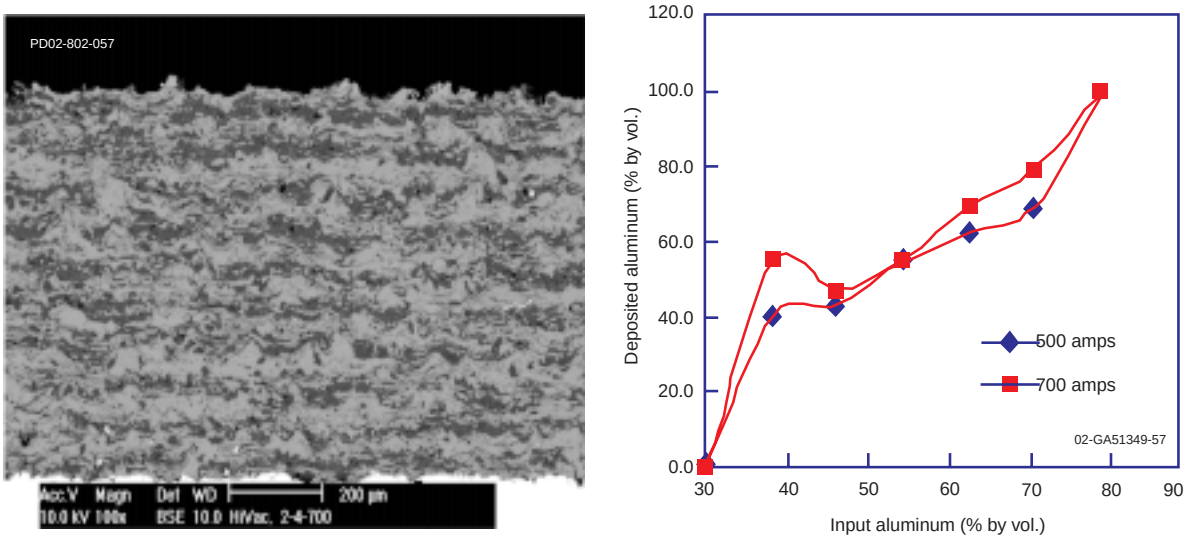


*FIGURE 2. Micrograph of a sectioned coating comprised of non-reacting aluminum and alumina. Also shown is a plot of aluminum deposited as a function of the amount of aluminum fed into the system by volume.*

aqueous powder over spray collection (water wash curtain and filtration system), exhaust system and acoustic enclosure.

The MSSL thermal spray lab is a functioning lab complete with tools, torch spare parts, bench and storage cabinets, and utilities.

Energetic materials offer a wide array of practical applications. Commercial uses include welding ground wires and railroad rail ends, emergency illumination, remote cutting, food warming, thermal destruction, and many more. These materials offer power to perform work without electricity in remote locations. When handled responsibly, such materials are simple and safe to use without special training or qualifications.

While many applications already exist, they are currently limited to those using loose powder mixtures in reaction chambers to control, direct, and/or contain the energy. The use of energetic materials could be dramatically expanded if containerless, complex-shaped parts could be produced more easily and at lower cost.

Plasma spray offers a powerful new fabrication tool for rapidly making any shape. Multiple molds could potentially be sprayed during the same run. Molds would be removed and reused. Container waste and disposal cost would be eliminated. If the permanent substrate were also a fuel material (for example, aluminum sheet), the entire device could be consumed and contribute to the reaction. The substrate could provide not only shape but also strength. Still no container waste would remain after use.

The INEEL leads the field in several areas of energetic materials development and applied research in associated arts. These materials and systems are important to national security missions. This LDRD represents a critical enabling technology applicable to several valuable national security program interests. National security customers often require rapid responses to energetic materials needs. This unique technology offers a significant leap forward in rapid forming of complex shapes.

# Assessment of Long-Term Variations in Soil Moisture and Regional Groundwater Flow Patterns within the Snake River Plain Aquifer System in Response to Potential Climate Changes

*Michael Szpakiewicz, Richard Smith, Michael Rohe*

## *How climate changes can affect groundwater contamination*

ES107

Safeguarding the Snake River Plain Aquifer System (SRPAS) from injected and buried nuclear and chemical wastes beneath the INEEL is of critical importance to the DOE long-term stewardship goals. Isolating these radioactive wastes from the biosphere and hydrosphere on time scales of centuries to millennia requires consideration of the impact of climate changes on the regional hydrologic cycle.

Atmospheric models indicate that by the year 2050 eastern Idaho will experience a 3.2° C annual temperature rise and a 27% increase in atmospheric moisture levels. Unfortunately, the potential for these simulated climate changes to mobilize buried wastes remains almost entirely unknown. While regional groundwater flow models have been successfully developed for the SRPAS, these have not focused on past or future climate change issues. Better representations of land surface and subsurface hydrologic conditions are needed to quantify the effects of predicted climate change on watershed hydrodynamics.

This LDRD is assessing the impact of climate change on the subsurface hydrology and aquifer vulnerability of the 500 x 280 km eastern Snake River watershed, which encompasses the Eastern Snake River Plain Aquifer, INEEL, and surrounding mountain ranges including the southwestern part of the Yellowstone Plateau. A Pleistocene lake called Lake Terreton covered a large portion of the present INEEL site during its high stands. Review of paleoclimatic literature for the region indicates that groundwater levels beneath Lake Terreton have fluctuated more than 200 feet several times over the past 120,000 to 160,000 years. The investigators on this LDRD are currently determining if a groundwater/surface water model calibrated to modern hydrologic stresses can reproduce these large water-level fluctuations using available paleoclimatic data. Potential effects of future climate change could then be assessed for 2050-2100 using output from atmospheric GCM models under assumptions of $CO_2$ doubling associated with continued fossil fuel burning.

Technical objectives for fiscal year 2002:

- Analyze spatial and temporal pollen data to reconstruct Pleistocene climate at INEEL.
- Evaluate the influence of past, current and future climate conditions on soil moisture distribution and groundwater flow patterns.
- Develop 3-D saturated flow model to determine feasibility of reproducing large water level fluctuations using available paleoclimatic data.

To reconstruct Pleistocene climate at INEEL, spatial and temporal pollen data from lake sediments across the Western USA were analyzed. A relationship between modern climate and modern lake pollen percentages was found using the multiple regression methodology. The 15 most abundant pollen types from 45 lacustrine records were statistically related to mean annual January and July temperatures and precipitation using the backward elimination multiple regression technique. The investigators applied the pollen transfer functions to dated sediment cores from Carp Lake (elevation 714 m MSL) in Western Washington and Cub Creek Pond (elevation 2,363 m MSL) in Yellowstone National Park – the two lakes nearest to INEEL from which Pleistocene pollen data are available.

Results indicate that conditions became cooler and drier in the Western USA beginning about 10 ka. January temperatures declined from about 31° F to 19° F and 21° F to 17° F for Carp Lake and Cub Creek Pond, respectively. July temperatures dropped from between 74° F to 62° F and 62° F to 58° F, respectively. Annual precipitation dropped from 25 to 20 in. and 15 to 10 in., respectively. These conditions had a net effect of reducing recharge to the SRPAS by about 53%.

The pollen data were only available back 33 ka. Earlier, more qualitative paleoclimatic reconstructions are available from published studies for Lake Terreton and Carp Lake. These authors analyzed the sediment facies and ostracode assemblages from three Lake Terreton cores (Fig. 1 next page), and used thermoluminescence and infrared stimulated luminescence to determine that the timing of lake level high stands was at 84 ka (± 6 ka), 130 ka
(± 12 ka), and 135 (± 13 ka). Two of these lakes level high stands correlate with Pleistocene Lake Bonneville high stands. Pollen data from Carp Lake indicated that overall conditions in the Western USA were drier than present for much of the late Pleistocene and Holocene but that there were at least two periods of wetter/cooler conditions between 43 to 56 ka and 93 to 117 ka. These

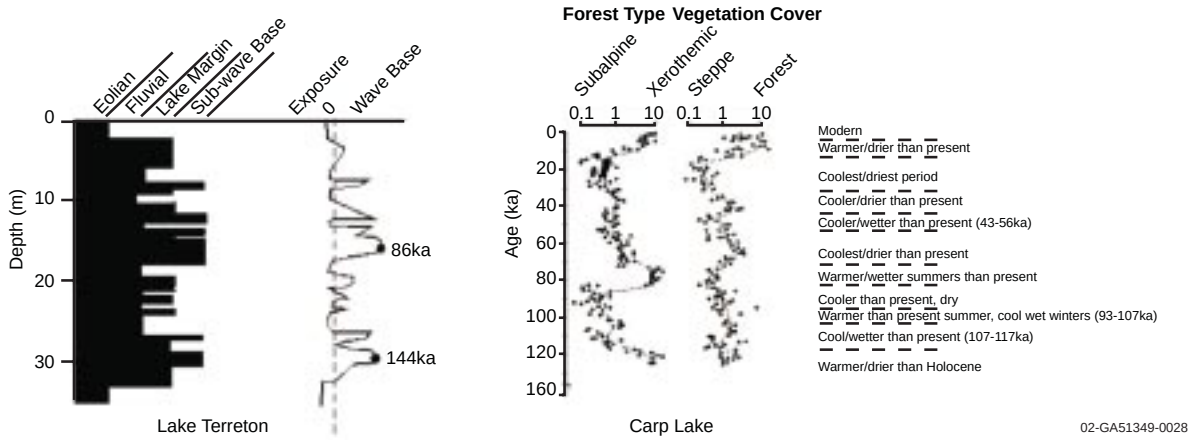


*FIGURE 1. Paleoclimatic data from Lake Terreton and Carp Lake cores. The Lake Terreton sediment facies data indicate as many as five periods of lake level high stands during the past 160ka. Pollen data from the Carp Lake cores reveal at least two periods between 43-56ka and 93-117ka when climatic conditions in the northwestern USA were cooler and wetter than modern conditions.*

studies indicate that the climate was both cooler and wetter than modern conditions during the past 160 ka and that this could explain the repeated Lake Terreton high stands.

Today, Lake Terreton is dry and the water table is between 200 ft to 250 ft below land surface. Since geostatistical analysis of lithofacies beneath INEEL reveals no laterally extensive confining units, the investigators infer that Lake Terreton high stands represent periods when the water table reached the land surface within the Big Lost Trough sub-basin that encompasses much of the INEEL facility. A specific goal of this study has been to determine what increase in recharge would have filled Lake Terreton in the past.

The influences of past, current, and future climate conditions on soil moisture distribution and groundwater flow patterns were evaluated in two steps. First, the Thornthwaite method was used to estimate monthly average recharge rates (precipitation minus evapotranspiration) over the model domain for current conditions and reconstructed climate conditions for 10 to 33 ka based on the pollen transfer functions described above. Second, MWT3D, a 3-D free-surface model that is uniquely suited for representing large ($10^2$m) water table fluctuations, was used to simulate saturated groundwater flow throughout the Eastern Snake River watershed. Because available pollen data only extend back 33 ka and this was a time when Lake Terreton was not believed to have been present, MWT3D was used to assess recharge rates required to cause the water table to intersect the land surface. In this sensitivity study, the estimated current rate of recharge was ramped up to a factor of 64, which is the ratio of simulated recharge to total precipitation in the vicinity of the INEEL.

Results of this preliminary modeling suggest that the model is an effective tool in evaluating these changes and that modifications of the recharge in the area within a plausible range could lead to the formation of a lake in the INEEL area again in the future. The small triangles on Figure 2A indicate areas within the model where seepage at the ground surface is indicated by the model under current climate conditions. Simulated seepage is limited to the discharge zone for the Eastern Snake River Plain aquifer system, which is generally consistent with observed conditions. The small circles indicate areas in which the water table remained below ground surface during all of the sensitivity model runs. The large squares

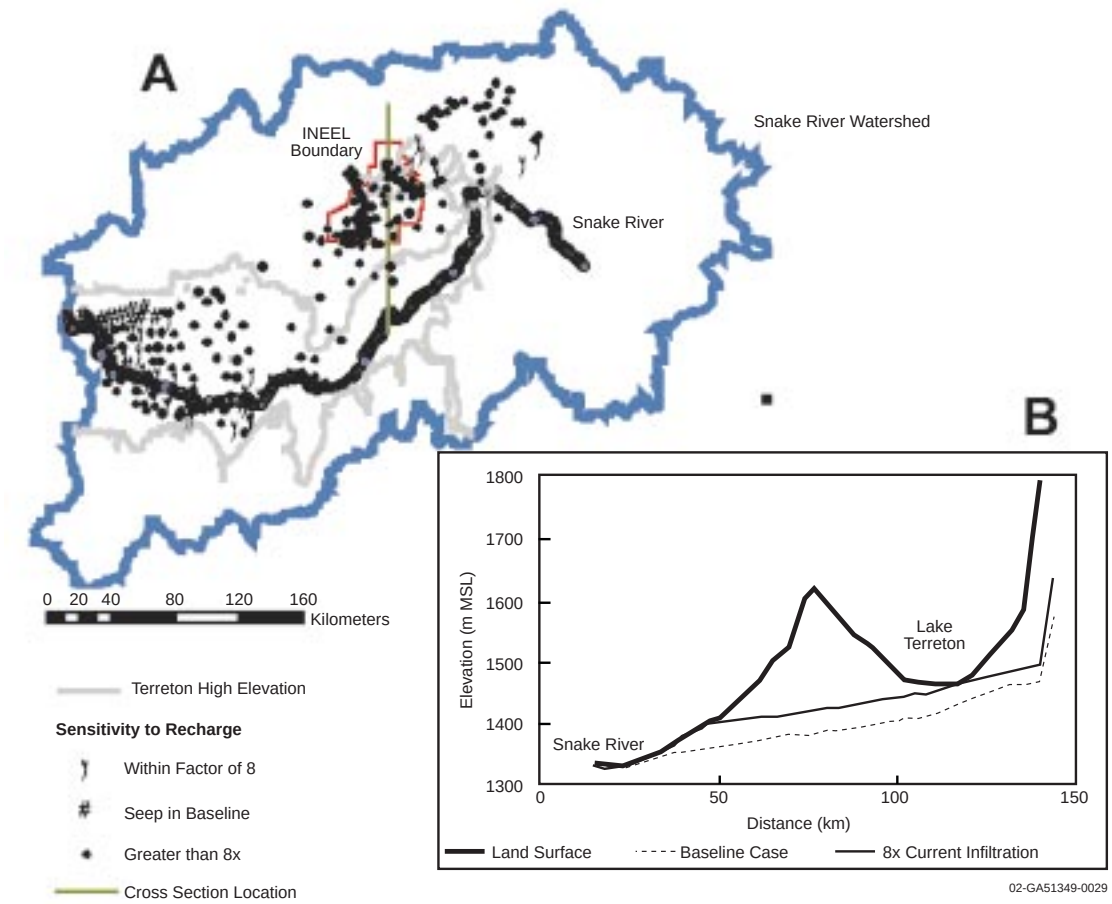


*FIGURE 2. (A) Map of sensitivity to changes in recharge to the water table over the Eastern Snake River Watershed. (B) Cross-section from the Snake River through the INEEL showing simulated water table positions under two recharge scenarios.*

are the areas where the simulated water table reached the ground surface by increasing the rate of recharge by 2- to 8-fold current simulated rates.

In the vicinity of the INEEL, the areas in which the simulated water table reaches the ground surface under increased recharge are limited to within the footprint of Pleistocene Lake Terreton (Figure 2B). In other words, the sensitivity study indicates that a 2- to 8-fold increase in recharge probably caused formation of Lake Terreton. This result also was verified using a 1-D analytic solution. Such an increase in recharge is plausible for the Snake River Plain, where 1% to 5% of precipitation actually reaches the aquifer. An 8-fold increase of recharge in the higher elevations would require greater annual precipitation. If GCM predictions of increased atmospheric

moisture lead to commensurate increases in recharge, Lake Terreton could be formed again in the future.

The vulnerability of the SRPAS to groundwater contamination also was assessed using a semi-quantitative ranking scheme. The INEEL facility currently is only moderately susceptible to groundwater contamination. Areas of high contamination potential are to the south and west along the Snake River. If increases in atmospheric moisture forecasted for 2050-2100 lead to increased recharge to the SRPAS, its vulnerability to contamination would obviously increase.

Future work on this project includes developing more numerically efficient algorithms to represent evapotranspiration and unsaturated flow under conditions of climate change, analysis of pollen assemblages from the Lake Terreton cores to provide a site-specific climate record, and continued development of the 3-D saturated flow model to incorporate surface water interaction and the ability to simulate mass transport and heat transport. In addition, assessment will be made of the vulnerability of the SRPAS to contamination under conditions of climate change.

This LDRD is helping to place the INEEL at the forefront of the development of hydrogeologic modeling that incorporate predicted global climate change. If successful, this work will provide the basis for developing future proposals for the Office of Science for refinement and adaptation to other locations.

# Mechanisms of Liquid Metal Embrittlement in Steels

*Terry C. Totemeier*

## *Understanding metal's reduced strength when exposed to a second liquid metal*

NS125

Liquid metal embrittlement (LME) is a phenomenon in which the strength and ductility of various metals are significantly reduced in the presence of a second liquid metal. LME has had a significant impact in the aerospace field, and may play an important role in the behavior of structural components exposed to liquid metal coolants in advanced nuclear reactor designs. Despite considerable research, the mechanisms of LME are still unclear. One of the limitations of previous research is the use of tensile test data rather than more intrinsic measures of material behavior, such as fracture toughness.

The objective of this LDRD is to measure the fracture toughness of steels in LME conditions using fracture-mechanics-based test methods. An innovative approach to introducing the liquid metal to the tip of a sharp precrack was developed and used to measure the fracture toughness of a structural steel as a function of tempering temperature in a liquid metal environment, thus determining the effect of metallurgical conditions on LME susceptibility for this steel. The results show that the fracture toughness of this steel is considerably reduced in LME conditions, and that the extent of reduction is strongly affected by tempering temperature. Work in FY03 will focus on completing the initial set of tests and examining the effects of strain rate.

Technical objectives for fiscal year 2002:

- Develop a test procedure to measure the fracture toughness of steels in liquid metal environments.
- Measure the fracture toughness of steel in a liquid metal environment as a function of tempering temperature.

To develop a test procedure to measure fracture toughness, specimens of standard fracture toughness test geometry were obtained that contained sharp, embrittler-filled precracks. To obtain a true measure of the base metal fracture toughness in the presence of the liquid metal, it is important that the precrack terminate in the base metal at the correct crack length.

After considerable experimentation it was discovered that cracks running through the base metal could be arrested using selective reinforcement of the specimen. The reinforcement technique uses a three-point bend specimen of standard geometry (Fig. 1). A shallow notch is machined into one side, and two steel reinforcement plates are attached to the sides of the specimen with high-strength epoxy. The specimen is loaded in displacement control at a temperature above the embrittler melting point until the load begins to drop (indicating crack initiation and growth). The specimen is immediately unloaded, arresting the precrack, and cooled to room temperature. The reinforcement plates are removed and the length of the embrittler-filled precrack is marked. The final loading to failure is again performed above the embrittler melting temperature. The final loading configuration meets requirements for a standard fracture toughness test in the LME environment.

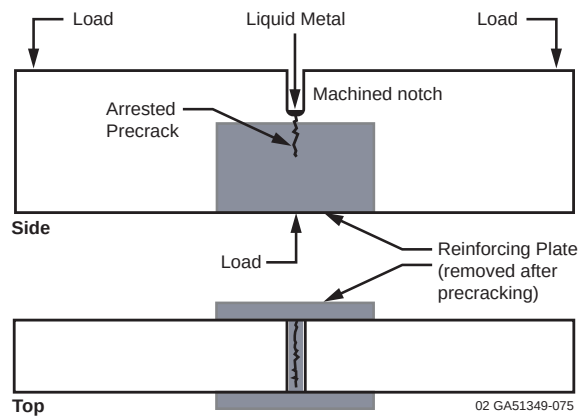


*FIGURE 1. Schematic of a reinforced 3-point-bend fracture toughness specimen after precracking.*

This technique was successfully applied to the measurement of fracture toughness of steel. For steel tempered at 1000° F, some plasticity was associated with the propagation of the precrack. The resulting critical stress intensity factor for propagation ($K_c$) did not meet the requirements of the ASTM test standard for valid $K_{Ic}$. Figure 2 (next page) is a plot of the variation in $K_{Ic}$ or $K_c$ as a function of tempering temperature. The toughness values for tempering temperatures of 300° F to 800° F

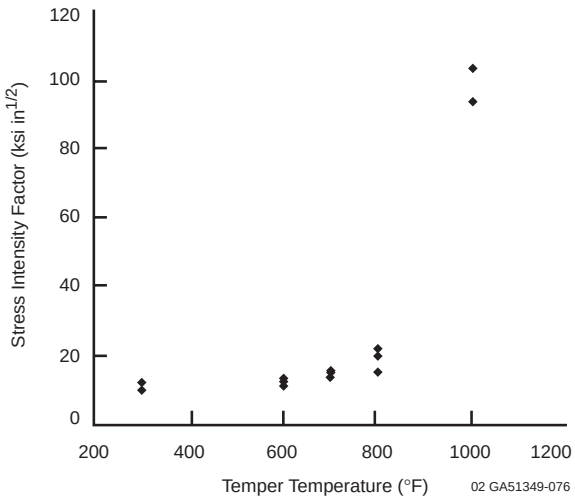


*FIGURE 2. Fracture toughness of steel in a liquid metal environment as a function of tempering temperature.*

are quite low and increase slightly from 9 ksi √in at 300° F to approximately 20 ksi √in at 800° F. There is a dramatic increase in toughness at 1000° F to values of nearly 100 ksi √in.

The development of the technique described for measuring fracture toughness in liquid metal environments is believed to represent a significant advance in the field of LME. This technique should be applicable to a number of embrittlement couples, and will enable a number of fundamental studies of LME. Efforts are currently underway to continue fundamental LME research through DOE-Sandia Corporation and the DOE-Nuclear Engineering – Nuclear Energy Research Initiative program. The current data is insufficient for a substantial, peer-reviewed publication. Completion of the research outlined for the second year of this LDRD is expected to result in publication.

# Porous Crystalline Silica (Gubka) Based Ion Exchange Sorbents

*Troy Tranter, Terry Todd*

## *Removing target radionuclides from waste*

ES105

Inorganic ion exchange media typically exist as fine powders, making large-scale use impractical, unless the media can be affixed to an appropriate matrix. Likewise, organic chelating agents are typically dissolved in a solvent and absorbed into porous matrices for use in extraction chromatography. The most common matrices used in both cases are organic materials that are not compatible with high-radiation fields or acceptable as final waste forms.

Recent investigations have shown that ion exchange and chelating agents can be effectively loaded within a porous crystalline silica (Gubka) matrix. This approach allows for target radionuclides to be adsorbed into a porous microcrystalline glass matrix that encapsulates the contaminant and becomes the final waste form. Subsequent to adsorption of the radionuclides, the Gubka matrix can be compressed in a hot uniaxial press to further reduce the amount of waste for disposition.

This LDRD is the result of a collaborative research program between the V.G. Khlopin Radium Institute (KRI), St. Petersburg, Russia, and the INEEL. In the first year of the project (FY01) the primary focus was the selective removal of cesium from acidic matrices with only cursory investigation into actinide removal. In FY02, octyl(phenyl)-N-N-diisobutyl-carbamoylmethylphosphine oxide (CMPO) for the removal of lanthanides and actinides from acidic liquid, was successfully incorporated into Gubka matrices. Tests for plutonium removal using CMPO-Gubka also were conducted.

Technical objectives for fiscal year 2002:

- Develop a technique for synthesizing an actinide extraction compound inside the hollow Gubka cenospheres.
- Perform batch contacts with the newly developed composite material to obtain equilibrium data.
- Perform at least one dynamic column test with Gubka in a fixed-bed configuration to determine radionuclide removal efficiency and decontamination factors.
- Collaborate with Khlopin Radium Institute to perform thermal stability testing of the loaded Gubka matrix in their laboratory to provide data on the volatility of the nuclides as well as the energy released during thermal treatment.

Gubka, or “sponge” in Russian, is an open-cell glass crystalline porous material that is produced from hollow glass crystalline microspheres (cenospheres) formed as small mineral slag particles in fly ash from coal combustion. The cenosphere sizes typically range from 0.1 to 0.5 mm in diameter. Average compositions of the cenospheres used to prepare Gubka include mainly the minerals common in glass, including up to 65 wt.% silicon oxide, 25 wt.% aluminum oxide, and lower amounts of iron, calcium, magnesium, potassium and titanium oxides ranging from less than one to five percent.

The method of preparing Gubka includes separating the cenospheres into fractions based on size, density, magnetic or non-magnetic, and perforated or non-perforated characteristics. Selected cenosphere portions are molded and agglomerated by sintering with or without a binder at high temperatures. The porous Gubka matrix consists of two types of porous openings: intraglobular pores in the cenosphere walls of 0.1-30 micrometers, and interglobular pores between the cenospheres of 20-100 micrometers. Depending on the cenosphere fractions selected, sintering conditions and additional treatments, Gubka is formed with a total open-cell porosity ranging from 40%-90%. Gubka has an apparent density of 0.3-0.6 g/cm$^3$ and a compressive strength in the range of 1.2-3.5 MPa. The Gubka material is chemically stable in concentrated nitric, hydrochloric, sulfuric, and phosphoric acids at boiling temperatures.

Techniques for synthesizing the selective actinide/lanthanide extraction compound octyl(phenyl)-N-N-diisobutyl-carbamoylmethylphosphine oxide (CMPO) inside the hollow cenospheres have been developed resulting in approximately 40% loading by mass.

Equilibrium experiments have been performed with the newly developed material using simulated solutions of INEEL acidic tank waste spiked with $^{239}$Pu. To measure the efficacy of the composite material for plutonium uptake, distribution coefficients were calculated for each of the batch contacts according the following formula:

$$K_d = \frac{(C_0 - C_e)}{C_e} * \frac{V}{M}$$

Where:

$C_0$ = Initial concentration of the ion in solution before contacting sorbent.

$C_e$ = Final equilibrium concentration of the ion in solution after contacting sorbent.

$V$ = mLs of solution

$M$ = Grams of sorbent material contacted.

The resulting $K_d$ values are listed in Table 1. These values are quite high indicating that the new composite material has high separation efficiency for plutonium.

Several bench-scale column tests have been completed with the CMPO-Gubka material to determine the capacity and kinetic properties of the sorbent during dynamic conditions. One of these tests was performed with a 1.5 $cm^3$ column using 2 M $HNO_3$ spiked with $^{239}Pu$ (Fig. 1).

These data are very promising and show that the new material has very high sorption capacities while maintaining good flow characteristics and mechanical stability. These preliminary column test data indicate that the feed solution can be processed at flow rates exceeding 5 bed volumes (BV) per hour before any column "slip" of the plutonium is seen. At the higher flow rate (10.7 BV/h), the $^{239}Pu$ in the effluent stream is not a result of exceeded column capacity, but rather due to the fact that the flow velocity has surpassed the kinetic capabilities of the column. This parameter can be further improved and optimized by proper column design.

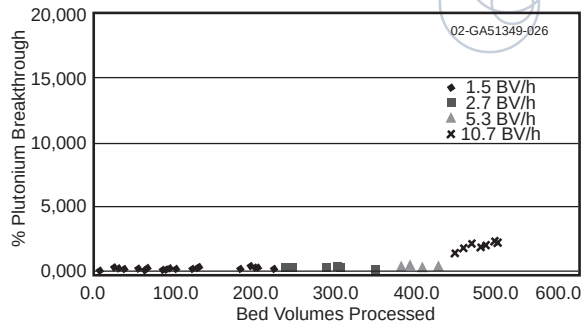


*FIGURE 1. Dynamic column test with CNPO-Gubka and 2 M $HNO_3$ - $^{239}Pu$ feed solution.*

Another advantage of the Gubka-sorbent material is that it can be compressed and calcined to obtain a waste form acceptable for a final repository, thus eliminating the need to elute the radionuclide and perform subsequent stabilization by vitrification, grouting, etc. To this end, it is necessary to study the radionuclide volatility and energy released during the heating and compressing of the composite material. This activity was done at the Khoplin Radium Institute. A Gubka-CMPO block loaded with americium was calcined at $1000^{B}C$ and a differential thermal analysis (DTA) and thermogravimetric (TG) measurement was performed during this process. An americium trap also was incorporated to determine total

| Feed | Weight (g) | Vol(mL) | Vol/Mass | $K_d$ |
|---|---|---|---|---|
| Simulated Tank Waste | 0.025 | 15.0 | 600 | 9293 |
| Simulated Tank Waste | 0.050 | 15.0 | 300 | 10824 |
| Simulated Tank Waste | 0.10 | 15.0 | 150 | 10543 |
| Simulated Tank Waste | 0.20 | 15.0 | 75 | 12491 |
| Simulated Tank Waste | 0.30 | 15.0 | 50 | 9317 |
| Simulated Tank Waste | 0.40 | 15.0 | 38 | 10426 |

02-GA51349-025

*TABLE 1. Plutonium distribution coefficients in simulated INEEL tank waste for the CMPO-Gubka composite.*

americium loss. The total mass loss for the Gubka impregnated with CMPO was 26%, with the majority of the mass loss taking place in the temperature range between 200ºC and 360ºC as shown by the TG curve in Figure 2. This mass loss is due to the decomposition of CMPO and the volatilization of the resulting products. The DTA curve in Figure 2 shows there is an acceptable exothermic energy release in the 200ºC to 540ºC range. The total americium released during the process was 0.3% of the amount adsorbed into the Gubka-CMPO. An X-ray analysis showed that the phase compositions of the initial Gubka and Gubka impregnated with CMPO are the same. This result indicates that phosphorus does not react with the Gubka material to form crystallized compounds.

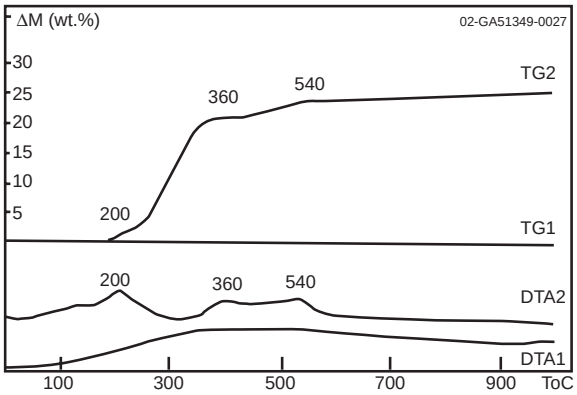


*FIGURE 2. DTA and TG measurements of initial Gubka (1) and Gubka impregnated with CMPO (2).*

This research has provided very promising results in that a novel inorganic matrix has been combined with a transuranic (TRU) extractant to successfully remove target TRU radionuclides from liquid radioactive waste. This matrix is very stable in high radioactive, temperature, and acid environments, unlike the organic polymers typically used for this purpose. It also has been demonstrated that this material can be treated thermally to yield a very stable ceramic waste form. This result is exceptionally important because it eliminates the current practice of stripping or eluting the radionuclides from the sorbent bed, which results in increased waste and requires further stabilization.

This new technology has great potential for the treatment and stabilization of radioactive waste solutions in the DOE complex as well as in Russia. Two patents on the Gubka material have been awarded in the U.S. and Russia. An additional patent disclosure is currently in the filing process in both countries. Peer-reviewed papers were presented at the Material Research Society conference in Boston, November 2001, and the 14th Radiochemical Conference at Marianske Lazne, Czech Republic, in April 2002.

The U.S. collaboration with Russian scientists has been very effective in establishing a synergistic approach to treating and stabilizing cold war legacy wastes within each country. After sufficient refinement at bench scale, a semi-scale experiment is expected to be performed on actual waste at the Tank Retrieval and Closure Demonstration Center (TRCDC) in Zheleznogorsk, Russia. This will provide confirmatory data on the newly developed technology and produce essential engineering data for a pilot scale prototype.

# Exploring Applications of Wavelet Theory: Groundwater Dynamical Systems, Gamma Spectral Analysis, Acoustic Resonance Spectrometry

*Maria Elena Velasquez, Charles V. McIsaac, Leo Van Ausdeln*

## *Applying wavelet theory for counter-terrorism solutions*

NS114

Wavelets are a versatile tool with very rich mathematical content and great potential for many applications. The objective of this LDRD is to explore the application of wavelet theory (multi-resolution analysis) to gamma-ray spectrometry, groundwater dynamical systems, and acoustic resonance spectrometry. During this year the research concentrated on refining the wavelet signatures developed during the first year and examining the application of wavelet signatures to the fields of Analytical Chemistry and Nuclear Physics.

Technical objectives for fiscal year 2002:

- Conduct detection and quantification research using wavelet signatures and mathematical/statistical models.
- Prepare publications and presentations of research results.

The application of wavelet theory to the analysis of gamma-ray spectrometry will improve the accuracy of spectral analysis results and the performance of software codes currently used at the INEEL and other DOE sites, aiding the laboratory in environmental cleanup efforts. Automated assays of radionuclides in chemical waste by passive gamma-ray spectroscopy, wavelet signatures and chemometrics were researched. It was determined that a computer-based intelligent system would provide real-time interpretation and avoid subjective biases that often lead to over-estimation of radionuclide concentration when interpreted by experts. The system is summarized using five steps: data input, wavelet signature preparation, classification and estimation, result display and user action (Fig. 1).

Inverse Least Square (ILS), a statistical method, was used for the classification and estimation. The model for ILS is as follows:

$C = PA$

Where:

$C$ = concentration matrix (known, for single isotopes)

$P$ = constant matrix (unknown, need it for quantification and unfolding of composite spectra)

$A$ = single isotope signature matrix (known, standards)

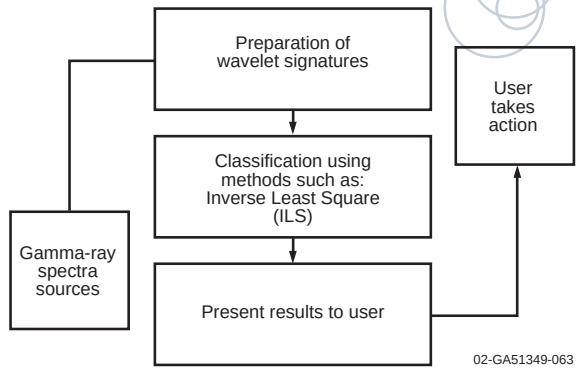


*FIGURE 1. Graphical representation of a computer-based intelligent system (five-step process).*

Using the standards for each isotope, the equation can solve for $P$ by $P = CA^{+}$ where $A^{+}$ is the pseudo-inverse of A. Once $P$ has been obtained, it and the ILS model can be used to determine the presence or absence of given isotopes in the composite spectra. For this step of the process a threshold on the concentration estimates is imposed.

$\tilde{C} = P\tilde{A}$

Where:

$\tilde{C}$ = concentration estimates matrix (unknown)

$P$ = concentration matrix (known, it was obtained in the prior step)

$\tilde{A}$ = measured spectra matrix (known, collected composite spectra data)

The model was tested on composite spectra (Drums) obtained from the cleanup program at the INEEL. (Results in table on following page).

The results are promising for "statistical detection" for most of the isotopes of interest. Yet U238 presents a challenge. Both the ILS model and the soft threshold technique used in the research need to be further analyzed.

This work was presented at the International Conference for Analytical Chemistry (September 2002).

| | | | | | | |
|---|---|---|---|---|---|---|
| **False Positive**<br>**False Negative** | **Co57**<br>14.29<br>14.29 | **Co60**<br>0<br>0 | **Eu152**<br>14.29<br>0 | **Am241**<br>0<br>28.57 | **Ra226**<br>0<br>0 | **U238**<br>14.29<br>42.86 |
| | **Co57**<br>0<br>0 | **Co60**<br>0<br>1 | **Eu152**<br>0<br>1 | **Am241**<br>0<br>0 | **Ra226**<br>0<br>0 | **U238**<br>0<br>0 |
| | -1<br>1 | 0<br>1 | 0<br>1 | 0<br>0 | 0<br>0 | 0<br>0 |
| | 1<br>0 | 0<br>1 | 0<br>0 | 0<br>0 | 0<br>0 | 0<br>0 |
| | 0<br>0 | 0<br>0 | 0<br>1 | 0<br>0 | 0<br>0 | 1<br>0 |
| | 0<br>0 | 0<br>0 | 1<br>0 | -1<br>1 | 0<br>1 | -1<br>1 |
| | 0<br>0 | 0<br>1 | 0<br>0 | 0<br>0 | 0<br>1 | -1<br>1 |
| | 0<br>0 | 0<br>1 | 0<br>1 | -1<br>1 | 0<br>1 | -1<br>1 |

02-GA51349-064

***Improving sensitivity, resolution, signal-to-noise ration and detection of CdZnTe detectors by rectifying hole-trapping with the use of wavelet theory*** – The investigators evaluated a class of gamma-ray detectors known as "room-temperature semiconductor detectors." Room-temperature semiconductor detectors have better resolution than NaI(Th) detectors, but poorer resolution than HPGe detectors. The most promising of these semiconductors is cadmium zinc telluride (CdZnTe).

Preliminary research on detecting the hole-trapping behavior in the CdZnTe detector was completed. The work consisted of testing and selecting the appropriate wavelet filters (transforms) for the detection of the hole-trapping effects on the spectra signal. Once the hole-trapping event is detected, by smoothing techniques, that section of data is excluded from the signal, thereby improving sensitivity and resolution of the detectors and signal-to-noise ratio in the resulting gamma-ray spectra.

This field of research has direct application to the U.S. effort to fight, identify, and mitigate the effect of terrorist activities.

***Improving sensitivity, resolution and signal-to-noise ratio of CdZnTe detectors by rectifying hole-trapping –*** Mathematical techniques of wavelet transforms and pattern recognition were used to rectify the hole-trapping effects in Cadmium/Zinc/Telluride detectors to improve sensitivity and resolution of the detectors, and signal-to-noise ratio in the resulting gamma-ray spectra. Challenges in this effort include collecting detector output signals, both with and without hole-trapping, and identifying representative signatures; i.e., extending the concepts and software for a global solution over many isotopes, and exploring the possibility of isotope recognition directly from pre-amp digital output.

***Detection of single isotopes using room temperature detectors: application of wavelet theory to gamma-ray spectral analysis –*** Wavelet theory and Non-Parametric Statistical methods will be used to develop signature extraction for gamma-ray spectra and simplified isotope detection software techniques for gamma-ray data from Cadmium/Zinc/Telluride gamma-ray (CdZnTe) detectors. The suite of radiation detection devices available to the counter-terrorism community to identify and mitigate terrorist threats would be augmented significantly by successful application of this research to improve the analysis and isotopic detection on data obtained from low-cost room-temperature semiconductor detectors.

***Rapid detection of pathogenic microbes using matrix-assisted-laser desorption/ionization time-of-flight mass spectrometer –*** Rapid detection of pathogenic microorganisms is important for maintaining public security. The facile identification of pathogens from environmental samples is important for securing hygiene in health facilities such as hospitals, for food hygiene in process-

ing plants, to counter bioterrorist attacks, and to prevent outbreaks of germicidal resistant microbes; e.g., super-bacteria that are genetically resistant to antibiotics. Matrix-Assisted-Laser Desorption/Ionization Mass Spectrometry (MALDI-MS) is a viable method for the characterization of bacteria that has played a key role in the analysis and investigation of large bio-molecules. Analysis using the MALDI-MS methods only takes a second to complete. This short analysis time coupled with throughput advantages give MALDI-MS advantages that surpass competitive methods such as polymerase chain reaction. In addition, the MALDI-MS method is very sensitive, allowing the detection of low ($10^{-15}$ –$10^{-18}$) mole quantities of sample with accuracy of (0.1 – 0.0010); i.e., data may be obtained from small quantities of bacteria (1,000 cells). Recent developments on a wavelet-based classification method that allows mixtures of bacteria to be classified give a strong basis for this work. This research seeks to optimize the MALDI-MS experiment for detecting bacteria from environmental samples and develop a robust automated identification system.

***Investigation of bacteria on dust using a high-resolution imaging ion microprobe –*** Dust particles have conveyed bacteria across continents causing detrimental effect on the environment. It has been suggested that the interplanetary transport of bacteria by cosmological dust might have provided the foundations for the origins of life on Earth. Dust particles provide a well-suited tool to terrorists for dissemination of biological agents. Besides trans-global transport, dust also might be used for localized attacks in cities or other areas of high population density (e.g., sporting events).

This project will use the high-resolution imaging secondary ion mass (SIMS) spectrometer instrument located at the Ohio Center of Excellence for Surface and Thin-film Analysis (CESTA) at the University of Cincinnati to study microorganism transport by dust particles. This instrument has sub-micrometer resolution and each pixel in the image is a high-resolution mass spectrum. A typical SIMS image is 1.5 GB in size, so data compression and modeling are important aspects of this project.

This effort will lead to better understanding of the characteristics of dust and bacteria that make transport under harsh environmental conditions possible, and development of a method for rapid identification of bacteria that pose environmental threats on airborne dust particles. A key component to this research will be building a hyperspectral imaging system that can locate and identify target microbes on dust particles.

This LDRD has generated an article for publication (under review) and resulted in a presentation at the International Conference on Chemometrics and Analytical Chemistry.

# Advanced Computing & Simulation Initiative

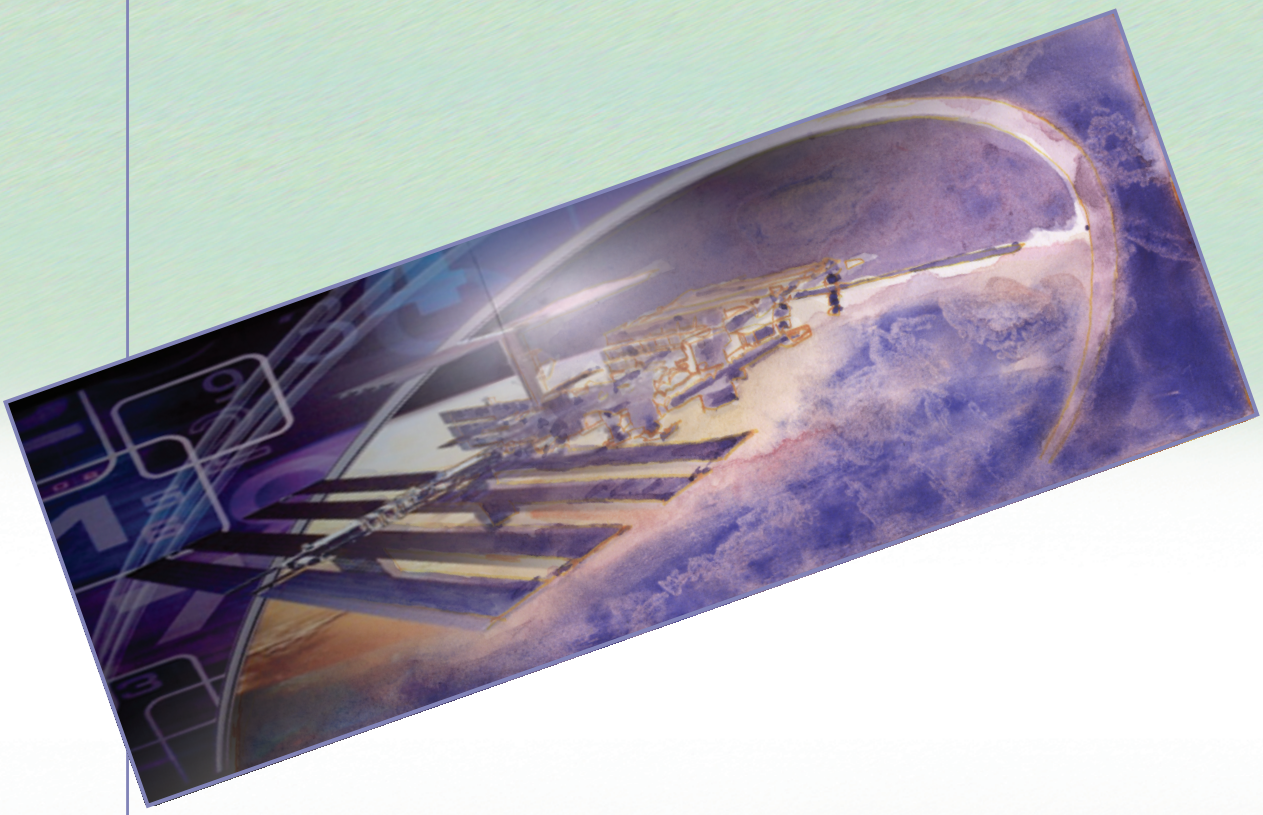

## LDRD Annual Report for FY-2002

Idaho National Engineering & Environmental Laboratory

# Development and Validation of Advanced Simulation and Collaboration Capability

*L. Eric Greenwade*

## *Advancing computational and collaborative work at INEEL*

AC104

An ever more robust, advanced computer simulation and collaboration environment is needed at the INEEL to promote additional scientific and engineering work. This LDRD establishes and validates the five fundamental components of an advanced computing and collaboration capability at the INEEL. These components are terascale data management, data abstraction models, performance optimization, parallelization, and visualization. Specific aspects of each are being developed and validated as well as an overall integration of all components. The near-term focus of this effort is on subsurface science. However, flexibility and extensibility for application to other mission areas, such as critical infrastructure protection and nuclear energy, are being incorporated.

Technical objectives for fiscal year 2002:

- Acquire new expertise in scientific programming.
- Complete collaborative environment specification.
- Develop and validate data abstraction model in subsurface code. Deliver to users.
- Implement and validate application-independent visualization tool for subsurface code.

In FY02, this project was successful in achieving all four of the year's goals. These four activities made substantial improvement in the advanced computing and collaboration capability at the INEEL.

Peter Cebull was hired in mid September to provide new expertise in scientific programming to the lab. With more than a decade of programming experience with scientific applications in a variety of environments, particularly those in use at the INEEL, Mr. Cebull rapidly integrated with the rest of the High Performance Computing and Visualization Group and immediately served as a resource to the group and users. His expertise will be key to the development of user sophistication in high performance computing and expansion of HPC efforts in nuclear engineering as well as other lab initiative areas.

An integrated design specification for a combined AccessGrid and powerwall system was completed, building on previous efforts of the Ohio Supercomputer Center, the National Center for Supercomputing Applications, the Princeton Plasma Physics Laboratory and the DOE Advanced Simulation and Computing Program. A combined equipment list for the integrated system was developed and validated with a number of these institutions. Necessary equipment was purchased to form a complete AccessGrid and powerwall integrated display system.

A data abstraction model for subsurface flow and transport codes was developed incorporating all known data elements for current and future models. The data abstraction model was based on the Hierarchical Data Format 5 (HDF5). This data model was implemented in the TETRAD subsurface code and used to create application-independent output files. These files will be accessible from a number of subsequent analysis and visualization processes and packages. To provide continuity with ongoing activities, both a native write and file translation capability were implemented. This capability gives users the choice of moving to the new environment provided by the data abstraction model (as time, scope and necessity dictate) or remaining with the traditional environment.

The advanced visual systems (AVS) commercial visualization package has been in widespread use across the DOE complex for 10 years and at the INEEL for eight years. While the package provides for a number of visualization options, many INEEL subsurface codes use proprietary file formats that preclude the use of AVS for these applications. A generalized reader was designed to translate the various data constructs used by the subsurface codes into the primitives provided within AVS. Additional logic routines were devised to handle those elements that did not have a direct representation within the AVS data format. Users from the international AVS-user community were polled, as several had similar

applications. The experience of these users was leveraged along with the knowledge gained at the INEEL to provide a fully functional interface design. The reader based on this design was implemented in several of the Numerical Simulation Laboratory's (NSL) HPC systems and provided to internal users. A couple of iterations were required to fully implement all necessary functionality.

This fiscal year's activity was the initial portion of a proposed three-year project. Although funding arrived late in the year, substantial progress was made on all fronts. The necessary milestones for FY02 were met, which positions the FY03 activities favorably for a successful start. A great deal of new and rekindled interest was generated from multiple lab initiative areas and all four components of R&D as a result of the work accomplished in this LDRD. These interests represent a variety of possible new directions that cover a gamut of applications, including subsurface science, nuclear engineering, critical infrastructure protection, and bioinformatics. This new work will drive the continued development of the advanced simulation and collaboration activity, continuing to advance the state of scientific research and engineering at the INEEL.

# Parallel Computing with Cluster Technology

*Thomas K. Larson, Charles R. Tolle*

## *Advancing high-performance computing*

AC101

Revitalization and advancement of high-performance computing (HPC) is a critical component of the INEEL Institutional Plan that supports all laboratory research and development activities. This LDRD is conducting a group of tasks to facilitate development and use of a more robust HPC capability. This work will support a cross-section of initiatives and users. However, initial emphasis is on the INEEL Subsurface Science Initiative, a fundamental laboratory activity for the immediate future. Tasks for this LDRD represent a multi-pronged capability evaluation and development effort to address some of the major stated computing needs, including parallel computing tools and distributed architectures, computational methods, and data visualization and repository. The primary effort will center on improving understanding and use of distributed computing or cluster technology where appropriate and possible. An over-arching driver in this work is low-cost high-performance computing – in other words, to minimize hardware cost and maximize computer performance for the specific problems of interest. This work is being conducted by INEEL in collaboration with universities and other institutions to leverage relevant ongoing research.

Technical objectives for fiscal year 2002:

- Investigate methods to achieve performance and scalability using inexpensive components and a systematic methodology to optimize cluster topology and connectivity for specific computational problems.
- Investigate tools to help the average scientist focus more on the task of algorithm development than on parallel implementation.
- Begin review, selection, and evaluation of cluster file- and load-balancing systems.
- Initiate building additional INEEL computational fluid dynamics (CFD) modeling and simulation capability using an existing particle method and high-perfor mance computing.
- Review integrated scientific data management and expanded visualization capability at the INEEL.

INEEL instigated a collaboration with the University of California Santa Barbara (UCSB) and MetaHeuristics LLC (Santa Barbara, CA) to study performance and scalability of computer cluster topology and connectivity for specific computational problems. Problems of interest include solution of the Navier-Stokes equations coupled with scalar transport equations, and phase-field systems involving solutions of a separate nonlinear partial differential equation. In these types of problems, large grid sizes (~$10^9$) and thus large memory and efficient communications between processors are necessary. Cluster issues addressed include optimization of communications between processors to avoid network bottlenecks and scaling issues as the number of CPUs is increased

During FY02, MetaHeuristics developed and tested a code to optimize communications between personal computers (PC) organized in a cluster. The purpose of the code is to simulate transfer of data between the processors in the cluster such that the wiring pattern and routing arrangement will minimize the time delays involved in passing data. The main features of this code include a simple user interface for input of hardware parameters and display of wiring patterns, code to generate different classes of wiring patterns for a flat network neighborhood topology (Fig. 1 next page) such that each PC is connected to every other PC in the cluster, and use of an artificial intelligence algorithm (currently simulated annealing), to find arrangements of the connections that will give optimal performance for each class of wiring patterns for given communication patterns. To benchmark the optimization code, UCSB constructed a four-node eight-processor Linux cluster with two D Link 1008T 8-port Gigabit switches and installed various parallel libraries. Software was also constructed for testing the performance of the cluster and generating data on bandwidth, latency, and communication frequency between nodes. The optimization code successfully ran using all four nodes and all eight processors. The code has been written to enable user optimization of the processors whether each node has one or more CPUs. Results to date indicate that optimization is worthwhile but a larger cluster is needed to generate more accurate performance data. Refinement of the optimization code using information from the small cluster will be continued in FY03 using different NIC drivers and cluster resource management systems. Scalability studies also will be conducted in FY03 using a larger cluster (likely a 32-processor cluster) to test different communication patterns and the channel-bonding concept.

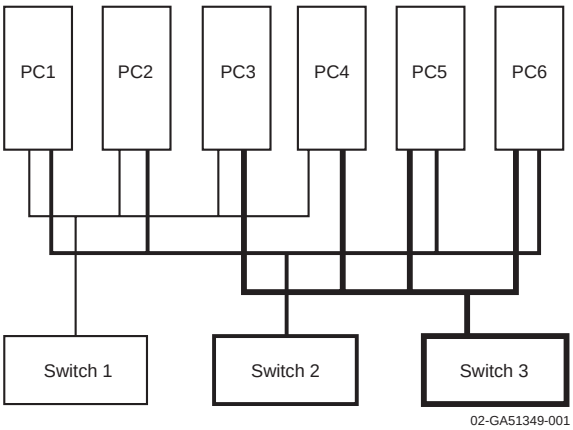


*FIGURE 1. Flat network neighborhood with six PCs and three 4-port switches.*

The Cilk compiler was chosen as a starting point for investigation of tools. Initial studies focused on evaluation of Cilk tool predictions for parallel scaling on a shared memory 64-processor Silicon Graphics Inc. (SGI) computer for two classes of algorithms. The first algorithm class was a highly distributed memory problem that could be implemented through a compartmentalized approach. The sample code for this series of tests was a newly implemented computational fluid dynamics (CFD) particle code. The algorithm's scalability was tested via a series of increasingly parallel code implementations (i.e., parallelism is distinguished from efficiency and thus measures different aspects of parallel code implementation). The base implementation was akin to the traditional Domain Decomposition (DDC) method where the problem is broken into a series of separate boxes over which local processor calculations can be made. The second implementation further parallelized the code by dividing the problem into individual particle update calculations. Likewise, a third implementation further parallelized the code by taking into account every particle-particle interaction as a separate parallel calculation. Figure 2 shows the results of these tests for varying numbers of CPUs.

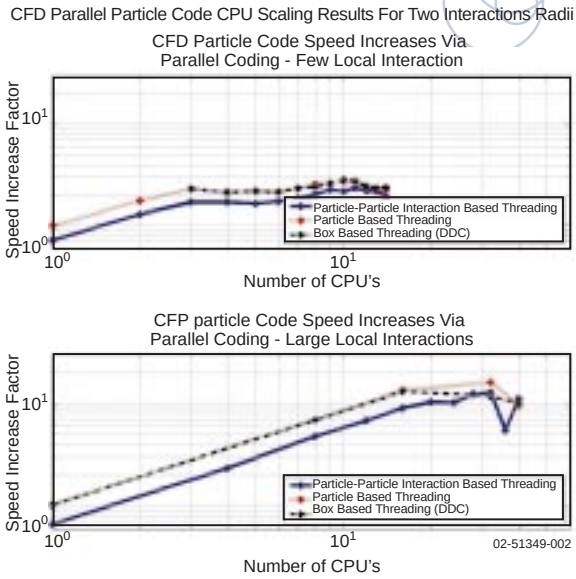


*FIGURE 2. Parallel scaling results of particle CFD code implemented within Cilk using normalized execution times based on the Particle Based Threading implementation.*

The first noteworthy result of this scaling study was that parallel scalability of the code changes dramatically by simply changing the range over which local particle interactions are allowed. For example, increasing the interaction range by a factor of ten changed the scalability from three processors to more then 30 processors. The code was not modified or recompiled for this change. Through use of the Cilk profiling tools, peak performance versus number of CPUs was accurately estimated using only two processors (i.e., the estimates can be made on small Linux and MacOS X implementations before the code is ported to a larger scale machine) for the particle-particle implementation. The profile tools used to estimate the peak performance were the critical path and total work estimations, which allow calculation of the code parallelism. A second result of the study showed that as parallelism in the code was increased the performance appeared to decrease, not increase as expected. On further investigation, this result appears to be machine architecture dependent. The large-scale SGI machine used for testing the code does not truly imple-

ment across-the-board, shared-memory architecture, as does the traditional dual-processor Linux or MacOS X machine. Architecture issues are better demonstrated using the second code class. This algorithm exhibits a high degree of common memory and requires complete exchange of the full memory space after each iteration. The program chosen to demonstrate this type of code was a traditional Fuzzy-C Means algorithm. On a MacOS X dual-processor 1.25GHz machine, the sample code runtime was 79.6 s for one CPU and 41.0 s for two CPUs, as was expected. However, on the SGI large-scale machine, the sample code ran in 108.2 s for one CPU and 237.2 s for two CPUs. It is believed that the code slowdown is due to arbitrary scheduling of the threads on non-memory-co-located CPUs. This result will be explored further in FY03.

Software layers developed to aid in the usability, performance, and administration of Linux compute clusters have been improving rapidly and the international Linux cluster community is in the process of transitioning from home-brewed solutions to distributions packaged by others. INEEL personnel initiated review, selection, and evaluation of several different cluster Distributed Resource Managers (DRM) and Distributed File Systems (DFS) to gain insight on implementation and performance issues and learn how to take full advantage of the products. A portion of an existing INEEL cluster (20 nodes of the 'dawulf' Athlon cluster) is being used for continuing product evaluations.

Most institutions with compute clusters use DRMs consisting of the Load Sharing Facility (LSF), the Portable Batch System pro/Open Portable Batch System (PBSpro/OpenPBS), or the Sun Grid Engine (SGE). LSF is popular if purchase cost is not an issue. Other solutions exist, such as Condor, and have a smaller but still significant installed base. Many institutions have been moving from OpenPBS to SGE because of the need for fail-over capability or the need to launch a massive number of jobs in a short time period.

Because of the cost and support structure, the INEEL has concentrated on evaluating SGE and OpenPBS. INEEL requirements for a DRM include support for Solaris, IRIX, and Linux operating systems, parallel job support (Message Passing Interface (MPI) and Parallel Virtual Machine (PVM)), job Checkpoint/Restart, complex resource allocation rules (e.g., consumable licenses), file staging, and high availability. Highly desired but not absolutely required features include inexpensive (or free) cost, source code availability, a large, active user community, and a web interface. Given INEEL requirements, SGE has several advantages relative to OpenPBS. For example, SGE supports Solaris, IRIX, Linux, Mac OSX, and has partial support for MS Windows. Parallel job support in SGE is superior and it provides checkpoint/restart hooks with better examples than OpenPBS. SGE can be configured to use complex resource allocation policies and, unlike OpenPBS, it can be installed with a "shadow master" for high availability. Another advantage SGE has over OpenPBS is that the free version has the same feature set as the current commercial version. Furthermore, the documentation for SGE is more thorough and readable than OpenPBS.

While Linux clusters have, for the most part used the traditional Unix Network File System (NFS), it is generally agreed that NFS has scalability and performance issues. Distributed File Systems are desirable for cluster compute systems because they make the system more efficient and easier to use. Thus, DFS is an active field of research supported by the DOE and other branches of the U.S. government. Many DFS in various stages of completion currently exist. For example, Lustre is targeted toward meeting the needs outlined by the DOE National Nuclear Security Administration and the DOD National Security Agency. Intermezzo, a relatively lightweight Linux-only distributed file system fits the INEEL cluster hardware better than Lustre. Intermezzo supports disconnected operation (i.e., high availability), has built in support in the Linux kernel, and is easy to install. Coda, a file system based on the original Andrew File System (AFS), supports more operating systems than Intermezzo, but is not yet suitably stable for operating in a production environment. OpenAFS, a file system open sourced by IBM, is now being developed and supported by an active community. While perhaps the most widely used DFS, it is complicated to install and configure. The Parallel Virtual File System (PVFS), while not a general-purpose cluster file system, is a good high-performance parallel file system for Linux and is easy to install and use. The Los Alamos

Cluster Research Laboratory is developing V9FS for Linux. OpenGFS, a distributed file system for shared-disk clusters, and the Global File System (GFS) are related file systems both targeted toward computer systems with shared disk arrays, which the current INEEL clusters do not have. Cluster File System (CFS) is the file system included with Single System Image (SSI) Clusters for Linux project. CFS has not been thoroughly tested and it does not implement file locking.

In summary, OpenAFS appears most suited for use across different computer architectures, but PVFS should work better for Linux clusters because of the ease of configuration. The Los Alamos V9FS approach to cluster file systems should be further evaluated as it may possibly offer a better solution than more traditional approaches. Evaluation and testing of DRM and DFS will continue in FY03.

Development of CFD modeling this year centered on validating the particle CFD code against an exact solution to the Navier-Stokes equations. A Poiseuille flow problem was set-up and executed on a single processor in preparation for operation on multiple processors. The problem domain consisted of a 10 x 250 grid with 4 particles per cell. The flow was driven by a pressure differential of $0.2P_0$, where $P_0$ was chosen to be 0.03 $N/m^2$. A small value for the pressure differential was chosen to minimize known difficulties encountered when particles flow into the top boundary and out of the bottom boundary. Test cases were run to determine the best methodology for solving the momentum equations. Past work by Los Alamos National Laboratory and the University of New Mexico solved the momentum equation on the grid and performed two sets of interpolations (from the grid to the particles and back from the particles to the grid) every time step. Even when velocity updates rather than total velocity values were mapped, the solution exhibited excessive dissipation and the analytic solution could not be achieved. However, when a different approach to solving the momentum equation was implemented, the analytic solution was achieved. This finding will produce significantly more accurate solutions with these types of methods. Tests also were run with different discretizations of the viscous terms in the Navier-Stokes equations. It was found that certain discretizations led to stability limitations and thus required the use of smaller time-steps. Research during FY03 will address implementation of no-flow boundary conditions, development of methods for handling boundaries and computational interfaces, and domain decomposition for implementation on multiple processors.

In an effort to address integrated scientific data management and expanded visualization capability needs at the INEEL, pilot studies were conducted to evaluate the Landmark Graphics Corporation (LGC) product suite's applicability to INEEL needs. The goal of the pilot study was to provide an opportunity for participants from various disciplines to evaluate LGC products and provide recommendations for requirements development. Prior to conducting pilot studies, LGC personnel demonstrated products that addressed the needs of the diverse technical disciplines at the INEEL. Group and individual consulting sessions were provided by LGC during the pilot program while participants were working on their chosen projects. As expected, the participants provided differing reviews, but none concluded that the LGC suite was a solution to all of the INEEL data management and visualization needs. However, many suggested that it was a powerful tool that would meet many of their individual visualization and analysis needs. A universal concern was the steep learning curve for the LGC product that would require specific, continual training and persistent use to develop and maintain proficiency. Some participants noted that retrofitting environmental data into petroleum industry formats would be required since the application is used in the petroleum industry. All of the participants expressed a desire to review additional tools and applications with more emphasis on environmental data. Documentation of the pilot study results will be conducted in FY03.

# Aerospace Situation Awareness and Risk Monitor Tool

*Steven D. Novack, Scott Hartley*

## *Developing a functional model to support operational personnel*

AC103

The original proposal for this LDRD was to develop situation awareness and risk monitoring software to support aeronautics and space missions. This software and decision tool would be applied to the systems analysis programs for hands-on integrated reliability evaluation (SAPHIRE) models for the space shuttle and the International Space Station that are being developed by NASA. Due to a funding reduction from $209,000 to $20,000, the original objectives of this LDRD have been modified. After meetings with Johnson Space Center (JSC) Safety Director Dr. Holsonback, the emphasis in FY02 was directed to developing a Functional model that could be used to support operational personnel and the safety console in the Mission Evaluation Room (MER) while providing a front-end for the Risk Monitor.

Technical objectives for fiscal year 2002:

- Develop a Functional model for the International Space Station (ISS).
- Provide example 3-D models to visualize functional system states.

The functional model was developed in ScienTec's REVEAL_W. This model represents the primary roles that the U.S. and Russian modules play in the ISS. An example of the top-level functional tree is seen in Figure 1.

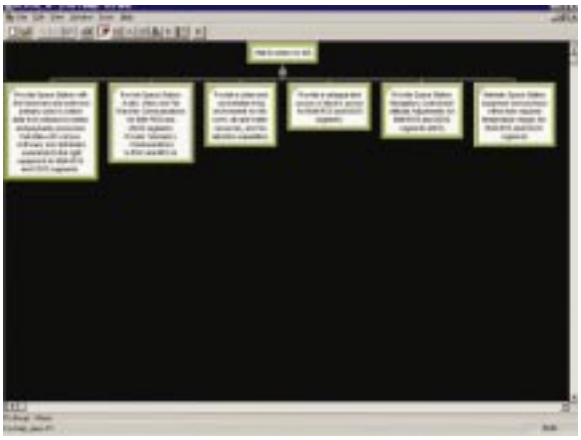

*FIGURE 1. Top-level functional tree.*

Figure 2 shows the relationships between mission demands and system functions.

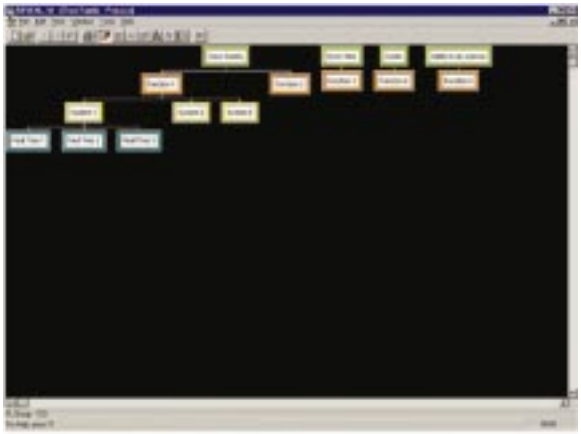

*FIGURE 2. Mission demands vs system functions.*

Figure 3 shows a sample section of a system functional diagram. The REVEAL modeling software was chosen for its ability to graphically display success paths within the functional diagram.

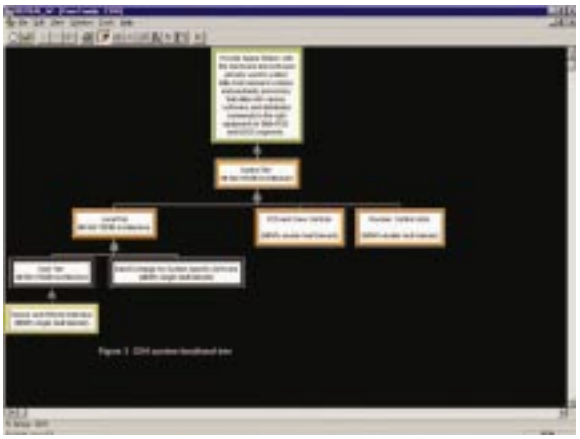

*FIGURE 3. Sample system functional REVEAL model.*

In a parallel effort, 3-D graphic models of the ISS systems were created for use in the graphical user interface with the risk monitor software. Starting with the full station (Fig. 4), graphic models are being produced that will enable users to visualize system-level impacts to functional requirements.

Face-to-face meetings with potential users of this software indicate a need to measure both safety and performance risk in a manner that is intuitive and can be summarized with indicators that display functional performance in a simple fashion. This requires the software to digest considerable performance detail, compare it to functional requirements, and grade performance.

Through this LDRD, contacts with NASA have been established at the national level with Michael Stamatolatos in Washington, D.C. and the Johnson Space Center in Houston. Future opportunities with NASA include monitoring situational risk for the ISS and the space shuttle.

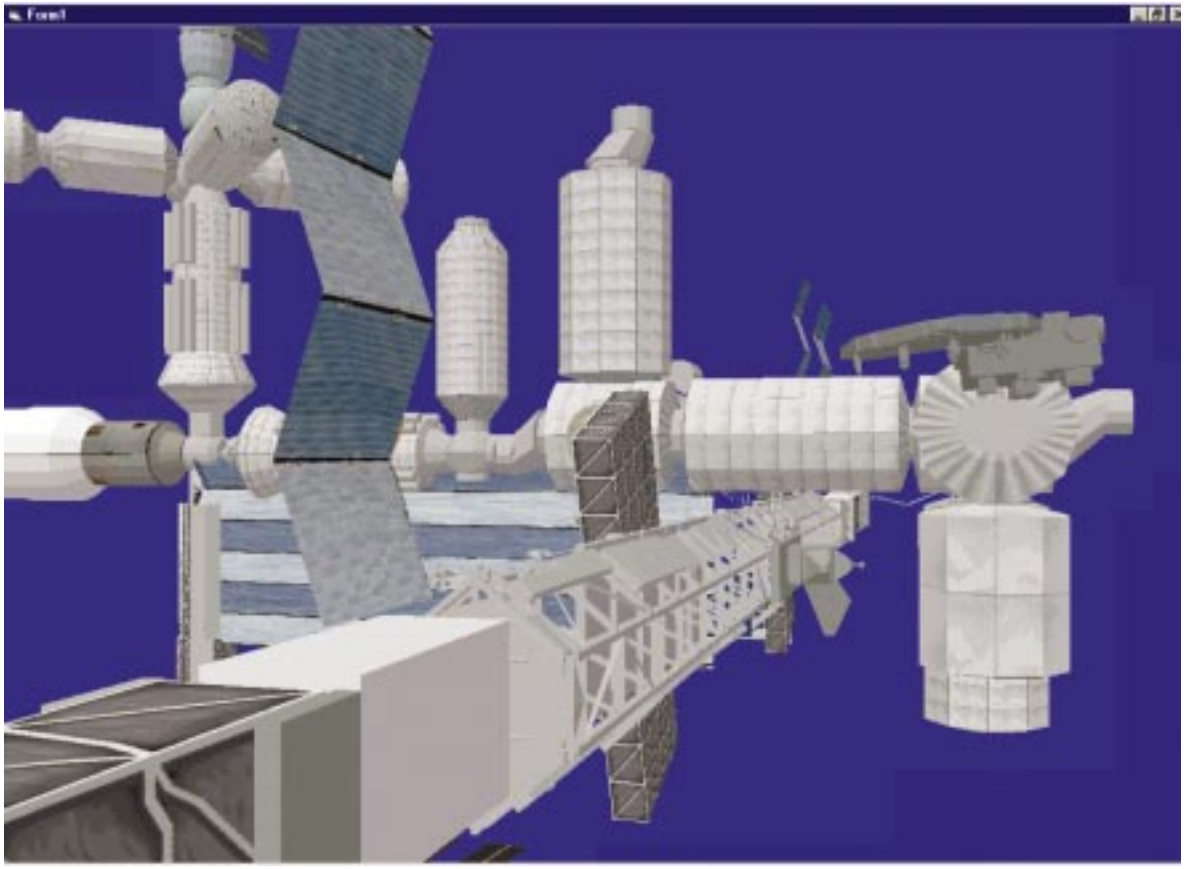

*FIGURE 4. Model of the International Space Station.*

# Improving Numerical Model Efficiency of a Simulation Model

*G. Michael Shook, Swen O. Magnuson*

## *TETRAD updated to meet INEEL research needs*

AC102

The numerical model TETRAD (Vinsome and Shook, 1993) is used in a variety of studies at the INEEL, including Environmental Restoration (ER), Geothermal Engineering, and Oil and Gas. Due to design considerations that were valid a decade ago but are no longer, TETRAD runs relatively slowly on "typical" ER model studies. This LDRD project is identifying ways of improving TETRAD to increase its efficiency as a tool for INEEL research. This effort involves identification of several code modifications that can increase TETRAD's efficiency, and identification of a suite of problems representative of ER model studies to test these modifications. The target speedup for the two-year project is to decrease the CPU runtime by at least 1 order of magnitude on test problems supplied by the ER Waste Area Group 7 (ER-WAG 7). First year efforts resulted in speedups of about 6-fold. The goal of 10-fold speedup is expected to be readily achieved in FY03.

Technical objectives for fiscal year 2002:

- Implement a component-specific, material balance convergence criterion to account for the vast differences in expected mass fractions of various components.
- Evaluate the possibility of implementing sequential implicit formulations for multicomponent simulation.
- Identify a set of test problems sufficiently complex to evaluate the relative speedup of proposed modifications. Test code changes.

As with any fluid flow model, TETRAD is based on the conservation of mass, energy and momentum. In order to describe the current limitations in TETRAD efficiency and solutions that can make it more robust, it is helpful to discuss conservation of mass.

The conservation of component i (for i=1, total number of components, or $N_c$) can be written as:

$$E_i = \frac{\partial}{\partial t}\left(\sum_{j=1}^{Np} \varphi\rho_j S_j \omega_{ij} + (1-\varphi)\rho_s\omega_{is}\right) + \vec{\nabla}\left(\sum_{j=1}^{Np} \rho_j \vec{u}\omega_{ij} - \vec{K}_{ij}\cdot\vec{\nabla}(\rho_j\omega_{ij})\right) + q_i - R_i = 0$$

The first term in Equation 1 above is the accumulation of component i, the second is the net flux (which includes advection and dispersion), $q_i$ is the source/sink of component i, and $R_i$ is formation/destruction of i from reaction or decay. The solution of these $N_c$ coupled equations is accomplished through a Newton-Raphson procedure as shown below.

$$\tilde{E}(t+\Delta t,x) = \tilde{E}(t,\tilde{x}) + \frac{\partial\tilde{E}}{\partial\tilde{x}}\cdot\delta\tilde{x} = \tilde{E}(t,\tilde{x}) + J(\tilde{x})\cdot\delta\tilde{x} = 0$$

For a variety of reasons, instead of solving Equation 2 to identically zero, the equations are solved to some predetermined convergence tolerance, $E_i < \varepsilon$. In the current version of TETRAD, $\varepsilon$ is a scalar. From material balance considerations, it must be substantially less than the smallest concentration being solved. However, there is no reason that mass balance convergence cannot be specie-dependant. Therefore, the first code modification investigated was to implement convergence criteria on a per-specie basis. This modified convergence criteria will be referred to below as $\varepsilon(i)$ for each of $i=1,N_c$ components.

Also investigated in FY02 was a means to implement a sequential implicit scheme for solving the mass balance equations. Noting that water and air alone dictate the pressure, saturation, and flow field (i.e., trace contaminants do not affect phase behavior), implicitly solving only these two mass balance equations was considered — determining the flow field and solving the balance of the equations explicitly. Implicit formulations have the advantage of being unconditionally stable. However, solving all conservation equations implicitly requires simultaneous solution of $N_c$ equations (the sequential implicit scheme requires two equations solved simulta-

neously and $N_c$-2 solved sequentially). Thus, while there are potential time step-size limitations, sequential implicit formulations were investigated.

During FY02, species-dependant convergence criteria were implemented in a test version of TETRAD. Code modifications included introducing a scale factor, SCALE(I), for each of the $N_c$ conservation equations. Mass balance convergence criteria for each component is the product of ε*SCALE(I). The revised model was then run on a variety of test problems provided by the ER-WAG 7 modeling group. As expected, the speedup of the revised code was strongly dependant on the relative value of the convergence criteria. An example 3-D simulation involved a 19x19x24 grid with a total simulation time of 54,000 days. Five species were simulated: water, two aqueous contaminants (e.g., radionuclides), air, and an organic liquid contaminant. A variety of tests examined the importance of the relative convergence criteria. In all cases, the benchmark results were run on the original version of TETRAD in which all convergence criteria were the same. The revised model used relaxed convergence for water and air. The contaminants' convergence criteria were the same as in the original version. An example of this comparison is given for $\varepsilon = 10^{-7}$ in Table 1.

Note that, while convergence criteria for water and air have increased, their relative accuracy (i.e., their mass balance accuracy) is the same as the other components (0.1%). Relative speedup of the revised code for a range of convergence tolerances is summarized in Figure 1. Even at relatively large convergence tolerance ($10^{-5}$), factors of 5+ increases in speed are observed. A stability

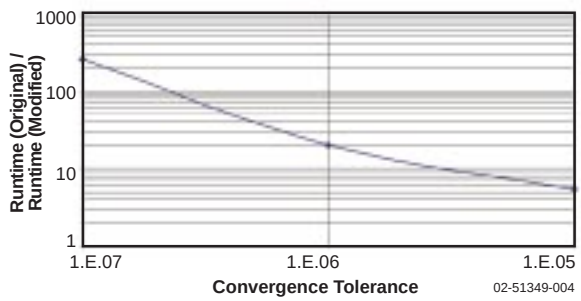


*FIGURE 1. Relative speed of revised code.*

analysis was conducted to evaluate the utility of sequential implicit schemes for these sample problems. The analysis indicated that relatively small increases in runtime could be expected primarily due to relatively large flow rates (Courant numbers exceeding 1). A limited numerical study was conducted. Results indicated that speedups of about 30% could be expected. This is well below this project's targeted reduction, so the sequential implicit schemes were abandoned.

The goal of the proposed work was to reduce runtimes of TETRAD by 1 order of magnitude in FY02-03. To date, speedups of approximately 6 orders of magnitude have been achieved. Further analysis of the problem indicates two distinct paths forward. Means of scaling the conservation equations will continue to be evaluated to reduce either the number of equations solved implicitly or the accuracy of the solutions. Modification of TETRAD also will be evaluated to develop a more specific program to meet INEEL needs. It is expected that no less than order-of-magnitude reductions in runtime will be accomplished.

| Component | Order of magnitude mol fraction | Original Version | Revised Version | | |
|---|---|---|---|---|---|
| | | $\varepsilon_2$ | $\varepsilon_2$ | SCALE (I) | $\varepsilon_2$(i) |
| Water | 0.1-1. | $10^{-7}$ | $10^{-2}$ | 1. | $10^{-2}$ |
| Air | 0.1-1. | $10^{-7}$ | $10^{-2}$ | 1. | $10^{-2}$ |
| Aq. Contam. #1 | $10^{-4}$ | $10^{-7}$ | $10^{-2}$ | $10^{-5}$ | $10^{-7}$ |
| Aq. Contam. #2 | $10^{-4}$ | $10^{-7}$ | $10^{-2}$ | $10^{-5}$ | $10^{-7}$ |
| NAPL or "oil" | $10^{-4}$ | $10^{-7}$ | $10^{-2}$ | $10^{-5}$ | $10^{-7}$ |

02-51349-003

*TABLE 1. Comparison in convergence criteria for original vs. modified TETRAD.*

# Advanced Waste Management Solutions Initiative

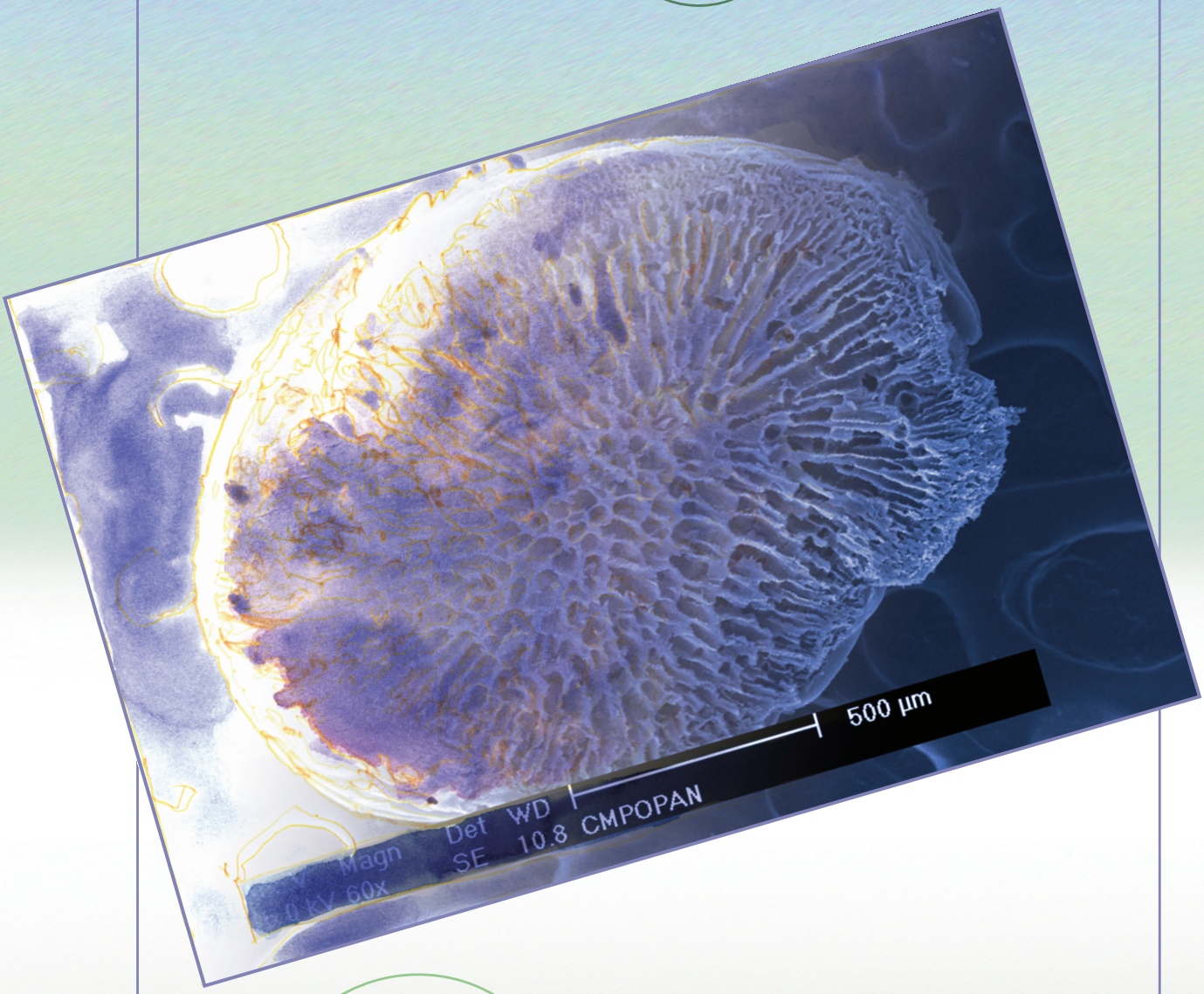


## LDRD Annual Report for FY-2002

Idaho National Engineering & Environmental Laboratory

# An Energy-Dispersive, X-Ray Fluorescence Excitation Source for In-Field Analysis

*John D. Baker, Robert J. Gehrke*

## *Faster, more sensitive assays of environmental media*

WT106

In-field elemental assay of environmental media and waste could be significantly enhanced with faster, more sensitive methods. $^{93m}$Nb has great potential as an in-field x-ray fluorescence excitation source (EDXRF) for this purpose. Based on the decay properties of this radionuclide, it is ideal for assay by x-ray fluorescence of the RCRA (Resource, Conservation and Recovery Act) elements arsenic, selenium, mercury, and lead at sub part per million concentrations with a 5 mCi source and a 15-minute count time – a feat that no other radioisotopic source has been able to claim. Another potential application is the analysis of erbium (Er), an element of interest for nuclear weapons applications. The strong merits of this excitation source are its long half-life (16.1 y), ideal energy of the niobium K x-rays (16.5 to 18.9 keV), its small size, and the purity of its spectrum (no other x, bremsstrahlung, $\gamma$, or beta radiation emitted from a prepared source). Production of high-purity, high-specific activity $^{93m}$Nb is from high burnup (>50%) fissile $^{239}$Pu with the $1.5 \times 10^6$ y $^{93}$Zr being separated from the mixed fission products that are normally disposed as waste. After a suitable grow-in period the $^{93m}$Nb can be repeatedly separated from the $^{93}$Zr parent indefinitely.

This LDRD is investigating the feasibility of producing pure $^{93m}$Nb for an acceptable cost, in high-specific activity, and in sufficiently high-activity levels to perform routine elemental analyses in a few minutes on samples containing sub ppm concentrations of the elements of interest. In FY01, the best method of production of 16.1-year $^{93m}$Nb was identified to be recovery of the fission product parent $^{93}$Zr from high burnup $^{239}$Pu obtained from assemblies irradiated years ago at the Savannah River National Laboratory at high flux and for high burnup of the $^{239}$Pu target. After suitable purification and grow-in period, the $^{93m}$Nb would be separated from its parent $^{93}$Zr. This would yield high-specific activity (carrier-free) $^{93m}$Nb material in millicurie quantities. This process could be repeated every six to twelve months indefinitely. In FY02, the effort has focused on identification of the effluent stream containing the zirconium, and developing a method to recover the $^{93}$Zr without impacting the primary process run for Los Alamos National Laboratory of recovering the $^{242}$Pu.

Technical objectives for fiscal year 2002:

- Agree on an Interagency contract with Chuck Alexander, an Oak Ridge National Laboratory (ORNL) employee and senior member of the Radiochemical Engineering Development Center (REDC), to modify the ORNL Mark 42 assembly chemical separations process for the recovery of fission product zirconium-93.
- Identify the effluent stream containing all or the bulk of the fission product zirconium.
- Run the modified process when a Mark 42 campaign is being conducted and analyze the recovered and collected product for zirconium-93 using ICP-mass spec.4.
- Further purify the collected $^{93}$Zr so that after suitable grow-in of the daughter, $^{93m}$Nb, high-specific activity, high chemical and radiochemical purity $^{93m}$Nb are obtained for the preparation of an x-ray fluorescence source.

Even though it has great potential as an in-field x-ray fluorescence excitation source, use of $^{93m}$Nb has not been reported in the literature due to the difficulty in producing pure $^{93m}$Nb for an acceptable cost, in high-specific activity, and in sufficiently high-activity levels to perform routine elemental analyses in a few minutes on samples containing sub ppm concentrations of the elements of interest. Of the many nuclear reactions that can be used to produce high purity, high-specificity $^{93m}$Nb in millicurie quantities, this research has found two reactions that can achieve these specifications: $^{93}$Nb(n, n') $^{93m}$Nb and Ac(n, f) $^{93}$Zr $\rightarrow$ $^{3m}$Nb, where Ac is a fissile actinide (production by charged particle reactions has been found to be impractical). The first reaction requires an irradiation facility in a high fast flux reactor such as the Advanced Test Reactor (ATR). The second reaction requires the fissile material to be irradiated for a long time at high neutron flux to achieve high burnup. Of these two methods of production, harvesting the $^{93}$Zr and $^{93m}$Nb from mixed fission products yields highest purity, near-carrier-free $^{93m}$Nb with the ability to replenish it indefinitely by periodically

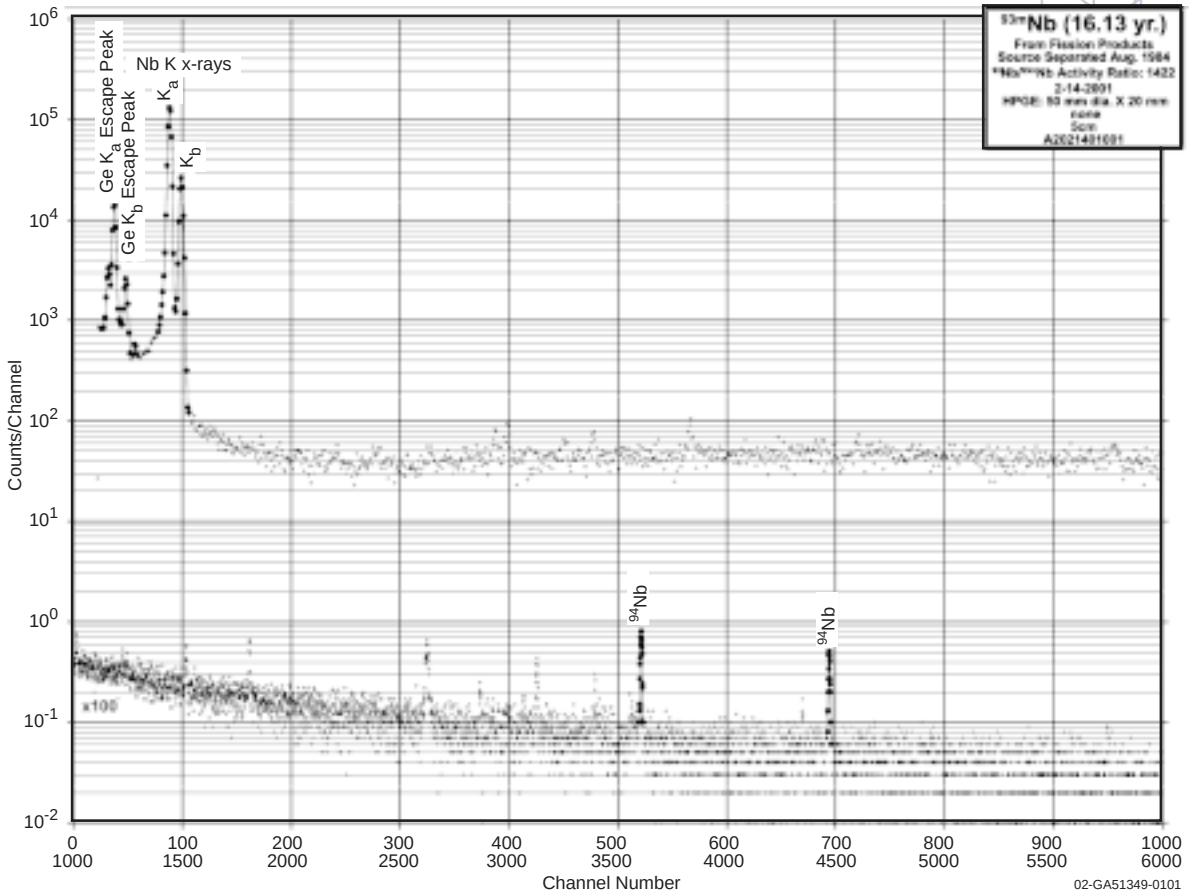


*FIGURE 1. Spectrum of $^{93m}$Nb as recovered from mixed fission products (not "milked" from the parent $^{93}$Zr).*

separating $^{93m}$Nb from the long half-life parent, $^{93}$Zr. Figure 1 is a spectrum of high-specific activity $^{93m}$Nb, produced from fission, with low levels of the contaminant $^{94}$Nb. By recovering the parent $^{93}$Zr and after suitable grow-in separating the daughter $^{93m}$Nb, a source free of any $^{94}$Nb can be achieved.

Mark 42 plutonium assemblies irradiated years ago in the Savannah River Production Reactors at high flux and for high (>50 %) burnup of the $^{239}$Pu target are being processed for Los Alamos National Laboratory at Oak Ridge National Laboratory (ORNL) for the $^{242}$Pu with the fission products being disposed as waste. Investigators in this LDRD have negotiated with ORNL to recover, as a side effort, the $^{93}$Zr fraction under an Interagency Contract for Services. Since 300 g of zirconium and 38.8 g $^{93}$Zr have been calculated by ORIGEN to be present in each plutonium assembly, there is more than sufficient $^{93}$Zr and $^{93m}$Nb to meet the needs for an in-field x-ray fluorescence source for environmental cleanup.

Because the use of hydrofluoric acid inside of their hot cell is strongly discouraged due to undesirable corrosion problems, developing a chemical separation process that

did not require hydrofluoric acid was one of the challenges confronting this year's effort. After several discussions with ORNL personnel it was determined that the most likely effluent stream to contain the majority of the zirconium fission product material is in the organic output from the Cleanex extraction process that follows the Purex separation step. The separation scheme that was developed consisted of contacting the organic phase with 1 M Oxalic acid. This solution would complex the Zr and remove it from the organic extractant. Further purification would be necessary, but this could likely be performed in a hood or glove box. To date, two modified separation schemes were conducted with the first unsuccessful due to insufficient flushing of the tank in which the Oxalic acid was mixed. $HNO_3$ apparently was left in the tank, making the Oxalic acid strip too acidic to effectively complex the Zr. The investigators are waiting for the analytical results from the second run of the modified and improved separation scheme. However, the radioactivity and mass of material in the Oxalic strip indicate that weighable amounts of some element were removed from the extractant.

While the recovery of the zirconium from the Mark 42 assemblies has proven to be more difficult than originally envisioned, this method of production is still expected to be successful. Preparation of the x-ray fluorescence source and demonstration of its capability will not difficult. These activities are expected to be completed next fiscal year.

The commercial value of $^{93m}$Nb as a radionuclide XRF excitation source was recognized before the best production mechanism was realized and a Patent Idea Record (B-160) was submitted. Success in the cost-effective production of millicurie quantities of high-purity, high-specific activity $^{93m}$Nb has immediate application for the production of radioisotopic excitation sources. The fact that $^{93m}$Nb can be periodically separated from its parent $^{93}$Zr allows for an ongoing supply at minimal cost (once the $^{93}$Zr is recovered and purified from the Mark 42 assemblies). This LDRD has resulted in collaboration with ORNL to develop the radiochemical procedures, simplifying the ability to make $^{93m}$Nb available to DOE on a first-priority basis.

# Enhanced Sample Based Modeling Techniques for Non Destructive Analysis and Long-Term Stewardship

*Gail A. Cordes, M. Elena Velasquez, Leo Van Ausdeln*

## *Using pattern recognition and analysis to improve process system operations*

WT108

This LDRD project is providing an important addition to a software suite that is available for INEEL customers and INEEL operations in nondestructive waste analysis (NDA) and long-term stewardship. The new software is based on pattern recognition and analysis, and promises to add safety, stability, consistency of product quality, and validation and verification of operations to process systems while reducing costs and schedules. It will benefit not only INEEL operations, but also DOE and other customer operations beyond INEEL. The software package is named the Advanced Data Validation and Verification System, Version 2, (ADVVS V2). It includes an INEEL shell and the year 2000 version of the computational kernel named Universal Process Modeling (UPM-2). During FY01 work on this LDRD project, the computational kernel was licensed from Triant Technologies Inc. of Nanaimo, B.C., Canada, and the kernel performance was successfully demonstrated in simple proof-of-concept tasks.

Technical objectives for fiscal year 2002:

- Monitoring and control — Apply the UPM-2 algorithms of ADVVS V2 to nondestructive analysis tools to monitor equipment health and provide automated multivariate feedback control.
- Measurement data analysis — Interpret gamma-ray spectrometry measurement data, using wavelet preprocessing of data and ADVVS V2 and other algorithms for pattern recognition and analysis.
- Understanding the past and predicting the future — Consider whether ADVVS V2 algorithms can be applied to data mining and predictive emergent computation for specific NDA waste and long-term stewardship and subsurface science problems.
- Designing an integrated system — Look ahead to long-term stewardship for EM and the needs for data quality verification, long-term data acquisition, and long-term monitoring of sensor systems through a conceptual design of an integrated system.

Much success was seen in FY02 due in great part to the collaborative approach and enthusiasm of the research team. The work was accelerated into the first half of the year to take advantage of this success by writing follow-on proposals and publishing papers. The relationship established in FY01with Triant Technologies, Inc. is ongoing, with the company continuing to provide technical support to the LDRD research under a Business Development Agreement. The principal investigator visited Triant Technologies to brief their new CEO on the pattern-based data processing approach of this project and the work that was accomplished in FY01 using the Universal Process Modeling kernel licensed to INEEL. Triant Technologies promised rapid turnaround when a third party licensee was identified for deployment of the INEEL shell and the UPM-2 kernel.

The project sponsored a three-hour tutorial on wavelet transform theory and techniques — added work scope at no extra cost. About 26 people attended at least one class and 19 completed the requisite two of three classes to receive recognition for this technical short course in the INEEL Train system. The instructor was Dr. Pete Harrington of Ohio University. The class targeted engineers and scientists with an engineering math background (Fourier transforms) and provided them enough information to use tools such as the MatLab wavelet toolkit.

Data were recorded from the Varitron accelerator operating at 6 MeV and 7 MeV energies, and ADVVS reference files were prepared to augment the data gathered earlier at 8 MeV. The reference files were used in experimental feedback control studies to demonstrate proof-of-concept for this use of ADVVS V2 at multiple energies. The test runs were successful. During all of the test runs, the monitoring capability of ADVVS V2 was demonstrated. The test results were documented in an external report. Two papers were presented on this objective.

Gamma-ray data were recorded for U-235, U-238, Am-241, Eu-152, Co-60 and Co-57, both singly and in combination. Wavelet-based signatures were prepared, and the capability of ADVVS-V2 to recognize the individual isotopes within the combination data sets was demonstrated. These isotopes were selected because they are of interest to SWEPP operations.

Wavelet-based signatures were prepared from gamma-ray spectral data available for 12 of over 100 SWEPP drums. The drums were previously subjected to destructive chemical analysis. Some progress was made in recognizing the presence of the six isotopes within the real waste management data. The study did not continue to include the total of 30 drums. A paper was presented, having been submitted for review and accepted last year. The team was not able to collect useful data from operating continuous air monitors. This prevented further progress on this subtask, and that milestone was not met.

Discussions were initiated with Savannah River on the topic of data mining using pattern recognition. Correspondence included a preliminary writeup of a one-page white paper.

A paper was presented in December 2001 that summarized the LDRD progress and discussed it in the context of an integrated system for waste management. Another paper was presented to the ANS June 2002 Annual Meeting in Hollywood, FL. The material expanded on the concept of using pattern recognition and analysis to provide stability and safety to any process system with attendant cost and schedule savings. A one-page white paper on the integrated system approach was written for outside distribution. A manuscript for a Nuclear Technology Journal article was recommended for publication by the reviewers and will appear in the January 2003 issue.

# Direct Dissolution of Plutonium and Neptunium Using Complexing Agents in Carbon Dioxide

*Robert V. Fox*

## *Extracting radionuclides from contaminated soils*

WT107

Radionuclide contamination of soil is a significant problem facing the DOE. The significance is due to the large amount of environmental media that is contaminated, the variety of radionuclide contaminants present, the wide ranging concentrations of contaminants found, the difficulty of removing strongly sorbed and chemically recalcitrant radionuclide forms from soil, and the potential threat of further spread of contamination. Few options are available for efficient, safe and publicly acceptable treatment of radionuclide-contaminated soils. In-situ treatment schemes rely on temporary sequestration and retardation of the spread of contaminants, but do not lead to permanent removal or isolation of the contaminant. There are a number of ex-situ techniques that rely on various physical and/or chemical means to permanently separate the contaminant from the soil. Ex-situ techniques suffer from high cost and safety concerns related to handling of contaminated soils, but primarily because of poor extraction efficiency. For the past decade there has been an increased emphasis on development of ex-situ treatment schemes that can overcome the technical limitations that lead to extraction inefficiencies.

In 1999 researchers at the INEEL performed a series of extraction experiments on plutonium-spiked INEEL soil samples using tributyl phosphate and beta-diketones dissolved in carbon dioxide. The extraction method demonstrated the ability to remove as much as 83% of the plutonium in the samples without any significant effort to optimize the technique. Americium was removed to below detection limits also without much attempt to optimize the extraction parameters. Although the findings are of great significance, of even greater significance is the fact that no loss of soil mass was detectable.

This LDRD seeks to build on the INEEL's preliminary results from 1999. In order to improve the extraction efficiency, there must first be a better understanding of the fundamental chemical reaction processes occurring in the given carbon dioxide solvent system. The current body of knowledge related to metal complexation reactions in carbon dioxide is shallow. Therefore, this LDRD will develop techniques to study and measure the chemical reaction/extraction phenomena.

Technical objectives for fiscal year 2002:

- Develop spectroscopic techniques for examining metal complexation chemical reactions in carbon dioxide solvent.
- Study well-known metal complexation chemical reactions in carbon dioxide solvent and acquire a basis data set using selected lanthanide metal salts.
- Determine how reaction components and solvent conditions uniquely influence metal complexation chemical reactions in carbon dioxide solvent. Compare those results to what is known in conventional solvent extraction literature.
- Study the matrix influence on extraction efficiency.
- Propose ways to overcome the matrix influence without destroying the matrix.
- Publish results in peer-reviewed journals, and present results at relevant national meetings to disseminate the findings.

Praseodymium nitrate, neodymium nitrate and holmium nitrate salts were chemically reacted with tributyl phosphate (TBP) and other selected neutral organophosphorus complexants in supercritical carbon dioxide. The products of the different chemical reactions were analyzed using UV-Vis and Raman spectroscopic techniques. The amount of complexed metal dissolving into the supercritical fluid phase was determined. The mole ratio method was used to calculate the stoichiometry of the soluble products. Equilibrium constants were calculated from spectral data and information obtained from the mole ratio plots. The praseodymium nitrate hexahydrate-tributyl phosphate and neodymium nitrate hexahydrate-tributyl phosphate systems both show a 1:4 lanthanide:TBP complex in supercritical carbon dioxide at 35°C. The heavier lanthanide, holmium nitrate pentahydrate, gave rise to a 1:2 Ho:TBP complex and a 1:4 Ho:TBP complex. The effects that pressure, temperature and the counter-anion species have on the chemical reaction were studied. Pressure was determined to have an effect only on solvent density and did not cause any detectable alterations to the complex stoichiometry as additional pressure was applied. Temperature was found to cause the organophosphorus complexes to fall apart and the combined complexation/solvation phenomena was found to be net exothermic.

The effects of increasing the basicity of the organophosphorus complexing agent was shown by reacting neodymium nitrate with TBP, tributyl phosphite ($TBPO_3$) and tributyl phosphine oxide (TBPO). Whereas the Nd:TBP system showed a 1:4 limiting stoichiometry, the Nd:$TBPO_3$ system showed a 1:9 stoichiometry, and the Nd:TBPO system formed a 1:5 Nd:TBPO complex. Neodymium triflate was chemically reacted with tributyl phosphate in supercritical fluid carbon dioxide at 35°C and formed a 1:4 complex. That reaction demonstrated that water did not necessarily need to be present and intrinsically attached to the metal center for the metal to be susceptible to chemical attack by tributyl phosphate in supercritical carbon dioxide. Neodymium carbonate hydrate and neodymium oxide were exposed to the different organophosphorus complexants in supercritical carbon dioxide at 35°C. Those two metal forms demonstrated no reactivity. Visual observation showed that neither the oxide nor the carbonate powders were physically changed in the presence of the augmented solvent. Synergistic chemical reactions using TBP and the beta-diketone complexants thenoyltrifluoroacetylacetone and hexafluoroacetylacetone were investigated for the praseodymium, neodymium and holmium nitrate salts. The products of the synergistic chemical reactions were analyzed using UV-Vis spectroscopic techniques and the mole ratio method was used to determine complex stoichiometry. Equilibrium constants were calculated for the different synergistic reactions.

The LDRD achieved a number of objectives this fiscal year. UV-Vis and Raman spectroscopic techniques have been developed for examination of lanthanide complexation reactions in carbon dioxide solvent. The mole ratio method has been used to determine the stoichiometry of various lanthanide complexes. Equilibrium constants have been calculated from the spectral data and the results have been compared to metal complexation reactions in conventional solvents. The effect of pressure on metal complexation reactions has been investigated. The effect of the counter anion on the metal complexation reaction and subsequent extraction process has been determined as well as the effect of temperature on the equilibrium constant. The effect of increasing the basicity of the complexing agent on complex stoichiometry and equilibrium constant also has been determined. The carbon dioxide solvent system has been compared to conventional solvent extraction systems and has been found to excel. Synergistic chemical reactions have been studied with use of TBP and the beta-diketone complexants thenoyltrifluoroacetylacetone (TTA) and hexafluoroacetylacetone (HFA). The role of water in the chemical reaction has not been fully elucidated and will be investigated in year three. Manuscripts have been prepared for peer-reviewed publications and presentations have been given at national societal meetings. A critical mass of experimental evidence has been acquired and three peer-reviewed manuscripts are being prepared but will not be finished in FY02. The primary goal for FY03 is twofold: a) conduct a minimum of laboratory tests to acquire data sets related to the role of water, and b) write and publish four papers.

The basic research resulting from this LDRD has grown INEEL expertise and capabilities in the area of understanding chemical reaction processes in supercritical fluids, positioning the INEEL as a leader in research in this area. The importance in the near future is in the direct involvement with Generation IV supercritical water chemistry. Since the INEEL has become affiliated with nuclear energy at DOE-HQ, the materials chemistry issues related to the Generation IV reactor will begin to play a predominant role in the direction of research. This LDRD can contribute to determining the effects of radiation on water and reactor materials in the supercritical fluid environment. The spectroscopic techniques developed in this LDRD will benefit those investigations significantly.

# Cold-Crucible Design Parameters for Next Generation High Level Waste Melters

Dirk Gombert, Grant Hawkes, John Richardson, John Morrison

## *Solving challenging melting concerns*

WT101

The cold-crucible induction melter (CCIM) design eliminates many materials and operating constraints inherent in joule-heated (JH) melter technology, which is currently the baseline technology for vitrification of DOE high-level waste. The internal surfaces of the new melter technology are water cooled, establishing a cold-skull of the melt material that isolates the crucible from corrosion while allowing melt temperatures much greater than the metallic surfaces could normally withstand. The cold-crucible design is smaller, less expensive, and generates much less waste for ultimate disposal. It also has the potential to increase the waste loading in glass and to decompose problematic salts such as sulfates. The CCIM design is applicable to solving challenging industrial melting concerns such as very high temperature, corrosive, or high purity materials.

The first year of this LDRD focused on evaluating the CCIM design. In FY02, this work was extended to modeling a cold-crucible induction melter system to give insight into system operation and provide information necessary for design. Electromagnetic, thermal, and fluid modeling of the CCIM supports two issues: engineering design of pilot or full-scale waste processing systems, and furthering understanding of how to configure and operate a CCIM to maintain product quality.

The modeling in FY02 was a successful collaboration with scientists at the Electrotechnical University (ETU) in St. Petersburg, Russia, and Montana Technical University (MTU) in Butte, MT. The activities focused on the development and validation of models representing energy deposition, temperature, and residence time for various melter configurations and waste formulations, and the model basis for the design of the power deposition and control system. At their current state of development, both the lumped parameter model and the finite element model generate useful results.

Technical objectives for fiscal year 2002:

- Complete and test the preliminary hybrid model.
- Compare benchmark tests using the analytical model against Russian results.
- Submit results to relevant journals for publication.

As part of this research into the feasibility of CCIM technology, both simplified bulk electrical properties and finite-element models for the concept are being developed that can eventually be used as a basis for design and control. The bulk electrical properties model represents the melt as a single-load conductance across the induction coil. The INEEL and MTU are developing this model jointly. The finite element model simulates the internal state and processes in the melt, including temperature profiles and inactive regions. This model is being reviewed and revised with the help of the ETU in St. Petersburg, Russia.

These models, when validated, will be used to investigate and optimize various configurations, parameter settings, melter productivity, etc. Ultimately, the two models should be developed sufficiently to estimate comparable results, thereby internally validating the theoretical bases for both models, estimating the same response from two completely independent modeling approaches. Beginning with a basic theoretical approach, gives the investigators a greater understanding of the technology for design and control, and for application of the technology to new areas such as specialty glasses. The combined modeling, design, and test capability will have no equal in the DOE complex, and probably all of North America.

Various modeling options were investigated to support condition monitoring and real-time control of a CCIM melter. The geometry of the melter is given in Figure 1. Current techniques are based on secondary or inferred measurements and do not work well when glass quality is a requirement. Two examples are 1) inferring melt core temperature by measuring surface temperature and guessing emissivity, and 2) inferring melt temperature by observing changes in output frequency of the power supply. The investigators concluded that an interactive one-dimensional model could be developed that would allow melter conditions to be reflected in the electrical characteristics of the primary inductor, allowing automated and accurate control of the melter by measuring and controlling these electrical characteristics. Such a model was developed and successfully operated in FY02.

The melter model consists of three coupled but independent models: electrical equivalent circuit, electromagnetic, and thermodynamic. The overall model incorporates dynamic changes of physical parameter

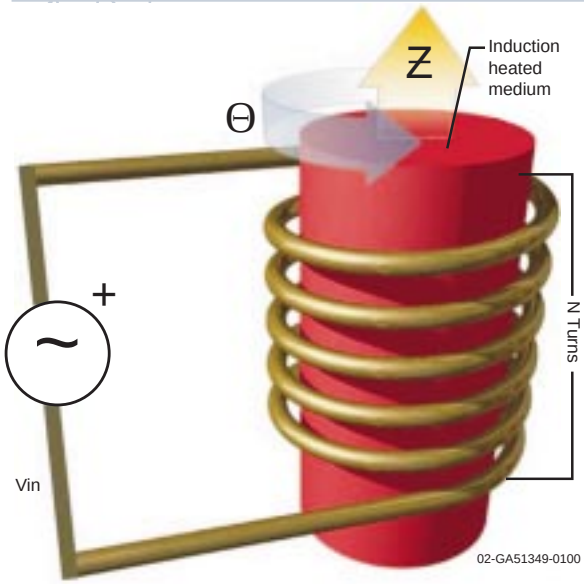


*FIGURE 1. Simplified melter geometry.*

values with temperature sensitivities. It reaches its solutions by iteratively calculating successive melter conditions. The CCIM model is implemented in a commercial software package, MATLAB, and can be made capable of near real-time operation to support a melter control system by conversion into an industry standard such as C or C++ language.

Further work needs to be done so that the model can be used as basis for a control algorithm. First, accurate physical parameter data on glass electrical and thermodynamic characteristics must be obtained. Representative data from other development efforts were used in FY02, but their accuracy for anticipated waste forms is questionable. Second, the electrical equivalent circuit used for the generator should incorporate a Thevenin model that accounts for changes in induction coil voltage with power. This is specific to the power system but can be determined using standard circuit analysis techniques. With these enhancements, the model can be used to develop control schemes and ultimately be implemented into a control algorithm as a high level language of choice.

The commercial finite element heat transfer code FIDAP was used to compute the electromagnetic field and heat transfer. This model calculates the magnetic vector potential that has a real and imaginary component. The purpose of this model is to deterministically assess the transient startup of a melt configuration. The coil is taken as a solid copper bar with the same cross sectional area as a six-turn copper tube coil. The material in the crucible is PSCM-20 glass and has been used in other melters. An initial hot region that is above the melting temperature of the glass is implemented to start the melt. The electrical conductivity is sufficient to produce heat and permit the melt to grow. This model does not include natural convection of the glass, as this will be added in the future. Figure 2 shows the real and imaginary components of the magnetic vector potential on the top row, followed by the temperature and heat generation field on the bottom row at a time of one hour. The molten region grows and melts more of the glass with time. FIDAP solved the magnetic equations as a set of highly coupled steady state equations and used this information as a heat source for the transient heat transfer model. A history of the power generated in the glass shows an initial drop-off in power while the melt region shrinks, followed by a rise in power as the melt region slowly grows.

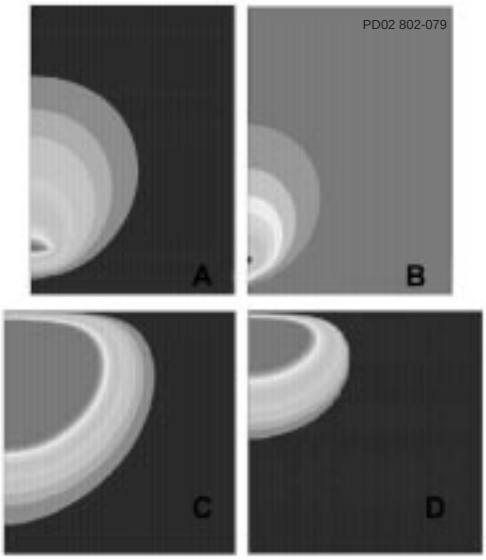


*FIGURE 2. Real (A) and imaginary (B) components of the magnetic vector potential, temperature (C) and heat generation (D) field at a time of one hour.*

Preliminary results indicate that the modeling effort agrees with earlier efforts by Russian colleagues, though additional discussions have been postponed. Unfortunately all communication with the Electrotechnical University has been done remotely. A trip was planned for the Russian scientists to visit the INEEL at the end of September, but was cancelled due to visa problems. This collaboration will continue in FY03, and the visit will be rescheduled if visas can be obtained.

The work performed in this LDRD has been an intensive collaboration between the INEEL, ETU, and MTU. The modeling approach is believed to be unique, and represents a capability to support cold-crucible design and control that may certainly result in intellectual property. The potential for the model application will be verified through a complimentary project funded by the Environmental Systems Research and Analysis Program at the INEEL to build and operate a pilot CCIM. The modeling capability from this LDRD effort provides the INEEL with greater insight into evaluating the technology for DOE applications, and significant credibility in dealing with industry. The models will help determine the limits of the technology without the expense of specific tests under all conditions.

# Steam Reforming in Micro Rectors for Destruction of Hazardous Organic Materials

*Dirk Gombert, Nick Soelberg, Mason K. Harrup, Stuart Janikowski*

## *Designing a versatile, mini-waste destruction system*

WT105

Incineration is a highly controversial yet standard process used to destroy volatile organic compounds commonly found in hazardous waste. New treatment methods are needed that can reduce the safety hazards, secondary waste, and cost of management and oversight associated with standard incineration methods. This LDRD evaluates a new waste treatment technology that uses heat, water, and catalysts to destroy volatile organic compounds, offering an attractive alternative to incineration. The project goal is to investigate steam reforming in a micro-reactor, using bi-metallic coupons coated with precious metal catalysts, to determine its effectiveness at destroying halocarbons and other organics. These reactors consist of catalytic sheet material closely packed in a laminar arrangement within a small conventional-style reactor casing. They facilitate higher reaction rates than their lower-temperature conventional analogs because of the obvious higher temperatures, increased reactivity on the surfaces inside the reactor, and inherently better mass transfer characteristics. The observed rate enhancement is therefore much greater than what would be expected from just downsizing conventional reactors to the micro-scale size. The small design also increases the reactor's suitability to remote operations, use in small-scale applications, and potentially as personal power supplies for military and civilian use.

Developing this technology increases the options for waste treatment problems faced within the DOE Complex, while providing a small package to accomplish waste destruction and reduce secondary waste generation. There are three focal areas to this research: development of coupon materials, application of the catalyst to the coupons, and performance testing of the catalyst/micro-reactor system at the INEEL.

Technical objectives for fiscal year 2002:

- Establish collaborative research and development arrangements with Oregon State University and the Albany Research Center to build a diverse research team. Establish roles and responsibilities.
- Modify the existing reactor and analysis system to better accommodate real-time and grab-sample analyses for off-gasses.
- Test and evaluate coupons having three different bi-metallic formulations impregnated with palladium catalyst.
- Determine destruction efficiency in the reactor/system for carbon tetrachloride, methylene chloride, and toluene at temperatures ranging between 200° C and 800° C.
- Present experimental data and results at the 2002 National Laboratory Catalysis Meeting.

The principal investigators for the INEEL project team met with the Oregon State University (OSU) collaborators early in the year to establish division of labor, extent of involvement of OSU students, and subcontract arrangements with the Albany Research Center (ARC) for providing coupons made from base materials previously identified as well-suited for high-temperature micro-reactor applications. A contract was placed and work toward the technical objectives began.

The bench-scale test system was designed and constructed. A micro-reactor was built with design criteria enabling its use at temperatures up to 800° C. The design holds up to seven coupons (2" x 2" x 1/4" thick) with variable inter-coupon spacing. The primary solvent used, carbon tetrachloride, represents the most difficult to treat halocarbon likely to be encountered in wastes. This solvent dominates the chlorinated organic constituents in TRU wastes at the INEEL, Rocky Flats, and Los Alamos. Halogenated and aromatic compounds are typically difficult to treat in oxidative processes. The three solvents chosen for testing are vastly different and the results should be transferable to a wide range of compounds.

The solvents were introduced with steam into the reactor at 10 mole %. This resulted in a very high percentage of chlorine, in the case of $CCl_4$ and $CH_2Cl_2$, or carbon in the case of $C_6H_6CH_3$, that would have swamped other treatment processes and resulted in very low yields. Yet the micro-reactor system performed extremely well.

Inter-metallic materials were chosen for coupon construction because they offer three main advantages over other materials. First, they offer superior corrosion

resistance in an environment that is certain to be harsh due to the formation of hydrohalic acids and the high temperatures. Second, they are durable through a very high temperature range. Third, they provide a unique type of surface that can attach the catalysts firmly under both harsh chemical and physical conditions. Three bi-metallic combinations were chosen for the coupons. Their compositions were: Ni/Al, Ti/Al, and Fe/Al in roughly equal volume ratios. The coupons were impregnated with Pd.

Reactions began at temperatures below 200° C with the formation of carbon monoxide, which is consistent with known mechanisms associated with steam reforming. The rate and conversion increased with temperature, estimated to be greater than 99.99% destruction efficiency between 500° C and 750° C. Products from the reactions with halocarbons included methane, hydrochloric acid, carbon dioxide, carbon monoxide, and hydrogen. Reaction products resulting from the destruction of toluene were similar except that no halogens were present to form the associated hydrohalic acids.

New knowledge was gained through this work that can benefit the DOE, and the INEEL in particular. Specifically, the concept of incorporating catalysts in a micro-reactor for the purpose of destroying hazardous compounds under steam reforming conditions was firmly established. Further, it was demonstrated that the appropriate choice of coupons and construction materials could affect prolonged operation under extremely severe corrosive and temperature conditions. The rate and extent of reaction are both higher for the given through-put and high concentration of halocarbon than for other competing technologies. Coupled with the small size of the reactor, these other features combine to make an extremely versatile waste destruction system. The new system has application for treating off-gasses from stored wastes and rendering them acceptable for permanent disposal without further treatment, and it can be used to treat off-gasses from underground storage tanks that will help make them ready for removal from service while leaving them in the ground. The technology also can be used for treating wellhead off-gasses in remote areas because the small size translates into low energy requirements that could easily be met by portable power units or solar panels. Beyond the technical accomplishments, the experience and expertise gained through this LDRD will benefit numerous other projects at the INEEL.

This LDRD has established collaborations between the INEEL, Oregon State University, and the Albany Research Center. ARC develops the bi-metallic materials suitable for this application and supplies the coupons to OSU. OSU in turn modifies the coupons by coating them with catalyst in a unique process that imbeds the catalytic material into the coupons, imparting high durability and making them potentially long-lived. The INEEL receives the coupons from OSU and provides the performance testing and feedback to OSU and ARC, creating a synergy among the three organizations that capitalizes on each of their strengths.

Results demonstrating the benefits of this technology in FY02 were significantly positive to warrant continuation and growth in two directions. One part of the proposed development will remain in-house, using the INEEL's existing partners to move the project closer to implementation for the treatment of drummed wastes. The second part will be directed at developing small-scale energy sources for portable and remote applications suitable for DOE and DOD applications. Intellectual property involving various aspects of 1) the reactor design, and 2) chemical processes for waste destruction, chemical synthesis, and energy production will be jointly developed and shared with project partners.

# Model-Based Decision Making

*Jerry L. Harbour*

## *Turning decision models into valuable decision-support tools*

WT104

There is a need to better understand how decision models can be effectively translated into decision tools. This LDRD is addressing this question, with particular attention to those tools that are being used by field operations-type personnel. The insight gained from this investigation will then be used to develop a prototype, computer-based decision tool that can readily support users in operational planning, analysis and execution in computer-assisted environments. The prototype system would offer time and probability modeling in a graphical, intuitive, easy-to-use, and field-deployable environment. Specifically, it would assist decision makers in modeling and assessing emergency response capabilities, physical security vulnerabilities and counter-response capabilities, and time-critical hazardous operations.

Technical objectives for fiscal year 2002:

- Conduct comprehensive survey of existing decision tools.
- Use gained insights to design and develop a computer-based prototype decision tool.
- Demonstrate potential application of prototype.
- Present findings at conferences.

A comprehensive survey of existing decisional tools, regardless of type or application domain, was completed. Particular attention was given to those tools that are clearly being used by field operations personnel. Shared characteristics of such tools include:

- A well-structured and understandable underly ing model base that readily lends itself to tool development.
- A simple and easy-to-use, yet powerful and transparent, tool base.
- A limited application domain base.
- An easily accessible "look up" knowledge base.
- A means for problem exploration and understanding.

It appears that users make decisions by gaining insight from the use of the tool. That is, the tool does not make the decision (as in artificial intelligence or expert-based type systems), but rather the users make decisions based on their interaction with the tool. Additionally, highly ranked tools appear to have both high usability (e.g., user friendliness) and high usefulness (e.g., domain application).

Based on gained insights from the comprehensive survey, a prototype computer-based decision tool (version 1.0) was developed, named *RapidOps*. *RapidOps* is a time- and probability-modeling tool especially well suited for time-critical, hazardous operations. The prototype system links time and probability modeling in a graphical, intuitive, easy-to-use, and field-deployable computer-assisted work environment (Fig. 1 next page). Specifically, *RapidOps* can assist decision makers in modeling and assessing emergency response capabilities, physical security vulnerabilities and counter- response capabilities, and time-critical hazardous operations.

The ability to use *RapidOps* to assess physical security vulnerabilities and counter-response capabilities is of special note. For such applications, *RapidOps* uses event pathways, probabilities, and activity times to generate various scenarios and assess system vulnerabilities. An event pathway represents a succession of activities (and associated steps) executed upon a set of objects under varying conditions through space and time. There are two basic types of event pathways: "threat" and "response." A threat pathway's primary objective is to cause harm (i.e., an attack sequence). Conversely, a response pathway's primary objective is to prevent, contain or limit the degree of harm. Creating event pathways under differing conditions permits the analysis of various generated scenarios by:

- Identifying and sequencing required attack or response activities and all associated activity steps.
- Calculating required elapsed times (e.g., total response times).
- Modeling the probability of a successful response by a defensive or countering force.
- Modeling physical security vulnerabilities and counter-response capabilities.

A cumulative-risk index of generated scenarios can then be created, graphically depicting response probability, consequence of loss, and identified threat level. The goal of *RapidOps* is to combine real or conceptual physical models with various performance metric models to make better design and planning decisions.

The work completed under this LDRD has generated considerable interest by various government agencies, including the DOE, Army Corps of Engineers, and the Nuclear Regulatory Agency. The Army Corps of Engineers will likely become a beta test site in FY03 with the potential of an application-specific *RapidOps* being developed as a follow-on activity. After successful beta testing in FY03, the possibility of developing customized versions of *RapidOps* exists. For example, a customized version of *RapidOps* can be developed to assist in dam vulnerability assessments, an interest of the Army Corps of Engineers. Potential applications outside of the security realm, such as emergency response support or time-critical operational planning, assessment, and execution support, have yet to be explored.

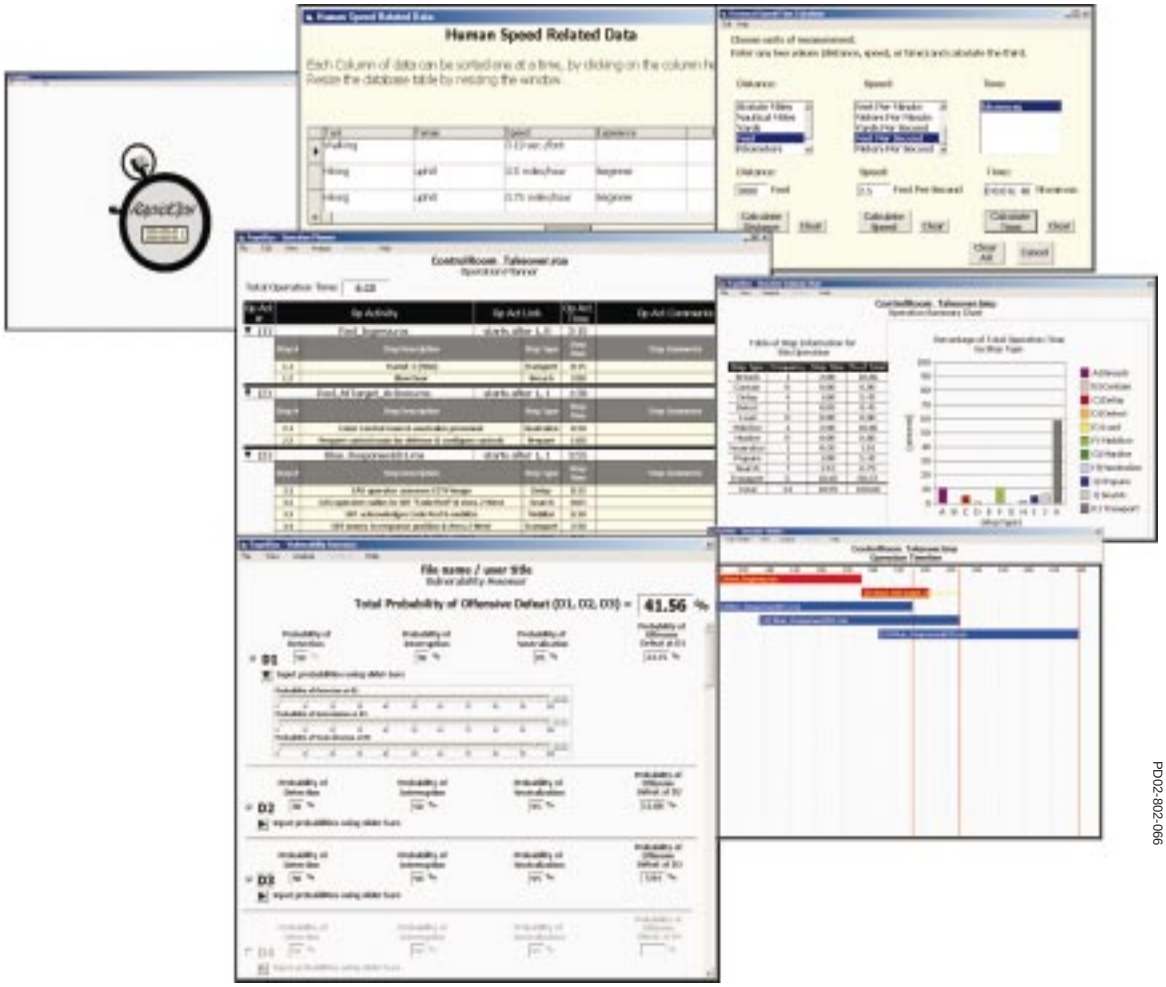


*FIGURE 1. Screen shots depicting some of the capabilities of RapidOps.*

# Advanced Formulation for Homogenization of Refractory Components in Glass and Ceramic Phases

*Swami V. Raman*

## *Developing unique glass molecular structures for durable waste containment*

WT110

Understanding interactions among components as a function of processing variables is fundamental to developing a viable process and material for treatment and containment of nuclear wastes. High-level and mixed nuclear wastes, such as the calcined granules and sodium-bearing waste found in Idaho, are composed of components that have varying solubility in borosilicate liquids. Waste immobilization technologies currently practiced at DOE sites do not directly apply to these wastes, which differ significantly in physico-chemical characteristics.

The primary aim of this LDRD is to evolve scientific basis for management and mitigation of the chemical component solubility problems encountered in waste processing and dispositioning. Two basic science approaches along the principles of phase equilibria and molecular vibrations were adopted in this research to elucidate the impact of component interactions on waste processing, waste loading, and waste form composition and durability. The results are shown as phase diagram and vibrational spectra. The plot of the calcine composition on the phase diagram outlines with certainty the chemical tuning that would be needed to transform the calcine into a compatible waste form, eliminating the speculative addition of components often practiced in empirical approaches. The vibrational spectra in turn, presents the molecular basis for component interactions and predicts the durability of the waste form on the basis of chemical bonding and atomic oscillations.

Technical objectives for fiscal year 2002:

- Develop formulation diagram to minimize physico-chemical uncertainties in nuclear waste processing and dispositioning.
- Apply molecular vibrational (Raman) spectroscopy to develop scientific basis for rapid and remote characterization methods.
- Evolve fundamental understanding among material structure, molecular and lattice vibrations, and properties to improve nuclear waste processing and dispositioning.
- Contribute to cutting-edge science and technology by presenting results in leading international journals and professional meetings.

The strength of the fundamental science approach is here demonstrated using the chemical components of the calcined wastes and sodium-bearing wastes of Idaho as model examples. The components dominating the waste streams were selected as candidates. These components are $ZrO_2$, $CaF_2$, $Na_2O$ and CaO. As several experimental results have demonstrated, empirical mixing among these components and additives has led to many uncertain results that in turn leave a large expanse of intensive and extensive variables for treatment and containment in suitable materials. To circumvent this problem, the experimental effort in this LDRD has emphasized building relations among phase equilibria, waste component loading, material structure, and durability. The high temperature phase equilibrium experiments on a crucible scale are conducted to extract information on component interactions, material composition, and waste loading. This experimental step is a necessary one for it provides much-needed data for chemically tuning the actual wastes, irrespective of the melting method adopted.

The INEEL institutional plan currently emphasizes cold crucible melting, the products of which are expected to be crystalline, non-crystalline, or their combinations, as in any other melting technology. Phase equilibrium studies form the fundamental basis for predicting the formation of such products as a function of waste stream and containment material composition and processing parameters. Clearly the project is a large one and so it must be addressed in definite steps by constraining the experimental conditions. The constraints here are 1) a constant processing temperature of 1200$^{o}$C in ambient atmosphere, 2) a constant calcium oxide content of 3 wt%, and 3) a constant composition for the base boroalumniosilicate glass in molar ratio: $26.5B_2O_3$:$4.5Al_2O_3$:$69SiO_2$. The results of this system are shown as projection onto the ternary surface $Na_2O$-$ZrO_2$-$CaF_2$ from boroaluminosilicate apex in Figure 1 (next page). The diagram shows the various phase relations, phase boundaries, and stability fields of glass, ceramic, and glass-ceramic waste forms. A calcine composition is shown to plot in the sintered ceramic regime, predicting its containment in a liquid phase sintered ceramic of composition zircon+fluorite+quartz.

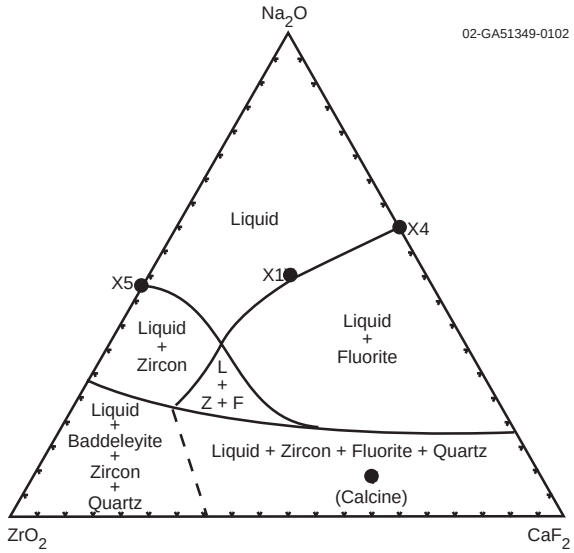


*FIGURE 1. Isothermal Projection at 1200° C and at 3 wt% CaO. The diagram shows composition of calcined waste relative to the stability fields of various phases.*

It is possible to tune the chemistry of the calcine on this diagram using lever rule to position its composition in a predictable field for forming glass or crystalline waste forms. The diagram is also useful for predicting the waste loading. It is a formulation diagram that is based on the principle of phase equilibria, and eliminates several uncertainties associated with additive component selection, component solubility, waste loading, waste composition, etc., that are commonly noted in the empirical approaches. The diagram is also of importance in ceramics for it covers the relations between two important ceramic materials, zircon and fluorite, and has the potential of becoming useful in the ceramic industry with testing of appropriate properties.

The next stage of this LDRD project involved exploring the component interactions at the molecular level. This is a detailed approach envisioned for improving the process and properties. The method involves relating molecular vibrations to material composition and properties as a function of processing. Because of the occurrence of both crystalline and non-crystalline phases, conventional Raman spectroscopy was selected to conduct systematic spectroscopic examination of materials. This part of the project commenced in collaboration with the Raman Spectroscopy Laboratory under the direction of Professor R.S. Czernuszewicz. Vibrational spectroscopy was selected because it is emerging as a routine characterization method. With advancement in instrumentation and data reduction technology, it has the potential of becoming a state of the art characterization method for rapid quantitative and qualitative analysis of diverse materials without involving intensive sample preparation. At present its application faces barriers stemming from the depth of scientific knowledge demanded in the interpretation of results. The method is even more challenging because of the complex composition of the nuclear waste. However, an important corollary of this effort is the contribution to both

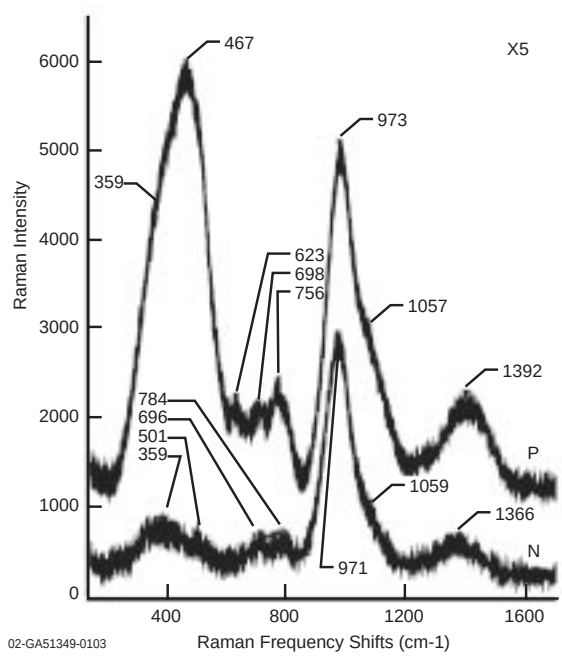


*FIGURE 2. Structure of quenched liquid/glass of composition X5 in Figure 1, showing covalent anisotropy in the normal scattering mode (N). This structure has higher durability than other glasses.*

fundamental and applied research, as the methodology commences from probing the nature of the chemical bond and atomic arrangement. In this direction, Figure 2 reveals the relative contributions of covalent and ionic bonding on molecular anisotropy. In conjunction with durability tests, the structure in Figure 2 imparts higher durability to glass. Yet another important finding has been the development of a unique glass structure that indicates intermediate atomic order and thus a higher durability.

Two important contributions to the scientific literature have emerged from this LDRD, as summarized in Figures 1 and 2. These contributions place the method of processing and immobilization of nuclear waste on a firmer scientific basis, and mitigate the generation of undesirable results such as melter freezing that may become very expensive to remedy. The unique scientific results of this research have resulted in a proposal for the DOE Office of Science, emphasizing the significance of molecular vibrations in developing nuclear waste compatible materials.

# Polyacrylonitrile-Based Ion Exchange Sorbents

*Terry A. Todd, Nick R. Mann, Troy J. Tranter, Ferdinand Sebesta*

## *Concentrating contaminants in the field*

WT103

Environmental contaminants in water exist in such small amounts that current methods to sample and analyze them require large samples (up to a few hundred gallons). These large samples must be transported to a laboratory, concentrated by evaporation or liquid/liquid extraction, and then analyzed.

The use of ion exchange sorbents for the treatment of waste and/or contaminated water is widespread. Polyacrylonitrile (PAN) in particular, is very effective at immobilizing ion exchange materials into useful forms such as spherical beads, because it is highly porous and can accommodate very high loadings of ion exchange material (5-95 wt %) into the PAN matrix. The process of incorporating the ion exchange material in the PAN matrix is entirely aqueous-based, greatly minimizing waste volume and treatment relative to processes that require organic-based solvents.

This LDRD explores using polyacrylonitrile-based sorbents/solid phase extractants to concentrate contaminants from water in the field and remove contaminants from various analytical or waste streams. The solutions are pumped through a small filter disk or beads, which are then transported to the laboratory. The filter disks and beads may be directly analyzed for contaminants by liquid scintillation spectrometry or proportional counting. The ability for direct analysis would eliminate the multiple, time-consuming, costly preparation procedures that are the current state of the art, reducing analysis time, tranportation costs, and waste volume generated in the concentration and sample analysis tasks. These attributes could be especially benefical to international efforts to quantify and track contamination levels resulting from past activities in Russia and countries of the former Soviet Union as well as national security programs tasked with assessing the emerging nuclear capability of countries hostile to the U.S.

Technical objectives for fiscal year 2002:

- Characterize octyl (phenyl)-N,N diisobutylcarbamoylmethylphosphine oxide (CMPO)-PAN and AMP-PAN materials using scanning electron microscope.
- Demonstrate reproducibility of several batches of CMPO-PAN and CMPO-PAN filter media.
- Obtain nitric acid and hydrochloric acid dependency curves for Am, Pu and Eu on CMPO-PAN.
- Evaluate Fe, U and Pu removal from simulated radioactive wastes using CMPO-PAN.
- Develop and test Aliquat-336-PAN (beads and filter media) for selective separation of Pu over Am and lanthanides.

Physical characterization of ammonium molybdophosphate (AMP)-PAN and CMPO-PAN were completed using a scanning electron microscope (SEM) and BET surface area analysis. Both materials are macroporous, exhibiting surface areas of approximately 10 $m^2$/gram. Scanning electron microscope micrographs of CMPO-PAN beads are shown in Figures 1 and 2. General observations about the beads are that they are spherical in shape and have no apparent "deposits" of CMPO, but rather it appears the CMPO is dispersed in the PAN matrix. In contrast, AMP-PAN micrographs clearly show deposits of AMP particles trapped within the pores of the PAN matrix.

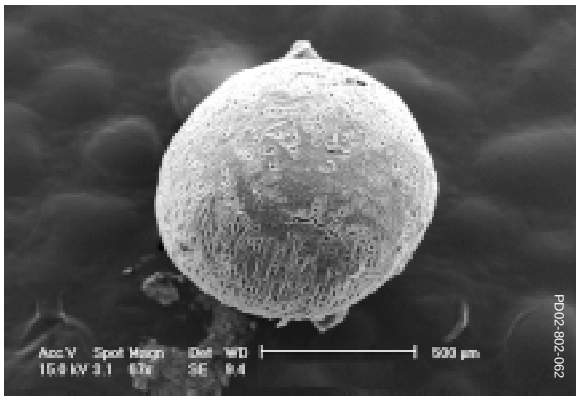


*FIGURE 1. SEM micrograph of CMPO-PAN bead.*

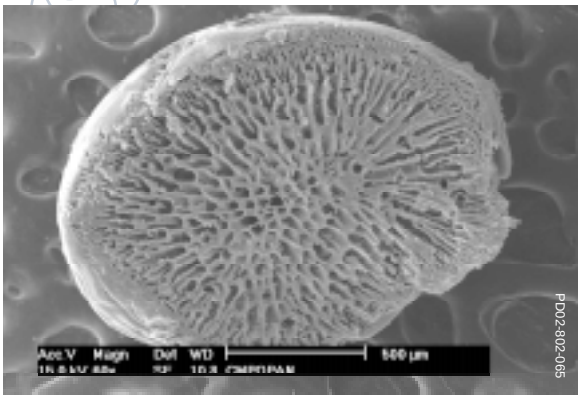


*FIGURE 2. Cross-section of CMPO-PAN bead.*

Uranium uptake by CMPO-PAN is of prime importance. An isotherm was generated to measure uranium uptake from 2.5 M nitric acid using CMPO-PAN. The isotherm data indicate CMPO-PAN has a maximum capacity for U of 120 mg U/g CMPO.

In analytical applications, the presence of non-radioactive matrix metals such as iron can interfere with the removal of the actinide species. This results in effectively loading the CMPO-PAN with the matrix metal, which substantially lowers the overall capacity of the CMPO-PAN. A similar isotherm was generated for Fe (III) from 2.5 M nitric acid. CMPO-PAN has a high affinity for uranium and iron as well as plutonium and americium. The high wt% loading of CMPO in CMPO-PAN gives it a much higher capacity that makes it less sensitive to the presence of matrix metals. However, the presence of matrix metals cannot be ignored when using CMPO-PAN.

In addition to CMPO-PAN, another very successful extraction chromatography resin was based on the extractant Aliquat-336. Samples of Aliquat-336-PAN (or A336-PAN) were prepared and tested to determine the efficacy of removing Pu, Am and Tc. The A336 extractant is selective to tetravalent ions over trivalent ions; therefore, it should extract Pu and not Am. It is also known to extract Tc as the pertechnatate anion. Results of batch contact tests with A336-PAN and nitric acid solutions spiked with Pu-239 or Am-241 are shown in Table 1. The Table shows that A336-PAN readily removes Pu over a broad range of nitric acid concentrations, but does not remove Am. Technetium batch contact results as a function of pH also were measured. Technetium was quantitatively removed from solutions with pH above 3 and distribution coefficients dropped as the pH was lowered below 3.

| Radioisotope | Nitric acid concentration (M) | Distribution Coeff. mL/g |
|---|---|---|
| AM-241 | 0.01 | 0 |
| AM-241 | 1.0 | 0 |
| Pu-239 | 0.1 | 3250 |
| Pu-239 | 1.0 | 5560 |

02-GA51349-103A.ai

*TABLE 1. A336-PAN batch contact results for Am and Pu.*

The results shown are based on dispersed particles or beads of PAN-based sorbents/solid phase extractants. Another useful form developed for these materials is impregnated filter media. Gelman glass fiber filters (49 mm) were impregnated with dissolved PAN containing a suspension of either CMPO or A336. The PAN suspension was imbedded in the glass filter matrix, providing a porous filter media with the capability to remove ions dissolved in solutions. Scanning electron micrographs of Gelman filters, before and after impregnating with CMPO-PAN, are shown in Figures 3 and 4 (next page).

By concentrating the contaminants on the small filter surface, the impregnated filter disk enables larger volumes of samples to be analyzed without transporting the entire sample to the lab. The filter disk can be analyzed directly by gas proportional counting or gamma spectroscopy, reducing or eliminating the secondary wastes generated during conventional sample analysis.

Several batches of CMPO-PAN and CMPO-PAN filter disks were prepared and tested to determine the reproducibility of the preparation methods. In all cases, the reproducibility was within the uncertainty of the measurements and analysis used to analyze for the radionuclides (typically 5-10%).

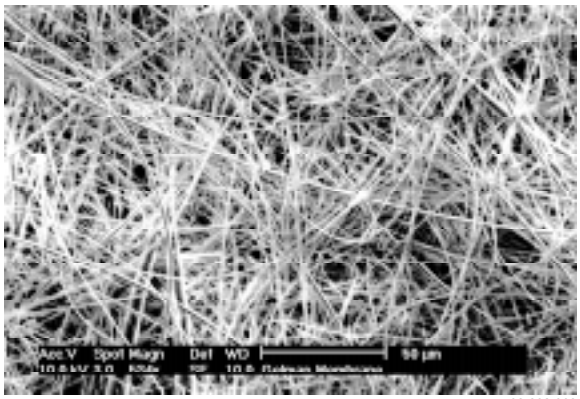


PD02-802-063

*FIGURE 3. Gelman glass fiber filter.*

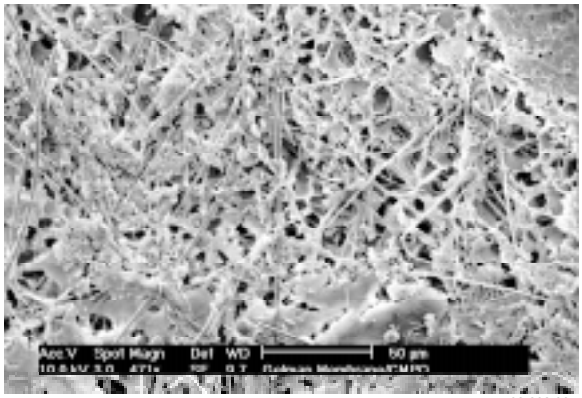


PD02-802-064

*FIGURE 4. Gelman filter impregnated with CMPO-PAN.*

With increasing awareness and concern over the quality of groundwater, surface water and drinking water, the need to rapidly and cost effectively sample and analyze water for contaminants is critical. As a result of this LDRD, new solid-phase extractants based on organic chelating agents were developed and prepared that offer significantly increased capacity over existing extraction chromatography resins. These sorbents offer the potential to treat secondary radioactive waste streams and render them non-TRU, or to analyze environmental samples and directly concentrate and analyze the sample based on PAN- impregnated filter media. The results of this LDRD research can greatly reduce sample transportation costs, concentration time and cost, and secondary waste generated in the sample analysis effort.

# Critical Infrastructure Protection Initiative

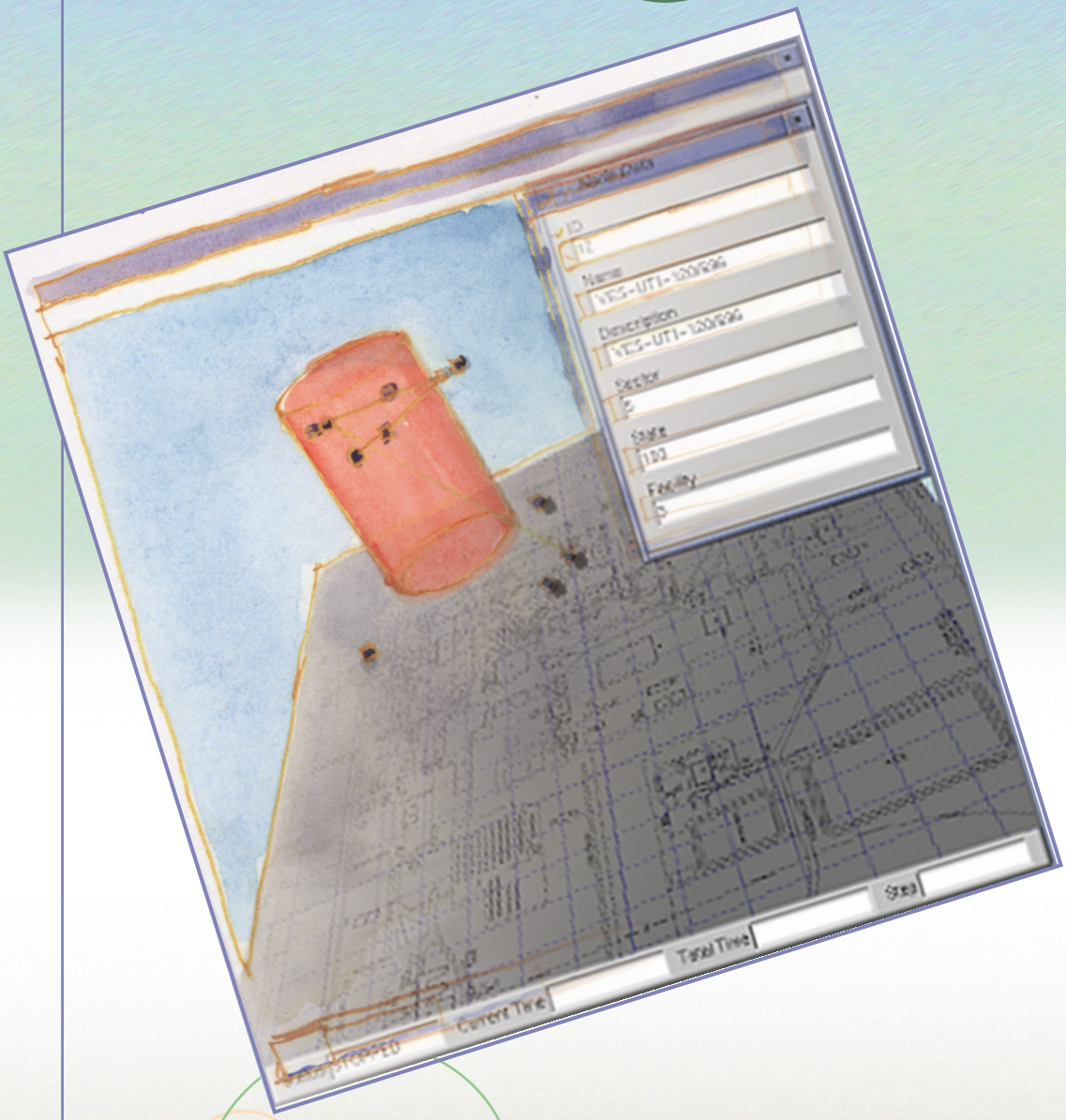


## LDRD Annual Report for FY-2002

Idaho National Engineering & Environmental Laboratory

# Use of Thermally Sprayed Traces for Damage Detection and Data Transmission

*Robert A. Carrington, Karen Moore, John Richardson*

## *Protecting pipeline infrastructure with spray-on sensors*

CS115

The ability to monitor pipeline operation in near real time is one of the major research objectives of the pipeline industry and is vital to pipeline infrastructure reliability and security. This LDRD research continues work initiated in fiscal year 2001 using a secure "smart pipe" configuration to monitor pipelines. In this research approach, the sensors and data communication pathways are inherent in the pipe using thermally sprayed sensors and data communication traces applied directly to the pipe wall. The electrical properties of thermally sprayed metals electrically behave differently than solid metal wire when subjected to physical conditions such as strain or temperature. This phenomenon, which is observed in very thinly applied traces, can be used to build a sensor and data communications network distributed along the length of the pipeline.

Technical objectives for fiscal year 2002:

- Characterize the electrical effects of temperature changes applied to certain thermally sprayed resistive and conductive traces.
- Integrate pwith the trace system.

The research in FY02 focused on using thermally sprayed temperature sensors and investigating the potential to embed other types of microsensors in the sprayed trace. Temperature measurement was chosen as the parameter to demonstrate the ability to thermally spray-form a usable sensor. Temperature measurement in the pipeline immediately downstream of the compressor stations is used to monitor operation of compressors and can be used along the pipeline to detect conditions in which hydrate formation or condensates can occur. For this application a temperature range from 0º C to 100º C was assumed.

To test the hypothesis that there is a functional time-invariant relationship between bulk resistivity and temperature for sprayed metallic traces, 80 traces were tested representing five sets of the sixteen various combinations of materials and manufacturing variables. The materials used were a nickel aluminum and copper.

The machine parameters affect several variables that in turn effect trace resistivity and potential performance as a temperature sensor. These attributes include content of phases, physical distribution of phases, stress distribution between phases, and relative volume of phases. Attributes were determined by the five machine parameters used to prepare the test coupons. These parameters were:

- Traverse speed of the gun.
- Distance of nozzle to the substrate.
- Surface temperature of the substrate.
- Oxide content due to gasses being used.
- Energy at the nozzle from flow rates and temperatures.

The desired result from the experiment was to be able to determine data trace fabrication specifications for both conductive traces and resistive traces. The conductive traces would be insensitive to temperature change and the resistive traces would showing a strong change in resistance for a change in temperature.

Figure 1 shows data collected on eight of the 80 coupons as the temperature was ramped from ambient to 100° C and back to ambient. The traces exhnibitedexhibited relative resistivity changes ranging from 30% to 46% for the resistive nickel aluminium traces with only a 16% change for the copper trace to 46% for the various nickel aluminum traces. over the temperature range of 26° C to 100° C. Furthermore the change of resistance with temperature showed no apparent hysterisis effects through the temperature cycle.

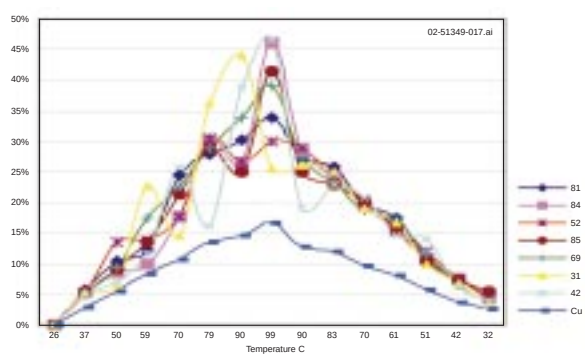


*FIGURE 1. Percent change of resistance with temperature.*

Complete analysis on all 80 traces is continuing by examining the cross-sectional areas to further distinguish

the different traces. Initial observations are that the greater percentage of oxide allows a greater initial resistance and a greater change in resistance. While speed and power do not greatly affect the percentage change, some analysis is needed to understand the different slopes in the curves. Trace thickness and width were constant for all traces measured (Table 1).

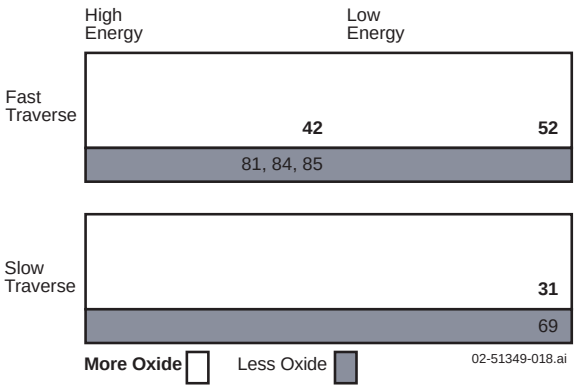


31 Low Energy, Slow Transverse, **More Oxide**
69 Low Energy, Slow Transverse, Less Oxide
42 High Energy, Fast Transverse, **More Oxide**
52 Low Energy, Fast Transverse, **More Oxide**
81, 84, 85 High Energy, Fast Transverse, Less Oxide

*Table 1: Machine parameters of traces.*

A sensor survey was conducted and various planar sensors were identified as candidates for experimentation. These sensors included stand-alone units as well as units with integrated network communications capability. A stand-alone unit, Analog Devices AD-590C, was selected for testing. Included in the sensor package were an individually trimmed (calibrated) temperature transducer and a temperature-current signal conditioner. This microchip is a planar design approximately 2mm x 4mm in physical dimensions with a thickness of 0.5mm. The device is a two-leaded analog device that operates independently of trace or lead resistance.

The AD-590 was attached to two thermally sprayed traces (by solderinged). Temperature testing was performed to validate sensor performance over a range of 20° C to 45° C (Fig. 2).

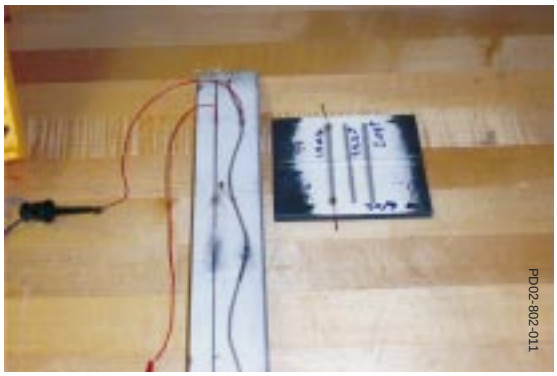


*FIGURE 2. Sprayed and embedded microsensor.*

Both solder and electrically conductive epoxy were evaluated to attach electrical and instrument leads. During soldering occasional trace debonding from the substrate was experienced. The solution to this problem was found through the use of low temperature silver solder. Even with this type of solder the operation was still very time-consuming and highly dependent on the skill of the person performing the work.

An alternative to soldering directly to traces is soldering to a prepared, sprayed copper pad. Test coupons with thermally sprayed copper pads were prepared and soldered electrical attachments evaluated. This technique provided easier soldering and lower contact resistances. Due to the easier soldering, less skill was required and faster connection times could be achieved. However, preparation of the copper pads significantly increased the cost and time required to manufacture the sample coupons.

High conductivity silver epoxy was evaluated as an electrical attachment method. This method worked very well. While not achieving the low contact resistances of the solder method, it was less time-consuming and

required significantly less skill in application. Also, employing the use of four-wire measuring techniques for monitoring trace resistances proved to be the most reliable attachment means for for measuring trace resistance during subsequent testing and was independent of contact resistance. The use of this material will be constrained by compatibility between the epoxies and the pipeline media (e.g., oil, natural gas, etc.).

Silver solder paste is a fourth technique proposed but that may be practical. Because silver solder "paste" is actual solder, most material compatibility issues should go away, contact resistances should be low and application techniques simplified. Assembly requires a lead wire, the solder paste, and a heat source such as a heat gun or oven for batch processing. Silver solder was not tested during the project.)

The work performed in this LDRD can increase the INEEL's capability in the use of thermal sprayed metals as an electromechanical signal source and data communications application. The INEEL is uniquely positioned to integrate expertise from several areas such as instrumentation, thermal spray parameters, materials characterization, and remote sensors to implement several innovative applications. The work done in FY02 on use of thermally sprayed traces for strain measurement has increased the role of the INEEL in working with the DOE-National Energy Technology Laboratory Natural Gas Infrastructure Reliability program.

The ability to solder wires reliably to such thin layers is of great use to the spray industry. The potential for intellectual property is being explored. The metallographic analysis conducted as part of this work is being used to support a University of Idaho Masters thesis project being conducted by Karen Moore.

In addition, the INEEL will increase it's relationship with the Department of Transportation and work with the Office of Pipeline Safety (OPS) to develop applications for the sensor to increase the security, reliability and operability of pipelines.

# Development of Blast- and Penetration-Resistant Materials and Systems for Comprehensive Protection of Vehicles, Personnel and Buildings

*Henry Chu, Tom Lillo*

## *Lightweight, high-performance armor solutions*

CS116

There is an increasing need to develop blast- and penetration-resistant materials and systems for the protection of various vulnerable areas on vehicles, personnel and buildings. This LDRD is establishing a comprehensive R&D and engineering program at the INEEL, under the auspices of National Security Critical Infrastructure Protection Initiative, to investigate new materials and systems to meet the nation's security needs in this area.

This specific research is establishing "proof of concept" of a low-cost high-volume pressureless sintering process to produce armor-quality monolithic SiC plate for personnel and vehicle protection. Though the whisker-reinforced SiC composite investigated in this project requires further process refinement to achieve full potential and surpass the performance of the monolithic SiC, a prototype encapsulated armor system was designed and fabricated using the INEEL's unique spray-forming technology. Live-fire testing of the encapsulated armor system showed excellent ballistic performance and multiple-hit capability. Further improvement in system performance is expected by replacing the present alumina core with reinforced or non-reinforced SiC.

This validation of the spray-form encapsulated armor concept would give the INEEL expertise to support various military branches and security needs.

Technical objectives for fiscal year 2002:

- Investigate advanced reinforced ceramic matrix composites.
- Determine best methods for low-cost direct-reactive sintering of aluminum oxynitride for transparent armor application.
- Spray-form an encapsulated ceramic armor system.
- Establish proof-of-concept for a blast- and penetration-resistant system based on integration of pumice and devitrified nanocomposite steel mat.

Because of a mid-year reduction of 20% in funding, the second and fourth tasks were eliminated from the above work scope. The remaining two tasks were continued because of the potential for meeting national security requirements in the near term.

The first task was to incorporate modified SiC whiskers into a SiC matrix. The whiskers were developed previously under a separate LDRD. The whiskers were heat-treated to produce a small knob on each end to aid in anchoring them in the matrix and eliminate sharp corners on the whiskers that might act as stress concentrators. The whiskers were wet-mixed with the matrix SiC powder that had been previously coated with a binder and boron carbide as sintering aid, dried and slightly crushed. The resulting powder was cold-pressed into green disks. The binder was thermoset during a heat treatment at 600° C and followed by pressureless sintering at 2100° C for 30 minutes.

The dynamic properties of pressureless sintered whisker-reinforced SiC composite and SiC matrix with no whiskers was evaluated and compared to two commercial hot-pressed SiC materials. Table 1 presents a summary of the depth-of-penetration (DOP) test results of various SiC samples. The figure-of-merit of the DOP test is mass efficiency, which is a measure of the thickness or mass of material required to stop a projectile from perforating, and therefore the dynamic strength and hardness of the material are inferred. The DOP test was performed with 30-caliber armor-piercing M2 rounds, impacting at 2800 ft/sec at zero degree obliquity and at 2-ft standoff. Three-inch-thick 6061-aluminum witness blocks were used to gage the depth of residual penetrations.

| Test Sample | Density (g/cc) | Thickness (cm) | Mass Efficiency |
|---|---|---|---|
| SiC matrix without whiskers | 3.165 | .447 | 5.4 |
| Whisker reinforced SiC | 3.051 | .401 | 3.5 |
| CoorsTek hot-pressed SiC | 3.200 | .635 | 5.6 |
| CerCom hot-pressed SiC | 3.217 | .445 | 6.5 |

02-51349-020

*TABLE 1. Machine parameters of resistance with temperature.*

The results in Table 1 indicate that the dynamic mechanical properties of pressureless sintered SiC matrix without whiskers was on par with the two commercial hot-pressed SiC, while that of whisker-reinforced SiC composite was below par.

The degradation of the performance of the whisker-reinforced SiC composite was investigated and the findings are as follows. Microstructural observations of the sintered disks revealed extensive grain growth. The grains grew in an elongated manner and were larger/longer than the whiskers that had been added. Two such grains are identified with arrows in Figure 1. It is thought that the elongated grains that developed during grain growth dominated the mechanical and ballistic properties of the sintered material. In essence, the detrimental effects of the large elongated grains masked over any benefit offered by the whiskers.

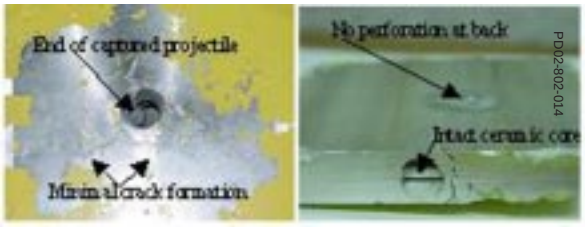


*FIGURE 1. Low-magnification optical micrograph (a) and TEM bright field (b) of SiC microstructure.*

Current thinking is that these elongated grains are responsible for the mediocre bend strength, approximately 300 MPa, and ballistic properties that fall short of commercial SiC. Efforts were initiated to reduce grain growth through the use of a different sintering atmosphere. Reports in literature suggest that a nitrogen-sintering atmosphere aids in preventing grain growth. Preliminary results produced material with a grain size in the 2-3 micron range without the presence of elongated grains, showing that nitrogen does, indeed, reduce grain growth. Efforts in this area will continue.

Microstructural observations using Transmission Electron Microscope (TEM) were made to further aid in decisions on paths forward to eliminate the extensive grain growth and improve mechanical and ballistic properties. These TEM observations (Fig. 1) revealed the presence of carbon-containing inclusions, thought to be graphite particles, on the order of 1-2 microns (black arrow) and much finer inclusions, <0.3 microns, containing significant quantities of molybdenum, titanium and vanadium (white arrows). Future work will concentrate on reducing or eliminating the carbon inclusions and eliminating the fine, metal-containing inclusions completely by reducing the carbon-containing binder content and eliminating cross-contamination during mixing, respectively.

A live-fire test was performed to further gage the ballistic performance of the pressureless sintered SiC material in a standard open-face, teo component armor system configuration. Several commercial pressure-assisted densified (PAD) SiC armor materials were used in a similar configuration as performance benchmarks. The ballistic performance test was performed by the Armor Mechanics Branch of the U.S. Army Research Laboratory (ARL). In this test, the projectiles used were 14.5 mm heavy machine gun-firing tungsten carbide cored projectiles (BS41). This test projectile is designated by the U.S. Army as the threshold threat requirement for the Future Combat System (FCS). Figure 2 summarizes the ballistic result of the live-fire test.

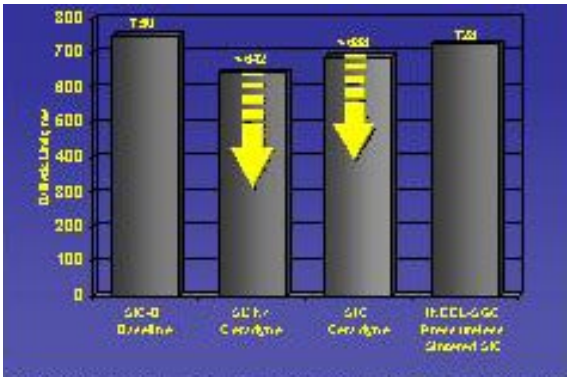


*FIGURE 2. Comparison of the ballistic limit of various SiC armor materials.*

The live-fire test results indicated that the INEEL pressureless-sintered SiC performed closely to the industrial benchmark PAD SiC-B material manufactured by Cercom, while exceeding the SiC and $Si_3N_4$ manufactured by Ceradyne. All benchmark materials are currently more expensive than the pressureless-sintered SiC. Cost

analyses indicate this process could potentially yield final products five- to six-times cheaper than current hot-pressed methods. Moreover, the production rate of this process is expected to be several orders higher and with low scrap rate.

An encapsulated ceramic armor prototype system was designed and fabricated using the INEEL spray-form process. The prototype system was constructed of a 1/8”-thick, 90%-pure alumina tile core encapsulated with 5083 aluminum on all six sides. The line-of-fire (LOF) areal density of the prototype was estimated to be 8 lb/sq ft. (Areal density is the product of the LOF thickness of the armor system and the volumetric density of the materials.) This prototype system was originally designed to defeat an NIJ Level 4 threat. In the initial live-fire verification test, the prototype armor system was struck with an AK47 7.62 x 39 mm 1943 PS ball round with a mild steel core at a standoff distance of 20 ft and with a muzzle velocity of about 2400 ft/sec at zero degree obliquity. The results of this test are shown in Figure 3.

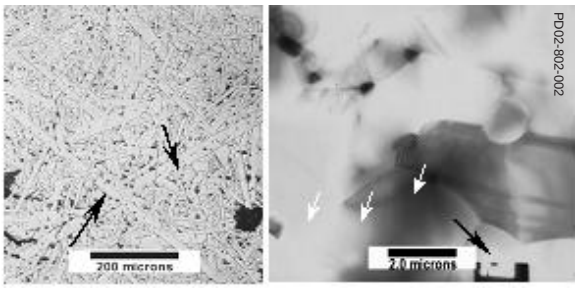


*FIGURE 3. Spray-formed encapsulated ceramic armor system (a) frontal impact face (b) back face and side view.*

For comparison purposes, previous tests have shown that approximately 14 lb/sq ft (equivalent to 1”-thick) of 5083-armor-grade aluminum would be required to trap the same projectile. Previous tests also have shown that the 1/8”-thick alumina without any encapsulation generally could not stop this projectile. The projectile also could perforate the same 1/8”-thick alumina mounted with adhesive on a 1/4”-thick 5083 aluminum as a standard open-face, two-component armor system. (Note: in Figure 3a there is no evidence of extensive crack formation on the impact face of the system. The alumina core also appears to be mostly intact inside the encapsulation in Figure 3b. These results confirm the multiple-impact capability of the design and fabrication process.)

This effort successfully demonstrated that the spray-form technology developed at the INEEL could be used to perform a one-step encapsulation of an otherwise undersized ceramic core, transforming it into a high-performance armor system. The one-step spray-form process is believed to be cost-effective against the current encapsulated armor fabrication method that consists of machining, electron-beam welding and hot-isostatic pressing.

The investigators plan to improve the system in FY03 by replacing the alumina core with the lighter and harder silicon carbide material. Also, the 5083 aluminum alloy encapsulation will be replaced with an aluminum-lithium alloy, offering higher tensile strength and stiffness per unit weight.

At a recent classified ground vehicle survivability conference, representatives from the U.S. Army Research Laboratory (ARL) pointed out that the encapsulated ceramic systems remain the only viable lightweight, high-performance armor solution that can be deployed in the short term, provided the manufacturing costs can be brought to a reasonable level and the throughput is sufficiently high. This successful demonstration of the INEEL spray-form encapsulated ceramic armor system may lead to immediate deployment of the systems in the Interim Armored Vehicle and the Future Combat System programs.

This research program encompasses advanced materials research and design, process development and engineering efforts as well as live-fire testing methods. The LDRD leverages in-house scientific and engineering capabilities and previous LDRD results to deliver proof-of-concept systems and materials prototypes. As a result of these efforts, a CRADA was established with Superior Graphite Company, Chicago, on the development of the pressureless sintering of silicon carbide and silicon carbide composite. This CRADA is expected to continue in FY03. In addition, the successful live-fire ballistic test by ARL resulted in Boeing (the lead system integrator for the Future Combat System) inviting an unsolicited R&D white paper and proposal from the INEEL.

A patent application is under preparation for the spray-formed encapsulated ceramic armor system.

Two presentations are scheduled for FY03 on the research results of this LDRD – one at the 27th American Ceramic Society Conference, the other at the 23rd Army Science Conference.

# Critical Infrastructure Critical Sub-network

*Don Dudenhoeffer, Miles McQueen*

## *Reducing vulnerabilities of critical national assets*

CS114

Critical infrastructures are physical and cyber-based systems essential to the minimum operation of the economy and government. They include telecommunications, energy, banking and finance, transportation, water systems and emergency services.

Due to advances in information technology and the necessity of improved efficiency, infrastructures have become increasingly automated and interlinked. Most modern commercial infrastructures are composed of a collection of interconnected networks that serve different purposes and have different owners. Even parts of the information residing on a single sub-network may have different purposes and different owners.

Critical information is passed between these component elements to coordinate necessary functions. The complexity and interdependency of this critical information flow introduces vulnerabilities into the entire critical infrastructure. Deliberate attacks or accidental system failures may result in serious consequences to the nation.

This LDRD is researching the interdependencies that exist between multiple infrastructure networks. The approach is to gain an understanding of these intricacies through modeling, simulation and algorithmic development. Specifically, this research seeks to identify the "irreducible critical sub-network," the smallest part of an infrastructure that can still execute its critical function, as well as identify "emergent behaviors" that result from interdependencies between infrastructures (e.g., water systems, emergency services, transportation, Supervisory Control and Data Acquisition [SCADA] systems, etc.). Through these insights, approaches and methodologies can be developed to assist in vulnerability assessment, resource allocation, and remediation against knowledgeable and capable attacks.

Technical objectives for fiscal year 2002:

- Develop a modeling and simulation framework to support infrastructure analysis.
- Collect data and develop models to support initial algorithmic development and method analysis.
- Develop an understanding of current infrastructure architectures and interdependencies.
- Present project results to peer groups for constructive feedback and comment.

This research has evolved from the National Security Division initiative addressing the broad needs of Critical Infrastructure Protection established by Presidential Decision Direction 63 (May 1998) and Presidential Executive Order 13231: Critical Infrastructure Protection in the Information Age (October 2001). The issue of critical infrastructure protection is a vital research area to support critical national assets.

The interweaving of infrastructure elements creates a complex system. A complex system is defined as "one whose component parts interact with sufficient intricacy that they cannot be predicted by standard linear equations; so many variables are at work in the system that its overall behavior can only be understood as an emergent consequence of the holistic sum of all the myriad behaviors embedded within." (Levy 1992) These interactions result in emergent behaviors.

The objective is to understand these behaviors and, specifically, the vulnerabilities they create. The decision-support tools being developed to gain this understanding and quantify vulnerabilities will consist of a modeling and simulation framework coupled with analytical methods. Using this framework, decision tools will be used in wargame-like scenarios in which attack vectors target selected infrastructure elements within defined critical missions. The simulation will be interactive to allow scripted events and/or user-inserted events.

The shear mass of data to be analyzed and the complexity of computations require this framework to be constructed using parallel computing architectures. Using the INEEL's high-performance computing capabilities, this framework is being developed for use on the SGI Origin computer or a Linux computer cluster. Figure 1 represents the parallel simulation architecture.

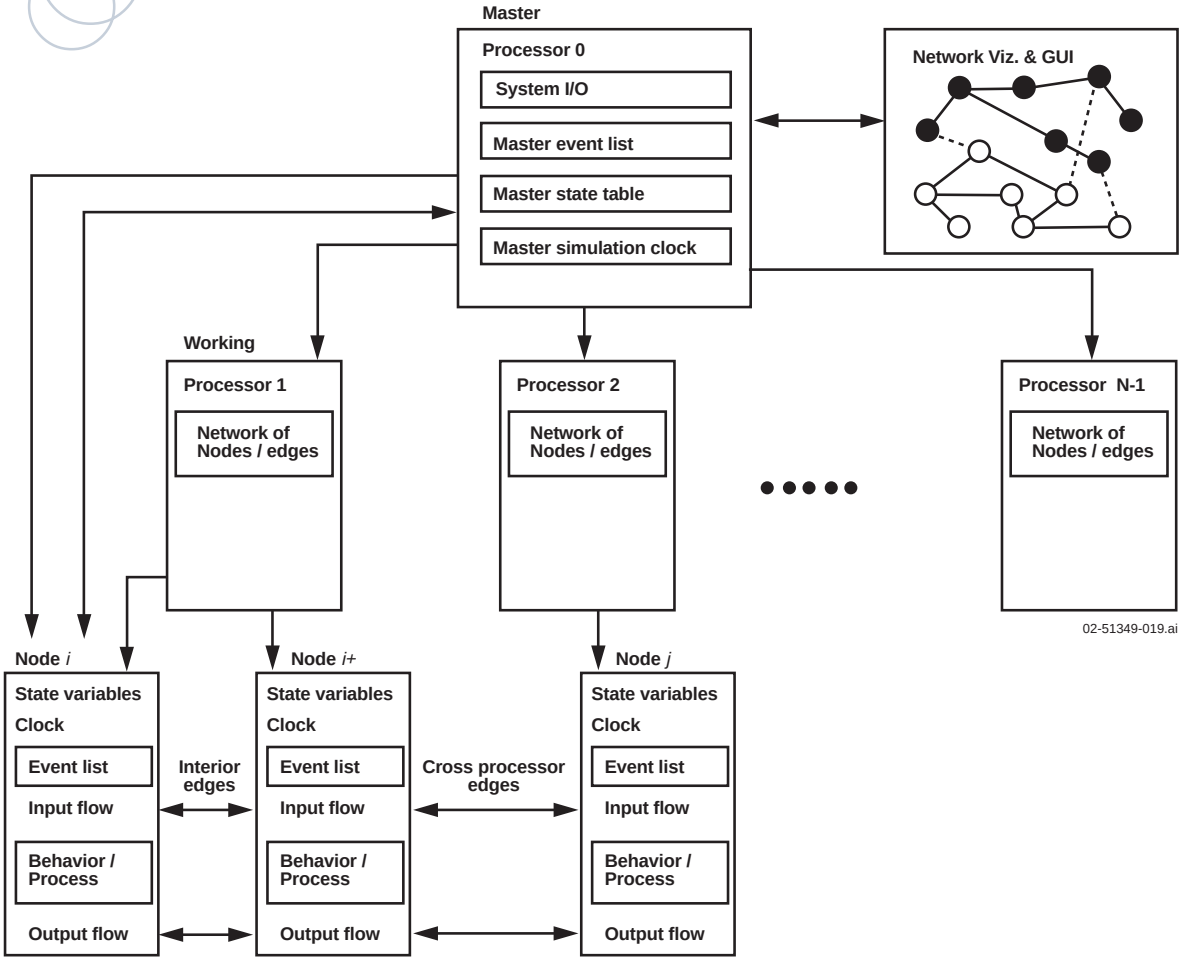


*FIGURE 1. Parallel simulation architecture.*

Individual networks are divided across multiple processors within this architecture. The networks are represented using graph and agent theory. A master processor controls simulation synchronization while an additional processor controls user interaction including 3-D visualization.

Capabilities developed this first year include:

- Modeling and simulation framework to support the analysis of large-scale cross networks.
- Advanced visualization techniques to identify interdependencies and observe emergent behaviors.
- Expertise in national infrastructure vulnerabilities.
- Initial infrastructure database to support modeling and algorithmic development. Currently 200 nodes are populated. The ultimate goal is 10,000 nodes.
- Increased INEEL expertise in high-performance computing and parallel programming.

Many challenges exist in this project including the development of parallel algorithms, data management in

terms of shear mass and quality, visualization and information presentation, and simulation model development.

Figure 2 represents the visualization being developed to support user interaction. Pictured are infrastructure elements. The cubes represent infrastructure assets. Vertical separation between nodes illustrates the various infrastructures being modeled. The edges between nodes represent flow paths (e.g., roads, pipes, wires, etc.).

The visualization is presented in a 3-D environment. The user can select edges or nodes to examine their state and can change various parameters. The cylinder represents a radius of impact potentially showing the infrastructure assets affected by an explosion. During the simulation, the nodes and edge change color to represent a change of state. This presents a visual representation of emergent system behavior.

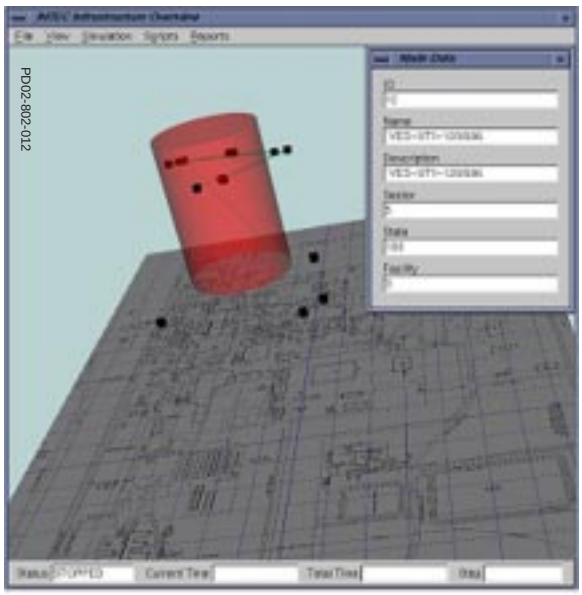


*FIGURE 2. Simulation visualization.*

One of the objectives this year has been to discuss this project with peer groups in the infrastructure modeling and analysis field. The National Institute of Standards and Technology (NIST) and Sandia National Laboratories have related efforts in this area. These efforts are complementary and address different levels of focus while possessing different analytical methods. Both NIST and Sandia's work represent potential collaboration opportunities that can support the objectives of DOD, DOE, or the Office of Homeland Security.

The insights gained from this project also may support the development of the National SCADA Testbed that is currently in the program-planning phase. This is a joint INEEL and Sandia project to research and evaluate SCADA vulnerabilities and mitigation/prevention plans.

# Survivable Networks of Dynamic Systems

*Miles A. McQueen*

## *Fending off malicious attacks to computer networks*

CS103

Surviving attacks on computers and networks is the focus of a very new field that is a superset of traditional computer and network security. The basic approach is to harden the systems by means of redundancy that can be partitioned into time, information, and physical redundancy. However, runtime analysis of attacks requires that all components making up a survivable system can exchange information accumulated at individual sites and use that information collaboratively to make real-time strategic decisions regarding system survivability as a whole and as individual machines within the network.

This LDRD is investigating the use of a system of autonomous mobile agents as a mechanism to enhance the survivability of a network of machines. For this research, the investigator augmented low-level signature recognition using mobile software agents to demonstrate the real-time performance and timing behavior of a two-level, survivability architecture. The lower level of the architecture includes attack analysis based on kernel attack signatures. The potential for fast response to and recovery from malicious attacks was the main motivation to implement attack detection and survivability mechanisms at the kernel level. The higher level survivability mechanism was implemented using migratory autonomous agents and motivated by the need for a slightly slower but more complex response mechanism.

A timing analysis is presented that suggests the real-time feasibility of the two-level approach. The limits to real-time response are identified from the host and network point of view.

The experimental data derived from this research is important for risk management and analysis in the presence of malicious network and computer attacks.

Technical objectives for fiscal year 2002:

- Use enhanced attack profiles (developed through LDRD CS105) as a low-level kernel, attack-recognition engine.
- Demonstrate the efficacy of a two-level survivability architecture using intrusion-detection profiles to support system and data integrity, system robustness, and system survivability for critical system infrastructures.
- Develop experimental results indicating the timing characteristics of both the low- and high-level response mechanisms.
- Present the two-tier survivability architecture experimental results at peer-reviewed conferences.

During FY02 this LDRD achieved all significant objectives identified for the year. A prototype, two-tier survivability architecture was designed and implemented as an experimental platform for assessing the validity of the proposed architecture. At the heart of the two-tiered architecture is the Signature Analysis engine. It is directly involved in the generation and analysis of the attack signatures. Signatures are collected in, and accessed from, an Attack Signature Library. At runtime, signatures are compared to the runtime system profile in an attempt to recognize attack signatures. Pending recognition, Event Handlers are called that implement the kernel-based survivability mechanisms. Simultaneously, the Agent Interface selects specific agents to propagate reactionary survivability measures.

The signature model described above is situated at the low level (i.e., kernel level). The high-level survivability features are implemented using agents. The agent migration system chosen for this architecture was Aglets, a Java-based migration system developed by IBM Research Laboratory Japan. Figure 1 gives an overview of the specific agent architecture.

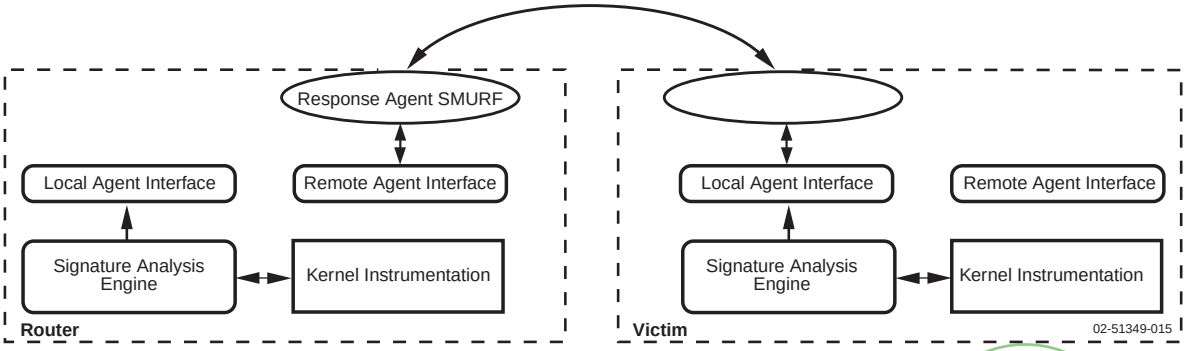


*FIGURE 1. Two-tier architecture components.*

The Signature Analysis Engine is the component of the survivability architecture that conducts real-time comparisons between the stored Attack Signature Library and the Kernel Instrumentation. Upon detecting an attack in progress, it passes the attack information (i.e., attack likelihood and attack type) to the Local Agent Interface. The attack likelihood refers to the probability of the attack being underway.

The Local Agent Interface is responsible for communicating between the Signature Analysis Engine and the Response Agents. Given the information regarding the attack from the Signature Engine, this component will make a decision whether to respond to an attack or not. For example, a "port sweep" is not likely to warrant much response, whereas a "smurf attack" requires a quick response. If the Local Agent Interface chooses to respond to the attack, it directs one of several Response Agents to apply appropriate action.

The Response Agents apply high-level survivability features. They are individual migratory agents that respond to attacks, each with a unique response for the specific attack it is defending against. For example, a smurf attack might require a router to turn off packet forwarding, whereas a port sweep might simply require warning other hosts in the network that there is a potential future attack. A response to a specific observed exploit might be to apply a patch.

Although Response Agents are created on one system, the so-called home host, in many circumstances it is desirable for them to migrate to another host to take specific action. For example, a Denial of Service (DoS) attack might require the router to take additional filtering action. However, a long-standing issue with respect to migratory agents deals with the security and trustworthiness of these agents. This issue is addressed in the current architecture by not allowing migratory agents any direct control over a host. This is the function of the Remote Agent Interface, which evaluates the trustworthiness of the agent and takes action on the local machine, if deemed necessary. Response Agents themselves have no capability to control a host.

Using the previously described architecture, a careful and thorough event sequence and timing analysis was undertaken. A general event sequence of the two-tier architecture is shown in Figure 2. Timing data was collected and analyzed for each sub-event shown. The timing results indicated good, near-real-time performance. Based on system call time, overall performance of the kernel is reduced by 14.3%. This degradation only occurs when instrumented functions are called, and so appears worse than it is. There will be no performance degradation if network functions are not used. Elapsed time is in some ways more accurate, as this is what a user sees. Overall degradation appears to be just .971% when elapsed time is used instead of system time.

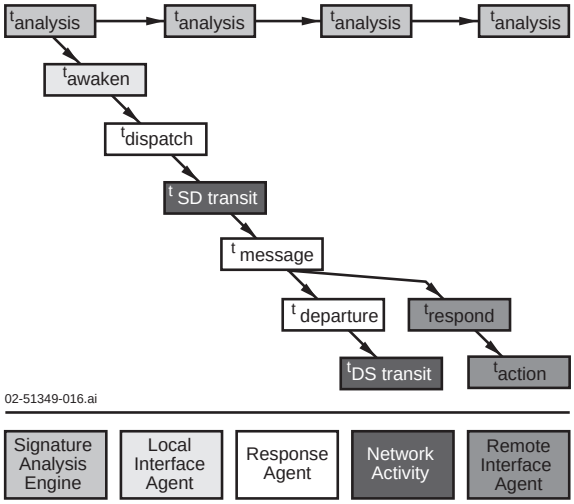


*FIGURE 2. Event sequence overview.*

The Signature Analysis Engine performs at O(1) in the best case, and O(k) in the worst case, where k is the number of signatures being compared. This worst case could perhaps be made more efficient by using a more sophisticated comparison algorithm. However, even with 100 signatures in the library, the comparisons took very little time. The execution times for the various agents were, overall, quite low even under high-load conditions.

Although the router was not loaded, similar results as loading the victim will be seen if the router is loaded.

The true bottleneck in the system for this test was the transmit time of the migratory agent. A DoS attack (like smurf) is specifically designed to congest the network and represents a “worst-case” situation. Such an attack is going to degrade overall performance greatly because migratory agents are used that must contend with the attack for network bandwidth. Even in these situations of extreme network loading (95% load), it is reasonable to assume that the attack will be responded to within one minute.

To culminate this year’s research, four refereed publications were accepted and presented to international conferences.

This LDRD supports INEEL’s objective of developing a recognized capability in information assurance and survivability. The LDRD has fostered research collaboration with the University of Idaho Computer Science Department (Dr. Scott Harrison and Dr. Axel Krings) that may lead to opportunities with the Technical Support Working Group.

# Environmental Stewardship Initiative

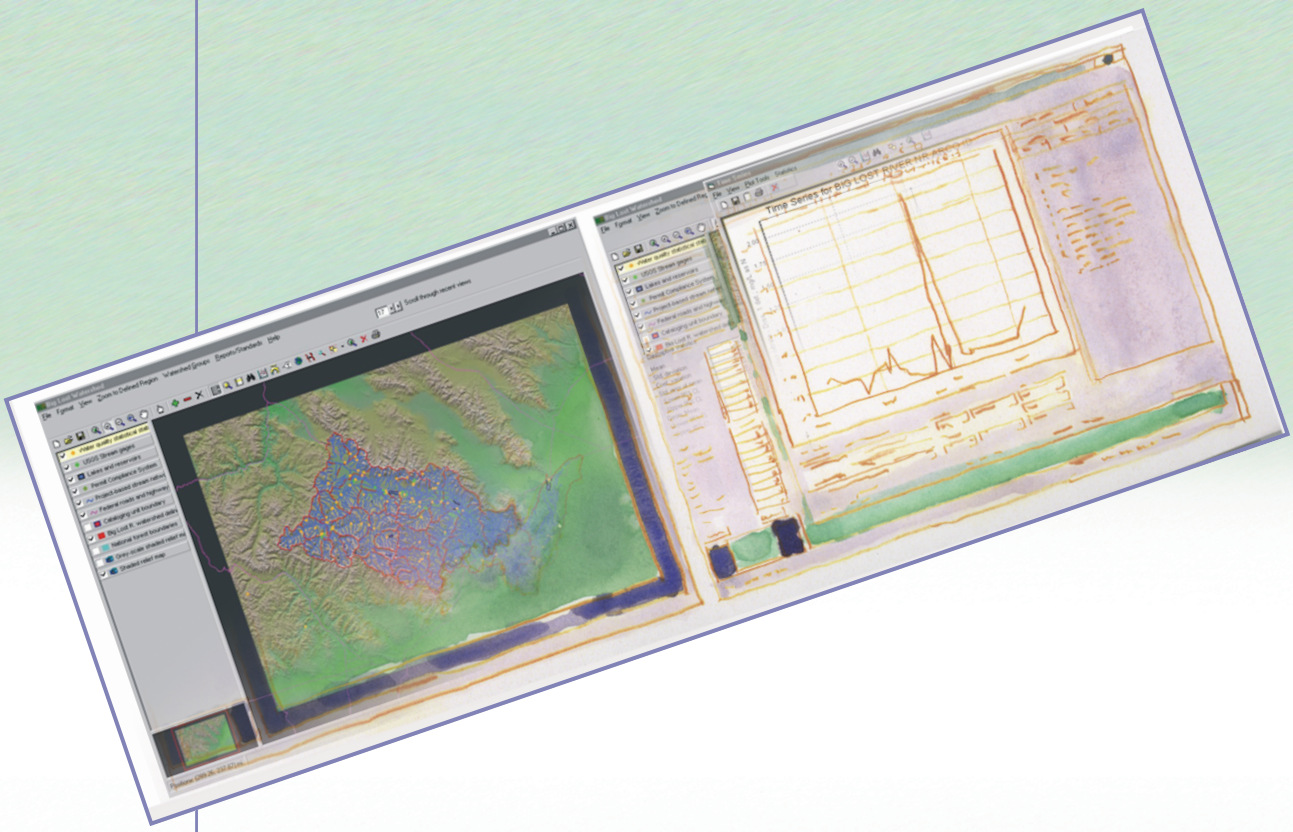

## LDRD Annual Report for FY-2002

Idaho National Engineering & Environmental Laboratory

# Airborne Contaminant Gradient Mapping System

*David A. Atkinson, Greg J. White, Ron C. Rope*

## *Field detection of chemical vapors*

ST102

Ion mobility spectrometry (IMS) has become an important analytical tool for trace organic detection. With the current paradigm shift of moving analytical measurements from the laboratory to the field, IMS is leading the way with highly sensitive, handheld instrumentation that can provide real-time data.

Many applications, especially in the environmental and national security arenas, require that chemical concentration data be tied to geographic position (GPS) data to be useful. This LDRD involves integrating portable IMS equipment with handheld GPS to provide a field-deployable prototype unit for geographic mapping of chemical vapor data. The integrated system provides chemical vapor data (simultaneous positive and negative mode IMS spectra) tagged with position information with a resolution of about 20 feet (on average) in a highly portable package.

Technical objectives for fiscal year 2002:

- Integrate IMS with GIS/GPS to provide airborne chemical concentration data.
- Use this data to develop concentration gradient maps.
- Optimize the system.
- Demonstrate the effectiveness of the system at the Seneca Nation site.

A handheld IMS (Graseby LCD-ABBII) was integrated with handheld GPS (Garmin III+) using a laptop computer and RS-232 serial interface protocol. Both the GPS and IMS use the RS-232 communications protocol in their off-the-shelf configuration. Integration of the system was carried out using the LabView programming environment.

Labview can read RS-232 from multiple ports, display the data, and provide instrument control. The software was written to handle simultaneous data sets and provide real-time feedback on chemical information and position. This software also can export the data into standard GIS shape files, which means that data sets can be read and manipulated by a number of off-the-shelf GIS software systems and easily shared between users.

The final GPS-IMS package was deployed in a laptop carry bag that could be easily carried for field operation. The handheld IMS was typically carried in-hand; however, a sampling tube could be mounted on it so the instrument could rest in the bag, leaving the user's hands free. Both the IMS and the GPS are tied together through the same system clock on the computer (or to the satellite clock via the GPS signal), so data sets are synchronized (Fig. 1).

*FIGURE 1. System in deployed configuration using laptop carry bag.*

GIS technology was used to develop and display coverages of the area of interest and map sampling grids/lines, and to analyze, query and display results of the chemical analysis. The chemical data can be displayed either as contours, a colored and/or 3-D surface based on sensor readings, or as individual points that can be color coded based on the numerical values from the sensor output.

The GIS also can query the results and display only the "hot spots" of interest based on some selected value. This display can be provided in the field immediately following the sampling effort to allow the sampling team to immediately return to hot spots if desirable. Digital 1:24,000 orthophotos, aerial imagery, and digital elevation models all can be used to map the instrumental data when needed.

A performance measure of the project was to demonstrate the system on Seneca Nation lands located in western New York. These lands were active natural gas and oil production sites during the first half of the twentieth century. Production began at the site during the first decade of the century, and effectively ceased during the 1940s.

Most of the gas and oil wells located on the Reservation were improperly plugged and abandoned. As a result, the wells are leaking methane, H2S, and other gases to the atmosphere, and also may be contaminating surface and ground waters in the area. Furthermore, the locations of only about half of the estimated 200 wells drilled are currently known.

This situation provides the perfect testbed for the integrated GPS/GIS/IMS system. The sour gas wells provide a fairly constant source of organosulfur and organonitrogen gases that respond well in IMS. Vapor data was taken at the Seneca site to verify that the gradient mapping concept works on this application. Geographic mapping of the IMS signal provided confirmation that this system could be used to find the abandoned wells, although very high-density data coverage is needed for location accuracy (Fig. 2).

Apart from high-density sampling performed by walking with the system, tests were performed for deployment of the system in a vehicle so that larger areas could be covered. These tests worked well, and proved the effectiveness of the system for vehicle deployment once the investigators addressed a major problem. The problem occurred when the IMS peaks began to shift as the vehicle increased its velocity. This problem was due to the pressure increase in the IMS as the vehicle's velocity forced air into the detector. The issue was resolved by using the IMS system's internal pressure sensor, which is read by the software system. All of the spectral data was then adjusted for pressure changes "on the fly" by calculating a pressure corrected spectrum.

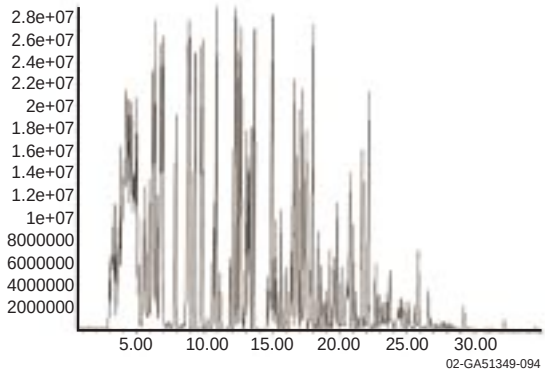


*FIGURE 2. Total ion chromatogram from GC/MS analysis of well vapor.*

Sensitive, field-deployable chemical detectors are the wave of the future for environmental and national security needs. IMS fulfills these needs, but there is also a strong requirement to correlate the chemical data with position information. This LDRD provides that capability. Now, chemical information can be obtained and visualized spatially. This new chemical vapor-mapping capability allows IMS to be used effectively and to its full potential. The INEEL IMS research group is well positioned to take advantage of the technique and its potential to satisfy DOE mission needs.

# Long Term Record Storage For Long Term Stewardship

*Sharon Berrett*

## *Using barcodes to store site-specific records*

ST108

Long-term record storage and retrieval will become increasingly important as the DOE moves toward Long Term Stewardship (LTS) where the ability to track and recover pertinent data is measured by decades rather than years.

This LDRD investigates two new automatic identification technologies – touch memory buttons and 2-D barcodes - coupled with handheld, portable computing devices to develop a prototype demonstrating how these issues might be resolved. Effectively, these devices will allow container or facility-specific database records to be stored directly on the container or facility itself, thus saving both time and money as well as relieving the dependence for information retrieval on remote computer systems. Both storage devices have the potential to maintain information in excess of 100 years. The application will be a self-contained standalone function, eliminating the need for connection to a remote system or dependence on electrical power.

Technical objectives for fiscal year 2002:

- Determine information likely to be retained for LTS sites.
- Develop a conversion module to align and reduce data into a format suitable for storage in a memory button using compression algorithms.
- Develop a desktop prototype to access a database, and pipe the data through the conversion module for downloading to the button memory and 2-D barcode.
- Develop a handheld computer application that accesses the memory buttons using a contact wand to download or retrieve stored data.
- Demonstrate desktop and handheld prototype applications.

This LDRD project uses standard desktop and handheld hardware platforms, operating systems, and software development environments. Some modifications to algorithms, cables, applicators, etc. were necessary. Vendors of the hardware devices have provided direct access to their support staffs when necessary.

Two primary software applications were created, one to run on the desktop and one to run on the handheld device. Each application provides a variety of functions, some of which are duplicated (e.g., both have the ability to display the information) and some of which are unique (e.g., only the desktop communicates the existing database).

A desktop application was developed to transfer pertinent LTS information to a 2-D barcode. Information that is static, such as historical data, was encoded and printed on the barcode. Information that is dynamic, such as monitoring information, was downloaded to the handheld computer to be transferred to the button after the button is attached at the location.

The handheld application allows the user to view information (using a Pocket PC) that is stored on the 2-D barcode and the button memory. This allows for on-site viewing of emergency information or procedures.

The FY03 phase of this LDRD will develop the ability for the application to be stored on the button itself. This ability will allow a user (with the proper authorization) to view information without previously having the application loaded on the Pocket PC. Next year this project also will investigate remote devices such as Radio Frequency tags that may be used to perform a similar function from remote locations; i.e., helicopter, vehicle, etc. In addition, GIS technology will be evaluated to determine integration and applicability.

The application being approached in this LDRD is virtually a self-contained information-retrieval system that addresses the problem of retaining access to information long after technology has advanced. This technology can benefit the INEEL, DOE and any agency faced with long-term stewardship tasks and the information-management challenges that come with that responsibility.

Discussions have been held with both EPA and DOD to use the technology from this LDRD in conjunction with Institutional Controls for Long Term Stewardship.

# Uptake and Translocation Patterns of Strontium by Sagebrush Steppe Ecosystem Plants

*Melinda A. Hamilton*

## *Using plants as bio-indicators*

ST108

Radionuclides and heavy metals are primary contaminants of concern at the INEEL and many DOE sites. Soil and groundwater contaminated with Strontium-90 pose a significant challenge in environmental restoration and long-term stewardship. Two essential components to long-term management of legacy waste sites are: 1) monitoring sites in which residual hazards remain after cleanup is completed, and 2) reducing the technical uncertainty associated with predictions of contaminant fate.

Plants may play a critical role both as a tool for monitoring contaminants and as an agent for affecting their potential migration. Although phytoextraction (plant uptake of metals/radionuclides) is widely known to occur, only gross uptake data has been published and many assumptions are used when trying to use plants as bio-indicators.

This LDRD is developing a scientific basis for using plants as accurate and reliable indicators of surface and near-surface contaminant concentrations, and changes in contaminant mobility over time. The first objective is to develop a fundamental understanding of the impacts of environmental factors and plant physiology on Sr-90 uptake and translocation. This new information will aid in the development of accurate and reliable predictive models that could elucidate changes in contaminant risk based on combinations of environmental and seasonal factors.

The second objective is to develop a non-destructive, aboveground imaging system that will provide information about changes in plant development and biomass concentrations of $^{90}$Sr.

Technical objectives for fiscal year 2002:

- Complete hydroponic experiments to quantify uptake and translocation patterns for Sr in crested wheatgrass.
- Complete biomass and solution analysis to correlate plant physiological parameters (leaf area index, biomass, etc.) representative of various stages of plant growth with contaminant concentrations in plant biomass fractions (roots, shoots, leaves).
- Initiate development of a method that uses imaging techniques to aid in future development of a model to predict both above- and belowground biomass as well as above- and belowground contaminant mass.

To understand and ultimately predict Sr-90 uptake and translocation in crested wheatgrass, actual Sr uptake rates and extents, Sr translocation patterns, and Sr effects on crested wheatgrass must first be understood. Studies to elucidate these phenomena, as well as parallel studies designed to define the ability to identify Sr presence in leaves with spectral imaging techniques, were undertaken during this first year of this work.

Working collaboratively with Dr. Bruce Bugbee of Utah State University (USU), two hydroponic greenhouse trials were completed with crested wheatgrass. In trial 1, three available Sr concentrations were compared, 0, 100, and 1000 micromolar with 4 replicates of each treatment in a randomized block design. In trial 2, four Sr concentrations were included, 0, 3, 10, and 100 micromolar with 3 replicates of each treatment in a randomized block design.

Crested wheatgrass seedlings were planted in quarter-strength Hoaglands nutrient solution and grown under constant greenhouse conditions. Strontium was added to the desired solution concentration as Sr-Cl salt. Calcium concentration was maintained at 1mmol available solution Ca in all treatments. Nitric acid (HNO3) was added to maintain pH.

Temperature, humidity, and solution pH were monitored continuously. Throughout these studies, weekly samples of leaves, stems, and roots were collected and analyzed for Sr and Ca concentrations, other trace metal and nutrient concentrations, and biomass (dry weight). Plant growth was measured by several methods including biomass, radiation capture, transpiration, and NO3 addition requirements. The heads of the plants also were analyzed once they appeared at about seven weeks.

These studies ran until the crested wheatgrass plants were approximately nine weeks old. Results indicate that the concentrations of Sr tested had little to no effect on measured parameters of plant growth, with the possible exception of the highest concentration (1 mmol). Sr uptake was similar to Ca uptake on a molar basis and on a translocation basis. Both Sr and Ca were found to concentrate primarily into the crested wheatgrass leaves (50% w/w) with stems, roots, and heads containing lower concentrations respectively. Sr uptake was fairly constant with biomass increase (Fig. 1).

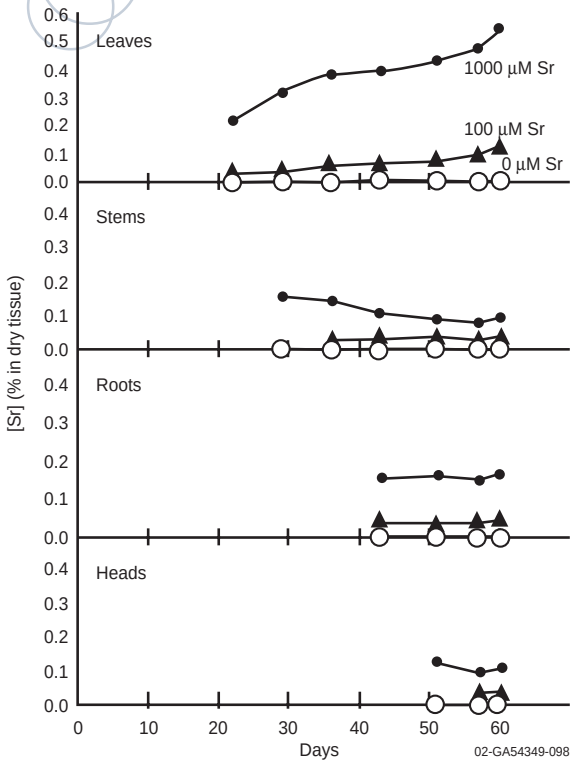


*FIGURE 1. Sr partitioning in crested wheatgrass plant structures over time of growth.*

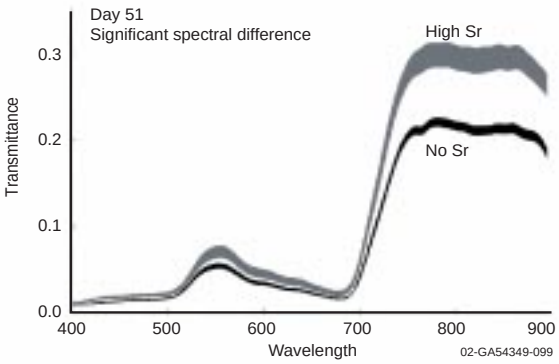


*FIGURE 2. Comparison of transmittance measurements for crested wheatgrass leaves with and without Sr incorporated.*

Spectral imaging to determine if the presence of Sr in the plant leaves could be detected by light transmittance/reflectance measurements, also was conducted at USU's Crop Physiology Lab. Spectral reflectance measurements were performed on crested wheatgrass leaves that contained high Sr concentrations due to plant uptake. The results were compared to control plant leaves that were grown in the absence of Sr. Wavelengths of 450 through 850 (nm) were used for these measurements and compared by standardizing to 820nm.

The development of a capability to detect high concentrations of Sr in crested wheatgrass leaves was not completed during this first year of work. While spectral reflectance varied with Sr concentrations, the differences were not statistically significant at the low Sr concentrations used. It is expected that by using a broader range of wavelengths (up to 2350 nm), spectral signals at these low Sr concentrations will be more pronounced and significant differences will be detected. Development of this method will continue in next year's work (Fig. 2).

Results of this research indicate that Sr is readily taken up by crested wheatgrass (like Ca); however, it does not result in easily detectable physiological or morphological changes in the plant. This suggests that crested wheatgrass growing in Sr-90 contaminated areas is likely to be taking up Sr-90, but until nondestructive measurement techniques are developed, would require harvesting, digesting, and analyzing the samples to verify uptake rates and extents. Therefore, research to date still indicates a need for a "screening method" and some predictive tools for determining the rate of Sr-90 uptake and entry into the food chain. This LDRD is on track to provide these tools.

Long-Term Stewardship of DOE sites in the West will need to rely on low-cost methodologies to constantly evaluate risks associated with leaving low-levels of contaminants in place. This LDRD is designed to provide a basis for doing just that for Sr-contaminated surface

soils initially, and potentially for other contaminants of concern. The first step toward this goal was to establish baseline data for Sr uptake by crested wheatgrass. This goal was accomplished during the first year of research, and the data indicate that the need for predictive tools and cost-effective screening methodologies is real.

Three areas for follow-on work are being considered and will be evaluated as the research progresses. The three topics are: follow-on fieldwork at a Sr-contaminated site at INEEL to validate the model, greenhouse studies with other sagebrush steppe ecosystem plants and other contaminants and expansion of the model to include these plants and contaminants, and development of remote sensing for bio-indicator applications. In addition to continuing the established collaboration with Utah State University this project intends to collaborate with remote sensing projects at the INEEL to explore approaches for remotely obtaining spectral data that can be used to estimate plant concentrations of contaminants.

# DOE Complex-Wide Long-Term Stewardship Options Analysis System

*Jacob J. Jacobson, Sharon Berrett*

## *Visualizing end-state site scenarios at INEEL*

ST107

The INEEL does not have a common repository or quick-retrieval method for documents for the multitude of operable units pertaining to waste site management. Currently, if documents need to be reviewed for a particular site, personnel have to search through archives trying to locate site identification numbers and documents.

This LDRD is researching a web-based application that can provide map-based near-real-time information on current INEEL waste sites. The application gives users access to contact information, on-line access to related documents, status of activities, contamination constituents, as well as proposed cleanup activities. In addition, this application can examine, from a more holistic perspective, the cleanup activities at multiple sites to determine if the cleanup work at each site is compatible with the entire area and with INEEL end-state planning.

This research is innovative in several ways. First, it combines several new technologies (computer simulation, Geographical Information System (GIS), Internet) into a comprehensive, powerful simulation tool that is visually appealing, intrinsically easy to operate, and runs over an Internet browser. Browser access bridges the computer operating system limitations and allows access to anyone with a network or modem connection.

Secondly, this work broadens the use of System Dynamics and computer simulations into the environmental management areas. The research also takes advantage of GIS's ability to allow data management and access through a graphical display. Finally, the end product could be applicable to a wide range of areas.

Technical objectives for fiscal year 2002:

- Create relational database for storing cleanup and long-term stewardship information with external links to already developed information sources.
- Develop a web application that allows users to visualize conditions, status and activities on area waste sites.
- Develop the web application to access documents (Word, PDF, PowerPoint, etc.) associated with waste area groups, operable units, and individual waste sites.
- Develop a tool to analyze proposed cleanup activities to identify conflicting or non-cohesive activities.
- Develop a simulation application that allows users to test different cleanup scenarios to support strategic planning for site-wide cleanup activities. Identify and test the application on an area at the INEEL.

The application area for this project was identified and confirmed with both DOE Long-term Stewardship (LTS) and INEEL LTS. The initial GIS map page has been created, GIS server identified and access granted (Fig. 1). The investigators successfully created the relational database this year. Some operational unit data has been entered. Record of Decision (ROD) data was identified and also entered. A simplified version of an ActiveX Web-enabled simulation interface was completed. To increase the modeling and simulation capabilities at the INEEL, the principal investigator also completed a four-semester Graduate Level Certification in System Dynamics at the Sloan School of Management. The model was presented at a System Dynamics Meeting sponsored by Massachusetts Institute of Technology in June. Presentation to operation personnel was made in August, and the GIS Application was presented at Spectrum 2002. The investigators met with the EPA-HQ LTS program manager this year to discuss use of this application on EPA's proposed multi-agency LTS program.

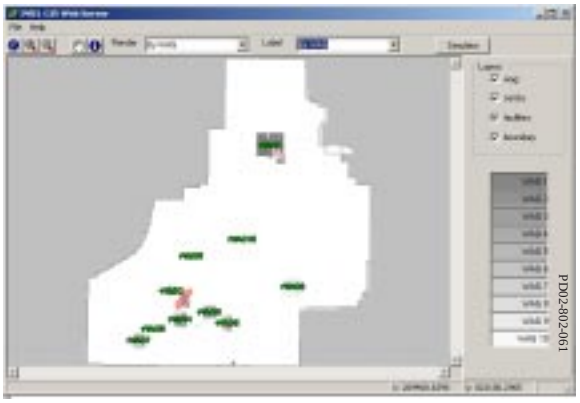


*FIGURE 1. The GIS interface allows the user to select different features for viewing and information retrieval.*

By centralizing vital information in a web-based, easily accessible form, this type of tool will be valuable at INEEL, other DOE facilities as well as DOD and other Federal waste sites. Some elements of this research will later fall under site operations (database management and upkeep). Currently, this tool is being leveraged with other research in the Long-term Stewardship Initiative.

In addition to waste management activities, this type of tool will be helpful and is being looked at for other management areas such as flood and fire control. Discussions have begun with EPA and the Department of Interior over potential uses with each of their respective long-term stewardship programs.

# Development of an Integrated Watershed Information Management Tool for Long-term Facilities Stewardship

*Ron Rope, Jerry Sehlke*

## *Making better water resource decisions*

ST105

Significant watershed management issues occur throughout the world, many crossing national boundaries. Given the current stresses on natural systems, resulting from both anthropogenic and natural events, watershed issues are being discussed internationally. A system that could help manage these issues would be extremely timely.

The goal of this LDRD is to provide DOE with Integrated Watershed Information Management Tools (IWIMT) that integrate and leverage water and environmental management information leading to improved long-term stewardship decision-making on the INEEL and within the associated watersheds. The tools and methods being developed are transferable to other DOE and federal facilities and to address national/global watershed management issues. Key components of the system include data management, access and analysis tools, a Bayesian Decision Network (BDN), web-enabled communication applications and options analysis/decision support capabilities.

The approach is structured around a BDN description of the Big Lost River (BLR) watershed and that portion of the Pioneer Basin on the INEEL that is influenced by the BLR. The BDN will be developed for integrated water and environmental management, and to identify and account for uncertainties associated with the physical systems, water quantity/quality, alternative long-term management options and socio-economic impacts of management decisions.

Work has involved data collection and database development for disparate data sources in the watershed and development of disciplinary data analysis and mathematical modeling tools to the Upper and Lower BLR and INEEL. These tools will be integrated into a coherent whole, termed an Integrated Watershed Information Management Tool, using BDN and the information flow structure that incorporates data and modeling uncertainty into the decision process. A systems dynamic model for the BLR is also a component of the system.

This tool will enable facilities managers to develop a suite of management alternatives that support water resource management decisions and communicate those decisions to stakeholders.

Technical objectives for fiscal year 2002:

- Collect data and develop a regional database and data access tools for surface and subsurface hydrology and water quality.
- Develop key water-land-environmental relationships and socioeconomic impacts of the INEEL site and associated watershed management decisions for use with specific applications within the region.
- Develop a BDN for the BLR, to identify data gaps and to allow for the prioritization and filling of data gaps with mathematical modeling efforts and future data collection.
- Use the BDN to aid design of data gathering networks and identify uncertainties in data, environmental and surface/subsurface relationships, and identify stewardship management options.
- Determine and implement tools for communication and ranking of management alternatives for decision-making.

Most water quality/quantity data for the system have been compiled. These data are now being documented and incorporated into databases and models as they are completed. A Microsoft Access database was produced that contains tables listing all of the GIS and temporal data needed for water quality and quantity management, and modeling in the BLR basin. This database includes data descriptions, physical locations of data, responsible persons, and a binary field that holds and files supporting information and documention such as critical metadata information files. The database is undergoing a final round of data entry at the INEEL and Utah State University and will be one of the more critical, useful and informative deliverables of this project.

Much of the data described in the aforementioned database has been incorporated into a standalone GIS-enabled spatial and temporal data visualization system for the BLR watershed. This tool, the BLR DataViewer (Fig. 1 next page), provides a level of access to a variety of data types not previously attainable through other methods. In addition to data visualization, the BLR DataViewer allows users to perform a large number of

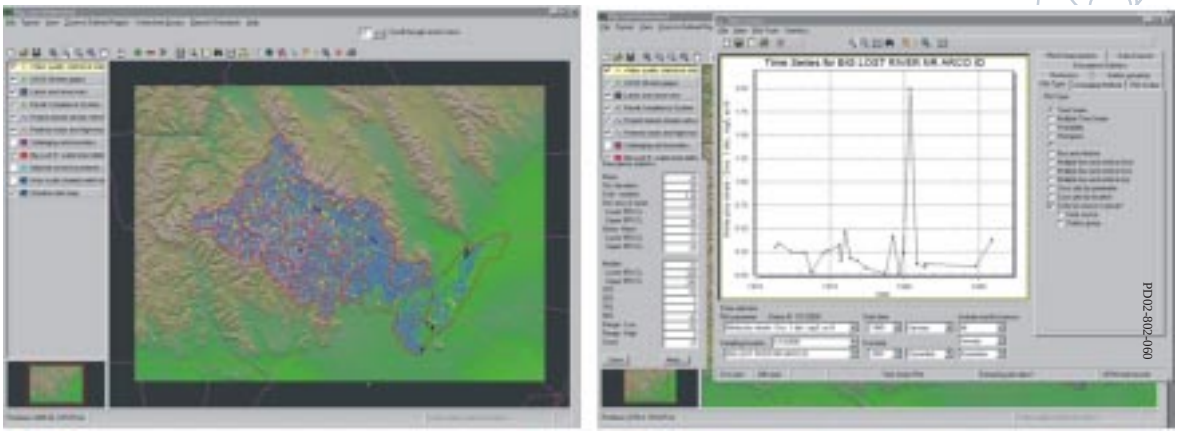


*FIGURE 1. Screen captures of BLR Data Viewer. (Left) BLR watershed with water quality and quantity monitoring stations identified. (Right) Trend analysis graphic for one of many parameters measured at one of the stations.*

simple and complicated data analyses and plots to help understand the data. This tool will serve as a backbone for the full IWIMT that is the final deliverable of this project.

GIS coverages were developed for the the "Pioneer Basins" (the seven watersheds that drain water to/from the INEEL) and specifiically for the BLR basin. Additional GIS coverages are still being developed (flood zone map, precipitation/snow fall data). Coverages not specific to the BLR watershed may be included in the BLR DataViewer and IWIMT to support a more integrated and holistic view of the factors contributing to water quality and quantity in the surrounding ecosystem and at the INEEL.

An initial BDN for flow management at the INEEL was populated with anecdotal and expert-based data and information. This was done to provide the BDN with a valid set of "Bayesian priors" or initial estimates of the conditional and marginal probability distributions at all nodes. In the next phase of this project, observations or hard data ("Bayesian evidence") will be used to update the prior probabilities and produce more robust "posterior" conditional and marginal probability distributions in the BDN.

An initial proof-of-concept software package based on the core technology of the IWIMT was completed this year and installed at the INEEL for testing and business development purposes. This software, Avalanche Hazard Mapper, exploits many of the core technologies of the IWIMT, including grid manipulation and calculation, integrated spatial data visualization and analysis, and custom GIS-enabled software deployment.

A complete set of GIS programming components was completed and prepared for installation and use on both internal and external computer systems running Microsoft Windows. This set of programming components, called MapWindow, allows users to embed GIS functionality directly in custom software applications with a degree of customizability, functionality and low-level data manipulation previously not available, yet critical to the success of IWIMT.

Several extensions (termed "plug-ins") to the MapWindow GIS system were produced this year including:

- Legend Editor for customizing the appearance of GIS data layers.
- Feature Identifier for exploring the attribute data associated with spatial data sets.
- Table Editor for modifying attribute data.
- TIN Builder/Viewer for converting grid-based terrain data into triangulated irregular networks and viewing the data in a 3-D environment.
- Network Editor for converting poly-line data sets into regular unidirectional networks (for stream analysis).

- Terrain Analysis Using Digital Elevation Models (TAUDEM) for analyzing terrain data, identifying drainage networks and flow paths, delineating watersheds and computing downstream accumulation values needed for non-point source pollution modeling.
- Database Manager for associating temporal data stored in a Microsoft Access database with spatially referenced points.
- Photo Viewer for associating photographs, descriptions and comments with spatially referenced points.
- Bayesian Network Viewer for viewing and running BDN models from within the MapWindow (and hence IWIMT) system.

Key web-site addresses for project tools include:

- MapWindow system and plug-ins: http://www.tmdl.org/toolkit/mapwin.htm
- TAUDEM: http://www.tmdl.org/toolkit/taudem.htm
- Avalanche Hazard Mapper: http://www.tmdl.org/toolkit/avalanche.htm
- DataViewer: http://www.tmdl.org/toolkit/dataviewer.htm

A Systems Dynamics Model was developed for the BLR incorporating watersheds, stream flow and aquifer flows. The stream flow component is operational; the watershed and aquifer components are being populated.

Installation of the BLR Watershed Data Viewer was completed this year. This data viewer includes all water quality and quantity data for the BLR integrated into a GIS-based data access and graphic display tool.

The investigators conducted a Bayesian Decision Network Workshop for INEEL and groups outside the INEEL in January. This included approximately 30 participants from over 10 different INEEL organizations. Four abstracts have been submitted for conference presentations/journal articles and the investigators have participated in the Lost Rivers National Learning Site in Holistic Management core group.

The tools, methods and approaches resulting from this LDRD are beneficial to any agency or organization involved in watershed and natural resources management. These tools and methods are being used to inform the water, natural resources and infrastructure managers at the INEEL and could be used for the same purpose at any DOE or other state/federal facility. Variations of these tools have been developed for EPA (e.g., Nooksack Watershed, USFS [Avalanche], and the Bureau of Reclamation).

The investigators are presently engaged with the Idaho Department of Environmental Quality in developing an EPA Watershed Initiative proposal in which a number of the tools and approaches developed in this project will be used to help analyze water quality and water use in the Bear River Basin. Discussions are also being conducted with the Idaho Department of Water Resources to use this LDRD system's dynamics methods for analyzing water use and flow in the Big Lost River and Bear River Basins. Discussions have begun with EPA's division of Watershed Assessment and Protection about using some of these methods and approaches for integrating water data/knowledge on a watershed basis. Discussions also have been held with the Governor's Natural Resources Chief about potentially assisting in the development of a statewide natural resources/energy plan.

Through this work, contacts and potential university collaborations have been made with Utton Transboundary Resource Center and with the University of Wyoming and the University of New Mexico.

# Use of Genetic Markers for Ecological Risk Assessment

*Angelica I. Stormberg*

## *Burrowing animals provide clues to contaminant exposure*

ST104

Radiological and hazardous waste have been disposed of at the INEEL since 1952. Spread of radionuclides and hazardous constituents from uncontained wastes, deteriorating waste containers, and waste disposal practices has resulted in contamination of the subsurface soils in the Subsurface Disposal Area (SDA) and at other facilities. To assess the risks to human and environmental health, the potential impacts of contaminant exposure on identified receptors must be determined.

Burrowing and excavation of the soil by small mammals, including deer mice (*Peromyscus maniculatus*), have been shown to be responsible for some radionuclide transport through the SDA environment; however, the genomic effects of exposure to contaminants at the INEEL are not known. Research is needed to develop new techniques to determine exposure to contaminants and the effects of that exposure to the genome of individuals so that environmental and remedial actions can be properly implemented.

The purpose of this LDRD is to explore the utility of molecular genetic techniques as screening tools for evaluating the risk to natural populations from contaminant exposure. These tools can be used to help evaluate site remediation needs. If remediation is implemented, genetic characterization of populations can provide insight on the effectiveness of the remediation through long-term monitoring.

Technical objectives for fiscal year 2002:

- Continue to sample mice populations at Radioactive Waste Management Complex (RWMC), SL-1 and the control areas of Atomic City and Burns during FY02.
- Obtain tissue samples from pregnant mice females and embryos.
- Extract and isolate DNA.
- Start DNA amplification of 16 microsatellite markers.

The null hypothesis to be tested is that there are no quantifiable differences between mammal populations that have been exposed to hazardous or radioactive contaminants and populations from uncontaminated locations.

Two control sites representing uncontaminated areas and two sites with known surface/subsurface contamination were selected for sampling. The two contaminated sites were outside the Comprehensive Environmental Response, Compensation and Liability Act (CERCLA) boundaries of RWMC and SL-1. The two control areas were located near Atomic City, approximately 3.3 miles east of the INEEL boundary, in an area called Burn, which is located on Highway 22 about 10 miles southeast of Howe, Idaho.

For each location, approximately 300 museum special snap-traps, baited with peanut butter and rolled oats, were used from March through June. Trap location, species, sex, weight and reproductive condition was recorded and tissue samples from females and embryos were collected. Pregnant females captured in RWMC and SL-1 were preserved in ethanol and will be submitted for radiological analysis in FY03. Genomic DNA was used as a template for specific amplification of microsatellite markers via standard PCR (polymerase chain reaction) technology. An ABI 377 Genetic Analyser (Applied Biosystems) was used for fragment analysis and then allelic data was scored.

The ratio of microsatellite mutant alleles vs. the non-mutant alleles (m/nm) was used as a direct assessment of mutation, using parent/offspring comparison of allele differences. Allele scoring was performed with 16 microsatellite markers for females and offspring from the four locations. Fetal genotypes that were inconsistent with the mother were scored as mutations. All genotypes scored as mutations will be reanalyzed to ensure data validation during FY03. The proportion of mutant alleles from each population was compared and tested for significant differences using the Fisher's exact test.

The total number of deer mice captured during the spring of 2002 was 519 individuals, from which 13.87% (n= 72) were pregnant females. The total number of embryos obtained for this field season was 375 (Table 1). To date, genetic data generated from these samples are being analyzed and compiled. Results will be presented in the next progress report.

| Area | No. of Pregnant Females | No. of Embryos |
|---|---|---|
| Atomic City | 40 | 205 |
| Burn | 5 | 27 |
| RWMC | 12 | 61 |
| SL-1 | 15 | 82 |
| Total | 72 | 375 |

02-GA51349-095

*TABLE 1. Number of mice females and embryos collected during spring 2002.*

Genotype data from samples collected during the spring of FY01 was updated (16 loci) genotype. All mutant alleles will be independently re-analyzed to ensure their validity. Mutation rates were calculated for the combined set of loci for this preliminary assessment.

Table 2 summarizes the combined mutation rate for sixteen microsatellites loci used in this study. The mutation rates for each of the study populations (SL-1 and RWMC) were significantly higher in comparison with Atomic City or Burn. No significant difference was found between SL-1 and RWMC or between the two control areas. These preliminary conclusions will be assessed with the additional analysis and second year results.

The preliminary data falsify the null hypothesis that deer mice populations in contaminated areas have similar levels of germline mutation rates for microsatellites loci. These results may be due to exposure to radioactive materials present in the environment. In addition, this study suggests that deer mice are genetically sensitive to exposure to anthropogenic contaminants. The species seems to constitute an ideal biological indicator for environmental monitoring of contaminants and long-term stewardship, as well as ecotoxicological studies.

Developing genetic techniques for application to ecological risk assessment and long-term stewardship builds unique capabilities at the INEEL and puts the laboratory at the forefront of scientific work and the application of genetics to environmental problems. This research also opens numerous new lines of scientific inquiry related to the application of genetics to environmental issues. The experience and capabilities residing at the INEEL will provide future collaborative research opportunities with universities, other government agencies, and other national laboratories.

Long-term stewardship is one of the three proposed initiatives in the Environmental Quality mission area. Key elements of the stewardship program include site monitoring, maintenance and environmental monitoring. This research will directly contribute to the key elements by providing a mechanism to assess the long-term impacts of DOE activities on ecosystems and biological

| | Burn | SL-1 | RWMC | Atomic City |
|---|---|---|---|---|
| Burn<br>*m = 0.59%* | — | ***p* = 0.0000005** | ***p* = 0.0000005** | *p* = 0.5 |
| SL-1<br>*m = 8.36%* | Non-mut mut<br>Burn 336 2<br>SL-1 263 24 | – | *p* = 0.2663 | ***p* = 0.0000002** |
| RWMC<br>*m = 6.36%* | Non-mut mut<br>Burn 336 2<br>RWMC 574 39 | Non-mut mut<br>SL-1 263 24<br>RWMC 574 39 | – | ***p* = 0.0000009** |
| Atomic City<br>*m = 1.24%* | Non-mut mut<br>Burn 336 2<br>AC 637 8 | Non-mut mut<br>SL-1 263 24<br>AC 637 8 | Non-mut mut<br>RWMC 574 39<br>AC 637 8 | – |

02-GA51349-096

*TABLE 2. Fisher Exact Test of Independence is presented above the diagonal. Number of mutant alleles and non-mutant alleles are summarized for each pair-wise population comparison below the diagonal. m= represents the percentage of mutant alleles in each of the populations.*

processes. Collaborative efforts include Idaho State University and Savannah River Ecology Laboratory. Future collaborative efforts are anticipated with USGS-Biological Resources Division and the U.S. Fish and Wildlife Service.

Follow-on work is expected as a result of this LDRD project. This research is part of a long-term plan for building a capability at INEEL in the use of genetic markers to address environmental issues. Once the technology is established, numerous applications using other species as environmental monitoring indicators can be explored. For example, an evaluation of the effects of contaminants on mutation rates of local plants would be useful for monitoring effects on crops, such as corn or wheat, which are common in the vicinity of the site. Other applications for this technology include: monitoring of mutation rates in birds that are in potential contact with contaminated soil, such as the burrowing owl and barn swallows, as well as studies of the ecological impacts on threatened and endangered species or candidate species, such as sage grouse. The technology developed as a result of this research has the potential to determine if mutation rate changes have occurred. This information will help researchers focus resources and efforts on environmental monitoring of radiological waste disposal sites.

# Development of Collaborative Approaches to Long Term Environmental Stewardship

*Greg J. White, William Keener*

## *Understanding natural systems in the intermountain west*

ST106

Stewardship of biological resources at the INEEL is critical, yet a lack of understanding of fundamental ecological patterns and processes is a significant barrier to the development of sustainable management practices. To address local and regional environmental issues associated with long-term environmental stewardship, a collaborative research program has been established through this LDRD between Idaho State University (ISU) and the INEEL. Both ISU and the INEEL have significant scientific expertise and distinct complementary capabilities to meet these varied environmental challenges.

The research effort is focused on two areas: 1) development of enzyme-specific probes for screening and characterization of environmental samples, and 2) assessment of the effects of climate change on the stability of protective caps for isolating buried hazardous wastes.

These efforts are representative of the approaches needed to meet environmental challenges and support the DOE goal of long-term stewardship at the INEEL.

Technical objectives for fiscal year 2002:

Development of Enzyme-Specific Probes:

- Complete microcosm application testing of an oxygenase probe.
- Continue development of a chloride probe.
- Publish or present results of research in this area.

Climate Change – Effects on Protective Caps:

- Measure soil profile development on the Protective Cap Burial Experiment (PCBE) plots. Compare results in various microsites, including under sagebrush plants and away from shrub canopies.
- Complete report relating the soil profile development to the seedling recruitment in the PCBE plots.
- Determine soil profile development in relation to litter standing crop and litter fall rates in the PCBE plots.
- Develop a method for testing options for soil pretreatment to remove inorganic carbon with acid so that total carbon by combustion corresponds to organic carbon.
- Develop a protocol to measure separately the inorganic orthophosphate in solution, the organic phosphorus in solution, and the colloidal phosphorous in soil extracts.
- Publish or present results of research.

***Development of Enzyme-Specific Probes*** – FY02 research focused on the development of probes and assays to evaluate microbial processes related to bioremediation in subsurface environments. Novel approaches have been incorporated into this work, including molecular probe and coupled fluorescence microscopy techniques. The purpose for these combined approaches is to begin to move this technology into the field.

Toward that end, collaboration was established with Kent Sorenson and Ryan Wymore of NorthWind Environmental, Inc. in Idaho Falls. NorthWind provided groundwater samples from wells at the INEEL Test Area North site. The samples were used to generate field-relevant probe data and enable preliminary inferences relative to microbial activity within the system.

The investigators exposed the cells from these groundwater samples to a variety of their enzyme activity probes. One significant result, using coumarin as a probe for methane monooxygenase, was a measurable level of activity in the aerobic zone of the aquifer. This observation has relevance, since the aquifer is contaminated with TCE, which is co-metabolized by methanotrophs that produce this enzyme.

Other accomplishments in FY02 included verification of the chloroperoxidase enzyme assay to detect chlorinated solvent degradation, characterization of the 3-ethynl benzoate probe for toluene side chain monooxygenase activity detection, development of DNA and RNA probes for all 5 toluene oxygenase pathways, and evaluation of INEEL-TAN groundwater using enzyme activity probes specific for toluene oxygenases and methane monooxygenase. Four papers describing this research were published or submitted during FY02.

***Climate Change – Effects on Protective Caps*** – A manuscript on the effects of shrub removal and nitrogen addition on soil water balance in sagebrush steppe is undergoing final revisions following inclusion of data

from the 2002 field season. Vegetation was sampled again in 2002 and soil moisture measurements were taken at two to three week intervals during the growing season.

Effects of shrub removal and nitrogen addition on the quantity and distribution of soil moisture in the top 190 cm of soil have remained consistent over the last four years (Fig. 1). Shrub removal plots have more soil moisture, particularly at depths of 80 – 120 cm, and nitrogen addition plots have significantly less moisture at those same depths. These results suggest that management of vegetated caps over buried hazardous wastes might include a moderate level of nitrogen addition to maintain lower levels of soil moisture and reduce the likelihood of moisture moving through the soil and becoming contaminated by buried wastes.

Soil samples for examining the development of resource islands under sagebrush plants are now ready for analysis with completion anticipated by November 2002. Soil samples collected on the PCBE plots in the fall of 2001 have been divided into six depth fractions and sieved. Analyses of these samples are ongoing. Results will be used to assess soil profile development on the PCBE plots.

The results of a study on soil profile development in relation to seedling recruitment in the PCBE plots was presented in August 2002 at the Ecological Society of America annual meeting in Tucson, AZ, by Terence McGonigle (ISU) and Lawrence Cook (INEEL).

The capability of performing the Walkley-Black organic carbon analysis system recommended by the U.S. Department of Agriculture has been established in the laboratory. This technique is now being used routinely at ISU, providing a method for determining total soil carbon. The investigators are now comparing newly developing approaches to this standard method. A protocol for measuring the inorganic orthophosphate, the organic P, and the colloidal P in soil solution or soil extract has been established using an ICP-AES analysis system.

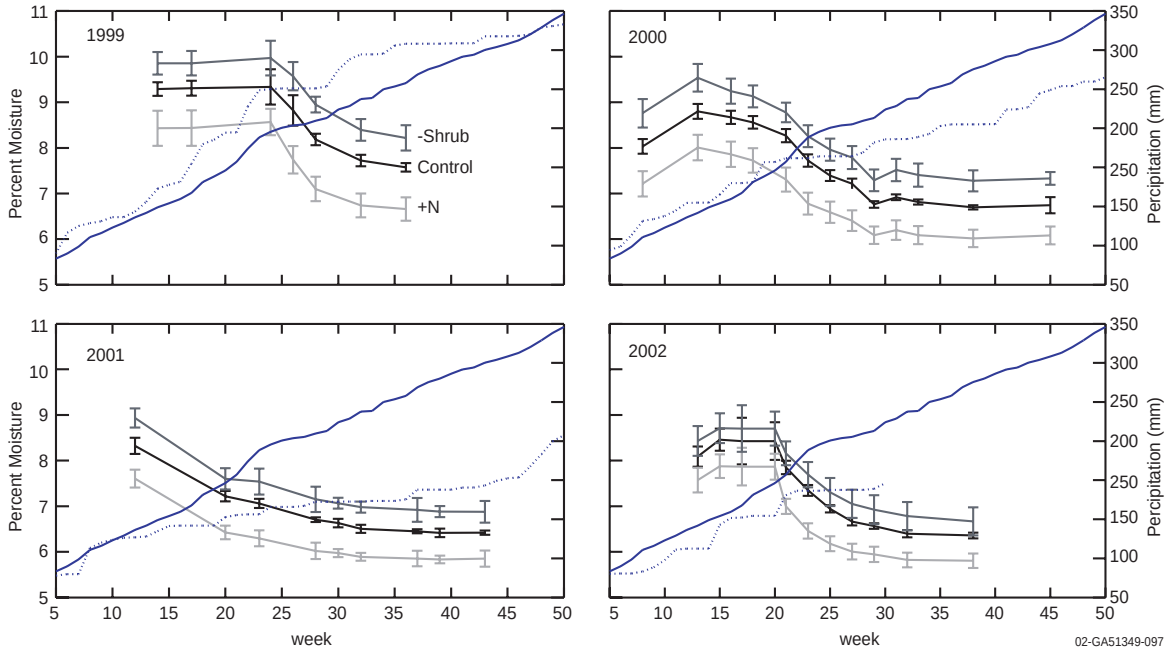


*FIGURE 1. Average soil moisture from 30 – 190 cm. The solid blue line in each graph shows average.*

Collectively, research conducted under these two tasks benefits the INEEL, and therefore the DOE and nation, by providing a better understanding of how the natural systems in the intermountain west can be managed to help protect human health and natural systems from hazardous and radioactive wastes. The research has provided an increased bank of useful subsurface techniques including subsurface microbiology methodologies, a field that is still in its infancy and expected to grow substantially over the next decades. The research has resulted in increased visibility for both the INEEL and for ISU, and the completion of several more advanced degrees by INEEL employees.

# Generation IV Nuclear Reactor Initiative

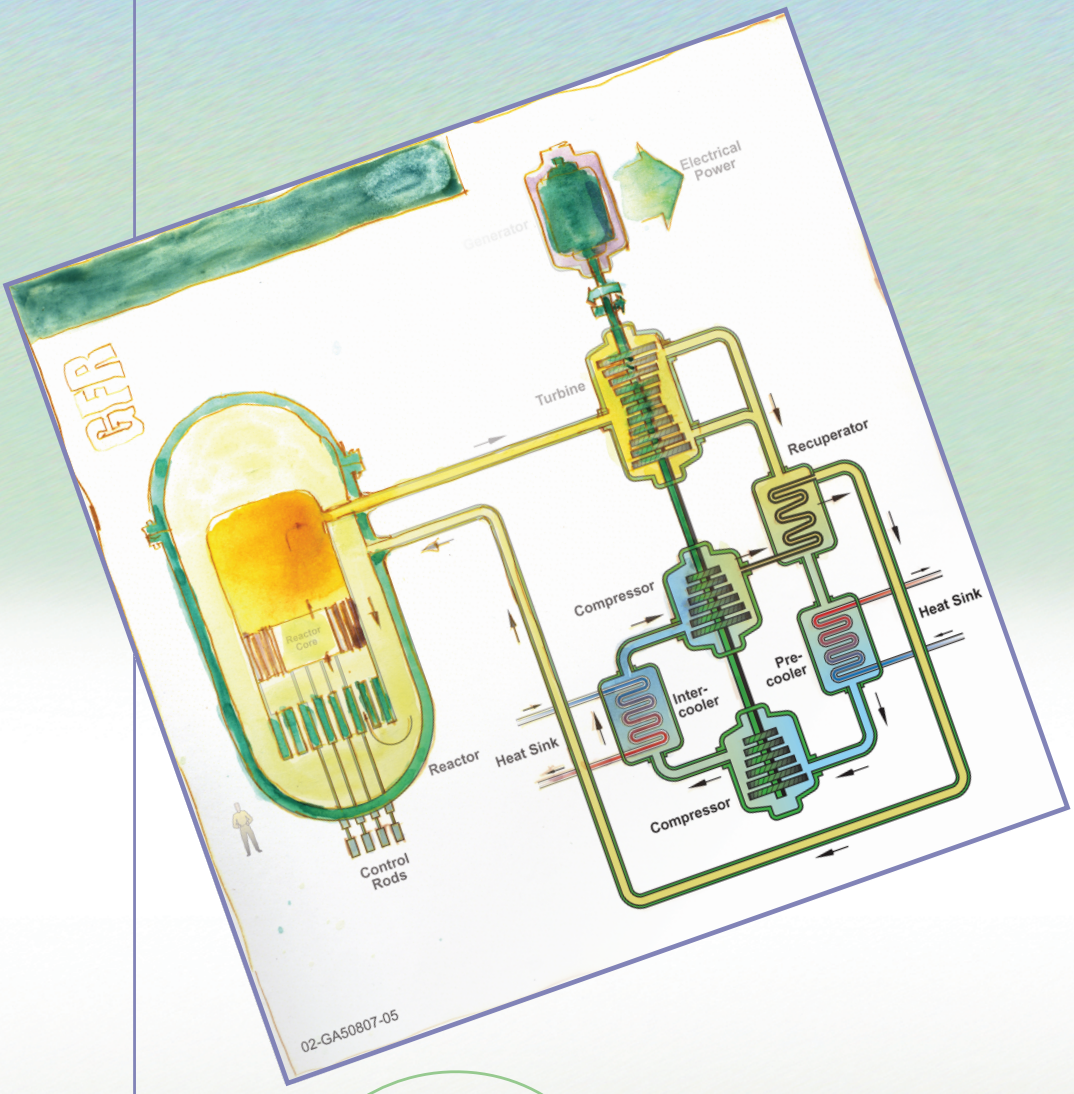


## LDRD Annual Report for FY-2002

Idaho National Engineering & Environmental Laboratory

# Advanced Transient Analysis Capabilities for Generation IV Reactors

*Edwin. A. Harvego*

## *Supporting advanced nuclear reactor concepts*

GE102

The importance of nuclear energy as a vital and strategic resource in the U. S. energy supply mix has led to the need to develop and demonstrate new and improved reactor technologies. Generation IV reactor concepts are expected to substantially improve the economics, safety, proliferation resistance and waste characteristics of current-generation reactors. Although a number of light water reactors (LWRs) have been proposed as Generation IV candidates, the majority of these concepts have fundamentally different characteristics than current operating LWRs. The intent of this three-year LDRD project is to develop and/or extend current INEEL transient analysis capabilities to support future Generation IV reactor design, development and assessment needs. The review and identification of transient analysis requirements to support new reactor technologies was completed in FY01. The development of additions/extensions to existing INEEL capabilities was initiated this past fiscal year.

Technical objectives for fiscal year 2002:

- Complete detailed conceptual designs of modeling extensions for transient analysis of gas-cooled reactors.
- Submit and present peer-reviewed technical paper for ICONE-10 conference on transient analysis of Generation IV reactors.
- Complete model development Task 1 (modeling of graphite oxidation in air and water).
- Complete model development Task 2 (heat transfer and flow losses through pebble-bed reactor cores).
- Complete model development Task 3 (conduction and radiation heat removal from a pebble-bed or graphite-block reactor core).

A review of proposed Generation IV reactor concepts, performed in the first year of this three-year LDRD project, led to the identification of both near-term and long-term transient analysis needs. The near-term development needs were those required to establish a basic capability to support anticipated DOE needs during the initial Generation IV evaluation process. The long-term development needs were those that would allow more refined analyses of the complex phenomena that will become more important as the reactor system designs evolve.

Based on the results of this LDRD's first-year study, a model design or description report was prepared defining the modeling and implementation requirement for four high-priority modeling improvements. These modeling improvements were directed at improving INEEL analysis capabilities supporting Generation IV gas-cooled reactor concepts. Although the initial intent was to focus on the pebble-bed modular reactor (PBMR) design, it was subsequently decided to develop a more general analysis capability that would allow transient modeling of both pebble-bed and graphite-block reactor core designs.

Three of the four modeling tasks outlined in the model design report were successfully implemented into the SCDAP/RELAP5-3D (severe core data analysis package/ Reactor Excursion and Leak Analysis Program) code in fiscal year 2002. The three models completed were 1) graphite oxidation in air and water, 2) heat transfer and flow losses through a pebble-bed reactor core design, and 3) 2-D conduction and radiation heat removal from a pebble-bed or graphite block reactor core following a complete loss-of-coolant accident.

The modeling of graphite oxidation includes oxidation of graphite in the core region, and in the bottom, top and side reflector regions. To evaluate the graphite oxidation modeling in SCDAP/RELAP5-3D, a simple pebble-bed reactor core model was developed and calculations were performed for two different rates of air ingress, namely 0.033 m/s and 0.066 m/s. The reactor core modeled in this case was 8.5 m in height and 3.5 m in diameter, and consisted of 90 axial nodes and 19 radial nodes (10 radial nodes in the core, 3 in the inner reflector, and 6 in the outer reflector). The fluid in the core was modeled with 90 RELAP5-3D control volumes. The results of the SCDAP/RELAP5-3D calculations with the two different air ingress rates are shown in Figure 1, which includes the temperature response of the reactor core at the 0.06-m and 0.56-m elevations above the bottom of the core. This plot shows that the heat-up of the bottom part of the core (0.06-m elevation) increases significantly with respect to the rate of air ingress. But at the 0.56-m elevation, the reactor core temperature response is not significantly influenced by the ingress of air. This

behavior is the result of graphite oxidation being limited by the bulk flow-rate of the air. For these rates of air ingress, a significant amount of the oxygen in the air was calculated to be consumed by oxidation of the graphite reflector below the fueled part of the reactor core, and virtually no oxygen was available for oxidizing graphite at the higher reactor core elevations above about the 0.2-m elevation.

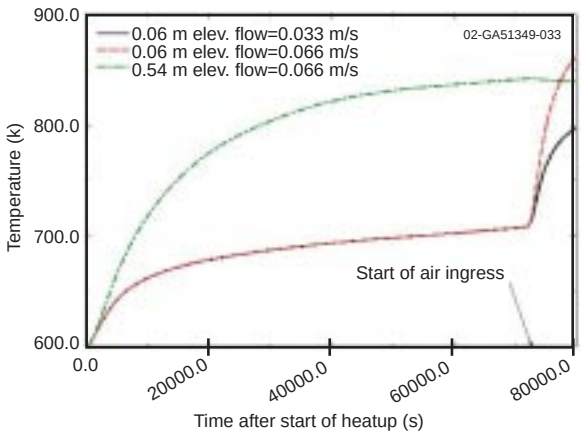


*FIGURE 1. Calculated reactor core temperature responses due to graphite oxidation.*

The results of Figure 1 also reflect extensions in SCDAP/RELAP5-3D for modeling of heat transfer and flow losses through a pebble-bed reactor core. This capability was added primarily to address PBMR gas-cooled reactor designs. Limited testing of this modeling capability has been performed for a large-break loss-of-coolant accident in a pebble-bed helium-cooled gas reactor using available helium and air properties in SCDAP/RELAP5-3D. This modeling capability also could be applied to other gas-cooled pebble-bed reactor designs (e.g., $CO_2$-cooled reactor designs), as well as supercritical-water or liquid-metal reactor concepts with pebble-bed core configurations, provided that the appropriate thermodynamic properties and convective heat transfer correlations were added to the code.

The modeling of 2-D conduction and radiation heat transfer was added specifically to address the transient response of the high heat capacity gas-cooled graphite reactor core designs following a complete loss-of-coolant accident. Under these conditions, removal of decay heat from the reactor core is primarily by conduction and radiation from the core, through various gaps and structures of the reflector region, core barrel, reactor vessel, and containment to the surrounding earth. The capability for 2-D modeling of these conduction/radiation heat transfer paths was initially developed for pebble-bed reactor designs, but was subsequently extended to include graphite-block reactor core designs.

The above described model development activities have established a basic capability to analyze the various helium-cooled gas reactor concepts recommended for continued development under the Generation IV reactor initiative. The only remaining modeling capability included in the initial design report, but not implemented in SCDAP/RELAP5-3D, is the ability to calculate the transport of air or water from a reactor primary system break to the reactor core by molecular/mass diffusion. This modeling capability was not added because of the reduced LDRD funding in FY02, but will be considered along with other remaining model development needs for inclusion in the FY03 work scope.

As the lead laboratory for Nuclear Energy, INEEL is in a position to provide strong technical leadership in support of DOE's Generation IV reactor initiative. Although INEEL is a recognized leader in light water reactor safety analyses, the laboratory's capability to perform transient analyses of other reactor concepts is limited. Therefore, the advanced transient analysis capabilities being developed through this LDRD will position the INEEL for major roles in support of DOE's Generation IV reactor initiative and related missions. The development of these essential capabilities is intended to coincide with the evolving development of Generation IV reactor concepts so that the INEEL capabilities will be available when needed by DOE and its Generation IV partners.

In addition to potential follow-on work associated with DOE's Generation IV reactor initiative, the development of advanced reactor transient analysis capabilities may lead to externally funded collaborative research and development in other areas.

# Advanced Nuclear Fuels for Enhanced Proliferation Resistance

*J. Stephen Herring*

## *Investigating Thorium-based fuels for light water reactors*

GE104

Advanced fuels for thermal reactors will be needed in the future to reduce the production of plutonium for proliferation resistance and to create robust fuel/waste forms. The fuel/waste form matrix holds the fission products and actinides in a permanent repository or in temporary storage waiting reprocessing. Thoria ($ThO_2$) fuels appear promising as a matrix for plutonium and the minor actinides during mono recycling in light water reactors (LWR). Thorium-based fuels reduce the total amount of plutonium produced and produce a mixture of plutonium isotopes high in $^{238}$Pu. Because of the high decay heat and spontaneous neutron generation of $^{238}$Pu, this isotope provides intrinsic proliferation resistance. Thoria also is difficult to dissolve, making the diversion of spent fuel for weapons production more difficult.

This LDRD is determining if thorium-based fuels can be used to further increase the proliferation resistance of light water reactor (LWR) fuels. Some of the proliferation concerns in the world today stem from plutonium that has already been separated from spent fuel. Currently, separated plutonium is being incorporated in $UO_2$-$PuO_2$ mixed oxide (MOX) fuel. However, because MOX fuel contains ~90 wt % $^{238}$U, substantial amounts of $^{239}$Pu are produced in the MOX fuel and net plutonium burnup rates are only 30% to 40% per cycle. The incorporation of plutonium into a $ThO_2$ matrix consumes already-separated plutonium without breeding additional $^{239}$Pu. The minor actinides (MA) (e.g. neptunium, americium, curium, berkelium, californium, etc.) are included in the $ThO_2$ to further reduce the long-term radiotoxicity of the fuel cycle. The overall result of a single transmutation cycle using thorium-based fuels in an LWR is a reduction of fissile plutonium of 67% and of the minor actinides by 58% to 81%.

Technical objectives for fiscal year 2002:

- Analyze the Th-U-Pu-MA oxide fuel to determine spatial and temporal evolution of isotopic content while in multiple cycles in a light water reactor.
- Determine spatial fission profiles and reactor kinetic parameters for the proposed fuel array.
- Present different aspects of the proposed fuel cycle at technical meetings.

The goals of this recycling strategy are to reduce overall inventories of plutonium, to render the resulting spent fuel as proliferation-resistant as possible through the accumulation of $^{238}$Pu, $^{240}$Pu, $^{242}$Pu and $^{232}$U, to consume the minor actinides, and to produce a very robust waste form. A schematic of the mono-recycling strategy is shown in Figure 1. In this fuel cycle, the LWR fuel assembly consist of 89% standard $UO_2$ fuel rods with a $^{235}$U enrichment of 4.95 wt %. The plutonium and minor actinides produced in earlier standard rods are separated and placed in thoria-urania pins occupying 11% of the positions in the fuel assembly. The goal of the mono-recycling strategy, or "twice-through fuel

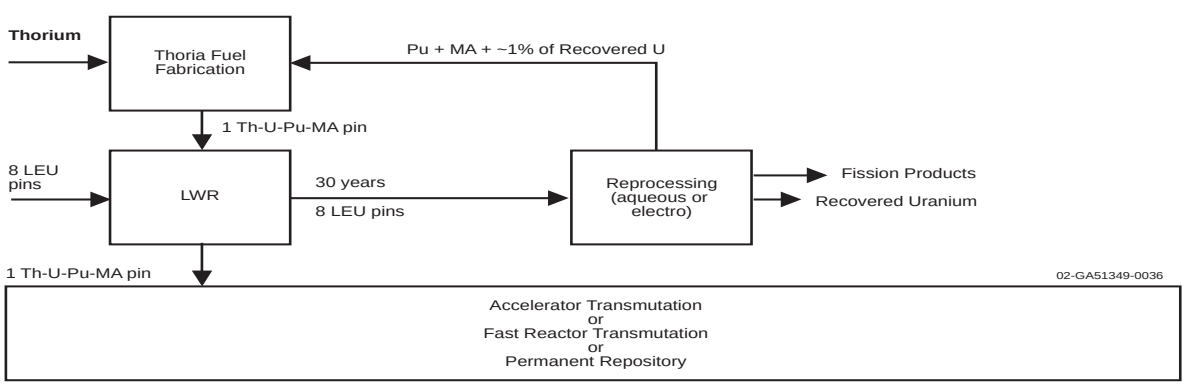


*FIGURE 1. Mono-recycling strategy for light water reactors.*

cycle," is to transmute the majority of the long-lived actinides in existing LWRs and to discharge a fuel-form that is a very robust waste form with an isotopic content that is very proliferation resistant.

In this project, a model has been used consisting of nine fuel pins, eight of which are standard $UO_2$ pins and one of which is a $(Th\text{-}U\text{-}Pu\text{-}MA)O_2$ transmuter pin. The plutonium and minor actinides are derived from $UO_2$ fuel irradiated to 45 MW-d/kg and reprocessed 30 years after discharge. In the various cases analyzed, the center pellet contained 0-10 wt% recovered uranium and 6-15 wt% Pu+MA. The recovered uranium (98.5 wt% $^{238}U$) was included to denature the $^{233}U$ below the 12 wt % limit for low enrichment uranium (LEU). For these analyses, the burnup code MOCUP, which uses the Monte Carlo transport code MCNP, and the exponential matrix generation and depletion code ORIGEN2, were used. MOCUP was used with 60-day timesteps, and tracked the generation and depletion of 50 fission products and 38 actinides. The model has white reflecting boundaries to simulate an infinite array. The eight outer pins are modeled as eight individual fuel zones and the center pin is divided into 20 equal-volume zones.

An example of the inventory variations of the $^{233}U$/total U, $^{238}Pu$/total Pu and $^{239}Pu$/total Pu for the center pellet, which at BOL contained 10% wt % recovered uranium and 15 wt % Pu+MA, is shown in Figure 2. Note that the $^{239}Pu$ as a fraction of total plutonium decreased from 70% to 20%. At the same time, the $^{238}Pu$ fraction of the total plutonium increased from about 2% to 20%. Thus, any plutonium extracted from the discharged fuel would have high decay heat and spontaneous neutron production, and would not be attractive for use in weapons. In addition, $^{233}U$ as a fraction of the total uranium content remains below 12%, making the uranium very resistant to weapons use.

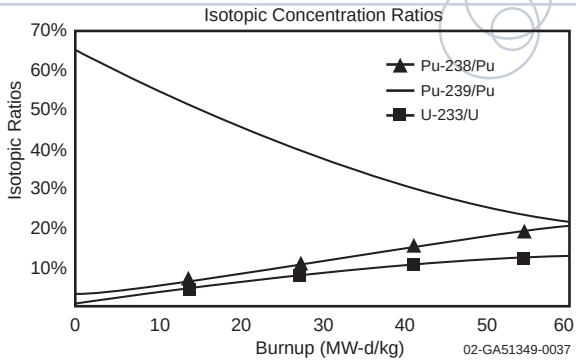


*FIGURE 2. Isotopic concentration ratios of importance to proliferation resistance.*

Use of thorium-based fuels contributes to the development of fuels with increased proliferation resistance. In particular, the intrinsic resistance of plutonium mixtures with high $^{238}Pu$ is enhanced through high-decay heat and spontaneous neutron production. Use of thorium-uranium fuels, and perhaps fuels with non-fertile matrices, shows promise as LWR transmuter fuels that would significantly reduce the amount of plutonium, neptunium and its precursors going to a permanent repository or to long-term interim storage. Furthermore, these transmuter fuels used in mono recycling significantly decrease the volume of spent fuel going to a repository while greatly increasing the proliferation resistance and waste form durability of the resulting fuel. Work continues in the analysis of non-fertile and thorium-based LWR transmuter fuels.

This LDRD research is contributing to the Advanced Fuel Cycle Initiative (AFCI). The goal of the AFCI is to greatly reduce the repository capacity needed for a continuing, sustainable nuclear fuel cycle.

# Design of an Actinide Burning, Lead or Lead-Bismuth Reactor That Produces Low Cost Electricity

*Philip E. MacDonald, Jacopo Buongiorno, Cliff Davis, Steve Herring, Eric Loewen, Kevan Weaver*

## *Safely meeting the world's expanding energy needs*

GE105

As the earth's population grows so will the demand for energy. Simply expanding energy use based on today's mix of production options will continue to have adverse environmental impacts and potential long-term consequences from global warming. Currently nuclear power plants produce 16% of the world's electricity. However, new and better reactor designs are needed to compete economically with coal-and natural gas-fired power plants while maintaining safety, increasing proliferation resistance and minimizing waste.

The purpose of this LDRD is to investigate a lead or lead-bismuth cooled fast reactor for producing low-cost electricity as well as for actinide burning. A reactor system of this type could potentially provide sustainable energy generation that meets clean air objectives, minimizes and manages its nuclear waste to reduce long-term stewardship concerns, excel in safety and reliability with a very low likelihood and degree of reactor core damage in the event of an accident, as well as other benefits. This LDRD is identifying and analyzing the key technical issues in core neutronics, materials, thermal-hydraulics, fuels, and economics associated with the development of this reactor concept.

Technical objectives for fiscal year 2002:

- Design a heavy metal-cooled reactor core for the Actinide Burner Reactor (ABR) that can achieve excellent safety and a high transuranic destruction rate.
- Assess the feasibility of a gas-lift pump approach for the ABR.
- Determine the response of the ABR to a variety of transients.
- Design the pumps needed for the ABR.
- Redesign the heat exchangers and assess their behavior during accidents.
- Optimize the recuperator and develop preliminary designs for the main components used in the supercritical-$CO_2$ Brayton cycle for the secondary side.
- Determine the ABR capital cost.
- Determine the corrosion behavior of commercially available and tailored fuel cladding and core structural materials.
- Complete the studies on polonium-hydride kinetics.
- Design a rare-earth filter that removes polonium from the lead-bismuth eutectic coolant.
- Assess polonium removal by alkaline extraction.

Work has been accomplished in four major areas of research: core neutronic design, plant engineering, material compatibility studies, and coolant activation. About 50% of the work was performed at the Massachusetts Institute of Technology (MIT) under subcontract to the INEEL. The ABR design was essentially completed during FY02.

***Neutronic design:*** The major focus of the neutronic analyses in FY02 was on the design of a core that can achieve excellent safety through self-controllability (as in the Integral Fast Reactor [IFR]) and high transuranic destruction. The analyses were performed for metallic thorium-based fuel (Th-U-Pu-MA-Zr) in a once-through cycle assuming that the discharged fuel from the ABR remains in temporary storage before multi-recycling is introduced.

Using thorium as the prime fertile material was found to be an effective means to reduce the large reactivity swing occurring in fertile-free cores while still allowing a high net actinide destruction rate per MWth. In addition, thorium use increased the Doppler feedback in comparison with fertile-free fuels and reduced the coolant density reactivity coefficient. Both the Doppler and fuel thermal expansion feedbacks were negative and their values were comparable to those for the IFR fuel.

The ABR destruction rate of actinides per MWth-yr was ~35% less than the destruction rate in the fertile-free critical ABR but only 20% less than in an accelerator-driven facility (due to the higher capacity factor in the ABR). This is a very appealing feature considering the simplicity of the proposed reactor versus the more complex accelerator-driven system.

The discharged fuel from the ABR satisfied proliferation constraints for both the plutonium and uranium compositions. Plutonium isotopics were significantly degraded from that of the pressurized water reactor (PWR) spent fuel vector making it virtually weapons unusable. Also, the fraction of in-bred U-233 remained

below 12% if depleted uranium was mixed with the thorium (~30wt% of uranium in the U+Th mixture).

The high coolant void worth typical of liquid metal-cooled fast reactors (especially those with minor actinide fuel) can be effectively mitigated by the employment of streaming fuel assemblies yielding a negative coolant void worth and a very small positive coolant temperature coefficient.

The combination of reactivity coefficients satisfied the requirements of self-control throughout the cycle so that, in concert with the passive decay heat removal design, all transients without scram led to an inherent shutdown without exceeding safe fuel and structural temperature limits.

The fuel cycle cost of the once-through cycle was found to be significantly higher than that of the multi-recycle scheme (about 30 versus 15 mills/kW-hr, best estimate). Therefore, considering fuel cycle economics and the small potential for reduction of long-term radiotoxicity and heat load on the repository from the wastes of the LWR (light water reactor)/ABR system, the once-through fuel cycle was discarded from future considerations. In comparison with an accelerator-driven facility, the fuel cycle cost of the ABR in the multi-recycle scheme was slightly smaller, but both the accelerator-driven facility and ABR fuel cycle costs were well above current LWR fuel cycle costs, even if lower bound values were used (the lower bound value for both the accelerator-driven facility and the ABR is about 9 mills/kW-hr versus about 3 mills/kW-hr for light water reactors).

In summary, the proposed design of the seven-year life core for burning transuranics from spent LWR fuel appears to be very promising and deserving of future refined analyses and optimization. It offers high consumption of actinides, excellent safety characteristics, and has the potential to have low electricity generation cost due to its modularity, simplicity, and high capacity factor. The only drawback is a high fuel cycle cost, which is inherent to all actinide-burning systems because of the currently high fuel reprocessing costs.

***Plant engineering:*** The feasibility of a gas-lift pump approach for the ABR was assessed. Gas-lift pumping of the lead-bismuth-eutectic (LBE) coolant in this case will require generation of a 53% void fraction in the chimney resulting in 2.3 m swelling of the liquid level. Such a large swelling of the liquid level would require design of a much longer vessel. The gas flow rate required to sustain a 53% void fraction in the chimney is 1.6 kg/s. The gas would be injected at the bottom of the chimney at a pressure of about 800 kPa. The pumping power would be about 5.1 MW versus 3.8 MW for a mechanical pump. Finally, the 1.6 kg/s helium mass flow rate corresponds to a 28 $m^3$/s volumetric flow and to a 3.8 m/s helium superficial velocity at the free liquid surface, enough to entrain considerable amounts of LBE, which would then have to be removed before the compressor inlet. These results clearly demonstrate that a gas-lift pump approach is not feasible for the ABR.

The ATHENA code was used to determine the response of the ABR to a variety of transients, including pump trip, station blackout, reactivity insertion, heat exchanger tube rupture, turbine stop valve closure, steam line break, loss of feed-water preheating, and loss of coolant from the reactor cleanup system. The transients were simulated without reactor scram to demonstrate the safety margins inherent in the reactor design. The ABR design successfully met the identified cladding, fuel, and guard vessel temperature limits for each of the transients analyzed. The cladding temperature was always closer to its limit than the fuel and guard vessel temperatures. The most limiting transient is initiated by a station blackout. The station blackout coupled with a failure to scram produced a peak cladding temperature that was equal to the transient limit. A steam line break does not result in significant overcooling in the actinide-burner reactor. The overcooling potential is limited by the small water inventory in the heat exchangers compared to the heat capacity of the lead-bismuth coolant. The transient initiated by a heat exchanger tube rupture resulted in the highest cover gas pressure of the cases evaluated. Because of the high pressure on the secondary side of the heat exchangers, a relief valve will be required to protect the reactor vessel. The maximum pressure is governed by the relief valve capacity and set point. It was set to open at 0.2 MPa in this analysis. Also, a loss-of-coolant accident (LOCA) sequence involving the coolant cleanup system was analyzed and the ABR was again found to be passively safe.

During FY02 two major improvements were made to the metal-fuel model developed in FY01, and the revised model was benchmarked with metal-fuel irradiation data from the IFR development program. First, better constitutive equations for the irradiation creep and thermal creep of the cladding material HT-9 were added to the code. The second improvement allowed for non-constant temperature, dose, and linear heat generation rate during irradiation. The new version of the model can simulate the behavior of a metal fuel pin with arbitrarily changing operating conditions.

Work on pump selection illustrated that a centrifugal pump can meet the ABR pumping needs. These needs also can be met by two pumps that will neatly fit within the 1.05 meter annular gap between the reactor vessel and the core chimney.

The reevaluation of the heat exchangers reaffirmed that the 700 MWth of core power can be transmitted to the power cycle. The new design is a baffled, cylindrical shell and tube heat exchanger with a modular design. Eight cylindrical heat exchangers have replaced the two original kidney-shaped components identified in the FY01 design. Each heat exchanger is 9.0 meters in length with an inside shell diameter of 1.0 meters. As before, the LBE coolant circulates on the shell side and the secondary coolant in the tubes, which have a triangular pitch. Three secondary-side heat exchanger variants were presented: superheated steam, supercritical steam, and supercritical $CO_2$. The worst-case heat exchanger accident with either a steam or $CO_2$ cycle was assessed. The hazardous result investigated was formation of lead oxide (PbO) in the primary coolant system, which could block or disrupt flow paths. The investigators determined that reactions that could lead to lead oxide formation were too slow to result in significant oxide formation in the event of a tube rupture.

An initial investigation of a supercritical steam cycle was performed to determine if it is a desirable alternative to either the superheated steam or supercritical $CO_2$ power cycles. The net efficiencies obtainable with the supercritical steam cycle were competitive with those of the supercritical $CO_2$ power cycle. However, the balance of plant design with the $CO_2$ power cycle is much simpler.

Work was performed during this fiscal year to optimize the recuperator and develop preliminary designs for the main components used in the supercritical-$CO_2$ Brayton cycle. The need for effective recuperators led to consideration of compact heat exchangers. To accommodate the high pressure differential across the recuperator, printed circuit heat exchangers manufactured by HEATRIC were selected. The most important factors for the performance evaluation were the heat exchanger geometry and flow arrangement. The diameter of the semicircular channels was selected as 1 mm. The heat conduction characteristic length was assumed to be equal to the plate thickness, even though it is likely to be smaller. The precooler design is significantly simpler than the recuperator design. However, the same type of heat exchanger is used. The precooler is designed to minimize the pumping power of the cooling water and pressure drop on the gas side and still have an acceptable size.

The preliminary design of the turbo-machinery was completed. A very encouraging finding is that the turbo-machinery size is miniscule compared to any other currently used fluid — about 30 times smaller than conventional steam turbines and about 5 times smaller than helium turbo-machinery. The preliminary efficiency calculation results are close to 92% efficiency (accounting for kinetic energy losses). The size of a 300 $MW_e$ turbine is about 1 m long and 0.8 m in diameter with approximately five stages. A similar evaluation was performed for the compressors, giving on the order of two and three stages for the main and recompressing compressors respectively. Overall, the cycle components are compact and their design should not impose significant requirements on research and development.

A capital cost analysis for the ABR was performed. The basis for this analysis was the 1994 Advanced Liquid Metal Reactor (ALMR) capital cost analysis. The table below presents a realistic comparison of the capital costs of the ABR and the ALMR. (The plant type labeled F is a first-of-a-kind plant and the type labeled N is a nth-of-a-kind plant. The number (1 or 3) distinguishes between power plants with one or three power blocks.)

The ALMR report costs were adjusted and scaled to account for differences between the two plants. Major differences include the absence of an intermediate heat transport loop in the ABR, differences in materials due to corrosion concerns, and the differences between the reactor vessels and heat exchangers. There is some uncertainty in the capital cost analysis due to the incomplete information available on the ALMR capital cost analysis. This uncertainty was quantified and a range of values for the capital cost of the ABR was provided. In all but the worst cases, the ABR is competitive with the ALMR plant. In many cases, the ABR has a capital cost advantage on a dollars per kilowatt-electric basis.

**Comparison of ALMR and ABR capital cost (constant *F* = 0.25)**

| Plant Type | ALMR Total Cost (2002 $/kWe) | ABR Total Cost (2002 $/kWe) |
|---|---|---|
| F1 | 2,761 | 2,542 |
| F3 | 2,120 | 1,991 |
| N1 | 2,196 | 1,938 |
| N3 | 1,801 | 1,661 |

02-GA51349-038

*TABLE 1. Comparison of ALMR and ABR capital cost (constant F = 0.25)*

***Material studies:*** LBE corrosion tests of several commercially available U.S. steels were performed in FY02 in which measurements were taken of the interaction layer with respect to time, temperature, and alloy type to quantify the damage rates. Corrosion coupons of HT9, 410, 316L, F22, and iron with three different level of silica (1, 2 and 3 wt.%) were tested at 550° to 700° C at time steps of 100, 300, 600, 700, and 1,000 hours inside corrosion cells made from hafnium stabilized zirconium alloy and 410 stainless steels. Only detailed results from the zirconium corrosion cells were obtained in FY02. Various zirconium alloys also were tested for 100 to 1000 hours at 550° to 700° C. At low temperatures (<550° C) zirconium has good corrosion resistance to LBE due to the presence of an adherent oxide layer. At higher temperatures (650° C and above), the zirconium alloys are easily dissolved by the LBE. The oxygen potential was controlled within a range of about $10^{-27}$ to $10^{-40}$ atm, using solid carbon to remove excess oxygen as carbon dioxide and reduce any PbO formed. Scanning electron microscope (SEM), energy dispersive X-ray (EDX), and inductively coupled plasma (ICP) analyses were performed on the samples to determine the depth of the interaction (corrosion) layer, and the composition of the LBE and interaction layer.

The pre-oxidized hafnium stabilized zirconium corrosion cells resulted in a liquid phase chemistry that affected the sample corrosion/dissolution in the loop, especially during Experiment 11 (650° C). The zirconium in solution in the LBE slows down the corrosion of some of the alloys by forming a layer of zirconium compounds on the surfaces and by consuming excess $O_2$. It was observed that the interaction layer formation rates of the HT9 and 316-stainless steel at 550° and 650° C are best represented by a logarithmic fit to the data. The 316L stainless steel interaction layer formation rates at 550° C were relatively low. However, the 316L stainless steel had relatively large interaction layers at 650° C. This degradation of the 316L stainless steel seems to be connected to the mass transfer of the Ni, as indicated by the ICP results. The interaction layer formation rates of the F22 low alloy steel and the 410-stainless steel at both temperatures were approximately linear. The F22 low alloy steel exhibited the highest interaction layer formation rate at 550° C but the lowest rate at 650° C. This result is probably due to the presence of the zirconium/hafnium layers on the samples in the 650° C test.

During this past year the effort also has been focused on the testing of selected refractory metals and initial testing of model Fe-Si alloys. This testing is part of an effort to develop a science-based alloy development program with the goal of developing an advanced iron-based alloy specifically optimized for Pb and Pb-Bi service. Two rotating electrode facilities have been built to conduct dynamic corrosion tests in Pb or Pb-Bi alloy coolants under isothermal conditions. The oxygen potential is controlled using the equilibrium reaction between $H_2$, $H_2O$ and $O_2$ and a mixing and monitoring system. The systems are capable of operating at temperatures up to 1000° C.

The refractory metals exhibit very little degradation when exposed to liquid Pb or Pb-Bi. However, the attack of pure iron by lead is quite severe and thus confirms the need for protective measure for the iron when operating at low oxygen potentials. The depth of the interaction layer on the Fe-1.24% Si alloy exposed to Pb for 100 hours at 600°C under reducing conditions was about 20~28 µm. The Fe-2.25% Si alloy was exposed for 100 hours in molten lead at 600° C and the reaction with the Pb was very minor with no intergranular penetration observed. There also was some enrichment of the silicon on the surface. The surface layer for the Fe-3.82% Si material showed a more compact interaction layer when compared with those with lower silicon content and enrichment of silicon in the surface region. These results suggest that greater than 2.25% silicon will be needed to protect iron-based alloys from molten lead.

An SEM micrograph of a Fe-1.24% sample tested in Pb-Bi eutectic (44.5% Pb, 55.5% Bi) for 100 hours indicated that bulk materials (mainly iron oxide formed during the heat-up period) were removed from the sample surface and incorporated into the deposited Pb-Bi layer leaving a compact but severely damaged interface between the Pb-Bi and bulk metal. The interaction layer of a Fe-2.55% Si alloy sample after exposure to Pb-Bi eutectic at 600° C for 100 hours consisted of a detached iron oxide layer with Pb-Bi at the interface with the metal. It is believed that the iron oxide formed during the heat process. Based on a comparison with the Pb case, it appears that Pb-Bi is more aggressive than Pb alone. The results of the Fe-Si series of tests show very promising behavior, especially in molten lead. As expected, a silicon-rich layer formed on the surface during exposure due to the selective dissolution of the iron. Since the solubility of silicon is much lower than iron in Pb and Pb-Bi, it is expected that the enriched layer will continue to grow during exposure and limit further dissolution. If the oxygen potential is high enough there will come a point where $SiO_2$ is stable and a protective oxide layer will form.

***Coolant activation*:** Studies on polonium-hydride kinetics were completed. The kinetic constants for the polonium-hydride formation reaction were calculated and found to be roughly independent of temperature and increase with hydrogen concentration. Sorption of polonium on rare earth (i.e., praseodymium) foils also was explored as a means to remove polonium from the LBE coolant. The formation of a praseodymium oxide film on the surface of the foil greatly impaired sorption, and should be avoided. Conceptual design of a rare-earth filter that removes polonium with an efficiency of 92% was completed. Also polonium removal by alkaline extraction was investigated using tellurium as chemical surrogate. Preliminary experiments show that alkaline extraction can be effective in cleaning up LBE, as the tellurium concentration in the LBE was reduced by three to four orders of magnitude upon contact with molten sodium hydroxide at around 500° C. Furthermore, five candidate materials (graphite, alumina, nickel, nickel-chromium and zirconium) were evaluated for the reaction crucible, which has to withstand high-temperature molten LBE and NaOH for up to 24 hours. SEM and ICP analyses indicate that zirconium has the best compatibility for this application.

The DOE has recently completed a technology roadmap for Generation IV nuclear energy systems, identifying six concepts that have the potential to meet the energy needs mentioned above in a more sustainable, economic and safe manner than current reactors. One of those six concepts is the Lead-cooled Fast Reactor System that has been the subject of this LDRD project for the last two years. The work done in this LDRD puts the INEEL in an excellent position to support the development of this reactor concept for the DOE.

# Development of a Nodal Diffusion Method for the General Cylindrical Geometry Reactor Core

*Abderrafi M. Ougouag, William K. Terry*

## *Creating new analytical tools to study new reactor physics*

GE106

The Pebble-Bed Reactor (PBR) is a leading candidate for near-term deployment as a simple alternative to complex water-cooled nuclear reactors. This reactor is essentially a cylindrical vat filled with billiard-ball-size fuel pebbles that move slowly from the top to be removed at the bottom. Thus, its core is inherently cylindrical, unlike the cores of water-cooled or prismatic gas-cooled reactors. It follows that the analytical tools for reactor physics studies of PBRs must be based on cylindrical geometry.

The PBR core will not generally be axisymetric. If control or emergency shutdown rods are present, they will occupy discrete azimuthal locations. Since recirculated pebbles are dropped onto the entry plane somewhat randomly, it is certain that some azimuthal asymmetries will develop in the distribution of burnup. In fact, the potential for development of "hot spots" is a serious regulatory concern. Therefore, complete analysis of reactor physics in PBRs requires fully 3-D treatment in cylindrical geometry.

Numerical techniques for solving the neutron diffusion equation include finite-difference and nodal methods. Nodal methods are greatly preferred over the older finite-difference methods both for their superior accuracy and greater computational efficiency. Nodal methods solve the equation analytically in a coarse spatial mesh to achieve much greater accuracy in much shorter computation times. However, no computer code presently exists that is based on a rigorous, fully analytical mathematical formulation of a nodal method in 3-D cylindrical geometry because of a mathematical impasse that led all previous investigators either to fail or to appeal to heuristic approximations.

The objective of this LDRD is to produce a computer code that solves the neutron diffusion equation in azimuthally asymmetric 3-D cylindrical geometry by the nodal method.

Technical objectives for fiscal year 2002:

- Obtain solutions for the center node and the external boundaries. The rigorous mathematical solution for the interior nodes had been found in FY01, but the central node and external nodes require a different treatment.
- Write a computer code to implement the nodal solution obtained in this work.

There are two approaches to the implementation of a nodal method. One approach is a completely nodal formulation of the solution. The investigators' FY01 accomplishments are fully amenable to this approach. However, all the coding required for this solution approach would have to be written from scratch. The other approach is called a Coarse-mesh Finite-Difference (CMFD) formulation. In the CMFD method, the framework of an existing finite-difference diffusion solver can be applied, using a coarser mesh description in the geometrical input than what is needed in regular finite-difference solutions. Information from the nodal solution is cast into the form required by the finite-difference solver. The total shift from a full, standalone nodal implementation, and one based on the CMFD approach also was made necessary by the midyear reduction of this LDRD budget. (The coding of full standalone nodal code not relying on the CMFD formulation remains a desirable goal, as it would ultimately provide a computationally more robust method.)

As a result of a separate LDRD, a finite-difference solver specifically formulated for cylindrical geometry was already available in PEBBED. In FY02, the finite-difference solver was upgraded to three dimensions using a formulation developed in the present LDRD. Originally, application of the CMFD approach to the NESTLE solver in the RELAP5 code was considered. It was decided that that application would not be as fruitful for this investigation as the implementation in PEBBED.

The CMFD approach to implementing the nodal solution was pursued. This decision required a reformulation of the nodal solution, which has been accomplished. The reformulated solution is now being coded within PEBBED. The implementation of the CMFD technique in PEBBED had to wait on the completion of PEBBED's 3-D finite-difference solver. The coding will continue in FY03.

In the mid-year progress report, it was stated that the nodal solution found in FY01 had been described in detail in a draft external report and summarized in a technical note to be submitted to an archival journal. The external report has been issued, but publication or presentation was postponed awaiting numerical results.

As part of the development of the nodal method, benchmarks must be prepared for comparison with other methods. To that end, calculations are being performed with the Monte Carlo code MCNP. These calculations are related to issues of practical interest in PBR technology. The results obtained from these calculations have been published.

In summary, the following goals were accomplished this fiscal year:

- Solutions for the center node and external boundaries were found.
- The 3-D cylindrical-geometry finite-difference equations were coded in PEBBED.
- The nodal portion of the CMFD was formulated.
- The CMFD code architecture was established.
- Five papers were presented or accepted for presentation at conferences to present the work from MCNP and PEBBED calculations.

Future work on development of the nodal method and the related PBR project will continue. The LDRD work scope for next year investigates kinetics issues in PBRS – i.e., the analysis of short-time-scale transients in which the motion of the fuel can be ignored.

# Modular Pebble Bed Reactor

*David Petti*

## *Benchmarking core design tools*

GE101

The Modular Pebble-Bed Gas-Cooled Reactor (MPBR) is a leading Generation IV reactor concept for an electric generation station, the viability of which has been proven by the operation of experimental MPBR reactors. However, many technical issues must be addressed before construction of MPBR reactors becomes commercially practical. This LDRD explores some of these issues, building on the strong capabilities at INEEL and Massachusetts Institute of Technology (MIT) for reactor core neutronics, thermal hydraulic design, and nuclear safety analysis. INEEL and MIT are involved in the development of fuel performance, neutronics, thermal hydraulics, and safety analysis computational models necessary to design the MPBR. This work is focused on developing and benchmarking these core design tools so that INEEL can assess the key technical issues associated with the technology.

- Technical objectives for fiscal year 2002:
- Improve the flux solution in the PEBBED code by adding azimuthal (q) dependence to the (r,z) geometry.
- Support the Georgia Institute of Technology in developing its perturbation technique into a cylindrical-geometry module for calculating cross sections.
- Install a more comprehensive set of equations to track the evolution of actinide isotopic species for proliferation studies.
- Continue air ingress studies on pebble-bed reactors, including sensitivity studies.
- Develop a fission product chemistry module for the fuel performance code PARFUME.

Research in FY02 focused on advancements in the PEBBED code and the application of PEBBED and the Monte Carlo code MCNP to address problems of practical interest in pebble-bed reactor (PBR) technology. The advancements in PEBBED include development of a 3-D version, improvements in the matrix formulation of pebble recirculation, enhancements of the depletion solver, and development of heat-transfer models.

Development of a 3-D version of PEBBED (PEBBED3) was begun. In PEBBED3, there are two options for the solution of the neutron diffusion equation in general 3-D cylindrical geometry. The first option is a standard finite-difference solution. This option is now fully operational. The second option is a nodal solution that is still being implemented.

Many pebble-bed core designs feature a two-zone core that may yield improved fuel economy and heat transfer over randomly loaded single-zone cores like the HTR Modul. For example, the South African PBMR consists of a graphite central zone and a fueled outer zone. The relative sizes of the zones are determined by the relative flow rates of pebbles through the inner and outer loading tubes. There is no physical barrier between the zones. In burnup-dependent two-zone cores, pebbles are loaded fresh into one zone and, at some point in their burnup history, transferred to the other zone. Previously, such cores were modeled in PEBBED by manually generating the recirculation matrix “off-line” and reading it into the code. The matrix algorithm was upgraded in PEBBED3 to generate the recirculation matrices internally and automatically for multiple pebble types, tracing independent paths through two-zone cores. Complex cores of this type can be modeled and optimized through the manipulation of a few key parameters in the input deck.

In PEBBED2, only one fissile nuclide could be specified in the fuel. The accuracy obtainable in modeling pebble-bed cores with high burnup or multiple fuel types was improved by enabling the code to compute fission yields for up to three fissile isotopes. Most core designs contain uranium-235 as the dominant fuel type, but in high-burnup cores a significant buildup of Pu-239 can occur. Cores containing fertile thorium will build-in a large amount of fissile U-233. The fission product yields of these fuel isotopes differ; thus, different fuel mixes will produce different nuclide distributions and discharge isotopics. PEBBED3 is able to compute and track depletion and buildup in multi-fuel cores.

A 1-D heat transfer model implemented in PEBBED2 has been improved for PEBBED3. The fuel temperature module was improved by adding a graphite thermal conductivity correlation dependent on temperature and neutron fluence. The correlation, developed at Oak Ridge National Laboratory, accurately accounts for the thermal conductivity in a pebble given its irradiation history. Coupled with the zone-dependent axial coolant

temperature calculation, the correlation gives good approximations of pebble fuel temperature throughout the core and over the history of a given pebble type.

In addition, post-accident fuel temperatures, as a result of a loss of coolant flow, were estimated using a 1-D (radial) transient heat conduction/radiation module implemented in PEBBED3. The temperatures were shown to be a strong function of the steady-state core power density. This feature allows a core optimization study to include the post-accident peak temperature as one of the parameters in an overall objective function.

The subcontract work with the Georgia Institute of Technology continued in FY02. The codes originally planned for use in cross-section processing, COMBINE and TORT, were shown in FY01 to be unsuitable. This year, the codes WIMS and EVENT were selected, tested, and shown to be appropriate.

Since PEBBED is being developed as a practical tool to answer questions about the performance of real PBRs, it is appropriate to test its capabilities at each stage in its development by applying it to address practical issues. During FY02, PEBBED was used to investigate questions on the deployment of PBRs in remote locations and on the susceptibility of PBRs to be used for nuclear weapons proliferation. The work on nonproliferation of nuclear weapons has shown that the PBR is a poor choice for overt or covert production of nuclear weapons material.

Work continued from the previous year in the area of air ingress into pebble bed reactors. A loss-of-coolant accident (LOCA) has traditionally been considered a design-basis accident for helium-cooled pebbled bed reactors. Following helium depressurization, it is anticipated that unless countermeasures are taken air will enter the core through the break and then, by molecular diffusion and ultimately by natural convection, cause oxidation of the in-core graphite structure and graphite pebbles. Thus, without any mitigating features, a LOCA will lead to an air ingress event. The investigator studied such an event with two well-respected light water reactor transient response codes: RELAP5/ATHENA and MELCOR. The RELAP5/ATHENA code was used to model convective heat transfer from the pebbles to the helium coolant using the heat conduction enclosure model for large break LOCAs. This model represents radial and axial heat transfer from the pebbles to the side, bottom, and top graphite reflectors. The side reflector and the core barrel were modeled as a composite heat structure. The radiation enclosure model was used to represent radiation between the core barrel, reactor vessel, and containment wall. The steady-state calculations agree very well with design values.

To study the degree of core oxidation occurring in a beyond-design-basis air ingress accident, a MELCOR model of the reference design was constructed. A modified version of MELCOR developed at INEEL that includes graphite oxidation capabilities and molecular diffusion of air into helium was used for these calculations. Results show a long time delay between the time that the decompression phase of the accident is over and the time that natural circulation air through the core occurs. Up until the onset of natural convection, the temperature of the pebbles remains below 1600° C, which agrees with the RELAP5/ATHENA calculations; however, once air starts to flow through the core the pebbles in the lower sections of the core begin to oxidize. Depending on the location and extent of oxidation, temperatures greater than 2200° C are calculated in the lower reflector locations of the reactor. The fueled region of the reactor is not affected; thus, fission product release is not anticipated.

The timing of the onset of natural convective flow in the reactor core and the beginning of core oxidation is very sensitive to the modeling of the molecular diffusion process, the magnitude and timing of heat loss from the vessel, and the oxidation rate for the graphite. All sensitivity calculations show the same phenomenological behavior with differences in timing associated with different boundary conditions and assumptions about oxidation and molecular diffusion. Work will continue in FY03 focusing on benchmarking the model against Japanese and German experiments where possible.

A major activity in FY02 was to develop a fission product chemistry model for the fuel performance model termed PARFUME. The purpose of this study was to estimate the chemical forms of fission products formed by fission of U-235 in a fuel kernel containing a mixture of $UO_2$ and $UC_2$ at various $UC_2$ fractions, enrichments,

burnup values, and temperatures, and to estimate the partial pressures of CO, $CO_2$, and noble gases in the kernel-buffer zone of the fuel particles. These results are needed to calculate stresses and fission product transport in the TRISO-coated particle fuel.

Two chemical equilibrium codes, HSC and FACTSAGE, were compared. For a test case, the concentrations of substances predicted by the two codes agree in general, but HSC shows a spread of valence distributions while FACTSAGE does not. HSC was chosen for subsequent computations. The 30 dominant fission products were combined into 12 groups to facilitate computations.

Equilibria have been calculated for a system with $UO_2$, $UC_2$, Pu, C, $O_2$, and 12 fission product groups, for which 241 output substances are possible. The equilibria have been computed at 5 values of fuel enrichment, 8 $UC_2$ fractions, 7 values of fuel burnup, and 18 temperatures, yielding a database of about 4600 equilibria. The CO concentration predicted by HSC varies slowly with burnup and fuel enrichment, but strongly with temperature. The CO yield is high with no $UC_2$ present, but drops rapidly to a plateau at $UC_2$ fractions above 10%, then drops to zero as the $UC_2$ fraction approaches 100%. There also is a substantial yield of $CO_2$ in pure $UO_2$ fuel, but not in UCO fuel. At T > 1500°K the ability of lanthanides to bind oxygen decreases, so the yield of CO could exceed simplified estimates that assume firm binding by lanthanides at all temperatures.

Algorithms are derived to predict the CO and $CO_2$ yields (molecules per fission) in pebble bed fuels as functions of $UC_2$ fraction, fuel enrichment, burnup, and temperature. Pressures of CO, $CO_2$, and noble gases are calculated for a specific fuel particle design. The $CO_2$ pressure is negligible in UCO fuel, but it can be significant in pure $UO_2$ fuel. For a case with pure $UO_2$ fuel the CO *yield* predicted by HSC exceeds the predictions of empirical algorithms based on CO *release* data after fuel particle crushing, but agrees with a theoretical estimate of *yield* assuming trivalent lanthanides.

This LDRD has enhanced the stature of the INEEL in the international PBR research community. The investigators have published eight papers in archival journals, refereed conference proceedings, and participated as invited guests in panel discussions.

# Generation IV Gas-Cooled Reactor System Analysis Tools

*Richard R. Schultz*

## *Coupling two software codes to create one powerful analysis tool*

GE103

To study advanced nuclear plant behavior, as well as thermal-hydraulic behavior of advanced systems in other industries, new analysis tools are needed. Currently, the Fluent Computational Fluid Dynamics (CFD) code is designed to perform detailed analyses of system components, predicting and analyzing the three-dimensional behavior of the working fluid. However, Fluent has no accommodations to handle rapidly changing boundary conditions at the component inlet and exit to analyze the component during a rapid transient as part of a system.

This LDRD created a new thermal-hydraulic analysis tool comprised of the Fluent CFD code coupled with the RELAP5-3D (Reactor Excursion and Leak Analysis Program) advanced systems analysis code. This tool offers unique capabilities and features, and has the ability to model the steady-state and transient fluids/heat transfer behavior of entire systems; portions in great detail with CFD; and, the remainder in sufficient detail to track the system behavior and provide accurate boundary conditions to the CFD code as a function of time. It also is capable of using a multitude of working fluids when the fluid properties are the same in both Fluent and RELAP5-3D. Prior to coupling Fluent and RELAP5-3D, these capabilities were not available to engineers and scientists but are sorely needed to study advanced nuclear plant behavior, to assist in ultimately licensing such systems, and to understand the thermal-hydraulic behavior of other advanced systems. This research also incorporates a first-round validation and verification (V&V) of the new tool. The V&V study will show that Fluent and RELAP5-3D have been coupled correctly, define how the interface between Fluent and RELAP5-3D should be constructed, and outline the strengths and limitations of the new tool.

Technical objectives for fiscal year 2002:

- Complete the linkage of the Fluent CFD software to the RELAP5-3D advanced system's analysis code to create a new advanced thermal-hydraulics analysis tool: the coupled Fluent/RELAP5-3D code.
- Debug the coupled Fluent/RELAP5-3D code.
- Perform coupled V&V analyses and round out the V&V matrix.

The investigators linked Fluent and RELAP5-3D using an Executive Program that monitors the calculational progression in each code, determines when each code has converged, governs the information interchanges between the codes, and issues permission to allow each code to progress to the next time step. The Executive Program was interfaced with Fluent and RELAP5-3D using user-defined functions. User-defined functions also were used to ensure the fluid properties used by Fluent and RELAP5-3D are equivalent. The Executive Program uses the Parallel Virtual Machine (PVM) as the control medium. The linked codes are being studied using simple problems (Figs. 1 and 2) that consist of a pipe modeled using RELAP5-3D coupled to a downstream section of the pipe modeled using Fluent coupled to a further downstream section of pipe modeled using RELAP5-3D.

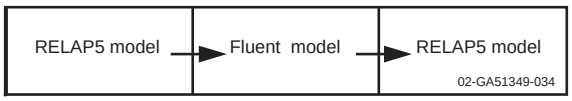


*FIGURE 1. Model to study fully developed turbulent pipe flow using coupled codes.*

The code has been debugged and the investigators are able to perform calculations. Debugging was completed using the model shown in Figure 2 (next page). The linked code's capability was defined to allow interfaces between either a two-dimensional and a one-dimensional RELAP5-3D model or a three-dimensional Fluent model and a one-dimensional RELAP5-3D model.

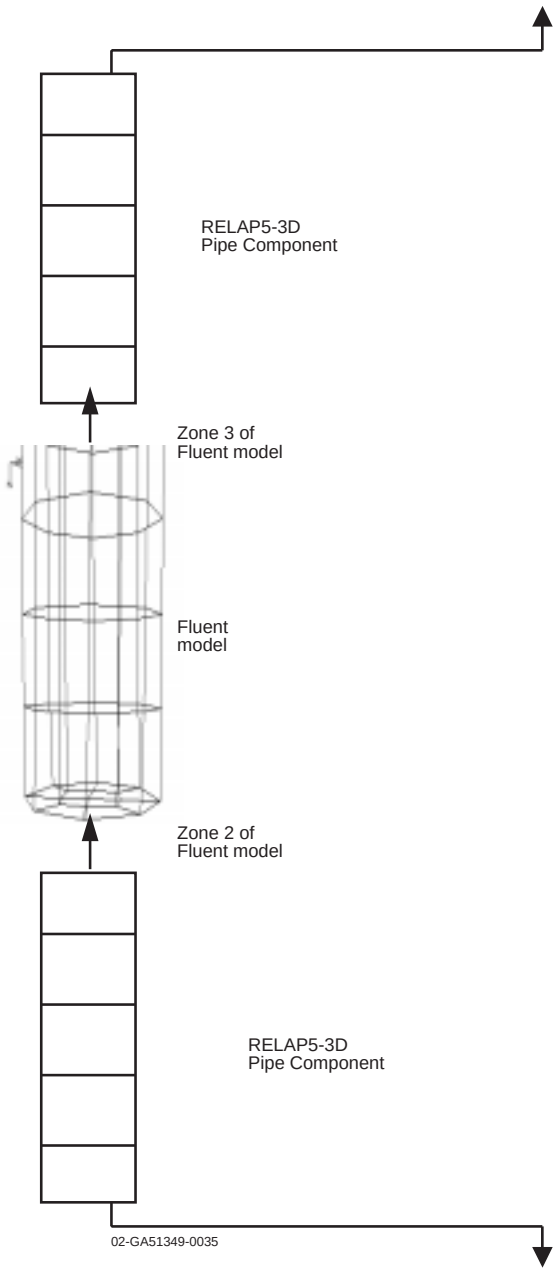


*FIGURE 2. Portion of nodalization used to debug Fluent-RELAP5-3D coupled code.*

The first coupled V&V calculation is ongoing (Fig. 1), i.e., fully developed pipe flow with helium as the working fluid. A user guideline document is being written based on performing the first V&V case and the debugging effort completed using the model shown in Figure 2. The effort is approximately 80% complete. The second V&V calculation (backward facing step with heat transfer) has been performed using Fluent alone. This calculation is based on a working fluid of air. During this work it was determined that a linked calculation cannot be performed until a simple process is created for using fluids, which RELAP5-3D presently doesn't include on its working fluid list (air is not included). Air introduces additional complications since it is a gas mixture.

Based on the experience with the second V&V calculation, work is being done on a means to enable users to input their own fluid properties for both RELAP5-3D and Fluent. In the past this approach was not used in the RELAP5-3D code because a complete definition of fluid properties for RELAP5 includes the fluid behavior in liquid form, two-phase saturated form, and vapor form. However, there are many applications, particularly for single-phase systems such as gas reactors where the working fluid remains in only the vapor phase and the thermodynamic conditions never approach the saturated condition. Therefore, it is important that accomodations be made to enable users to input working fluids easily to avoid unnecessary complications for potential commercial users.

The V&V matrix reported in the FY01 year-end report has been supplemented with an additional case: the Gas Turbine-Modular Helium Reactor (GT-MHR) system proposed by General Atomic (GA). Although there are no three-dimensional data for the system, GA has done extensive investigations into the behavior and performance of their design to determine the conditions at each

equipment stage. Consequently, GA has an intimate knowledge of the general system behavior such as the system pressure and average temperature at the inlet and exit of the lower plenum. GA has agreed to provide their GT-MHR RELAP5 model to the investigators so they can perform a V&V case that would enable INEEL to model the lower plenum using Fluent, couple the Fluent model to the RELAP5 model of the remainder of the plant, examine the coupling conditions at the inlet and outlet plenum, and examine the mixing characterisitics in the lower plenum.

The coupled Fluent/RELAP5-3D code enables researchers and analysts to perform analyses of present and advanced plant systems in a way that was impossible prior to the existence of this tool. By coupling RELAP5 and Fluent the balance-of-system can be modeled using RELAP5 such that boundary conditions can be provided to the Fluent model time step by time step. Thus Fluent linked to RELAP5 enables researchers to analyze the behavior of a system component in great detail in a system undergoing a rapid transient.

A final product of this LDRD research is a new thermal-hydraulic analysis tool comprised of the Fluent CFD code coupled with the RELAP5-3D/ATHENA advanced systems analysis code. Outgrowths of this LDRD include:

- A cooperative relationship with the Fluent Corporation.
- Follow-on work that may include the modeling of non-nuclear systems, advanced nuclear systems (Generation IV), and conventional nuclear systems.

During the second half of the fiscal year, an INEEL presentation was given at the Fluent User Group Meeting in Manchester, NH, regarding the coupled code capability. Fluent's sales network has found several Fluent users in the nuclear industry who are quite interested in using the coupled code. All interested parties are awaiting completion of several examples and also the publication of user guidelines.

# Subsurface Science Initiative

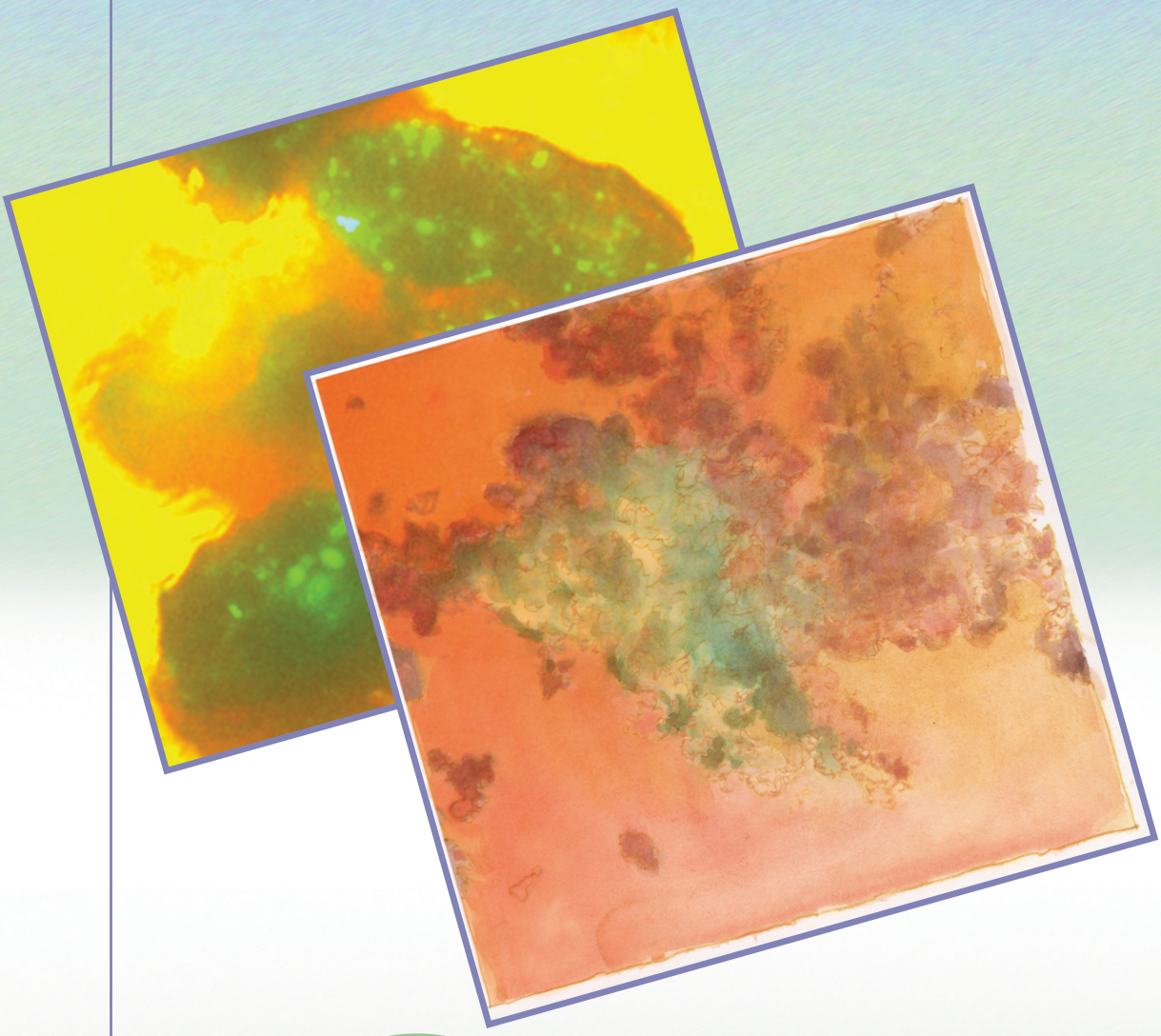

## LDRD Annual Report for FY-2002

Idaho National Engineering & Environmental Laboratory

# Development of Sensors for Detection of Metal-Reducing Bacteria in Mesoscale and Field Experiments

*William A. Apel, Frank Roberto, Joni Barnes*

## *Assessing bacteria's ability to reduce heavy metals*

GC142

Contamination of the subsurface with metals and radionuclides is a ubiquitous, difficult problem. Heavy metal and radionuclide contamination of groundwater and soils is a pervasive problem throughout the DOE complex. In addition, heavy metal contamination affects many non-government sites, with over 50% of all Superfund sites in the U.S. requiring significant heavy metal cleanup. The expense of this remedial activity will be high. According to a 2000 National Research Council report, cleanup across the DOE complex alone is expected to cost at least $200 billion dollars and will take decades to complete.

One method to address this problem is in situ metal/radionuclide transformations using indigenous bacteria. These transformations can take the form of either oxidations or reductions and, if performed selectively, can drastically affect metal/radionuclide mobility and sometimes toxicity.

In a previous LDRD, the investigators discovered members of the bacterial genus *Cellulomonas* to be present in subsurface sediments collected from the DOE Hanford site and demonstrated that these bacteria are capable of catalyzing the reduction of oxidized forms of chromium, uranium and iron. These results were unanticipated, as no *Cellulomonas* species had ever been reported to be capable of metal reduction.

The purpose of this LDRD, was to better assess the ability of these *Cellulomonas* isolates to reduce metals and to concurrently develop a molecular probe specific for *Cellulomonas*. The metal reduction information is important as it enables a more effective evaluation of whether *Cellulomonas* can be used to remediate subsurface heavy metal and radionuclide contamination. The molecular probe is equally important as it provides a method that can be used to readily detect whether *Cellulomonas* species are widely dispersed through the subsurface at a variety of locations or whether they are unique to Hanford.

Technical objectives for fiscal year 2002:

- Assess the ability of wild-type *Cellulomonas* isolates to reduce metals.
- Develop a molecular assay for the efficient identification of *Cellulomonas* species in subsurface samples.

Three strains of *Cellulomonas* (WS01, WS12, and ES06) isolated from Hanford subsurface samples were tested for their ability to reduce to trivalent chromium. This testing was done by culturing the organisms under anaerobic conditions in a minimal, simulated groundwater medium containing nitrate and hexavalent chromium. Laboratory cultures of a characterized *Cellulomonas* species, *Cellulomonas turbata*, and an organism phylogenetically and morphologically related to *Cellulomonas*, *Microbacterium laevaniformans*, were tested under the same conditions for comparative purposes.

All three Hanford strains of *Cellulomonas* actively reduced hexavalent chromium under the conditions employed. The laboratory strain of *Cellulomonas* (i.e. *C. turbata*) also actively reduced hexavalent chromium. Interestingly, under the same conditions, *M. laevaniformans* was incapable of reducing chromium, demonstrating that the ability to catalyze hexavalent chromium reduction is not necessarily inherent across all Gram (+) bacteria.

For the development of a molecular assay, DNA sequencing of the 16S ribosomal RNA genes of *Cellulomonas* strains WS01, WS12, ES5, and ES6 was performed on an ABI Prism Model 3700 (Applied Biosystems, Inc., Foster City, CA). Two hundred ng of purified PCR product was incubated with 2 µL Big Dye version 3 "ready reaction mix" (containing *Taq* FS polymerase, buffer, deoxynucleotides, and the 4 Big Dye fluorescent dideoxynucleotide terminators), 2 µL 2.5X dilution buffer, 1 µL of sequencing primer (to span the near full length gene, primers included 8F, 1492R, 515F, 907R, 1100R; 1.6 pmol) and water to a final volume of 10 µL. A consensus sequence was generated for each portion of the 16S ribosomal RNA gene based on a minimum of five independent sequence determinations with each primer. Overlaps between primer reads were used to assemble the final sequence used for subsequent analyses.

8F: 5'-agagtttgatcctggctcag-3'

1492R: 5'-ggttaccttgttacgactt-3'

515F: 5'-gtgccagcmgccgcggtaa-3'

907R: 5'-ccgtcaattcctttragttt-3'

1100R: 5'-agggttgcgctcgttg-3'

From comparison to the GenBank database using the Basic Local Alignment Search Tool (BLAST), the nearest neighbors to the *Cellulomonas* strains sequenced were *Cellulomonas* strain 1533 and *Cellulomonas hominis*, which have been isolated from human clinical samples.

Primers Cel1F (5'-TGG GGA GCG AAC AGG ATT AG-3') and Cel1R (5'-GGC AAC CAT CTC TGG AAG TTT C-3') were designed using MacVector™ 7.0 (Accelrys, San Diego, CA). Hybridization probes for *Cellulomonas* were designed using MeltCalc Professional version 2.06. This software package was developed specifically for the design of hybridization probes and allows the user to set reaction concentrations, $T_m$ values, and gap between probes. In addition, it screens for interactions among the probes and primers so that non-interacting oligonucleotides can be selected. Probes were selected with a gap of two base pairs between the acceptor and donor fluors. The upstream probe was labeled with fluorescein (Cel1Flu: 5'-GAT GCA ACG CGA AGA A-3') and the downstream probe was labeled with CY3 (Cel1CY3: 5'-TTA CCA AGG CTT GAC ATA C –3').

Roche LightCycler-FastStart DNA Master Hybridization Probe kits, optimized for use with glass capillaries and containing a hot start polymerase, were used as the master mix base for all reactions. All reactions were 20-ul and had final concentrations of 5.0 mM $MgCl_2$, 500 nM each primer, 300 nM Cel1Flu probe and 500 nM of Cel1Cy3 probe. Amplification was performed in Idaho Technology's Ruggedized Advanced Pathogen Identification Device (RAPID™). Melt-analysis curves were generated using the LightCycler® Data Analysis software supplied with the RAPID, with the digital filter enabled and a linear fit selected. Cycling regimes are shown in Table 1.

| Assay | Cycling parameters | | | | | | | |
|---|---|---|---|---|---|---|---|---|
| | | | | | | | | 02 GA51349-134 |
| Hybridization probes | | Hot Start | Amplification | | | Melt | | |
| | Cycles<br>Analysis Mode | 1<br>None | 55<br>Quantification | | | 1<br>Melt Curves | | |
| | | Segment 1 | Segment 1 | Segment 2 | Segment 3 | Segment 1 | Segment 2 | Segment 3 |
| | Target temperature (°C) | 95 | 95 | 45 | 72 | 95 | 35 | 75 |
| | Incubation time (s) | 600 | 0 | 4 | 12 | 60 | 120 | 0 |
| | Transition rate (°C/s) | 20.0 | 20.0 | 20.0 | 20.0 | 20.0 | 5.0 | 0.2 |
| | Acquisition mode | None | None | Single | None | None | None | Step |
| | Gains | | | Ch2=16 | | | | Ch2=16 |

*Table 1. Cycling regime for Cellulomonas hybridization probe assays preformed on the RAPID.*

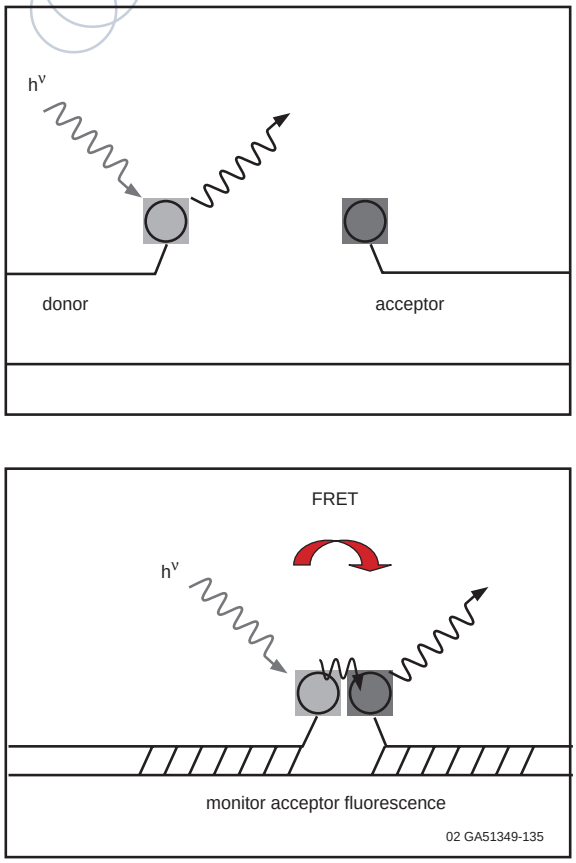


*FIGURE 1. Schematic of hybridization probe.*

Figure 1 depicts the strategy associated with the use of hybridization probes in real-time PCR. The use of two primers that must anneal adjacent to one another for fluorescence resonance transfer (FRET) to occur, provides additional specificity to the amplification reaction and provides a means of assessing product purity post-amplification during a melt analysis. The primer and hybridization probes designed from the 16S ribosomal RNA gene sequences of strains WS01, WS12, ES5 and ES6 successfully amplified DNA extracts from these strains. The purity of the resulting products was confirmed by melt-curve analysis where the coincidence of the melt peaks indicated that the same product was detected in all cases (negative controls did not produce discrete peaks).

The information generated by this LDRD contributed to a proposal titled "Long-term stewardship of mixed wastes: Passive reactive barriers for the simultaneous in situ remediation of chlorinated solvent, heavy metal, and radionuclide contaminants" submitted to the DOE Office of Science EMSP Program. That proposal resulted in funding for three years beginning in FY03.

This research also supported in part, two presentations and one publication.

# Use of Molecular Markers for Detection and Tracking of Environmental Bacteria

*Joni M. Barnes, Bill Bauer, Frank Roberto, Debby Bruhn*

## *Tracking microbe interaction with mineral surfaces*

GC124

At most DOE sites, groundwater contamination with radionuclides, heavy metals or chlorinated solvents is a problem. Subsurface microbes use minerals and mineral surfaces to facilitate metabolic processes. These processes in turn influence redox chemistry and pH of groundwaters and can affect the fate of contaminants such as chlorinated hydrocarbons, chromium, uranium, and plutonium. Therefore, information relative to the transport and fate of microorganisms in natural environments is important in the development of bioremediation strategies as well as predicting and monitoring natural attenuation.

Studies designed to assess the interaction of microbes with soil and mineral surfaces frequently use light, electron or confocal scanning laser microscopy to visualize the cells. However, sample preparation techniques can physically alter the sample, change bacterial surface properties and kill the cells. To eliminate these artifact problems, simple, non-invasive bacterial tagging agents are needed.

This LDRD investigates using molecular markers as a means to detect and track environmental bacteria. Over the past year, work has focused on the use of green fluorescent protein (GFP) as a non-invasive cell marker. Cells that have been genetically altered with the GFP gene produce a stable internal chromophore that fluoresces in the absence of other substrates or cofactors. Cells expressing GFP emit a bright green fluorescence that can be visualized using epifluorescent or confocal microscopy. In addition, several color variants of GFP and a red fluorescent protein (RFP) are commercially available, providing a method to simultaneously monitor mixed cell populations.

Technical objectives for fiscal year 2002:

- Determine the effect of GFP plasmid vectors on host cell metabolism.
- Assess the stability of the plasmid vector in GFP-tagged bacteria.
- Develop imaging techniques for monitoring surface colonization by GFP-tagged cells in a flowing system.
- Develop molecular techniques to chromosomally tag environmental bacteria with GFP.

This is the second year of a three-year project. In FY01, the investigators developed a plasmid vector (pRK415npt$_2$gfp) that provides an appropriate antibiotic resistance gene and an optimum promoter for environmental bacteria. The plasmid, which carries genes for tetracycline resistance and expresses GFP genes from a npt$_2$ promoter, can be introduced into the bacterium of choice via electroporation or conjugation. Using this approach, iron-reducing bacteria and nitrate-reducing bacteria were successfully labeled with GFP. In addition, effective epifluorescent and laser confocal microscopy methods were developed that enable detection of labeled cells. Using these tools, work in FY02 was done to assess the effect of the plasmid on host cell metabolism, determine plasmid stability and develop imaging techniques for real-time monitoring of GFP-tagged microbes. Work also was initiated in the development of molecular techniques for inserting GFP genes onto the bacterial chromosome.

*Shewanella putrefaciens* is a faculatative iron-reducing bacterium that is widely distributed in the environment. Under anaerobic conditions, *S. putrefaciens* can use an array of electron acceptors including ferrous and manganese oxide, nitrate, nitrite, thiosulfate, fumarate and elemental sulfur. Based on the distribution and versatility of this microbe, and its ability to switch between aerobic and anaerobic growth, *S. putrefaciens* was selected as a model bacterium for use in methods development.

First, *S. putrefaciens* cells were tagged with GFP using pRK415npt$_2$gfp as described above. The cells carrying the plasmid were found to emit strong green fluorescence that was easily detected by direct epifluorescent microscopy. Next, to assess the influence of pRK415npt$_2$gfp on the bacteria, the growth of *S. putrefaciens* was monitored in the presence and absence of the plasmid under aerobic and anaerobic conditions. No effect was found. In addition, under anaerobic conditions, the rate and extent of iron reduction by both strains was similar. Although these studies indicate that the presence of pRK415npt$_2$gfp places minimal stress on *S. putrefaciens*, due to the diversity of environmental microbes problems may be encountered following plasmid insertion into other bacterial strains. Hence, the affect of the plasmid on host metabolism must be determined on a strain-by-strain basis.

To assess the stability of pRK415npt$_2$gfp in *S. putrefaciens*, cells were grown to late log phase in mineral salts medium containing tetracycline (10 µg/ml). The culture was then diluted 100 fold in medium without antibiotic and allowed to grow overnight at room temperature. This procedure was repeated every 24 hours over a three-day test period. After each dilution, the ratio of fluorescent to non-fluorescent cells was determined microscopically, and the fluorescence intensity of the cells was measured using fluorometry. In these experiments, no plasmid loss was observed after 12 generations (24 hours) and 83% of the cells still retained the plasmid after 36 generations (72 hours) indicating that short-term studies can be conducted in the absence of antibiotic selection.

In an effort to develop appropriate imaging techniques for the detection and tracking of bacteria, biofilm studies using *S. putrefaciens* tagged with GFP were conducted. Bacteria were grown in simulated groundwater and pumped through a laminar flow cell that contained a hematite pellet. Throughout the experiment, cells that attached and adhered to the hematite surface were observed by placing the flow chamber directly on the stage of a Nikon Eclipse E600 microscope. The E600 is equipped with a water immersion objective lens (60x, NA=1.20), a 100-watt mercury arc lamp and a filter block fitted with a 465-495 nm excitation filter, a 505 nm dichroic mirror and a 510-555 nm emission filter. The surface of the hematite was indexed using the microscope stage coordinates and cells were imaged using a Peltier-cooled CCD camera (Olympus Magnafire). Using these techniques it was demonstrated that GFP provides an effective non-invasive means to monitor cell activity over time (Figure 1).

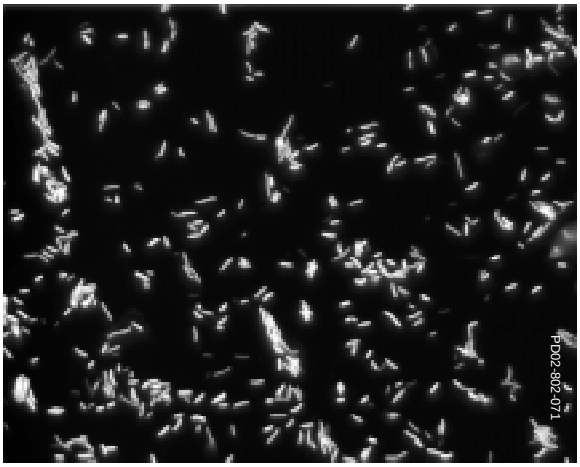


*FIGURE 1. Epifluorescence photomicrograph of* Shewanella putrefaciens *attached to a hematite surface. The cells, which are tagged with GFP, were grown for 44 hours in a laminar flow cell operated under aerobic conditions.*

Work to-date in this LDRD has shown that plasmid-based GFP vectors provide an effective means to tag environmental bacteria for use in short-term studies; however, to maximize genetic stability, bacterial strains used in long-term bench-scale or field studies should be chromosomally marked. In an effort to achieve this, the investigators are currently assessing transposon mutagenesis as a means to randomly insert the GFP gene onto the chromosome of *Shewanella* using a suicide transposon vector derived from Tn5. This work will be continued in FY03. In addition, the use of GFP-tagged cells in soil column studies and the use of GFP as a metabolic reporter will be assessed.

Ultimately, this work will provide a valuable research tool for evaluating the interaction of microbes with a variety of surfaces at the INEEL and other DOE sites. This work directly supports Subsurface Science Initiative projects that need to evaluate the role of bacteria in complex environmental samples and can be used to study biocorrosion and biofouling related to nuclear and conventional power systems.

# Characterizing Microbial Population Shifts in Response to Alternative Electron Donors and their Effect on Trichloroethylene Dechlorination Efficiency

*David E. Cummings, Kent S. Sorenson*

## *Creating dynamic bioremediation strategies*

GC131

Contamination of the subsurface environment with industrial chlorinated solvents such as trichloroethylene (TCE) threatens our nation's limited drinking water supplies. Some experts estimate that TCE is the most widespread subsurface contaminant in the U.S. and possibly the world. Active remediation of a TCE plume at the INEEL Test Area North (TAN) provides a unique opportunity for focused research on the mechanisms underlying the success of the biological treatment. Lactate is injected regularly into the subsurface plume to stimulate the indigenous microbial populations, maintaining anoxic conditions, and facilitating the reductive dechlorination of TCE to ethene.

This LDRD project is investigating how microbial population dynamics under different electron donor conditions affect the bioremediation of chlorinated solvents. The results are expected to provide mechanistic information as to the functioning of the dechlorinating community and significantly advance the ability to manage, remediate, and reclaim TCE-contaminated sites.

Technical objectives for fiscal year 2002:

- Apply molecular techniques developed in FY01 to characterize the microbial diversity in the aquifer beneath INEEL-TAN.
- Obtain consistent and reproducible TCE dechlorination in several laboratory bioreactors (developed in FY01) inoculated with TAN groundwater.
- Characterize the microbial diversity in the TCE-dechlorinating laboratory consortium (bioreactor) using molecular techniques.
- Examine the TAN and lab cultures for Dehalococcoides spp., the only known bacteria capable of complete dechlorination of TCE and thought to be essential for complete dechlorination in the field.

The aquifer beneath Test Area North has been receiving regular additions of lactate, an organic carbon and electron source, to stimulate the indigenous microbial community. The goal is to first remove all oxygen followed by the reductive dechlorination of trichloroethylene to the harmless by-product ethene, both biologically catalyzed reactions. Continued lactate additions maintain anoxic conditions and provide the electron source necessary to carry out the reductive dechlorination reactions. Very little is known about how the microbial community carries out reductive dechlorination. It is essential to understand the ecology of this system in order to optimize the current treatment with specific nutrients, respond to unexpected changes in performance of the treatment, and transfer the technology to other field sites.

The first goal of FY02 research was to identify and quantify as many of the various microorganisms as possible in the lactate-stimulated community. To accomplish this, state-of-the-art molecular biology techniques were applied to make use of microbial DNA as a fingerprint of the specific organisms present. Table 1 provides a summary of the microbial diversity discovered at TAN using clone libraries and T-RFLP of 16S rRNA genes. In summary, the Bacterial community is dominated by acetogens, strictly anaerobic bacteria that produce acetate as their primary metabolic end product. Likewise, the Archaeal community is composed exclusively of methanogens, microbes that convert $CO_2$ to methane. The methanogens comprising the Archaeal community at TAN are mainly acetoclastic. That is, they use acetate as their carbon and energy source. It appears that the lactate additions have selected for a syntrophic partnership between acetate-producing Bacteria and acetate-oxidizing Archaea.

Other TCE-dechlorinating systems that have been studied appear to be hydrogen driven; i.e., they are dominated by hydrogen-producing Bacteria and hydrogen-oxidizing Bacteria and Archaea. The implications of an acetate-driven system have yet to be rigorously explored, but are likely to be different from hydrogen-driven systems and may provide a new paradigm for the biological remediation of chlorinated solvent-contaminated sites.

As Table 1 indicates, other Bacteria present in the TAN aquifer include a small percentage of organisms known to have the ability to catalyze some steps in the dechlorination pathway, such as *Dehalospirillum* and *Trichlorobacter.* Additionally, a clone most closely related to *Dehalococcoides ethenogenes*, the only known complete TCE dechlorinator, was identified.

| Taxon | Frequency in Field | Presence in lab | Comments |
|---|---|---|---|
| **Bacteria** | | | |
| *Acetobacterium* spp. | 37% | + | Homoacetogenic |
| *Clostridium* spp. | 21% | + | Fermentative |
| CFB Group | 13% | + | Common soil organisms |
| Known dehalogenators | 5% | - | Reductively dechlorinate |
| Thermotogae | 5% | - | Fermentative, thermophilic |
| *Spirochaeta* spp. | 4% | + | Produce ethanol, acetate, and $H_2$ |
| *Syntrophomonas* spp. | 4% | - | Produce acetate and $H_2$ |
| *Acidaminococcus* spp. | 3% | + | Produce acetate and butyrate |
| Sulfate-reducing bacteria | 2% | - | Produce $H_2S$ |
| *Acholeplasma* spp. | 2% | - | Fermentative, no cell wall |
| Verrucomicrobia | 1% | - | Prosthecated |
| *Dehalococcoides* spp. | 1% | + | Complete TCE dechlorinator |
| **Archaea** | | | |
| *Methanosaeta* spp. | 53% | + | Utilizes acetate only |
| *Methanospirillum* spp. | 27% | + | Utilizes acetate only |
| *Methanosarcina* spp. | 11% | + | Utilize $H_2$ or acetate |
| *Methanoculleus* sp. | 9% | + | Utilize $H_2$ only |

02 GA51349-141

*TABLE 1. Bacterial and Archaeal 16S rRNA gene clones from TAN groundwater and a laboratory bioreactor.*

The second objective of FY02 was to obtain a laboratory culture that could completely and reliably dechlorinate TCE using groundwater from TAN as inoculum. As the ultimate goal of this LDRD project is to examine the effects of alternative electron donors on dechlorination efficiency and their effects on the microbial community structure and activities (work that is impractical at the field scale), such a consortium was critical for performing laboratory studies that provide field-relevant information. A bioreactor designed in FY01 was used as the laboratory vessel. This reactor was constructed in a fashion that allowed pressurization, maintained anaerobic conditions, and facilitated sample collection without compromising the culture conditions. Using groundwater collected from TAN, a consortium was established in the lab that dechlorinated TCE to ethene. This reactor consortium continues to operate today, and experiments with alternative electron donors are underway.

Once TCE dechlorination was established in the bioreactor, the molecular tools used to describe the microbial diversity in the field were applied to the lab consortium. In general, the lab consortium was comprised of a subset of the populations identified in the field. This is to be expected since the field community was the source of organisms supplied to the bioreactor. Since dechlorination was successful in the lab consortium it is reasonable to postulate that the organisms essential to the process were those common to both systems, i.e. field and lab. The commonalities included an apparently acetate-driven syntrophism, along with many of the same species. These findings improve this project's understanding of the roles of different organisms in the reductive dechlorination process. Further-

more, the metabolic activities of the known organisms provide clues as to how the biostimulation might be optimized.

It has been proposed recently that *Dehalococcoides ethenogenes*, the only known organism to completely reductively dechlorinate TCE to ethene, is essential for complete dechlorination to occur in the field. Thus, it was an important part of this study to interrogate the field and lab communities for the presence of *Dehalococcoides*-like organisms.

Using published PCR primers that are specific to the 16S rRNA gene of the genus *Dehalococcoides*, their presence in both the lab and field communities was established. Subsequent cloning and sequence analysis revealed two distinct species of *Dehalococcoides* present in both cultures. Since *Dehalococcoides* are hydrogen oxidizers and are not known to use acetate, the effects of an acetate-driven system on dechlorination need to be further explored. Apparently enough hydrogen is produced in the reactor by other metabolic pathways that these organisms can survive and, possibly, contribute to the dechlorination performance of the community.

In summary, the past year's efforts to characterize the microbial communities associated with reductive dechlorination of TCE at TAN and in the laboratory have been largely successful. The laboratory consortium is a subset of organisms found in the field, providing testable hypotheses about the role(s) of different species in the process, as well as providing the experimental unit for the final stage of research: testing the efficacy of alternative electron donors on dechlorination. *Dehalococcoides*-like organisms also were detected, supporting the recent sentiment that these organisms are critical to complete anaerobic dechlorination. Two manuscripts are now being prepared to share these findings with the public. The first describes in detail the microbial diversity of the TAN and lab communities and compares their TCE-dechlorinating performance. A second manuscript is forthcoming that will expand on the concept of an acetate-driven dechlorinating system, and its implications for remediation technologies worldwide.

TCE may be the most widespread groundwater contaminant in the world today. In fact, nearly all DOE-owned or managed sites are contaminated with TCE. The accomplishments of this LDRD project will not only contribute to solving the problem at Test Area North here at the INEEL, but also provide valuable information for the remediation of chlorinated solvents across the entire DOE Complex and beyond. The success of this work contributes to the international research reputation of INEEL, improves upon core competencies, and builds on INEEL's growing reputation in the field of remediation of chlorinated solvents.

# Characterization of Dense Non-Aqueous Phase Liquids Adsorption/Desorption to Geological Media

*Gary S. Groenewold, Jani C. Ingram*

## *Gaining insight into the impact of chlorinated solvent-soil interactions*

GC143

The fate of carbon tetrachloride (CT) and other chlorinated solvents in the vadose zone is controlled by complex interactions (partitioning) between the vapor, soil, and moisture phases. Slow desorption processes are particularly problematic because they contribute to plume broadening, and hamper vacuum extraction remediation. An improved understanding of the slow desorption processes is needed to accurately predict chlorinated solvent behavior in the vadose zone during remediation.

While the phenomenological understanding of chlorinated solvent mobility has improved significantly over the past decade, insights into the underlying mechanisms operative at the micron to molecular scales have been elusive. Specifically, identification of binding sites and competitive adsorption phenomena has been difficult to characterize analytically.

This LDRD, which was initiated in February 2002, is directly characterizing the surface interactions of carbon tetrachloride (CT) and other chlorinated solvents with INEEL soils and soil simulants to gain insights into their fate and transport in the vadose zone. The research addresses these knowledge gaps by directly interrogating the interactions at the soil surface using a combination of surface analysis techniques including Raman and infrared spectroscopies, secondary ion mass spectrometry, and microscopy. The correlated vibrational, mass, and morphological information is expected to result in significantly improved understanding of micron to molecular scale processes that are needed to explain phenomenological behavior and provide predictive capability extendable to other systems or system perturbations.

Technical objectives for fiscal year 2002:

- Using spectroscopy, characterize chlorinated solvent adsorption on soil simulant(s).
- Using spectroscopy, characterize chlorinated solvent adsorption on native INEEL soil. Use simulant results to aid interpretation.

The overall goal of this research is to characterize the interfacial interactions of chlorinated solvents with soils and soil simulants to gain insights into the impact of the interactions on fate and transport in the vadose zone. The research approach uses vibrational spectroscopy, static secondary ion mass spectrometry (SIMS), and other complimentary surface analysis techniques to characterize the interactions. An understanding of the bonding between the chlorinated solvents and the reactive sites will provide valuable insight into the adsorption mechanisms.

Vibrational spectroscopy is capable of investigating this specific and important aspect of adsorption due to its ability to interrogate subtle differences in bonding. Collection of information concerning the sorption and reactivity of molecules on oxide surfaces using Raman spectroscopy has been demonstrated. Static SIMS has been demonstrated in the laboratory as an effective tool for investigating interfacial chemistry of soils and natural minerals. The polyatomic projectile employed in the INEEL SIMS instrumentation is particularly well suited to this study because it is highly surface specific.

The specific milestones of this project are to characterize the soil surface chemistry of simulant and natural soils using surface analysis techniques. Soil simulants were provided by Washington State University (WSU) through collaboration with Drs. David Yonge and Brent Peyton. These simulants have well characterized, narrow pore size distributions and known surface functional groups. This information will enable correlation with transport behavior and analytical characterization of the reactive sites.

The first task centered on the use of soil simulants with specific pore sizes to investigate the fundamental soil characteristics that control chlorinated solvent sequestration and release. Silica dioxide particles, with a range of carefully defined intraparticle pore sizes between 20 and 100 angstroms, are being developed in the WSU laboratory. Particle development has been based on research pertaining to the production of mesoporous catalysts used in the chemical industry.

Pore size is controlled by using non-ionic organic surfactants as a “template” during the silica dioxide precipitation procedure. The pore-sized distribution is dependent on the molecular size of the surfactant. Once the organic template is removed by thermal combustion, chemical functional groups will be added to the surface using an additional precipitation process with an

organometallic compound. A focus of this task has been to characterize the pore size, surface area, and surface chemistry of the simulants to determine the most desirable method of synthesis. Eighteen different soil simulants were characterized by $N_2$ adsorption for surface area and pore-size distribution with a Micromeritics TriStar 3000 Surface Area and Porosimetry Analyzer. Additionally, these simulants were analyzed by SIMS to determine the surface cleanliness. From these results, modifications are currently being made to optimize the synthesis procedures.

Preliminary experiments were performed on two of the soil simulants. Tween 40 has a pore-size distribution of 20 to 30 Å, and Pluronic P65 has a pore-size distribution of 60 to 70 Å. The surfaces of these simulants were determined to be free of organic contaminants (Fig. 1).

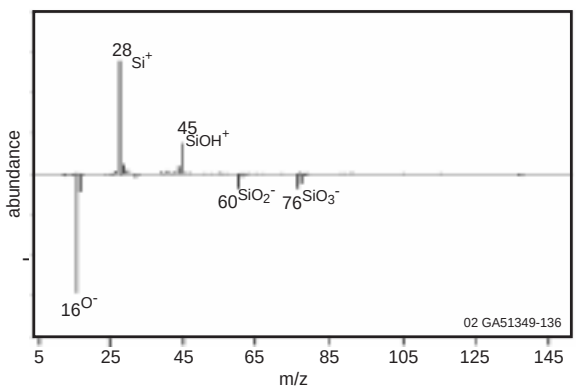


*FIGURE 1. SIMS analysis of Pluronic P65. (Similar spectra were observed for Tween 40).*

The objective of the experiment was to determine the strength of interaction between carbon tetrachloride ($CCl_4$) and the soil simulants. Raman scattering was used to measure the shift in vibrational energy of the sorbed $CCl_4$ compared to bulk $CCl_4$. The experimental approach was to place the soil simulant in a divot of a glass slide. Afterwards, 25 µl of neat $CCl_4$ was piped on top of the simulant and covered with a glass cover slip. The sample was analyzed by focusing on a small area of the simulant using a microscope equipped with a 50x long working distance (7 mm) objective. The Raman-scattered light was collected with an SA S3000 Raman microprobe using excitation from the 514.5 nm line of the $Ar^+$ ion laser. Spectra were collected over time to allow the bulk $CCl_4$ to evaporate, leaving the sorbed $CCl_4$.

A series of spectra for the $CCl_4$ on Pluronic P65 is shown in Figure 2. These data show the $CCl_4$ peaks at 219, 315, and 460 $cm^{-1}$, and decreases in intensity with evaporation; however no shifting in the peaks is observed. The peak at 488 $cm^{-1}$ originated from $SiO_2$. It is not clear what the surface coverage of the $CCl_4$ is on the surface of the Pluronic P65; however, these data suggest only physi-sorption interactions with the surface of the $SiO_2$ simulant. Similar results were observed for the Tween 40.

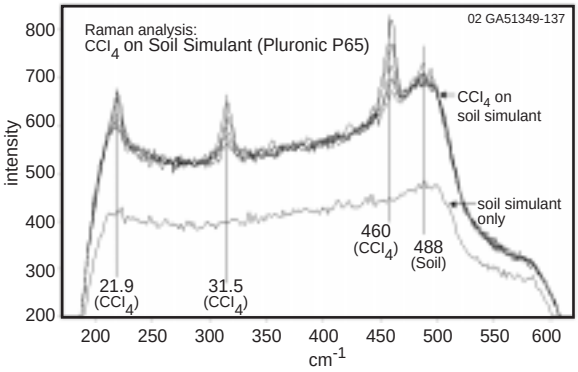


*Figure 2. Raman analysis of sorbed $CC1_4$ on the soil simulant Pluronic P65. Spectra taken during the $CC1_4$ evaporation process; bottom spectrum of P65 in absence of $CC1_4$.*

Another objective was to investigate the interactions of the chlorinated solvents with native INEEL soils using the soil simulant results to guide interpretation of the results. These experiments have not been initiated, but are planned for the beginning of FY03.

The results of this work will advance predictive capability for subsurface contaminant mobility. This information will not only assist regulatory agencies in setting achievable cleanup goals that are based on defensible information, but yield information critical to the effective management of contaminated sites across the country. The investigators expect to produce a minimum of two peer-reviewed publications reporting research results by the conclusion of the project. Additionally, collaboration between INEEL and WSU is being fostered through this project.

# Residual Hazards Management: Decisions Leading Toward Success or Failure

*Jerry L. Harbour, Kevin Kostelnik*

## *Developing a predictive decision network for long-term stewardship*

PH103

Numerous activities generate hazardous byproducts. In many instances, such hazards cannot be completely removed and must reside in the environment for extended periods of time. The environmental management of such hazards is termed "residual hazards management." Residual hazards management may be defined as the identification/delineation, assessment, selective removal, control, and/or monitoring and maintenance of an enduring source of danger.

Of particular interest is the long-term control of such hazards. This LDRD focuses on the areas of physical and institutional controls and the associated decisions that play a potential role in the failure of residual hazards management systems. Specifically, this project involves performing an investigative analysis to identify appropriate case studies (both DOE and non-DOE) that exemplify DOE plans for isolating subsurface residual hazards.

Case studies in which long-term protection has been maintained, as well as case studies in which system degradation and loss of control have occurred, are being identified and investigated. The key decisions influencing the system performance and/or system failure will be presented as a decision network for each case. These decision networks and their associated information will further be analyzed to determine similarities and differences between and among the cases, as well as notable lessons learned. A comprehensive decision network will be formulated based on selected case studies.

Technical objectives for fiscal year 2002:

- Develop initial residual hazards management model.
- Identify case studies and collect initial case study attributes.
- Present findings at a technical conference.

The goal of this research, which started mid-year FY02, is to improve the long-term management of residual hazards. This effort will be accomplished in three parts: 1) investigating how institutional and engineered control decisions have influenced hazards isolation; 2) applying relevant decision theory to this environmental management situation; and, 3) developing a useful and usable decision-analysis tool applicable to future residual hazardous sites.

The project focus is on the areas of physical and institutional controls and the associated decisions that play a potential role in the failure of residual hazards management systems. A residual hazards management model was developed (Fig. 1) showing that, ideally, residual hazards remain isolated from the biosphere. However, in the event of loss of institutional control and/or engineered control failure, unwanted residual hazard exposure may occur via either contaminant migration out of the system (i.e., egress) or external intrusion into the system (i.e., ingress).

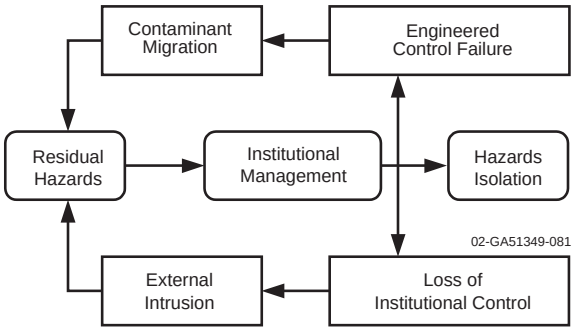


*FIGURE 1. Conceptual model for residual hazards management. Note: exposure can result from failures in both institutional and engineered controls.*

Key questions to be answered in this research include: Did system failure occur? If so, what aspect or aspects of the system actually failed? Is imminent system failure detectible and, if so, how? Are there consequences that result from failure (e.g., legal, financial, health)? What decisions played a role in the failure? Was one decision key to failure or was there an accumulation of minor decisions that formed a critical mass? Did 'decision irreversibility' occur? Was there adequate recovery time after making 'wrong' decisions? Are long-term planning assumptions valid? What are the long-term planning assumptions? Are these assumptions similar for all cases? What role do these assumptions play in system performance?

Various potential case studies have been identified for detailed analysis. Case study selection criteria was developed and defined as follows:

- End-state decision (e.g., ROD) defined and implemented.
- Known, contaminated hazards remain on-site in the shallow subsurface.
- Engineered and institutional controls are part of the end-state condition.
- Both historical and current system performance information is available.

Identified case studies and associated residual hazards included:

- Love Canal: dioxins, chlorides, and metals (e.g., lead).
- American University/Spring Valley: arsenic and chemically-filled munitions (e.g., chlorine, phosgene, and mustard agent).
- Cannonsburg UNTRA Disposal Cell: Radium-226.
- Maxey Flats Nuclear Disposal Site: Pu-238/239/240, Am-241, organics, and inorganics.
- Old Works/East Anaconda Development Area: Arsenic, Cadmium, and Lead.
- Rocky Mountain Arsenal: pesticides, chemical agents, VOCs, and unexploded ordnance.

To date, site visits have occurred at American University/Spring Valley and the Rocky Mountain Arsenal. From these case study investigations and site visits, some very preliminary lessons have been learned. Engineered and institutional controls can and will fail. Historic information management is often inadequate given current regulatory climate. Land-use and demographic changes occur fairly rapidly. Sustainable financial mechanisms are required for long-term institutional management. Multi-agency and public involvement strengthen and resolve residual hazards management issues. Innovative approaches to institutional management are being developed and tested, both at the national and international levels.

A paper on "Institutional Management of Residual Hazards – Examples from DOD" was presented by the investigators at the IEEE conference in September 2002.

Due to selected case studies, this particular LDRD effort has wide application across the nation, both within and outside of the DOE. Indeed, any agency responsible for the management of residual hazards will directly benefit from the study (e.g., EPA, Department of Interior, Army Corps of Engineers). Of particular importance is the very real potential for better understanding of what decision criteria (and associated types of engineered and institutional controls) lead to the continued isolation of known residual hazards and, just as importantly, to the failure and associated reintroduction of such hazards into the biosphere.

Ultimately, this project aims to develop a predictive decision network for application to the stewardship of both DOE and non-DOE residual hazards. This decision network would represent potential decision pathways, critical decision nodes, and the cause and effects relationships of key decisions. As such, this tool would aid resource planners, management, and stakeholders in defining and evaluating alternative residual hazards management strategies and end-states.

# Hybrid Nanocomposite Materials as Subsurface Permeable Reactive Barriers

*Mason K. Harrup, Robert T. Paine, Michael Jones, Linda Polson, Byron White*

## *Designing novel methods of contaminant containment*

GC111

The development of effective subsurface barriers could be a tremendous aid for the containment of contaminants in the vadose zone, directly solving one of DOE's toughes t problems at the INEEL Site.

This LDRD investigates the effectiveness of recently developed novel nanocomposite materials for subsurface permeable reactive barrier applications (PRBs). These new materials are Type I nanocomposites. That is, they are preformed organic polymers embedded in an inorganic matrix without significant covalent bonding between the components. The required properties for these materials to function efficiently are: 1) a tunable water passing rate to approximate the hydraulic conductivity of the subsurface environment where the PRB will be placed, 2) sufficient mechanical strength (both wet and dry) to maintain barrier integrity, 3) the ability to incorporate selective metal sequestration agents so that they remain active – yet do not leach from the barrier, and 4) to be deployable through direct injection methods such that trenching is not needed. Additionally, there is a need to keep the technology as low cost as possible, while remaining reliable.

Results obtained from the second year of this multi-year project show that the materials under investigation continue to show promise as novel PRB materials.

Technical objectives for fiscal year 2002:

- Establish collaboration with Dr. Robert Paine at the University of New Mexico to provide new sequestration agents for incorporation into the nanocomposites.
- Examine at least one new hydrophillic polymer family, formulate into nanocomposites, and compare to the existing systems.
- Investigate water uptake (swelling) behavior through the project's leading nanocomposites.
- Examine the leading nanocomposite formulations to better understand the systems and improve performance.

Hybrid molecular nanocomposites consisting of commercially available polymers, incorporated with a ceramic component, have been under investigation for the use as PRBs. Thorough characterization was made of both acid- and base-catalyzed nanocomposites for this project's leading polymer systems — polyvinyl alcohol (PVA) and polyvinyl acetate (PVAc) — containing ion sequestration agents selective for cesium. The nanocomposites were characterized using controlled-force testing, multiple- or single-frequency temperature ramp experiments, as well as creep recovery type dynamic mechanical analysis (DMA) experiments.

The acid-catalyzed nanocomposites appear to be mechanically superior to the base- or salt-catalyzed nanocomposites. Further, the cesium sequestration agent aminomolybdophosphate (AMP) was found to add strength to the nanocomposites, as indicated by controlled-force ramp studies and tan delta peak max test data.

Time temperature superpositioning (TTS) is a technique that can be used with multifrequency DMA experiments to predict material behavior at various use temperatures over theoretically impossible "laboratory test" time scales. This provides an invaluable predictive capability on the mechanical integrity and long-term behavior of these potential subsurface barriers.

The materials developed in this LDRD show great promise in that they are rheologically simple. In experiments with the AMP containing nanocomposites of both PVA and PVAc, the model fits for the Williams, Landel, and Ferry (WLF) theory and the Arhenius equation are quite good (< 30), suggesting these nanocomposites can be reliably characterized with this technique. Data gathered to date suggest that these barrier materials will perform very well over extended time periods and over the temperature ranges expected on the INEEL Site.

The interaction of metal ion laden solutions and the nanocomposite formulations is a critical element for these nanocomposites to function well as subsurface barriers. Last year's efforts provided the initial data from both PVA and PVAc systems that showed these materials were very effective at removing cesium from water. Additional experiments were conducted on these systems and the full results are to be published in the journal *Chemistry of Materials*.

The most important new data relates to the wet behavior of these nanocomposite systems. As shown in Figure 1 (next page), the two systems exhibit a wide

range of water swelling, and hence hydraulic conductivity. This result shows promise that these types of nanocomposite materials will be "tunable" to approximate a variety of subsurface environments.

Further, the total "scavenging" abilities of these systems are extremely good – removing down to as low as 300 parts per billion. Most importantly, the subsequent release of captured cesium is very low – only 1 to 3 parts per million.

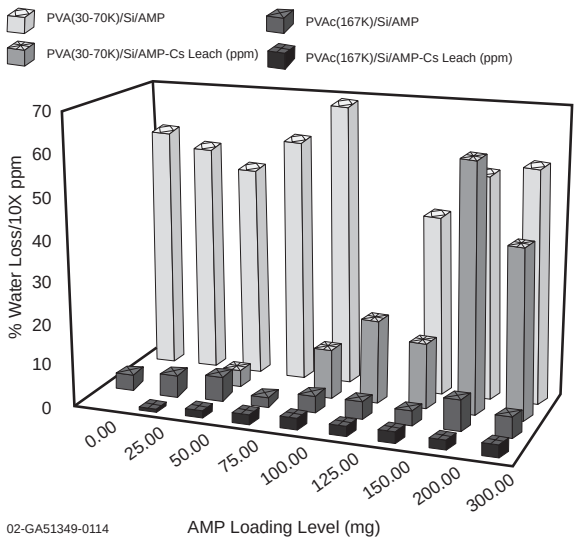


*FIGURE 1. Swelling and contaminant leaching data for the PVA and PVAc systems.*

The investigators entered into collaboration with professor Robert T. Paine at the University of New Mexico (UNM) to design, prepare and test nanocomposite materials for potential applications in subsurface barrier concepts. Prior work at INEEL had shown that nanocomposite materials could contain selective sequestering agents, while prior work at UNM had focused on designing actinide ion selective sequestering agents. The present project married the two laboratory efforts to obtain nanocomposite materials that function as specific actinide barriers.

During the first stage of the project, the UNM group prepared macroscopic quantities of 2,6-bis(diphenylphosphinomethyl) pyridine N, P, P - trioxide (TPNOPOPO). Of this material, 1.15 g was sent to INEEL for subsequent barrier material synthesis and testing. Difficulties with compatibility between 2,6-bis(diphenylphosphinomethyl) pyridine N, P, P - trioxide and the model barrier polymer material were revealed. The request was made to prepare additional amounts of the trioxide agent, which was accomplished. The samples were used in barrier syntheses and tests at INEEL. The results were somewhat disappointing. The TPNOPOPO was found to be only 10%-15% efficient in the PVA and PVAc systems versus 75%-85% active in the case of AMP in similar systems (*vide supra*). It was concluded that synthetic modifications to the nanocomposite sequestering agent would be needed in order to accomplish the long-term materials' performance goals. The UNM group will propose a second-generation ligand target for the nanocomposite.

New polymer systems that were explored were: polycaprolactam (PCL), poly-2-ethyl-2-oxazoline (POX), polyacrylonitrile (PAN), and polyethyleneoxide (PEO). Each of these systems met the prerequisites that they be amenable to incorporation into Type I nanocomposite systems and have appreciable hydrophilicity, up to and including complete water solubility. Some systems exhibit a much greater degree of swelling (like POX), unfortunately none of these systems has performed as well overall as the previously studied materials. After the collection of these empirical results, it was decided to use these data to form the basis of correlations between the solubility parameters that can be calculated, and water uptake/water permeability behavior of the nanocomposite formulations.

Specific chemical affinity of any molecule can be described as a summation of the individual "parts," as described by group contributions. Using the group contribution tool, chemical affinity of a molecule may be

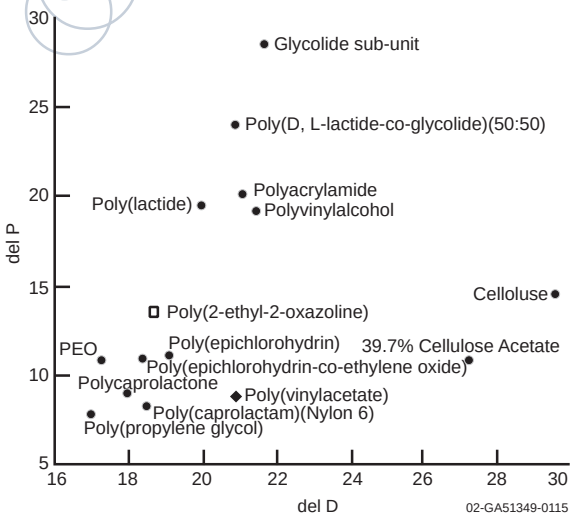


*FIGURE 2. Hanson solubility plot of new potential nanocomposite systems.*

described in terms of Hansen solubility parameters where the polar ($\delta_p$), dispersion ($\delta_d$) and hydrogen bonding ($\delta_h$) aspects of chemical affinity are represented. Since Type I nanocomposites were desired, and since one of the largest contributors to $\delta_h$ is the hydroxyl functionality, this parameter could reasonably be ignored for these initial studies.

Fourteen polymers (Fig. 2) were characterized for $\delta_p$ and $\delta_d$ using published procedures. Application of this method allows for numerical and graphical descriptions of chemical affinities that should yield a predictive capability such that intelligent design of new molecular nanocomposites with the "correct" water affinity may be accomplished.

This LDRD has resulted in the submission of an invention disclosure agreement.

# Advanced Technology for Mapping Subsurface Water Conductivity

*Gail Heath, John Svoboda*

## *Combining two techniques for better subsurface characterization*

GC108

Traditional subsurface resistivity or conductivity distribution mapping is a well-established subsurface characterization method. This method's potential resolution is not exploited to the fullest extent because the method is based only on bulk direct current (DC) resistance measurements between multiple pairs of two points with subsequent data processing to estimate the subsurface resistivity distribution.

This LDRD is developing a unique variation of this existing technology that combines the traditional DC resistivity measurements with surface magnetic field measurements where the magnetic field is generated by subsurface current flow. Resistivity measurements are accomplished by passing current through a system of permanently installed subsurface electrodes at varying depths in the volume of interest. Surface magnetic field measurements are made with a 3-axis flux-gate magnetometer's output that is synchronously detected with the transmitted subsurface current.

Magnetic field measurements are made at each map point for each frequency and electrode pair combination. Inversion algorithms will generate conductivity maps by using the spatial magnetic data as well as the resistivity data. This data will be used to determine the depth to groundwater, identification of contaminant plumes, and contaminant migration through comparison with background and historical conductivity values.

Technical objectives for fiscal year 2002:

- Design a synchronously detected, spatially resolved, 3-axis vector B-field measurement system incorporated into the operation of a Zonge GDP-32 resistivity measurement system for simultaneous surface magnetic field and subsurface electric field measurements.
- Continue refinement of the post-processing package required to prepare the magnetic field data for multi-dimensional inversion with the electric field data.
- Generate simulated electric and magnetic field data sets using a full physics model to validate inversion code development.
- Validate Multi-Phase Technologies' 3-D inversion code that incorporates electric and magnetic fields.

Electrical Resistance Tomography (ERT) is a technique for reconstruction of subsurface electrical resistivity distributions. The electrical resistivity distribution can lend information on the moisture content and distribution, movement of plumes, the geology, temperature, and most manmade materials present between the boreholes. ERT data provides good information on targets of interest between boreholes. The surface magnetic field measurements provide an orthogonal magnetic field surface view of the plumes and other conductive bodies between and outside the boreholes providing more information with less cost over existing systems.

The data sets are collected by transmitting electrical current into a pair of electrodes while the electrical potentials are measured at other electrode pair combinations and the magnetic field is measured at the surface. ERT and surface magnetic field data sets have been collected at the new Meso-scale test bed located at the Jefferson Canal Site. Baseline data collection was performed to test the INEEL B-field system and its incorporation into the Zonge ERT system. Software, primary field correction, and data interpretation have been tested using the data sets collected at the meso-scale site at Jefferson Canal Site. Three different algorithms (pre-processing, processing and inversion) are being developed for data interpretation. The integral equation solution of LaBrecque and Ward, (1987) was used to calculate steady-state results for a uniform half-space.

A synchronously detected, spatially resolved, 3-axis vector B-field measurement system was designed and incorporated into the operation of a Zonge GDP-32 resistivity measurement system for simultaneous surface magnetic field and subsurface electric field measurements. The magnetic field measurement system consists of a 3-axis flux gate magnetometer, three lock-in amplifiers, and a Zonge GDP-32 ERT receiver. Alternating current 50% duty cycle (8 Hz) is passed through the subsurface volume of interest via electrode pairs located at several depths in each borehole pair. The subsurface excitation current is controlled and transmitted via the

transmitter portion of the Zonge receiver. The Zonge receiver simultaneously measures the voltage across all non-transmitting electrode pairs. This constitutes the potential field data used by the inversion code. The 3-axis magnetometer output is fed to the lock-in amplifiers unknown input, which allows for synchronous detection of any AC magnetic fields that are synchronous with the subsurface current excitation. The lock-ins direct current output is fed to spare Zonge receiver inputs where the magnetic field data is measured and recorded with the potential data. This constitutes the magnetic field data used by the inversion code.

Synchronous detection allows for the extraction of extremely small signal levels buried in noise. The lock-in amplifiers derive their reference from the transmitted subsurface current signal. All other fields not synchronized with the reference are averaged to zero. This technique provides detection of vector magnetic field components due to milliamps of current flow through subsurface volumes.

A pre-processing package was developed that corrects the magnetic field vector data for sensor orientation, calculates the inphase and quadrature components, and corrects for the B-field associated with the surface conductors that deliver the subsurface current. During the data collection, it is difficult to keep the magnetometer aligned in the reference direction. However, this difficulty is overcome by recording the deviation angle, which is the angle between measurement direction and the true north. Given the fact that angle b is a known value, from measured angle c the deviation can be calculated and measurement can be reduced to reference plane. This reduction is called orientation correction. Orientation correction is the first correction done to the data.

The field data is collected in magnitude and phase of the magnetic field's x, y, and z components. To correct the primary magnetic field caused by current flow in the source wires, the data need to be converted to the InPhase and Quadrature component. The converted data then can be used to eliminate primary field.

A full physics 3-D forward model capable of modeling subsurface electric fields and surface magnetic fields due to subsurface current flow was developed by Dr. David Alumbaugh of the University of Wisconsin and Dr. Greg Newman of Sandia National Labs. The model is capable of calculating electric and magnetic fields in mediums characterized by conductivity, permeability, and permitivity. The Newman/Alumbaugh model and field data taken at the Jefferson Canal Site are being used as a source for generating data sets capable of testing inversion code robustness.

Closely related to ERT is the MagnetoMetric-Resistivity method (MMR) in which measurements are made on the magnetic fields generated by a more or less steady-state electric subsurface current. The MMR method has seen occasional use in mineral exploration but has seen little if any application in engineering or environmental applications. One problem is that the equipment is more expensive than standard resistivity equipment and is not readily available. As a stand-alone method, MMR has some significant limitations. Even for simple bodies, the MMR responses are fairly complicated and thus interpretation is more difficult. A fully 3-D inversion routine is necessary to interpret the ERT/MMR data in terms of subsurface conductivity. In addition, the interpretation of ERT/MMR results is non-unique. The problems in uniqueness can be overcome by combining the magnetic and electric measurements in the same inversion code.

Key to this research is that ERT is very good at delineating large structures such as layered earths whereas MMR is more sensitive to small, 3-D structures. Therefore, combining the two methods will improve the overall resolution of the ERT method alone.

This LDRD supported development of a fully 3-D inverse routine that combines magnetic and electric field measurements. The algorithm was designed and coded

by Multi-Phase Technologies of Reno, NV and is based on a 3-D finite difference forward algorithm. The magnetic fields were modeled by applying the reciprocity theorem to model the electric fields induced by a coil of unit moment at a frequency of one radian per second. Using this method allowed for an adjoint formulation for calculating sensitivities of both magnetic and electric fields with respect to changes in the conductivities of individual cells within the finite-difference mesh. In initial model studies, combined MMR/ERT surveys were better able to result 3-D structures than ether MMR or ERT alone. Therefore, combining the two methods will improve the overall resolution of the ERT method.

Successful completion of this project supports Environmental Quality and Energy Security by allowing for the mapping of subsurface contamination plumes and water, steam, and /or $CO_2$ floods. Current collaboration includes the University of Wisconsin and Multiphase Technologies of Reno, NV. Both are involved with inversion code development.

# Electrical Resistivity Imaging to Define Preferred Flow Paths in a Heterogeneous, Layered Vadose Zone

*Gail Heath, Russ Hertzog*

## *Understanding flow and transport in the vadose zone*

GC133

The DOE Vadose Zone Science Program is being developed to coordinate interdisciplinary research to improve understanding of processes occurring between land surface and underlying aquifers, and to develop the tools for using this knowledge to accurately predict and monitor the movement and transformation of contaminants. An important component of the hydrogeologic system at the INEEL is a thick (250 to 1,000 ft) unsaturated zone between the ground surface and the Snake River Plain Aquifer.

This unsaturated zone (or vadose zone) presents a significant hurdle to assessing the impact of operational activities, waste disposal, and past contaminant releases on the aquifer. To provide successful environmental management, scientific understanding of the processes important to predicting and controlling vadose zone transport and remediation must be enhanced.

A search of the DOE EM-50 Science and Technology Coordination Group (STCG) "Technology Needs" database identified 17 technology needs associated with flow and transport in the vadose zone at Los Alamos, Sandia, Hanford, Nevada, and the INEEL. This LDRD is addressing these technology needs to better understand vadose zone processes. Specific areas being investigated are: conceptual modeling of complex environments, predicting behavior of contaminants in dynamic transport processes and complex geology, innovative characterization techniques, and basic data or methods to support long-term decisions. The conceptual models developed in this project will provide a significant advancement toward meeting many vadose-zone science needs.

Technical objectives for fiscal year 2002:

- Install three monitoring wells along the Big Lost River for measurement capabilities on an intermittent infiltration source.
- Procure an Electrical Resistance Tomography (ERT) measurement system.
- Obtain a 3-D anisotropy inversion modeling routine for resistivity data.
- Design and develop an automation code for the resistivity system for automated data collection and a processing package for resistivity multi-dimensional inversion and imaging.

An MPT 2002 ERT measurement system was procured from Multi-Phase Technologies (MPT) of Sparks, NV, who also collaborated with researchers on development of the inversion code and hardware. ERT is a technique for reconstruction of subsurface electrical resistivity distributions. The electrical resistivity distribution can lend information on the moisture content and distribution, movement of plumes, geology, temperature, and most manmade materials present between the boreholes. The surface magnetic field measurements provide an orthogonal magnetic field surface view of the plumes and other conductive bodies between and outside the boreholes, providing more information with less cost over existing systems. Transmitting electrical current into a pair of electrodes while the electrical potentials are measured at other electrode pair combinations results in the data sets

The purpose of the project was to monitor infiltration on a pair of 61 m by 61 m ponds on the INEEL Site west of Idaho Falls, ID. The two ponds are separated by approximately 15 m and one pond is directly north of the other. The ponds lie on top of about 17 m of alluvial sand and gravel, and underlain, interbedded basaltic lava flows and sediments. There are significant sediment beds at around 40 m and 60 m within the basalt flows.

Prior to flooding the site, five electrode arrays were installed: three vertical electrode arrays (VEA), and two surface electrode. One of the VEA was centered between the ponds. The two surface arrays extend outward from this VEA along east-west lines between the ponds. Each surface array included thirty electrodes at 6 m intervals. The other VEA were located approximately 150 m apart in an east-west direction and 30 m south of the east-west line formed by the surface arrays. This positioned the VEA on each side of the south percolation pond, approximately 30 m distant from the pond, and the third at approximately one-third of the south extent of the pond. The depth of all three VEA was 70 m. Electrodes were placed at 2.5 m intervals.

Various electrical data were available for collection. The significant data that were collected during each time period include Schlumberger sounding/profiling along the surface arrays, common-well and cross well dipole-

dipole data, and cross-well horizontal transmitters with vertical dipole receivers. Pole-dipole-like data also was collected that used a vertical dipole in one VEA and a single electrode in a second well. The reference electrode was the bottommost electrode in the third VEA.

The data collection schedules included a pre-flood background dataset collected the morning of June 18, 2002. Subsequent data collection intervals were approximately every five hours. Continuous cycling over each 24-hour period resulted in five to six collection intervals per day. Each collection interval started and ended autonomously. Infiltration amounts are in the table below.

Conductivity changes in the subsurface show the speed of fluid movements as well as the location of ponding. The ERT data will be compared to the hydrologic information to provide more insight to the geophysics so quantification information can be extracted for the 3-D geophysics data and integrated into the hydrology point source data. This effort will provide a better, wide-scale picture of subsurface processes.

There are substantial advantages to applying a fully 3-D, autonomous system to long-term monitoring. Although all of the techniques possible with such a system have not been implemented, a prototype system successfully collected data using a variety of different arrays.

Data were collected over a two-week period essentially without an operator on the site. The data were used successfully to monitor the infiltration of the water in the interbedded sediment and basalts at the INEEL.

During the operation, the investigators determined there was a need to develop a more sophisticated operating system dedicated to autonomous operation. The existing system performs a number of self-monitoring operations. Using the menu-driven, operator-oriented operating system, the data collection system was designed to halt operation and inform the operator of any system problems. In the field trial, this was compensated for by collecting multiple data sets, thus assuring that one, or more, complete data set was collected during each day of operation. Our experience using this method suggests that, in autonomous systems, the system needs to be able to continue operations rather than halt for any situation that does not threaten to damage the system even in cases where only part of the data may be collected. Ideally, such a system should be able to adapt to problems and if necessary contact the operators remotely when problems occur.

This LDRD project is supporting Environmental Quality and Energy Security by enabling mapping of subsurface contaminant plumes, and water, steam, and / or $CO_2$ floods. Research completed to date is now being applied to an EPA monitoring project on an acid mine waste site in South Dakota.

| Data(s) | Water Added to North Pond ($m^3$) | Water Added to South Pond ($m^3$) |
|---|---|---|
| June 18-19, 2002 | 1020 | 3467 |
| June 20, 2002 | 0 | 907 |
| June 21, 2002 | 0 | 1927 |
| June 24, 2002 | 0 | 1240 |
| June 25, 2002 | 0 | 1158 |

02 GA51349-129

*TABLE 1. Data collection schedule.*

# Quantitative Deep-Reading Vadose Zone Moisture Characterization

*Russell C. Hertzog, Woo Yoon*

## *Enhancing neutron moisture tool accuracy with new interpretation methods*

GC137

Neutron tools are often preferred for moisture measurements in near-surface environmental research. However, current neutron moisture tools have very shallow depth-of-investigation and limited sensitivity to moisture content in vadose zone (unsaturated) environments. In addition, these tools are inadequately characterized and uncorrected for most near-borehole environmental factors, systematically affecting the measurement accuracy by as much as 30% to 50%.

This LDRD project investigates new, innovative methods to obtain quantitative measurements of subsurface fluid content in the vadose zone using neutron moisture tools. The research evaluates the hypothesis that enhanced moisture sensitivity can be derived from tools using large source-to-detector (S-D) spacing — consistent with larger slowing-down lengths encountered in unsaturated formations.

A Monte Carlo-based tool model will be developed for different tool configurations to compute the neutron count rate in these environments. Neutron response in terms of counting rates will be transformed into moisture content. A full moisture-response characterization will be developed for vadose zone formations, including basalts, sandstone, and interbeds containing complex clay minerals. In addition, a range of borehole conditions will be examined.

A second hypothesis evaluated in this project is to interpret moisture measurement made by the neutron tool based on formation, geochemical-based macroscopic neutron cross-sections — leading to a new, quantitative interpretation scheme or mixing law. If the new cross-section-based mixing law is successful, then quantitative moisture responses of conventional as well as new moisture tools can be extended to any arbitrary formation lithology, and each formation-component contribution can be quickly calculated from its elemental cross-sections. This interpretation scheme will extend the range of formation environments in which these tools can be used to quantitatively determine moisture.

Technical objectives for fiscal year 2002:

- Develop Monte Carlo model geometry for typical tools and new tool developments.
- Characterize the moisture-response of each different tool design.
- Develop new neutron-moisture interpretation for a wide range of environments.

The first step of this investigation consisted of surveying INEEL and U.S. Geological Service geophysicists and hydrologists who use moisture probes to determine the most common commercial neutron moisture probes currently in use and their physical-nuclear properties. The probes included the Campbell Pacific Nuclear International Inc. (CPN) Model 503 Hydroprobe Neutron Moisture Gauge and several (9055, 9057, 9073 and the 9072) neutron logging tools provided by Century Geophysical Corporation. Their properties, such as detector size, pressure, type (thermal or epithermal), and source-to-detector spacing and shielding are important for accurate Monte Carlo modeling simulations. As a starting point in this project, the CPN Model 503 Hydroprobe Neutron Moisture Gauge was selected because of its widespread use at the INEEL.

The first phase of neutron probe modeling used the internal design of the CPN Model 503 gauge, which is a short-spaced (3.89-in.) S-D configuration. However, in the interest of efficient use of this research effort, the investigation was extended to include larger S-D spacing configurations for each environmental condition (e.g. borehole fluid and casing, lithology, and grout thickness). This enabled evaluation of the effect of large S-D spacing designs and the potential use of multiple detectors on the moisture sensitivity for the same environmental conditions.

At the time of this report, ten different environmental conditions had been modeled resulting in 630 separate calculations, which are summarized in Table 1 (next page). Each model calculation simulated the effect of varying S-D spacing on the porosity response of fully saturated formations, and then the effects of S-D spacing on the water-saturation response to a 40% porous formation.

The first model determined the ultimate tool response to changes in porosity and water saturation in an ideal no-borehole, pure silica-sandstone environment. It provides a tool benchmark for subsequent results. The

| Model-Formation | Borehole | Tool Position | Casing Fluid |
|---|---|---|---|
| 1 — Silica Sandstone | no borehole | Centered | None |
| 2A — Silica Sandstone | 4" PVC, 1" Grout | Centered | Air filled |
| 2B — Silica Sandstone | 4" PVC, 1" Grout | Centered | Water filled |
| 2C — Silica Sandstone | 4" PVC, 1" Grout | Eccentric | Air filled |
| 2D — Silica Sandstone | 4" PVC, 1" Grout | Eccentric | Water filled |
| 2E — Basalt Formation | 4" PVC, 1" Grout | Centered | Air filled |
| 2F — Limestone | 4" PVC, 1" Grout | Centered | Air filled |
| 2G — Silica Sandstone | 4" PVC, no Grout | Centered | Air filled |
| 2H — Basalt Formation | 4" PVC, no Grout | Centered | Air filled |
| 2J — Silica Sandstone | 4" PVC, 2" Grout | Centered | Air filled |

02 GA51349-131

*Table 1. Summary of modeled formations and borehole environments completed in FY02.*

second model considered a 4" PVC borehole in a uniform porous media environment (silica sandstone, basalt and limestone). Note that limestone is the standard reference formation used universally in the oil and gas industry. Silica-based sandstone and basalt formations are commonly encountered in the INEEL vadose zone environment. The effects of air and water in the casing and different grout thickness (0" to 2") between the casing and porous medial formation were modeled and evaluated. Finally, the effect of logging tool position, centered or eccentric, was modeled and evaluated.

Quantitative moisture sensitivity and interpretation of the modeled data will start in the next phase of the project. However, initial results and interpretations give a good qualitative understanding of the moisture sensitivity obtained from this research. First, the computed count-rate response of the conventional single-detector, short-spaced CPN Model 503 to porosity variations in saturated water-filled porous silica-sandstone formations shows that for all borehole environments the porosity response is non-linear over the entire porosity range of 0% to 100%. It is also clear that the 4" borehole has a large impact on the ultimate porosity response of this tool, and that the porosity sensitivity diminishes greatly at porosity greater than 20%. Water-filled boreholes produce a response that is significantly shifted and anti-correlates with conventional air-filled response. Tool positioning is critical in a water-filled borehole shown by the large shift in response between the tool-centered and tool-eccentric response curves.

In addition, the computed count-rate response of a single 40-in. spaced detector, similar to the one in a CPN Model 503 tool, to porosity variations in saturated water-filled porous silica-sandstone formations shows substantial differences in the porosity responses for a long S-D tool design. The impact of the 4" borehole on the ultimate porosity response of this tool is significantly reduced, and the porosity sensitivity does not diminish nearly as much as the short-spaced tool design at large porosity. Water-filled and air-filled boreholes still produce a response that is shifted from the ultimate no-borehole response, but they both behave in a similar manner. There is an apparent loss of porosity sensitivity seen in air-filled boreholes for this detector configuration. Using appropriate neutron shields or a focused detector array could potentially alleviate this problem. Tool positioning is not as critical for the 40-in.-spaced tool, which is shown by the lack of shift in response between the tool-centered and tool-eccentric response curves for both water-filled and air-filled boreholes.

These and the other model computations enable evaluation of tool moisture sensitivity for S-D spacing from 3.89 in. to 40 in. These evaluations will enable consideration of multi-detector array designs for deeper reading and moisture profiling in near-borehole (up to 40 in.) environments.

This LDRD is generating new quantitative subsurface moisture-logging technology and interpretation methods that support the DOE mission need for quantitative "Moisture Characterization and Improved Monitoring." Successful application of the new science-based interpretation methodology, together with deeper-reading measurements, will enhance the ability to determine accurate moisture (water and organic solvents) content in the subsurface. Such advances may lead to higher technical success of DOE efforts to remediate or stabilize contamination migration.

This project also addresses the Science Needs and Opportunities statement ID-S.1.27 for enhancing and developing current in situ instrumentation, including greater analytical capabilities to determine fluid and contaminate transport in the subsurface. Science-based interpretation methodology, such as the one investigated in this research, can make moisture measurements substantially more quantitative and extend the range of formations that can be interpreted.

In addition, this research addresses the Technology Needs and Opportunities and Long-term Stewardship Needs statement, ID-6.1.27, for integrated suites of in situ instruments to determine fluid mass flux in the vadose zone. New, deep-reading tool designs coupled with comprehensive quantitative moisture interpretation can provide enhanced, integrated and more accurate mass analysis of subsurface fluids.

Follow-on work would lead to a wider range of quantitative moisture data and information for current and future logging at INEEL and other DOE sites. The new interpretation methodology developed in this project will be directly applicable to a wide range of current neutron moisture tools.

# Application of New Borehole Geophysical Methods for Stratigraphic Correlation and Identification of Non-Aqueous-Phase Contaminants

*Russell C. Hertzog, Richard Smith*

## *Defining new logging techniques for better subsurface characterization*

GC138

To improve environmental quality, more definitive methods are needed to correlate lava flow units in the subsurface through quantitative rock property information for in situ conditions, and for identification of non-aqueous contaminants in groundwater. This LDRD is investigating new methods that will give the INEEL a unique capability to analyze results of state-of-the-art borehole logging measurements in general, and specifically provide drill-rig support in INEEL wells for better characterization of the local subsurface.

The research addresses the difficult problems of stratigraphic correlation of lava flows and identification of non-aqueous phase organic contaminants in groundwater in the subsurface. Stratigraphic correlation in basaltic volcanic terrains is difficult because of the similarity of physical and chemical properties of lava flow units and the irregular 3-D geometry of lava flows. In addition, this research will support other geophysics work in subsurface science, including ongoing work at the Vadose Zone Research Park, and proposed electrical soundings for determination of aquifer and sediment interbed geometries.

Specific objectives of this LDRD include: deployment of an additional logging tool (nuclear magnetic resonance) that has the potential to differentiate between groundwater and non-aqueous-phase organic contaminants in the groundwater; providing expertise for interpretation of advanced geochemical borehole logging results; and providing drill-rig support for pulling and replacing pumps, and for setting and removing temporary plastic or fiberglass casing in wells selected for logging. The temporary casing is necessary because of the potential for losing logging tools with nuclear sources in uncased wells.

Technical objectives for fiscal year 2002:

- Add nuclear magnetic resonance (NMR) tool to provide discrimination criteria that are unavailable for any other logging method.
- Identify and refine new logging techniques that will increase confidence in stratigraphic correlation of basalts beneath INEEL and aid in defining the subsurface geometry of rock and sediment units that affect groundwater (both in the saturated and unsaturated zones) and contaminant movement.
- Provide drill-rig support for the logging campaign.

This project began in January 2002. The first step taken was to search the inventory of wells at the INEEL and surrounding region to identify wells of sufficient diameter, uncased footage, and appropriate status for logging. This task required preparatory work on short-listed wells that included removing pumping equipment and acquiring up-to-date video logs to verify the condition of the well and its casings.

The second task involved augmenting deployment of the geochemical logging tool with deployment of the nuclear magnetic resonance and magnetic susceptibility tools. The magnetic susceptibility tool will help characterize the magnetic state of the basalts and aid in the interpretation of remnant magnetic directions used for correlation of basalt lava flows. To date, a supplier of magnetic susceptibility logging tools or services has not been established.

The nuclear magnetic resonance tool provided by both Halliburton and Schlumberger measures the relaxation times of spinning protons contained in water and organic fluids in the formations. This relaxation time depends on the type of fluid and the environment in which the fluid is found. Each measurement produces a distribution of relaxation times for the fluid components in the formation. This enables one to distinguish tightly bound hydrated water in clay materials, capillary-bound water, and free water. Nuclear magnetic resonance tools also can distinguish water from other hydrogen-containing fluids (petroleum, gas and possibly organic solvents) by their different relaxation times. NMR logging measurements are traditionally used in oil and gas environments — typically saturated sandstone or carbonate formations. Schlumberger was contacted, and cost estimates to perform the logging measurements were obtained.

The third task required the development of new acquisition and processing protocols for the geochemical logging tool to account for its use in unsaturated and freshwater conditions. Schlumberger has developed geochemical-logging interpretations for saturated sedimentary environments such as those encountered by the oil and gas industry. Elsewhere, some interpretations for igneous and metamorphic terrains for the Ocean Drill Program (ODP) have been developed at the Lamont-Doherty Geological Observatory, Columbia University.

For INEEL unsaturated freshwater environments, a new interpretation model will be required. The INEEL vadose zone is comprised of unsaturated basalt formations and continental sediment interbeds with freshwater and possible DNAPL contaminates, unlike those in the ODP interpretation model or the marine clastic-sediment models developed for the oil field applications. Geochemical interpretation models combine measurements from various conventional logging tools with thermal-neutron capture, gamma-ray measurements from nuclear spectroscopy tools, nuclear physics, and geochemical information to determine elemental concentrations.

There are two major steps in developing geochemical interpretations. A new "Oxides-Renormalization Model" needs to be defined for freshwater basalt formations. This model is a critical component in converting nuclear spectroscopic measurements to elemental concentrations. Activity completed in FY02 resulted in assembling existing chemical and modal compositions of basalt data at INEEL. Following this, a new element-to-mineral transformation model will be developed for evaluating this environment. Cores and core data from the logged wells or nearby wells are in the process of being examined and analyzed for elemental concentrations and mineral content to develop and benchmark the new interpretation model.

This is a proof-of-principal project and demonstration of utility that can lead to the development of optimum tools for the shallow-subsurface, continental-basaltic environment. The research is contributing to environmental quality by providing a more definitive way to correlate lava flow units in the subsurface, by providing quantitative rock property information for in situ conditions, and by providing a heretofore-unavailable way of identifying non-aqueous contaminants in groundwater. In addition, this work will bring to bear the most advanced borehole logging techniques to problems of stratigraphic correlation in volcanic terrains, and has the potential to make significant advances in this problem area. Increasing the confidence in the correlation of units would be extremely valuable in the subsurface characterization of several DOE sites (INEEL, Hanford, Los Alamos, and perhaps others). Also, demonstration of the capability of detecting non-aqueous contaminants in groundwater would be beneficial at all DOE sites.

# A New Hydrogeophysical Method for Characterizing and Monitoring Preferential Flow Paths in Complex Layered and Fractured Basalt

*Russell C. Hertzog, Carolyn W. Bishop, Mike D. Knoll*

## *Improving non-invasive techniques for subsurface characterization*

PH106

At monitoring sites across the DOE complex, contaminant transport in the vadose zone has greatly exceeded predicted transport suggesting that current predictions contain serious errors. Prediction inaccuracy is related to computer model uncertainty. Model uncertainty is directly related to the ability to accurately describe the system being modeled. Specifically, the predictive failure can be attributed to scaling issues involved with hydraulic property estimation, limited ability to use proxy information, failure to understand vadose zone processes, and inability to monitor flow in preferential flow pathways.

The purpose of this LDRD is to evaluate and test an integrated hydrogeophysical methodology for identifying, characterizing and monitoring preferential flow paths in complex, layered and fractured basalt sequences. In particular, this research can lead to better techniques to characterize subsurface heterogeneity, estimate hydraulic properties, and characterize and monitor fluid flow and contaminant transport through extremely complex fractured rock systems.

Technical objectives for fiscal year 2002:

- Log TAN-34 and TAN-35 with the optical televiewer to provide an oriented visual image of the formation around the borehole, or virtual core.
- Assemble all geophysical well logs.
- Conduct crosshole radar and seismic tomography in TAN-34 and TAN-35.
- Use single-hole directional radar methods to image near-vertical features near the wells at the TAN site.

This LDRD research began in April 2002. Therefore, this report is of the first 6 months of a 36-month investigation. The project research is divided into two phases with the first part of each phase designated for data collection. The first steps were to prepare a work package to perform fieldwork at TAN, and to obtain waste generating permits. Required software also was purchased.

TAN-34 and TAN-35, wells approximately 125-m deep and spaced about 20 m apart, were logged with the optical televiewer. Because optical televiewer data had not been collected previously at the INEEL, it was not obvious that this technique would be successful here. However, operating and adjusting the televiewer to subsurface conditions at the INEEL was achieved, and data from the two boreholes were successfully collected.

The next step involved processing and analyzing the optical televiewer logs. Deeper water in these wells contains dark-colored residue — presumably a byproduct of the ongoing bioremediation activity in the aquifer. It was difficult to "see" the formation through the murky water. This was especially true for deeper portions of TAN-35. Thus, more enhancements may be required. Even given these difficulties, the televiewer data will have far-reaching implications for INEEL subsurface science.

The televiewer data were compared to archived TAN-34 core to demonstrate that it accurately represents the real core. In many ways, the televiewer data is superior to the core data — at a fraction of the cost. Clearly, this type of data will impact scientific understanding of aquifer dynamics, flow mechanics, remediation efforts, well drilling, etc.

Figure 1 shows a sample of a three-meter section (at 94- to 97-m depth) from TAN-34 that contains a rubble zone. Comparing the virtual core sample with the actual core, illustrates the utility of the televiewer. In recovering the actual core, this interval was largely lost with less than a half meter of core obtained. The structure of the actual core sample also was completely lost. The televiewer core, conversely, shows the actual structure of the rubble zone as it exists in the subsurface. This insight has the potential of enhancing scientific understanding of the structure, and how water and contaminants might move through it.

*FIGURE 1. Virtual core from TAN-34.*

In addition to information gained from a visual inspection of the aquifer, the planned scientific application of the data are to use it along with other data to map porosity and permeability between the two boreholes. Those tasks will be investigated in FY03.

Digital files for TAN-34 and TAN-35 geophysical well logs were collected and are being evaluated to determine whether they are of sufficient quality or whether additional logs will be required. Neutron, gamma-gamma, natural-gamma, temperature, and flow logs have been located. The sonic logs are unavailable and the density tool is not calibrated to the INEEL subsurface, which reduces its usefulness. Additional geophysical logging will be required, including sonic, temperature, and flow logs.

In September, seismic tomography surveys were run in TAN-34 and TAN-35. The data will be analyzed and processed in FY03. Radar reflection and radar tomography data have been collected previously. The intent is to convert the neutron logs into porosity logs. Radar can define the high and low porosity values, and be used to convert the neutron counts into porosity. The optical televiewer can serve as a guide to what portions of the neutron logs can be trusted

Training in WelCAD also was accomplished this year. An abstract describing the early results was submitted to the Symposium on the Application of Geophysics to Environmental and Engineering Problems (SAGEEP) for presentation in April 2003.

This LDRD is contributing to improved methods for imaging, characterizing and monitoring preferential flow paths in layered and fractured basalt. The research meets the science needs expressed by the National Research Council (NRC 2000) for improved understanding of subsurface processes, scale issues, and characterization and monitoring methods for DOE and other stakeholders. This project has fostered collaboration between the INEEL and Boise State University.

# Advanced Simulation Method Development

*Richard W. Johnson*

## *Updating numerical techniques for faster computing*

GC123

The ability of scientists and engineers to simulate complex processes is a function of the correctness of the mathematical model for the process, the accuracy and efficiency of the numerical method used for discretization, the speed and capacity of the computer, and the efficiency of the programming. It is well established that the numerical simulation of complex physical processes, such as flow in porous media and turbulence, has utility and can provide useful insight.

The INEEL uses numerical simulation to design and simulate subsurface remediation schemes and evaluate engineering equipment, such as nuclear reactor heat exchangers. While significant and continuing progress is being made in machine speed and computer programming, numerical techniques that were developed in the 60s, 70s and 80s are still in use. These techniques typically employ piece-wise linear "curves" to represent model solutions that are indeed complex curves.

B-spline collocation is a numerical method that can employ piece-wise continuous curves of degree "n" where "n" is arbitrary. The information needed to define such curves is usually far less than for piece-wise linear curves for representing the same actual curve. The details for using such versatile spline curves to approximate solutions to differential equations includes what degree "n" to use, which points to use for the evaluation (collocation) points, how best to manipulate the curve, and the best algorithm to find the solution. For the case of a simple 2-D fluid flow problem, it has been found the quartic B-spline curves are best, control-point collocation is best, and that a simple ad-hoc treatment works well to find a solution to the flow equations.

One of the DOE missions is to develop significant simulation codes for several different areas of interest to promote scientific discovery. That is, it is desired that numerical approximation be used to simulate, and hence understand the basic physics of complex processes such as combustion, turbulence in fluid dynamics, subsurface transport of pollutants and others. Simulations of such processes can require very long computational times and enormous memory resources for one simulation, or they can require a large number of simulations for calibration and design optimization.

B-spline collocation holds the promise of faster compute times and reduced storage requirements than traditional methods. This two-year LDRD is investigating and determining the most appropriate B-spline functions to use and the most effective ways in which they should be implemented.

Technical objectives for fiscal year 2002:

- Determine whether quartic B-splines are more efficient and effective for representing the solution to the second order differential equations that describe the test problem than are cubics for the same fineness of knot vector.
- Develop a novel knot insertion (refinement) algorithm for a 1-D test problem that inserts knots to improve the accuracy of the approximate solution, starting with only boundary knots.
- Submit journal papers for review for publication.

The traditional numerical methods of finite differences and finite volumes use piece-wise linear curves to represent solutions to differential equations. The standard finite element method typically uses linear elements, although it can apply higher degree basis functions. Usually however, the continuity of the basis functions is only $C^0$ continuous (has function continuity, but not derivative continuity) at element boundaries. B-spline curves are piece-wise polynomials that have $C^{n-1}$ continuity for 'n' degree B-splines (with simple knots). By using higher continuity at the segment junctions, or knots, B-spline curves/surfaces require less information for their definition than do curves with lower order continuity. For this reason, it is desirable to determine how efficiently and effectively B-spline-based solutions compare to the traditional methods.

A collocation method evaluates the differential equation at a finite set of (collocation) points on the approximating curve, Fairweather and Meade (1989). The points chosen for the collocation points characterize the collocation method. The choice of collocation points is crucial to the accuracy of the scheme. Collocation at the knots is called nodal collocation, while collocation at the Gauss integration points is denoted orthogonal collocation. In the present research, it has been found

that collocation at the same locations as the control points yields accurate results. For rectangular geometry, the control points are located at the Greville points. Carey and Oden (1983) indicate that collocation is actually a member of the finite element family, although it is not a standard approach.

Although spline collocation has been around for some time, it has usually been applied to simple 1-D equations. More recently, researchers have shown a renewed interest in collocation methods and have begun to extend their application to complex equations in multiple dimensions, such as equations that describe fluid dynamics.

Objectives for developing the numerical method are speed, accuracy, versatility and robustness. Developing, 2-D, incompressible, laminar channel flow is used for a test problem. Tensor product B-splines surfaces are used to represent the solution to the describing equations. After investigating cubic B-splines, it has been found that quartic B-splines yield more accurate solutions for the same knot vectors. This is attributed to the fact that second-order derivatives of quartic B-splines are quadratic B-splines. Second-order derivatives of cubic B-spline curves, on the other hand, are only piece-wise linear B-spline curves. The solution is found using Newton's method and a single matrix equation.

The control points of the velocity components at the boundaries are given by the boundary conditions. Knowing the boundary control points however, does not satisfy the differential equations on the boundaries because the solution is not the analytical solution. If both (Dirichlet) boundary conditions and boundary residuals are included in the solution, an over-determined system results. Such systems can be solved using optimization algorithms. Solutions have been found using the following approaches:

- A minimization solver employing the well-known BFGS update on a fine grid.
- A minimization solver employing BFGS update at the control points (Greville points).
- Newton's method & line search with residuals on the boundaries for the over-determined systems for $C^{n-1}$ and cubic $C^1$ splines curves; that is $C^2$ and $C^1$ cubics and $C^3$ quartics.
- Newton's method for an exactly determined system by eliminating equations for velocities at near-wall control points.

Figure 1 presents results for the test problem for the FIDAP finite element code, the fine grid BFGS solution, the BFGS solution at the Greville points, and the exactly and over-determined solutions. The FIDAP and BFGS

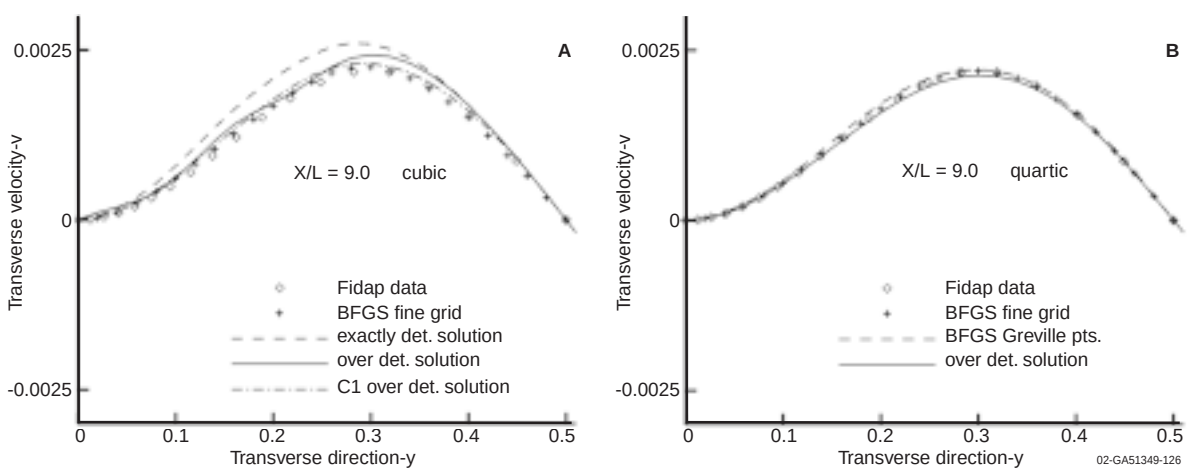


*FIGURE 1. Transverse velocity profile using (a) cubic and (b) quartic B-splines for the cases shown.*

fine-grid solutions, which closely match, are taken to be the most accurate solutions and are used for comparison purposes. Figure 1 results are for the transverse velocity profiles at x/L = 9.0. It can be seen that the quartic solutions are superior to the cubic ones and that the quartic over-determined solutions, which employ the special wall treatment, match the FIDAP and fine-grid BFGS results quite closely.

Time requirements for B-spline collocation are of interest to show the potential for speed. The time required for the setup and solution for the FIDAP and over-determined solutions for a single iteration is in the table below:

| | | B-spline Collocation (over-determined) | |
|---|---|---|---|
| | FIDAP v. 8.60 | C2 cubic | C3 quartic |
| Problem setup and Newton iteration | 1.2 sec | 0.5 sec | 1.5 sec |
| LU decomposition and solution | 4.0 sec | 0.7 sec | 1.4 sec |
| Total time | 5.2 sec | 1.2 sec | 2.9 sec |

02-51349-126B

The above cubic and quartic B-spline collocation schemes are faster than the bilinear FIDAP FEM solution. Solutions found using the BFGS optimization algorithm are significantly slower than the others and not competitive in a time-wise sense. This result is preliminary inasmuch as the B-spline collocation solution has not yet been fully optimized.

The implementation of quartic B-spline surfaces with a collocation scheme, using the control points for the collocation points and including residual information on the boundaries, is shown to yield accurate results. The method shows promise to be significantly faster for the same accuracy than traditional finite element methods. The present work includes collaborators at Brigham Young University who are well known in the field of computer aided geometric design, which develops advanced geometric functions.

This project seeks to develop a numerical method for quickly solving differential equations. Mathematical models that describe many physical processes are differential equations. Modeling is clearly important to the Subsurface Science Initiative, the Advanced Computational Simulation Initiative, Long-Term Environmental Stewardship Initiative, and the Generation IV Nuclear Energy Initiative. Numerical modeling is also important to DOE programs, including Office of Science advanced computing, EM programs and EREN interests in improving energy efficiency through understanding and modeling industrial processes through simulation-based design.

# Demonstration of Spatially Resolved Molecular Approach to Detect Specific Microbial Activity on Mineral Surfaces

*William K. Keener*

## *Understanding subsurface microbial processes*

GC139

The National Research Council has identified as a major scientific knowledge gap, the lack of understanding of processes operating in the subsurface, including microbiological processes and their effects on contaminant form and migration. As conditions change due to microbial enzymatic activities, changes in the microbial communities ensue. Particular members of subsurface communities (e.g., *Geobacter* spp., *Shewanella* spp.) attach to iron-containing minerals and can act directly on the iron, using it as an electron acceptor. Soluble contaminants (e.g., radioactive uranium) also can be reduced by bacterial enzymes and immobilized. By manipulating microbial processes to control contaminant migration in the subsurface, the eventual exposure of human populations to these toxic contaminants might be avoided.

The adaptation of recently reported molecular methods to subsurface samples provides a promising means of obtaining an understanding of subsurface microbial activities. This LDRD investigates the direct visualization of attached subsurface bacteria based on activity markers that may be spatially correlated with measurements of the results of their metabolic processes (such as the reduction of various metals and actinides), some of which represent contaminants of concern to DOE (e.g., uranium). The research is investigating attached microbial communities according to their activities and correlating this information with the spatial microanalysis of immobilized contaminants. The methodology involves visualization of bacteria based on direct, fluorescent labeling of cells through the polymerase chain reaction (PCR) occurring within the cells (in situ PCR). By amplifying bacterial nucleic acids encoding the metal-reducing enzymes, an indication of the microbial activity of interest is obtained. Though technically challenging, progress was made in improving this method during the project term.

Technical objectives for fiscal year 2002:

- Establish collaborations with Idaho State University (ISU).
- Further improve methodology and conduct in situ PCR experiments at the INEEL.
- Identify and label representative bacteria with improved specificity.

This project was a short-term LDRD (March -September 2002). To obtain the research objectives, it was decided to integrate existing methods and strengthen collaborations with people working in this field, such as Dr. Timothy Magnuson at ISU. Activities included several working visits to ISU and ensuing work at INEEL. As a result of this collaboration, it was determined there was a high background labeling of cells even in the absence of the PCR reaction. Hence, the experimental conditions would need to be improved to achieve PCR-dependent labeling and avoid nonspecific labeling of cells caused by the water-insoluble fluorescent probes (linked to dUTP nucleotides to allow incorporation into PCR products). Since the long-term applications include labeling of bacteria attached to substrata with varying affinities, it is undesirable to rely upon extensive washings to remove unreacted probe molecules. Washings also might dislodge bacteria and result in artifactual data, thus probes were sought that had decreased tendencies to adhere nonspecifically to cells.

The *E. coli* (target gene, *malE*) was selected by the principal investigator as a representative bacterium with which to refine in situ PCR methods. After testing various probes (Fig. 1 next page), it was found that Alexafluor-dUTP probes (Molecular Probes, Inc., Eugene, OR) enabled PCR-dependent labeling with only a single washing step to remove unincorporated probes. As a control, unlabeled nucleotides were omitted to prevent PCR product formation and demonstrate PCR dependence. It was later found that drying the labeled cells could improve their contrast (visibility) against the background (Fig. 1E).

At ISU, Dr. Magnuson tested a set of alternative probes with similar results. His representative microorganisms were *Geobacter pelophilus* and *G. sulfurreducens* (target genes, *ferA*, encoding an outer membrane metal reduc-

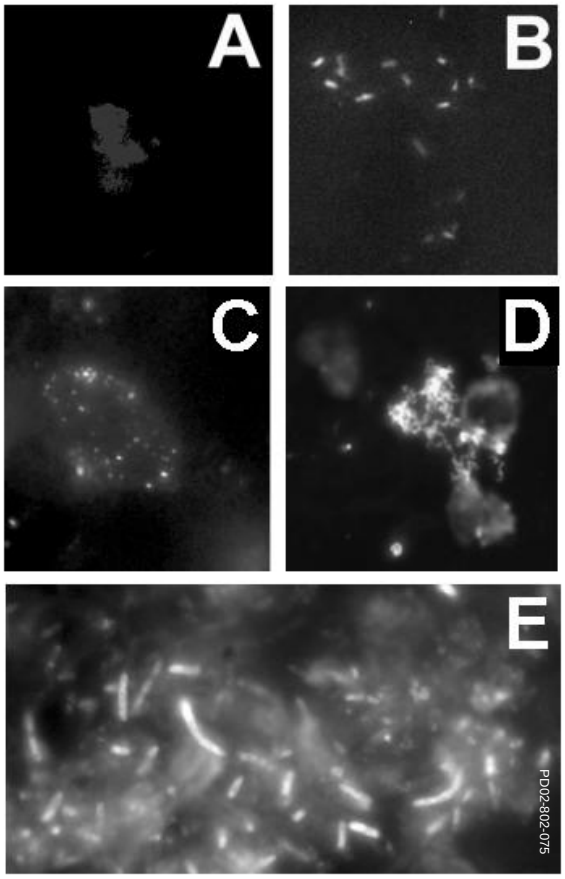


*FIGURE 1. In situ RT-PCR detection of cells using various fluorescently labeled nucleotides. (A) Negative control of mineral-attached* Geobacter pelophilus *with IRIS-labeled water-soluble nucleotide; (B) Positive reaction with attached* G. pelophilus *and IRIS-nucleotide; (C) IRIS-Fuchsia-dUTP positive reaction with attached* G. sulfurreducens*; (D) BODIPY-TR14-dUTP positive reaction with attached* G. sulfurreducens *(note non-specific binding of BODIPY dye to mineral surfaces); (E) labeling of* E. coli *by in situ PCR with Alexafluor-488-dUTP.*

tase). Cultures were grown on synthetic ferrihydrite mineral, and cells were then fixed and pretreated for reverse trancriptase-PCR (RT-PCR amplifies mRNA). Cells labeled by RT-PCR were visualized by fluorescence microscopy. It was clear that the water-soluble fluorescent probe IRS-Fuschia-dUTP performed better, in terms of labeling, with lower background and lower non-specific binding to the mineral (Fig. 1C, D). Labeled amplicons of RT-PCR were observed in gel electrophoresis experiments.

The knowledge and expertise gained from this short-term LDRD has enhanced the INEEL's capabilities in subsurface science research. The increased expertise in molecular techniques and considerations for environmental analysis has enabled INEEL scientists to develop new concepts for a microarray-based detection platform for DNA analysis with applications in environmental science, among others. As a result of this work, INEEL and ISU scientists are in a better position to pursue environmental applications of in situ PCR methodology. Future experiments would integrate other methodologies for detecting contaminant deposition caused by bacterial microcolonies.

This work is relevant to the DOE Environmental Quality Mission and addresses EM science needs: ID-S.1.01, Microbial Alteration of Heavy Metal and Radionuclide Partitioning at Mineral Surfaces; and ID-S.1.10, Geochemistry of Contaminants in the Vadose Zone.

# Nonaqueous-Phase Fluid Behavior in the Vadose Zone: Model Development & Testing

*Robert Lenhard*

## *Understanding "residual NAPL" for improved modeling*

GC132

To predict multiphase fluid flow behavior in the subsurface, relations among fluid relative permeabilities, saturations, and pressures (i.e., k-S-P relations) need to be known. In this LDRD, a hysteretic k-S-P model is being modified to account for immobile nonaqueous-phase liquid (NAPL) in the vadose zone. Because the NAPL is immobile, it is retained in the pore spaces of the vadose zone and serves as a long-term source of groundwater contamination. The NAPL that is retained in the vadose zone against gravity is commonly called "residual NAPL."

Current models describing k-S-P relations are unable to accurately predict the formation of residual NAPL. Typically, models that account for residual NAPL assume it is a constant value independent of saturation-path history. Recognizing the deficiency in current k-S-P models, the investigators developed an improved k-S-P model for predicting residual NAPL.

Furthermore, capabilities have been developed for continuing this research of subsurface NAPL behavior. An automated two- and three-phase saturation-pressure apparatus has been designed and constructed for investigating and quantifying relations between fluid pressures and saturations. Capabilities also were acquired for measuring important fluid properties that govern subsurface NAPL behavior.

This work is a valuable step toward developing computer codes at the INEEL that more accurately predict the behavior and distribution of contaminants in the vadose zone. Additionally, the research has resulted in capability at the INEEL to better investigate subsurface NAPL contamination problems at DOE sites, which are important environmental concerns to the nation.

Technical objectives for fiscal year 2002:

- Build a second experimental apparatus for automatically measuring relations between fluid pressures and saturations in either two- or three-fluid systems.
- Develop mathematical model to account for residual NAPL in k-S-P relations that can be used in numerical simulators for predicting subsurface NAPL behavior.
- Develop capabilities for measuring important fluid properties.
- Prepare manuscripts for scientific publication and present research at professional meetings.

Relations between fluid pressures and saturations are very important for predicting the subsurface behavior of NAPL. From these measurements, parameters are determined that reflect the distribution of pore sizes in a porous medium. Information about the pore-size distribution is used to predict how quickly fluids move through a porous medium. The relationships among fluid pressures, saturations, and fluid-conductance potential typically are referred to as relative permeability-saturation-pressure (k-S-P) relations and are required for modeling multiphase flow.

There are several k-S-P models commonly used in multiphase flow and transport numerical simulators. A deficiency in them is that they do not predict or account for residual NAPL. Laboratory experiments have clearly demonstrated the failure of current k-S-P models to predict residual NAPL, especially dense NAPL (DNAPL) in the vadose zone.

To improve predictions of subsurface DNAPL behavior at DOE sites, the investigators modified an existing k-S-P model for two- (air-water) and three-fluid (air-NAPL-water) systems. These modifications allow residual NAPL to be predicted based on the water and NAPL saturation-path histories. The modified model can be incorporated in multiphase flow and transport simulators to obtain a more accurate description of subsurface DNAPL contamination at DOE sites. Additionally, the simulators can be used to investigate remedial alternatives, the long-term groundwater contamination risks, and help develop plans for cost-effectively characterizing contaminated sites. Using well-formulated and scientifically sound predictive models can help to reduce the costs of managing legacy contamination at DOE sites.

The major modification made to the current k-S-P theory was to separate the NAPL that is not trapped and occluded by water into mobile and immobile components. Most current k-S-P theory assumes all NAPL that is not trapped by water is mobile. The investigators developed an expression to calculate the immobile NAPL

saturation as a function of the water and NAPL saturation-path histories based on fundamental considerations. The expression is

$$\bar{\bar{S}}_{rot} = \bar{S}_{rom}\left(\bar{\bar{S}}_t^{max} - \bar{\bar{S}}_w\right)^{0.5}\left(1 - \bar{\bar{S}}_w\right)^{1.5}$$

in which $\bar{\bar{S}}_{rot}$ is the apparent residual-NAPL saturation, $\bar{S}_{rom}$ is the effective maximum residual-NAPL saturation (a calibration term), $\bar{\bar{S}}_t^{max}$ is the historic maximum apparent total-liquid saturation, $\bar{\bar{S}}_w$ is the apparent water saturation. Predictions using equation (1) were compared to experimental data published in the literature. The predicted values were generally within 0.02 of the measured values, which suggests that this approach to predicting residual NAPL is appropriate. Equation (1) is a significant advancement for modeling residual NAPL, because different values are predicted depending on the prior wetting and drying history of the site. A constant value does not have to be employed in predictive models.

To predict how readily NAPL can move through the pore spaces, which may contain immobile NAPL, an integral expression was developed. A key element to the expression is that the NAPL relative permeability will be zero when the mobile NAPL saturation becomes zero. A NAPL relative permeability of zero means that the remaining NAPL is immobile. Both the tortousity-correction term and the integral expression will be zero when the mobile NAPL saturation is zero. The integral expression also includes a correction term for any air that might be trapped in the mobile NAPL. The expression is

$$k_{ro} = \bar{S}\,of^{0.5}\left\{\frac{\displaystyle\int_{\bar{\bar{S}}_w + S_{rot}}^{\bar{\bar{S}}_t} \frac{d\,\bar{S}_e}{h\,(\bar{S}_e)} \int_0^{\bar{S}_{atof}} \frac{d\,\bar{S}_{atof}}{h\,(\bar{S}_e)}}{\displaystyle\int_0^1 \frac{d\,\bar{S}_e}{h(\bar{S}_e)}}\right\}^2$$

in which $k_{ro}$ is the NAPL relative permeability, $\bar{S}_{of}$ is the effective mobile-NAPL saturation, $\bar{\bar{S}}_t$ is the apparent total-liquid saturation, and $\bar{S}_{atof}$ is the effective trapped-air saturation in the mobile NAPL.

A computer program was written using equations (1) and (2) to predict water and NAPL saturations and relative permeabilities. The program was used to test the modified k-S-P model. Saturations and relative permeabilities were predicted for a hypothetical scenario involving wetting and drying water and NAPL saturation paths. Results suggest that the modified k-S-P model is able to predict the formation of residual NAPL and how it affects NAPL movement. Use of the model at DOE sites is likely to provide a more accurate and reasonable description of subsurface NAPL contamination.

This LDRD supports the Subsurface Science Initiative at the INEEL. The work also supports the development of expertise, scientific knowledge, and capabilities for conducting research on DNAPL contamination at DOE sites. Manuscripts have been written for presentation/publication. In addition, this research has led to a proposal to the DOE's EM Environmental Management Science Program in collaboration with Auburn University and Pacific Northwest National Laboratory.

# Investigation of the Movement and Fate of Chlorinated Hydrocarbons

*Robert Lenhard*

## *Using mesoscale experiments to model contaminant behavior*

GC135

The Subsurface Science Initiative at the INEEL emphasizes the need for mesoscale experimental investigations to better understand processes occurring in the field. Too frequently, poor predictions of contaminant flow and transport result when data and parameters from small-scale experiments are used to predict field behavior. This occurs because many of the complicated and interdependent factors that govern flow and transport behavior in the field do not manifest themselves in small-scale experiments in a meaningful manner.

At the INEEL Subsurface Disposal Area (SDA), waste has been buried from DOE's Rocky Flats site that contains carbon tetrachloride ($CCl_4$) in a gel-type form. Over time, $CCl_4$ vapors from this waste have moved through the subsurface, resulting in groundwater contamination. The purpose of this LDRD is to help understand and predict $CCl_4$ contamination in groundwater at the SDA by developing mesoscale experiments. The experimental system will be approximately 3-m long by 2-m wide by 2-m high. The movement of $CCl_4$ in the gas phase through simulated layers of sediments and basalt to the capillary fringe will be measured as well as microbial-assisted transformation of $CCl_4$. The resulting data will be used to help predict the subsurface fate of $CCl_4$ in the SDA and test the predictive model.

The work effort this year was focused on designing and constructing the experimental system and evaluating the potential use of measuring systems to quantify the chemical composition of the aqueous and gas phases in porous media.

Technical objectives for fiscal year 2002:

- Determine the dimensions of the experimental system with computer modeling studies.
- Design and construct the experimental system.
- Test and evaluate measurement systems to use in the experiments.

To help reduce costs for cleaning up contaminated DOE sites across the nation, experiments are needed to better understand the complex subsurface processes that affect contaminant fate, and predictive models need to be tested against the resulting data.

This research investigates the movement of $CCl_4$ vapors through porous media with a structure similar to the subsurface beneath the SDA – mainly alternating layers of unconsolidated sediments and fractured basalt. The data collected is being used to better understand $CCl_4$, and to test the predictive model that forecasts future behavior.

To conduct this investigation, mesoscale experiments are being used. The size of the experimental domain was determined by a combination of practicality and computer model simulations of $CCl_4$ behavior. It was determined that an experimental system 3-m long by 2-m high by 2-m wide would likely be sufficient. An experimental cell was designed to enable simulation of groundwater flow and provide for a vadose zone of significant thickness (Fig. 1).

*FIGURE 1. The 3-m long by 2-m high by 2-m wide experimental cell.*

To investigate microbial-assisted transformation of $CCl_4$, microbial cultures were prepared for the experiments. These laboratory cultures were developed from microorganisms collected from vapor extraction wells at the SDA. The cultures were grown in serum vials and diluted to $1x10^5$ cells/ml of growth medium. The cultures will be used in the experiments and in tests to evaluate the effects microbes may have on measurement of chemical concentrations.

In all experiments, measurement systems need to be used that can quantify the changing chemical environment. These measurement systems must nondestructively determine chemical concentrations over long time periods with minimal maintenance. Dakota Technologies, Inc., was engaged through a subcontract to evaluate the feasibility of using their new measurement system in mesoscale experiments (Fig. 2). The measurement system consists of hollow-fiber membrane sensors that will be used to quantify $CCl_4$ concentration in the gas and aqueous phases in partially water-saturated porous media. Pulses of carrier gas are flushed through the headspace of the hollow-fiber membranes and analyzed by a gas chromatograph. The concentrations of gases in the headspace of the hollow-fiber membranes are related to the concentrations in the porous media through Fick's and Henry's Laws.

The conclusion of the initial feasibility study is that the hollow-fiber membranes can be used to quantitatively measure $CCl_4$ concentrations in porous media.

This LDRD is building unique capabilities and expertise at the INEEL to conduct mesoscale experiments that will lead to a better understanding of contamination problems at DOE sites, including the $CCl_4$ contamination problem at the INEEL.

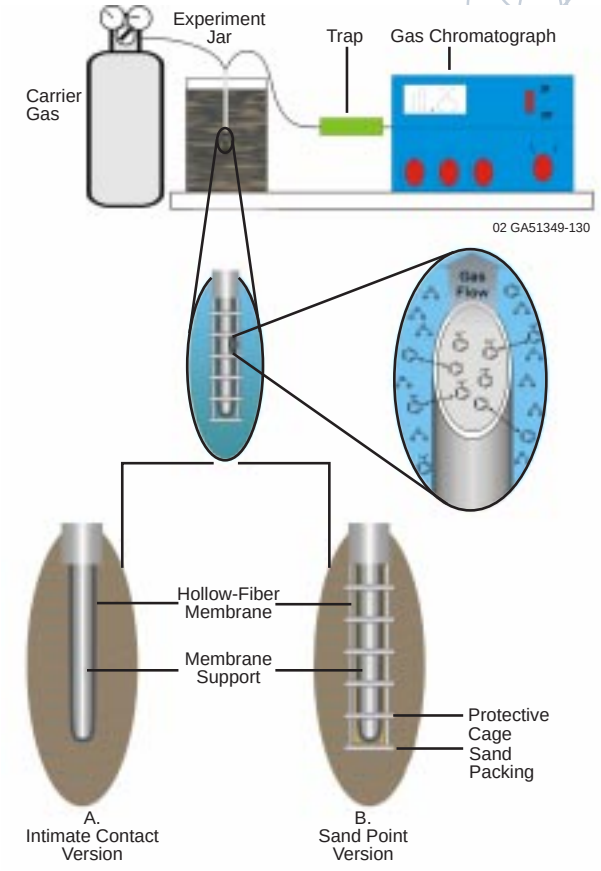


*FIGURE 2. Schematic of measurement system from Dakota Technologies, Inc.*

# Investigation of the Effects of Microbial Growth on Unsaturated Hydraulic Properties

*Earl D. Mattson, Carl D. Palmer, Michael A. Plummer, Kristine E. Baker*

## *Examining complex subsurface contaminant migration with a centrifuge*

GC146

Access to chemical sorption sites, delivery of microbial nutrients, and net solute residence time within the vadose zone depends on the pore-scale flow structure and the porous media. One conceptual model used to describe the early arrival and long tailing of solute breakthrough curves (BTC) in unsaturated media is the mobile-immobile water model. In this conceptual model, the water contained in the soil pores consists of two portions: a mobile fraction contributing to the advection of solute through the unsaturated soil and an immobile water fraction that is stationary and acts as a solute source/sink term.

Published research results have shown that at low moisture contents, only a small fraction (< 20%) of total soil water contributes to advective transport in an unsaturated soil. These small fractions lead to enhanced-solute velocity as compared to that calculated using the average pore-water velocity. An immobile water fraction of 0.80 implies that solute is being transported five times faster than calculated using the classical BTC analysis. Transfer of the solute between the mobile and immobile water fractions is assumed to be diffusion limited and accounts for the long tailing of BTCs.

In addition to affecting the solute BTC, less studied aspects of the mobile-immobile water model are the secondary effects of the solute transfer into the immobile regions affecting microbial growth and kinetically controlled chemical processes. These coupled processes can have a major impact upon the effectiveness of engineered contaminant remedial solutions, prediction of solute transport through surface and subsurface barriers, contaminant migration in unsaturated soil, and release rates from waste sites. The implication of these secondary effects upon contaminant transport in a centrifugal field has not been sufficiently explored or quantified.

This LDRD project is investigating methodologies, tools, and expertise for examining complex subsurface contaminant migration processes through the use of a centrifuge. This centrifuge experimental approach has two distinct advantages over conventional methods. First, experimental data is collected over much shorter time periods, resulting in a more complete evaluation of various chemical conditions and materials. Second, the increased forces in the centrifuge allow experiments to be conducted over a wider range of moisture regimes.

Although the results of the proposed research applies to all DOE sites, those with deep vadose zones in arid climates, such as the INEEL, Hanford, the Nevada Test Site (NTS), and Yucca Mountain, will benefit the greatest.

Technical objectives for fiscal year 2002:

- Design geocentrifuge experimental protocol to conduct solute transport experiments.
- Conduct suite of geocentrifuge experiments.
- Build quantitative tools to analyze experiments.

The transfer of solutes between the mobile and immobile water fractions is often described by a first-order rate coefficient ($\alpha$). This coefficient is a fitting parameter of the solute BTC and is generally assumed to be a constant independent of both the velocity of the fluid in the mobile water fraction as well as the moisture content at which $\alpha$ is determined.

The assumption of a constant $\alpha$ is questionable. Conceptually, since solute flow pathways are dynamically related to moisture content, diffusion between mobile and immobile water should also be related to moisture content. Secondly, the potential effect of mobile-water velocities on the diffusion of solutes between mobile and immobile water has not been evaluated. Although the $\alpha$ parameter is determined through solute BTC analysis under a known flux, under the current conceptual model, the value of $\alpha$ should be determined at zero velocity.

A review of the literature indicates a lack of data from which to calculate $\alpha$ as a function of moisture content and of mobile pore water velocities for a single porous medium. This issue is further obscured through the limited ranges that can be observed using traditional laboratory column BTC methods and the frequent stopping of the centrifuge to obtain effluent samples for chemical analysis. Due to these incomplete data sets and experimental limitations, it is unclear if $\alpha$ is dependent upon moisture content and what the limitation of ignoring the velocity effect has on the estimated magnitude of the mobile-water fraction. This LDRD is examining methodologies, tools and expertise that can be used to conduct suites of experiments to answer these questions.

Developing geocentrifuge experimental protocol to conduct solute transport experiments was accomplished using the INEEL unsaturated flow apparatus (UFA) centrifuge. One limitation of the UFA identified by researchers at PNNL (Pacific Northwest National Laboratory) was the frequent stoppage of the UFA to collect effluent for chemical analyses. Through this LDRD, the investigators have worked with engineers at Beckman-Coulter and the INEEL to design and build a wireless electrical conductivity sensor system that can be used in the UFA to analyze the electrical conductivity of the effluent while the centrifuge is in flight. Unfortunately, the final prototype was delivered at the end the fiscal year so the new capability was not available to collect the solute breakthrough curve (BTC) in these experiments.

The solute transport experiments were conducted using a blend of Ottawa sand with a median grain size of 150 mesh. Ottawa foundry sand is nearly pure crystalline silica and exhibits little sorptive capacity on its surface. The sand was pretreated with a nanopure water rinse to remove excess dissolved salts and pre-compacted in the centrifuge prior to conducting a solute BTC experiment. A flux of water was passed through the soil sample at a constant rotation speed until a steady-state condition was reached. Next, the influent was switched to a 2000 ppm sodium bromide solution and the effluent was collected for chemical analysis. An example of a typical BTC is shown in Figure 1.

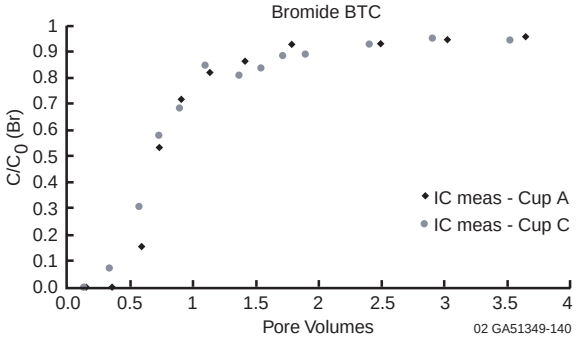


*FIGURE 1. Bromide breakthrough curve effluent chemical analysis for the 25 ml per hour for unsaturated Ottawa sand at approximately 14% volumetric moisture content.*

A set of quantitative tools was developed to design and interpret the centrifuge experiments. The investigators worked with Dr. Jirka Simunik (University of California, Davis) modifying HYDRUS 1D and replaced the uniform gravity term in his code with a centrifugal acceleration term. This modification enabled use of HYDRUS 1D as a quantitative tool to interpret the bromide BTC results and evaluate the effects of the non-uniform centrifugal force on moisture distribution and solute transport in the soil sample. Due to the success of these modifications, HYDRUS 2D also was modified to examine potential effects of the diverging flow lines and heterogeneities.

During this research, appropriate methodologies were developed to conduct solute breakthrough experiments, resulting in a new capability to measure the solute breakthrough concentrations (i.e. the electrical conductivity) in real time while the UFA is spinning. A set of solute breakthrough experiments was conducted to examine the mass transfer coefficient in unsaturated soil. Finally, existing quantitative numerical tools were modified to examine flow and transport in centrifugal experiments.

The INEEL has initiated an environmental thrust area to study subsurface coupled-processes using the centrifuge approach. Currently, the INEEL has a small 0.012-meter and a large 2-meter centrifuge for this purpose. Results from this LDRD support this INEEL emphasis through the development of the basic tools and physical modeling of coupled processes in the centrifuge. Examples of such coupled processes include microbial distribution relationship to the mobile-immobile water phases and its reliance on the net transfer of solutes between these water phases in unsaturated soil. Chemical sorption is dependent upon the mineral type and its size distribution in the porous media. Depending upon these distributions, the solute interaction with these sorption sites depends upon the mobile and immobile water fractions.

This LDRD project has contributed to the INEEL's growing expertise in centrifugal hydrologic techniques, and to improving understanding of contaminant migration processes that is relevant to all DOE site clean-up efforts.

# Modeling of Flow and Colloid Behavior in Subsurface Fractures

*Paul Meakin*

## *Using particle-based methods to model multiphase flows*

GC136

Fractures are omnipresent in the upper part of the Earth's crust. The ability to model the fate and transport of subsurface contaminants with sufficient accuracy and reliability depends on our understanding of fluid flow in fracture apertures and on our ability to develop scientifically defensible conceptual models for the long-range flow of fluids in the fractured subsurface. Important contaminants, such as radionuclides, have been found to travel much further and faster than predictions based on the science of a few decades ago. This is usually attributed to the focusing of flow into preferred pathways such as fractures and fracture networks, and in some cases, to the transport of contaminants associated with colloids along similar preferred pathways. If scientists are to reduce the uncertainties in computer-based predictions of subsurface contaminant behavior, computational tools must be developed to model fluid flow in fractured porous media under the wide range of conditions that are encountered in the subsurface. More accurate models would reduce the cost of long-term monitoring and stewardship, and facilitate the development and deployment of more effective remediation technologies.

This LDRD is investigating and testing computational methods that can be used to simulate flow in complex fracture apertures under a wide range of flow conditions. For single-phase flow processes the traditional finite-element and finite-difference approaches are, in most cases, the most computationally efficient and accurate. However, in multiphase flows these methods are extremely difficult to apply because of the difficulty of tracking complex dynamical interfaces. Under these circumstances, the computer code becomes complex (and consequently error prone), computational efficiency is seriously degraded, and a particular approach to interface tracking can only be applied to a narrow range of problems.

An alternative approach is to use particle-based methods that allow fluid-fluid interfaces to evolve with only a modest increase in code complexity and degradation of efficiency. In addition, the particle-based methods used to model multiphase flows can usually be applied to a very wide range of processes and conditions.

Technical objectives for fiscal year 2002:

- Develop realistic computer models for complex fracture apertures.
- Determine which approaches can best be used to model single-phase and multiphase flow in complex fracture apertures.
- Attempt to develop improved conceptual models for fluid flow in fracture apertures.
- Work with experimentalists to design, motivate and interpret laboratory-scale and larger scale experiments.

A variety of particle-based methods are under development for application to multiphase flow on complex fracture apertures. These include 1) lattice-Boltzmann models, 2) molecular dynamics models with very soft inter-particle interactions, and 3) smoothed-particle hydrodynamics models.

The lattice-Boltzmann method is based on the idea that the local properties of a fluid are determined by the velocity distribution function. In this modeling approach, the continuous velocity distribution is approximated by the fractions of the "particles" at a particular node on the lattice that are traveling in a discrete number of directions with discrete velocities that ensure all of the particles will travel from one node to an adjacent node in exactly the same amount of time. The algorithm consists of a sequence of translation steps and collision steps during which the particle velocity distribution relaxes (or over-relaxes) toward the local equilibrium determined by the local fluid velocity.

Despite these drastic simplifications, the model fluid conforms to the Navier Stokes equation, providing that the model has sufficiently high crystallographic isotropy to ensure that fourth-order tensors appear to be isotropic. (For a fluid, all directions are equal; this is not true of a lattice. However, provided that the fourth-order viscosity tensor is crystallographically isotropic, the hydrodynamics can be described to a good approximation by the Navier Stokes equation.)

The lattice-Boltzmann fluid can be induced to undergo a phase separation into a high-density and a low-density fluid by including short-range fluid-fluid

interactions that depend on the fluid densities. Figure 1 shows the results of a lattice Boltzmann simulation of the gravity-driven flow of a phase-separated fluid through a complex fracture aperture.

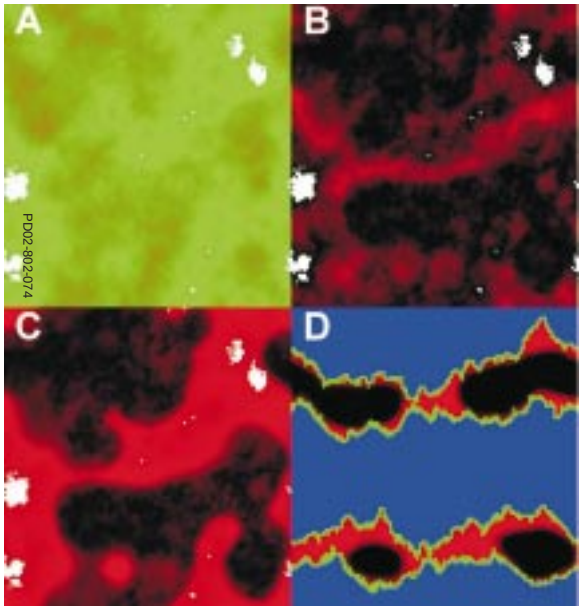


*FIGURE 1. A lattice-Boltzmann simulation of two-phase flow in a complex-fracture aperture. Part A shows the fracture aperture (the color scale ranges from red to green as the aperture decreases, and occluded regions are white). Part B shows the depth-integrated fluid density. Part C shows the depth-averaged fluid density. Part D shows cross-sections through the center of the aperture in the horizontal (top) and vertical (bottom) directions. In parts B-D, the color changes from black to red as the fluid density increases. Gravity acts from left to right. The aperture is the gap between a self-affine fractal surface with a Hurst exponent of 0.7, and a replica that has been translated both horizontally and vertically.*

Lattice-Boltzmann simulations also have been carried out to simulate single-phase flow and advection-diffusion in the cells that are being used by Daphne Stoner (LDRD GC134) and her collaborators to investigate the effects interactions between biofilm growth and fluid flow. Good agreement was obtained between the lattice-Boltzmann simulations and dye-tracer experiments.

A computer model has been developed to simulate fluid flow using a molecular dynamics approach with soft, repulsive interaction potentials. This approach depends on the universality of the fluid flow equations. The flow of all simple fluids (even model fluids with unrealistic interaction potentials) can be described to a good approximation by the Navier Stokes equation. For the simple case of flow in a smooth-walled channel at low velocities, the velocity profile approaches the theoretical parabolic form as the particle density increases (and the mean free path decreases). If attractive interactions are included, the fluid forms dense droplets embedded in a low-density fluid (essentially a vacuum).

A smoothed-particle hydrodynamics model is also under development. Although this model is operationally equivalent to a molecular dynamics model with multi-body interaction potential, the philosophy behind the model is much different. In smoothed-particle hydrodynamics, the forces that move the particles are calculated from approximations to the continuum equation of motion for the fluid. At this stage, a simple smoothed-particle hydrodynamics program has been written but not tested.

Progress also has been made toward the goal of developing more realistic fracture-aperture models. For example, the fractal model illustrated in Figure 1 has been combined with a statistical model and void-distribution model to obtain a model for the fractures in vesicular basalts. A further improvement would be to use the lattice-Boltzmann approach to simulate the void distributions prior to fracture.

The research resulting from this LDRD is contributing to the build-up of a critical mass of researchers and facilities at INEEL in the area of fluid flow in complex confined geometries. This is an area of considerable scientific and practical importance for applications ranging from the fundamental physics of flow in complex systems to applications in environmental management and fossil fuel extraction.

# Natural and Synthetic Subsurface Colloids

*Glenn A. Moore, George Redden*

## *Understanding colloid transport*

GC125

To effectively model and/or perform meso-scale investigations involving colloid-facilitated contaminant transport, one must first understand the nature of the colloid species present and their dynamic properties. Therefore, characterization of colloids in the subsurface is of interest to both geoscience experimentalists and modelers alike.

This LDRD is establishing the requisite capabilities at the INEEL for collecting and analyzing the natural colloids that are present in vadose zones, perched water zones, and the Eastern Snake River Plain Aquifer (ESRPA). To date, colloids have been extracted from Spreading Area B soil samples and perch aquifer water/silt samples within the Subsurface Disposal Area. Colloid samples have been initially characterized for particle size, electrophoretic mobility, morphology, and mineralogy. Colloid mobility experiments have been initiated using a bench-scale sand column, a field-flow fractionation instrument, and a centrifuge system referred to as the Unsaturated Flow Apparatus (UFA). These experiments are expected to provide valuable insight on the conditions needed for colloid-facilitate contaminant transport in the soil matrices of interest.

A second component of this project involves the synthesis of engineered colloids — manmade colloids that mimic the mobility characteristics of natural colloids. To date, mesoporous silica, poly(propylene carbonate), and polyphosphazene colloids have been prepared in the laboratory. Ongoing colloid synthesis activity is focused on controlling particle size and incorporation of fluorescent markers. The properties of these engineered colloids will be established using a suite of particle characterization instruments and via soil-column experiments.

Technical objectives for fiscal year 2002:

- Enhance INEEL capabilities to collect and characterize colloids present in vadose zone, perched water zones and ESRPA.
- Develop synthetic colloids tailored to subsurface investigations at the INEEL.

A frit-outlet Field Flow Fractionation (FFF) instrument produced by Postnova Analytics, Salt Lake City, UT, was configured with a Hitachi L-4200H High Sensitivity Series UV-VIS detector. This new capability is being used to characterize and compare the mobility of natural and synthetic colloids. The instrument separates particles based on their diffusion in a laminar flow channel.

Smaller particles, having greater local diffusion, have a higher probability of escaping the boundary layer at the membrane surface where they are initially concentrated. Thus, the smallest colloids pass more quickly than larger colloids through the channel. Charge-based particle membrane interactions also play a role in this separation scheme. The influence that electrophoretic mobility plays in the fractionation of natural and synthetic colloid suspensions is being examined.

Particle fractions can be collected after passing through the detector, providing samples that can be analyzed to determine if certain mineral types in mixed-mineral colloid samples are more mobile than others. Figure 1 shows FFF data for 50, 100, and 450 nm silica microspheres, and a colloid sample isolated from an inner-bed silt sample.

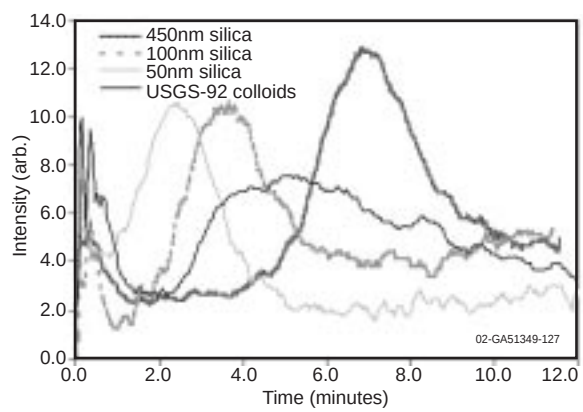


*FIGURE 1. FFF data sets for three sizes of silica microspheres and colloids extracted from an INEEL inner-bed silt sample.*

In January 2002, an automated particle analysis program was procured and installed on the Jeol 8900-R electron microprobe. This particle analysis software provides a means of obtaining submicron-sized particle size distributions, particle aspect ratios, and semi-

quantitative chemical analysis using energy dispersive spectroscopy. To date the natural and synthetic colloid samples have been characterized using a submicron particle size analyzer, an electrophoretic mobility (Zeta potential) instrument, scanning electron microscopy (SEM), transmission electron microscopy (TEM), and FFF. Colloid sample preparation techniques being used include: sedimentation, centrifugation, and stirred-cell filtration.

Environmental water samples collected from in-place lysimeters around the INEEL are a potential source of natural colloid samples for this project. These lysimeters use a porous ceramic or metal element able to hold a partial vacuum. The negative pressure within the lysimeter provides a driving force for the migration of water from the unsaturated soil matrix. The nominal pore size of these porous elements is typically 1µm. It is expected that most colloidal matter will be screened or filtered out before it can pass through the cross section of the lysimeter. Colloidal analyses of several lysimeter samples are currently underway. Centrifugation and/or dialysis filtration techniques will be used, as needed, to isolate/concentrate the colloids so that they can be characterized.

Late in FY02, a selection of dual tube sampling accessories was procured from AMS, American Falls, ID. The sampling hardware will be used with the INEEL's direct-push sampling system. The dual-tube sampling hardware (AMS PowerProbe) provides a means of collecting minimally disturbed soil samples inside two-inch-diameter plastic sleeves at discrete depths of the subsurface. The sleeves can then be brought to the laboratory and configured with end caps for use in colloidal transport studies and as a means of collecting the natural colloid samples under saturated or unsaturated conditions. Such experiments are planned for FY03.

A 2.25" ID column was configured to conduct saturated and unsaturated colloid mobility experiments. The base configuration consists of an IV pump, an acrylic tube column, a permeate sampling autocollector, and a vacuum chamber to facilitate sample collection under unsaturated flow conditions. To date, samples have been collected from saturated flow experiments and analyzed using a submicron particle size analyzer and a UV-VIS spectrophotometer. Future experiments will use an in-line-configured UV-VIS HPLC detector and/or an HPLC fluorescence detector. The fluorescence detector will be used for detection of fluorescent-tagged synthetic colloids.

At the start of FY02, colloid synthesis activity was focused on mesoporous silica colloids — surfactant-templated mesoporous silica particles ranging from 50-500 nm in diameter. Unlike silica microspheres that are dense, mesoporous silica has an interconnected 3-5 nm pore structure. Both types of particles are prepared using sol-gel techniques. The mesoporosity can be used to host fluorescing dyes or other suitable signature chemicals that facilitate subsurface transport studies.

The sol-gel process used here involves the hydrolysis and condensation of a tetraethyl orthosilicate (TEOS) in the presence of a surfactant at a level above its critical micelle concentration. Research focused on obtaining like results in the 200-600 µm size range. While the investigators were able to easily produce particles in this range, the distributions were quite broad, typically 0.2-1.5 µm. Additionally, surfactant removal at 550°C resulted in significant sintering, "necking," of the submicron particles. Thus, in the second quarter of FY02, synthesis activity shifted to organic-polymer based colloids.

Presently poly(propylene carbonate) and polyphosphazene polymers are being investigated. These polymers are soluble in solvents such as acetone and tetrahydrofuran (THF) but not soluble in water. When a polymer/solvent solution is mixed with water, the polymer condenses and a colloidal suspension is formed. Filtration or rotary evaporation is then used to remove the solvent, leaving an aqueous colloidal suspension.

This LDRD is enhancing the INEEL's environmental capabilities.

# Fundamental Studies on Gas Contaminant Mobility in the Vadose Zone from Atmospheric Pressure Fluctuations

*Chang Oh*

## *The effects of atmospheric pressure on long-term cleanup strategies*

GC101

Subsurface soil-gas concentration data taken from a large vadose-zone contaminant plume 150 feet below land surface at the Radioactive Waste Management Complex (RWMC) at the INEEL have been found to vary at a single point by as much as an order of magnitude. Variations appear to correlate with atmospheric pressure fluctuations. Preliminary analysis suggests that changes in soil pressure compress and expand the contaminant plume. In addition, results from a vadose-zone tracer study indicate gas-phase transport is significantly influenced by atmospheric pressure changes, and rates of migration are faster than those indicated by diffusive transport alone. These two findings suggest that current understanding of soil-gas dynamics is incomplete, and that management decisions committing considerable time, effort, and finances to remediation may be based on improper assumptions.

This LDRD is focused on understanding and describing the effect of fluctuations in atmospheric pressure on the shape and dynamics of contaminant vapor plumes in the vadose zone. Laboratory and modeling studies have been initiated to more closely study the influence of pressure fluctuations on soil-gas migration under controlled conditions.

Technical objectives for fiscal year 2002:

- Determine the propagation of atmospheric pressure changes downward through homogeneous and heterogeneous porous media and dense and fractured bedrock.
- Mathematically describe the time lag and amplitude suppression of pressure waves through subsurface geologic materials.
- Gain a basic understanding of the kinetics of contaminant partitioning induced by naturally occurring pressure gradients from sequestered phase changes (soil surfaces, organic components, and moisture).
- Create a computer simulation of the effects of daily and weather cyclic pressure fluctuations on vertical and horizontal soil vapor plume movement in heterogeneous porous media.

A piezometer nest containing six ports, each terminated at different depths below land surface, was instrumented to collect soil-gas concentration data and soil pressure data at rotating intervals at each port. The intent was to correlate atmospheric pressure changes and subsequent pressure propagation down through the soil/basalt profile with real-time contaminant concentration changes. Resultant data are the first ever collected describing the influence of atmospheric pressure fluctuations on vadose zone contaminant plumes.

The data from this experiment is seen in Figure 1. Soil

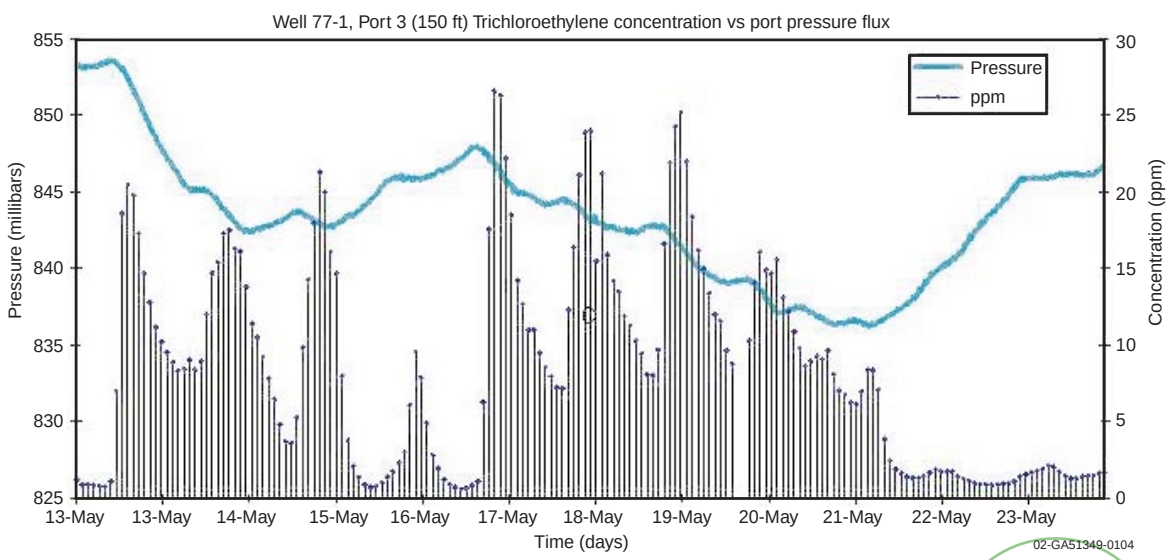


*FIGURE 1. Real-time atmospheric pressure fluctuation and TCE concentration 150 ft below land surface.*

pressure and trichloroethylene concentrations are measured at the same point in the subsurface. An increase in soil pressure was observed to correlate with a decrease in trichloroethylene concentration. Trichloroethylene concentrations were observed to vary over an order of magnitude at a point. One possible interpretation is that increasing and decreasing pressures compress and expand the contaminant plume. In other words, soil vapor plumes are dynamic in nature responding to pressure fluctuation. This would make conventional diffusion theory inadequate to completely explain vapor-phase transport. This finding and mathematical interpretation should change the way risk to groundwater from vadose-zone plumes is calculated.

Three ports each in two piezometer wells 25 feet apart were instrumented to collect both pressure and concentration data. A tracer test was implemented on March 7, 2002. Sulfur hexafluoride ($SF_6$) was injected 112-ft below surface in one well until March 24, 2002. Tracer concentration measurements were made at ports in both wells. Results of the tracer test were analyzed to estimate gaseous diffusion parameters for modeling contaminant transport at the RWMC. A well-respected analytical solution to the transient diffusive transport equation was fitted to the tracer results. Figure 2 shows tracer breakthrough at a port located 151-ft below surface. Also shown are results of the fitted Carslaw and Jaeger equation. Values for $\tau D_o$ of $7x10^{-4}$, $1x10^{-3}$, and $1.5x10^{-3}$ were used (top to bottom) in the fitted expressions. These values are two to three orders of magnitude higher than values expected by diffusion alone, and suggest other mechanisms play a role in contaminant transport.

Tracer breakthrough was observed to correspond to changes in atmospheric pressure, and a plot of atmospheric pressure and tracer arrival showed that tracer concentrations decreased as subsurface pressure at the port depth rose, and increased when pressures decreased. Modeling work and laboratory experiments under

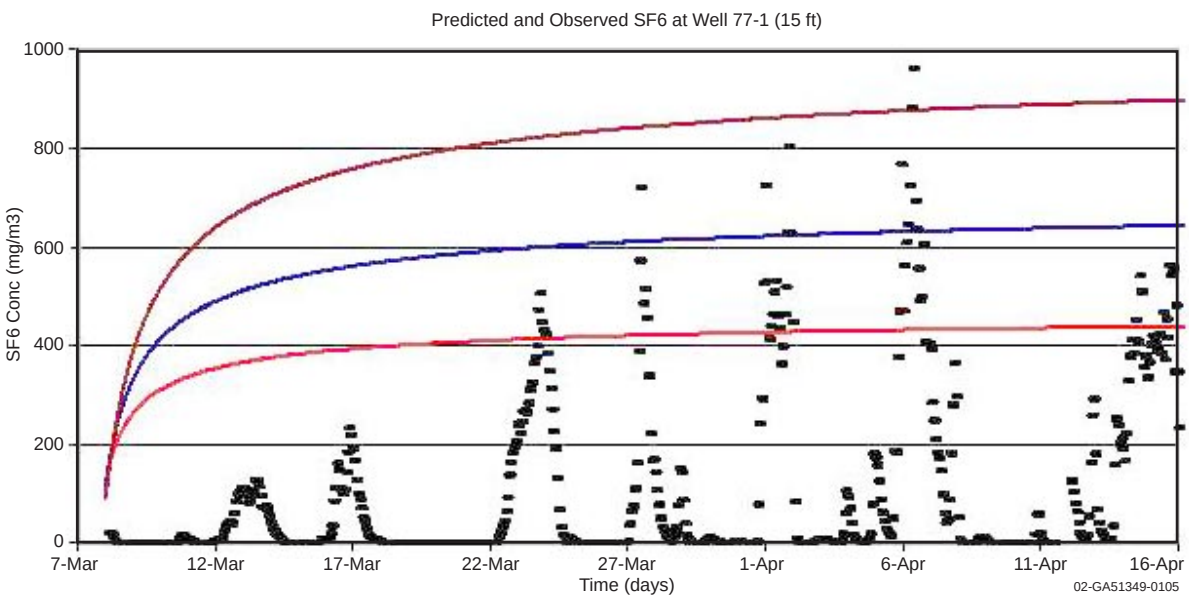


*FIGURE 2. $SF_6$ breakthrough data and Carslaw and Jaeger fitted diffusion expression at Well 77-1, Port 3 (151-ft. bls).*

controlled conditions are in progress to correlate changes in subsurface pressure with expected contaminant migration.

This LDRD research is being performed in collaboration with co-investigators Wayne C. Downs and W. Vincent Wilding, both of Brigham Young University. In addition, an affiliation has been established with researchers at the DOE Sandia Laboratory to investigate contaminant migration under the influence of varying pressure. Investigators will use Sandia's newly developed vapor detector. The detector measures vapor concentrations without removing a volume sample, which would distort the pressure profile. Sandia is lending this project the detector along with support of its installation. The investigators will test the detector's pressure extremes.

Next year's work will focus on analysis of FY02 field data and laboratory work. It is expected that the laboratory work will illuminate a dispersive mixing process never before reported in the literature, and that the mathematical description that will come from the laboratory work will be successfully applied to the field tracer data. A journal article describing the effect of atmospheric pressure fluctuations on contaminant plumes is in preparation. Laboratory experiments and computer simulation are expected to result in another article. By the end of FY03, the investigators anticipate using the knowledge resulting from this LDRD to assist in the RWMC soil vapor extraction program and in management decisions involving the long-term cleanup on the vadose-zone plume there.

# Enhanced Techniques for Evaluating Colloidal Processes

*Judy K. Partin, George D. Redden*

## *New sensing technology offers in situ characterization and detection*

GC106

The analysis of colloidal matter, and its role in contaminant mobility, is an important need for DOE sites with significant quantities of buried mixed wastes. In particular, colloidal-facilitated transport may be responsible for the presence of radionuclides occasionally detected in groundwater samples at the INEEL.

Current monitoring and characterization methods for subsurface colloids rely on light scattering techniques or the collection of particulate by conventional or ultrafiltration, followed by standard analytical analyses including inductively coupled plasma, scanning electron microscopy, and energy dispersive spectroscopy. Light scattering techniques are not sensitive enough to detect low-concentration suspensions. The filtration techniques are very costly and labor-intensive, and also may not accurately sample colloidal materials in the very small particle size ranges or at the appropriate times to detect significant events. Most sampling methods are prone to generating artifacts due to physical disturbances, such as pumping, that can remobilize colloids, or collecting fine particles associated with drilling.

This LDRD investigates a new sensing technology for the in situ characterization of low-density colloidal suspensions, combining features of laser-induced breakdown spectroscopy and acoustic detection. The technique offers the possibility of not only detecting the presence of sub-micron particles at very low number densities, but also determining their species composition.

Technical objectives for fiscal year 2002:

- Complete laboratory proof-of-concept testing and evaluation of colloidal materials.
- Design prototype, integrating monitoring instrumentation with remote sampling head.

This LDRD involves a new monitoring capability (Fig. 1) based on the interaction of small particles with a high-energy laser pulse. When a particle is introduced into the focal volume of such a laser, the particle is vaporized and ionized, producing luminous plasma and a pressure wave, or acoustic signal. The spectroscopic analysis of the plasma can be used to determine the elemental composition of the particle. The amplitude of the acoustic signal, as a function of the laser energy, can be used to determine the particle size. The particle concentration, or number density, is then determined by measuring the number of signals as function of laser shots for a given energy.

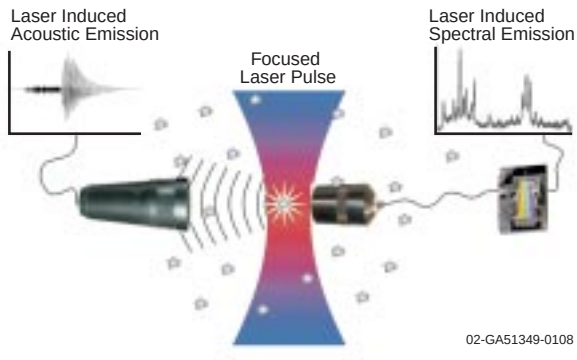


*FIGURE 1. Laser-induced breakdown detection principle.*

In FY01 a series of scoping experiments were performed to establish the ability of the laser-induced breakdown technique to detect various types of sub-micron metallic oxide particulate dispersed into aqueous solutions. During FY02, this testing was expanded to include other colloidal matrices of interest to subsurface applications, including actinide surrogates. These proof-of-concept experiments successfully demonstrated the ability of the technique to detect and characterize the presence of various types of colloids at low number densities. As an example, the spectral and acoustic data for ~ 0.5 micron diameter uranyl particulate, precipitated from a salt solution and diluted to a concentration of around 20 ppm, is presented in Figure 2. Emission lines, characteristic of uranyl ion, are clearly seen in the spectral data. The acoustic data also shows signal levels above background, or threshold, indicating the presence of particulate.

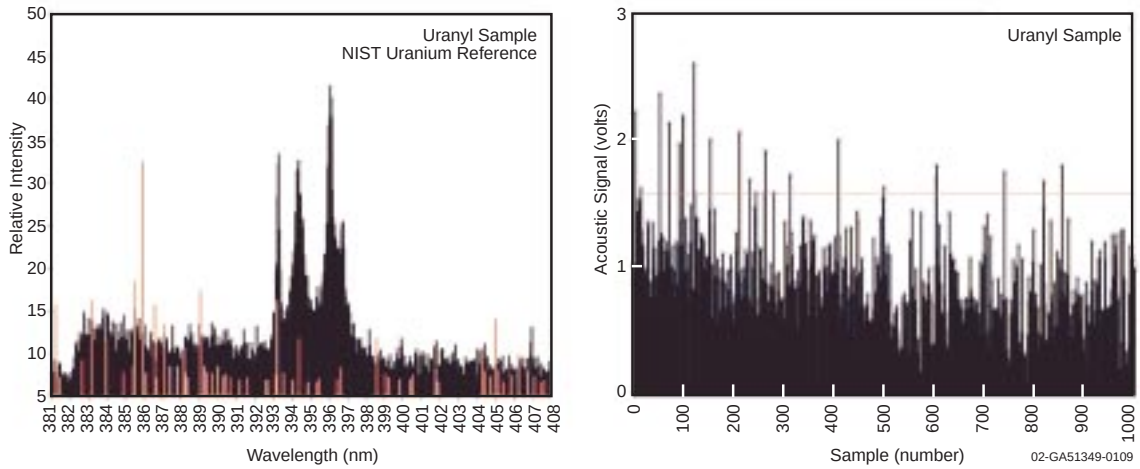


*FIGURE 2. Spectral and acoustic signatures for a 20-ppm concentration suspension of 0.5-micron diameter uranyl particulate.*

The ability to correlate signals with particle size also was established. Experiments were conducted to determine if small amounts of material adsorbed into the colloidal matrix could be detected. The presence of the adsorbates could be detected on colloidal powders but could not always be seen with good signal-to-noise when suspended in aqueous solutions with the existing experimental set-up. In some cases, reliable detection may require the use of resonant, or wavelength-specific, excitation.

In addition to the laboratory proof-of-concept experiments, the practicality of designing and fabricating a system for down-hole deployment was explored. The goal was to determine if the basic features of the laboratory system could be implemented into a device that could be deployed in a borehole and used for the in situ detection and characterization of colloids. The principal design requirements were as follows: the sampling head should be less than 100 millimeters in diameter, the optical and electrical signals should be capable of being transmitted and received over distances up to 500 meters and still be able to detect colloids at very low densities, and the instrumentation used in the measurements must be sufficiently robust to be used in the field environment. The conceptual design for a remote sampling head meeting these requirements has been developed. The remote head could be easily fabricated and integrated into a field deployable instrument using off-the-shelf components.

The unique monitoring capability investigated in this LDRD may have a number of other applications in addition to predicting and evaluating contaminant transport from buried waste sites. The detection and control of suspended fine solids is important to a number of manufacturing processes, including the semiconductor and biochemical engineering industries. The control of boiler water quality is very important in power production in order to prevent damage to turbine blades, or other critical components. The ability to detect very small levels of various metals could allow an assessment of the health of the plant operation. Mining and mineral recovery operations also could benefit from this technology. The work could also be valuable to national and homeland security agencies for use in detecting or monitoring for aerosol emissions from biological or dirty bomb threats.

# Chemical Modification of Atomic Force Microscope Probes for Imaging Patterned Molecular Architectures

*Patrick J. Pinhero*

## *Understanding the surface chemistry of environmental contaminant*

GC113

Surface chemistry is a strong component in the development of an understanding for the fate and transport of potential contaminant streams within the subsurface vadose zone. Adsorption of chemical species to a host substrate surface can occur by either physical interactions (physisorption) or by covalent bonding (chemisorption). Characterization of these interactions on a molecular scale provides information about the strength of interaction and helps develop insight into potential environmental remediation strategies.

The analytical toolbox commonly used to characterize environmental contamination consists of spectroscopy, chromatography and mass spectrometry. These techniques suffer by the lack of spatial resolution required to adequately determine how molecules interact with the structure of a surface. Atomic force microscopy (AFM) provides the necessary spatial component but has traditionally lacked chemical specificity.

This LDRD is researching extremely high-resolution techniques for characterizing chemical species at surfaces. The project seeks to satisfy the limitations of the current state of the art by decoupling the forces indicative of specific chemical interactions from the conventional force signature – i.e., surface topographic deflection signal. By separating out this component of the force measurement and modulating it both electronically and chemically, a complete multidimensional image of the surface and its chemical composition can be acquired. This image may potentially elucidate important information about processes such as biotransformation of toxic solutes, that are required to understand vadose zone processes.

Technical objectives for fiscal year 2002:

- Develop technique for increasing chemical sensitivity of AFM.
- Increase understanding of AFM probe chemical modification.
- Produce AFM probes and cross-test with combinations of substrate surfaces.

To address the issue of increasing the chemical sensitivity of AFM, a chemical procedure was used in which AFM probes were modified with organofunctional silanes, as shown in Figure 1. Silylation was the preferred modification procedure because it enables exploitation of the native chemistry of the AFM probe, which is based on single-crystal silicon possessing a silica (SiO2) / silicon hydroxide (SiOH) outer surface. Organofunctional silanes can be commercially obtained with varying chain lengths and terminal functional groups. Additionally, it is quite easy to synthesize other organofunctional silanes through simple organic chemistry.

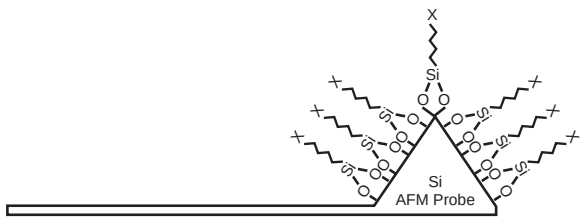


**X = RY**
R = $(CH_2)a$
Y= $CH_3$, $NH_2$, Porphyrin, phenyl, Cl, F, OH, COOH, $SO_3$, vinyl, epoxy, ect.

02 GA51349-116

*FIGURE 1. Illustration of an AFM probe modified by silylation.*

Modification of AFM probes by silylation occurs by displacement of an active hydrogen, in the hydroxyl group located at the probe's surface, by an organosilyl group. By accomplishing this modification, it was possible to impart hydrophobicity or organic nature to an inorganic surface. The silylation also provided a method to place reactive groups on a stable insoluble substrate. Since the modification was achieved by covalent bonding, it is assumed that the resulting "couple" is very strong and thus resistant to removal by organic solvents or by water.

Interest in developing AFM-based techniques has grown parallel to, and well connected with, the study of self-assembled monolayers (SAMs). This technology has led to a revolution in surface science and the designing of unique surface-bound molecular architectures. The ability to visualize these surfaces is due to AFM measurements. One area for application of this technology is the imaging of biomolecular surfaces that mimic those in nature (biomimetics). An example of this application is biomineralization in subsurface environments.

Building on the progress of FY01, the investigators sought to increase their understanding of the modification process and apply it to characterizing surfaces of mixed composition in FY02. A significant amount of success was achieved, including an invitation to a special symposium of the Fall 2002 Materials Research Society (MRS) conference in Boston, where the investigators were to present their results (canceled due to project termination). Additionally, the investigators acquired enough data to furnish a graduate student with a MS Thesis (University of Idaho, Department of Mechanical Engineering).

In brief, this project used a combination of AFM probe chemical modification, with the novel Pulse Force Mode (PFM) technique of AFM. PFM has been discussed elsewhere, and will be defined as a method by which an adhesive force of interaction between the AFM probe and the surface of interest can be measured. PFM highlights regions on the surface where the adhesion is strongest. Using the old adage that similar compounds have more favorable (attractive) interactions than those compounds that are dissimilar, it is easy to see the motivation in modifying AFM probes and using PFM as a measuring tool.

There were several points requiring clarification in FY02 with respect to the modification procedure. First, was it possible to detect if the AFM probes and corresponding substrate surfaces (Si single crystal semiconductor wafers) had been actually modified? Second, if the modification had occurred, how thick was the modification? It was hoped that the modification was only one monolayer (a single molecule) thick, because that would ensure that the functional group pointed outward. If it was more that a monolayer thick, then other techniques needed to be used to determine which way the functional group was pointing to understand the measured interaction between the AFM probe and substrate surface.

A number of techniques were used to characterize the modification process. These techniques included scanning electron microscopy (SEM), X-ray photoelectron microscopy (XPS), contact angle measurements, and nuclear magnetic resonance (NMR). Figure 2 displays SEM images of three modified tips along with their corresponding contact-angle measurements. Contact-angle measurements provide information about the surface-free energy of the modified material, with larger contact angles being indicative of lower surface-free energies and greater hydrophobicity in the case of water test drops.

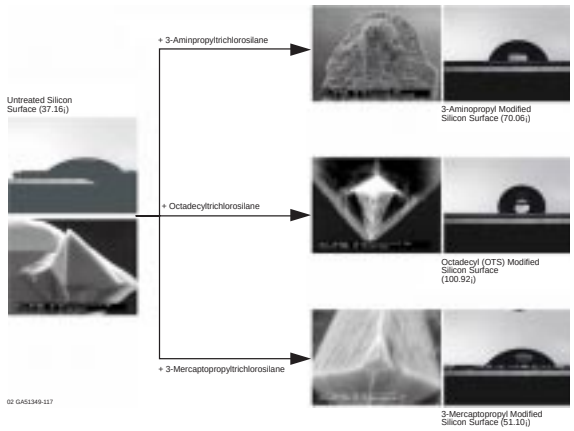


*FIGURE 2. SEM and contact-angle images for three different silylations. At left is the unmodified probe and substrate. On the right are 3-aminopropotrichlorosilane (top), octadecyltrichlorosilane (middle), and 3-mercaptopropotrichlorosilane (bottom).*

Figure 2 demonstrates that a chemical modification is present at the surface of the AFM probes (SEM images) and Si substrates (contact angle images). It is apparent that there is variation in the amount of material present. Since deposition is a function of both the concentration of silane available for reaction (limiting case) and the time of deposition (kinetic requirement), much effort was devoted to developing deposition profiles in order to best determine the correct parameters for forming the thinnest overlayer without compromising the PFM-AFM adhesion measurement. Other surface analytical tools such as XPS and scanning auger microprobe (SAM) were used to confirm that a surface modification was present.

For additional characterization, infrared (IR), ultraviolet / visible (UV/Vis) and NMR spectroscopies have been employed. Both NMR and IR will provide needed information about the orientation of the modified surface

as to whether the functional groups are, in fact, pointing away from the substrate. By rotating the degree of polarization of the IR beam, it is possible to determine whether the axes of the molecules comprising the overlayer are parallel or perpendicular to the surface normal. By examining a combination of nuclei ($^{29}Si$, $^{13}C$, and $^{1}H$) with solid state NMR, it is hoped a determination can be made whether the modification is indeed covalently bound to the substrate.

Together the information gathered through the characterization studies will lead to design modifications that provide the best chemical detection. For example, the investigators are interested in the effect of varying the chain length (denoted "R" in Fig. 1) of the silanes in order to yield maximum performance in the PFM-AFM adhesion measurements.

In FY02, the majority of the PFM-AFM adhesion measurements were gathered from single-component surfaces. AFM probes were produced with a variety of functional groups and cross-tested with combinations of substrate surfaces derived from the same modifications. Table 1 shows the results of these tests. There are two adhesion values provided in the table. The first are values measured from a software-captured AFM force curve oscilloscope image, and the second are values extracted directly from the PFM-AFM adhesion image. The force curve measurements represent sets of eight samples acquired from various regions on the surface, whereas the data extracted from images contains 65,536 points.

The obvious question when examining the data in Table 1 is how these values compare with actual

| MODIFIED AFM PROBE / SUBSTRATE SURFACE | $F_{adhesion}$ (nN) from force curve | $F_{adhesion}$ (nN) from adhesion image |
|---|---|---|
| Chloroproposilyl- / Chloroproposilyl- | 32.130 ± 0.68 | 29.902 ± 1.44 |
| Octatrichlorosilyl- / Octatriclorosilyl- | 26.597 ± 0.84 | 21.977 ± 1.42 |
| Thiolproposilyl- / Thioproposilyl- | 18.278 ± 0.09 | 19.021 ± 0.82 |
| Aminoproposilyl- / Aminoproposilyl- | 18.885 ± 1.10 | 18.528 ± 2.58 |
| SiOx / SiOx | 17.541 ± 0.72 | 13.487 ± 0.39 |
| Chloroproposilyl- / SiOx | 25.585 ± 0.74 | 23.790 ± 1.40 |
| Chloroproposilyl- / Aminoproposilyl- | 24.217 ± 1.96 | 21.192 ± 2.07 |
| Chloroproposilyl- / Octatrichlorosilyl- | 37.485 ± 1.96 | 26.304 ± 5.64 |
| Octatriclorosilyl- / SiOx | 14.221 ± 0.15 | 12.841 ± 0.70 |
| Octatriclorosilyl- / Aminoproposilyl- | 13.358 ± 1.47 | 13.034 ± 2.22 |
| Octatriclorosilyl- / Chloroproposilyl- | 18.475 ± 0.67 | 15.858 ± 1.46 |
| Aminoproposilyl- / SiOx | 20.635 ± 0.92 | 18.432 ± 0.70 |
| Aminoproposilyl- / Octatrichlorosilyl- | 27.192 ± 1.96 | 27.803 ± 3.24 |
| Aminoproposilyl- / Chloroproposilyl- | 26.567 ± 1.27 | 27.450 ± 1.99 |
| SiOx / Aminoproposilyl- | 7.735 ± 0.66 | 7.576 ± 0.93 |
| SiOx / Octatrichlorosilyl- | 7.183 ± 0.04 | 6.390 ± 0.57 |
| SiOx / Chloroproposilyl- | 11.989 ± 0.05 | 10.003 ± 0.41 |
| SiOx / Thioproposilyl- | 17.255 ± 0.92 | 16.915 ± 0.66 |
| Thiolproposilyl- / SiOx | 17.713 ± 0.98 | 18.193 ± 1.06 |

02 GA51349-118

*TABLE 1. Cross-testing results of AFM probes.*

adhesion force values, and whether this technique can in fact be used to identify chemical species located at a surface? The short answer is that the investigators are attempting to reconcile these values with literature values, as well as model adhesion forces with a simple code being developed at the INEEL. Much of the interpretation is dependent upon fully understanding the modification process, which motivated the extensive characterization of the surface after modification.

In summary, this LDRD project has made major progress in the fundamental science of adhesion. It has produced a technique to measure the adhesion between very small ensembles of molecules. The feasibility of this technique for increasing the chemical sensitivity of AFM is demonstrated through the combination of results for the first two years of the project.

This project is contributing to a better understanding of the fate and transport of potential contaminant streams within the subsurface vadose zone to meet the cleanup challenges of the INEEL and other DOE sites.

# Evaluating Microelectrodes and Fiber-Optic Probes for Use in Mesoscale Experiments

*Patrick J. Pinhero, Tedd E. Lister, William F. Bauer, George D. Redden*

## *Providing long-term, real-time collection of chemical data*

GC117

Subsurface environments are notoriously complex as demonstrated by the fact that many systems classified as homogeneous can have heterogeneous transport properties on different scales. To establish links between laboratory observations and the complex systems found in the field, the INEEL has given high priority to mesoscale demonstration projects. Mesoscale projects will be designed on scales necessary to study complex coupled processes. Many of the processes to be studied are largely influenced by chemical parameters that are variable due to heterogeneities inherent to or that develop within the system being studied. To derive the most benefit from the mesoscale experiments, it is necessary to acquire spatially and temporally resolved data using various sensors strategically placed within the experiment.

This LDRD addresses the issues related to in situ measurement of chemical parameters during the course of such a mesoscale experiment. Specifically, available microelectrode and fiber optic sensor technologies are being evaluated to determine how they may be effectively incorporated into mesoscale experiments to provide long-term, real-time collection of chemical data. When the desired performance is not achieved, adaptations of the sensor technologies are being made to maximize the performance for long-term investigations of the subsurface using mesoscale experiments.

Technical objectives for fiscal year 2002:

- Evaluate fibers and probes for UV applications to directly determine tracers and nutrients.
- Evaluate microelectrodes.
- Program LabView for optimal data collection from the microelectrodes and Ocean Optics Spectrometers.
- Prepare fluorescence-based fiber-optic pH sensors using sol gel method.
- Modify soil column for better incorporation of microelectodes and flow characteristics.

Other than the fiber optic oxygen sensors offered by Ocean Optics, the investigators found no commercially available “optodes” for chemical-specific sensing other than probes offered for standard transmission, reflectance or fluorescence spectroscopy. The pH-specific probes offered by Ocean Optics either have not worked at all or worked unreliably at best. There is, however, a multitude of literature concerning the development of chemical-specific fiber-optic probes.

Among the more promising types of fiber-optic probes for subsurface applications are those similar to the oxygen sensor, which incorporates a fluorophor (ruthenium complex) into a sol gel on the end of an optical fiber. Similar techniques have been used to make other chemical-specific optodes. Following this lead, pH-sensing optodes were made incorporating the pH-sensitive dye seminaphthorhodamine-1 carboxylate (SNARF-1C) in a sol gel using the methods described by Grant and Glass (1997). Testing of these optodes is pending.

The lack of chemical-specific optodes also led to the development of a fiber-optic-based direct UV spectroscopic method for determining water quality parameters and common infiltration tracers. The primary problems with this methodology have been with the lack of optical transmission of common solarization-resistant optical fibers. The investigators had been using transmission probes acquired from Ocean Optics, however the optical transmission across the entire spectrum was less than desirable and the probes were somewhat bulky. Because of the extremely poor transmission of these probes below 250 nm, long integration times were required and a bandpass produced by a simple monochrometer centered on 220 nm was necessary to avoid extreme oversaturation of the CCD array detector at the longer wavelengths. Better optical components are, therefore, necessary to make this technique viable.

Better fibers were obtained from Polymicro Technologies, LLC and optimally configured probes using these fibers were obtained from C-Technologies, Inc. Figure 1 demonstrates the advantages on the UVM fibers from Polymicro and the probes assembled by C-Technologies. The UVM test fiber obtained directly from Polymicro behaved exactly as predicted by their literature. The probes made with UVM fibers performed consistently and showed very little, if any, degradation at any wavelength with time. Conversely, the Ocean Optics probes rapidly solarized at less than 250 nm with the relative transmission being <20% after 6-10 hours of use.

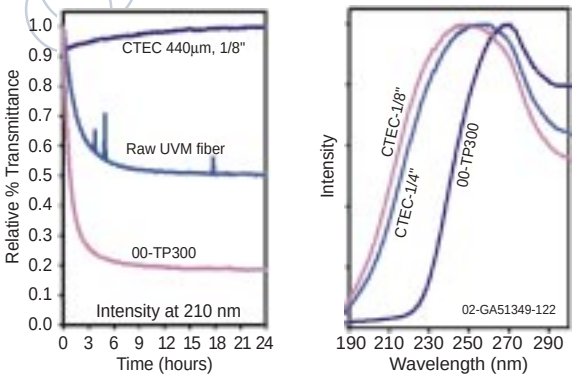


*FIGURE 1. Left: Transmission degradation at 210 nm of fibers and fiber probes upon exposure to a deuterium lamp. Right: Normalized single-beam spectra from an ocean Optics TP300 probe and the CTEC probes with the UVM optical fibers after at least 24-hour exposures to a deuterium source.*

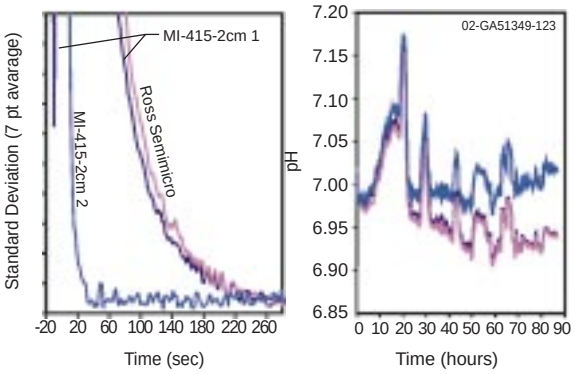


*FIGURE 2. Left: Time required to reach equilibrium as determined from the standard deviation of a moving boxcar average. Right: The long-term stability of the microelectrodes vs the standard Ross semimicro combination pH electrode.*

Previously tested microelectrodes from Unisense were far too fragile to be incorporated into a soil column and were somewhat noisy. Similar microelectrodes from Microelectodes, Inc. appear to be somewhat more rugged and are available in a variety of useful configurations. Figure 2 compares a Microelectodes, Inc. combination pH microelectrode with a diameter of 0.75 mm to a standard combination pH electrode (Ross semimicro). The microelectodes take as much as four minutes to come to complete equilibrium while the standard electrode takes less than 30 seconds. Stability of all electrodes is quite good and varies primarily with temperature. The mean measured pH of a pH 7 buffer after 87 hours was 6.97±0.05 for each of the two microelectrodes and 7.01±0.04 for the standard electrode.

The INEEL mission statement includes a directive to improve the understanding of subsurface environments. This LDRD is directly contributing to that objective by improving methods of chemical data collection.

# In Situ Bioremediation of Explosives in the Vadose Zone

*Corey Radtke*

## *Assessing remediation methods for hazardous waste cleanup*

PH101

Explosives contamination is widespread throughout the DOE complex, including environmental problems at Pantex, Los Alamos and the INEEL, as well as over 1200 DOD and private sites in the U.S. and abroad. These sites typically harbor a surface soil or vadose zone source contributing to continuing groundwater contamination. For example, firing ranges are exceedingly difficult to remediate and may contaminate groundwater via vadose-zone leaching.

This LDRD is evaluating the design, optimization and field-testing of an in situ, vadose zone. The lab work has progressed through flask and column studies, and the technology is currently being tested in a 30'X30'X30' explosives-contaminated field site at the Pantex facility.

Additionally, a microcosm reactor has been developed to test remediation at the lab scale, but in the field. The microcosm is an in situ, flow-through reactor, easily deployed and applicable to both vadose and saturated zones. Amendment additions and effluent sampling could be performed in either continuous or batch modes, and the treatment added could be diluted with subsurface gasses or groundwater to any desired concentration. The technology is expected to be ideally suited to assessing remediation methods for most hazardous waste cleanup sites.

Technical objectives for fiscal year 2002:

- Finish lab work portion of this project.
- Design and install field carbon delivery system. Begin testing.
- Build second prototype of the in situ microcosm and test in the subsurface.
- Submit a patent for an in situ microcosm.
- Develop and implement a solid-phase microextraction (SPME)/GC-MS method for soil vapor investigation.
- Present technical results through presentations and/or publication.

Experiments show that the addition of gaseous carbon sources should greatly improve in situ remediation of explosives in the vadose zone. For example, downflow columns receiving 1000 ppm n-propyl acetate in nitrogen gas for three months revealed an almost 50% RDX removal (Fig. 1). The RDX degradation was uniform throughout the reactor, which shows that the n-propyl acetate had an effective range of at least 45". This is important when considering the zone of influence in the field. Nitrogen gas controls revealed no significant degradation (data not shown). A column receiving another carbon source, ethanol, showed quick high-explosive remediation yet little effective range through the soil column.

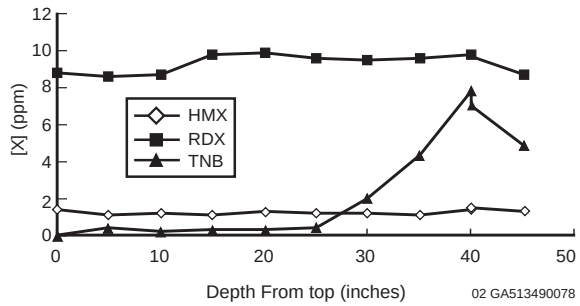


*FIGURE 1. Sectional analysis for trace explosives of a soil column receiving 1000 ppmv n-propyl acetate for 3 months. The gas flow was downwards at a linear velocity of 1 cm/min, the same as the flow rate estimated in the field site. Note 1,3,5-trinitrobenzene (TNB) degraded more quickly toward the source of the gas, while RDX fell to about 8.5 ppm. RDX was initially at 15.1 +/- 1.3 ppm (n=5) in thoroughly homogenized soil.*

The field site is a five-spot (square footprint with wells like the five-spot arrangement on a die) with injections at the corners and extraction in the center. Three corners are receiving approximately 2000 ppmv of an organic vapor in a nitrogen stream, with a fourth staying as a nitrogen gas control.

The field site has been receiving gaseous carbon sources for over 25 weeks. Several gas-sampling wells have shown breakthrough of the carbon sources and their daughter products. Soil samples will be taken in FY03 for explosives analysis, which will be the best indication of the effectiveness of this treatment system.

The DOD has recently started characterizing the contamination at firing ranges. The technology resulting from this LDRD research could be ideally suited for application at these sites. This in situ vadose work will also benefit other hazardous waste arenas.

# Kinetics and Mechanisms of Inter-Surface Transfer, and Solid-Solution Partitioning, of Surface-Complexed Metals in Colloidal Systems

*George Redden*

## *Understanding colloid-facilitated contaminant transport rates*

GC114

Colloidal particles have been implicated as agents for accelerating the transport of heavy metals and radionuclides in subsurface environments. In addition, colloids and reactive nanoparticles are increasingly being considered as a nano-technology with potentially valuable applications in the treatment and monitoring of subsurface contaminants and subsurface characterization.

A critical aspect of modeling colloid-facilitated transport of surface-reactive solutes is how solutes partition between mobile colloids, stationary surfaces and the solvent phase. Specifically, the rate of contaminant exchange between mobile and immobile phases is one factor controlling rate of transport of contaminants by colloids. Very little is known about the kinetics or mechanisms of sorbate transfer between colliding surfaces. Yet, this information is a necessary component for modeling colloid-facilitated transport solutes, especially in systems that involve flow rates that are fast relative to the kinetics of solute-solution partitioning.

This LDRD is attempting to interpret the rate of transfer of solutes between mineral surfaces in terms of mass transfer limitations (desorption, diffusion, adsorption), thermodynamics (reversibility of sorption and evolution of surface complexes with time), and surface contact frequency and energy. The hypothesis is that surface-surface contact can promote inter-surface transfer of adsorbed chemical species.

To date, the primary activity has involved setting up, testing and using a rotating disk reactor to establish quantifiable contact frequencies between colloids in suspension and an iron oxide surface (the disk). The analytical model for the reactor has been developed, iron particles (hematite) of suitable dimensions have been synthesized, and the reactor is now being used for this task.

During the final year of this project, the bulk transfer kinetics using two populations of colloids will be conducted in parallel with the disk reactor experiments. While the rotating disk reactor offers more quantitative control and interpretations of the solute transfer kinetics, the batch studies are simpler to conduct and can be applied to more types of materials.

Technical objectives for fiscal year 2002:

- Set up rotating disk experiments.
- Develop extensions of the rotating disk model.
- Continue work on the synthesis process to produce larger diameter particle populations.
- Investigate procedures to coat glass disks with hematite particles.
- Present results at technical conferences.

In FY02, the experimental set-up for the rotating disk experiments was completed. Preliminary tests were performed with benzoic acid disks dissolving into aqueous solutions using pH as the analytic indicator. These tests were necessary to quantify the hydrodynamic and mass transfer characteristics of the reactor. In this system, the dissolution rate is expected to be controlled exclusively by convective mass transfer from the disk into the solution.

Figure 1 (next page) shows the concentration of benzoic acid in the liquid as a function of time for one of these experiments. Figure 2 (next page) shows the dissolution rate as a function of the square root of the disk's rotational speed. The linearity of this relation validates the theory of mass transfer from the disk under laminar flow conditions.

A rotating disk model to simulate the mechanisms underlying solution/colloid/disk interactions was extended in this year's work to include:

- Kinetic step for surface-surface transfer from attached colloid to disk.
- Rate of transport of colloids to rotating disk without resulting adhesion.
- Kinetic step for colloid-to-disk solute transfer through liquid film separating surfaces when colloid/disk interaction occurs without adhesion.

The model has been employed to predict the appropriate experimental conditions to study solute transport in colloidal systems with the rotating disk apparatus. Simulations indicate colloid mediated solute transfer dominates mass transfer only for strongly sorbing

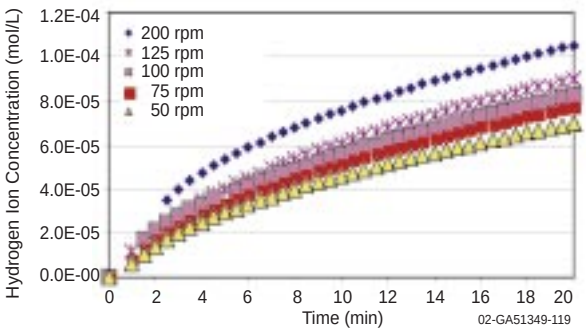


*FIGURE 1. Benzoic acid dissolution – rotating disk verification pH measurements, 20° C.*

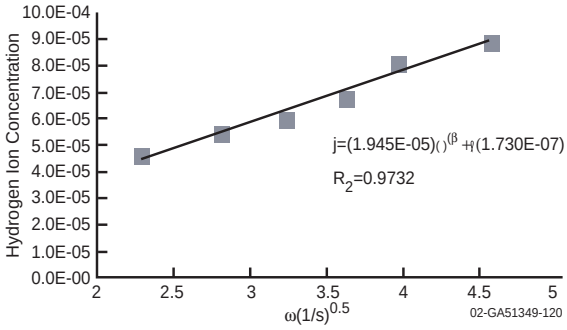


*FIGURE 2. Benzoic acid dissolution – rotating disk verification Levich's Relationship.*

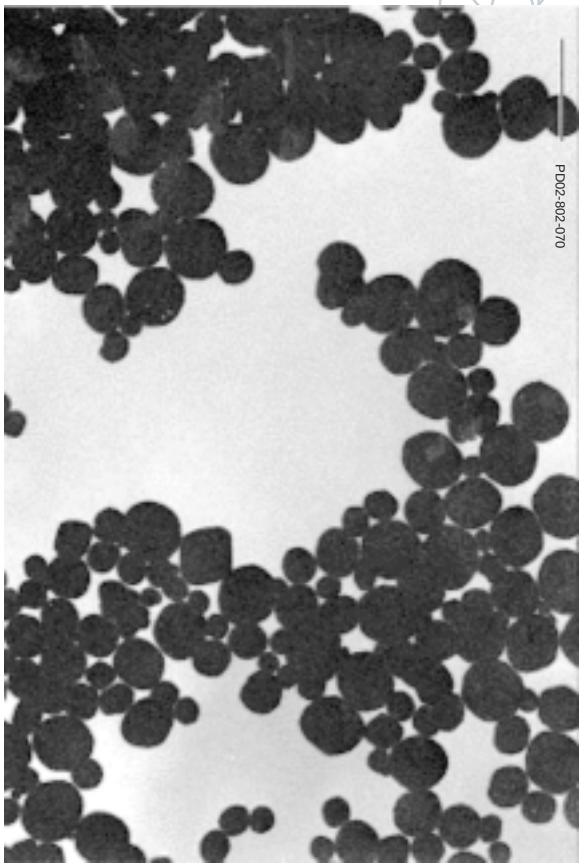


*FIGURE 3. Micrograph of colloid morphology and size distribution.*

species, and the rate of transfer is sensitive to the rate of solute transfer from non-aggregating, close-approach colloid/disk interactions.

The synthesis process implemented in the previous year to obtain near-spherical hematite colloids was extended to produce particle populations with appreciably larger diameters (300 nm and 600 nm). Colloid morphology and size distribution have been verified using transmission electron microscope (TEM). A representative micrograph is shown in Figure 3. These particles will be used in rotating disk experiments. A gravimetric separation method was developed and used to separate the populations of different size particles.

The solute to be used in the rotating disk experiments must be a species that sorbs strongly onto the colloids. This means that concentrations of solute in the liquid will be relatively low. For analytical reasons, possible solutes were identified that might be used along with the analytical techniques that should be employed to measure their concentration. At this point, the following possible solutes/analytical techniques are being considered: phenanthrene/gas chromatography, PCB/gas chromatography, and pyrene/fluorescence spectroscopy.

Experimental procedures were explored for coating the glass disks to be used in the rotating disk experiments with hematite particles. One procedure involves depositing particles from a colloidal dispersion onto the disk surface by solvent evaporation. The coating structure was analyzed by optical microscopy and SEM.

Future work in this LDRD includes incorporating into the model nonlinear isotherms that better quantify the behavior of the systems to be used in the rotating disk experiments. The investigators also plan to perform rotating disk experiments with hematite colloids and a selected solute to quantify the relative importance of the transport mechanisms. Bulk transfer measurements using dual colloid populations of iron oxide particles with separation by centrifugal filtration also will be performed.

Results from this research to-date have resulted in two presentations before American Institute of Chemical Engineers.

# Organic Co-Solvent and Co-Contaminant Effects on Sorption of Uranyl and Cesium to Metal Oxide Surfaces

*George Redden*

## *Predicting contaminant behavior in the presence of co-contaminants*

GC116

Solute partitioning between dissolved and sorbed states is governed by the chemical and physical interactions with other dissolved components, the solvent phase, and characteristics of the solid phase. Synthetic and natural organic complexing agents can significantly affect partitioning, and are common constituents of radioactive wastes as well as natural waters. Recent studies have demonstrated that simple generalizations about the degree and direction of the changes in metal partitioning caused by organic ligands cannot yet be made. The additional complexity of effects induced by changes in the solvent medium is relatively unexplored.

The presence of co-solvents that are miscible with water can potentially influence every parameter that governs the transport of solute species in soil and groundwater, including shifts in chemical speciation and reaction kinetics, changes in hydrodynamic properties of the solution phase, changes in soil structure, and effects on biological activity. For systems containing metal(oxy) ions, organic complexing ligands and oxide surfaces, the ability to predict chemical and partitioning behavior is necessary, but generally difficult or not yet possible. Thermodynamic issues make translation of knowledge about aqueous systems to mixed solvent systems difficult (or erroneous when neglected or incorrectly applied).

This LDRD addresses the effects of organic co-solvents on the chemical interactions between ionic solutes that are representative of environmental contaminants at DOE sites and on metal oxide (mineral) surfaces. The objectives of this project are to study the surface chemistry and sorption of metals on representative mineral oxides in the presence of: 1) highly miscible organic co-solvents (ethanol and acetone) 2) a co-solvent that is highly soluble but only partially miscible such that a saturation limit exists at higher concentrations (n-butyl alcohol, benzene or phenol), and 3) organic chelating ligands (EDTA, CDTA, NTA, citric acid).

The metals being investigated, uranium(VI) and cesium(II), are significant components of stored radioactive wastes. The solid oxides, goethite and kaolinite, are representative of important mineral components of aquifer solids.

Technical objectives for fiscal year 2002:

- Study speciation using Raman spectroscopy and EXAFS (Extended X-ray Absorption Fine Structure).
- Examine the distribution of $UO_2$-citrate species as a function of pH.
- Complete characterization of species.
- Perform EXAFS study of the Uranyl-citrate system at high pH.

To date, the pH dependence of uranyl(VI) complexation by citric acid has been investigated using Raman and attenuated total reflection-FTIR spectroscopies, as well as electrospray ionization mass spectrometry (ESI-MS). The pH-dependent changes in the $\nu_s(UO_2)$ vibrational envelope indicate the presence of three major $UO_2$-citrate complexes with progressively increasing U=O bond lengths over a pH range from 2.0 to 9.5. The first species, which is the predominant form of uranyl(VI) from approximately pH 3.0 to pH 5.0, contains two $UO_2$ groups in spectroscopically equivalent coordination environments, and corresponds to the $(UO_2)_2Cit_2$ complex previously known to exist in this pH range. At higher pH values, $(UO_2)_2Cit_2$ undergoes a pH-related interconversion to form $(UO_2)_3Cit_3$ and $(UO_2)_3Cit_2$, which are important at pH > 6.5.

ESI-MS studies combined with alteration of uranyl(VI) and citrate ratios, pH, solvent, and solution counter anion were successfully used to confirm complex stoichiometries. Results from surface-specific ATR-FTIR spectroscopy indicate that $Al_2O_3$-citrate interactions are stronger than those of citrate with $UO_2$, resulting in a structural transformation of the $UO_2$-citrate complex upon adsorption. An EXAFS study of the Uranyl-citrate solution complex, which has not yet been resolved in the literature, also was initiated using the Advanced Photon Source (APS) at Argonne National Laboratory. This data will be used to corroborate and constrain structural interpretations from the infrared analysis.

Spectrochemical titrations were performed to determine the pH dependence of $UO_2$-citrate complex formation. Much earlier work by Feldman et al. (1954) concluded on the basis of potentiometric and spectrophotometric studies that the 2:2 $UO_2$–citrate species undergoes a reaction at higher pH to form complexes with ratios of 3:3 and 3:2. A Raman band at 812 $cm^{-1}$ has been tentatively assigned to a species containing a 3:2 mole ratio of $UO_2$:citrate. A Raman band at 795 $cm^{-1}$, while a candidate for the 3:3 complex, cannot be definitely assigned because the spectra response to changes in mole ratios does not show a clear change at this ratio, although the relatively low frequency of this

mode suggests that this species is more highly oligomerized than either the dimer or the 3:2 complex. EXAFS spectra have been obtained and will be used to constrain the species interpretation.

Raman spectrochemical titration data was used to examine the distribution of $UO_2$-citrate species as a function of pH for a solution 50 mM each in $UO_2$ and citrate (Fig. 1). Based on the results, general-solution equilibria can be represented as:

$$6UO_2^{2+} + 6Cit^{3-} \rightleftharpoons 3(UO_2)_2Cit_2^{2-} \rightleftharpoons 2(UO_2)_3Cit_2 + 2Cit^{3-} \rightleftharpoons 2(UO_2)_3Cit_3$$

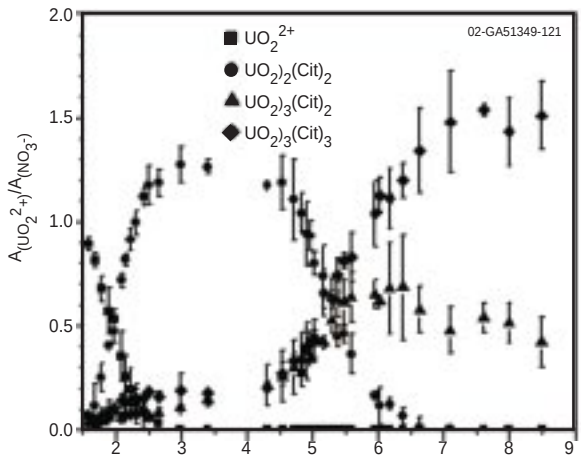


*FIGURE 1. Raman spectrochemical titration showing $UO_2$-citrate speciation as a function of pH.*

The existence of hydroxo- or oxo-bridging groups, as previously proposed based on results from $^{13}C$ and $^{1}H$ NMR spectroscopy, are clearly precluded. The formation of surface-adsorbed, hydrolyzed $UO_2$ species is a likely scenario once the citrate hydroxyl group is removed from the $UO_2$ coordination sphere in order to become attached to the $Al_2O_3$ surface.

An analysis of the uranyl-citrate system using EXAFS at the Advanced Light Source at Argonne National Laboratory was completed this year. This work was made possible through the generous offer of facility time by the Pacific Northwest Consortium group at the APS. This data will be used to help constrain the interpretation of the uranyl-citrate species and establish the viability of the analysis technique.

In conclusion, Raman, ATR-FTIR, and ESI-MS have proven to be powerful tools for the elucidation of both solution and surface speciation of $UO_2$-ligand complexes. The results of this LDRD definitively indicate the presence of three structurally distinct $UO_2$-citrate complexes in dynamic equilibrium over an environmentally relevant pH range. These pH-induced structural changes can now be used to explain such phenomena as the pH-dependence of $UO_2$-citrate complex biodegradation and photo degradation, both processes under investigation for the remediation of uranium in soils.

Results from surface-specific ATR-FTIR spectroscopy indicate that $Al_2O_3$-citrate interactions are stronger than those of citrate with $UO_2$, resulting in a structural transformation of the $UO_2$-citrate complex upon adsorption. The strong interactions of citric acid with $Al_2O_3$ and the association of $UO_2$ with adsorbed citrate may have broader implications for the remediation of uranium in soils, as the nature of the $UO_2$-citrate-$Al_2O_3$ ternary complex may affect uranium extraction efficiency.

The final year of this project will focus on sorption studies in co-solvent systems, studied in batch systems, while expanding the speciation studies to characterize co-solvent effects on the formation of uranyl-citrate complexes, both in solution and on oxide surfaces. In particular, the effects of one or more of the miscible and partially organic co-solvents ethanol and TCE will be investigated.

Results from this LDRD are expected to provide answers to two important issues:

- Heavy metal and actinide contamination associated with subsurface buried wastes are often associated with organic solvents in complex waste mixtures. This study may reveal how this association affects near-field transport or release in modeling source terms, information that to-date is essentially unknown.
- Application of Raman IR to the study of surface complexation is important since there are very few methods available that do not require vacuum conditions where water will not be present. The notable exception is X-ray spectroscopy made possible by synchrotron light sources. The spectroscopic speciation part of this study will be compared to EXAFS data in order to establish the viability of the technique.

This LDRD research will be generally applicable for waste treatment strategies and for predicting the behavior of contaminant mobility in soils and groundwater.

# Computational Experiments of Hysteretic Chemical and Moisture Migration

*Annette Schafer*

## *Understanding the history-dependence of flow transport*

GC140

Numerical transport predictions form the primary technical basis underlying environmental management decisions by providing a means of interpreting field data, integrating empirical observations, and testing conceptual models. Transport predictions, based on steady-state assumptions, distribute precipitation recharge uniformly over 365 days rather than assigning spring snowmelt and rainfall to the few days during which they occur, resulting in temporally uniform transport. However, during transient infiltration into dry soils, increasingly larger pores are filled beginning with small pores. The actual wetting order and distribution is dependent on infiltration history, implying that flow direction is a transient, spatially variable, hysteretic property.

This LDRD studies the influence of repeated infiltration events on the transport of reactive solutes through variably saturated, heterogeneous, porous media. The premise is "in as much as water flow paths are history dependent, geochemical reactions should be history dependent." In dry conditions, the large reactive surface area available in the fine-grained material will allow one reaction path, with a less reactive pathway becoming available as the larger-pores are filled with increasing saturation. This availability of reactive surface area should translate into time- and history-dependant effective reactivity (e.g., temporally hysteretically and spatially varying retardation).

Study of this phenomenon follows the approach of: 1) implementing hysteresis into a simulator ported to the high-performance computing facilities at INEEL, 2) conducing numerical experiments to assess the range of conditions influencing transport predictions, and 3) designing physical experiments to test the hysteretic relationships incorporated into the model.

The research will enable quantification of uncertainty in contaminant transport predictions incurred by neglecting the effects of transient infiltration through heterogeneous geologic materials.

Technical objectives for fiscal year 2002:

- Perform finite difference implementation of the 3-D Richard's equation.
- Condition soil columns for hysteretic studies.

In FY02, the first technical objective was finite difference implementation of the 3-D Richard's equation:

$$\nabla \bullet [K(\theta)\nabla h] = -pg\left(\frac{d\theta}{d\psi}\right)\frac{\partial\theta}{d\psi} = \frac{\partial K}{dz} + \frac{\partial\theta}{\partial t}$$

$$P_t = \frac{h}{1+\beta h}$$

modified using the 2-D Pan-Wierenga transform variable:

resulting in: This code that considers single-phase water flow, heterogeneous properties, and transient

$$\frac{\partial\theta}{\partial t} = \nabla \bullet K^* \nabla P_t - \frac{\partial K}{\partial z}$$

boundary conditions in three dimensions. The modified form of Richard's equation was adapted to reduce the nonlinearity in the pressure-saturation relationships. This modification has been implemented in a 3-D finite difference code to result in a regular matrix structure that lends itself to multi-grid and parallel solvers. These faster methods of solution will enable the Monte Carlo simulations necessary to quantify uncertainty. The non-linear iteration implemented thus far is based on a Newton method.

Testing of this code has shown that in 2-D it currently performs faster than the available finite element codes and is more robust than the standard finite difference implementation of Richard's Equation. However, the implementation did not converge for many of the synthetic realizations of stochastic hydrogeologic parameters. This method is based on a fully implicit approach using a modified pressure head as the primary variable. As a result, it requires estimates of soil hydraulic properties at the new time level, giving a non-linear system solved by Newton iteration. Under conditions involving sharp contrasts in saturation, the iteration is prone to convergence difficulties. Options for stabilizing the iteration include increasing the diagonal dominance of the matrix, searching for optimal relaxation parameters, or implementing the time-derivative term via the

method of Celia et al. (1990) and the diffusive term via the Picard method. The investigators are in the process of implementing these alternatives for testing with the stochastically generated random fields.

***Conditioning soil columns for hysteretic studies.*** Hysteresis phenomena in soils refers to differences in unsaturated hydraulic properties that occur between wetting and drying (Fig. 1) for the capillary pressure and saturation. Because the capillary pressure is a function of the radius of curvature: $Pc=2\sigma/r$, and the surface area in contact with the transported solute is a function of radius: $A=\pi r^2$, the adsorption should be hysteretic.

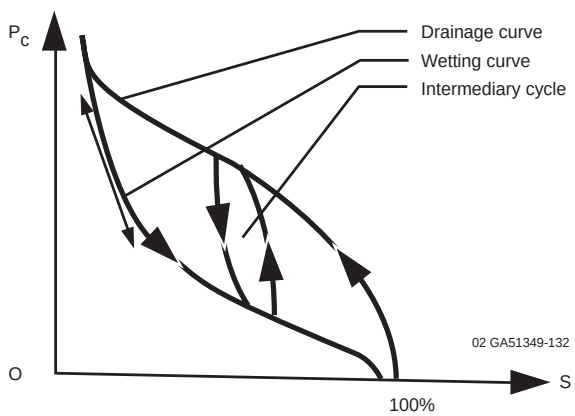


*FIGURE 1. Hysteresis: capillary pressure versus saturation.*

To assess the chemical adsorption properties as a function of the wetting and drying history, the investigators used a fixed flow rate, fixed water content infiltration and drainage experiment. For the flow component, the water potential will be the independent variable, and will be measured for each drainage and imbibition cycle. This will enable determination of the K-theta, and P-theta relationships using conventional means. Given the flow rate, permeability, and porosity transport through the column will yield a breakthrough curve that can be analyzed using the advection-dispersion equation, which will be interpreted to obtain the dispersion coefficient and retardation factor for a solute undergoing linear-equilibrium adsorption. Multi-valued retardation behavior will be used to infer the effective reactive surface area, assuming a constant surface-area based adsorption relationship.

The relatively small hysteresis typically observed in the hydraulic conductivity-water content function enables the experiment to be run either on the wetting loop or drying loop. Starting with a dry soil, infiltrating water at a constant rate until a uniform distribution of soil water is achieved gives one point on the hysteresis curve. Increasing the infiltration rate, and then lowering it to the same value as when wetting, results in a value on an adjacent scanning curve. Thus, a column can be conditioned to exist at the same water content and flow rate but with different soil water pressures depending on the point at which the drainage cycle is changed to imbibition. Similar hysteresis is expected in the effective reactive surface area.

To date, four valve-less pumps with a wide range of settable flow rates have been acquired. These have been attached to soil columns in the configuration shown in Figure 2 (next page). Recognizing that delineating the hysteresis relationships will require reproducible and constant flow rates over periods of up to several weeks, the selection of tubing and fittings was made to minimize variation in observed flow rate. The sandy loam soil placed in the columns was selected to produce widely separated scanning curves.

These characterization and verification experiments are being conducted currently. The chemical characterization of the soils will occur during the first quarter of FY03. Results from these 1-D infiltration experiments will be used to characterize the chemical hysteresis for verification of simulator performance. Tasks in FY03 will include expanding the physical columns to the 2nd and 3rd dimensions.

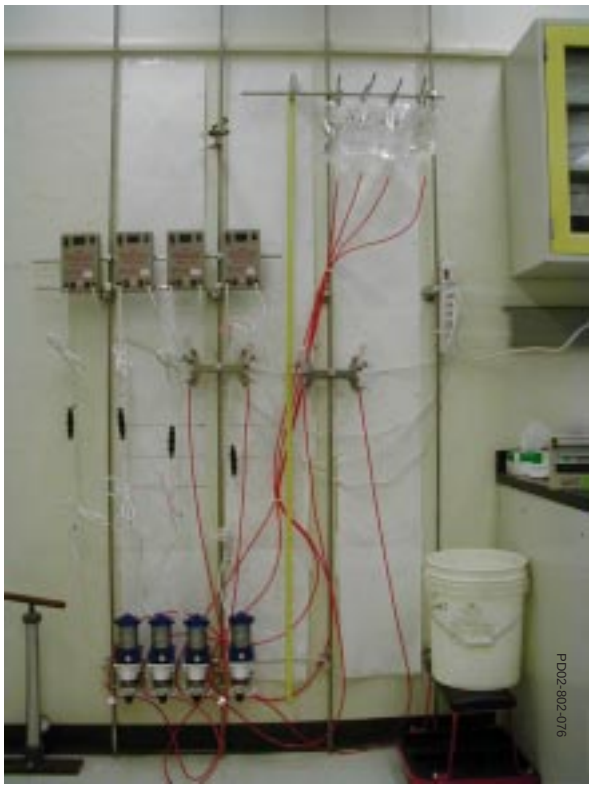


*Figure 2. Pumps attached to soil columns.*

The simulator and experiments developed in this research can help make inroads into quantifying the uncertainty underlying contaminant management and waste disposal decisions at INEEL and contribute to the success of the subsurface science program. Currently, the INEEL does not claim ownership of computational tools that can be used to simulate vadose zone flow or transport. In developing this tool, the research community will have access to a powerful and stable computational resource that can be modified and adapted to assist in experimental design and evaluation of experimental results. Further, the INEEL has limited expertise in conducting mesoscale transport experiments in geochemically and hydraulically heterogeneous media. This is especially true in transient observation mode. There is a need to develop and expand the laboratory's capabilities in this area.

The combined experimental and code development activities of the second year of this LDRD will greatly expand the technical capabilities of the INEEL. In total, this project has the potential to contribute to the long-term technical advance of the subsurface program at INEEL. Application of this code will lead to peer-reviewed publications, and thus will benefit DOE by contributing to the general scientific knowledge base.

# Development of Imaging Fourier Transform Mass Spectrometer Capabilities for Analyses of Complex & Heterogeneous Samples

*Jill R. Scott, Paul L. Tremblay, Timothy R. McJunkin*

## *Multipurpose instrument enables 3-in-1 measurement*

GC119

There is significant need at the INEEL and throughout the DOE complex for technology that can analyze complex heterogeneous environmental and biological samples. This LDRD focuses on the development of a unique, multi-purpose instrument capable of providing both mass spectral and optical imaging of complex, heterogeneous sample surfaces. This new instrument will provide the INEEL with the capability to analyze samples using the high resolution and mass accuracy of the laser desorption Fourier transform mass spectrometer (FTMS), while adding processes for illuminating the structure and environment of chemical species on the samples and retaining the spatial context necessary for imaging.

This project has three tasks: 1) enhance the imaging laser desorption FTMS capabilities, 2) integrate surface fluorescence detection within FTMS, and 3) incorporate Raman detection within FTMS.

Under the first task, an individual mass spectrum, obtained by the laser desorption Fourier transform mass spectrometer, will be correlated to its x, y-position; thereby, retaining the contextual relationship among all the spectra obtained from the sample. Tasks two and three will take advantage of the unique laser scanning system to allow incorporation of fluorescence and Raman imaging, respectively. This instrument will be capable of collecting the data equivalent of three separate instruments from the same sample. The optical and mass spectral imaging of complex samples will provide complementary information for complete sample characterization.

Technical objectives for fiscal year 2002:

- Perform collaborative studies for mapping minerals, microbes, soils, etc.
- Enhance software intelligence for image data analysis and display.
- Investigate new sample probe/inlet to accommodate real-life samples.
- Integrate fluorescence detection within FTMS.
- Coordinate fluorescence software with imaging FTMS software.
- Investigate feasibility of incorporating Raman detection with imaging system.
- Publish and present research results as appropriate.

During FY02, both the optical (fluorescence) and chemical (mass spectrometry) imaging were linked into one instrument that is now referred to as the INEEL Laser-based Optical and Chemical Imager (LOCI). The fluorescence imaging uses the same unique laser scanning system that was developed for the chemical imaging; however, lower laser powers are used so that the fluorescence imaging is non-destructive, unlike the chemical imaging that requires part of the sample to be desorbed into the gas phase for mass spectral analysis. Additionally, the automated data acquisition and analysis software was improved this year. LOCI can acquire 7200 files/hour. The inference engine used for automated data interpretation can interpret the 7200 files in approximately 20 minutes. The software seamlessly transforms the raw data into the spectra that are then classified to produce the images, a task that would require approximately 120 hours if it had to be done manually by an analyst. The 3-inch probe bar has proved useful for accommodating a wide variety of samples. Through collaborations, the investigators began analyzing real samples.

Figure 1 (next page) shows two images obtained from a single location on a basalt thin section exposed to *Burkholderia cepacia* G4 for approximately two days, then rinsed and analyzed by depth-profiling using the LOCI. Figure 1A is from the first scan with the microbes on the basalt thin section. The image of the second pass, Figure 1B, shows that plagioclase was the mineral beneath most of the microbes. Figure 1B shows that there are some residual microbes on the sample, possibly from incomplete laser ablation of the first layer. Alternatively, the microbes in the second pass might be associated with pores in the basalt sample.

Each dot in Figures 1A and 1B is the product of a single laser shot. Figures 1C and 1D show typical spectra used by the automated inference engine for assigning a mineral type and representative color to the respective dots. Figure 1C is a spectrum obtained from the microbes on the surface of the mineral. Because the

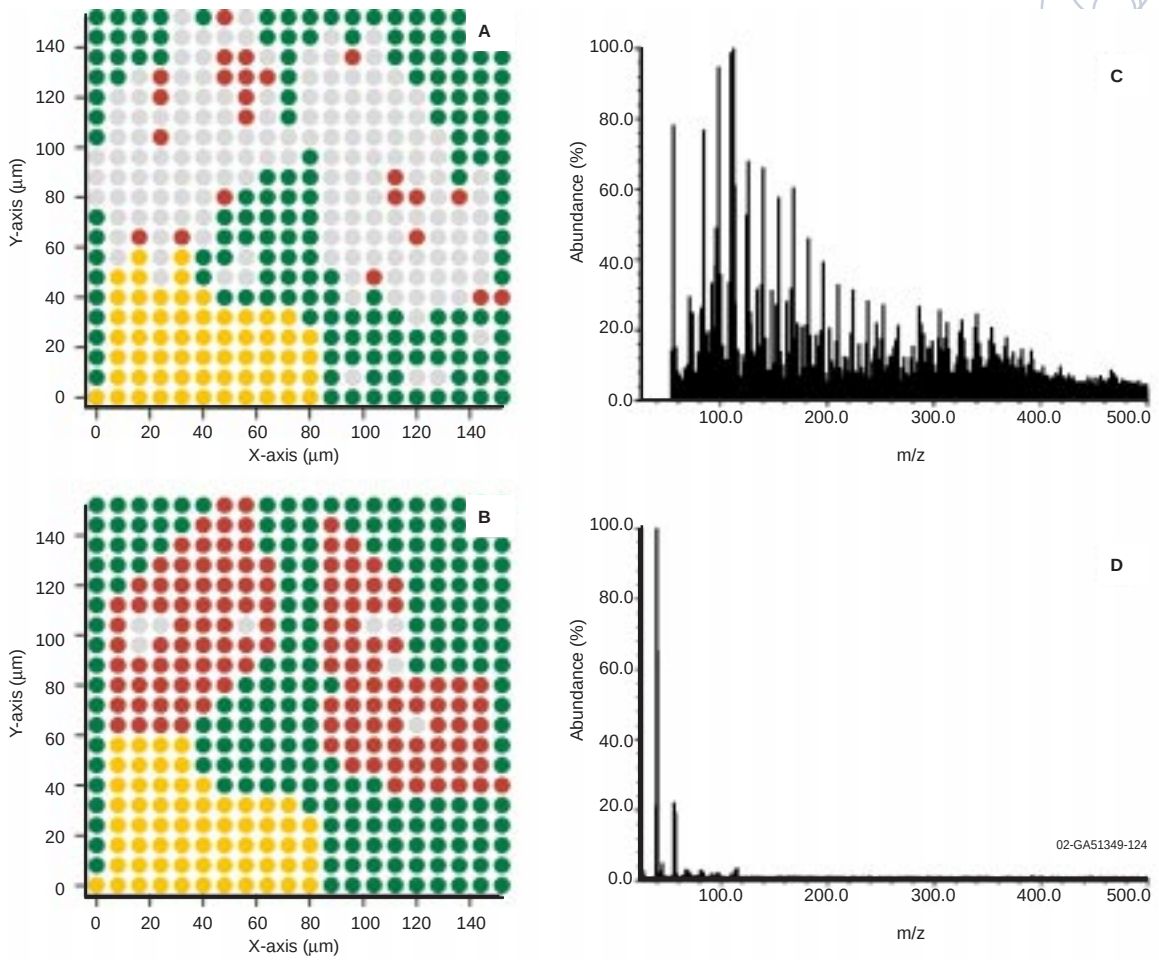


*FIGURE 1. Chemical images produced from depth-profiling a basalt thin section exposed to* Burkholderia cepacia *G4: A) first scan and B) second scan. Gray = microbe, Red = plagioclase, Green = olivine, and Yellow = augite. FTMS spectra taken from the same location during two sequential scans: C) FTMS spectra of* Burkholderia cepacia *G4 on basalt, and D) FTMS spectrum of the basalt (plagioclase) underneath the bacteria.*

sample was exposed only to a single microbe type, the FTMS parameters were set to merely detect biogenic molecular ions, as opposed to looking at the higher m/z range necessary to fingerprint the exact type of microbe. Figure 1D is the spectrum of the mineral (plagioclase) taken from the same spot as Figure 1C, but during a second scan of the sample.

Figure 2 illustrates the use of combined surface fluorescence and mass spectrometry detection for analyzing uranium contaminants. Figure 2A is the fluorescence emission spectrum from a 10 µm spot on a stainless steel surface exposed to uranyl phosphate excited at 355 nm. The fluorescence emission spectrum is characteristic of the uranyl species ($UO_2^{2+}$). Minerals with this species show the same basic shape with a shift in wavelength dependent on the equitorial ligands of the

uranyl species. ( LOCI's inference engine also classifies fluorescence spectra and correlates them to their x,y-coordinates to produce images or maps similar to the chemical image shown in Figure 1, but this particular sample was virtually homogenous, so an image would not have been meaningful.) Figure 1B is the mass spectrum obtained from a subsequent laser desorption event. The presence of gas-phase species, $UO_2^{1+}$, $UO_2^{2+}$ and $UO_2^{3+}$, is evident in the mass spectrum as m/z 270.0402, 135.0198, and 90.0130, respectively.

In general, the non-destructive fluorescence detection is acquired first. If the contaminant fluoresces, then it is not only detected, but information allowing its speciation also is obtained. Then the depth-profiling capability of the laser desorption chemical imaging can be used to interrogate the underlying surface. However, if the contaminant does not fluoresce (either naturally or due to quenching), then chemical imaging via mass spectrometry can be used to at least determine its presence or absence and provide information that can be used to infer speciation when compared to spectra of "knowns" obtained from similar surfaces. The speciation from mass spectra can only be indirectly inferred, because many gas-phase species (such as $UO_2^{1+}$ and $UO_2^{3+}$) rarely correlate with the surface species. In fact, desorption ionization inherently produces a majority of singly charged species, as shown in Figure 1B. Therefore, it is usually impossible to determine the surface oxidation state of an element from the mass spectrum.

This LDRD addresses several needs of the INEEL and DOE. Development of this technology will directly support Subsurface Science Initiative projects that need to analyze complex, heterogeneous environmental and biological samples. Although the imaging FTMS is not a field instrument, it can be used to analyze field samples and bolster confidence in field measurements obtained by less capable, portable instrumentation. This technology also provides the opportunity to obtain a suite of measurements on the same sample to more thoroughly understand complex samples of interest to DOE: environmental, biological, and material (nanotechnology).

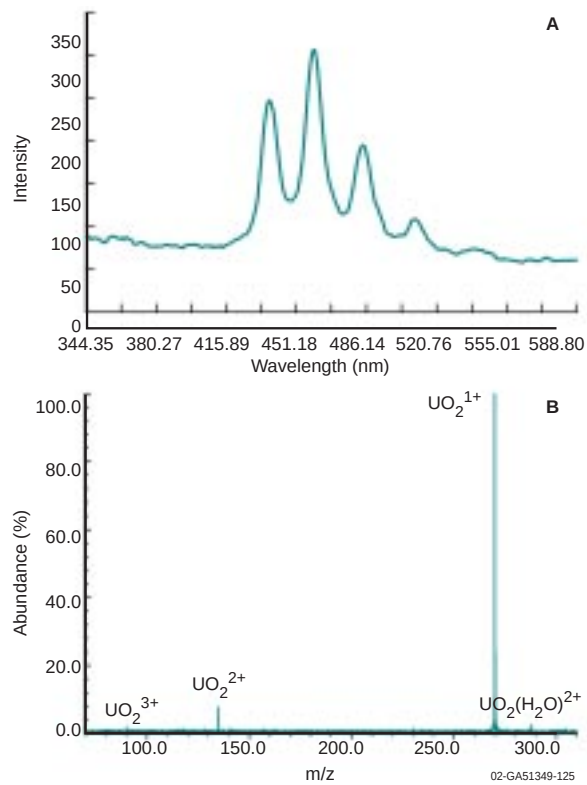


*FIGURE 2. Results of two-step LOCI analyses of uranyl ($UO_2^{2+}$) on stainless steel surface: A) non-destructive fluorescence spectral analysis showing surface speciation of uranium and subsequent, and B) destructive laser desorption mass spectral analysis showing the presence of uranium.*

This project also has led to external collaborations. In FY02, collaboration with Montana State University's Professor Inskeep was initiated with ACE Fellowship support of a student, Mary Kauffman, for mineral and microbe studies using various techniques including the imaging FTMS system. As appropriate, proposals will be submitted to DOE programs, such as EM and SC, as well as outside sources.

# Dual Electrodes and Defining the Electrically Disturbed Region in Induced Polarization Measurements

*Clark Scott*

## *Using electrical behavior to locate contamination*

GC145

With the arrival of the geocentrifuge and the Subsurface Geosciences Laboratory (SGL), methods of imaging and characterization lab-scale experiments are required. At larger scales there are continuing needs for characterization technologies in the DOE clean-up process. Of the many physical properties that can be measured, the electrical behavior of the system is one of the most promising for locating the often-subtle signature of contamination.

The current state of the art in sensor development/deployment, data collection/processing, modeling and interpretation/inversion is technologically inadequate for the range of studies envisioned for the INEEL. Examples of this inadequacy include electrodes that are too invasive and leak contaminants into the experiments, and sensor deployment that minimizes the noise due to electro-chemical disturbance using large spatial separations or time-consuming data collection schemes.

This LDRD addresses the need for a complex-resistivity (CR) capability at the INEEL for use in contaminant and flow experiments at the lab and field scale. The project approach is to develop a non-polarizing two-electrode device incorporating independent source and receiver electrodes in one robust deployable assembly. The major issue to be addressed is the necessary separation distances between sensor and source in typical soils to achieve electrochemical independence while satisfying geometric equivalence of the two electrodes at various scales.

A modeling and experimental approach will be used to address optimal sensor deployment for an automated, less labor intensive, and fast surveying system for the different environments envisioned for this application; i.e., tank, mesoscale and field surveys.

Technical objectives for fiscal year 2002:

- Complete design and acquisition of laboratory complex-resistivity system.
- Develop theoretical description of electrically disturbed zone.
- Evaluate electrode materials.
- Collect data to test theory of disturbed zone.
- Prepare paper describing disturbance zone work.

Several factors have influenced the design of the laboratory complex-resistivity setup including a data collection mechanism that will enable multiple channel data collection at low frequencies while maintaining accurate results at the higher frequencies. The system will be somewhat portable so that experiments can be easily run in different labs. The system as a whole, or as parts, can be integrated with other data streams in support of the mesoscale experiment process.

The low frequencies present the problem of taking three to four hours to collect data from a single channel. The solution was to include matrix switching to simultaneously collect data from a group of channel pairs. The data are, in a sense, multiplexed and software is used to de-multiplex the data stream at the recording computer. This solution will work until a threshold frequency of around 1 hertz is met.

Above 1 hertz the switching is too slow to collect enough data points from multiple channels to accurately reconstruct the phase. At these higher frequencies it becomes more efficient to record the data from one channel at a time. As measurement frequencies continue to increase there will come a point where the digitizing card in the computer cannot digitize fast enough. At these higher frequencies the signal will be fed into a lock-in amplifier and then to the computer. The final design is shown in Figure 1.

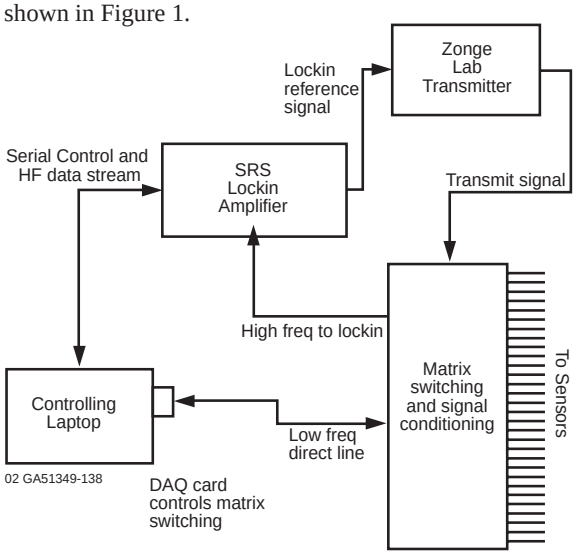


*FIGURE 1. Schematic of the laboratory complex-resistivity system final design.*

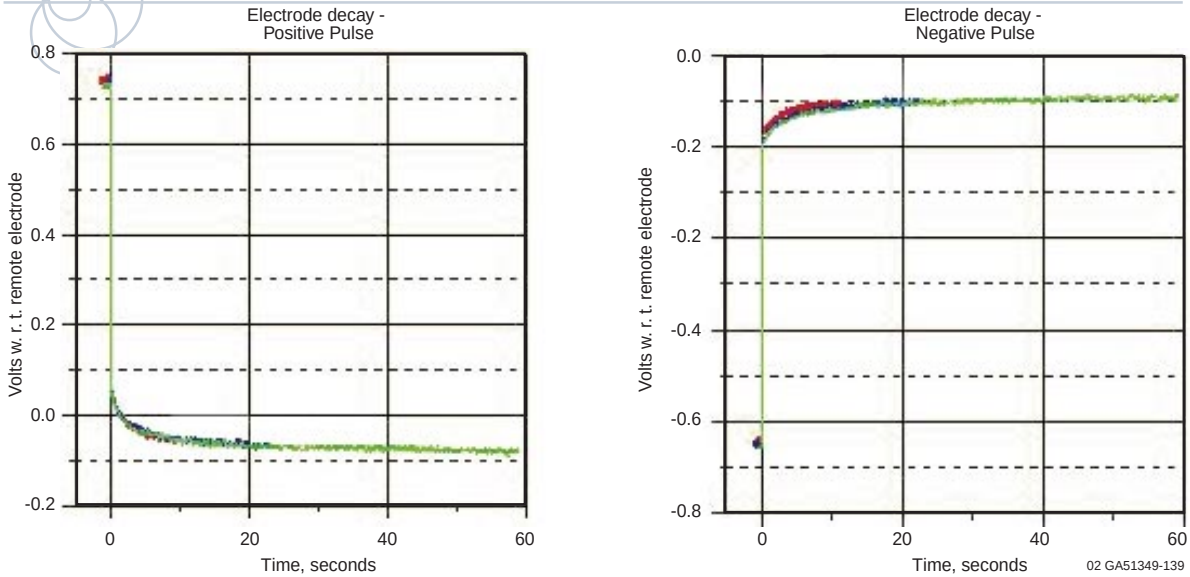


*FIGURE 2. Plots of the measured decay curves from metal (iron steel) electrodes. Data shown was taken after a one-minute charge time. Note the offsets persist for long periods and the apparent asymmetry between the positive and negative pulse.*

Electrode development has begun on two issues. At the INEEL, testing different polymerizing agents for the gelling of Cu-SO4 solutions was begun and several porous materials (plastic and ceramic) for the containment of the final gelled solution were acquired. Through collaboration with Dr. William Frangos at James Madison University (JMU) in Virginia, JMU has begun the testing of standard electrode materials including metal and Cu-So4 electrodes. These initial tests are investigating the metal polarization effects and have shown the expected strong polarization behavior of metal-transmitting electrodes (Fig. 2). The next step is to develop a non-polarizing transmitting electrode that can be used to investigate what the investigators call "the weak polarization of the surrounding medium." Standard metal electrodes overpower this weaker signal and standard porous pot electrodes have very high impedances making them unsuitable as transmitting electrodes.

Initial theoretical development has followed a path that is leading to a more comprehensive description of polarization effects in complex-resistivity measurements. Current theory, and geophysical lore, has typically treated polarization in measurement as two separate phenomena: the polarization of the transmitting electrode (strong polarization), and the polarization of the surrounding medium (weak polarization). In most of the project work, the main obstacle to good data has been the strong polarization effect. This fact has long been recognized by the industry and past efforts have been in developing the theory around strong polarization. In the development of a dual electrode, the investigators came to realize that the weak polarization phenomena may be a considerable effect and are starting to focus their efforts in that area.

This LDRD is leading to the capability for 3-D characterization of geometrically and electrically complex systems. This capability can be applied at the INEEL and at other DOE sites around the country for contaminant studies. Initially complex resistivity may be applied in lab, mesoscale, and field experiments concerning contaminant flow/characterization and scaling experiments central to SSI goals. Beyond these goals, the capabilities developed in complex resistivity also show promise in areas such as discrimination in UXO and mine detection, and in remotely quantifying corrosion in metal drums, tanks, and pipes.

# Improving Soil Water Flux Estimates in the Deep Vadose Zone

*James B. Sisson, Joel M. Hubbell*

## *Decreasing uncertainty on contaminant transport at the INEEL*

PH105

Dissolved contaminants are transported with soil water. Thus, knowing the in situ flux of soil water is a crucial variable for predicting contaminant transport in the vadose zone. Soil water flux has been estimated using a variety of indirect techniques (e.g., mass balance, empirical, soil physics approaches) and direct measurement techniques (e.g., lysimeters, tracers). All of these methods require monitoring soil water variables over long periods of time.

Soil water data collected throughout the deep vadose zone at the INEEL and other DOE facilities indicate that the variation found over time decreases with depth. This reduced variability enables substantial improvements in the accuracy and precision of indirect and direct approaches for estimating soil water flux. In addition, the availability of low-cost, high-precision sensors and new instrument installation techniques for placing instrument packages below the zone of large temperature fluctuations provides the opportunity to make precise and repeatable measurements.

The objective of this LDRD is to improve estimates of soil water flux in the deep vadose zone. The work being done can lead to new and improved methodologies for measuring soil moisture flux in the deep vadose zone and for collecting data to compare new and existing methods. Successful completion of this project will establish methods for estimating flux in the deep vadose zone and provide the tools required to estimate water movement at DOE, NRC, and commercial sites.

These tools and techniques can be employed to improve risk assessments and estimates of the aquifer recharge rates and quantities. The new tools would also be useful for validating remediation approaches that involve developing engineered control of soil water flux.

Technical objectives for fiscal year 2002:

- Obtain and evaluate data from deep vadose zone instrumentation to determine the limiting and controlling state variables for accurate estimates of moisture movement.
- Evaluate and summarize the attributes of existing flux estimation techniques that can be adapted or modified for use in deep vadose zones.
- Develop conceptual design requirements of physical tools and analytic techniques for use in flux measurement. Construct prototype instruments and conduct initial laboratory tests to prove feasibility of the concept and design.
- Prepare and submit intellectual properties (invention disclosure reports).

Information from field measurements in deep vadose zones suggests deep moisture flux should vary over a narrow range of values at any given location. Several methodologies have been deployed in this research to measure the state variables for moisture flux in the field, with tensiometers providing the most accurate measurement for flux estimation. The soil water potential measurements obtained from advanced tensiometers enable determination of hydraulic gradients and can be related to the moisture flux. The key unknown parameter is the unsaturated hydraulic conductivity of the material, which is an unknown function of water content. Field observations are providing a framework for estimating unsaturated hydraulic conductivity at ambient soil water condition.

Flux estimation techniques used in the shallow vadose zone were reviewed, and features are being used to design methodologies applicable for measurements in the deep vadose zone. Existing instruments originally developed for installation in the walls of excavations are being adapted for deployment in boreholes. Several direct measurement techniques have been extended to designs for use in deep vadose zones and this has resulted in several Invention Disclosure Records (IDR's) being filed to secure intellectual property rights for rapid and inexpensive flux estimation methods.

Based on the physical characteristics of the deep vadose zone, the investigators developed conceptual design requirements of physical tools and analytic

techniques. There was also a need for an analogous laboratory measurement that could be performed in the laboratory for core samples. A new technique was theorized and a prototype instrument constructed for testing. Two laboratory tests were conducted indicating the technique is feasible, the prototype instrumentation works, and additional testing is warranted. Further modification of this technique may yield a new low-cost laboratory test for accurate measurement of hydraulic properties representative of in situ conditions.

Three previously submitted IDR's describe methods and tools for measuring vertical soil water flux at any depth in sediments. These instrument designs and associated installation techniques were further evaluated for direct-point measurement of flux in the deep vadose zone.

The results and tools developed in this project support the Subsurface Science Initiative and will be used at DOE and commercial sites throughout the nation. This project supports the mission of the INEEL and DOE to ensure that past (and future) operations will not adversely impact the environment. This research should decrease uncertainty relating to contaminant transport and long-term waste management practices at the INEEL. The INEEL is collaborating with researchers from the University of Idaho and Clemson University on this project.

# Regional Setting and Flow Dynamics of the Snake River Plain Aquifer

*Richard P. Smith, Travis L. McLing, Michael J. Rohe*

## *Uncovering new insights into contaminant transport*

GC102

Improved understanding of groundwater flow in the Snake River Plain aquifer beneath the INEEL is key to more accurately predicting contaminant transport. Various geophysical, geochemical, and hydrologic data exist regarding the Snake River Plain, though much of it was collected for other purposes. This LDRD investigates an approach that analyzes, merges, and augments these existing data to uncover new insights on aquifer geometry and flow dynamics. The information gleaned from analysis of these databases is vital for current and future modeling of contaminant transport.

The focus of this research is on aquifer temperature distribution, water chemistry (both solute and isotopic compositions of Sr and U), and water level records. These extensive data sets provide independent means to test hypotheses of groundwater movement. Aquifer temperature distribution shows areas of major geothermal input from depth, allows determination of aquifer thickness variations, and helps to trace plumes of cold recharge water across the INEEL. Aquifer chemistry and isotopic ratios allow recognition of preferential flow paths and zones of slow water movement. The time histories of water levels in INEEL wells for the past 50 years enable calculation of aquifer gradient variations through time and aquifer response to climatic cycles, and provide predictive capability for future water levels and water table gradients.

Technical objectives for fiscal year 2002:

- Obtain 1960's vintage analog (strip chart recorder) temperature logs for 123 wells, digitized them, and add to the database of temperature logs for INEEL.
- Merge INEEL-area temperature data with that for the entire eastern Snake River Plain.
- Use observed temperature distribution to develop parameters and set up simple models to estimate the changes in permeability required to develop aquifer warm zones given a constant heat input at the base of the aquifer. Actual modeling to be done in FY03.
- Collect and analyze additional samples of uranium isotopes to increase the resolution of geochemistry-based preferential flow paths.
- Develop a new methodology for incorporating the effects of matrix diffusion on transport of natural and anthropogenic isotopes in the aquifer.
- Prepare an animation of groundwater elevation changes over time.
- Separate water level hydrographs for 215 regional aquifer wells into four distinct time scales. Prepare spatial distribution maps of water-level variance that occurs at these different time scales.
- Examine relative severity of downward trend in water table elevations as a function of location.
- Prepare and present papers on research.

In FY02, investigators successfully merged INEEL aquifer temperature data with that for the entire eastern Snake River Plain to provide a more complete understanding of aquifer recharge from adjacent highlands than was possible before. Previously unexplained ridges in the elevation of the water table were seen to be caused by mounds of cold recharge water from major drainages. High temperatures occur all around the margins of the aquifer except in places where major streams enter the Plain.

In addition to the narrow plume of cold recharge water from the Birch Creek drainage that penetrates southward into a high-temperature zone in the TAN area, a second cold recharge plume was identified by temperature distribution along the northeast margin of the INEEL near Mud Lake. The source of this cold recharge plume is Medicine Lodge Creek on the south side of the Centennial Range. The elongate narrow shapes of these cold plumes indicate they are preferential flow paths (probably fracture zones or interconnected rubble zones between lava flows) in which groundwater velocity is great enough to maintain low temperature in areas that otherwise have lower impermeability.

This year's research led to the generation of a new double-porosity mathematical model that incorporates diffusive processes along with traditional chemical effects in fractured rock media. The new procedure simultaneously models the effects of diffusion and reactions of the individual isotopes in fracture-bounded blocks and advective pathways, and then derives the isotopic ratios to be expected. The approach of this LDRD differs from other methods because it uses

multiple coupled equations to model the system. This effort provides a better estimation of the isotope ratios to be expected and the flow velocities experienced along individual flow paths.

The four different characteristic shapes of INEEL-area hydrographs (Fig. 1) can be related to response of the aquifer to different recharge conditions. Wells in north-central INEEL (near TAN) exhibit low-amplitude long-term cycles and strong seasonality, showing the relative stability of the Birch Creek recharge with varying climatic conditions. Wells in eastern INEEL have similar hydrographs but with a more abrupt rise in the mid-1980s and smaller amplitude annual cycles, probably because of great distance from major recharge sources. Wells in northwestern INEEL, near the mouth of the Little Lost River, exhibit unusually large changes in water table elevation at the low-frequency time scale, reflecting strong recharge due to underflow from the drainage and strong response of the drainage to climatic variations. Wells in central INEEL, near the Big Lost River, are similar to those in northern and eastern INEEL, but have strong spikes only during times when the river flows for long periods onto the INEEL. Underflow recharge from the Big Lost River enters the aquifer down gradient of INEEL.

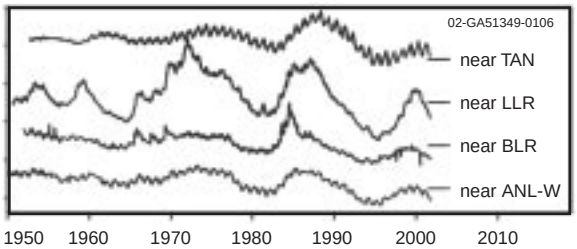


*FIGURE 1. Four characteristic hydrograph shapes for INEEL-area wells are shown. The strong difference between the response from the Big Lost (BLR) and Little Lost (LLR) rivers reflects differences in the manner of recharge from each and, perhaps, different irrigation practices between the two basins.*

This LDRD research supports the Subsurface Science Initiative, the site-wide groundwater modeling efforts of the Environmental Management program, and long-term stewardship activities at INEEL. It addresses problems of prediction of contaminant transport in the aquifer by providing input parameters and uncertainty limits for models, and by increasing understanding of aquifer geometry and flow characteristics. This project has fostered collaborations with Southern Methodist University, University of Idaho, University of Mississippi, and Los Alamos National Laboratory that provide increased peer acceptance of results. This LDRD positions the INEEL to apply the developed techniques and concepts to other sites where groundwater contamination occurs in complex aquifers.

# Development of Techniques for In situ Measurement of Groundwater Contaminant Source Strength

*Robert C. Starr, Carl D. Palmer*

## *Improving predictability of contaminant transport and fate*

GC130

Rate coefficients for reactions that affect groundwater contaminants are needed to simulate the transport and fate of contaminants in aquifers. Mass transfer coefficients govern the generation of contaminated groundwater plumes from subsurface contaminant sources, and decay coefficients govern the rate of contaminant dissipation. For contaminants that undergo substantial decay in the subsurface, rate coefficients are often the most important simulation parameter. Rate coefficients vary over orders of magnitude. Existing methods for determining rate coefficients are problematic. Typical methods include back-calculating by simulating existing contaminant plumes, extrapolation from laboratory studies, and field-scale measurement. Field measurements are the most desirable, but also the most difficult.

This LDRD is investigating a method for measuring in situ reaction rates to improve predictions of contaminant transport and fate in the subsurface, and to design, implement, and assess the performance of groundwater remediation programs. The effectiveness of remediation can be monitored by measuring the rate of relevant reactions and comparing the pre- and post-treatment rate of dissolved-contaminant generation. The mathematical theory, procedures, and equipment for in situ measurement of first-order chemical processes are being developed. The existing theory for making such measurements with single-well push-pull tests (SWPPTs) has been extended to more general cases, including several rate laws and multiple-rate coefficients in different parts of the physical system. The mathematical solution for the first-order decay case is being validated via laboratory-scale experiments. A series of laboratory tests at sequentially larger scale and of greater complexity will be used to validate solutions for additional rate equations, and develop the procedures and equipment for in situ measurement of rate coefficients.

Technical objectives for fiscal year 2002:

- Derive a general mathematical method for determining reaction coefficients from single-well push-pull test data.
- Validate the method for first-order decay using laboratory studies.

Single-well push-pull tests have been developed as a practical method for making field measurements. These tests are conducted by preparing a tracer solution that contains both a non-reactive tracer and the solute for which rate constants are needed. The tracer solution is injected into an aquifer using a single well (the push phase), allowing a quiescent period for reactions to occur, and then an extraction (pull) phase in which the tracer solution is pumped out of the aquifer using the same well. Dispersion affects both tracers, and reactions additionally affect the reactive tracers. Using the ratio of the concentrations of both tracers, rate coefficients can be determined from the test data.

Mathematical solutions have been developed for several cases, including zero and first-order dissolution and decay, second-order decay, and Monod kinetics. These solutions are more general than previously published solutions, and are not based on the restrictive or unrealistic assumptions made in previous solutions. This set of solutions allows SWPPTs to be used for measuring rate coefficients for a wide range of processes important to contaminant migration in groundwater.

The first-order decay case is being experimentally validated using laboratory scale model aquifer studies. A model aquifer was built with geometry and boundary conditions consistent with the mathematical solution; i.e., a homogeneous radially symmetric system with constant head at the outer circumference and a well at the center. Sorption studies were conducted to identify materials for constructing the model that did not sorb the tracers.

The general approach was to use a reactive tracer whose decay coefficient is known *a priori* to conduct a SWPPT in the model aquifer, then to calculate the rate coefficient from the SWPPT data. Close agreement between the known and measured rate coefficients would indicate that the solution was valid.

Selection of the tracers was a critical component of this experiment. Technetium-99m (Tc-99m) was used as the decaying tracer. Its desirable characteristics include suitable geochemical behavior, a half-life (six hours) that is convenient for this study, and ready availability. Tc-99m is routinely used for tracing inside the human body

by the nuclear medicine community. Aliquots of Tc-99m were obtained for these studies from isotope sources that had decayed so much that they were no longer useful for medical imaging, but still had sufficient activity for this research. Tritiated water was used as the conservative tracer.

One experiment has been performed to date. Additional experiments are planned to more completely validate additional aspects of the first-order decay solution and solutions for other rate orders. The results of the first-order decay validation experiment (Fig. 1) yielded a measured decay half life of 4.6 hours, compared to the accepted value of 6.01 hours, with an error of about 24%. Considering that reaction rate coefficients range over orders of magnitude, obtaining a measured value this close to the true value in the first attempt is encouraging. Correction of minor problems with the experimental apparatus is expected to yield measured values that are closer to the known value. Additional experiments are planned to validate special cases of the general first-order decay solution.

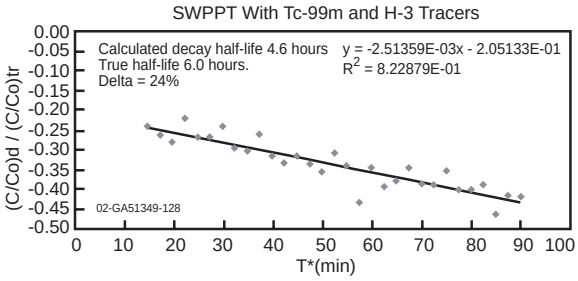


*FIGURE 1. Results from lab-scale single-well push-pull test with a radiotracer.*

Subsequent research will include validating solutions for rate laws other than first-order decay, and for scaling up the experimental apparatus for use at the meso and field scales. Development and validation of a suite of solutions will facilitate use of single-well tests for measuring defensible rate coefficients. This effort will yield better simulations of contaminant transport in groundwater, enabling better-informed decisions on groundwater resource protection and remediation.

The familiarity and expertise developed with Tc-99m as a non-sorbing decaying tracer are expected to be used in subsequent laboratory and meso-scale experiments for groundwater zone and vadose zone research.

Two collaborations are being formed as the result of this research. The Health Physics department at Idaho State University (ISU) has been instrumental in the radiotracer studies performed to validate the first-order decay solution. Development of this collaborative relationship provides hydrogeologists at INEEL with a broader suite of techniques for investigating subsurface processes and provides Health Physicists at ISU with more applications for radiotracer techniques. In addition, researchers at Boise State University are interested in collaborating with INEEL to provide a well-characterized and instrumented field site for developing expertise in field-scale deployment, in exchange for additional characterization of bioactivity in the root zone within the shallow aquifer.

This LDRD project is leading to the development of a practical and robust method for in situ measurement of rate coefficients. This new method potentially has broad applicability, including use at numerous government and private-sector sites where more accurate parameterization of contaminant transport models would lead to better decisions. The same technique also can be used to assess the effectiveness of strategies intended to remediate subsurface sources of groundwater contaminants. Improved predictions and performance assessment of environmental restoration sites will lead to reduced costs and enhanced effectiveness of groundwater remediation programs.

# Improved Osmotic Tensiometer Components and Parameters

*Mark Stone*

## *Designing longer lasting groundwater sensors*

GC107

Osmotic tensiometers are used as groundwater sensors to obtain data for mapping subsurface water movement and content. They operate on the principle of osmotic transport through a semipermeable membrane. The porous tensiometer bulb is filled with water, attached to a pressure-measuring device, and placed in the ground. When water (a component of the fill fluid) passes in or out of the membrane, it results in a pressure change that is measured.

One problem with the present technology is that the fill fluids currently used tend to leak or degrade over time. Another problem is that the membranes do not last as long as desired. This LDRD addresses these two weaknesses while considering other sensor enhancements.

Technical objectives for fiscal year 2002:

- Test alternative fill fluids.
- Investigate better long-lasting membranes.
- Investigate alternative bulbs/supports.
- Start work toward developing a miniature tensiometer.

The initial membrane selected for investigation was a reverse osmosis membrane composed of a thin polymer layer adhered to a paper backing. A one-inch diameter circle was cut from a sheet, placed in the cell, and secured by screwing on the threaded cap. The first set of experiments looked at concentration-dependence of the fill solution. A series of three sucrose solutions in water (1%, 10% and 20%) were loaded into three separate cells and immersed in water at room temperature (Fig. 1). The effects of concentration are quite dramatic — both the rates of response and the ultimate pressures attained were affected. Several steep drops in the 20% curve also were noted. In order to protect the transducer, when the cell pressure increased to over 200 psi, the cell was momentarily removed from the water, opened briefly to relieve the pressure, resealed, and placed back in the water.

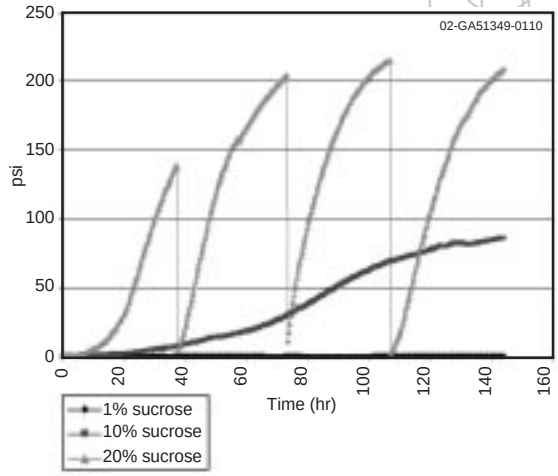


*FIGURE 1. Concentration effects on pressure build-up in the osmotic tensiometers.*

Sintered stainless steel discs were used that were 1/8" thick by 1" in diameter but with differing pore sizes (from 0.5 to 100 µm). The results of the different pore sizes were dramatic, and as expected, the larger the pore size the more rapid the response. In the case of the 100 µm pores, the pressure rose more than 300 psi in less than two hours.

One aspect of this work was to explore better configurations for construction of the osmotic apparatus. In a regular tensiometer, a porous bulb is filled with water, attached to a pressure-measuring device and placed into the ground. The pressure starts out at zero. As water moves out of the bulb into the surrounding soil, a vacuum is created. Since the bulb starts out in a saturated condition, no pressures higher than zero can be observed.

An osmotic tensiometer typically has a semipermeable membrane that works in combination with a solute that cannot permeate the membrane. The apparatus is placed into a supply of pure water until an ultimate osmotic pressure is attained. Once this has occurred, the apparatus is placed in the ground. Because the system starts out at a positive pressure, a wider range of pressure measurements can be made.

As an alternative approach to apparatus design, this LDRD explored eliminating the membrane and instead using a small-pore-sized bulb and a molecule too large to pass through. A series of molecules were synthesized and checked in a regular cell using a membrane to see if the molecules were osmotically active. Polyethylene glycols of various weights have been studied as fill fluids. These molecules were tethered together to see if they would still be osmotically active. A series of methyl esters substituents having molecular weights (MW) of 350, 550, 750, 2000, and 5000 were produced and attached to a cyclic phosphazene backbone. Testing showed that the 350, 550, 750, and 2000 MW hexasubstituted cyclic phosphazene materials were osmotically active (Fig. 2). Testing of the 5000 MW material was scheduled but not performed because the project was stopped. The goal of these final tests was to see if the larger molecules could be loaded into a fine-pored ceramic cup and pressurized without the use of a membrane coating in the bulb. If that were possible it would make a tensiometer that could measure over wider moisture ranges.

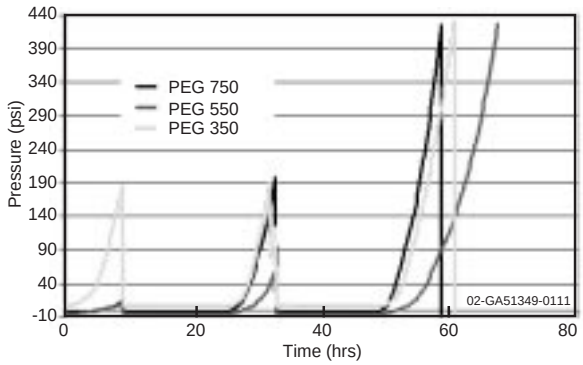


*Figure 2. Pressure build-up vs. time for three of the methyl ester cyclic phosphazene trimers.*

This LDRD research is expected to lead to an improved osmotic tensiometer that could have a significant impact on all general types of moisture-measuring applications. These applications include INEEL site aquifer measurement/monitoring, groundwater determinations and agricultural applications (when irrigation is required). Monitoring water movement and water content fluctuations is a vital part of environmental responsibilities.

# Development and Application of Custom Flow Models for Understanding Flow in Porous and Fractured Matrices with Biological Components

*Daphne Stoner, Vance Deason, Paul Meakin, Randall LaViolette*

## *Creating repeatable and reliable modeling techniques*

GC134

Key to designing cost-effective, efficient remediation strategies is an understanding of the mechanisms of fluid flow and contaminant transport through porous and fractured matrices, and the impact of microbial activity and growth. Better information will provide the framework necessary to resolve critical issues regarding water resources, materials transport and the use of microorganisms for in situ processes such as enhanced oil recovery, mineral dissolution and recovery, and remediation technologies.

The goal of this multidisciplinary LDRD project is to investigate methodology and computational modeling techniques for repeatable and reliable determination of the effects of geometry, surface condition, and biofilm growth on flow and materials transport. In this effort, stereolithographic methods were used to reliably produce well-characterized structures. These physical models allowed examination of localized and system-wide hydrodynamics and of the impact microbial biofilm formation has on these processes. Computational analysis of fluid flow in the physical models was used to evaluate theory and provide the foundation for the design of future experiments.

The project's short-term goal of developing reproducible physical models and experimental systems to examine the impact of microbial biofilm growth on fluid flow behavior is relevant to DOE and INEEL missions. In situ environmental remediation technologies rely on naturally occurring or enhanced microbial communities to degrade organic pollutants and to transform or immobilize inorganic or radioactive contaminants. This research enhances understanding of biofilm formation and the impact on fluid flow.

Technical objectives for fiscal year 2002:

- Evaluate a variety of plastic media for use in the fabrication of flow cell models.
- Assemble an experimental and data acquisition system.
- Initiate experiments examining the impact of biofilms on flow.
- Initiate the development and evaluation of computational models.

A number of light-transparent models were designed, fabricated and tested for examining the impact of biofilm formation on localized and system-wide behavior of fluid flow (Fig. 1A and 1B).

Plastic models were designed using 3-D computer-aided drafting programs and fabricated using laser-based stereolithography. The models were fitted with a glass plate and gasket system to allow flow testing and viewing at the macro- and microscale. The physical models were integrated with flow delivery and monitoring systems. The flow delivery system consisted of a syringe pump and a pressure control module. Time-lapse images were acquired with a high-resolution digital still camera interfaced with a computer data acquisition system. Analysis of system-wide and localized flow effects was accomplished by observing time-sequenced movies of the flow and by comparing it to the computational models. A series of time-course studies was conducted to evaluate localized and system-wide flow of water and low-nutrient media in the physical models with and without biofilms (Fig. 1C).

An initial assessment of the appropriate modeling techniques to develop and apply was made. In a separate LDRD program, investigator Paul Meakin has been working on developing computer models for multiphase flow in complex fracture apertures. As a step towards this goal, lattice Boltzmann models for single phase have been developed and applied to a variety of flow geometries. Results of simulations (Fig. 1D) were comparable to results of the dye tracer experiments carried out in this program. These studies demonstrate that the lattice Boltzmann approach can be applied to this project's experiments.

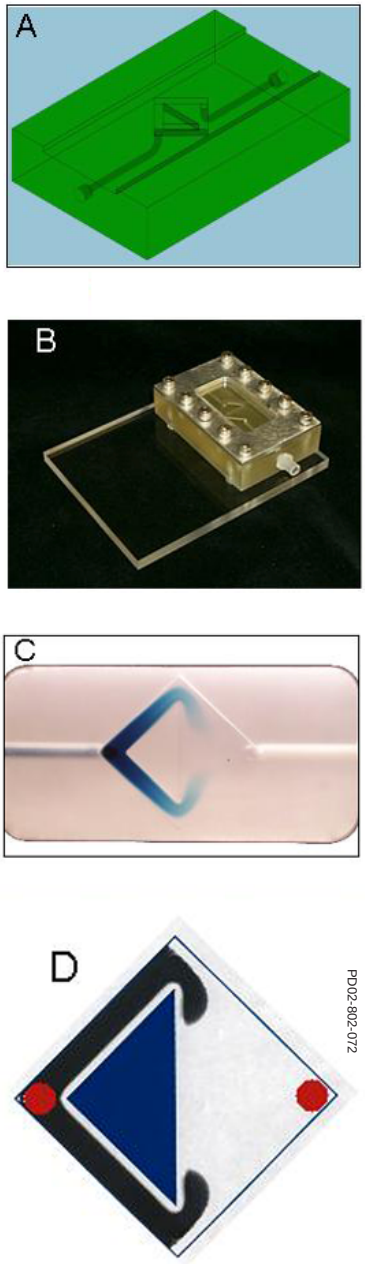


*FIGURE 1: A) 3-D rendering of a computer-aided design file used to fabricate the flow cell. B) Stereolithographically fabricated flow cell fitted with glass window and stage mount. C) One of a series of time-lapse images of flow cell with dye to visual the flow field. D) One step in a simulation of the flow field based on the lattice Boltzmann model. Red circles are the tubes coming into the flow region; the blue diamond is the triangular obstacle; black is the simulated dye in the flow field.*

Technical articles and presentations are in production to disseminate the results of this research. Future work will include development of custom models based on surface scans of actual fracture surfaces. This will entail the ability to convert among the surface scans, stereolithographic- and the computational format files. Coating methods will be developed that enable deposition of a mineral layer on to the custom models, allowing investigation of the impact biogeochemical reactions on fluid flow. Additionally, models will be developed that can simulate biofilm effects on fluid flow.

This LDRD is developing integrated experimental and computational methods for analyzing biofilm formation and its impact on fluid flow. This understanding is of significance because of the importance of water resources, materials transport and the potential use of microorganisms for in situ processes such as mineral dissolution and recovery, enhanced oil recovery and remediation technologies. Accordingly, the research will support DOE Basic Energy Sciences, Fossil Energy, Environmental Research, and Environmental Management programs.

# Characterization of Nonlinear Complex Resistivity Spectra during Biochemical Reduction of $Cr^{+6}$ to $Cr^{+3}$

*Gregory J. Stormberg, Birsen Canan-McGlone, William A. Smith, John Svoboda.*

## *Exploring minimally or non-invasive monitoring and validation techniques*

GC144

Measurement of direct and indirect geochemical, biochemical, and geophysical properties and processes is among the challenges associated with monitoring and validation of remedial actions. Meeting this challenge will require long-term investment but can lead to a better understanding of the relationship between chemical and biological properties and processes and physical phenomenon that can be measured with existing technology. In addition, this research investment can help determine the key measurements required to validate model and system behaviors, the spatial and temporal resolution at which such measurements must be obtained, and the extent to which surrogate data can be used in validation efforts.

Electrical properties are useful in the earth sciences in a variety of ways as they are one of the easiest of all physical properties to measure and are one of the most sensitive to changes in material and environmental conditions. This extreme sensitivity can be a problem or advantage depending on the technique used to measure electrical properties. For example, it can be an advantage when the widest possible numbers of electrical parameters are measured as a function of variables that are easily controlled by the experimenter. Typically, this involves the use of frequency of measurement as a variable.

This LDRD is developing lab measurement capabilities to study a geophysical method, Nonlinear Complex Resistivity (NLCR). NLCR takes advantage of this sensitivity issue leading to the development of a minimally invasive or non-invasive technique to map, monitor, and validate microbiologically-mediated chemical reactions, particularly $Cr^{+6}$ reduction to $Cr^{+3}$, in contaminated, heterogeneous subsurface environments.

Technical objectives for fiscal year 2002:

- Procure a 16-channel data acquisition card, an IOTech WaveBook/516, and two Stanford Research function generators.
- Design and construct interface electronics and calibration kit, i.e. instrumentation amplifier and resistor boards.
- Design and manufacture sample columns and electrodes.
- Develop software for NLCR data acquisition and processing.
- Test and validate NLCR hardware and software system with electrically well-known samples.

Complex resistivity (CR) is a geophysical method similar to electrochemical impedance spectroscopy that allows study of chemical processes in the laboratory or in the field. The technique involves the passage of an electric current through a material, and the measurement of the electric voltage generated by the resistance to that current flow. The ratio of the voltage response to the current stimulus is called impedance. Measured at finite frequencies, there is an observable shift in time between the stimulus and the response. The voltage current amplitude ratio is the magnitude, and the shift is the phase of the impedance. The impedance is normalized by the measurement geometry, and then it becomes complex resistivity.

CR nonlinearity is determined by analysis of the stimulus waveform and the column response. If a pure sine wave is the stimulus used to excite the system and a distorted sine wave is the response, then the Total Harmonic Distortion (THD) is characterized by the square root of the sum of squares of the harmonic content. If the real and imaginary parts of the complex resistivity as a function of frequency are not related to each other by the Hilbert Transform, then the discrepancy may be used to characterize another independent parameter of nonlinearity called Hilbert Distortion (HD). THD and HD are the discriminating elements in NLCR in addition to the resistivity magnitude and the phase from linear CR.

Even though NLCR has been studied extensively at the laboratory scale and in some field applications for monitoring organic contaminant movement via their reactions with soil, it has not been applied to $Cr^{+6}$ contaminated and remediated environments. It is possible to apply this technique to biologically mediated, oxidation-reduction reactions such as the ones proposed to remediate contaminated soils at the INEEL and other DOE facilities. This project is investigating the use of

NLCR for microbially remediated $Cr^{+6}$ reduction to develop proof of principal for future development that could be applicable for in situ real-time monitoring and validation efforts of $Cr^{+6}$ remediation.

This project has two coordinated parts. FY02 concentrated on building test and measurement equipment to acquire NLCR data of microbially stimulated $Cr^{+6}$ reduction and developing software to collect and process NLCR data. FY03 will concentrate on preparing samples, measuring NLCR, and doing periodic chemical and biological analyses of the sample columns. The outcome will be to establish qualitative and quantitative relationships between $Cr^{+6}$ reduction and the NLCR spectrum. The NLCR spectrum will be used to monitor and validate the remediation effort of $Cr^{+6}$ in situ. Following are a summary of this year's accomplishments.

***Data Acquisition Procurement*** – One IOTech WaveBook/516 data acquisition system and two Stanford Research function generators constitute the core of the data acquisition and column excitation capability. A key specification for this research that was met by the manufacturer is the requirement for "simultaneous sampling" of all 16 analog input channels in synchronization with the excitation frequency. Simultaneous sampling is necessary for accurate THD and HD analysis of the small non-linearities present in the column response. Sequential sampling (the norm for most data acquisition systems) introduces unacceptable measurement system-induced errors into the THD and HD calculations.

***Interface Electronics and Calibration Design*** – Key to the accurate measurement of each column's non-linear response to $Cr^{+6}$ reduction is the requirement that the measurement system does not load the potential electrodes with anything but very highly resistive impedance. Capacitive or inductive loading is to be eliminated. An Analog Devices' high-end instrumentation amplifier with double driven shields was selected for the solution. The amplifier is rated at $10^{+9}$ ohms of resistive input impedance that places it far above the inherent column impedance. The driven shields virtually eliminate any amplifier-to-column signal cable capacitance by driving the signal to shield voltage to zero. A calibration stick, consisting of seven precision resistors connected in series, was designed and used to simulate typical column resistances for system calibration. The instrumentation amplifiers are disconnected from the columns and attached to the calibration stick. The system then measures the simulated purely resistive column response over the normal range of frequencies, and system errors are calculated and stored for subtraction from column measurements.

***Sample Column and Electrode Design*** – Three columns were constructed, each consisting of a 7 cm inner diameter and 65 cm length cast plastic flow cell with eight 10 cm long MP35N electrodes electrically connected to the internal soil medium (Fig. 1). MP35N was selected for electrode material due to its high

*FIGURE 1. NLCR test columns with instrumentation amplifier and resistor board.*

corrosion resistance properties. Current is driven between the two outer most electrodes while the electrical potential is measured between the three electrode pairs located between the driven electrodes of each column. All the columns will have non-reactive quartz sand, $Cr^{+6}$ and simulated groundwater. Column one is considered a control column. Column two will have an inorganic reductant of $Cr^{+6}$ and is considered a control column. Column 3 will have biotic reductant and is the unknown column. A solution of different concentrations of $Cr^{+6}$ is pumped through each column. Fluid samples pumped out of the columns are periodically collected and analyzed for their chemical and biological content. In FY03, samples of contaminated soil from Hanford site will be tested, instead of quartz sand.

***NLCR Data Acquisition and Processing Softwares*** – To be able to continuously measure ongoing biochemical reactions taking place in the sample columns, the data acquisition software has to be custom made to fit the research needs. The developed NLCR program accomplishes this task. After initial desired inputs are set, the program continuously acquires input and output waveform data for 19 sets of given frequencies between 0.001 Hz to 1 KHz. When all the measurements are done for the frequency range given, the program pauses enough to give the experimenter a chance to change samples or settings. During this time, if the experimenter chooses to continue to measure the existing sample with existing settings, the program keeps running unless it is stopped.

The data-processing software, written in C language, calculates the components of NLCR, i.e., magnitude and phase, THD, and percent magnitude of and phase of HD.

***NLCR System Testing and Validation*** – System operational testing has been accomplished by measuring the NLCR spectrum of calibration resistors and an electrically well-defined liquid sample of 0.001 Mole of KCl water electrolyte. The measurement of calibration resistors has shown that the system works very well without causing major cable coupling effects. The result of this test measurement also allows system gain calibration. The results from the KCl water electrolyte will be used to calculate the columns geometric factor. Both tests became a standard test for system check before and after each series of measurements for different sample conditions.

The focus of this research is on monitoring and validation. Improvements in the ability to locate contaminants and validate performance of remedial actions will greatly enhance technical success of DOE efforts to remediate or stabilize and contain contamination. This LDRD research may ultimately lead to the development of a technique that will establish quantitative and qualitative relations between NLCR spectra and the microbiochemical reduction reactions of $Cr^{+6}$ to $Cr^{+3}$. Establishing this relationship will lead to investigation of the remediation of other contaminants present at the INEEL and at other contaminated sites of DOE across the U.S. It will have application to any number of contaminants that can lend themselves to bacterial-mediated remediation.

# Development of Biosensors for Environmental Applications

*Vicki Thompson, Yoshiko Fujita and Eric Peterson, Thomas A. Luther*

## *Testing remediation effectiveness*

GC109

An issue commonly encountered during characterization, remediation, and long-term stewardship of contaminated sites is the lack of comprehensive data regarding contaminant locations and concentrations. This LDRD is researching design, construction and testing of biosensor technologies based on immobilized enzymes for the determination of chemical species in the subsurface.

The first design will be a sensor for detection of urea concentrations in groundwater and will be tested in conjunction with an existing Environmental Management Science Program (EMSP) project at INEEL. Urea will be injected into INEEL groundwater to cause bacterially induced precipitation of calcite with co-precipitation of $Sr^{90}$ and Co contaminants. The urea sensor will enable real-time monitoring of bacterial activity in the subsurface as a measure of remediation effectiveness.

In outlying years of this project, other types of biological sensors will be examined and constructed for monitoring environmental contaminants such as organics, explosives, and heavy metals.

Technical objectives for fiscal year 2002:

- Continue development of polyphosphazene matrix for urease entrapment.
- Develop and characterize biosensor.

In FY02, two additional MEEP-type polymers for crosslinking studies with urease were synthesized and characterized by NMR spectroscopy ($^{1}H$, $^{13}C$, and $^{31}P$). The polymers have a random mixture of methoxyethoxyethoxy (MEE) and allyloxyethoxyethoxy (AEE) pendant groups. The use of AEE allows the formation of covalent crosslinks between the polymer strands and the enzyme, and the formation of polymer interstrand crosslinks through thermal free-radical initiation. The syntheses followed the general synthetic route that has been successfully developed for MEEP using the sodium salt of AEE along with the sodium salt of MEE.

The synthesis starts with reacting allyloxyethoxyethanol with sodium hydride in tetrahydrofuran (THF) to generate the sodium allyloxyethoxyethoxide. Freshly sublimed hexachlorocyclotriphosphazene was heated in a sealed, evacuated glass reaction vessel at 250° C for approximately 24 hours to generate the polydichlorophosphazene. Upon cooling, the polydichlorophosphazene was dissolved in THF and slowly added to the THF solution of the sodium allyloxyethoxyethoxide.

A second flask was used to prepare sodium methoxyethoxyethoxide under similar conditions using sodium hydride and methoxyethoxyethanol in THF. The sodium methoxyethoxyethoxide/THF solution was added to the reaction mixture and the reaction was monitored by $^{31}P$ NMR spectroscopy.

Upon completion of the reaction, the crude polymer was precipitated into hexanes, collected, and re-dissolved in nanopure $H_2O$. Isolation and purification was accomplished by exploiting the phase transition behavior associated with the lower critical solubility temperature of the polymer. The $^{31}P$ and $^{1}H$ NMR spectra of the two MEEP polymers was determined. By integration of the $^{1}H$ NMR spectra, it was determined that the polymers have AEE:MEE pendant group ratios of 10:90 (10%-XLMEEP) and 20:80 (20%-XLMEEP). The 10%, 20% and 32% (produced in FY01) MEEP polymers were swelled in a HEPES pH 8 buffer, containing urease enzyme, overnight at 4° C. The polymers were then exhaustively washed with HEPES buffer to remove enzyme that had not been entrapped by the polymer. The concentration of urease in the washes is shown in Figure 1. It can be seen that the 10% MEEP polymer retained the most urease (the smallest amount washed out). This polymer will be used in subsequent sensor studies in FY03.

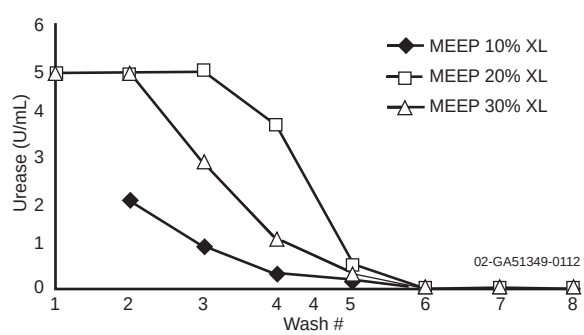


*FIGURE 1. Concentration of urease in washes.*

Initially a subcontract with Dr. Siddhartha Duttagupta at Boise State University was to be placed for design and development of a sensor. However, Dr. Duttagupta left the university before the subcontract could be placed. An examination of the literature was conducted to determine alternative sensor designs for the urea sensor. A design based on use of a pH probe was selected. A glass pH probe system designed for connection to a computer through a PC card was selected so that data could be collected in real time. Solution phase studies were used initially to determine the response time of the pH probe system. In these studies, 20 Units/ml urease was added to urea solutions of various concentrations and the response of the pH probe was assessed. It was determined that the probe response was approximately 30 seconds, the dynamic range was 0.1 to 3 mg/ml urea and the limit of detection for the system was 0.1 mg/ml urea.

Next, immobilization of urease to the pH probe was examined. A 2% alginate solution containing 40 Units/ml urease was prepared and placed in a cell culture insert that was slightly larger than the tip of the pH probe. The culture inserts have a 10,000 molecular weight cutoff membrane on the bottom that allows low molecular weight substances such as urea to diffuse to the probe surface while retaining the high molecular weight urease molecules. The pH probe was inserted into the culture insert and placed into a 0.1 M solution of calcium chloride. The calcium chloride crosslinked the alginate into a polymer with the urease enzyme trapped inside the matrix. After the alginate was fully crosslinked, the probe was placed in a solution of urea and the pH change was monitored.

Typical probe response for three different concentrations of urea is shown in Figure 2. The initial slope of the response varies sharply with urea concentration and shows that the probe is able to measure urea concentrations between 0.1 and 10 mg/ml, a larger dynamic range than the solution phase case. The response time of the immobilized urease was significantly longer than for solution phase urease (30 seconds compared to 10-15 minutes). This is probably due to diffusion limitations introduced by immobilization of the urease enzyme. The alginate-immobilized urease probe could be regenerated by brief immersion in acid solution; however, this often resulted in denaturation of the enzyme and was not an optimum regeneration method. Immobilization with glutaraldehyde was examined as an alternative. Response times of the sensor were much faster (approximately 1-2 minutes) probably due to less diffusion resistance offered by the thinner layer of glutaraldehyde-immobilized urease. The glutaraldehyde based probe also could be regenerated by soaking in a pH 7 solution for 20-30 minutes, which was preferable to the alginate immobilization.

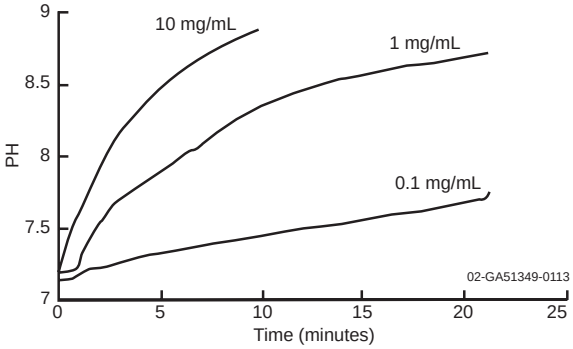


*FIGURE 2. Probe response for differing concentration of urea.*

Studies were initiated using an ion-select field effect transistor pH probe (ISFET). In these studies, urease was immobilized onto the probe surface by glutaraldehyde. This probe has the advantage of being more robust than a conventional glass pH probe and more suitable for field applications. Initial studies with this probe indicate that it has a response similar to the glass pH probe. Studies in FY03 will focus on using MEEP polymers to immobilize urease onto the ISFET pH probe surface.

This LDRD is providing the foundation for the development of a new line of innovative, cost-effective monitoring technologies for subsurface investigations,

and directly supports the INEEL's mission as a leader for environmental technologies. Additionally, this work will provide the basis for development of sensors that can be used for monitoring any contaminated site. This work constitutes a significant milestone in the INEEL's excellence in biologically compatible polymer synthesis for the development of new environmental technologies.

This project plans to use the urea sensor to monitor urea concentrations in support of mesoscale studies of ureolytically induced calcite precipitation and ultimately field-scale studies where urea is directly injected into the Snake River Plain Aquifer for stimulation of ureolytic activity by native microorganisms. This activity is part of an ongoing remediation effort to sequester contaminant metals and radionuclides

# Calibration and Enhancement of Geophysical Imaging Tools in a Mesoscale Experimental Facility

*Roelof Versteeg, Russell Hertzog, Cal Christensen, Gail Heath*

## *Creating automatic, semi-autonomous systems*

GC141

Effective contaminant remediation and mitigation depends on knowledge of past and future contaminant behavior as well as on insights into the effectiveness of a range of treatment approaches. This knowledge hinges on understanding of subsurface processes, which in turn requires the ability to observe, model and predict these processes.

Observational data on processes will have to come from large numbers of noninvasive (geophysical) measurements, reinforced with strategically chosen invasive measurements. Interpretation of this data will require the ability to quantitatively link geophysical data to hydrological, geochemical and biological processes. Developing this ability requires simultaneous measurement of geophysical signatures of processes and direct invasive measurements of these processes in a controlled environment. These measurements will enable the quantitative interpretation and calibration of geophysical data to subsurface processes.

This LDRD focuses on the calibration of geophysical imaging tools to quantify geophysical data in terms of subsurface processes. Field-scale implementation of process imaging techniques will require automated semi-autonomous systems. Thus, a core technical component of this research is the development of techniques to collect, process, and interpret geophysical and auxiliary data automatically.

Technical objectives for fiscal year 2002:

- Design a framework for automated, semi-autonomous collection, processing, and interpretation of geophysical and auxiliary data.
- Implement a general lab- and field-applicable system for automated data acquisition and processing for electrical resistivity.
- Design an integrated lab acquisition system (including automated sensor and material emplacement systems), and assemble the components (including several soil tanks).

The goal of this research is quantification of geophysical data in terms of subsurface processes. The first step was to design a conceptual framework (Fig. 1) that would enable this quantification. This framework links together the different elements of geophysical data acquisition in a controlled environment, and provides a rigorous, certifiable structure in which the contribution of each element to the final result can be traced. The elements in the framework are partly hardware (soil tanks, acquisition systems, sensors) and partly software. In FY02 the general software structure for this framework was completed.

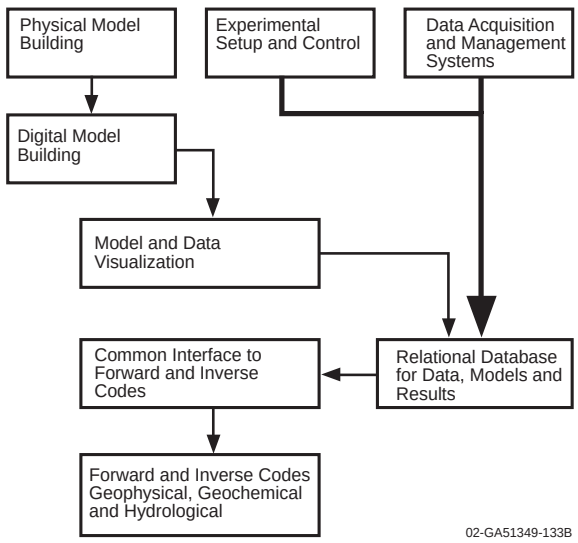


*FIGURE 1. Elements of the geophysical mesoscale design.*

The software structure uses discrete programs for each task with communications between all programs done through TCP/IP. This structure provides for maximum flexibility of the system and allows different elements of this environment to be located in geographically different locations.

Constructing the comprehensive structure for all components was quite complex. Thus, there was a strong incentive to test the concept on a realistic (but limited) geophysical case. The second objective of this project was to implement the framework for electrical resistivity measurements. These measurements are both relatively easy to do remotely (as the sensors are in fixed locations)

and are among the most relevant to make (as electrical resistivity changes are often related to contaminant movements and these measurement can be translated into 3-D maps of processes). This objective was achieved through the construction of custom-created, remotely controllable Labview interfaces that interact with off-the-shelf resistivity acquisition systems. Acquisition in the field is controlled through a dedicated program that synchronizes its local database to a remote central database. The central database is queried by a processing module that inverts the data and writes the result to the database. From there, a visualization module takes the data and makes both static and animated imagery. Finally, a web front-end provides access to data, and processes results and imagery. This work resulted in the first completely automatic geophysical acquisition and processing system, and proved many of the concepts underlying Figure 1. This system is currently in use both in a laboratory and several field settings.

A third objective was the design of an integrated in-lab acquisition system and initial assembly of the components. To observe processes, there is a need to have tight control of the processes (model control and boundary control) and of the sensors used to measure these processes. An infrastructure integrating a broad range of sensors for multi-sample point measurement of physical, chemical and hydrological properties was designed. The associated components are currently being integrated. In addition a large soil tank (8 x 8 x 16 foot) was designed and purchased.

Contaminant remediation and monitoring is an extremely expensive task on which DOE spends about $6 billion a year. Other federal and state agencies spend similar amounts: for example, DOD is responsible for many bases that have been contaminated; and EPA has some 1220 sites on the National Priority List (Superfund), each of which typically will cost tens of millions of dollars to remediate. In addition to this, there are some 450 thousand estimated brown field sites for which cleanup responsibility and cost is, in most cases, carried by state or local agencies. Permanent, autonomous monitoring systems that provide quantitative information on processes would provide significant benefits to all of these sites.

# Fracture Prediction, Characterization, and Detection in Snake River Basalts – A Modeling and Field Approach

*David Weinberg, Stephen Novascone, Phil West, Richard Smith, Eric Larson, Jodie Boyce*

***Providing scientifically based direction to remediation and stewardship***

GC103

Spatial variability of hydraulic properties and geologic controls within the vadose zone at the INEEL and most DOE sites in the western United States is poorly described because instrumentation typically measures only at borehole locations. Borehole televiewer tools use high-frequency acoustic transducers to image the inner borehole surface, but are limited to detecting only those fractures that actually intersect the borehole. Research conducted to investigate the potential for improving subsurface logging using orbital vibrators (OV) has focused on detecting vertical extents and azimuthal orientations of vertical to near-vertical fractures. Earlier work has shown that the concept of using an orbital vibrator as a fracture-detection tool depends on tool-fluid-borehole interactions. Currently these interactions are only poorly understood and have hampered the ability to optimize tools for various applications.

This LDRD explicitly addresses the development of models that will adequately predict fractures in basalt, characterize the OV tool and its interactions with boreholes, and provide field demonstration of the technology.

Technical objectives for fiscal year 2002:

- Develop predictive model for the spatial orientation of fractures in basalt that are the result of the cooling of the flow.
- Create a methodology for using that model in conjunction with sparse subsurface data to predict fracture patterns between wells.
- Develop a model that describes the interaction of the OV with its subsurface environment for the purpose of detecting presence and azimuth of permeable fractures in cased and uncased wells.
- Field-test the OV and the predictive fracture model.

Fieldwork was performed at the University of Idaho (UI) with collaborators Dr. Simon Kattenhorn and Conrad Schafer to incorporate a range of lava flow morphologies, particularly flow aspect ratio as viewed in cross section view, into the analysis of fracture distribution in Eastern Snake River Plain (ESRP) flows (Fig. 1). The fieldwork involved development and refinement of specific fracture growth models for all fracture types within lava flows, with emphasis on parametric controls on fracture that were summarized in a presentation at the 2002 Annual Meeting of the Geological Society of America. Additional work addressed statistical characteristics of fracture density distributions in flows of variable aspect ratios.

*FIGURE 1. Fractured lava flow in Box Canyon, Eastern Snake River Plain (ESRP), and showing upper and lower colonnade separated by a densely fractured entablature.*

The second part of the UI project work involved initiation and development of thermal-mechanical models of cooling lava flows that test the effects of flow shape on heat loss from a flow, as well as the competing effects of conductive, convective and radiative heat loss into the surrounding media. The effects of perturbations to the thermal field also were addressed in an effort to explain the variation in fracture styles in many ESRP flows that cannot be simply attributed to conductive cooling (the typical approach to lava cooling in previous investigations). Initial model results clearly demonstrate the importance of convective heat loss through inflation fractures (Fig. 2.) in controlling the thermal field within a cooling flow, and hence the thermal stress distribution.

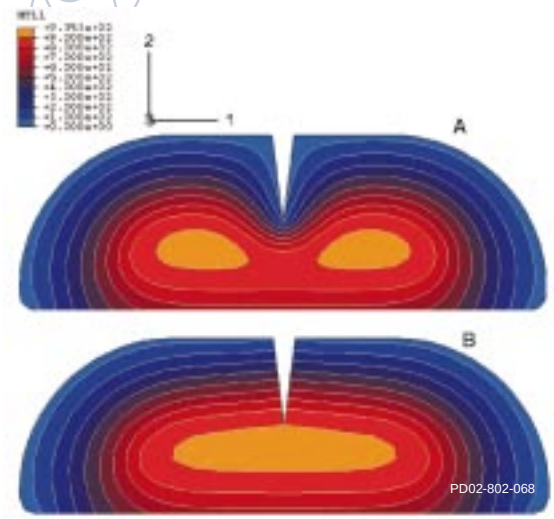


*FIGURE 2. (A) Thermal perturbation due to convecting inflation fracture penetrating a lava flow. The lava core has been divided into two distinct pods that will ultimately form separate entablatures. (B) Only minor thermal perturbation is produced by a penetrating fracture that does not permit convective cooling of the lava flow.*

At the University of Arkansas with collaborator Dr. Robert Reynolds, the investigators proceeded with development and verification of the finite element modeling code through second quarter of 2002. However, it was found that fundamental flaws in the portions of the adopted code prevented it from correctly reproducing several analytical test cases. As these problems lay in the fundamental structure of the code (as adopted from the public domain), it was decided to revise the project strategy and employ a new library of finite element subroutines that provided more flexibility and accuracy in the code development. This new library is also in the C++ language, but better conforms to ANSI standards, abides the Open Source code development guidelines much more faithfully, and continues to be actively developed by a large community of researchers from around the world.

Using this library, a new code has been written that already successfully models the wave propagation problem in the fluid and solid (i.e. rock) domains in two and three dimensions. The only remaining tasks involve implementing the fluid-solid interaction and the ability to import finite element meshes from the programs already in place at the INEEL. This work is underway and the final code is expected to be online soon. Key features of the code include:

1. Wave propagation in unbounded domains (e.g. subsurface environments).
2. Transient analyses.
3. Higher order elements (up to 4$^{th}$ order).
4. Multi-processor capability (for use on large computers).
5. Distribution of library routines under the Gnu Public license:
   - Ability to include error estimation & adaptive meshing
   - Extensible

Computer code developed at the INEEL in Labview™to set vibrator run parameters and control the programmable power supply (hence controlling frequency sweep, data acquisition, and an algorithm to calculate the best-fit to the data) were written and tested in the laboratory and in the field. This work was done in preparation of performing the field experiments in the fall. These trials were forfeited by the funding cut. However, preliminary testing done in north central Oklahoma demonstrates that the orbital vibrator is sensitive to lithology changes. As this LDRD has been terminated, further data analysis will have to be postponed until new funding can be procured. To date, seven peer-reviewed/refereed publications have resulted from this project.

This LDRD supports the goal of the Subsurface Science Initiative to provide scientifically based direction to environmental remediation and stewardship activities. The project helped develop a unique capability within the DOE laboratory complex, namely a technique and modeling capability for using a very simple device to provide mechanical insight into the properties of the earth. Including both the University of Arkansas and the University of Idaho with the more engineering-focused work at the INEEL, resulted in a far broader scientific base for understanding, detecting and, some day, predicting fractures in the subsurface, especially those related to the cooling of basaltic lavas.

# Advanced Borehole Seismic Sources for High-Resolution Subsurface Imaging and Characterization for Environmental Applications

*Dr. David Weinberg, Stephen Novascone, Phillip West, Eric Larsen*

***Improving subsurface characterization for long-term cost savings***

GC105

The INEEL Environmental Restoration (ER) program is concerned with all aspects of investigating and cleaning up contaminated locations on the Site that may pose a threat to human health or the environment. Substantial savings in characterization and long-term monitoring costs can be achieved in this effort by the accurate determination of spatial variability of flow of contaminants over large scales in the vadose zone. Determination of large-scale properties allows better estimates of risk to groundwater and potential receptors. Assessment of future risk and selection of remedial options for at least two DOE sites (INEEL, Hanford) requires fate and transport modeling through a thick, fractured rock and sedimentary vadose zone. However, current technologies do not provide large-scale measurements required for modeling.

The technical problems associated with "seeing" or imaging the subsurface to provide better large-scale measurements lie within two general areas, namely the physical properties of the earth materials through which one wants to image, and the resolution available based on the interrogation technique. Subsurface characterization can be performed in a multitude of geophysical ways, but as ever-finer vertical and horizontal resolution is required, acoustic (seismic) techniques have become the overall standard method, especially for 3-D imaging. This LDRD is investigating several borehole seismic sources specific to these environmental applications.

Technical objectives for fiscal year 2002:

- Design, fabricate and deliver both an AC-motor orbital vibrator (AC OV) and an electromagnetic vertical shear wave (VSH) vibrator. Acquire wireline and truck capable of being used with various borehole sources, if funding permits.
- Develop both 2-D and 3-D finite element models (FEMs) with infinite elastic medium with and without borehole.
- Develop hybrid FEM and Boundary Element Model (BEM).
- Develop 2-D analytical model with a liquid-filled annulus and incorporate anisotropy in analytical model.
- Test 4.5-inch dual-motor DC OV and a 3.5-inch single-motor DC OV at Seneca Lake and in a liquid-filled, steel cased, cemented well.

Work in FY02 was quite successful. Three new borehole sources were designed, fabricated and delivered. Some additional support equipment remains to be acquired, but the INEEL is now in possession of a truly unique set of borehole vibratory seismic sources (Fig. 1).

*FIGURE 1. Vibratory borehole seismic sources. (A) AC OV: 64 inches long by 4.5 inches in diameter and weighs 58 pounds. (B) dual-motor DC OV: 34 inches long by 4.5 inches in diameter and weighs 25 pounds. (C) single-motor DC OV: 19.5 inches long by 3.5 inches in diameter and weighs 9 pounds. (D) electromagnetic vertical shear wave (VSH) source: 54 inches long by 4.5 inches in diameter and weighs 202 pounds.*

The new vibrators were designed and fabricated in collaboration with Dr. Jack Cole of Cole Engineering: a single-motor (SM), small-diameter DC OV, an AC-motor OV, and an electromagnetic vertical shear wave vibrator. The SM DC OV can be run on the INEEL's existing seven-conductor wireline. The AC and VSH vibrators require a special wireline. Prior to testing in FY03, such a wireline will be acquired or leased.

Numerically, both 2-D and 3-D FEM models with infinite elastic medium (with and without a borehole) were developed. A 2-D analytical model of an infinite elastic isotropic earth with a liquid-filled annulus was developed. From these models, investigators derived an expression for velocity of OV in terms of properties of surrounding geologic medium. This has never been done despite the use of orbital vibrators for seismic surveys for over a decade.

Tests at the U.S. Navy's Seneca Lake test facility were completed with the SM DC OV. Data collected with the hydrophone validated expectations of OV output as

compared to impulsive sources. Intermittent electrical problems with the rented hydrophone string prevented the tests from being as useful as they could have been. But overall, the tests were sufficient. Tests using the SM DC OV at the INEEL were largely "shakedown" tests of surface power-supply and data acquisition equipment. Without corroborating information (fracture or lithology variation data), no conclusions could be reached as to the efficacy of the OV in a monolithologic situation. However, the equipment performed as designed and the tests were successful from that perspective. Earth properties testing in a single well with an OV was accomplished at a "well of opportunity" offered by Seismic Recovery, LLC. This well in the North Burbank field in Osage County Oklahoma provided an excellent opportunity to run both the dual-motor (DM) DC OV and the SM DC OV in direct comparison to each other. These tests resulted in significant modifications being made to the design of the more powerful AC-motor vibrator (ACOV), to be delivered to the INEEL in late FY03. The initial analysis of the Oklahoma data set showed that the velocity response of the OV is sensitive to changes in lithology in a liquid-filled, steel-cased cemented well. This analysis validates a long-standing hypothesis that has never before been examined even though OVs have been used as borehole seismic sources for more than a decade. This discovery will be the subject of at least two papers in refereed journals.

The data in Figure 2 underscores the need to extensively integrate the design of the tool with the application of the source. The DM DC OV is considered an excellent seismic source within the petroleum industry for use in reflection seismic and vertical seismic profiles. However, it clearly cannot be used for lithology discrimination. The increased sensitivity of the SM DC OV led to the significant design change apparent in the AC OV (Fig. 1A), which separates the heavy motor from the rotating eccentric mass by means of a flexible shaft. This added power without the weight is expected to result in higher sensitivity and deeper penetration.

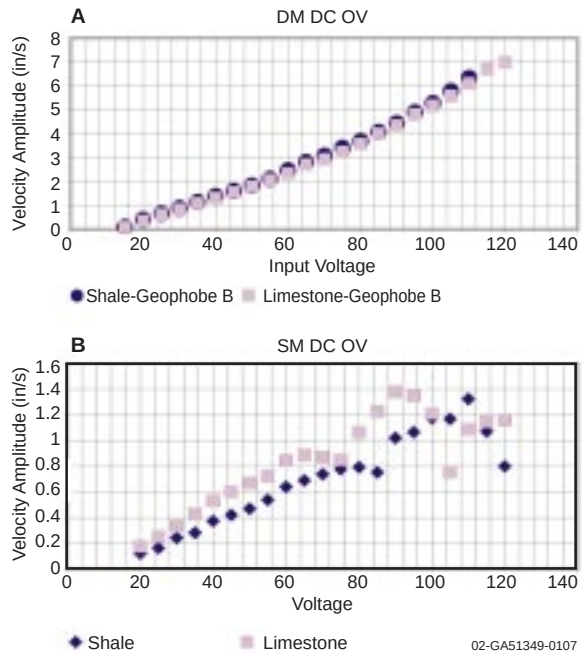


*FIGURE 2. Velocity amplitude plots of the two DC OV sources. The top chart (A) plots the longer and heavier DM source while the shorter and lighter SM source is plotted on the bottom chart (B). Data was taken at the same points in the well. The dark points are data with the OV surrounded by shale. The pink points are data taken in limestone. The input voltage is the independent variable in both plots. The data differences in the plot on the right are statistically significant, validating the hypothesis that the OV source behaves differently in different lithologies.*

Additional modifications will eventually need to be made to allow this configuration to achieve the hoped-for 1.0 to 1.2 kHz frequencies.

This project supports development of internal expertise in processing of borehole seismic data, and interpretation of surface seismic and other borehole data.

# Modeling an Earth-Borehole System for Physical Property Determination in Shallow Subsurface Environments with Emphasis on Vadose Zone Applications

*David Weinberg, Stephen Novascone*

## *Using orbital vibrators as a physical-properties-logging tool*

PH104

Flow properties of porous and fractured subsurface earth materials affect flow and transport of such things as organic pollutants, heavy metals, and radionuclides. Subsurface flow properties are related to subsurface elastic properties. Thus, characterizing elastic properties of the subsurface is important when developing models of subsurface flow and transport.

Early experimental evidence suggests that driving-point impedance measurements can be used to characterize a volume of elastic earth medium surrounding a liquid-filled well (Cole, 1997). Driving-point impedance measurements are obtained by recording the velocity amplitude of a down-hole orbital vibrator (OV) as a function of frequency. An OV is a rotating eccentric mass contained within a closed tube whose frequency of rotation is controllable. When operating in air, the OV displays a circular orbit of constant amplitude throughout its frequency range. Internal cross-polarized geophones (a velocity-measuring device) are sufficiently sensitive to measure the velocity amplitude of that motion. It has been shown experimentally, although qualitatively, that when the OV is placed in a liquid-filled well, both orbit amplitude and shape can change because of loading induced by the elastic properties of the well and the medium surrounding the well. This measurable orbit-change phenomenon gives the OV potential for use as a physical-properties-logging tool.

This LDRD is conducting experiments to provide quantifiable evidence of the sensitivity of the OV to the surrounding elastic medium.

Technical objectives for fiscal year 2002:

- Characterize driving-point impedance response of an OV in air and a liquid-filled well.
- Develop analytical model that predicts velocity amplitude of OV in terms of elastic properties of the surrounding geologic medium.
- Conduct experiments of OV in a liquid-filled well at two lithologically different locations.
- Compare analytical model response with experimental data.
- Submit papers on experimental results to technical conferences and/or referred journals.

Applying Newton's second law, a model predicting the motion of an OV in contact with arbitrary surroundings can be derived. The rotating eccentric mass plus the resistance of the surroundings cause the forces applied to the OV. For steady-state harmonic motion, the velocity amplitude of the OV is derived from Newton's second law

$$|\mathbf{V}| = \left| \frac{-jm_o ec\omega}{Z + j\omega m} \right|$$

where $j=\sqrt{-1}$, $m_o$ is the eccentric mass, $ec$ is the size of the eccentricity, $m$ is the total mass of the OV, $\omega$ is the frequency of the rotating mass, and V is the complex valued velocity of the OV. Z is the overall impedance of the medium surrounding the OV and is generally a complex number. Note that the medium surrounding the OV includes the liquid in the well, the steel case, the cement bond, and the geologic medium. This equation (above) can be used to provide insight to experimental measurements of driving-point impedance.

Two sets of experiments were conducted: one of the OV running in air, and one with the OV running in a fluid-filled well (surrounded by fractured basalt and located at the INEEL). In both sets of experiments, different voltages were applied to the OV motor with geophone signals recorded at each corresponding steady state frequency.

The data from these experiments are presented in Figure 1. This plot shows OV velocity amplitude vs. voltage (where voltage corresponds to frequency) applied to the DC motor. The velocity amplitude vs. voltage is linear over the voltage range 15V to 60V. This means that the driving-point impedance is characterized as inertial. Inertial driving-point impedance means that the response of the OV in the well is equivalent to the response of the OV in air with added mass. Understanding this is important when using the OV as a physical-properties logger because the differences in lithology will manifest as differences in slope on the OV velocity amplitude vs. voltage plot.

The results of this experiment were submitted to the Society of Exploration Geophysicists (SEG) 2002 annual conference. The paper passed technical peer review and was accepted. Stephen Novascone, one of two collabora-

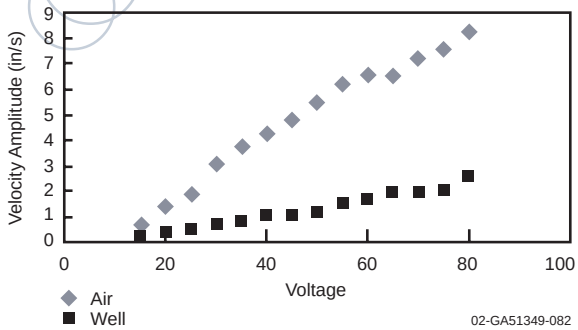


*FIGURE 1. Velocity amplitude of the OV is linear with applied voltage indicating inertial driving-point impedance.*

tors on this project from the University of Idaho, presented the paper at the SEG conference in October 2002.

A similar set of experiments was conducted in a liquid-filled well in shale and limestone. This well was steel-cased and cemented. The purpose of this experiment was to determine if the OV velocity signal was sensitive to changes in lithology (i.e. differences in elastic properties of the surrounding geologic medium).

Figure 2 presents a plot of OV velocity amplitude vs. applied OV motor voltage for shale and limestone. The plot shows that the slopes and velocity amplitudes are different thus indicating that the OV velocity signal is sensitive to changes in the elastic properties of the geologic medium surrounding a liquid-filled, steel-cased cemented well.

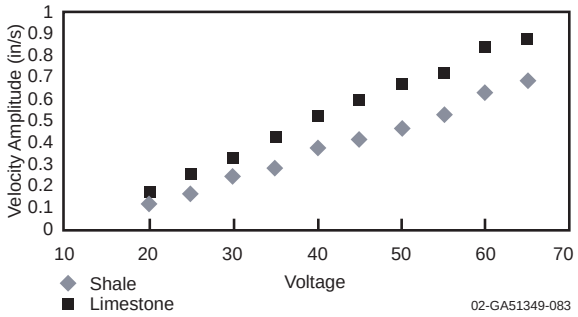


*FIGURE 2. OV velocity amplitude slope in shale is different than the slope in limestone.*

A 2-D model of the OV in a liquid-filled annulus surrounded by an infinite elastic medium was developed. This model was first proposed by Reynolds and Cole (2002), and was used to develop an algebraic expression for OV velocity amplitude as a function of the elastic properties of an infinite medium. In simplified terms the OV velocity amplitude expression is

$$|\mathbf{V}| = \left| \frac{m_o ec\, \omega^2 - f(\mathrm{Z})}{j\omega m} \right|$$

In the above equation, the $f(\mathrm{Z})$ term contains elastic properties of the geologic medium. This 2-D model was compared with the experimental data from the OV velocity amplitude in shale and limestone. This model predicted inertial impedance but underestimated the observed effect of the elastic medium on the OV velocity signal. The 2-D model also predicts that the OV can "sense" changes in elastic properties two meters from the center of the annulus (Reynolds and Cole, 2002).

A 3-D finite element model could account for the 2-D model underestimation of the elastic medium effect. The 3-D finite element model is a planned activity for FY03. The results from the shale and limestone experiment and the 2-D modeling effort are being prepared for a paper to be submitted to the SEG journal in FY03.

It is important to note that while other methods and tools exist for physical-properties logging, the OV can log through a steel-cased, cemented well over a relatively large volume surrounding the well. This capability is unique to this approach.

The Environmental Restoration (ER) program is concerned with all aspects of investigating and cleaning up contaminated locations. These activities require modeling contaminant flow in the vadose zone and, as explicitly called out on the Site Technology Coordination Group's list of technology needs, development of sensors for large earth-volume measurements. A major shortcoming of the science of vadose zone modeling is the inability to accurately predict contaminant transport, which originates with input parameters derived from site characterization.

This LDRD research has demonstrated that the driving-point impedance of the OV is inertial. Driving-point impedance measurements can be used to distinguish shale and limestone in a cased well. Further development of analytical and numerical modeling can provide a way to take an OV velocity measurement and translate that to a geologic elastic property measurement. The elastic properties can then be used to determine porous and fracture properties. The porous and fracture properties can be used as inputs to subsurface flow models to accurately predict contaminant transport.

This work may enable DOE to meet its obligations to the State of Idaho regarding environmental clean up. Results of this work also can be applied to other national labs and private industry, providing national benefits.

# Carbon Fractionation Potential of Soils Via $CO_2$/ Water Gradient Fractionation

*Gregory J. White, Harry W. Rollins, David A. Atkinson*

## *Measuring carbon storage in soils*

GC104

Various strategies have been proposed to reduce atmospheric $CO_2$ by transferring carbon to soil organic matter for long-term sequestration. Traditional methods for measuring soil carbon focus on total organic carbon without considering the tremendous inherent heterogeneity. Methods are needed for quantifying different carbon compounds based on their longevity in the soil. Recent research has focused on the application of nuclear magnetic resonance (NMR) for this purpose. However, NMR has low resolution, high cost, and is not field portable.

The research conducted in this LDRD investigates the development of an alternative technique for quantifying carbon fractionation in soils using high-temperature, high-pressure, $CO_2$/water supercritical fluids extraction. Extracts have been recovered from several different soil types, and efforts were made to identify the compounds in the extracts. Field tests with additional soils collected from a well-characterized ecological research site were also conducted. Although considerable additional research is necessary, the technique shows some promise in advancing measurement of carbon in soils by enabling a method of rapid, tunable analysis of soil carbon fractions that is both more sensitive and more cost effective than current techniques. In turn, this could help refine models of subsurface contaminant transport.

Technical objectives for fiscal year 2002:

- Complete construction of the extraction system.
- Continue to test and tune the extraction system to maximize organic extracts from representative soils.
- Develop a technique for identifying key organic compounds.
- Test the system with a suite of soil samples collected from a well-characterized ecological research site.

The objective of this research is to develop an analytical technique for assessing carbon in soils by various key carbon fractions. Accurate prediction of carbon cycling in soils is difficult because soil organic matter consists of a complex array of carbon compounds ranging from highly labile water-soluble compounds (e.g., simple sugars, amino acids and aliphatic acids) to less labile carbohydrates (e.g., cellulose and hemicellulose) to highly refractory materials (e.g., lignin and “humus”). Humus is a generic term for a range of largely unidentified and variable polymeric compounds that are highly aromatic and aliphatic in composition. The accumulation and distribution of soil organic matter is dependant on the quantity and distribution of organic inputs, rates of decay, and the ability of the soil to protect soil organic matter. Since different carbon fractions possess dramatically different residence times in soil, this will allow for better assessment of the actual carbon storage capacity for a soil.

During FY02, a variety of soils were extracted using water at a series of temperatures up to 350° C. These included soils from a wide variety of sites collected the previous year (garden, lawn, and fallow agricultural soils from the Idaho Falls area; soils from quaking aspen and lodgepole pine forests in eastern Idaho; a sample from a saltwater marsh in South Carolina, and soils from redwood and live oak forests in California). The carbon from these various soils was expected to yield distinctly different carbon profiles. Additional samples were collected from the Cedar Creek Long-Term Ecological Research Site in Minnesota during FY02. These samples represented soils of the same type, but which differed in terms of management history. They included samples from abandoned agricultural sites (ranging from 20 to 80 years since abandonment), along with adjacent forest and savanna locations. For the Cedar Creek samples, similar carbon profiles were expected, showing differences in the range necessary for the technique to be broadly applicable.

The soil extracts were characterized using a wide variety of analytical methods including UV-visible absorption spectroscopy, FT-IR absorption spectroscopy,

and NMR spectrometry. Figure 1 shows FT-IR spectra of extracts of a typical soil sample obtained at temperatures of 50° C, 100° C, and 150° C. The efficiency of extraction was determined gravimetrically for a series of samples and found to increase with increasing temperature and to vary with soil type (see Table 1). The more efficient extraction at higher temperatures was reflected in the strength of the transitions in the FT-IR spectra. At lower temperatures a variety of oxygen-containing

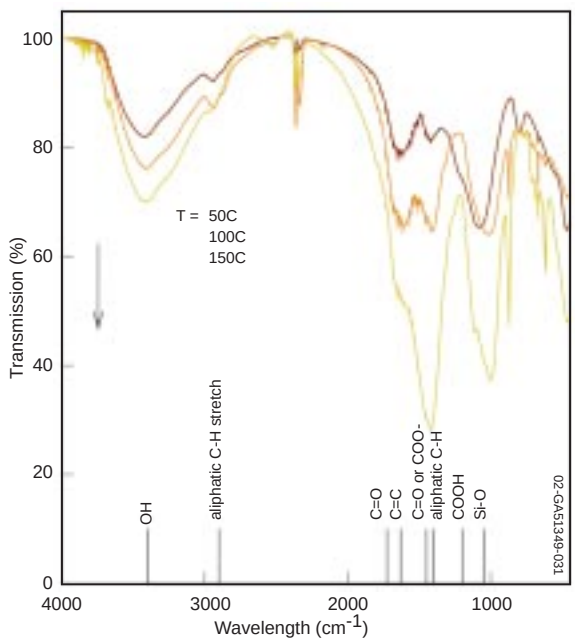


*FIGURE 1. Effect of temperature on the properties of extracts. Transitions for various functional groups are shown for comparison.*

compounds were readily extracted. Increasing the extraction temperature to 150° C resulted in a large increase in the relative proportion of aliphatic carbon material that was extracted. This is seen in the large increase in the intensity of the band that is at ~ 1400 – 1450 $cm^{-1}$. UV-visible absorption spectroscopy was also used to determine the effects of temperature on the extract properties. The ratio of absorbance at 465 nm to

| SOIL | E4/E6 100 | E4/E6 150 | Efficiency (wt%) 150 |
|---|---|---|---|
| Old Field 29 | 8.59 | 6.06 | 2.73 |
| Savanna | 8.21 | 5.74 | 0.25 |
| Forest | 7.10 | 5.46 | 0.89 |
| Old Field 22 | 6.30 | 5.28 | 1.84 |
| Old Field 69 | 6.43 | 5.21 | 1.05 |

02-GA51349-032

*TABLE 1. Efficiency of extraction for a series of samples at different temperatures.*

665 nm (E4/E6) has been shown to correlate with the molecular weight of humic and fulvic acids, with smaller values corresponding to larger molecular weights.

The E4/E6 ratio for a series of soil samples obtained from the Cedar Creek Long-Term Ecological Research site was determined for extraction temperatures of 100° C and 150° C. For all of the soil samples, the E4/E6 ratio for the extracts obtained at 150° C was higher than for those obtained using an extraction temperature of 100° C. This data agrees well with the FT-IR results indicating the extraction of higher molecular weight material at higher temperatures. This is also consistent with the decreasing polarity of water with increasing temperature. The previously cultivated soils (#22, #29, and #69) contained a larger quantity of extractable material than the uncultivated soils. The savanna soil (which had been burned fairly regularly) had the least extractable quantity of material. $^{13}C$ and $^{1}H$ nuclear magnetic spectroscopy also was used to characterize the extracts. NMR spectra for all the samples were similar and showed several broad peaks in the alkyl region with little or no signal in the aromatic regions.

All of the extracts contain a mixture of a large number of different chemical species. To quantify the various species more precisely, several separation strategies were employed. Due to the low volatility of the components, the extracts were derivatized to the corresponding ester

and analyzed using GC-MS. Volatility of the samples was still low making the gas chromatography problematic. The soil extracts were then separated using size exclusion chromatography, which separates samples based on molecular weight. Chromatograms of different extracts all showed similar features and had a broad distribution of molecular weights. Molecular weight distributions for the extracts were not determined due to a lack of suitable standards and interactions of the extract materials with the solid phase of the size exclusion chromatography column.

Although the driving need for the analytical capability investigated in this LDRD is to improve measurement and predictability of carbon storage in soils relating to global climate change, the technique may also substantially enhance the predictive ability of models of subsurface transport of contaminants, and therefore is applicable to the Subsurface Science Initiative and Long-Term Stewardship issues.

According to the recent U.S. DOE document "Carbon Sequestration – State of the Science," research is needed in the area of terrestrial carbon sequestration *"…that will lead to an ability to understand, predict, assess, measure, and implement substantially increased sequestration of carbon in soil and vegetation systems."* Current efforts to quantify, predict, and verify the capacity of soils to store C are hampered by (1) the complexity of soil organic matter; (2) difficulties in predicting C turnover times; and, (3) the lack of accurate, cost-effective, field-portable analytical tools for measuring different C compounds or classes of compounds in the soil. Methods are needed that will allow for the accurate assessment of carbon storage or sequestration in soils. The research conducted under this LDRD will develop such a technique that, if successful, can lead to dramatic improvements in the measurement and prediction of carbon sequestration in soils.

To date, this LDRD has resulted in collaborations with researchers at Idaho State University and the University of Maine. In the future, collaborations with researchers involved with the Free Air $CO_2$ Enrichment (FACE) and the AmeriFlux programs, both of which are sponsored in part by DOE, also will be pursued.

# Appendices

| | |
|---|---|
| **Appendix A** | Authors |
| **Appendix B** | Refereed Publications |
| **Appendix C** | Key Terms |
| **Appendix D** | Project Performance |
| **Appendix E** | Relevance to Major DOE Missions |
| **Appendix F** | Relevance to Major National Programs |

LDRD Annual Report for FY-2002

Idaho National Engineering & Environmental Laboratory

## *Appendix A–*
## *Authors*

## Appendix A–Authors


| Project ID | Principal Investigator | Page # |
|---|---|---|
| | A | |
| ET110 | Abbott, M. L. | 91 |
| ET108 | Alessi, R. S. | 94 |
| NE120 | Anderson, R. P. | 25 |
| ET105 | Apel, W. A. | 97 |
| GC142 | Apel, W. A. | 299 |
| S028 | Appelhans, A. D. | 100 |
| NS109 | Aryaeinejad, R. | 153 |
| ST102 | Atkinson, D. A. | 259 |
| SC105 | Atkinson, D. A. | 103 |
| | B | |
| WT106 | Baker, J. D. | 221 |
| GC124 | Barnes, J. M. | 302 |
| NS123 | Bauer, S. G. | 156 |
| NS102 | Benson, M. T. | 159 |
| ST108 | Berrett, S. | 261 |
| NE121 | Boardman, R. D. | 27 |
| ET116 | Bruemmer, D. | 107 |
| | C | |
| CS115 | Carrington, R. A. | 243 |
| CS116 | Chu, H | 246 |
| WT108 | Cordes, G. A. | 224 |
| GC131 | Cummings, D. E. | 304 |
| | D | |
| SC113 | Deason, V. A | 110 |
| NS104 | Derr, K. | 162 |
| CS114 | Dudenhoeffer, D. D. | 250 |
| H062 | Dudenhoeffer, D. D. | 113 |

| Project ID | Principal Investigator | Page # |
|---|---|---|
| | E | |
| PH102 | Eide, S. D. | 116 |
| NE108 | Evans, R. P. | 31 |
| | F | |
| NC102 | Fincke, J. R. | 118 |
| WT107 | Fox, R. V. | 226 |
| ET114 | Fujita, Y. | 119 |
| NE115 | Gering, K. L. | 33 |
| | G | |
| WT101 | Gombert, D. | 228 |
| WT105 | Gombert, D. | 231 |
| AC104 | Greenwade, L. E. | 209 |
| GC143 | Groenewold, G. S. | 307 |
| | H | |
| ST109 | Hamilton, M. A. | 262 |
| WT104 | Harbour, J. L. | 233 |
| PH103 | Harbour, J. L. | 309 |
| NE112 | Harrup, M. K. | 35 |
| GC111 | Harrup, M. K. | 311 |
| NE117 | Hartwell, J. K. | 38 |
| GE102 | Harvego, E. A. | 279 |
| GC108 | Heath, G. | 314 |
| GC133 | Heath, G. | 317 |
| GE104 | Herring, J. S. | 281 |
| GC137 | Hertzog, R. C. | 319 |
| GC138 | Hertzog, R. C. | 322 |
| PH106 | Hertzog, R. C. | 324 |
| CE102 | Hess, J. R. | 41 |
| CE110 | Hoskinson, R. L. | 44 |

## Appendix A–Authors


| Project ID | Principal Investigator | Page # |
|---|---|---|
| | J | |
| ST107 | Jacobson, J. J. | 265 |
| SC114 | Johnson, K. B. | 122 |
| GC123 | Johnson, R. W. | 326 |
| NS122 | Jones, J. L. | 165 |
| | K | |
| GC139 | Keener, W. K. | 329 |
| NS129 | Kenney, K. L | 168 |
| ES101 | Kong, P. C. | 169 |
| NS119 | Kotter, D. | 172 |
| NS124 | Kotter, D. | 175 |
| NS110 | Kunerth, D. C. | 177 |
| | L | |
| AC101 | Larson, T. K. | 211 |
| GC132 | Lenhard, R. | 331 |
| GC135 | Lenhard, R. | 333 |
| NE125 | Lessing, P. A. | 47 |
| NC103 | Lessing, P. A. | 126 |
| NE124 | Liang, J. T. | 49 |
| PH107 | Liang, J. T. | 52 |
| | M | |
| GE105 | MacDonald, P. E. | 283 |
| GC146 | Mattson, E. D. | 335 |
| CS103 | McQueen, M. A. | 253 |
| GC136 | Meakin, P | 337 |
| NE109 | Mecham, D. | 55 |
| ES102 | Moore, G. A. | 179 |
| GC125 | Moore, G. A. | 339 |

| Project ID | Principal Investigator | Page # |
|---|---|---|
| | N | |
| ES106 | Novack, S. D. | 181 |
| NS131 | Novack, S. D. | 183 |
| AC103 | Novack, S. D. | 215 |
| | O | |
| NE110 | O'Brien, J. E. | 57 |
| NS127 | O'Brien, M. H. | 184 |
| GC101 | Oh, C. | 341 |
| GE106 | Ougouag, A. M. | 288 |
| | P | |
| GC106 | Partin, J. K. | 344 |
| GE101 | Petti, D. | 290 |
| ET106 | Piet, S. J. | 128 |
| GC117 | Pinhero , P. J. | 350 |
| GC113 | Pinhero, P. J. | 346 |
| | R | |
| PH101 | Radtke, C. | 352 |
| WT110 | Raman, S. V. | 235 |
| GC114 | Redden, G. | 353 |
| GC116 | Redden, G. | 356 |
| NE114 | Richins, W. D. | 60 |
| NS118 | Roberto, F. | 185 |
| NC104 | Rollins, H. | 130 |
| NS121 | Roney, T. | 187 |
| ST105 | Rope, R. | 267 |

## Appendix A–Authors


| Project ID | Principal Investigator | Page # |
|---|---|---|
| | S | |
| GC140 | Schafer, A. | 358 |
| GE103 | Schultz, R. R. | 293 |
| GC145 | Scott, C | 364 |
| SC111 | Scott, J. R. | 132 |
| GC119 | Scott, J. R. | 361 |
| NS128 | Shewmaker, A. | 190 |
| AC102 | Shook, M. | 217 |
| ET107 | Silverman, H. | 135 |
| PH105 | Sisson, J. B. | 366 |
| NE111 | Smartt, H. B. | 63 |
| GC102 | Smith, R. P. | 368 |
| GC130 | Starr, R. C. | 370 |
| CE108 | Steffler, E. D. | 65 |
| GC107 | Stone, M. | 372 |
| S472 | Stoner, D. | 137 |
| GC134 | Stoner, D. | 374 |
| ST104 | Stormberg, A. I. | 270 |
| GC144 | Stormberg, G. | 376 |
| NS107 | Swank, D. | 192 |
| ES107 | Szpakiewicz, M. | 195 |
| | T | |
| D437 | Telschow, K. | 68 |
| NE118 | Telschow, K. | 71 |
| NC101 | Telschow. K. | 139 |
| SC104 | Thantu, N. | 142 |
| CE101 | Thompson, D. N. | 74 |
| GC109 | Thompson, V. | 379 |
| WT103 | Todd, T. A. | 238 |
| NE122 | Tolle, C. R. | 78 |
| NS125 | Totemeier, T. C. | 199 |
| ES105 | Tranter, T. | 201 |
| | V | |
| SC112 | Van Siclen, C. | 144 |
| NS114 | Velasquez, M. E. | 204 |
| GC141 | Versteeg, R. | 382 |
| | W | |
| CE105 | Ward, T. E. | 81 |
| NE122 | Weaver, K. D. | 83 |
| GC103 | Weinberg D. M. | 384 |
| NE123 | Weinberg, D. M. | 86 |
| GC105 | Weinberg, D. M. | 386 |
| PH104 | Weinberg, D. M. | 388 |
| ET115 | White, G. J. | 147 |
| ST106 | White, G. J. | 273 |
| GC104 | White, G. J. | 391 |

## *Appendix B–*
## *Refereed Publications*

## Appendix B–Refereed Publications

*Apel, ET105 - Biologically Based Catalysts for Processing and Detection in Harsh Service Conditions*
W. A. Apel, A. Aiken, B. Peyton, J. Petersen, "Heavy Metal Induced Inhibition of Aspergillus Niger Nitrate Reductase: Applications for Rapid Contaminant Detection in Aqueous Samples," Analytica Chimica Acta, Volume 480, pp. 131-142, 2003.

*Apel, GC142 - Development of Sensors for Detection of Metal-Reducing Bacteria in Mesoscale and Field Experiments*
W. A. Apel, W. Smith, B. Peyton, J. Petersen, "Effect of Carbon and Energy Source on Bacterial Chromate Reduction," Bioremediation Journal, Volume 6, Issue 1, Jan 11, 2002, pp. 205-215.

*Appelhans, S028 - New Ion Injection Technologies for Ion Trap Secondary Ion Mass Spectrometry (SIMS)*
A. D. Appelhans, D. A. Dahl, "Measurement of External Ion Injection and Trapping Efficiency in the Ion Trap Mass Spectrometer and Comparison with a Predictive Model," Int J Mass Spectrom, Volume 216, pp. 269-284.

*Appelhans, S028 - New Ion Injection Technologies for Ion Trap Secondary Ion Mass Spectrometry (SIMS)*
A. D. Appelhans, M. B. Ward, J. E. Olson, "Electron Flood Charge Compensation Device for Ion Trap Secondary Ion Mass Spectrometry," Int J Mass Spectrom, Volume 221, Issue 1, pp. 21-38.

*Aryaeinejad, NS109 - Second Generation of Neutron/ Gamma Sensor*
R. Aryaeinejad, E. Reber, D. Spencer, "Development of a Handheld Device for Simultaneous Monitoring of Fast Neutrons and Gamma Rays," IEEE Transactions on Nuclear Science, Volume 49, Issue 4, Aug-02.

*Aryaeinejad, NS109 - Second Generation of Neutron/ Gamma Sensor*
R. Aryaeinejad, E. Reber, D. Spencer, "Using the Cockroft-Walton Voltage Multiplier with Small Photomultipliers," IEEE Transactions on Nuclear Science, Volume 49, Issue No. 3, pp. 1150-1153.

*Atkinson, SC105 - Ion Mobility Spectrometry*
D. A. Atkinson, K. A. Daum, R. G. Ewing, "The Role of Oxygen in the Formation of TNT Product Ions in Ion Mobility Spectrometry," International Journal of Mass Spectrometry, Volume 214, Issue 2, p. 259.

*Atkinson, SC105 - Ion Mobility Spectrometry*
D. A. Atkinson, C. Wu, W. E. Steiner, P. S. Tornatore, L. M. Matz, W. F. Siems, H. H. Hill, "Construction and Characterization of a High-Flow, High-Resolution Ion Mobility Spectrometer for Detection of Explosives after Personnel Portal Sampling," Talanta, Volume 57, Issue 1, p. 123.

*Benson, NS102 - Selected Release of Polymer Degradation Agents by Photoinitiation*
M. T. Benson, "Density Functional Investigation of Melamine-Formaldehyde Crosslinking Agents - Part 1: Partially Substituted Melamine," Industrial Engineering Chemistry Research, submitted for publication.

*Bruemmer, ET116 - Advanced Control Architectures for Human-Robot Synergy in Complex, Multi-Operation Domains*
D. J. Bruemmer, J. L. Marble, M. O. Anderson, M. D. McKay, D. D. Dudenhoeffer, "Dynamic-Autonomy for Remote Robotic Sensor Deployment," Spectrum 2002, Reno, Nv., August 2002.

*Bruemmer, ET116 - Advanced Control Architectures for Human-Robot Synergy in Complex, Multi-Operation Domains*
D. J. Bruemmer, J. L. Marble, D. D. Dudenhoeffer, "Intelligent Robots for Use in Hazardous DOE Environments," PerMIS 2002, Gaithersburg, Mc., August 2002.

*Bruemmer, ET116 - Advanced Control Architectures for Human-Robot Synergy in Complex, Multi-Operation Domains*
D. J. Bruemmer, D. D. Dudenhoeffer, J. Marble, "Dynamic-Autonomy for Urban Search and Rescue," AAAI Mobile Robot Workshop, Edmonton, Canada, August 2002.

## Appendix B–Refereed Publications

*Bruemmer, ET116 - Advanced Control Architectures for Human-Robot Synergy in Complex, Multi-Operation Domains*
D. J. Bruemmer, J. L. Marble, D. D. Dudenhoeffer, "Mutual Initiative in Human-Machine Teams," Human Factors and Power Plants, Scottsdale, AZ, September 2002.

*Bruemmer, ET116 - Advanced Control Architectures for Human-Robot Synergy in Complex, Multi-Operation Domains*
D. J. Bruemmer, J. L. Marble, D. D. Dudenhoeffer, M. O. Anderson, M. D. McKay, "Mixed-Initiative Control for Remote Characterization of Hazardous Environments," HICSS 2003, Waikoloa Village, Hawaii, January 2003.

*Derr, NS104 - Information Visualization By Query*
K. Derr, K. Rohde, "Information Visualization by Query," ACM Conference Proceedings, Companion, Oct-01.

*Dudenhoeffer, CS114 - Critical Infrastructure Critical Subnetwork*
D. Dudenhoeffer, M. Permann, E. Sussman, "A Parallel Simulation Framework for Infrastructure Modeling and Analysis," Proceedings of the 2002 Winter Simulation Conference.

*Dudenhoeffer, H062 - Behavioral and Control Modeling for Large Scale Micro-Robot Systems*
D. Dudenhoeffer, D. Bruemmer, M. Davis, "Modeling and Simulation For Exploring Human-Robot Team Interaction Requirements," Proceedings of 2001 Winter Simulation Conference.

*Evans, NE108 - Two-Phase Mass Flow Measurement for Geothermal Wells*
R. P. Evans, J. Blotter, "Mass Flow Measurement Using Flow-Induced Pipe Vibration," 48th International Instrumentation Symposium.

*Fox, WT107 - Direct Dissolution of Plutonium and Neptunium Species Using Chelated Agents in Carbon Dioxide*
R. V. Fox, B. J. Mincher, "Supercritical Fluid Extraction of Plutonium and Americium from Soil," ACS Symposia Series.

*Gering, NE123 - Characterization of Methane Hydrate Deposits*
K. Gering, "Simulations of Methane Hydrate Phenomena over Geologic Timescales. Part I: Effect of Sediment Compaction Rates on Methane Hydrate and Free Gas Accumulations," Journal of Earth & Planetary Science Letters.

*Gombert, WT101 - Cold-Crucible Design Parameters for Next Generation High Level Waste Melters*
D. Gombert, J. R. Richardson, "Cold Crucible Induction Melter Design and Development," Nuclear Technology, Volume 141, Issue 3, March 2003.

*Harrup, NE112 - Novel Solid Electrolyte Materials for Lithium Batteries*
A. Luther, M. K. Harrup, F. F. Stewart, "NMR Spectroscopic Study of Ion Conducting 15N Labeled Polyphosphazenes," American Chemical Society Symposium, Advances in the NMR Spectroscopy of Polymers, Volume 834, Issue 31.

*Harrup, GC111 - Hybrid Nanocomposite Materials as Subsurface Permeable Reactive Barriers*
M. K. Harrup, A. K. Wertsching, M. G. Jones, "Preparation and Characterization of Novel Polymer/Silicate Nanocomposites," Functional Condensation Polymers, Volume 1, Issue 1, p. 43.

*Harrup, GC111 - Hybrid Nanocomposite Materials as Subsurface Permeable Reactive Barriers*
A. K. Wertsching, G. B. Cotten, M. K. Harrup, "Examination of the Physical Properties of Polyphosphazene Silicate Nanocomposites Using Novel Synthetic Strategies," Composite Interfaces, Volume 9, Issue 1, p. 77.

## Appendix B–Refereed Publications

*Herring, GE104 - Advanced Nuclear Fuels for Enhanced Proliferation Resistance*
J. S. Herring, K. D. Weaver, "Criticality Issues in Advanced Fuel Cycles," Transactions of the American Nuclear Society, Volume 86, Issue, p. 289.

*Herring, GE104 - Advanced Nuclear Fuels for Enhanced Proliferation Resistance*
K. D. Weaver, J. S. Herring, "The Effect of the Hydrogen to Heavy Metal Ratio (H/HM) on Reactivity and Discharge Isotopics of Homogeneous Thoria-Urania Fuel," Proceedings of the Tenth International Conference on Nuclear Engineering, accepted for publication.

*Hurley, NC101 - Nanostructure Characterization for Sensing*
D. H. Hurley, K. L. Telschow, "Picosecond Surface Acoustic Waves Using a Suboptical Wavelength Grating," Phys. Rev. B Brief Reports.

*Johnson, GC123 - Advanced Simulation Method Development*
R. W. Johnson, J. Zheng, T. Sederberg, "Least Squares Methods for Solving Differential Equations Using Bezier Control Points," Applied Numerical Mathematics, submitted for publication.

*Johnson, GC123 - Advanced Simulation Method Development*
R. W. Johnson, "High-Order B-Spline Collocation at the Greville Abscissae," Applied Numerical Mathematics, under review for publication.

*Johnson, GC123 - Advanced Simulation Method Development*
R. W. Johnson, "A B-Spline Collocation Method for Solving the Navier-Stokes Equations," Computers & Fluids, under review for publication.

*Johnson, K, SC114 - High Intensity Perrhenate Ion Gun for use as a Primary Ion Beam in SIMS*
K. B. Johnson, J. E. Delmore, "High Intensity Perrhenate Ion Gun for use as a Primary Ion Beam in SIMS (Secondary Ion Mass Spectroscopy)," International Journal of Mass Spectroscopy.

*Lenhard, GC132 - Nonaqueous-Phase Fluid Behavior in the Vadose Zone: Model Development & Testing*
R. J. Lenhard, M. Oostrom, C. Hofstee, T. W. Wietsma, "Flow Behavior and Residual Saturation Formation of Liquid Carbon Tetrachloride in Unsaturated Heterogeneous Porous Media," J. Contaminant Hydrology, accepted for publication.

*Lenhard, GC132 - Nonaqueous-Phase Fluid Behavior in the Vadose Zone: Model Development & Testing*
R. J. Lenhard, M. Oostrom, "Carbon Tetrachloride Flow Behavior in Unsaturated Hanford Caliche Material: An Investigation of Residual NAPL," Vadose Zone Journal, 2003, Issue 2, pp. 25-33.

*MacDonald, GE105 - Design of an Actinide Burning Lead or Lead Bismuth Reactor that Produces Low Cost Electricity*
K. D. Weaver, P. E. MacDonald, J. S. Herring, "Reactivity and Isotopic Assessment of Fertile Fuels for Proliferation-Resistant,Actinide-Burning Lead or Lead-Bismuth Cooled Fast Reactors," MIT-ANP-TR-074.

*MacDonald, GE105 - Design of an Actinide Burning, Lead or Lead-Bismuth Cooled Reactor that Produces Low Cost Electricity*
C. B. Davis, "Assessment of the ATHENA Code for Calculating the Void Fraction of a Lead-Bismuth/Steam Mixture in Vertical Upflow," MIT Nuclear Engineering Dept., Volume 133, pp. 187-193.

*MacDonald, GE105 - Design of an Actinide Burning, Lead or Lead-Bismuth Cooled Reactor that Produces Low Cost Electricity*
J. Buongiorno, M. S. Kazimi, N. E. Todreas, "Heavy-Metal Aerosol Transport in a Lead-Bismuth Cooled Fast Reactor with In-Vessel Direct-Contact Steam Generation," MIT-ANP-TR-079,CANES/MIT.

## Appendix B–Refereed Publications

*MacDonald, GE105 - Design of an Actinide Burning, Lead or Lead-Bismuth Cooled Reactor that Produces Low Cost Electricity*
J. Buongiorno, B. D. Hawkes, "Seismic Analysis of Heavy-Liquid-Metal-Cooled Reactor Vessels," CANES/MIT Nuclear Engineering Dept.

*MacDonald, GE105 - Design of an Actinide Burning, Lead or Lead-Bismuth Cooled Reactor that Produces Low Cost Electricity*
J. Buongiorno, K. R. Czerwinski, C. L. Larson, "Experimental Investigations on Vapor Pressure of Lead Polonide at Low Temperature & Thermodynamics of Polonium Hydride," MIT-ANP-TR-080.

*MacDonald, GE105 - Design of an Actinide Burning, Lead or Lead-Bismuth Cooled Reactor that Produces Low Cost Electricity*
P. Hejzlar, M. J. Driscoll, M. S. Kazimi, "Conceptual Neutronic Design of a Lead-Bismuth Cooled Actinide Burning Reactor," Nuclear Science & Engineering, Volume 139, 18-Jan.

*MacDonald, GE105 - Design of an Actinide Burning, Lead or Lead-Bismuth Cooled Reactor that Produces Low Cost Electricity*
J. Buongiorno, N. E. Todreas, M. S. Kazimi, "Heavy-Metal Aerosol Transport in a Lead-Bismuth Cooled Fast Reactor with In-Vessel Direct-Contact Steam Generation," Nuclear Technology, Volume 138, pp. 30-43.

*MacDonald, GE105 - Design of an Actinide Burning, Lead or Lead-Bismuth Cooled Reactor that Produces Low Cost Electricity*
C. B. Davis, D. Kim, N. E. Todreas, M. S. Kazimi, "Core Power Limits for a Lead-Bismuth Natural Circulation Actinide Burner Reactor," Nuclear Engineering and Design, Volume 213, pp.165-182.

*MacDonald, GE105 - Design of an Actinide Burning, Lead or Lead-Bismuth Cooled Reactor that Produces Low Cost Electricity*
J. Buongiorno, K. R. Czerwinski, C. L. Larson, "Speciation of Polonium Released from Molten Lead Bismuth," Radiochimica Acta, Issue 2, volume 91, 2003.

*MacDonald, GE105 - Design of an Actinide Burning, Lead or Lead-Bismuth Cooled Reactor that Produces Low Cost Electricity*
J. Buongiorno, N. E. Todreas, M. S. Kazimi, "Neutronic Design for a Pb-Bi-Cooled Actinide Burner Fast Reactor," Proceedings of ICONE-8, Volume No. 8739.

*MacDonald, GE105 - Design of an Actinide Burning, Lead or Lead-Bismuth Cooled Reactor that Produces Low Cost Electricity*
C. B. Davis, A. S. Shieh, "Overview of the Use of ATHENA for Analysis of Lead-Bismuth Cooled Reactors," 8th International Conference on Nuclear Engineering.

*MacDonald, GE105 - Design of an Actinide Burning, Lead or Lead-Bismuth Cooled Reactor that Produces Low Cost Electricity*
E. P. Loewen, C. B. Davis, P. E. MacDonald, "A Technique for Dynamic Corrosion Testing in Liquid Lead Alloys," Proceedings of the 8th International Conference on Nuclear Engineering ICONE-8.

*MacDonald, GE105 - Design of an Actinide Burning, Lead or Lead-Bismuth Cooled Reactor that Produces Low Cost Electricity*
K. D. Weaver, J. S. Herring, P. E. MacDonald, "Performance Modeling of Metallic and Nitride Fuels in Advanced Lead-Bismuth Cooled Fast Reactors," Proceedings of the 8th International Conference on Nuclear Engineering ICONE-8.

## Appendix B–Refereed Publications

*McQueen, CS103 - Survivable Networks of Dynamic Systems*
M. A. McQueen, A. W. Krings, W. S. Harrison, N. Hanebutte, "On the Performance of a Survivability Architecture for Networked Computing Systems," 35th Hawaii International Conference on System Sciences.

*McQueen, CS103 - Survivable Networks of Dynamic Systems*
M. A. McQueen, A. W. Krings, W. S. Harrison, "Shifting the Focus of Survivability: Back to the Basics," Information Survivability Workshop, (ISW-2001), Vancouver, BC Canada, Oct. 15-17..

*McQueen, CS103 - Survivable Networks of Dynamic Systems*
M. A. McQueen, A. W. Krings, W. S. Harrison, M. H. Azadmanesh, "The Impact of Hybrid Fault Models on Scheduling for Survivability," International Workshop on Scheduling in Computer and Manufacturing Systems.

*O'Brien, NE110 - High-Temperature Flow Measurement of Molten Salts*
J. E. O'Brien, "Techniques for Molten Salt Transfer, Sampling, and Flow Measurement," Proceedings, 15th Topical Meeting on the Technology of Fusion Energy.

*Oh, GC101 - Fundamental studies on gas contaminant mobility in the vadose zone from atmospheric pressure fluctuations*
C. Oh, W. Downs, "Gas Contaminat Mobility at Subsurface Disposal Facility," Material Research Society, Volume JJ, Issue 235, p.242.

*Ougouag, GE106 - Development of a Nodal Diffusion Method for Cylindrical-Geometry Reactor Cores*
W. K. Terry, H. D. Gougar, and A. M. Ougouag, "Direct Deterministic Method for Neutronics Analysis and Computation of Asymptotic Burnup Distribution in a Recirculating Pebble-Bed Reactor," Annals of Nuclear Energy, Volume 29, Issue 7, pp. 1345 –1364.

*Ougouag, GE106 - Development of a Nodal Diffusion Method for Cylindrical-Geometry Reactor Cores*
A. M. Ougouag, R. R. Schultz, W. K. Terry, A. G. Stephens, "Preliminary Investigation of an Optimally Scramming Control Rod for Gas-Cooled Reactors," ICONE-10.

*Ougouag, GE106 - Development of a Nodal Diffusion Method for Cylindrical-Geometry Reactor Cores*
A. M. Ougouag, W. K. Terry, H. D. Gougar, "Examination of the Potential for Diversion or Clandestine Dual Use of a Pebble-Bed Reactor to Produce Plutonium," HTR-2002, pp. 52-57.

*Ougouag, GE106 - Development of a Nodal Diffusion Method for Cylindrical-Geometry Reactor Cores*
H. D. Gougar, W. K. Terry, A. M. Ougouag, "Matrix Formulation of Pebble Circulation in the PEBBED Code," HTR-2002, pp. 80-85.

*Ougouag, GE106 - Development of a Nodal Diffusion Method for Cylindrical-Geometry Reactor Cores*
H. D. Gougar, W. K. Terry, A. M. Ougouag, C. B. Neill, "Matrix Formulation for Automated Modeling of Pebble Circulation in the PEBBED Code," Transactions of the ANS, Volume 85, pp. 108-109.

*Ougouag, GE106 - Development of a Nodal Diffusion Method for Cylindrical-Geometry Reactor Cores*
A. M. Ougouag, H. D. Gougar, "Preliminary Assessment of the Ease of Detection of Attempts at Dual Use of a Pebble-Bed Reactor," Transactions of the ANS, Volume 85, pp. 115-117.

*Petti, GE101 - The Modular Pebble-Bed Reactor*
W. K. Terry, H. D. Gougar, A. M. Ougouag, "Direct Deterministic Method for Neutronics Analysis and Computation of Asymptotic Burnup Distribution in a Recirculating Pebble-Bed Reactor," Annals of Nuclear Energy, Volume 29.

## Appendix B–Refereed Publications

*Petti, GE101 - The Modular Pebble-Bed Reactor*
A. M. Ougouag, W. K. Terry, H. D. Gougar, "Examination of the Potential for Diversion or Clandestine Dual Use of a Pebble-Bed Reactor to Produce Plutonium," Proceedings of HTR 2002, 1st International Topical Meeting on High Temperature Reactor Technology (HTR).

*Petti, GE101 - The Modular Pebble-Bed Reactor*
A. M. Ougouag, W. K. Terry, H. D. Gougar, "Proliferation Resistance of the Pebble-Bed Reactor Concept: Examination of the Potential for Diversion or Clandestine Dual Use to Produce Plutonium," Nuclear Engineering and Design.

*Petti, GE101 - The Modular Pebble-Bed Reactor*
R. L. Moore, C. H. Oh, B.J. Merrill, D. A. Petti, "Studies on Air Ingress for Pebble Bed Reactors," Proceedings of HTR 2002, 1st International Topical Meeting on High Temperature Reactor Technology (HTR).

*Petti, GE101 - The Modular Pebble-Bed Reactor*
G. K. Miller, D. A. Petti, J. T. Maki, "Development of an Integrated Performance Model for TRISO-Coated Gas Reactor Particle Fuel," Proceedings of HTR 2002, 1st International Topical Meeting on High Temperature Reactor Technology (HTR).

*Petti, GE101 - The Modular Pebble-Bed Reactor*
H. D. Gougar, W. K. Terry and A. M. Ougouag, "Matrix Formulation of Pebble Circulation in the PEBBED Code," Proceedings of HTR 2002, 1st International Topical Meeting on High Temperature Reactor Technology (HTR).

*Raman, WT110 - Advanced Formulation for Homogenization of Refractory Oxides in Glass and Ceramic Phases: Implications for Dispositioning of Idaho High Level Waste Calcine and Sodium Bearing Waste Liquid*
S.V. Raman, "Raman Spectra ..... Glass Network," Philosphical Magazine, Volume 5, Issue 15, p. 2002.

*Schultz, GE103 - Generation IV Gas-Cooled Reactor System Analysis Tools*
R. R. Schultz, K. W. Weaver, A. M. Ougouag, W. Wieselquist, "Validating & Verifying a New Thermal-Hydraulic Analysis Tool," Proceedings of the International Conference on Nuclear Engineering 10.

*Scott, GC119 - Development of Imaging Fourier Transform Mass Spectrometer Capabilities for Analyses of Complex & Heterogeneous Samples*
J. R. Scott, P. L. Tremblay, "Highly Reproducible Laser Beam Scanning Device for an Internal Source Laser Desorption Microprobe Fourier Transform Mass Spectrometer," Review of Scientific Instruments, Volume 73, Issue 3, pp. 1108-1116.

*Scott, GC119 - Development of Imaging Fourier Transform Mass Spectrometer Capabilities for Analyses of Complex & Heterogeneous Samples*
T. R. McJunkin, P. L. Tremblay, J. R. Scott, "Automation and Control of an Imaging Internal Laser Desorption Fourier Transform Mass Spectrometer (I2LD-FTMS)," Journal of the Association for Laboratory Automation, Volume 7, Issue 3, pp. 76-83.

*Stoner, S472 - Integrated Experimental and Mathematical Analysis of Complex Chemical and Biological Systems*
C. R. Tolle, T. R. McJunkin, D. T. Rohrbaugh, R. A. LaViolette, "Optimal Cover-Based Definition of Lacunarity for Ramified Data Sets," Physical D.

*Thantu, SC104 - Trace Chemical Species Detection and Analysis Using Femtosecond Optical Heterodyne Detected Raman Induced Kerr Effect Spectroscopy*
N. Thantu, R. S. Schley, D. McMorrow, J. S. Melinger, "Coherent Two-Photon Absorption in the Third-Order Ultrafast Spectroscopy of Aniline," Chemical Physics Letters, submitted for publication.

## Appendix B–Refereed Publications

*Thompson D., CE101 - Removal of Minerals from Wheat Straw for Increased Straw Utilization for Bioenergy and Bioproducts*
D. N. Thompson, P. G. Shaw, J. A. Lacey, "Post-Harvest Processing Methods for Reduction of Silica and Alkali Metals in Wheat Straw," Applied Biochemistry and Biotechnology, accepted for publication, April 2003.

*Todd, WT103 - PAN-Based Ion Exchange Sorbents*
N. R. Mann, T. A. Todd, T. J. Tranter, F. Sebesta, "Development of Novel Composite Sorbents for the Removal of Actinides from Environmental and Analytical Solutions," Journal of Radioanalytical and Nuclear Chemistry, Volume 254, Issue 1, pp. 41-46.

*Todd, WT103 - PAN-Based Ion Exchange Sorbents*
T. A. Todd, N. R. Mann, T. J. Tranter, F. Sebesta, J. John, A. Motl, "Cesium Sorption from Concentrated Acidic Tank Waste Using Ammonium Molybdophosphate-polyacrylonitrile Composite Sorbents," Journal of Radioanalytical and Nuclear Chemistry, Volume 254, Issue 1, pp. 47-54.

*Tranter, ES105 - Porous Crystalline Silica (Gubka)-Based Ion Exchange Sorbents*
T. J. Tranter, D. A. Knecht, T. A. Todd, J. Macheret, A. S. Aloy, N. V. Sapozhnikova, A. A. Tretyakov, A. G. Anshits, "Porous Crystalline Silica (Gubka) as a Inorganic Support Matrix for Novel Sorbents," Scientific Basis for Nuclear Waste Management XXV, Volume 713, Issue 1, pp. 907-913.

*Tranter, ES105 - Porous Crystalline Silica (Gubka)-Based Ion Exchange Sorbents*
T. J. Tranter, N. R. Mann, T. A. Todd, F. Sebesta, "Evaluation of a Novel Solid Phase Extraction Composite for the Removal of Actinides from Acidic Nuclear Waste Solutions," Czech Journal of Physics, accepted for publication.

*Weinberg, NE123 - Characterization of Methane Hydrate Deposits*
D.W. Reed, Y. Fujita, M. Delwiche, D. B. Blackwelder, F. Colwell, P.P. Sheridan, T. Uchida, "Microbial Communities from Methane Hydrate-Bearing Deep Marine Sediments in a Forearc Basin," Appl. Environ. Microbiol, Volume 68, pp. 3759-3770.

*Weinberg, NE123 - Characterization of Methane Hydrate Deposits*
F.S. Colwell, R. P. Smith, "Unifying Principles of the Deep Terrestrial and Deep Marine Biospheres," Amer. Geophys. Union Monograph - Subseafloor Biosphere at Mid-Ocean Ridges.

*Weinberg, GC103 - Fracture Prediction, Characterization, and Detection in Snake River Basalts - a Modeling and Field Approach*
D. M. Weinberg, C. D. Christensen, S. R. Novascone, J. H. Cole, R. R. Reynolds, "Driving Point Impedance—A New Paradigm For Detecting Fracture And In Situ Stress In Boreholes," Mining Engineering, accepted for publication.

*Weinberg, GC103 - Fracture Prediction, Characterization, and Detection in Snake River Basalts - a Modeling and Field Approach*
R. R. Reynolds, J. H. Cole, Z. Yuan, "The Pressure Field around a Vibrating Cylinder in a Fluid Annulus," Proceedings of Annual Meeting 2002, Volume 11, p. 1.

*Weinberg, GC103 - Fracture Prediction, Characterization, and Detection in Snake River Basalts - a Modeling and Field Approach*
R. R. Reynolds, "Effects of Geometry on the Performance of a Downhole Orbital Vibrator," Proceedings, Volume 124, Issue 2, pp. 77-82.

*White, ST106 - Integrated Environmental Analysis: Development of Collaborative Approaches to Long Term Environmental Stewardship*
A. Miller, F. Roberto, W. Keener, M. Watwood, "Development of a Fluorescence-Based Assay for Soluble Methane Monooxygenase," Applied Microbiology and Biotechnology, Volume 2002.

## *Appendix C–*
## *Key Terms*

# Appendix C–Key Terms

## Symbols

93mNb 221

## A

acidophilic bacteria 81
acoustic 86
acoustic detection 344
acoustic resonance spectrometry 204
acoustic wave propagation 110
Actinide Burner Reactor (ABR) 283
actinide burning 283
adaptable alternatives 128
adhesive-related proteins 135
Advanced Data Validation & Verification System, 224
Advanced Test Reactor (ATR) 68, 71
agent migration system 253
air infiltration 60
air pathway transport 91
air pollutant fallout 91
Air Quality 93
air-coupled ultrasound 177
aniline 142
Aquifer chemistry 368
aquifer recharge 368
aquifer temperature distribution 368
arc plasma synthesis 47
armor-quality monolithic SiC 246
automatic identification technologies 261
automotive manufacturing industry 192

## B

B-spline collocation 326
barcodes 261
battery-operated sensor 153
Bayesian Decision Network (BDN) 267
benzoic acid 353
Beowulf clusters 190
beta-diketones 226
better large-scale measurements 386
“bi-material” structures 63
biocatalysts 97
bioenergy and bioproducts 74
bioenergy production processes 78
bioenergy source 44
biofilm formation 137, 374
biofouling 137
biomass 44
biomass feedstocks 81
biomass fractionation/flow regime 41
biomass separation 41
biomimetic glue products 135
bioprocess 81
bioremediation of chlorinated solvents 304
biosensor technologies 379
biosensors 97
bioterrorism agents 185
biotransformation of toxic solutes 346
borehole logging measurements 322
borehole seismic sources 386
Boron neutron capture therapy 38

## C

calcined granules 235
Cancer treatment 38
carbon nanotubes 47
carbon sequestration 49
carbon tetrachloride 231
carbon tetrachloride (CCl4) 333
Cellulomonas 299
cellulosic crops 65
centrifuge 335
ceramic films 126
cereal genotypes 65
cermet filters 169
chemical and biological weapon agent destruction 169
chemical identification 165
chemical vapor 259
chemical vapor-mapping 260
chemical-specific fiber-optic probes 350
chemometrics 204
chlorinated solvent adsorption 307
chlorinated solvent-soil interactions 307
classified projects 190
climate change 273
climate changes 195

cluster computer 191
co-solvents 356
Co2 recovery of coal bed methane 49
Co2 sequestration technology 52
coal bed methane (CBM) reservoirs 52
coal permeability 52
coal-strain measurements 52
Coarse-mesh Finite-Difference (CMFD) 288
code modifications 217
cold-crucible induction melter (CCIM) 228
colloid-facilitated contaminant transport 339
colloid-facilitated transport 353
colloidal-facilitated transport 344
combustion synthesis 169
command and control (C2) architectures 113
Complex resistivity (CR) 376
complex-resistivity (CR) capability 364
comprehensive decision network 309
comprehensive risk framework 116
Compton Backscatter (CBS) 187
computational fluid dynamics 55
Computational Fluid Dynamics (CFD) 293
computer simulation 209
computer-based decision tool 233
contained information-retrieval system 261
contaminant behavior and mobility 356
controlled delivery of drugs 159
core neutronics 283
cost-effective sorbents 27
Critical Heat Flux 55
critical heat flux (CHF) 55
Critical infrastructure 250
Critical Infrastructure Protection 250
Critical Infrastructure Protection Initiative 246
crop residue feedstocks 41
cylindrical geometry 288

## D

data abstraction models 209
data visualization and repository 211
decay coefficients 370
decision science 128
decommissioning-stewardship-waste decisions 129
Dehalococcoides 304
detection and characterization of unexploded ordin 177
differential quartz reactor 27
distributed architectures 211
DNAPL contaminates 323
Doppler feedback 283
driving-point impedance measurements 388
dynamic mechanical analysis (DMA) 311

## E

Eastern Snake River Plain Aquifer (ESRPA) 339
ecological patterns and processes 273
electrical behavior 364
Electrical Resistance Tomography (ERT) 314, 317
electrically disturbed zone 364
electron- and energy-transfer modalities 132
elemental assay 221
emergent behaviors 113
emission control strategies 91
encapsulated armor system 246
end-state planning 265
energetic compositions 192
energetic materials 184
energy use 60
enhanced coal bed methane (ECBM) production 53
environmental bacteria 302
environmental colloid science 119
environmental management 265
environmental restoration 262
environmental samples 273
environmental waste 116
enzymatic biosensors 97
enzyme-specific probes 273
erbium (Er) 221
Extremophilic microbes 97

## F

femtosecond laser source 142
fertilization regime 44
fiber-optic probes 350
finite element modeling code 385

flow noise 31
flowmeter 57
fluid flow in fractured porous media 337
fluid-fluid interfaces 337
fluorescent labeling 329
flux estimation methods 366
formation lithology 319
Fourier transform mass spectrometer (FTMS) 132, 361
fractal dimension 137
fracture (cleat) system 52
fracture toughness of steels 199
fracture-detection 384
fracture-mechanics-based test 199
Friction Stir Welding (FSW) 63
fuel cell technology 47

## G

gamma-ray spectrometry 204
Gas Contaminant Mobility 341
gas phase ion/molecule reactions 103
gas-cooled fast reactors 83
Generation IV reactor 279
geo-location technologies 156
geocentrifuge 335
geochemical borehole logging 322
geochemical-based macroscopic neutron cross-sectio 319
geologic Co2 sequestration 51
geophysical imaging tools 382
geothermal well 31
global climate change 49
granular disorder 144
Granular materials 144
green fluorescent protein (GFP) 302
Ground penetrating radar 177
groundwater dynamical systems 204
Gubka matrix 201

## H

halocarbons 231
heavy metal contamination 299
heterogeneous robotic platforms 113
Hierarchical Data Format 209
High Performance Computing 209
high-efficiency cutting 184
high-level waste 228
high-performance computing 211
high-performance computing (HPC) 190
human systems science 94
Human-Robot Synergy 107
hybrid electric vehicles 33
hydrate-containing sediments 86
hydrodynamics 374
hydrogen economy 47
hydrogen production 25
hydrogen storage 47
hydrogeophysical methodology 324
hysteretic property 358

## I

imaging laser desorption FTMS 361
Imaging Patterned Molecular Architectures 346
in situ bioremediation 119
in situ characterization/monitoring technologies 86
in situ microcosm 352
in situ reaction rates 370
Information Visualization by Query (IVBQ) 162
infrastructure architectures and interdependencies 250
Integral Fast Reactor, IFR 283
Intelligent robots 107
inter-surface transfer of adsorbed chemical specie 353
Intercalated Graphite 47
interfacial chemical dynamics 142
interfacial interactions 307
interferometric detection scheme 68
International Space Station 215
Ion Exchange Sorbents 201
ion injection 100
Ion mobility spectrometry (IMS) 103, 259
Ion trap secondary ion mass spectrometry (IT-SIMS) 100
ionic solutes 356
ionization mechanism 103
irreducible critical sub-network 250

## K

k-S-P models 331
kernel-based survivability mechanisms 253
kerogen release kinetics 28
Khlopin Radium Institute (KRI) 201
KONVERGENCE framework 128

## L

lacunarity 137
land mines 110
lanthanide complexation reactions 227
Large Eddy Simulation (LES) 31
laser ablation system 118
laser light pipe apparatus 68
Laser Ultrasonic Camera 110
Laser ultrasonics 71
laser ultrasonics 68
Laser-based Optical and Chemical Imager (LOCI) 361
Laser-Compton Scattering (LCS) 165
laser-induced breakdown spectroscopy 344
lattice-Boltzmann models 337
lead or lead-bismuth cooled fast reactor 283
legacy risk 116
light water reactors (LWR) 281
light-transparent models 374
Liquid metal embrittlement (LME) 199
Lithium Batteries 35
long-term stewardship 116, 262
loss-of-coolant accident (LOCA) 291
loss-of-coolant/loss-of-flow accidents 83

## M

magnetic field measurements 314
magnetic susceptibility tools 322
MagnetoMetric-Resistivity method (MMR) 315
malicious network and computer attacks 253
map-based near-real-time 265
Mapping Subsurface Water Conductivity 314
mass flow measurement 31
Mass transfer coefficients 370
material probing 165
matrix-assisted laser desorption/ionization (MALDI 132
medical radiation therapy 165
MEEP polymers 379
memory buttons 261
mesoscale experiments 350
Metal Matrix Fuel 84
metal reduction 299
micro-reactor 231
microantenna-array technology 175
microbial biofilm formation 374
microbial enzymatic activities 329
microbiologically-mediated chemical reactions 376
microcosm reactor 352
microcrystalline glass matrix 201
microelectrodes 350
microwave plasma system 118
minor actinides 281
Mission Evaluation Room (MER) 215
mobile nuclear sensor system 172
mobile software agents 253
mobile-immobile water model 335
Modular Pebble-Bed Gas-Cooled Reactor (MPBR) 290
moisture measurements 319
moisture-response characterization 319
molecular markers 65, 302
molecular probe 299
molten-salt flowmeter 57
molten-salt flows 57
Multipath fading 156
multipath propagation 156
multiphase flows 337
multivariate mixture models 91

## N

nano-crystalline grain boundaries 126
nanocomposite materials 311
nanomaterials 130
Nanoscale Phonon Dynamics 139
Nanoscale Photon Dynamics 139

nanosensors 185
nanostructure 118
nanostructured materials 139
nanotubes 118
Nanowires 118
NASICON-type ceramic compositions 126
natural gas hydrates 86
Navier Stokes equation 337
Neutron energy spectroscopy 38
neutron moisture tools 319
neutron probe modeling 319
neutron spectroscopy 38
neutron-based radiotherapy 38
neutron/gamma detection system 153
neutron/gamma separation 153
Neutronics of Pebble Fuel 83
nodal methods 288
non-aqueous contaminants 322
nondestructive waste analysis (NDA) 224
Nonlinear Complex Resistivity (NLCR) 376
Integrated Watershed Information Management Tools 267
nuclear magnetic resonance (NMR) 147, 391
nuclear magnetic resonance (NMR) tool 322
nuclear plant behavior 293
nuclear safety analysis 290
numerical simulation of complex physical processes 326
Numerical transport predictions 358
nutrient delivery 119

## O

oil shale pollutant sorption reactions 27
optical televiewer 324
orbital vibrator 386
orbital vibrator (OV) 388
orbital vibrators (OV) 384
organic acids 81
organic chelating ligands 356
organic ligands 356
ormogels 185
Osmotic tensiometers 372
osmotic transport 372

## P

parallel computing tools 211
parallelization 209
pattern recognition and analysis 224
PBMR gas-cooled reactor 280
pebble-bed helium-cooled gas reactor 280
Pebble-Bed Reactor (PBR) 288
permeable reactive barrier applications (PRBs) 311
perrhenate anion 122
perrhenate anion (ReO4-) emitter 122
Phase change materials (PCM) 33
Photo-initiated degradation 159
photon beam generation 187
physical-properties-logging tool 388
phytoextraction 262
pipeline infrastructure reliability and security 243
plants as bio-indicators 262
plasma spray coating 192
plasma-assisted chemical vapor deposition (PACVD) 118
plasmid purification techniques 135
Polyacrylonitrile (PAN) 238
polyacrylonitrile-based sorbents/solid phase extra 238
Polymer Degradation Agents 159
polymerase chain reaction 329
polymerase chain reaction (PCR) 135
polymeric precursor chemistry 126
polythiophosphazene SPE 35
polyvinyl acetate (PVAc) 311
polyvinyl alcohol (PVA) 311
porosity engineering 169
pressureless sintering process 246
public participation 94
Pulse Force Mode (PFM) 347
pulse shape discrimination (PSD) 153

## Q

quantification of geophysical data 382

## R

Radiation Detection Tracking System (RDTS) 172
radionuclide contamination 299
radionuclide-contaminated soils 226
radionuclides 344
Raman spectroscopic 226
RapidOps 233
Rate coefficients 370
RCRA (Resource, Conservation and Recovery Act) 221
reactor core neutronics 290
real-time in-pile kinetic data 71
recombinant proteins 135
record storage and retrieval 261
reductive dechlorination 304
repeated infiltration events 358
residual hazards management 309
residual NAPL 331
reverse osmosis membrane 372
Richard's equation 358
risk analyses 116
risk monitor 215
robotic systems 107
robotics 113
robots 113
rotational ultrafiltration system 179
Russian nuclear power plants 181

## S

SAPHIRE-based risk monitor 181
Secondary Ion Mass Spectrometry 100
Secondary Ion Mass Spectrometry (SIMS) 122
seismic technologies 86
semiconductor quantum dots 139
Shewanella putrefaciens 302
single-pass harvester 41
single-phase flow processes 337
single-well push-pull tests (SWPPTs) 370
Smart Antenna" technologies 156
smart pipe 243
Snake River Plain Aquifer 317
Snake River Plain aquifer 368
Snake River Plain Aquifer System (SRPAS) 195
sodium-bearing waste 235
Soil water flux 366
soil-gas dynamics 341
sol-gels 185
solid polymer electrolyte (SPE) 35
Solute partitioning 356
spatial element identification 165
Spatial variability of hydraulic properties and ge 384
species-dependant convergence 218
standoff monitoring 175
steam reforming 231
stereolithographic methods 374
Stewardship of biological resources 273
stratigraphic correlation of lava flows 322
stress chains 144
Strontium-90 262
sub-micron and sub-nanometer structures on silicon 165
subsurface 386
subsurface barriers 311
subsurface biogeochemical systems 137
subsurface bioremediation 119
subsurface contaminant migration processes 335
subsurface NAPL behavior 331
Supercritical Co2 Power Plant 84
supercritical fluid processing techniques 130
superheated drop detectors 38
support non-intrusive and nondestructive inspectio 187
surface-reactive solutes 353
survivability architecture 253
synthetic biofilm images 137
synthetic colloids 119, 339
System Dynamics 265
System's Analysis Programs for Hands-on Integrated 181
systems analysis programs for hands-on integrated 215

## T

teleoperated robotic systems 107
terascale data management 209
terpene release 159
TETRAD 217
TETRAD subsurface code 209
thermal hydraulics 290
thermal infrared (IR) emissions 175
thermal management system (TMS) for HEVs 33
thermal spray coating 192
thermal-hydraulic behavior 293
thermal-hydraulics 283
thermal-mechanical models 384
thermally sprayed sensors and data communication 243
thermitic cutting compositions 184
Thermus brockianus 97
thioether pendant groups 35
Thoria (ThO2) fuels 281
thorium 283
Time temperature superpositioning (TTS) 311
trace organic detection 259
trace toxins 100
transient analysis 279
transient fluids/heat transfer behavior 293
transport of reactive solutes 358
transposon mutagenesis 303
tributyl phosphate 226
trichloroethylene 142
trichloroethylene (TCE) 304
tunable x-ray sources 165
Two-Phase Mass Flow Measurement 31

## U

Ultrafast nonlinear optical techniques 142
ultrasonic imaging techniques 110
unmanned autonomous forces 113
unsaturated flow apparatus (UFA) centrifuge 336
unsaturated hydraulic conductivity 366
unsaturated zone 317
urea 379
urea sensor 379

## V

Vadose Zone 317
vadose zone 331
vitrification 228
volatile organic compounds 231

## W

Waste immobilization technologies 235
waste site management 265
waste treatment projects 91
water-splitting processes 25
watershed hydrodynamics 195
watershed management 267
wavelet signatures 204
wavelet theory (multi-resolution analysis) 204
wheat straw 44
wheat straw residue 74
whisker-reinforced SiC composite 246
wireless local-area network (WLAN) 156

## X

x-ray fluorescence excitation source (EDXRF) 221
x-ray-imaging systems 187

## Y

Yellowstone Plateau 195

## Z

Zircaloy corrosion in nuclear reactors 71
zirconium 221

## *Appendix D–*
## *Project Performance*

## Appendix D–Project Performance

| Project ID | Principal Investigator | Project Title | FTE | Other Students | Post Docs | Faculty | Crada | WFO | IDR | Patents Awarded | Copyrighting/Trademark | License | Publications | Presentations | Symposia | Awards |
|---|---|---|---|---|---|---|---|---|---|---|---|---|---|---|---|---|
| ET110 | Abbott, M. L. | Elemental Tracers and Multi Variate Receptor Modeling Methods in Assessing Air Pollution | 0.59 | | | | | | | | | | 1 | | | |
| ET108 | Alessi, R. S. | Improving Stakeholder Interactions: A Stakeholder Based Research Methodology for Reaching Decisions on Polarized Issues | | | | 1 | | | | | | | | | | |
| NE120 | Anderson, R. P. | Hydrogen Production from High Temperature Nuclear Reactors | 0.32 | | | | | | | | | | | | | |
| NE125 | Anderson, R. P. | Hydrogen Technologies | 0.98 | | | 1 | | | | | | | | | | |
| ET105 | Apel, W. A. | Biologically Based Catalysts for Processing and Detection in Harsh Service Conditions | 1.45 | 1 | | 1 | | | 1 | | | | 1 | | | |
| GC142 | Apel, W. A. | Development of Sensors for Detection of Metal-reducing Bacteria in Mesoscale and Field Experiments | 0.55 | | | | | | | | | | 2 | | | |
| S028 | Appelhans, A. D. | New Ion Injection Technologies for Ion Trap Secondary Ion Mass Spectrometry | 0.6 | | | | | | | | | | 2 | | | |
| NS109 | Aryaeinejad, R. | Second Generation Neutron/Gamma Sensor | 0.75 | | | | | | | | | | 2 | 3 | | |
| SC105 | Atkinson, D. A. | Ion Mobility Spectrometry | 2.1 | | | 2 | | | | | | | 2 | 2 | 1 | |
| ST102 | Atkinson, D. A. | Airborne Contaminant Gradient Mapping System | 0.2 | | | | | | | | | | | 1 | 1 | |
| WT106 | Baker, J. D. | Energy-Dispersive, X-Ray Fluorescence Excitation Source for In-Field Analysis | 0.25 | | | | | | | | | | | | | |
| GC124 | Barnes, J. M. | Use of Molecular Markers for Detection and Tracking of Environmental Bacteria | 1.05 | | | | | | | | | | | | | |
| NS123 | Bauer, S. G. | Multipath Propagation Analysis, Simulation, and Prediction in Wireless Environments | 1.29 | | | | | | | | | | | | | |
| NS102 | Benson, M. T. | Selected Release of Polymer Degradation Agents by Photo initiation | 1.11 | | | | | | | | | | 2 | | | |
| ST108 | Berrett, S. | Long-Term Record Storage for Long-Term Stewardship | 0.7 | | | | | | | | | | | 1 | | |
| NE121 | Boardman, R. D. | Co-Firing of Coal and Refuse-Derived Fuel with Oil Shale for Control of Environmental Contaminants and Improved Energy Production: Laboratory Studies | 1.5 | 2 | 1 | 1 | | | | | | | | | | |

## Appendix D–Project Performance

| Project ID | Principal Investigator | Project Title | FTE | Other Students | Post Docs | Faculty | Crada | WFO | IDR | Patents Awarded | Copyrighting/Trademark | License | Publications | Presentations | Symposia | Awards |
|---|---|---|---|---|---|---|---|---|---|---|---|---|---|---|---|---|
| ET116 | Bruemmer, D. J. | Advanced Control Architectures for Human-Robot Synergy in Complex, Domains | 1.9 | | | | | | | | | | 5 | 3 | 1 | 1 |
| CS115 | Carrington, R. A. | Use of Thermally Sprayed Traces for Damage Detection and Data Transmission | | 1 | | | | | | | | | | | | |
| CS116 | Chu, H. S. | Development of Blast and Penetration Resistant Materials and Systems for Comprehensive Protection of Vehicles, Personnel and Buildings | 1 | | | | 1 | | | | | | | 3 | | |
| WT108 | Cordes, G. A. | Enhanced Sample Based Modeling Techniques for Nondestructive Analysis and Long-term Stewardship | | | | | | | | | | | | | | |
| GC131 | Cummings, D. E. | Characterizing Microbial Population Shifts in Response to Alternative Electron Donors and their Effecton Trichloroethylene Dechlorination Efficiency | 0.49 | 1 | | | | | | | | | | | | |
| SC113 | Deason, V. A. | Detection of Buried Objects using Imaging Laser Acoustics | 0.5 | | | | | | | | | | | | | |
| NS104 | Derr, K. W. | Information Visualization By Query | 1 | | | | | | | | 1 | 2 | 1 | 1 | | |
| CS114 | Dudenhoeffer, D. D | Critical Infrastructure Critical Subnetwork | 3.15 | | | | | | | | | | 1 | 1 | | |
| H062 | Dudenhoeffer, D. D | Behavioral and Contro lModeling for Large Scale Micro-Robot Systems | 0.6 | | | 1 | | | | | | | 2 | | | |
| PH102 | Eide, S. A. | Characterization of Legacy Risk | 0.8 | 1 | | 1 | | | | | | | | | 1 | |
| NE108 | Evans, R. P. | Two Phase Mass Flow Measurement for Geothermal Wells | 0.11 | 1 | | 2 | | | 1 | 1 | 1 | | | | | |
| NC102 | Fincke, J. R. | Controlled Growth of Nanowires | 1 | | | | | | | | | | | | | |
| WT107 | Fox, R. V. | Direct Dissolution of Plutonium and Neptunium Species Using Complexing Agents in Carbon Dioxide | 1 | | | | | | | | | | 1 | 1 | | |
| ET114 | Fujita, Y. | Use of Engineered Nano-Particles for Nutrient Delivery and Bioremediation in Subsurface Environments | 1.05 | | | | | | | | | | | | | |
| NE115 | Gering, K. L. | Clean Cold Start Technology for Conventional, Electric, and Hybrid Vehicles | 1 | | | | | | 1 | | | | | | | |

## Appendix D–Project Performance

| Project ID | Principal Investigator | Project Title | FTE | Other Students | Post Docs | Faculty | Crada | WFO | IDR | Patents Awarded | Copyrighting/Trademark | License | Publications | Presentations | Symposia | Awards |
|---|---|---|---|---|---|---|---|---|---|---|---|---|---|---|---|---|
| WT101 | Gombert, D. | Cold-Crucible Design Parameters for Next Generation High Level Waste Melters | 1.7 | | | 2 | | | | | | | 3 | 2 | | |
| WT105 | Gombert, D. | Steam Reforming in Micro-Reactors for Destruction of Hazardous Organic Materials | 0.9 | | | 1 | | | | | | | 1 | 2 | | |
| AC104 | Greenwade, L. E. | Development and Validation of Advanced Simulation and Collaboration Capability | | | | | | | | | | | | | | |
| GC143 | Groenewold, G. S. | Characterization of Dense Non-aqueous Phase Liquids Adsorption/Desorption to Geological Media | 0.25 | 1 | 1 | 1 | | | | | | | | | | |
| ST109 | Hamilton, M. A. | Uptake and Translocation Patterns of Strontium by Sagebrush Steppe Ecosystem Plants | 0.2 | | | 2 | | | | | | | | | | |
| PH103 | Harbour, G. L. | Residual Hazards Management: Decisions Leading Toward Successor Failure? | 0.7 | | | 1 | | | | | | | | 1 | | |
| WT104 | Harbour, G. L. | Model-Based Decision Making: Conceptual Framework and Environmental-Related Application Development | 0.5 | 1 | 3 | | | | | | | | | | | |
| GC111 | Harrup, M. K. | Hybrid Nanocomposite Materials as Subsurface Permeable Reactive Barriers | 2.05 | | | 1 | | | | | | | 2 | 2 | | |
| NE112 | Harrup, M. K. | Novel Solid Electrolyte Materials for Lithium Batteries | 1 | | | | | | | | | | 2 | 2 | | |
| NE117 | Hartwell, J. K. | Active Neutron Spectroscopy for Neutron Capture Beam Characterization | 0.35 | | | | | | | | | | | | | |
| GE102 | Harvego, E. A. | Advanced Transient Analysis Capabilities for Generation IV Nuclear Reactors | 1 | | | | | | | | | | | 2 | 1 | |
| GC108 | Heath, G. L. | Advanced Technology for Mapping Subsurface Water Conductivity | | | | | | | | | | | | | | |
| GC133 | Heath, G. L. | Electrica lResistivity Imaging to Define Preferred Flow Paths in a Heterogeneous Layered VadoseZone | 0.55 | | | | | | | | | | | | | |
| GE104 | Herring, J. S. | Advanced Nuclear Fuels for Enhanced Proliferation Resistance | 0.8 | | | 1 | | | | | | | 3 | 4 | 1 | 1 |
| GC137 | Hertzog, R. C. | Quantitative Deep-Reading Vadose Zone Moisture Characterization | 0.56 | 1 | | | | | | | | | 1 | 1 | 1 | 1 |

## Appendix D–Project Performance

| Project ID | Principal Investigator | Project Title | FTE | Other Students | Post Docs | Faculty | Crada | WFO | IDR | Patents Awarded | Copyrighting/Trademark | License | Publications | Presentations | Symposia | Awards |
|---|---|---|---|---|---|---|---|---|---|---|---|---|---|---|---|---|
| GC138 | Hertzog, R. C. | Application of New Bore-hole Geophysical Methods for Stratigraphic Correlation and Identification of Non-Aqueous-Phase Contaminants | 0.3 | | 1 | | | | | | | | | | 1 | |
| PH106 | Hertzog, R. C. | A New Hydrogeophysical Method for Characterizing and Monitoring Preferential Flow Paths in Complex Layered and Fractured Basalt | 1.01 | 1 | | 1 | | | 1 | | 1 | 1 | 1 | 1 | 1 | 1 |
| CE102 | Hess, J. R. | Characterization and Modeling of a Grain Combine Harvester | 0.4 | | | 1 | | | 2 | | 1 | 1 | 1 | 1 | 1 | 1 |
| CE110 | Hoskinson, R. L. | Development of Analytical Decision-Making Tools or Energy Efficient Agricultural Biomass Production | 1 | | | | | | | | | | 1 | 1 | | |
| ST107 | Jacobson, J. J. | DOE Complex-Wide Long-Term Stewardship Options Analysis System | 1.5 | | | | | | | | | | | 3 | | |
| SC114 | Johnson, K. B. | High Intensity Perrhenate Ion Gun for Use as a Primary Ion Beamin Secondary Ion Mass Spectroscopy | 0.25 | | | | | | | | | | 1 | | | |
| GC123 | Johnson, R. W. | Advanced Simulation Method Development | 1 | | 1 | 2 | 3 | | | | | | | | | |
| NS122 | Jones, J. L. | A Compton-Backscatter Photon Source for Tunable, Monoenergetic, Hard X-Rays | 1 | | | 1 | | | | | 1 | 1 | 1 | 1 | 1 | |
| GC139 | Keener, W. K. | Demonstration of Spatially-Resolved Molecular Approach to Detect Specific Microbial Activity on Mineral Surfaces | 1 | | | 1 | | | | | | | | | | |
| NS129 | Kenney, K. L. | Mechanical, Physical and Metallurgical Factors Affecting Liquid-Metal Embrittlement of Steels | 1 | | | | | | | | | | 1 | 1 | 1 | 1 |
| ES101 | Kong, P. C. | Cermet Filters for Hazardous Material, Chemical and Biological Agent Destruction | 2.2 | | | | | | 2 | | | | 1 | | | |
| NS119 | Kotter, D. K. | Distant Neutron Source Detection and Location | 0.31 | | | | | | 1 | | | | | | | |
| NS124 | Kotter, D. K. | Microantenna Infrared Tags | 0.45 | | | 1 | | | 1 | | | 1 | | | | |

## Appendix D–Project Performance

| Project ID | Principal Investigator | Project Title | FTE | Other Students | Post Docs | Faculty | Crada | WFO | IDR | Patents Awarded | Copyrighting/Trademark | License | Publications | Presentations | Symposia | Awards |
|---|---|---|---|---|---|---|---|---|---|---|---|---|---|---|---|---|
| NS110 | Kunerth, D. C. | Ultrasonic Detection and Characterization of Buried Objects: Air-Coupled Techniques | 0.6 | | | | | | | | | | | | | |
| AC101 | Larson, T. K. | Parallel Computing with Cluster Technology | 1.6 | 1 | 1 | 1 | | | | | | | | | | |
| GC132 | Lenhard, R. J. | Nonaqueous-Phase Fluid Behavior in the Vadose Zone: Model Development & Testing | 0.7 | | 1 | | | | | | | | 2 | 1 | | |
| GC135 | Lenhard, R. J. | Investigation of the Movement and Fate of Chlorinated Hydrocarbons | 1.15 | | | 1 | | | | | | | | | | |
| NC103 | Lessing, P. A. | Enhanced Transport in Nanocrystalline Ceramic Films | 1 | | | | | | | | | | | | | |
| NE124 | Liang, J. | Carbon Dioxide Sequestration in Geologic Coal Formations | 0.4 | | | | 1 | | | | | | | 1 | 1 | |
| PH107 | Liang, J. | Dependence of Coal Bed Permeability on Pore Pressure and Adsorbed Gas Content | 1 | | | 1 | | | | | | | | | | |
| GE105 | MacDonald, P. E. | Design of an Actinide Burning, Lead or Lead-Bismuth Reactor that Produces Low Cost Electricity | 1.2 | 3 | | 7 | | | | | | | 35 | | | |
| GC146 | Mattson, E. D. | Investigation of the Effects of Microbial Growth on Unsaturated Hydraulic Properties | 0.25 | | | 1 | | | | | | | | 1 | | |
| CS103 | McQueen, M. A. | Survivable Networks of Dynamic Systems | 2.75 | 2 | 2 | 4 | 1 | | | | | | | | | |
| GC136 | Meakin, P. | Modeling of Flow and Colloid Behavior in Subsurface Fractures | 1 | | | | | | | | | | | 1 | 1 | |
| NE109 | Mecham, D. C. | Thermal Studies of Potential Increased Advanced Test Reactor Power Margins | 1 | | | 1 | | | | | | | | | 1 | |
| ES102 | Moore, G. A. | Novel Cyclodextrin-Based Sorbent Materials for Waste Separation Needs | 0.7 | | | | | | | | | | | | | |
| GC125 | Moore, G. A. | Natural and Synthetic Subsurface Colloids | 0.75 | 2 | 1 | | | | | | | | | | | |
| AC103 | Novack, S. D. | Aerospace Situation Awareness and Risk Monitor Tool | 0.2 | | | | | | | | | | | | | |
| ES106 | Novack, S. D. | Probabilistic Risk Monitoring Software for SAPHIRE | 1.1 | 1 | | | | | | | | | | | | |
| NS131 | Novack, S. D. | Technical Advancement of the INEEL Critical Infrastructure Protection Supervisory Controland Data Acquisition Test Bed | 0.7 | | | | | | | | | | | | | |

## Appendix D–Project Performance

| Project ID | Principal Investigator | Project Title | FTE | Other Students | Post Docs | Faculty | Crada | WFO | IDR | Patents Awarded | Copyrighting/Trademark | License | Publications | Presentations | Symposia | Awards |
|---|---|---|---|---|---|---|---|---|---|---|---|---|---|---|---|---|
| NE110 | O'Brien, J. E. | High-Temperature Flow Measurement of Molten Salts | 0.5 | | | | | | | | | | 1 | 1 | | |
| NS127 | O'Brien, M. H. | Cutting of Structural Materials using Energetic Materials | 0.4 | | | | | | | | | | | | | |
| GC101 | Oh, C. H. | Fundamental Studies on Gas Contaminant Mobility in the Vadose Zone from Atmospheric Pressure Fluctuations | 0.82 | 2 | | 2 | | | 1 | | 1 | 1 | 1 | 2 | 1 | 1 |
| GE106 | Ougouag, A. M. | Development of a Nodal Diffusion Method for Cylindrical-Geometry Reactor Cores | 1 | | | | | | 2 | | | | 6 | 2 | | |
| GC106 | Partin, J. K. | Enhanced Techniques for Evaluating ColloidalTransport Processes | 0.75 | 1 | | | | | | | | | | | | |
| GE101 | Petti, D. A. | The Modular Pebble-Bed Reactor | 2.25 | 2 | 9 | 1 | | | | | | | | | | |
| ET106 | Piet, S. J. | Making Sustainable Decisions Using the *K*ONVE*R*GENCE Framework | 1 | 1 | 1 | | | | | | | | | | | |
| GC113 | Pinhero, P. J. | Chemical Modification of Atomic Force Microscope Probes for Imaging Patterned Molecular Architectures | | | | | | | | | | | | | | |
| GC117 | Pinhero, P. J. | Evaluating Microelectrodes and Fiber-Optic Probes for Use in Meso-Scale Experiments | | | | | | | | | | | | | | |
| PH101 | Radtke, C. W. | In Situ Bioremediation of Explosives in the Vadose Zone | 2.3 | 3 | | 2 | | | 1 | | | | | 2 | | |
| WT110 | Raman, S. V. | Advanced Formulation for Homogenization of Refractory Components in Glass and Ceramic Phases | 1.5 | 2 | 1 | | | | | | | | | | | |
| GC114 | Redden, G. D. | Kinetics and Mechanisms of Inter-Surface Transfer, and Solid-Solution Partitioning, of Surface-Complexed Metals in Colloidal Systems | 0.9 | 1 | | 1 | | | | | | | | | 2 | |
| GC116 | Redden, G. D. | Organic Co-Solvent and Co-Contaminant Effects on Sorption of Uranyl ndCesium to Metal Oxide Surfaces | 1.15 | 1 | | 1 | | | | | | | | | | |
| NE114 | Richins, W. D. | Energy Efficient Building Simulation and Technologies | 0.85 | 2 | | 2 | | | 1 | | | | | 1 | | |
| NS118 | Roberto, F. F. | Novel Selective Matrix for Collection and Identification of Priority Pathogens | 0.74 | | | 1 | | | | | | | | | | |

## Appendix D–Project Performance

| Project ID | Principal Investigator | Project Title | FTE | Other Students | Post Docs | Faculty | Crada | WFO | IDR | Patents Awarded | Copyrighting/Trademark | License | Publications | Presentations | Symposia | Awards |
|---|---|---|---|---|---|---|---|---|---|---|---|---|---|---|---|---|
| NC104 | Rollins, H. W. | Nucleation and Growth of Nanoparticle Materials in Supercritical Fluid Processes | 1 | | | | | | | | | | 2 | 1 | | |
| NS121 | Roney, T. J. | Imaging Applications of Photon Beams Produced with Compton Back scatter of Laser Beams | 0.35 | | | 1 | | | | | | | | | | |
| ST105 | Rope, R. C. | Development of an Integrated Watershed Information Management Tool for Long-Term Facilities Stewardship | 3.51 | 10 | | 2 | | | | | | | 1 | 11 | | |
| GC140 | Schafer, A. L. | Computational Experiments of Hysteretic Chemical and Moisture Migration | 0.5 | | | 1 | | | | | | | | | | |
| GE103 | Schultz, R. R. | Generation IV Gas-Cooled Reactor System Analysis Tools | 0.8 | | | | | | | | | | 1 | 1 | 1 | |
| GC145 | Scott, C. L. | Dual Electrodes and Defining the Electrically Disturbed Region in Induced Polarization Measurements | 0.4 | 1 | | | | | | | | | | | | |
| GC119 | Scott, J. R. | Development of Imaging Fourier Transform Mass Spectrometer Capabilities for Analyses of Complex & Heterogeneous | 1.95 | 1 | | 1 | | | 1 | | | | 2 | 1 | | |
| SC111 | Scott, J. R. | Elucidating the Photo-Physics of Complex Metal Ions Trapped in a Fourier Transform Mass Spectrometer | 0.35 | 1 | | 1 | | | | | | | 1 | 1 | | |
| NS128 | Shewmaker, A. G. | Classified Cluster Computing | 0.75 | | | | | | | | | | | | | |
| AC102 | Shook, G. M. | Improving Numerical Model Efficiency of a Simulation Model | 0.2 | 1 | | | | | | | | | | | | |
| ET107 | Silverman, H. G. | Recombinant Adhesive Protein Production and Investigation in to Alternate Natural AdhesiveSystems in Marine Mussels | 0.76 | | | | | | 1 | | | | | | | |
| PH105 | Sisson, J. B. | Improving Soil Water Flux Estimates in the Deep Vadose Zone | 1 | | | 3 | | | 4 | | | | | | | |
| NE111 | Smartt, H. B. | Friction Stir Welding of Lightweight Materials | 0.9 | 1 | | 1 | | | | | | | | | | |
| GC102 | Smith, R. P. | Regional Setting and Flow Dynamics of the Snake River Plain Aquifer | 1.9 | 1 | | 2 | | | | | | | | 1 | | |
| GC130 | Starr, R. C. | Development of Techniques for In Situ Measurement of Groundwater Contaminant Source Strength | 1.64 | 1 | | | | | | | | | | 1 | | |

## Appendix D–Project Performance

| Project ID | Principal Investigator | Project Title | FTE | Other Students | Post Docs | Faculty | Crada | WFO | IDR | Patents Awarded | Copyrighting/Trademark | License | Publications | Presentations | Symposia | Awards |
|---|---|---|---|---|---|---|---|---|---|---|---|---|---|---|---|---|
| CE108 | Steffler, E. D. | Genetic Control of Straw Stem Ultrastructure that Affects the Biomechanics of Stem Separation | 0.75 | 1 | 1 | | | | | | | | | | | |
| GC107 | Stone, M. L. | Improved Osmotic Tensiometer Componentsand Parameters | 0.5 | | | | | | | | | | | | | |
| GC134 | Stoner, D. L. | Development and Application of Custom Flow Models for Understanding Flow in Porous and Fractured Matrices with Biological Components | 1.8 | | | | | | | | | | | | | |
| S472 | Stoner, D. L. | Integrated Experimental and Mathematical Analysis of Complex Chemical and Biological Systems | 1.15 | | | | | | | | | | 1 | | | |
| ST104 | Stormberg, A. I. | Use of Genetic Markers for Ecological Risk Assessment | 0 | | | | | | | | | | | 1 | | |
| GC144 | Stormberg/ McGlone | Characterization of Nonlinear Complex Resistivity Spectra During Biochemical Reduction of Cr to Cr+6+3 | 0.6 | | 1 | | | | 1 | | 1 | 1 | 1 | 1 | 1 | 1 |
| NS107 | Swank, W. D. | Plasma Spray Processing Development for Energetic Materials | 1 | | | | | | | | | | | | | |
| ES107 | Szpakiewicz, M. J. | Assessment of Long-Term Variations in Soil Moisture and Regional Ground water Flow Patterns in Response to Potential Climate Changes | | | | | | | | | | | | | | |
| D437 | Telschow, K. L. | Laser Ultrasonic Characterization of Irradiated Ceramics | 1.7 | | | | | | | | | | | 1 | | |
| NC101 | Telschow, K. L. | Nanostructure Characterization for Sensing | 0.57 | | 1 | 4 | 1 | | | | | | | | | |
| NE118 | Telschow, K. L. | Laser Ultrasonic Corrosion Monitor | 0.8 | | | | | | | | | | | 1 | | |
| SC104 | Thantu, N. | Trace Chemical Species Detection and Analysis Using Femtosecond Optical Heterodyne Detected Raman Induced Kerr Effect Spectroscopy | 0.9 | | | 1 | | | | | | | 1 | | 1 | |
| CE101 | Thompson, D. N. | Removal of Minerals from Wheat Straw for Increased Straw Utilization for Bioenergy and Bioproducts | 1 | | | | | | | | | | 1 | | | |
| GC109 | Thompson, V. S. | Development of Enzymatic Biosensors for Environmental Applications | 1.125 | | | | | | | | | | | | | |

## Appendix D–Project Performance

| Project ID | Principal Investigator | Project Title | FTE | Other Students | Post Docs | Faculty | Crada | WFO | IDR | Patents Awarded | Copyrighting/Trademark | License | Publications | Presentations | Symposia | Awards |
|---|---|---|---|---|---|---|---|---|---|---|---|---|---|---|---|---|
| WT103 | Todd, T. A. | Polyacrylonitrile-Based Ion Exchange Sorbents | 0.8 | | | 1 | | | 2 | | | | 2 | | | |
| CE109 | Tolle, C. R. | Computational Fluid Dynamics Model Based Control of Two-Phase Flow | 0.73 | | | | | | | | | | | | | |
| NS125 | Totemeier, T. C. | Mechanisms of Liquid Metal Embrittlement in Steels | 0.4 | | | | | | | | | | | | | |
| ES105 | Tranter, T. J. | Porous Crystalline Silica (Gubka)-Based Ion Exchange Sorbents | 0.41 | | | | 1 | 1 | 2 | 1 | 2 | | | | | |
| SC112 | VanSiclen, C . D. | Mechanical and Flow Properties of Dry Granular Media | 0.33 | | | | | | | | | | | | | |
| NS114 | Velasquez, M. E. | Exploring Applications of Wavelet Theory: Groundwater Dynamical Systems, Gamma Spectral Analysis, Accoustic Resonance Spectrometry | 0.5 | 1 | 1 | 1 | | | | | | | | | | |
| GC141 | Versteeg,R. J. | Calibration and Enhancement of Geophysical Imaging Tools in a Mesoscale Experimental Facility | 0.621 | 1 | | | | | | | | | | 1 | | |
| CE105 | Ward, T. E. | Acidophilic Bioprocess for Production of Organic Acids from Biomass | 0.7 | | | | | | 1 | | | | | | | |
| NE122 | Weaver, K. D. | An Innovative Gas-Cooled Fast Reactor | 1.3 | 3 | | 2 | | | | | | | | | | |
| Gc103 | Weinberg, D. M. | Fracture Prediction, Characterization, and Detection in Snake River Basalts-A Modeling and Field Approach | 0.6 | 1 | | 2 | | | | | | | 7 | | | |
| GC105 | Weinberg, D. M. | Advanced Borehole Seismic Sources for High-Resolution Subsurface Imaging and Characterization for Environmental Applications | 2.6 | 4 | | 2 | | | | | | | | 1 | | |
| NE123 | Weinberg, D. M. | Characterization Methane Hydrate Deposits | 1.2 | | | | | | 1 | | | | 4 | | | 1 |
| PH104 | Weinberg, D. M. | Modeling an Earth Borehole System for Physical Property Determination in Shallow Subsurface Environments with Emphasis on Vadose Zone Applications. | 0.5 | 1 | 1 | 1 | 1 | | | | | | | | | |
| ET115 | White, G. J. | Carbon Fractionation Potential of Soils via $CO_2$/Water Gradient Fractionation | 0.7 | | | | | | | | | | | | | |

## *Appendix D–Project Performance*

| Project ID | Principal Investigator | Project Title | FTE | Other Students | Post Docs | Faculty | Crada | WFO | IDR | Patents Awarded | Copyrighting/Trademark | License | Publications | Presentations | Symposia | Awards |
|---|---|---|---|---|---|---|---|---|---|---|---|---|---|---|---|---|
| GC104 | White, G. J. | Carbon Fractionation Potential of Soils Via $CO_2$/Water Gradient Fractionation | | | | | | | | | | | | | | |
| ST106 | White, G. J. | Development of Collaborative Approaches to Long-Term Environmental Stewardship | 0.9 | 5 | | 3 | | | | | | | 1 | | | |
| | | **Totals** | **119.5** | **69** | **28** | **81** | **9** | **1** | **28** | **2** | **9** | **8** | **111** | **75** | **21** | **9** |

## Appendix E–Relevence to Major DOE Missions

| Project ID | Principal Investigator | Project Title | Environmental Quality | Energy | Science and Technology | National Defense |
|---|---|---|---|---|---|---|
| ET110 | Abbott, M. L. | Elemental Tracers and Multi-Variate Receptor Modeling Methods in Assessing Air Pollution | X | | X | |
| ET108 | Alessi, R. S. | Improving Stakeholder Interactions: A Stakeholder-Based Research Methodology for Reaching Decisions of Polarized Issues | X | X | | |
| NE120 | Anderson, R. P. | Hydrogen Production from High Temperature Nuclear Reactors | | X | | |
| NE125 | Anderson, R. P. | Hydrogen Technologies | | X | | |
| ET105 | Apel, W. A. | Biologically Based Catalysts for Processing and Detection in Harsh Service Conditions | X | X | X | |
| GC142 | Apel, W. A. | Development of Sensors for Detection of Metal-Reducing Bacteria in Mesoscale and Field Experiments | X | | X | |
| S028 | Appelhans, A. D. | New Ion Injection Technologies for Ion Trap Secondary Ion Mass Spectrometry | X | | X | |
| NS109 | Aryaeinejad, R. | Second Generation Neutron/Gamma Sensor | | | X | X |
| ST102 | Atkinson, D. A. | Airborne Contaminant Gradient Mapping System | X | | X | |
| SC105 | Atkinson, D. A. | Ion Mobility Spectrometry | X | | X | X |
| WT106 | Baker, J. D. | Energy-Dispersive, X-Ray Fluorescence Excitation Source for In-Field Analysis | X | | X | |
| GC124 | Barnes, J. M. | Use of Molecular Markers for Detection and Tracking of Environmental Bacteria | X | | X | |
| NS123 | Bauer, S. G. | Multipath Propagation Analysis, Simulation, and Prediction in Wireless Environments | | | X | X |
| NS102 | Benson, M. T. | Selected Release of Polymer Degradation Agents by Photoinitiation | | | X | X |
| ST108 | Berrett, S. | Long-Term Record Storage for Long-Term | X | X | X | |
| NE121 | Boardman, R. D. | Co-Firing of Coal and Refuse-Derived Fuel with Oil Shale for Control of Environmental Contaminants and Improved Energy Production: LaboratoryStudies | X | X | X | |
| ET116 | Bruemmer, D. J. | Advanced Control Architectures for Human-Robot Synergy in Complex Domains | X | X | X | X |
| CS115 | Carrington, R. A. | Use of Thermally Sprayed Traces for Damage Detection and Data Transmission | | X | X | X |

## Appendix E–Relevence to Major DOE Missions

| Project ID | Principal Investigator | Project Title | Environmental Quality | Energy | Science and Technology | National Defense |
|---|---|---|---|---|---|---|
| CS116 | Chu, H. S. | Development of Blast and Penetration Resistant Materials and Systems for Comprehenisve Protection of Vehicles, Personnel and Buildings | | X | X | X |
| WT108 | Cordes, G. A. | Enhanced Sample Based Modeling Techniques for Nondestructive Analysis and Long-Term Stewardship | X | | | |
| GC131 | Cummings, D. E. | Characterizing Microbial Population Shifts in Response to Alternative Electron Donors and their Effect on Trichloroethylene Dexhlorination Efficiency | X | | X | |
| SC113 | Deason, V. A. | Detection of Buried Objects using Imaging Laser Acoustics | X | | X | |
| NS104 | Derr, K. W. | Information Visualization By Query | | X | X | |
| CS114 | Dudenhoeffer, D. D. | Critical Infrastructure Critical Subnetwork | | X | | X |
| H062 | Dudenhoeffer, D. D. | Behavioral and Control Modeling for Large Scale Micro-Robot Systems | X | | | X |
| PH102 | Eide, S. A. | Characterization of Legacy Risk | X | | | |
| NE108 | Evans, R. P. | Two-Phase Mass Flow Measurement for Geothermal Wells | | X | X | |
| NC102 | Fincke, J. R. | Controlled Growth of Nanowires | X | | X | |
| WT107 | Fox, R. V. | Direct Dissolution of Plutonium and Neptunium Species Using Complexing Agents in Carbon Dioxide | X | | X | |
| ET114 | Fujita, Y. | Use of Engineered Nano-Particles for Nutrient Delivery and Bioremediation in Subsurface Environments | X | | X | |
| NE115 | Gering, K. L. | Clean Cold Start Technology for Conventional, Electric, and Hybrid Vehicles | | X | X | |
| WT105 | Gombert, D. | Steam Reforming in Micro-Reactors for Destruction of Hazardous Organic Materials | X | | X | |
| WT101 | Gombert, D. | Cold-Crucible Design Parameters for Next Generation High Level Waste Melters | X | | X | |
| AC104 | Greenwade, L. E. | Development and Validation of Advanced Simulation and Collaboration Capability | X | | | |
| GC143 | Groenewold, G. S. | Characterization of Dense Non-Aqueous Phase Liquids Adsorption/Desorption to Geological Media | X | | X | |
| ST109 | Hamilton, M. A. | Uptake and Translocation Patterns of Strontium by Sagebrush Steppe Ecosystem Plants | X | X | | |

| Project ID | Principal Investigator | Project Title | Environmental Quality | Energy | Science and Technology | National Defense |
|---|---|---|---|---|---|---|
| PH103 | Harbour, G. L. | Residual Hazards Management: Decisions Leading Toward Success or Failure? | X | | | |
| WT104 | Harbour, G. L. | Model-Based Decision Making | X | X | | |
| GC111 | Harrup, M. K. | Hybrid Nanocomposite Materials as Subsurface Permeable Reactive Barriers | X | | | |
| NE112 | Harrup, M. K. | Novel Solid Electrolyte Materials for Lithium Batteries | X | | X | |
| NE117 | Hartwell, J. K. | Active Neutron Spectroscopy for Neutron Capture Beam Characterization | | | X | |
| GE102 | Harvego, E. A. | Advanced Transient Analysis Capabilities for Generation IV Nuclear Reactors | | X | | |
| GC133 | Heath, G. L. | Electrical Resistivity Imaging to Define Preferred Flow Paths in a Heterogeneous Layered Vadose Zone | X | | | |
| GC108 | Heath, G. L. | Advanced Technology for Mapping Subsurface Water Conductivity | X | | X | |
| GE104 | Herring, J. S. | Advanced Nuclear Fuels for Enhanced Proliferation Resistance | X | X | | |
| GC137 | Hertzog, R. C. | Quantitative Deep-Reading Vadose Zone Moisture Characterization | X | | | |
| GC138 | Hertzog, R. C. | Application of New Borehole Geophysical Methods for Stratigraphic Correlation and Identification of Non-Aqueous-Phase Contaminants | X | | X | |
| PH106 | Hertzog, R. C. | A New Hydrogeophysical Method for Characterizing and Monitoring Preferential Flow Paths in Complex Layered and Fractured Basalt | X | | X | |
| CE102 | Hess, J. R. | Characterization and Modeling of a Grain Combine Harvester | | X | | |
| CE110 | Hoskinson, R. L. | Development of Analytical Decision-making Tools for Energy Efficient Agricultural Biomass Production | | X | | |
| ST107 | Jacobson, J. J. | DOE Complex-Wide Long-Term Stewardship Options Analysis System | X | | | |
| SC114 | Johnson, K. B. | High Intensity Perrhenate Ion Gun for Use as a Primary Ion Beam in Secondary Ion Mass Spectroscopy | X | | X | X |

## *Appendix E–Relevence to Major DOE Missions*

| Project ID | Principal Investigator | Project Title | Environmental Quality | Energy | Science and Technology | National Defense |
|---|---|---|---|---|---|---|
| GC123 | Johnson, R. W. | Advanced Simulation Method Development | X | | X | |
| NS122 | Jones, J. L. | A Compton-Backscatter Photon Source for Tunable, Monoenergetic, Hard X-rays | | | X | X |
| GC139 | Keener, W. K. | Demonstration of Spatially-Resolved Molecular Approach to Detect Specific Microbial Activity on Mineral Surfaces | X | | X | |
| NS129 | Kenney, K. L. | Mechanical, Physical and Metallurgical Factors Affecting Liquid-Metal Embrittlement of Steels | | | X | X |
| ES101 | Kong, P. C. | Cermet Filters for Hazardous Material, Chemical and Biological Agent Destruction | | | | X |
| NS124 | Kotter, D. K. | Micro antenna Infrared Tags | | | | X |
| NS119 | Kotter, D. K. | Distant Neutron Source Detection and Location | | | | X |
| NS110 | Kunerth, D. C. | Ultrasonic Detection and Characterization of Buried Objects: Air-Coupled Techniques | X | | X | X |
| AC101 | Larson, T. K. | Parallel Computing with Cluster Technology | X | X | X | |
| GC132 | Lenhard, R. J. | Nonaqueous-Phase Fluid Behavior in the Vadose Zone: Model Development andT esting | X | | X | |
| GC135 | Lenhard, R. J. | Investigation of the Movement and Fate of Chlorinated Hydrocarbons | X | | | |
| NC103 | Lessing, P. A. | Enhanced Transport in Nanocrystalline Ceramic Films | X | X | X | |
| PH107 | Liang, J. | Dependence of Coal Bed Permeability on Pore Pressure and Adsorbed Gas Content | X | X | X | |
| NE124 | Liang, J. | Carbon Dioxide Sequestration in Geologic Coal Formations | | X | | |
| GE105 | MacDonald, P . E. | Design of an Actinide Burning, Lead or Lead-Bismuth Reactor that Produces Low Cost Electricity | | X | | X |
| GC146 | Mattson, E. D. | Investigation of the Effects of Microbial Growth on Unsaturated Hydraulic Properties | X | | | |
| CS103 | McQueen, M. A. | Survivable Networks of Dynamic Systems | | | | X |
| GC136 | Meakin, P. | Modeling of Flow and Colloid Behavior in Subsurface Fractures | X | X | X | |
| NE109 | Mecham, D. C. | Thermal Studies of Potential Increased Advanced Test Reactor Power Margins | | X | | X |

## Appendix E–Relevence to Major DOE Missions

| Project ID | Principal Investigator | Project Title | Environmental Quality | Energy | Science and Technology | National Defense |
|---|---|---|---|---|---|---|
| ES102 | Moore, G. A. | Novel Cyclodextrin-Based Sorbent Materials for Waste Separation Needs | X | | X | X |
| GC125 | Moore, G. A. | Natural and Synthetic Subsurface Colloids | X | | X | |
| NS131 | Novack, S. D. | Technical Advancement of the INEEL Critical Infrastructure Protection Supervisory Control and Data Acquisition Test Bed | | | | X |
| ES106 | Novack, S. D. | Probabilistic Risk Monitoring Software for SAPHIRE | X | X | X | |
| AC103 | Novack, S. D. | Aerospace Situation Awareness and Risk Monitor Tool | | X | | X |
| NE110 | O'Brien, J. E. | High-Temperature Flow Measurement of Molten Salts | | X | X | X |
| NS127 | O'Brien, M. H. | Cutting of Structural Materials using Energetic Materials | | | X | X |
| GC101 | Oh, C. H. | Fundamental Studies on Gas Contaminant Mobility in the Vadose Zone from Atmospheric Pressure Fluctuations | X | | X | |
| GE106 | Ougouag, A. M. | Developmentof a Nodal Diffusion Method for Cylindrical-Geometry Reactor Cores | | X | X | X |
| GC106 | Partin, J. K. | Enhanced Techniques for Evaluating Colloidal Transport Processes | X | | X | |
| GE101 | Petti, D. A. | The Modular Pebble-Bed Reactor | | X | | X |
| ET106 | Piet, S. J. | Making Sustainable Decisions Using the *K*ONVE*R*GENCE Framework | X | X | | |
| GC117 | Pinhero, P. J. | Evaluating Microelectrodes and Fiber-Optic Probes for use in Meso-Scale Experiments | X | | X | |
| GC113 | Pinhero, P. J. | Chemical Modification of Atomic Force Microscope Probes for Imaging Patterned Molecular Architectures | X | | X | |
| PH101 | Radtke, C. W. | In-Situ Bioremediation of Explosives in the Vadose Zone | X | | | |
| WT110 | Raman, S. V. | Advanced Formulation for Homogenization of Refractory Components in Glass and Ceramic | X | | | |
| GC114 | Redden, G. D. | Kinetics and Mechanisms of Inter-Surface Transfer, and Solid-Solution Partitioning, of Surface-Complexed Metals in Colloidal Systems | X | | X | |
| GC116 | Redden, G. D. | Organic Co-Solvent and Co-Contaminant Effects on Sorption of Uranyl and Cesium to Metal Oxide Surfaces | X | | X | |

## Appendix E–Relevence to Major DOE Missions

| Project ID | Principal Investigator | Project Title | Environmental Quality | Energy | Science and Technology | National Defense |
|---|---|---|---|---|---|---|
| NE114 | Richins, W. D. | Energy Efficient Building Simulation and Technologies | X | X | | |
| NS118 | Roberto, F. F. | Novel Selective Matrix for Collection and Identification of Priority Pathogens | | | X | X |
| NC104 | Rollins, H. W. | Nucleation and Growth of Nanoparticle Materials in Supercritical Fluid Processes | | X | X | |
| NS121 | Roney, T. J. | Imaging Application of Photon Beams Produced with Compton Backscatter of Laser Beams | | | X | |
| ST105 | Rope, R. C. | Development of an Integrated Watershed Information Management Tool for Long-Term Facilities Stewardship | X | | | |
| GC140 | Schafer, A. L. | Computational Experiments of Hysteretic Chemical and Moisture Migration | X | | X | |
| GE103 | Schultz, R. R. | Gas-Cooled Reactor System Analysis Tools | | X | | |
| GC145 | Scott, C. L. | Dual Electrode sand Defining the Electrically Disturbed Region in Induced Polarization Measurements | X | X | | |
| SC111 | Scott, J. R. | Elucidating the Photo-Physics of Complex MetalIons Trapped in a Fourier Transform Mass Spectrometer | X | | X | |
| GC119 | Scott, J. R. | Development of Imaging Fourier Transform Mass Spectrometer Capabilities for Analyses of Complex and Heterogeneous Samples | X | | X | |
| NS128 | Shewmaker, A. G. | Classified Cluster Computing | | X | | X |
| AC102 | Shook, G. M. | Improving Numerical Model Efficiency of a Simulation Model | X | X | | |
| ET107 | Silverman, H. G. | Recombinant Adhesive Protein Production and Investigation in to Alternate Natural Adhesive Systems in Marine Mussels | | | X | X |
| PH105 | Sisson, J. B. | Improving Soil Water Flux Estimates in the Deep Vadose Zone | X | | X | |
| NE111 | Smartt, H. B. | Friction Stir Welding of Lightweight Materials | | X | X | |
| GC102 | Smith, R. P. | Regional Setting and Flow Dynamics of the Snake River Plain Aquifer | X | | X | |
| GC130 | Starr, R. C. | Development of Techniques for In Situ Measurement of Groundwater Contaminant Source Strength | X | | X | |
| CE108 | Steffler, E. D. | Genetics Control of Straw Stem Ultrasound that Affects theBiomechanics of Stem Separation | | X | X | |

## Appendix E–Relevence to Major DOE Missions

| Project ID | Principal Investigator | Project Title | Environmental Quality | Energy | Science and Technology | National Defense |
|---|---|---|---|---|---|---|
| GC107 | Stone, M. L. | Improved Osmotic Tensiometer Components and Parameters | X | | X | |
| GC134 | Stoner, D. L. | Development and Application of Custom Flow Models for Understanding Flow in Porous and Fractured Matrices with Biological Components | X | | X | |
| S472 | Stoner, D. L. | Integrated Experimental and Mathematical Analysis of Complex Chemical and Biological Systems | X | | X | |
| ST104 | Stormberg, A. I. | Use of Genetic Markers for Ecological Risk Assessment | X | | | |
| GC144 | Stormberg/McGlone | Characterization of Nonlinear Complex Resistivity Spectra During Biochemical Reduction of Cr to Cr+6+3 | X | | X | |
| NS107 | Swank, W. D. | Plasma Spray Processing Development for Energetic Materials | | | X | |
| ES107 | Szpakiewicz, M. J. | Assessment of Long Term Variations in Soil Moisture and Regional Groundwater Flow Patterns in Response to Potential Climate Changes | X | | | |
| NE118 | Telschow, K. L. | Laser Ultrasonic Corrosion Monitor | | X | X | X |
| D437 | Telschow, K. L. | Laser Ultrasonic Characterization of Irradiated Ceramics | | | X | X |
| NC101 | Telschow, K. L. | Nanostructure Characterization for Sensing | X | | X | |
| SC104 | Thantu, N. | Trace Chemical Species Detection and Analysis Using Fem to second Optical Heterodyne Detected Raman Induced Kerr Effect Spectroscopy | X | | X | |
| CE101 | Thompson, D. N. | Removal of Minerals from Wheat Straw for Increased Straw Utilization for Bioenergy and Bioproducts | | X | X | |
| GC109 | Thompson, V. S. | Development of Enzymatic Biosensors for Environmental Applications | X | | X | |
| WT103 | Todd, T. A. | Polyacrylonitrile-Based Ion Exchange Sorbents | X | | X | |
| CE109 | Tolle, C. R. | Computational Fluid Dynamics Model Based Control of Two-Phase Flow | | X | X | |
| NS125 | Totemeier, T. C. | Mechanisms of Liquid Metal Embrittlement in Steels | | | X | X |
| ES105 | Tranter, T. J. | Porous Crystalline Silica (Gubka)-Based Ion Exchange Sorbents | X | | X | |
| SC112 | VanSiclen, C . D. | Mechanical and Flow Properties of Dry Granular Media | X | | X | X |

## *Appendix E–Relevence to Major DOE Missions*

| Project ID | Principal Investigator | Project Title | Environmental Quality | Energy | Science and Technology | National Defense |
|---|---|---|---|---|---|---|
| NS114 | Velasquez, M. E. | Exploring Applications of Wavelet Theory: Groundwater Dynamical Systems, Gamma Spectral Analysis, Accoustic Resonance Spectrometry | X | | X | |
| GC141 | Versteeg, R. J. | Calibration and Enhancement of Geophysical Imaging Tools in a Mesoscale Experimental Facility | X | | | |
| CE105 | Ward, T. E. | Acidophilic Bioprocess for Production of Organic Acids from Biomass | | X | X | |
| NE122 | Weaver, K. D. | An Innovative Gas-Cooled Fast Reactor | | X | | X |
| PH104 | Weinberg, D. M. | Modeling an Earth Borehole System for Physical Property Determination in Shallow Subsurface Environments with Emphasis on Vadose Zone Applications | X | X | X | X |
| NE123 | Weinberg, D. M. | Characterization of Methane Hydrate Deposits | | X | | |
| GC105 | Weinberg, D. M. | Advanced Borehole Seismic Sources for High-Resolution Subsurface Imaging and Characterization for Environmental Applications | X | | X | |
| GC103 | Weinberg, D. M. | Fracture Prediction, Characterization, and Detection in Snake River Basalts-A Modeling and Field Approach | X | | X | |
| ST106 | White, G. J. | Development of Collaborative Approaches to Long-Term Environmental Stewardship | X | | X | |
| ET115 | White, G. J. | Carbon Fractionation Potential of Soils via $CO_2$/Water Gradient Fractionation | | | | |
| GC104 | White, G. J. | Carbon Fractionation Potential of Soils via $CO_2$/Water Gradient Fractionation | X | | X | |

*Appendix F–*
## *Relevence to Major National Missions*

## Appendix F–Relevence to Major National Missions

| Project ID | Principal Investigator | Project Title | National Nuclear Security Administration | Environmental Management | EE - Industrial Technologies | FE - Fossil Energy | NE - Nuclear Energy | NR - Naval Reactors | SC - Office of Science |
|---|---|---|---|---|---|---|---|---|---|
| ET110 | Abbott, M. L. | Elemental Tracers and Multi-Variate Receptor Modeling Methods in Assessing Air Pollution | X | X | | | | | |
| ET108 | Alessi, R. S. | Improving Stakeholder Interactions: A Stakeholder-Based Research Methodology for Reaching Decisions on Polarized Issues | X | X | X | | X | | X |
| NE120 | Anderson, R. P. | Hydrogen Production from High Temperature Nuclear Reactors | | X | | X | X | | |
| NE125 | Anderson, R. P. | Hydrogen Technologies | | | X | X | | | |
| ET105 | Apel, W. A. | Biologically Based Catalysts for Processing and Detection in Harsh Service Conditions | | X | X | | | | X |
| GC142 | Apel, W. A. | Development of Sensors for Detection of Metal-Reducing Bacteria in Mesoscale and Field Experiments | | X | | | | | X |
| S028 | Appelhans, A. D. | New Ion Injection Technologies for Ion Trap Secondary Ion Mass Spectrometry | X | X | | | X | | X |
| NS109 | Aryaeinejad, R. | Second Generation Neutron/Gamma Sensor | X | X | | | X | | |
| ST102 | Atkinson, D. A. | Airborne Contaminant Gradient Mapping System | X | X | | X | | | X |
| SC105 | Atkinson, D. A. | Ion Mobility Spectrometry | X | X | | X | | | X |
| WT106 | Baker, J. D. | An Energy-Dispersive, X-ray Fluorescence Excitation Source for In-field Analysis | | X | | | X | | X |
| GC124 | Barnes, J. M. | Use of Molecular Markers for Detection and Tracking of Environmental Bacteria | | X | | | | | X |
| NS123 | Bauer, S. G. | Multipath Propagation Analysis, Simulation, and Prediction in Wireless Environments | X | | | | | | |
| NS102 | Benson, M. T. | Selected Release of Polymer Degradation Agents by Photoinitiation | X | | | | | | X |
| ST108 | Berrett, S. | Long-Term Record Storage for Long-Term Stewardship | | X | | | | | |
| NE121 | Boardman, R. D. | Co-Firing of Coal and Refuse-Derived Fuel with Oil Shale for Control of Environmental Contaminants and Improved Energy Production: Laboratory Studies | | X | X | X | | | |
| ET116 | Bruemmer, D. J. | Advanced Control Architectures for Human-Robot Synergy in Complex Domains | X | X | | | X | | X |
| CS115 | Carrington, R. A. | Use of Thermally Sprayed Traces for Damage Detection and Data Transmission | X | | | | | | |

## Appendix F–Relevence to Major National Missions

| Project ID | Principal Investigator | Project Title | National Nuclear Security Administration | Environmental Management | EE - Industrial Technologies | FE - Fossil Energy | NE - Nuclear Energy | NR - Naval Reactors | SC - Office of Science |
|---|---|---|---|---|---|---|---|---|---|
| CS116 | Chu, H. S. | Development of Blast and Penetration Resistant Materials and Systems for Comprehenisve Protection of Vehicles, Personnel and Buildings | X | | | | | | X |
| WT108 | Cordes, G. A. | Enhanced Sample Based Modeling Techniques for Nondestructive Analysis and Long-Term Stewardship | | X | | | | | |
| GC131 | Cummings, D. E. | Characterizing Microbial Population Shifts in Response to Alternative Electron Donors and their Effect on Trichloroethylene Dexhlorination Efficiency | | X | | | | | X |
| SC113 | Deason, V. A. | Detection of Buried Objects using Imaging Laser Acoustics | X | X | X | X | | | X |
| NS104 | Derr, K. W. | Information Visualization By Query | X | X | X | X | | | |
| CS114 | Dudenhoeffer, D. D. | Critical Infrastructure Critical Subnetwork | X | | X | X | X | | |
| H062 | Dudenhoeffer, D. D. | Behavioral and Control Modeling for Large Scale Micro-Robot Systems | X | X | | | | | X |
| PH102 | Eide, S. A. | Characterization of Legacy Risk | X | X | | | X | | |
| NE108 | Evans, R. P. | Two-Phase Mass Flow Measurement for Geothermal Wells | | | X | | X | | |
| NC102 | Fincke, J. R. | Controlled Growth of Nanowires | | X | | | | | X |
| WT107 | Fox, R. V. | Direct Dissolution of Plutonium and Neptunium Species Using Complexing Agents in Carbon Dioxide | | X | | | | | |
| ET114 | Fujita, Y | Use of Engineered Nano-Particles for Nutrient Delivery and Bioremediation in Subsurface Environments | | X | | | | | |
| NE115 | Gering, K. L. | Clean Cold Start Technology for Conventional, Electric, and Hybrid Vehicles | | | X | | | | X |
| WT105 | Gombert, D. . | Steam Reforming in Micro-Reactors for Destruction of Hazardous Organic Materials | | X | | | | | |
| WT101 | Gombert, D. . | Cold-Crucible Design Parameters for Next Generation High Level Waste Melters | | X | | | X | | |
| AC104 | Greenwade, L. E. | Development and Validation of Advanced Simulation andCollaboration Capability | X | X | X | X | X | | X |
| GC143 | Groenewold, G. S. | Characterization of Dense Non-Aqueous Phase Liquids Adsorption/Desorption to Geological Media | | X | | | | | |
| ST109 | Hamilton, M. A. | Uptake and Translocation Patterns of Strontium by Sagebrush Steppe Ecosystem Plants | X | | | | | | |

| Project ID | Principal Investigator | Project Title | National Nuclear Security Administration | Environmental Management | EE - Industrial Technologies | FE - Fossil Energy | NE - Nuclear Energy | NR - Naval Reactors | SC - Office of Science |
|---|---|---|---|---|---|---|---|---|---|
| PH103 | Harbour, G. L. | Residual Hazards Management: Decisions Leading Toward Successor Failure? | | X | | | | | |
| WT104 | Harbour, G. L. | Model-Based Decision Making | X | X | X | X | X | | |
| GC111 | Harrup, M. K. | Hybrid Nanocomposite Materials as Subsurface Permeable Reactive Barriers | | X | | | | | X |
| NE112 | Harrup, M. K. | Novel Solid Electrolyte Materials for Lithium Batteries | X | | X | | | | X |
| NE117 | Hartwell, J. K. | Active Neutron Spectroscopy for Neutron Capture Beam Characterization | | | | | X | | X |
| GE102 | Harvego, E. A. | Advanced Transient Analysis Capabilities for Generation IV Reactors | X | | | | X | X | |
| GC133 | Heath, G. L. | Electrical Resistivity Imaging to Define Preferred Flow Paths in a Heterogeneous Layered Vadose Zone | | X | | | | | X |
| GC108 | Heath, G. L. | Advanced Technology for Mapping Subsurface Water Conductivity | | X | | X | | | |
| GE104 | Herring, J. S. | Advanced Nuclear Fuels for Enhanced Proliferation Resistance | X | | | | X | X | |
| GC137 | Hertzog, R. C. | Quantitative Deep-Reading Vadose Zone Moisture Characterization | | X | | X | | | |
| GC138 | Hertzog, R. C. | Application of New Borehole Geophysical Methods for Stratigraphic Correlation and Identification of Non-Aqueous-Phase Contaminants | | X | | | | | X |
| PH106 | Hertzog, R. C. | A New Hydrogeophysical Method for Characterizing and Monitoring Preferential Flow Paths in Complex Layered andFractured Basalt | | X | | | | | |
| CE102 | Hess, J. R. | Characterizaiton and Modeling of a Grain Combine Harvester | | | X | X | | | X |
| CE110 | Hoskinson, R. L. | Development of Analytical Decision-making Tools for Energy Efficient Agricultural Biomass Production | | | X | | | | X |
| ST107 | Jacobson, J. J. | DOE Complex-Wide Long-Term Stewardship Options Analysis System | X | X | | | | | X |
| SC114 | Johnson, K. B. | High Intensity Perrhenate Ion Gun for Use as a Primary Ion Beam in Secondary Ion Mass Spectroscopy | X | X | | | | | X |

## Appendix F–Relevence to Major National Missions

| Project ID | Principal Investigator | Project Title | National Nuclear Security Administration | Environmental Management | EE - Industrial Technologies | FE - Fossil Energy | NE - Nuclear Energy | NR - Naval Reactors | SC - Office of Science |
|---|---|---|---|---|---|---|---|---|---|
| GC123 | Johnson, R. W. | Advanced Simulation Method Development | | X | | | | | X |
| NS122 | Jones, J. L. | A Compton-Back Scatter Photon Source for Tunable, Monoenergetic, Hard X-rays | X | | | | | | X |
| GC139 | Keener, W. K. | Demonstration of Spatially-Resolved Molecular Approach to Detect Specific Microbial Activity on Mineral Surfaces | | X | | | | | X |
| NS129 | Kenney, K. L. | Mechanical, Physical and Metallurgical Factors Affecting Liquid-Metal Embrittlement of Steels | X | | | | | | X |
| ES101 | Kong, P. C. | Cermet Filters for Hazardous Material, Chemical and Biological Agent Destruction | X | X | | | | | |
| NS124 | Kotter, D. K. | Microantenna Infrared Tags | X | | | | | | |
| NS119 | Kotter, D. K. | Distant Neutron Source Detection and Location | X | X | | | | | |
| NS110 | Kunerth, D. C. | Ultrasonic Detection and Characterization of Buried Objects: Air-Coupled Techniques | X | X | | | | | |
| AC101 | Larson, T. K. | Parallel Computing with Cluster Technology | X | X | | | X | | X |
| GC132 | Lenhard, R. J. | Nonaqueous-Phase Fluid Behavior in the Vadose Zone: Model Development and Testing | | | X | | | | |
| GC135 | Lenhard, R. J. | Investigation of the Movement and Fate of Chlorinated Hydrocarbons | | | X | | | | X |
| NC103 | Lessing, P. A. | Enhanced Transport in Nanocrystalline Ceramic Films | | X | X | X | | | X |
| PH107 | Liang, J. | Dependence of Coal Bed Permeability on Pore Pressure and Adsorbed Gas Content | | X | X | X | | | X |
| NE124 | Liang, J. | Carbon Dioxide Sequestration in Geologic Coal Formations | | | | X | | | |
| GE105 | MacDonald, P. E. | Design of an Actinide Burning, Lead or Lead-Bismuth Reactor that Produces Low Cost Electricity | X | | | | X | X | |
| GC146 | Mattson, E. D. | Investigation of the Effects of Microbial Growth on Unsaturated Hydraulic Properties | | X | | X | | | X |
| CS103 | McQueen, M. A. | Survivable Networks of Dynamic Systems | X | | | | | | X |
| GC136 | Meakin, P. | Modeling of Flow and Colloid Behavior in Subsurface Fractures | | X | | X | | | X |
| NE109 | Mecham, D. C. | Thermal Studies of Potential Increased Advanced Test Reactor Power Margins | X | | | | X | | X |

## Appendix F–Relevence to Major National Missions

| Project ID | Principal Investigator | Project Title | National Nuclear Security Administration | Environmental Management | EE - Industrial Technologies | FE - Fossil Energy | NE - Nuclear Energy | NR - Naval Reactors | SC - Office of Science |
|---|---|---|---|---|---|---|---|---|---|
| ES102 | Moore, G. A. | Novel Cyclodextrin-Based Sorbent materials for Waste Separation Needs | X | X | | | | | X |
| GC125 | Moore, G. A. | Natural and Synthetic Subsurface Colloids | | X | | | | | X |
| NS131 | Novack, S. D. | Technical Advancementof the INEEL Critical Infrastructure Protection Supervisory Control and Data Acquisition Test Bed | X | | | | | | |
| ES106 | Novack, S. D. | Probabilistic Risk Monitoring Software for SAPHIRE | | X | | | X | | |
| AC103 | Novack, S. D. | Aerospace Situation Awareness and Risk Monitor Tool | X | | | | X | | |
| NE110 | O'Brien, J. E. | High-Temperature Flow Measurement of Molten Salts | | | | | X | | |
| NS127 | O'Brien, M. H. | Cutting of Structural Materials using Energetic Materials | X | | | | | | X |
| GC101 | Oh, C. H. | Fundamental Studies on Gas Contaminant Mobility in the Vadose Zone from Atmospheric Pressure Fluctuations | | X | | | | | X |
| GE106 | Ougouag, A. M. | Development of a Nodal Diffusion Method for Cylindrical-Geometry Reactor Cores | X | | | | X | X | X |
| GC106 | Partin, J. K. | Enhanced Techniques for Evaluating Colloidal Transport Processes | | X | | | | | |
| GE101 | Petti, D. A. | The Modular Pebble-Bed Reactor | X | | | | X | X | X |
| ET106 | Piet, S. J. | Making Sustainable Decisions Using the *K*ONVE*R*GENCE Framework | | X | | | X | | |
| GC117 | Pinhero, P. J. | Evaluating Microelectrodes and Fiber-Optic Probes for use in Meso-Scale Experiments | | X | | | | | |
| GC113 | Pinhero, P. J. | Chemical Modification of Atomic Force Microscope Probes for Imaging Patterned Molecular Architectures | | X | | | | | X |
| PH101 | Radtke, C. W. | In Situ Bioremediation of Explosives in the Vadose Zone | | X | | | | | X |
| WT110 | Raman, S. V. | Advanced Formulation for Homogenization of Refractory Components in Glass and Ceramic Phases | | X | | | | | X |
| GC114 | Redden, G. D. | Kinetics and Mechanisms of Inter Surface Transfer, and Solid-Solution Partitioning, of Surface-Complexed Metals in Colloidal Systems | | X | | | | | X |
| GC116 | Redden, G. D. | Organic Co-Solvent and Co-Contaminant Effects on Sorption of Uranyl and Cesium to Metal Oxide Surfaces | | X | | | | | |

## Appendix F–Relevence to Major National Missions

| Project ID | Principal Investigator | Project Title | National Nuclear Security Administration | Environmental Management | EE - Industrial Technologies | FE - Fossil Energy | NE - Nuclear Energy | NR - Naval Reactors | SC - Office of Science |
|---|---|---|---|---|---|---|---|---|---|
| NE114 | Richins, W. D. | Energy Efficient Building Simulation and Technologies | | | X | | | | |
| NS118 | Roberto, F. F. | Novel Selective Matrix for Collection and Identification of Priority Pathogens | X | X | | | | | X |
| NC104 | Rollins, H. W. | Nucleation and Growth of Nanoparticle Materials in Supercritical Fluid Processes | | X | X | | | | X |
| NS121 | Roney, T. J. | Imaging Application of Photon Beams Produced with Compton Backscatter of Laser Beams | X | | | | | | X |
| ST105 | Rope, R. C. | Development of an Integrated Watershed Information Management Tool for Long-Term Facilities | | X | | X | | | X |
| GC140 | Schafer, A. L. | Computational Experiments of Hysteretic Chemical and Moisture Migration | | X | | | | | X |
| GE103 | Schultz, R. R. | Gas-Cooled Reactor System Analysis Tools | | | X | | X | X | |
| GC145 | Scott, C. L. | Dual Electrodes and Defining the Electrically Disturbed Region in Induced Polarization Measurements | | X | | | | | X |
| SC111 | Scott, J. R. | Elucidating the Photo-Physics of Complex Metal Ions Trapped in a Fourier TransformMassSpectrometer | | X | X | | | | X |
| GC119 | Scott, J. R. | Development of Imaging Fourier Transform Mass Spectrometer Capabilities for Analyses of Complex and Heterogeneous Samples | X | X | | | | | X |
| NS128 | Shewmaker, A. G. | Classified Cluster Computing | X | | | | | | X |
| AC102 | Shook, G. M. | Improving Numerical Model Efficiency of a Simulation Model | | X | X | X | | | |
| ET107 | Silverman, H. G. | Recombinant Adhesive Protein Production and Investigation into Alternate Natural Adhesive Systems in Marine Mussels | X | | X | | | | X |
| PH105 | Sisson, J. B. | Improving Soil Water Flux Estimates in the Deep Vadose Zone | | X | | | | | |
| NE111 | Smartt, H. B. | Friction Stir Welding of Lightweight Materials | | | X | | | | |
| GC102 | Smith, R. P. | Regional Setting and Flow Dynamics of the Snake River PlainAquifer | | X | | | | | X |
| GC130 | Starr, R. C. | Development of Techniques for In Situ Measurement of Groundwater Contaminant Source Strength | | X | | | | | |
| CE108 | Steffler, E. D. | Genetics Control of Straw Stem Ultrasound that Affects the Biomechanics of Stem Separation | | | X | | | | X |

## Appendix F–Relevence to Major National Missions

| Project ID | Principal Investigator | Project Title | National Nuclear Security Administration | Environmental Management | EE - Industrial Technologies | FE- Fossil Energy | NE - Nuclear Energy | NR - Naval Reactors | SC - Office of Science |
|---|---|---|---|---|---|---|---|---|---|
| GC107 | Stone, M. L. | Improved Osmotic Tensiometer Components and Parameters | | X | | | | | X |
| GC134 | Stoner, D. L. | Development and Application of Custom Flow Models for Understanding Flow in Porous and Fractured Matrices with Biological Components | | X | | | | | X |
| S472 | Stoner, D. L. | Integrated Experimental and Mathematical Analysis of Complex Chemical and Biological Systems | X | X | X | X | X | X | X |
| ST104 | Stormberg, A. I. | Use of Genetic Markers for Ecological Risk Assessment | | X | | | | | |
| GC144 | Stormberg/McGlone | Characterization of Nonlinear Complex Resistivity Spectra During Biochemical Reduction of Cr to Cr+6+3 | | X | | | | | X |
| NS107 | Swank, W D. | Plasma Spray Processing Development for Energetic Materials | X | | | | | | |
| ES107 | Szpakiewicz, M. J. | Assessment of Long-Term Variations in Soil Moisture and Regional Groundwater Flow Patterns in Response to Potential Climate Changes | | X | | | | | |
| NE118 | Telschow, K. L. | Laser Ultrasonic Corrosion Monitor | X | | X | | X | X | X |
| D437 | Telschow, K. L. | Laser Ultrasonic Characterization of Irradiated Ceramics | | | | | X | | X |
| NC101 | Telschow, K. L. | Nanostructure Characterization for Sensing | | X | | | | | X |
| SC104 | Thantu, N. | Trace Chemical Species Detection and Analysis Using Femtosecond Optical Heterodyne Detected Raman Induced Kerr Effect Spectroscopy | | X | | X | | | X |
| CE101 | Thompson, D. N. | Removal of Minerals from Wheat Straw for Increased Straw Utilization for Bioenergy and Bioproducts | | | X | | | | X |
| GC109 | Thompson, V. S. | Development of Enzymatic Biosensors for Environmental Applications | | X | | | | | X |
| WT103 | Todd, T. A. | Polyacrylonitrile-Based Ion Exchange Sorbents | | X | | | X | | |
| CE109 | Tolle, C. R. | Computational Fluid Dynamics Model Based Control of Two-Phase Flow | | | X | | X | | X |
| NS125 | Totemeier, T. C. | Mechanisms of Liquid Metal Embrittlement in Steels | X | | | | | | X |
| ES105 | Tranter, T. J. | Porous Crystalline Silica (Gubka)-Based Ion Exchange Sorbents | | X | | X | | | X |
| SC112 | VanSiclen, C . D. | Mechanical and Flow Properties of Dry Granular Media | X | X | X | | | | X |

## Appendix F–Relevence to Major National Missions

| Project ID | Principal Investigator | Project Title | National Nuclear Security Administration | Environmental Management | EE - Industrial Technologies | FE - Fossil Energy | NE - Nuclear Energy | NR - Naval Reactors | SC - Office of Science |
|---|---|---|---|---|---|---|---|---|---|
| NS114 | Velasquez, M. E. | Exploring Applications of Wavelet Theory: Groundwater Dynamical Systems, Gamma Spectral Analysis, Accoustic Resonance Spectrometry | X | X | | | | | X |
| GC141 | Versteeg, R. J. | Calibration and Enhancement of Geophysical Imaging Tools in a Mesoscale Experimental Facility | | X | | | | | X |
| CE105 | Ward, T. E. | Acidophilic Bioprocess for Production of Organic Acids from Biomass | | | X | X | | | X |
| NE122 | Weaver, K. D. | An Innovative Gas-Cooled Fast Reactor | | | | | X | | |
| PH104 | Weinberg, D. M. | Modeling an Earth Borehole System for Physical Property Determinationin Shallow Subsurface Environments with Emphasis on Vadose Zone Applications | X | X | | X | | | |
| NE123 | Weinberg, D. M. | Characterization of Methane Hydrate Deposits | | | | X | | | |
| GC105 | Weinberg, D. M. | Advanced BoreholeSeismic Sources for High-Resolution Subsurface Imaging and Characterization for Environmental Applications | | X | | X | | | |
| GC103 | Weinberg,D . M. | Fracture Prediction, Characterization, and Detection in Snake River Basalts-A Modeling and Field Approach | | X | | X | | | |
| ST106 | White, G. J. | Development of Collaborative Approaches to Long-Term Environmental Stewardship | | X | | | | | |
| ET115 | White, G. J. | Carbon Fractionation Potential of Soils via $CO_2$/Water Gradient Fractionation | | X | | X | | | X |
| GC104 | White, G. J. | Carbon Fractionation Potential of Soils via $CO_2$/Water Gradient Fractionation | | X | | X | | | X |

INEEL

Idaho National Engineering & Environmental Laboratory